NASA SP-7037 (268)
August 1991

AERONAUTICAL ENGINEERING

A CONTINUING BIBLIOGRAPHY WITH INDEXES

(NASA-SP-7037(268)) AERONAUTICAL ENGINEERING: A CONTINUING BIBLIOGRAPHY WITH INDEXES (SUPPLEMENT 268) (NASA) 131 p
CSCL 01B
N91-30077
Unclas
00/01 0038241

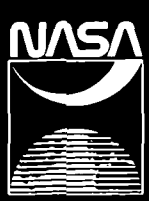

STI PROGRAM
SCIENTIFIC &
TECHNICAL
INFORMATION

NASA SP–7037 (268)
August 1991

AERONAUTICAL ENGINEERING

A CONTINUING BIBLIOGRAPHY WITH INDEXES

National Aeronautics and Space Administration
Office of Management
Scientific and Technical Information Program
Washington, DC 1991

INTRODUCTION

This issue of *Aeronautical Engineering—A Continuing Bibliography* (NASA SP-7037) lists 406 reports, journal articles, and other documents originally announced in July 1991 in *Scientific and Technical Aerospace Reports (STAR)* or in *International Aerospace Abstracts (IAA).*

Accession numbers cited in this issue are:

STAR (N-10000 Series)	N91-21059 — N91-23072
IAA (A-10000 Series)	A91-32449 — A91-36012

The coverage includes documents on the engineering and theoretical aspects of design, construction, evaluation, testing, operation, and performance of aircraft (including aircraft engines) and associated components, equipment, and systems. It also includes research and development in aerodynamics, aeronautics, and ground support equipment for aeronautical vehicles.

Each entry in the publication consists of a standard bibliographic citation accompanied in most cases by an abstract. The listing of the entries is arranged by the first nine *STAR* specific categories and the remaining *STAR* major categories. This arrangement offers the user the most advantageous breakdown for individual objectives. The citations include the original accession numbers from the respective announcement journals.

Seven indexes—subject, personal author, corporate source, foreign technology, contract number, report number, and accession number—are included.

A cumulative index for 1991 will be published in early 1992.

Information on availability of documents listed, addresses of organizations, and NTIS price schedules are located at the back of this issue.

PAGE ii INTENTIONALLY BLANK

CONTENTS

Category 01 Aeronautics (General) 543

Category 02 Aerodynamics 544
Includes aerodynamics of bodies, combinations, wings, rotors, and control surfaces; and internal flow in ducts and turbomachinery.

Category 03 Air Transportation and Safety 561
Includes passenger and cargo air transport operations; and aircraft accidents.

Category 04 Aircraft Communications and Navigation 563
Includes digital and voice communication with aircraft; air navigation systems (satellite and ground based); and air traffic control.

Category 05 Aircraft Design, Testing and Performance 570
Includes aircraft simulation technology.

Category 06 Aircraft Instrumentation 575
Includes cockpit and cabin display devices; and flight instruments.

Category 07 Aircraft Propulsion and Power 577
Includes prime propulsion systems and systems components, e.g., gas turbine engines and compressors; and onboard auxiliary power plants for aircraft.

Category 08 Aircraft Stability and Control 580
Includes aircraft handling qualities; piloting; flight controls; and autopilots.

Category 09 Research and Support Facilities (Air) 584
Includes airports, hangars and runways; aircraft repair and overhaul facilities; wind tunnels; shock tubes; and aircraft engine test stands.

Category 10 Astronautics 586
Includes astronautics (general); astrodynamics; ground support systems and facilities (space); launch vehicles and space vehicles; space transportation; space communications, spacecraft communications, command and tracking; spacecraft design, testing and performance; spacecraft instrumentation; and spacecraft propulsion and power.

Category 11 Chemistry and Materials 588
Includes chemistry and materials (general); composite materials; inorganic and physical chemistry; metallic materials; nonmetallic materials; propellants and fuels; and materials processing.

Category 12 Engineering 590
Includes engineering (general); communications and radar; electronics and electrical engineering; fluid mechanics and heat transfer; instrumentation and photography; lasers and masers; mechanical engineering; quality assurance and reliability; and structural mechanics.

PAGE iv INTENTIONALLY BLANK

Category 13 Geosciences 602
Includes geosciences (general); earth resources and remote sensing; energy production and conversion; environment pollution; geophysics; meteorology and climatology; and oceanography.

Category 14 Life Sciences N.A.
Includes life sciences (general); aerospace medicine; behavioral sciences; man/system technology and life support; and space biology.

Category 15 Mathematical and Computer Sciences 604
Includes mathematical and computer sciences (general); computer operations and hardware; computer programming and software; computer systems; cybernetics; numerical analysis; statistics and probability; systems analysis; and theoretical mathematics.

Category 16 Physics 606
Includes physics (general); acoustics; atomic and molecular physics; nuclear and high-energy physics; optics; plasma physics; solid-state physics; and thermodynamics and statistical physics.

Category 17 Social Sciences 608
Includes social sciences (general); administration and management; documentation and information science; economics and cost analysis; law, political science, and space policy; and urban technology and transportation.

Category 18 Space Sciences N.A.
Includes space sciences (general); astronomy; astrophysics; lunar and planetary exploration; solar physics; and space radiation.

Category 19 General 608

Subject Index A-1
Personal Author Index B-1
Corporate Source Index C-1
Foreign Technology Index D-1
Contract Number Index E-1
Report Number Index F-1
Accession Number Index G-1
Appendix APP-1

TYPICAL REPORT CITATION AND ABSTRACT

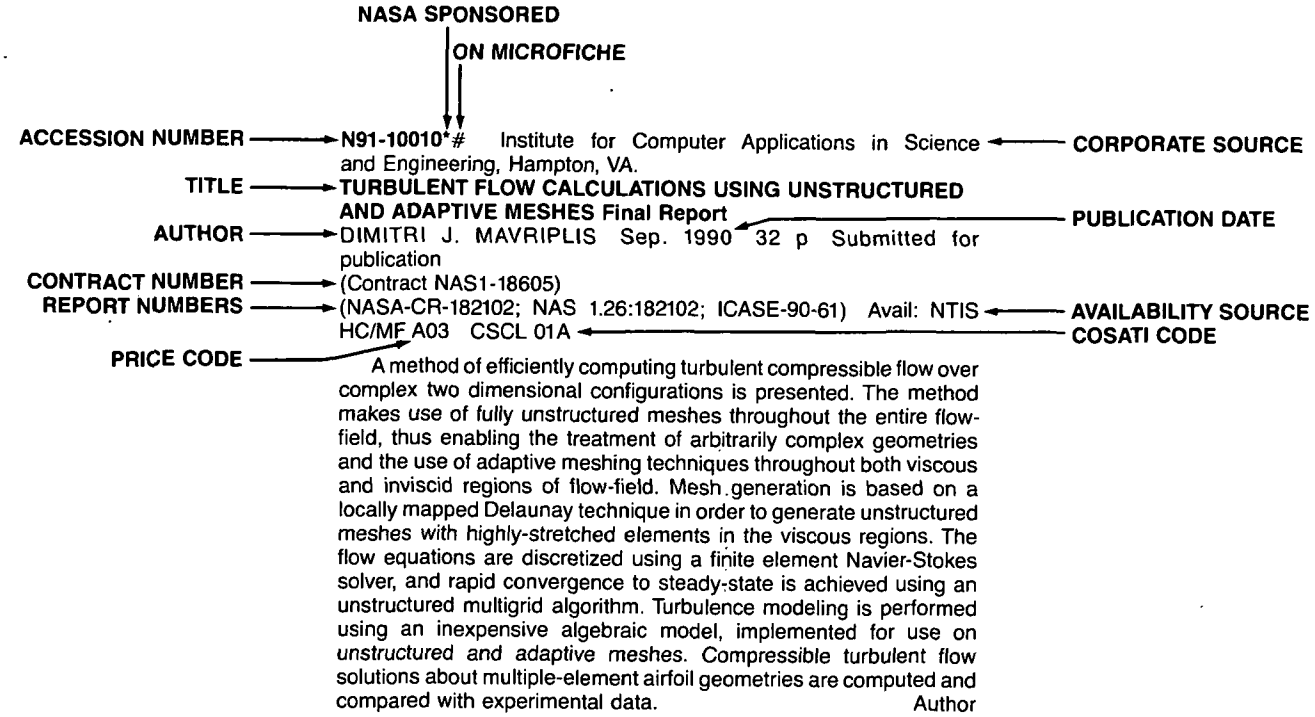

TYPICAL JOURNAL ARTICLE CITATION AND ABSTRACT

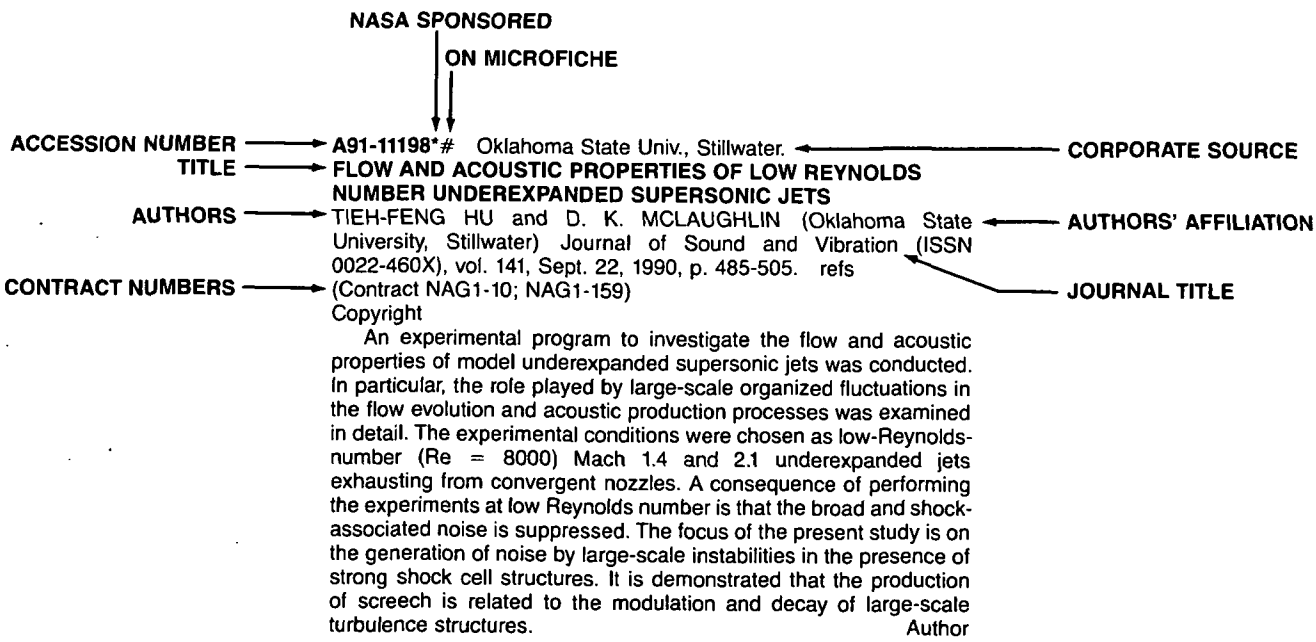

AERONAUTICAL ENGINEERING

A Continuing Bibliography (Suppl. 268)

AUGUST 1991

01

AERONAUTICS (GENERAL)

A91-32648
ADVANCED COMPOSITE TECHNOLOGY OF WEST GERMAN GENERAL AVIATION AIRCRAFT
KLAUS WOITHE (Industrieanlagen-Betriebsgesellschaft mbH, Ottobrunn, Federal Republic of Germany) IN: ICCM-VII; Proceedings of the 7th International Conference on Composite Materials, Guangzhou, People's Republic of China, Nov. 22-24, 1989. Vol. 3. *Beijing/Oxford, International Academic* Publishers/Pergamon Press, 1989, p. 391-397.
Copyright

General-aircraft projects under development or in operation, such as Grob G115, Gyroflug SC 01, and Seastar CD 02 are covered. Two composite technologies, low-pressure and high-pressure, are compared, and it is noted that the West Germany small-aircraft industry is utilizing the low-pressure composite (LPC) technology due to low manufacturing costs associated with low expenditures for the manufacturing equipment. Procedures for the verification of LPC-composite structures is outlined with emphasis on component and structural-part tests, as well as static and fatigue tests. The static strength, fatigue life, residual strength, and damage-tolerance behavior of the SC and G115 wings are measured and found to be within the American and West German certification requirements. V.T.

A91-33372
INTERDISCIPLINARY COOPERATIVE AEROSPACE RESEARCH - EXAMPLES OF SCIENTIFIC COOPERATION WITH BRAUNSCHWEIG TECHNICAL UNIVERSITY [INTERDISZIPLINAERE FORSCHUNGSKOOPERATION IN DER LUFT- UND RAUMFAHRT - BEISPIELE WISSENSCHAFTLICHER ZUSAMMENARBEIT MIT DER TU BRAUNSCHWEIG]
KARL-FRIEDRICH DOHERR, BERND GMELIN, PETER HAMEL, and BERND KRAG (DLR, Institut fuer Flugmechanik, Brunswick, Federal Republic of Germany) DLR-Nachrichten (ISSN 0937-0420), Feb. 1991, p. 23-25. In German.
Copyright

A91-35193
A FLEXIBLE ROBOTIC WORK CELL FOR THE ASSEMBLY OF AIRFRAME COMPONENTS
HOWARD B. OLSEN (Rohr Industries, Inc., Riverside, CA) IN: 1990 IEEE International Conference on Robotics and Automation, Cincinnati, OH, May 13-18, 1990, Proceedings. Vol. 2. Los Alamitos, CA, IEEE Computer Society Press, 1990, p. 1278-1283.
Copyright

A flexible robotic work cell for the assembly of airframe components is described. The key cell devices are two robots, a flexible fixture, a metrology system, an automatic fastening machine, and several end effectors. Software modules are found behind all cell devices. Other software components are found in the cell controller, planning utilities, and offline programming. The emphasis is on functional aspects of the cell and the associated software. I.E.

N91-22067# Aviation Planning Associates, Inc., Cincinnati, OH.
ECONOMIC IMPACT OF AVIATION IN PENNSYLVANIA Final Report
Mar. 1990 85 p Sponsored by Pennsylvania Dept. of Transportation, Harrisburg
(PB91-128264) Avail: NTIS HC/MF A05 CSCL 01/2

The output (gross sales, taxes, and capital expenditures) payroll, and employment generated by aviation activity in Pennsylvania in 1988 are identified. The Commonwealth's aviation network, which includes 146 public-use airports (17 commercial service and 129 general aviation), 350 private airports, and 300 heliports, is a major economic contributor and a simulator of business and industrial development. The direct economic contributions made by airports is identified, and also the induced impacts accrued when aviation dollars circulate throughout the economy, creating successive waves of spending, was estimated. Direct impacts were identified through data collected from major aviation-related groups. Induced impacts were estimated using economic multipliers supplied by the Pennsylvania State University. A major survey conducted for the study showed that the Commonwealth's businesses and industries rely heavily on aviation services. Businesses rated the availability of airports as the third most important of 10 key site selection criteria, and 85 percent said they use commercial air service. GRA

N91-22068# Federal Aviation Administration, Washington, DC. Office of Aviation Policy and Plans.
FAA AVIATION FORECASTS: FISCAL YEARS 1991-2002
Feb. 1991 281 p
(AD-A231721; FAA-APO-91-1) Avail: NTIS HC/MF A13 CSCL 17/7

This report contains the Fiscal Years 1991-2002 Federal Aviation Administration (FAA) forecasts of aviation activity at FAA facilities. These include airports with FAA control towers, air route traffic control centers, and flight service stations. Detailed forecasts were made for the major users of the National Aviation System: air carriers, air taxi-commuters, non-military and general aviation. The forecasts have been prepared to meet the budget and planning needs of the constituent units of the FAA and to provide information that can be used by state and local authorities, the aviation industry, and the general public. After a downturn in economic growth in 1991, caused largely by an escalation in oil prices, the overall outlook for the 12-year forecast period is for contiued economic growth, declining real fuel prices, and moderate inflation. Based upon these assumptions, aviation activity by fiscal year 2002 is forecast to increase by 27.4 percent at towered airports, 30.1 percent at air route traffic control centers, and 6.5 percent in flight services performed. Hours flown by general aviation are forecast to increase 17.5 percent and domestic revenue passenger miles (RPM's) are forecast to increase 62.6 percent, with scheduled international RPM's forecast to increase by 110.8 percent and regionals/commuters RPM's forecast to increase by 140.4 percent. GRA

02

AERODYNAMICS

Includes aerodynamics of bodies, combinations, wings, rotors, and control surfaces; and internal flow in ducts and turbomachinery.

A91-32958#
THREE-DIMENSIONAL FLOW NEAR THE BLADE/ENDWALL JUNCTION OF A GAS TURBINE - VISUALIZATION IN A LARGE-SCALE CASCADE SIMULATOR
J. T. CHUNG and T. W. SIMON (Minnesota, University, Minneapolis) ASME, Winter Annual Meeting, Dallas, TX, Nov. 25-30, 1990. 7 p. refs
(Contract F49620-85-C-0049)
(ASME PAPER 90-WA/HT-4)

A large-scale two half-blade facility for simulating a turbine cascade flow is presented. The simulator consists of two large half-blade sections, one wall simulating the pressure surface and the other wall simulating the suction surface; two parallel endwalls constitute the third and fourth walls of the channel. Various flow-visualization techniques including oil and lampblack, ink and oil of wintergreen, a single tuft probe, and a tuft grid are used to confirm that the important features of the cascade flow are replicated in the simulator. It is observed that the location of the saddle point and the track of the horseshoe vortex are not sensitive to the position of the side wall so long as the side wall is in place, inducing most of the flow to go through the passage between the blades. V.T.

A91-33369
PROGRESS IN THE PREDICTION OF THE LAMINAR-TURBULENT TRANSITION FOR LAMINAR WINGS - THE PROFILE AND WING GEOMETRIES DETERMINE THE FRICTION DRAG OF AN AIRCRAFT [FORTSCHRITTE BEI DER VORHERSAGE DES LAMINAR-TURBULENTEN UMSCHLAGS BEI LAMINARFLUEGELN - PROFIL- UND FLUEGELGEOMETRIE BESTIMMEN REIBUNGSWIDERSTAND EINES FLUGZEUGES]
GUENTER REDEKER and KARL H. HORSTMANN (DLR, Institut fuer Entwurfsaerodynamik, Brunswick, Federal Republic of Germany) DLR-Nachrichten (ISSN 0937-0420), Feb. 1991, p. 7-11. In German. refs
Copyright

The current status of DLR research on the transition to turbulence on laminar-flow aircraft wings is reviewed and illustrated with diagrams, graphs, and photographs. The relationship between Tollmien-Schlichting instability, cross-flow instability, and leading-edge transition is explained; the stability theory of laminar boundary layers is outlined; and flight tests are described in which the Tollmien-Schlichting and cross-flow N factors were measured for swept and unswept wings with different laminar-flow profiles (where N is the ratio of the instability amplitude A at a given point in the boundary layer to the initial amplitude A0). It is shown that the flight-test data can be incorporated into empirical models, permitting accurate predictions of the transition to turbulence during the design of laminar wings. T.K.

A91-33378*# National Aeronautics and Space Administration. Langley Research Center, Hampton, VA.
FLOWFIELD AND VEHICLE PARAMETER INFLUENCE ON RESULTS OF ENGINEERING AEROTHERMAL METHODS
KATHRYN E. WURSTER, E. VINCENT ZOBY, and RICHARD A. THOMPSON (NASA, Langley Research Center, Hampton, VA) Journal of Spacecraft and Rockets (ISSN 0022-4650), vol. 28, Jan.-Feb. 1991, p. 16-22. Previously cited in issue 18, p. 2763, Accession no. A89-43279. refs
Copyright

A91-33379#
COMPUTATION OF FLOWFIELDS FOR PROJECTILES IN HYPERSONIC CHEMICALLY REACTING FLOWS
KLAUS A. HOFFMANN (Wichita State University, KS), TING-LUNG CHIANG (Texas, University, Austin), and WALTER H. RUTLEDGE (Sandia National Laboratories, Albuquerque, NM) Journal of Spacecraft and Rockets (ISSN 0022-4650), vol. 28, Jan.-Feb. 1991, p. 23-30. refs
Copyright

A technique is presented for solving the inviscid, chemically reacting, hypersonic flowfield over axisymmetric blunt bodies. The Euler equations are solved using a fully implicit, flux vector splitting, finite-difference scheme. An approximate factorization scheme is also used in order to improve computational efficiency. Finite-rate chemical reaction calculations are decoupled from the gas dynamic equations in the current analysis. Complex blunt body shapes, including highly indented nose geometries, are analyzed for Mach numbers from 2 to 18. Author

A91-33380*# National Aeronautics and Space Administration. Ames Research Center, Moffett Field, CA.
FULLY COUPLED IMPLICIT METHOD FOR THERMOCHEMICAL NONEQUILIBRIUM AIR AT SUBORBITAL FLIGHT SPEEDS
CHUL PARK (NASA, Ames Research Center, Moffett Field, CA) and SEOKKWAN YOON (MCAT Institute, Moffett Field, CA) Journal of Spacecraft and Rockets (ISSN 0022-4650), vol. 28, Jan.-Feb. 1991, p. 31-39. Previously cited in issue 18, p. 2750, Accession no. A89-41818. refs
Copyright

A91-33382#
PREDICTION OF SLENDER BODY CONING CHARACTERISTICS
L. E. ERICSSON (Lockheed Missiles and Space Co., Inc., Sunnyvale, CA) Journal of Spacecraft and Rockets (ISSN 0022-4650), vol. 28, Jan.-Feb. 1991, p. 43-49. Previously cited in issue 21, p. 3252, Accession no. A89-47679. refs
(Contract F33615-87-C-3607)
Copyright

A91-33675
NUMERICAL SIMULATION OF COMPRESSIBLE EULER FLOWS
ALAIN DERVIEUX, ED. (INRIA, Valbonne, France), BRAM VAN LEER, ED. (Michigan, University, Ann Arbor), JACQUES PERIAUX, ED. (Dassault Aviation, Saint-Cloud, France), and ARTHUR RIZZI, ED. (Royal Institute of Technology, Stockholm, Sweden) Wiesbaden, Federal Republic of Germany/Hauppauge, NY, Friedr. Vieweg & Sohn/Ballen Books (Notes on Numerical Fluid Mechanics. Vol. 26), 1989, 368 p. No individual items are abstracted in this volume.
Copyright

Implicit, explicit, steady-state, and multigrid numerical solution methods for the Euler equations of compressible fluid dynamics are described and demonstrated in papers presented at a GAMM workshop held at INRIA in Rocquencourt, France, in June 1986. The problems posed to the workshop participants for analysis are stated; the basic numerical approaches are reviewed in introductory lectures; the individual methods are outlined; and the test-computation results are presented in extensive graphs and briefly characterized. D.G.

A91-33735
THE DYNAMIC BEHAVIOR OF A SHOCK-WAVE/TURBULENT BOUNDARY LAYER INTERACTION
MICHAEL S. SELIG and ALEXANDER J. SMITS (Princeton University, NJ) IN: Near-wall turbulence. New York, Hemisphere Publishing Corp., 1990, p. 190-197. refs
(Contract DAAG29-85-K-0255)
Copyright

Periodic blowing at frequencies up to 5 kHz was used to control the unsteadiness of a two-dimensional shock wave/turbulent boundary layer interaction. The interaction was formed by a 24-deg compression corner, and the periodic blowing was introduced into the shock-induced separation bubble. Measurements of the

fluctuating mass flux and wall pressure were made, and the unsteady flowfield was visualized through stroboscopic schlieren videography. Although the control of the shock wave ranged from negligible to strong, the turbulence amplification showed no substantial changes, suggesting that the unsteady shock was not the principal cause for the increased turbulence as had been previously thought. Instead, there is strong evidence to suggest that large-scale instabilities associated with inflectional velocity profiles in the downstream boundary layer contribute strongly to the large mixing observed downstream of the interaction. Author

A91-33747
CORRELATION MEASUREMENTS AND STRUCTURE ANGLES IN A TURBULENT BOUNDARY LAYER RECOVERING FROM CONVEX CURVATURE
AMY E. ALVING and ALEXANDER J. SMITS (Princeton University, NJ) IN: Near-wall turbulence. New York, Hemisphere Publishing Corp., 1990, p. 507-528. refs
(Contract AF-AFOSR-85-0126)
Copyright

Simultaneous, multiple point turbulence measurements were made in a boundary layer upstream and downstream of a 90-deg convex bend. Two-point space-time correlation coefficients were computed for several separation distances. For the undisturbed boundary layer, theta takes low values near the wall, increases to 30 - 40 deg in the central portion of the layer, and increases further near the boundary layer edge. At the exit from the convex curvature, theta is largely unchanged. In the relaxing boundary layer theta appears to increase over most of the boundary layer thickness. The sensitivity of the structure angle to the probe separation distance, and the significance of the results in terms of large-scale organized motions are discussed. The instantaneous structure angle can be defined in terms of short-time correlations, and some of the difficulties associated with this concept are also discussed. Author

A91-33802
EFFECTS OF HEAT TRANSFER ON AERODYNAMICS AND POSSIBLE IMPLICATIONS FOR WIND TUNNEL TESTS
D. G. MABEY (Royal Aerospace Establishment, Aerodynamics Dept., Bedford, England) Progress in Aerospace Sciences (ISSN 0376-0421), vol. 27, no. 4, 1990, p. 267-303. refs
Copyright

A review is made of the large effects of heat transfer on steady aerodynamics. Cooling the surface delays flow separation and thus is roughly equivalent to an increase in Reynolds number. Conversely heating promotes flow separation and is roughly equivalent to a decrease in Reynolds number. Cooling can also increase the extent of laminar boundary layers. These characteristics might be exploited to identify conditions for which large scale effects occur. The review has found no discussion of the effects of heat transfer on unsteady aerodynamics. From the steady effects some tentative suggestions are inferred about the probable influence of heat transfer on buffet excitation measurements in wind tunnels. Some preliminary wind tunnel tests and some predictive studies are recommended to clarify some of the issues discussed. Author

A91-33803
ON MANAGEMENT AND CONTROL OF TURBULENT SHEAR FLOWS
H. E. FIEDLER and H.-H. FERNHOLZ (Berlin, Technische Universitaet, Federal Republic of Germany) Progress in Aerospace Sciences (ISSN 0376-0421), vol. 27, no. 4, 1990, p. 305-387. DFG-supported research. refs
Copyright

An attempt is made to compile a major body of the available knowledge on flow control in separated and wall bounded turbulent flows. After a brief introduction of the basics of control theory and of the major flow structures and their stability characteristics, free and wall-bounded turbulent shear flows are discussed. This discussion summarizes the main relationships between structure and flow behavior, and shows possibilities of influencing properties of these flows, such as increasing mixing or avoiding separation. Author

A91-33920
EFFECT OF A SINGLE THREE-DIMENSIONAL SURFACE ROUGHNESS ON THE TRANSITION IN A SUPERSONIC BOUNDARY LAYER [VLIIANIE EDINICHNOI TREKHMERNOI SHEROKHOVATOSTI NA PEREKHOD V SVERKHZVUKOVOM POGRANICHNOM SLOE]
O. I. ZININ, A. A. MASLOV, V. E. NOVIKOV, and S. G. SHEVEL'KOV (AN SSSR, Institut Teoreticheskoi i Prikladnoi Mekhaniki, Novosibirsk, USSR) Akademiia Nauk SSSR, Sibirskoe Otdelenie, Izvestiia, Seriia Tekhnicheskie Nauki (ISSN 0002-3434), June 1990, p. 47-53. In Russian. refs
Copyright

The effect of a single surface roughness in the form of a projecting cylinder (0.3 mm in diameter) on the laminar-turbulent transition in a boundary layer on a flat plate was investigated experimentally at M = 2.0 for various wind tunnel regimes. The transition was observed by means of flow visualization techniques and measured by using pressure transducers and hot-wire anemometry. The results are in agreement with the results of Van Drist and Blumer (1962) obtained for a cone with surface roughness in the form of spheres. The evolution of turbulence in the wake of the roughness is examined. V.L.

A91-34033
LAMINAR SHOCK/BOUNDARY-LAYER INTERACTION - A NUMERICAL TEST PROBLEM
E. KATZER (Kiel, Universitaet, Federal Republic of Germany) IN: Numerical treatment of the Navier-Stokes equations; Proceedings of the 5th GAMM-Seminar, Kiel, Federal Republic of Germany, Jan. 20-22, 1989. Wiesbaden, Federal Republic of Germany/Hauppauge, NY, Friedr. Vieweg & Sohn/Ballen Books, 1990, p. 82-89. refs
Copyright

The interaction of an oblique shock with a laminar boundary layer has been used frequently as a test problem for comparing Navier-Stokes codes. This paper identifies various length scales of the interaction region which impose considerable restrictions on the numerical grid. It is shown that the wall pressure distribution is not useful for assessing the numerical accuracy. The pressure at the edge of the boundary layer is proposed as an expedient variable indicating the numerical accuracy. Local and global properties of the flow are analysed. A new similarity law for the length of the separation bubble facilitates an estimate of the global length scale and could be used for the generation of initial values for numerical calculations. Author

A91-34034
COMPARISON OF UPWIND AND CENTRAL FINITE-DIFFERENCE METHODS FOR THE COMPRESSIBLE NAVIER-STOKES EQUATIONS
B. MUELLER (DLR, Institut fuer theoretische Stroemungsmechanik, Goettingen, Federal Republic of Germany) IN: Numerical treatment of the Navier-Stokes equations; Proceedings of the 5th GAMM-Seminar, Kiel, Federal Republic of Germany, Jan. 20-22, 1989. Wiesbaden, Federal Republic of Germany/Hauppauge, NY, Friedr. Vieweg & Sohn/Ballen Books, 1990, p. 90-99. refs
Copyright

Two implicit second-order finite-difference methods are compared for the steady-state solution of the time-dependent compressible Navier-Stokes equations: a central spatial discretization scheme with added second- and fourth-order numerical damping and an upwind scheme, which reduces to first-order accuracy at extrema and is total variation diminishing for nonlinear one-dimensional scalar hyperbolic equations. The upwind scheme proves in general to be more robust and more accurate than the central scheme for subsonic flat plate flow, transonic airfoil flow, and hypersonic ramp flow. Using approximate factorization, the central scheme is more efficient than the upwind scheme. Author

A91-34052
A VORTEX-LATTICE METHOD FOR THE CALCULATION OF VORTEX SHEET ROLL-UP AND WING-VORTEX INTERACTION
R. BEHR and S. WAGNER (Muenchen, Universitaet der Bundeswehr, Neubiberg, Federal Republic of Germany) IN: Finite approximations in fluid mechanics II: DFG priority research programme results 1986-1988. Wiesbaden, Federal Republic of Germany/Hauppauge, NY, Friedr. Vieweg & Sohn/Ballen Books, 1989, p. 1-14. refs
(Contract DFG-WA-424/4)
Copyright

A vortex-lattice method is presented that allows the calculation of attached and separated flow over single or coupled thin wings of arbitrary planforms. Both lifting-surface and free vortex sheets are represented by a distribution of doublet elements of stepwise constant strength. Beginning with an impulsive start, the position of the vortex lines in the flowfield is obtained by a time-marching procedure so that no starting solution for the wake geometry is necessary. For a successful analysis of strongly rolled-up discretized vortex sheets within the time-dependent framework, a continuous velocity distribution all over the flowfield is indispensable. Due to the use of discrete vortices, the amount and direction of induced velocities close to the discontinuity surfaces calculated by the Biot-Savart law lead to unrealistic values. To overcome this problem, which all low-order panel methods have to face, some different numerical procedures are introduced. Results of this model are compared with measurements and other computational methods. Author

A91-34055
A METHOD TO CALCULATE THE INFLUENCE OF VORTEX ROLL-UP ON THE INDUCED DRAG OF WINGS
R. EPPLER and S. SCHMID-GOELLER (Stuttgart, Universitaet, Federal Republic of Germany) IN: Finite approximations in fluid mechanics II: DFG priority research programme results 1986-1988. Wiesbaden, Federal Republic of Germany/Hauppauge, NY, Friedr. Vieweg & Sohn/Ballen Books, 1989, p. 93-107. refs
Copyright

The theoretical basis and numerical implementation of a method developed by Eppler (1987) to determine the induced drag produced by vortex roll-up in the wake of an aircraft wing are reviewed. Consideration is given to the normalization of the parameters; the characteristic relations; the application of Munk's theorem; the wake iteration; and the calculation of lift, induced drag, and roll-up intensity. Results for wings with straight trailing edges, wings with upward- or downward-facing winglets, and wings with positive or negative sweep angle are presented in graphs and briefly characterized. D.G.

A91-34057
NUMERICAL CALCULATION OF THE UNSTEADY SEPARATING FLOW ON OSCILLATING AIRFOILS (DYNAMIC STALL)
W. GEISSLER (DLR, Institut fuer Aeroelastik, Goettingen, Federal Republic of Germany) IN: Finite approximations in fluid mechanics II: DFG priority research programme results 1986-1988. Wiesbaden, Federal Republic of Germany/Hauppauge, NY, Friedr. Vieweg & Sohn/Ballen Books, 1989, p. 125-141. refs
Copyright

The unsteady viscous flow on an airfoil undergoing light dynamic stall (up to 5 deg pitching-mode oscillations about mean angles of attack up to 15 deg) is investigated by means of numerical simulations. The theoretical basis of the method is discussed, with an emphasis on the treatment of the unsteady inviscid flow outside the airfoil boundary layer, direct viscous-inviscid coupling, and interactive-mode coupling. A global coupling procedure is outlined, and results for NACA 0012 and NLR 7301 airfoils, obtained using the FLARE approximation (Reyhner and Fluegge-Lotz, 1968) to avoid numerical instabilities, are presented in graphs. It is shown that direct coupling fails at the position of unsteady separation, but that this problem can be averted using strongly interactive coupling (with the external velocity distribution as an additional unknown). The applicability of the present analysis to oscillations of helicopter rotor blades is indicated. D.G.

A91-34063
CLOSED-COUPLED ZONAL SOLUTION FOR VISCOUS FLOW PROBLEMS
ERNST HEINRICH HIRSCHEL (Muenchen, Technische Universitaet; MBB GmbH, Munich, Federal Republic of Germany) and K. M. WANIE (MBB GmbH, Munich, Federal Republic of Germany) IN: Finite approximations in fluid mechanics II: DFG priority research programme results 1986-1988. Wiesbaden, Federal Republic of Germany/Hauppauge, NY, Friedr. Vieweg & Sohn/Ballen Books, 1989, p. 197-215. refs
Copyright

This paper reviews the development of a method of zonal solutions for viscous flow problems. Within the zonal approach local solutions of the Navier-Stokes equations in regions of strong viscous-inviscid interaction are closely coupled with solutions of the Euler and the boundary-layer equations in regions of weak interaction. Overall goal is to reduce the computational effort while improving the description of boundary-layer and separation phenomena. The governing equations, the leading principles and their numerical realization are described in detail. A wide range of applications demonstrates the feasibility of the method. Author

A91-34070
HYPERSONIC FLOW SIMULATION FOR BLUNT BODIES AT INCIDENCE
B. MUELLER, S. RIEDELBAUCH, and D. RUES (DLR, Institut fuer theoretische Stroemungsmechanik, Goettingen, Federal Republic of Germany) IN: Finite approximations in fluid mechanics II: DFG priority research programme results 1986-1988. Wiesbaden, Federal Republic of Germany/Hauppauge, NY, Friedr. Vieweg & Sohn/Ballen Books, 1989, p. 310-321. DFG-supported research. refs
Copyright

Laminar hypersonic flows over spherically blunted bodies and an ellipsoid at angle of attack are simulated by a semi-implicit finite-difference method. The central discretization of the thin-layer Navier-Stokes equations is explicit in the surface tangential directions and implicit in the normal direction. The scheme operates as a checkerboard line relaxation method, and requires only the conservative variables and the Cartesian coordinates to be permanently stored. The code is verified by comparison with axisymmetric computational results and with experiments. Primary and secondary separation vortices are simulated for hypersonic flow over an ellipsoid at 20 degrees incidence. Author

A91-34073
AIRFOILS IN TWO- AND THREE-DIMENSIONAL GUST FIELDS
S. SCHLECHTRIEM and J. BALLMANN (Aachen, Rheinisch-Westfaelische Technische Hochschule, Federal Republic of Germany) IN: Finite approximations in fluid mechanics II: DFG priority research programme results 1986-1988. Wiesbaden, Federal Republic of Germany/Hauppauge, NY, Friedr. Vieweg & Sohn/Ballen Books, 1989, p. 337-350. refs
Copyright

The numerical solution of the hyperbolic system of PDEs of the inviscid unsteady compressible flow around an airfoil is obtained by using an explicit second-order bicharacteristic method. The airfoil's wake is treated as a contact discontinuity which corresponds to a time-dependent vortex sheet emanating from the trailing edge. To overcome the difficulties arising from a combination of a fixed grid with an embedded time-dependent vortex layer, a moving grid is employed. The method is applied to study the interaction of discrete transverse and lateral gusts with an airfoil (profiles NACA 0012 and RAE 2822). Author

A91-34074
COMPUTATION OF UNSTEADY INCOMPRESSIBLE VISCOUS FLOW AROUND AIRFOILS
H. SCHUETZ and F. THIELE (Berlin, Technische Universitaet, Federal Republic of Germany) IN: Finite approximations in fluid

mechanics II: DFG priority research programme results 1986-1988. Wiesbaden, Federal Republic of Germany/Hauppauge, NY, Friedr. Vieweg & Sohn/Ballen Books, 1989, p. 366-380. refs
Copyright

The calculation of flow around airfoils with unsteady vortex shedding is based on the Navier-Stokes equations in the pure streamfunction formulation. For the finite approximation of the fourth-order differential equation, a Hermitian finite-difference and Euler-implicit 3-point-backward discretization is used for spatial and time derivatives, respectively. Applying Newton-Chord linearization, the algebraic system of equations obtained is directly solved by means of an L-U decomposition specially adapted to the structure of the coefficient matrix. Author

A91-34126#
VORTICITY EQUATION SOLUTIONS FOR SLENDER WINGS AT HIGH INCIDENCE
A. DAGAN (Rafael Armament Development Authority, Haifa, Israel) and D. ALMOSNINO (Rafael Armament Development Authority; Technion - Israel Institute of Technology, Haifa) AIAA Journal (ISSN 0001-1452), vol. 29, April 1991, p. 497-504. Previously cited in issue 18, p. 2751, Accession no. A89-41832. refs
Copyright

A91-34128#
CELL-VERTEX, MULTIGRID EULER SCHEME FOR USE WITH MULTIBLOCK GRIDS
M. T. ARTHUR, T. A. BLAYLOCK (Royal Aerospace Establishment, Farnborough, England), and J. M. ANDERSON AIAA Journal (ISSN 0001-1452), vol. 29, April 1991, p. 507-514. Previously cited in issue 09, p. 1281, Accession no. A89-25387. refs
Copyright

A91-34130*# Old Dominion Univ., Norfolk, VA.
INTERFERENCE-FREE MEASUREMENTS OF THE SUBSONIC AERODYNAMICS OF SLANTED-BASE OGIVE CYLINDERS
COLIN P. BRITCHER and CHARLES W. ALCORN (Old Dominion University, Norfolk, VA) AIAA Journal (ISSN 0001-1452), vol. 29, April 1991, p. 520-525. refs
(Contract NAG1-716)
Copyright

Drag, lift, pitching moment, and base-pressure measurements have been made, free of support interference, on a range of slanted-base ogive cylinders, using the NASA Langley Research Center 13-in magnetic suspension and balance system. Test Mach numbers were in the range 0.04-0.2. Two types of wake flow were observed, a quasi-symmetric turbulent closure or a longitudinal vortex flow. Aerodynamic characteristics differ dramatically between the two wake types. Drag measurements are shown to be in agreement with previous tests. A hysteretic behavior of the wake with varying Reynold's number has been discovered for the 45-deg base. An interaction between forebody boundary-layer state and wake flow and base pressures has been detected for higher slant angles. Author

A91-34135*# National Aeronautics and Space Administration. Lewis Research Center, Cleveland, OH.
ROLE OF ARTIFICIAL VISCOSITY IN EULER AND NAVIER-STOKES SOLVERS
APARAJIT J. MAHAJAN (NASA, Lewis Research Center, Cleveland, OH; Duke University, Durham, NC), EARL H. DOWELL, and DONALD B. BLISS (Duke University, Durham, NC) AIAA Journal (ISSN 0001-1452), vol. 29, April 1991, p. 555-559. refs
(Contract NAG3-724)
Copyright

A method is proposed to determine directly the amount of artificial viscosity needed for stability using an eigenvalue analysis for a finite difference representation of the Navier-Stokes equations. The stability and growth of small perturbations about a steady flow over airfoils are analyzed for various amounts of artificial viscosity. The eigenvalues were determined for a small time-dependent perturbation about a steady inviscid flow over an NACA 0012 airfoil at a Mach number of 0.8 and angle of attack of 0 deg. The method has been applied to inviscid flows here, but as discussed is also applicable to viscous flows. The movement of the eigenvalue constellation with respect to the amount of artificial viscosity is studied. The stability boundaries as a function of the amount cf artificial viscosity from both the eigenvalue analysis and the time-marching scheme are also presented. The eigenvalue procedure not only allows for determining the effect of varying amounts of artificial viscosity, but also for the effects of different forms of artificial viscosity. Author

A91-34136*# National Aeronautics and Space Administration. Ames Research Center, Moffett Field, CA.
EFFECT OF GEOMETRICAL DISTURBANCE ON VORTEX ASYMMETRY
DAVID DEGANI (NASA, Ames Research Center, Moffett Field, CA) AIAA Journal (ISSN 0001-1452), vol. 29, April 1991, p. 560-566. Previously cited in issue 06, p. 760, Accession no. A90-19937. refs
Copyright

A91-34139#
UNSTEADY FLOWFIELD BEHIND A VORTEX GENERATOR RAPIDLY PITCHED TO ANGLE OF ATTACK
HOWARD S. LITTELL and JOHN K. EATON (Stanford University, CA) AIAA Journal (ISSN 0001-1452), vol. 29, April 1991, p. 577-584. Previously cited in issue 07, p. 968, Accession no. A91-21330. refs
(Contract F49620-86-K-0020)
Copyright

A91-34179* Boeing Co., Seattle, WA.
SOLUTION ADAPTIVE LOCAL RECTANGULAR GRID REFINEMENT FOR TRANSONIC AERODYNAMIC FLOW PROBLEMS
MICHAEL B. BIETERMAN, JOHN E. BUSSOLETTI, CRAIG L. HILMES, FORRESTER T. JOHNSON, ROBIN G. MELVIN (Boeing Co., Seattle, WA) et al. IN: GAMM-Conference on Numerical Methods in Fluid Mechanics, 8th, Delft, Netherlands, Sept. 27-29, 1989, Proceedings. Wiesbaden, Federal Republic of Germany/Hauppauge, NY, Friedr. Vieweg & Sohn/Ballen Books, 1990, p. 22-31. refs
(Contract NAS2-12513)
Copyright

This paper describes the use of solution-adaptive local grid refinement in a numerical method for solving transonic flow problems about complex three-dimensional aircraft configurations. The method is implemented in the TRANAIR code, which has been applied to help solve many practical engineering problems. Attention is focused here on the principal components of the solution-adaptive grid algorithms currently being developed and on two applications that demonstrate the capabilities of the algorithms. Author

A91-34180
NUMERICAL SIMULATION OF LAMINAR HYPERSONIC FLOW PAST BLUNT BODIES INCLUDING HIGH TEMPERATURE EFFECTS
G. BRENNER, S. RIEDELBAUCH, and B. MUELLER (DLR, Institut fuer theoretische Stroemungsmechanik, Goettingen, Federal Republic of Germany) IN: GAMM-Conference on Numerical Methods in Fluid Mechanics, 8th, Delft, Netherlands, Sept. 27-29, 1989, Proceedings. Wiesbaden, Federal Republic of Germany/Hauppauge, NY, Friedr. Vieweg & Sohn/Ballen Books, 1990, p. 32-41. Dassault Aviation-supported research. refs
Copyright

Axisymmetric laminar hypersonic flows of perfect gas and equilibrium air past blunt bodies are simulated. The thin-layer Navier-Stokes equations are solved by a semi-implicit central finite-difference method. The thermodynamic and transport properties of equilibrium air are obtained from curve-fitting routines and from a Gibbs-energy minimization procedure. Results are obtained for a flow past a hemisphere and a hyperboloid.
Author

A91-34185
SOLUTION METHOD FOR VISCOUS FLOWS AT ALL SPEEDS IN COMPLEX DOMAINS
I. DEMIRDZIC (Sarajevo, University, Yugoslavia), R. I. ISSA (Imperial College of Science, Technology, and Medicine, London, England), and Z. LILEK (Unis-Institut, Sarajevo, Yugoslavia) IN: GAMM-Conference on Numerical Methods in Fluid Mechanics, 8th, Delft, Netherlands, Sept. 27-29, 1989, Proceedings. Wiesbaden, Federal Republic of Germany/Hauppauge, NY, Friedr. Vieweg & Sohn/Ballen Books, 1990, p. 89-98. refs
Copyright

An existing numerical method for the solution of laminar and turbulent incompressible flows in complex geometries is extended to the calculation of steady compressible flows. As a result a method is obtained which is equally valid for both incompressible and compressible flows, including transonic and supersonic regimes. The method is verified on a number of test cases, including inviscid and viscous both internal and external flows. The overall performance of the method may be considered good, except for the smearing of the shocks, which is the consequence of the currently employed first order differencing scheme. As an illustration of the capabilities of the method it is applied to the prediction of the flow around a projectile with and without base bleed. Author

A91-34187
HYPERSONIC LEESIDE FLOW COMPUTATIONS USING CENTERED SCHEMES FOR EULER EQUATIONS
PETER ELIASSON and ARTHUR RIZZI (Aeronautical Research Institute of Sweden, Bromma) IN: GAMM-Conference on Numerical Methods in Fluid Mechanics, 8th, Delft, Netherlands, Sept. 27-29, 1989, Proceedings. Wiesbaden, Federal Republic of Germany/Hauppauge, NY, Friedr. Vieweg & Sohn/Ballen Books, 1990, p. 109-118.
Copyright

A centered finite-volume scheme using artificial viscosity is applied to hypersonic flow past a sphere. The windside of the flowfield is characterized by the strong bow shock, and the leeside by separation and vortical flow. In order to obtain the correct bow shock standoff distance, this scheme has been improved in terms of conservation and viscosity switches. A number of computed examples of hypersonic flows past a sphere demonstrate these improvements and illustrate the features of the leeside flowfield. Author

A91-34191
NON-EQUILIBRIUM HYPERSONIC FLOW COMPUTATIONS BY IMPLICIT SECOND-ORDER UPWIND FINITE-ELEMENTS
N. GLINSKY, L. FEZOUI, M. C. CICCOLI, and J.-A. DESIDERI (INRIA, Valbonne, France) IN: GAMM-Conference on Numerical Methods in Fluid Mechanics, 8th, Delft, Netherlands, Sept. 27-29, 1989, Proceedings. Wiesbaden, Federal Republic of Germany/Hauppauge, NY, Friedr. Vieweg & Sohn/Ballen Books, 1990, p. 159-168. refs
Copyright

Second-order implicit schemes are constructured for the solution of steady hypersonic chemically-reacting inviscid flows. In a standard nonequilibrium model accounting for five species (N2, O2, NO, N and O), the Euler equations are coupled with species-convection equations. In a fractional-step approach, the set of fluid-motion equations and the set of chemical-kinetics equations are alternatively time-marched, both sets implicitly. The basic approximation method employs a finite-volume formulation applicable to arbitrary finite-element-type unstructured triangulations. The accuracy is enhanced by the MUSCL extrapolation, and quasi-second-order solutions are obtained by slope-limitation or TVD-averaging. The merits of the various proposed approximations are evaluated by numerical experiments, computing the hypersonic flows over a cylinder and around a model geometry for the Hermes space shuttle. Author

A91-34192* National Aeronautics and Space Administration. Ames Research Center, Moffett Field, CA.
A STREAMWISE UPWIND ALGORITHM APPLIED TO VORTICAL FLOW OVER A DELTA WING
PETER M. GOORJIAN and SHIGERU OBAYASHI (NASA, Ames Research Center, Moffett Field, CA) IN: GAMM-Conference on Numerical Methods in Fluid Mechanics, 8th, Delft, Netherlands, Sept. 27-29, 1989, Proceedings. Wiesbaden, Federal Republic of Germany/Hauppauge, NY, Friedr. Vieweg & Sohn/Ballen Books, 1990, p. 169-178. refs
Copyright

Improvements have been made to a streamwise upwind algorithm so that it can be used for calculating flows with vortices. A calculation is shown of flow over a delta wing at an angle of attack. The laminar, thin-layer, Navier-Stokes equations are used for the calculation. The results are compared with another upwind method, a central-differencing method, and experimental data. The present method shows improvements in accuracy and convergence properties. Author

A91-34193* Rome Univ. (Italy).
A NUMERICAL STUDY OF HYPERSONIC STAGNATION HEAT TRANSFER PREDICTIONS AT A COORDINATE SINGULARITY
FRANCESCO GRASSO (Roma I, Universita, Rome, Italy) and PETER A. GNOFFO (NASA, Langley Research Center, Hampton, VA) IN: GAMM-Conference on Numerical Methods in Fluid Mechanics, 8th, Delft, Netherlands, Sept. 27-29, 1989, Proceedings. Wiesbaden, Federal Republic of Germany/Hauppauge, NY, Friedr. Vieweg & Sohn/Ballen Books, 1990, p. 179-188. refs
Copyright

The problem of grid induced errors associated with a coordinate singularity on heating predictions in the stagnation region of a three-dimensional body in hypersonic flow is examined. The test problem is for Mach 10 flow over an Aeroassist Flight Experiment configuration. This configuration is composed of an elliptic nose, a raked elliptic cone, and a circular shoulder. Irregularities in the heating predictions in the vicinity of the coordinate singularity, located at the axis of the elliptic nose near the stagnation point, are examined with respect to grid refinement and grid restructuring. The algorithm is derived using a finite-volume formulation. An upwind-biased total-variation diminishing scheme is employed for the inviscid flux contribution, and central differences are used for the viscous terms. Author

A91-34194
VISCOUS, HYPERSONIC FLOWS OVER COMPRESSION RAMPS
WERNER HAASE (Dornier Luftfahrt GmbH, Friedrichshafen, Federal Republic of Germany) IN: GAMM-Conference on Numerical Methods in Fluid Mechanics, 8th, Delft, Netherlands, Sept. 27-29, 1989, Proceedings. Wiesbaden, Federal Republic of Germany/Hauppauge, NY, Friedr. Vieweg & Sohn/Ballen Books, 1990, p. 189-200. refs
Copyright

Steady, hypersonic viscous flow over two-dimensional compression ramps are computed. In order to gain insight into the influence of different Mach numbers, Reynolds numbers and ramp angles on the flow structure, results are presented for low and high Mach numbers, for low and high Reynolds numbers as wel as for different ramp angles. Furthermore, with respect to high Mach number flows, the influence of real gas effects is investigated. Computed surface pressure, skin friction and heat transfer distributions are compared with available measurements. Author

A91-34195* National Aeronautics and Space Administration. Ames Research Center, Moffett Field, CA.
SIMULATION OF GLANCING SHOCK WAVE AND BOUNDARY LAYER INTERACTION
CHING-MAO HUNG (NASA, Ames Research Center, Moffett Field, CA) IN: GAMM-Conference on Numerical Methods in Fluid Mechanics, 8th, Delft, Netherlands, Sept. 27-29, 1989, Proceedings. Wiesbaden, Federal Republic of Germany/Hauppauge, NY, Friedr.

Vieweg & Sohn/Ballen Books, 1990, p. 211-220. Previously announced in STAR as N90-11970. refs
Copyright

Shock waves generated by sharp fins, glancing across a laminar boundary layer growing over a flat plate, are simulated numerically. Several basic issues concerning the resultant three-dimensional flow separation are studied. Using the same number of grid points, different grid spacings are employed to investigate the effects of grid resolution on the origin of the line of separation. Various shock strengths (generated by different fin angles) are used to study the so-called separated and unseparated boundary layer and to establish the existence or absence of the secondary separation. The usual interpretations of the flow field from previous studies and new interpretations arising from the present simulation are discussed. Author

A91-34196
ASPECTS OF THE APPLICATION OF AN EULER-EQUATION METHOD TO THE SIMULATION OF LEADING-EDGE VORTEX FLOW

J. M. J. W. JACOBS and H. W. M. HOEIJMAKERS (National Aerospace Laboratory, Amsterdam, Netherlands) IN: GAMM-Conference on Numerical Methods in Fluid Mechanics, 8th, Delft, Netherlands, Sept. 27-29, 1989, Proceedings. Wiesbaden, Federal Republic of Germany/Hauppauge, NY, Friedr. Vieweg & Sohn/Ballen Books, 1990, p. 221-232. Netherlands Agency for Aerospace Programs-supported research. refs
Copyright

The flow about a 65-deg sharp-edged cropped delta wing is simulated by solving the Euler equations. Solutions are obtained for transonic vortex flow with and without shocks including cases with strong vortices. This paper concentrates on the assessment of the capability of the Euler method to simulate the details of the flow field, especially with respect to the influence of artificial dissipation and the influence of the computational mesh. Author

A91-34198
A NUMERICAL STUDY OF INTERFACIAL INSTABILITIES AT HIGH MACH NUMBERS

R. KLEIN (Princeton University, NJ), C. D. MUNZ (Kernforschungszentrum Karlsruhe GmbH, Institut fuer Neutronenphysik und Reaktortechnik, Federal Republic of Germany), and L. SCHMIDT (Karlsruhe, Universitaet, Federal Republic of Germany) IN: GAMM-Conference on Numerical Methods in Fluid Mechanics, 8th, Delft, Netherlands, Sept. 27-29, 1989, Proceedings. Wiesbaden, Federal Republic of Germany/Hauppauge, NY, Friedr. Vieweg & Sohn/Ballen Books, 1990, p. 242-251. refs
Copyright

Direct numerical simulations of high Mach number shear flow instabilities based on the two-dimensional Navier-Stokes equations are performed. To deal with the steep gradients and shocks which emerge after the growth of instabilities, modern high resolution shock capturing schemes are employed. Some peculiarities arising generally when shock capturing schemes are applied to shear flow stability problems in the limit of vanishing viscosity are pointed out. Streak lines are calculated to visualize the development of the instabilities. Author

A91-34201
3D EULER FLOWS AROUND MODERN AIRPLANES

J. L. KUYVENHOVEN (Fokker Aircraft, Schiphol, Netherlands) and J. W. BOERSTOEL (National Aerospace Laboratory, Amsterdam, Netherlands) IN: GAMM-Conference on Numerical Methods in Fluid Mechanics, 8th, Delft, Netherlands, Sept. 27-29, 1989, Proceedings. Wiesbaden, Federal Republic of Germany/Hauppauge, NY, Friedr. Vieweg & Sohn/Ballen Books, 1990, p. 283-292. refs
Copyright

The numerical simulation of flows around complex aircraft configurations like the Fokker 50 and Fokker 100, is described. In these simulations multiblock grids and a three-dimensional Euler-flow solver are used. The major features of the grid-generation procedure and flow solver are outlined. Results of the validation of the numerical-flow-simulation system for aerodynamic design work are presented. Author

A91-34203* National Aeronautics and Space Administration. Langley Research Center, Hampton, VA.
NUMERICAL SIMULATION OF TURBULENT FLOWS AROUND AIRFOIL AND WING

YVES P. MARX (NASA, Langley Research Center, Hampton, VA) IN: GAMM-Conference on Numerical Methods in Fluid Mechanics, 8th, Delft, Netherlands, Sept. 27-29, 1989, Proceedings. Wiesbaden, Federal Republic of Germany/Hauppauge, NY, Friedr. Vieweg & Sohn/Ballen Books, 1990, p. 323-332. refs
Copyright

During the last years the simulation of compressible viscous flows has received much attention. While the numerical methods were improved drastically, a satisfactory modeling of the Reynolds stresses is still missing. In this paper, after a short description of the numerical procedure used for solving the Reynolds equations, experiments with a promising simple turbulence model are discussed. Author

A91-34206
SPLIT-MATRIX MARCHING METHODS FOR THREE-DIMENSIONAL VISCOUS AND INVISCID HYPERSONIC FLOWS

S. MENNE and C. WEILAND (MBB GmbH, Munich, Federal Republic of Germany) IN: GAMM-Conference on Numerical Methods in Fluid Mechanics, 8th, Delft, Netherlands, Sept. 27-29, 1989, Proceedings. Wiesbaden, Federal Republic of Germany/Hauppauge, NY, Friedr. Vieweg & Sohn/Ballen Books, 1990, p. 353-362. refs
Copyright

Two split-matrix marching methods for hypersonic flow are presented: a space marching method for inviscid flow and a time-integration marching method for viscous flow. For both methods the solution algorithm is explained. Flow calculations of the hypersonic flow over a two-stage transport vehicle show that the methods allow an economic computation of flows over complex geometries with sharp shocks and no spurious oscillations without using any explicit artificial damping. Author

A91-34210
INVISCID FLOW ABOUT A DOUBLE ELLIPSE

GINO MORETTI (GMAF, Inc., Freeport, NY) and MAURO VALORANI (Roma I, Universita, Rome, Italy) IN: GAMM-Conference on Numerical Methods in Fluid Mechanics, 8th, Delft, Netherlands, Sept. 27-29, 1989, Proceedings. Wiesbaden, Federal Republic of Germany/Hauppauge, NY, Friedr. Vieweg & Sohn/Ballen Books, 1990, p. 401-410.
Copyright

The study addresses the need for a benchmark providing a standard of accuracy for the numerical analyses of a flow field about a double ellipse simulating the bow of a vehicle with a canopy. The lambda scheme for integrating the Euler equations at grid nodes and shock-fitting technique are utilized. Two different approaches are used for handling the shock generated the canopy: division of the flow field into two regions and a single region. The results obtained are consistent with a variety of free-stream Mach numbers and angles of attack. The paper concentrates on discrepancies found in the analysis, and such difficult areas as the neighborhood of the corner and the appearance of a consistent pattern that changes dramatically as the standoff distance decreases are assessed. V.T.

A91-34213
NUMERICAL SIMULATION OF VORTICES MOTION IN PRESENCE OF SOLID BOUNDARIES

PAOLO ORLANDI (Roma I, Universita, Rome, Italy) IN: GAMM-Conference on Numerical Methods in Fluid Mechanics, 8th, Delft, Netherlands, Sept. 27-29, 1989, Proceedings. Wiesbaden, Federal Republic of Germany/Hauppauge, NY, Friedr. Vieweg &

Sohn/Ballen Books, 1990, p. 436-445. refs
Copyright

A numerical simulation describing the behavior of large structures in the presence of bodies of different shapes is discussed. The N-S system of equations for a two-dimensional case is considered, where the vorticity-stream function formulation allows to reduce the number of operations. The vorticity-stream formulation is developed in order to transfer its qualities to the primitive variable formulation. As an intermediate step, an accurate method for treating high-Re flows is obtained. The motion of a dipolar vortex is considered for testing the importance of global conservation properties, and the time evolution of small perturbations starting from the plane Poiseuille flow at Re = 7500 is analyzed. A vortex dipole impinging a small cylinder and a dipole encountering a constriction in a two-dimensional channel are simulated as well. V.T.

A91-34215
ON THE RELATION BETWEEN TVD AND MESH ADAPTION AND APPLICATION TO NAVIER-STOKES CALCULATIONS

B. PALMERIO (Nice, Universite; INRIA, Valbonne, France), C. OLIVIER, and A. DERVIEUX (INRIA, Valbonne, France) IN: GAMM-Conference on Numerical Methods in Fluid Mechanics, 8th, Delft, Netherlands, Sept. 27-29, 1989, Proceedings. Wiesbaden, Federal Republic of Germany/Hauppauge, NY, Friedr. Vieweg & Sohn/Ballen Books, 1990, p. 454-463. refs
Copyright

Considering the TVD methods as accuracy-adaption methods, a strategy for deciding mesh refinements for TVD-approximated compressible flows is proposed. Both mesh enrichment and deformation are applied to two typical test cases involving boundary layers: a flow past a flat plate and a flow around an airfoil. Author

A91-34216
COMPUTATION OF THE VISCOUS FLOW PAST A PROLATE SPHEROID AT INCIDENCE

JEAN PIQUET and PATRICK QUEUTEY (Ecole Nationale Superieure de Mecanique, Nantes, France) IN: GAMM-Conference on Numerical Methods in Fluid Mechanics, 8th, Delft, Netherlands, Sept. 27-29, 1989, Proceedings. Wiesbaden, Federal Republic of Germany/Hauppauge, NY, Friedr. Vieweg & Sohn/Ballen Books, 1990, p. 464-473. refs
(Contract DRET-86-104)
Copyright

The computation of the three dimensional viscous flow past a prolate spheroid at incidence and its wake is investigated. An iterative technique resting on the fully elliptic mode is applied to the Reynolds-Averaged-Navier-Stokes-Equations (RANSE) written down in a nonorthogonal curvilinear body-fitted coordinate system. Results of the computations are compared to available experiments such as the DFVLR experiments and the ONERA experiments. Author

A91-34218
NUMERICAL INVESTIGATION OF THREE DIMENSIONAL LAMINAR FLOWS IN A CHANNEL WITH A BUILT-IN CIRCULAR CYLINDER AND WING-TYPE VORTEX GENERATORS

M. SANCHEZ, N. K. NITRA, and M. FIEBIG (Bochum, Ruhr-Universitaet, Federal Republic of Germany) IN: GAMM-Conference on Numerical Methods in Fluid Mechanics, 8th, Delft, Netherlands, Sept. 27-29, 1989, Proceedings. Wiesbaden, Federal Republic of Germany/Hauppauge, NY, Friedr. Vieweg & Sohn/Ballen Books, 1990, p. 484-492.
Copyright

Laminar flows around a circular cylinder in a rectangular channel with a pair of built-in vortex generators in form of delta winglets on the bottom plate of the channel have been investigated by solving the complete Navier- Stokes equations with a Marker-and-cell technique. Results show that longitudinal vortices from the vortex generators placed in the wake of the cylinder not only control the spread of the wake of the cylinder but also completely damp the periodic vortex street. Author

A91-34220
SOME ASPECTS OF THE NUMERICAL SIMULATION OF COMPRESSIBLE VISCOUS FLOW AROUND BLUFF BODIES AT LOW MA-NUMBER

B. SCHULTE-WERNING, U. DALLMANN, and B. MUELLER (DLR, Institut fuer theoretische Stroemungsmechanik, Goettingen, Federal Republic of Germany) IN: GAMM-Conference on Numerical Methods in Fluid Mechanics, 8th, Delft, Netherlands, Sept. 27-29, 1989, Proceedings. Wiesbaden, Federal Republic of Germany/Hauppauge, NY, Friedr. Vieweg & Sohn/Ballen Books, 1990, p. 503-512. refs
Copyright

A numerical code of the Beam-Warming type is used to simulate the two-dimensional symmetric form of the flow around a circular cylinder and a sphere. The calculations are based on the viscous compressible equations of motion. The first aim is an analysis of the solution behavior of the algorithm in the range of medium Re numbers and low Ma numbers to set up the limits for the simulation of steady separation structures. The influence of initial conditions and small compressibility on the solution are investigated. It is also shown to what extent stable and steady solutions can be derived from the unsteady procedure and how to resolve large gradients in the flow field. The second aim is to study the structure of the separation at higher Re in the axisymmetric sphere case. A comprehensive comparison is made with other numerical and experimental results. Author

A91-34229
AN INVERSE BOUNDARY LAYER PROCEDURE WITH APPLICATION TO 3-D WING FLOW

L. XUE and F. THIELE (Berlin, Technische Universitaet, Federal Republic of Germany) IN: GAMM-Conference on Numerical Methods in Fluid Mechanics, 8th, Delft, Netherlands, Sept. 27-29, 1989, Proceedings. Wiesbaden, Federal Republic of Germany/Hauppauge, NY, Friedr. Vieweg & Sohn/Ballen Books, 1990, p. 592-602. Research supported by MBB GmbH and BMFT. refs
Copyright

For three-dimensional boundary layers an inverse solution procedure is described to be used in connection with the interactive approach. Due to the finite-difference approximation applied the pressure gradients as well as the displacement thicknesses can be directly incorporated into the numerical scheme. For this reason the method developed differs only slightly from the direct mode with prescribed external velocity components. Calculations are reported for the turbulent flow over a flat plate and a wing flow. The results confirm that the inverse procedure provides accurate solutions within few iterations even in regions where the flow tends to separate. Author

A91-34398
A FUNCTIONAL METHOD FOR THE APPROXIMATE SOLUTION OF A TRANSONIC PROBLEM [UNE METHODE FONCTIONELLE DE RESOLUTION APPROCHEE D'UN PROBLEME TRANSSONIQUE]

MARC POGU (Ecole Nationale Superieure de Mecanique, Nantes, France) and GEORGES TOURNEMINE (Rennes I, Universite, France) Academie des Sciences, Comptes Rendus, Serie II - Mecanique, Physique, Chimie, Sciences de la Terre et de l'Univers (ISSN 0764-4450), vol. 312, no. 5, Feb. 28, 1991, p. 431-434. In French. refs
Copyright

A functional method for solving transonic-flow problems is developed, where the solution is reduced to the determination of a fixed point of a suitable mapping. An iterative algorithm provides a solution to the equation governing the velocity field. In addition, a constructive algorithm leads to the adjustment of the Kutta-Joukowski condition. B.J.

A91-34783#
MIXING IN AXIAL-FLOW COMPRESSORS - CONCLUSIONS DRAWN FROM THREE-DIMENSIONAL NAVIER-STOKES ANALYSES AND EXPERIMENTS
J. H. LEYLEK and D. C. WISLER (GE Aircraft Engines, Cincinnati, OH) ASME, Transactions, Journal of Turbomachinery (ISSN 0889-504X), vol. 113, April 1991, p. 139-156; Discussion, p. 156-160. refs
(ASME PAPER 90-GT-352) Copyright

The present experiments and numerical analyses of mixing phenomena in compressors of multistage axial-flow type encompass three-dimensional Navier-Stokes solutions with high-order turbulence modeling for flow through a compressor-blade row at both design conditions and conditions of enhanced, off-design loading. The analytical results demonstrate the development of spanwise radial and circumferential flows in the stator, as well as the change in location and extent of separated flow regions with increasing loading. Both secondary flow and turbulent diffusion are implicated in spanwise and circumferential mixing in axial-flow compressors; their relative importance is a function of configuration and loading levels. O.C.

A91-34784#
MIXING IN AXIAL FLOW COMPRESSORS. I - TEST FACILITIES AND MEASUREMENTS IN A FOUR-STAGE COMPRESSOR. II - MEASUREMENTS IN A SINGLE-STAGE COMPRESSOR AND A DUCT
Y. S. LI and N. A. CUMPSTY (Cambridge, University, England) ASME, Transactions, Journal of Turbomachinery (ISSN 0889-504X), vol. 113, April 1991, p. 161-172; Discussion, p. 172-174. Research supported by Rolls-Royce, PLC, Ministry of Defence of England, and British Council. refs
(ASME PAPER 90-GT-38) Copyright

The present investigation of the mixing mechanism in a four-stage axial-flow compressor proceeds by establishing that the mixing coefficient across the first and third stators are of comparable magnitude. Attention is given to the experimental apparatus and techniques employed. The first part of this work establishes the presence of substantial circumferential fluid motions in the compressor end-wall regions due to the effects of end-wall boundary layer skew and secondary flows. In the second part, attention is given to a two-dimensional rectangular duct flow which reveals the mixing mechanism in the corner region to be similar to those formed by blade surfaces and endwalls in a compressor; anisotropic inhomogeneous turbulent diffusion is primarily responsible for the nonuniform mixing in the corner region. O.C.

A91-34785#
A REVIEW OF PREDICTIVE EFFORTS FOR TRANSPORT PHENOMENA IN AXIAL FLOW COMPRESSORS
A. J. WENNERSTROM (USAF, Aero Propulsion and Power Laboratory, Wright-Patterson AFB, OH) ASME, Transactions, Journal of Turbomachinery (ISSN 0889-504X), vol. 113, April 1991, p. 175-179. refs
Copyright

An account is given of the historical development and current status of treatments of transport phenomena in axial-flow compressor throughflow calculations, highlighted by the contention between Adkins-Smith (1982) and Gallimore-Cumptsy (1986) approaches to radial transport. The resolution of this debate lay in the determination that both turbulent transport and convective secondary flows are involved in spanwise transport processes. The present discussion suggests substantial value in a reconsideration of the work of Kerrebrock and Mikolaiczak (1970) concerning circumferential transport. O.C.

A91-34786#
THREE-DIMENSIONAL WAKE DECAY INSIDE OF A COMPRESSOR CASCADE AND ITS INFLUENCE ON THE DOWNSTREAM UNSTEADY FLOW FIELD. I - WAKE DECAY CHARACTERISTICS IN THE FLOW PASSAGE. II - UNSTEADY FLOW FIELD DOWNSTREAM OF THE STATOR
C. POENSGEN and H. E. GALLUS (Aachen, Rheinisch-Westfaelische Technische Hochschule, Federal Republic of Germany) ASME, Transactions, Journal of Turbomachinery (ISSN 0889-504X), vol. 113, April 1991, p. 180-197. refs
(ASME PAPER 90-GT-21) Copyright

A multisensor hot-wire anemometry-based technique has been developed to ascertain turbulent flows' unsteady, three-dimensional velocity vector in the case of the passage and exit flow of an annular compressor cascade which is disturbed by the wakes of an upstream cylinder rotor. In part I of this investigation, attention is given to the decay of the rotor wakes, first without stator, and then through a stator passage. In the second part, an account is given of the time-dependent turbulent flow field downstream of the stator. The rotor wakes are found to have a major influence on the development of three-dimensional separated regions within the compressor cascade. O.C.

A91-34787#
EXPERIMENTAL AND NUMERICAL INVESTIGATION OF THREE-DIMENSIONAL VISCOUS FLOWS AND VORTEX MOTION INSIDE AN ANNULAR COMPRESSOR BLADE ROW
H. E. GALLUS, H. D. SCHULZ (Aachen, Rheinisch-Westfaelische Technische Hochschule, Federal Republic of Germany), and C. HAH (GE Research and Development Center, Schenectady, NY) ASME, Transactions, Journal of Turbomachinery (ISSN 0889-504X), vol. 113, April 1991, p. 198-206. refs
(ASME PAPER 90-GT-155) Copyright

A detailed experimental and numerical investigation was carried out to examine the three-dimensional flow field, secondary flows, and vortex motion in an annular compressor cascade. Various flow visualizations near the blade surface and endwalls, wall static pressure and loss measurements, as well as hot-film and hot-wire measurements inside the blade boundary layers were performed at various flow rates to understand the complex flow phenomena. A Reynolds-averaged Navier-Stokes equation was solved to investigate the flow numerically. The detailed comparison between measurement and numerical prediction indicates that the complex-three-dimensional flow phenomena (corner stall, vortex motion, radial mixing, etc.) are very well predicted with the numerical method. Author

A91-34788#
UNSTEADY RADIAL TRANSPORT IN A TRANSONIC COMPRESSOR STAGE
P. A. KOTIDIS and A. H. EPSTEIN (MIT, Cambridge, MA) ASME, Transactions, Journal of Turbomachinery (ISSN 0889-504X), vol. 113, April 1991, p. 207-218; Discussion, p. 218. USAF-supported research. refs
(ASME PAPER 90-GT-133) Copyright

A quasi-three-dimensional vortex-street wake model is proposed for a set of time-resolved measurements of spanwise fluid transport in a transonic compression stage which indicates a spanwise transport of several percent of total flow mass. When fit to the data to derive the vortex characteristics, the model predicts most of the inward fluid transport along a span of about 15 percent of the outward motion. It is suggested that most of the outward transport is concentrated in separated regions within the blade boundary layers. Spanwise fluid transport, by moving the loss experienced near the hub toward the rotor tip, renders hub-section performance apparently superior, and tip-section performance proportionately worse. O.C.

A91-34789#
TEMPORALLY AND SPATIALLY RESOLVED FLOW IN A TWO-STAGE AXIAL COMPRESSOR. I - EXPERIMENT
R. C. STAUTER, R. P. DRING, and F. O. CARTA (United Technologies Research Center, East Hartford, CT) ASME, Transactions, Journal of Turbomachinery (ISSN 0889-504X), vol. 113, April 1991, p. 219-225; Discussion, p. 226. refs
(ASME PAPER 90-GT-259) Copyright

A two-component LDV system has been used to investigate the temporal and spatial variations in the midspan aerodynamics of the second stage of a two-stage compressor. Spatial variations were examined by traversing the LDV probe volume through a

dense matrix of both axial and circumferential positions, while temporal resolution was achieved by acquiring data as a function of instantaneous rotor position; in this fashion, the data set reveals rotor and stator wake structure and decay in both the stationary and the rotating reference-frames. The data thus obtained compare favorably with pneumatic measurement previously acquired on the same compressor. O.C.

A91-34790#
THE INFLUENCE OF INLET SWIRL DISTORTIONS ON THE PERFORMANCE OF A JET PROPULSION TWO-STAGE AXIAL COMPRESSOR
W. PAZUR and L. FOTTNER (Muenchen, Universitaet der Bundeswehr, Neubiberg, Federal Republic of Germany) ASME, Transactions, Journal of Turbomachinery (ISSN 0889-504X), vol. 113, April 1991, p. 233-240. Research supported by BMVg and Bundesamt fuer Wehrtechnik und Beschaffung. refs
(ASME PAPER 90-GT-147) Copyright

The influence of inlet swirl distortions on the performance of a transonic two-stage axial compressor installed in a turbo-jet bypass engine is evaluated. A typical inlet swirl distortion was simulated by a delta wing in front of the engine. An experimental method was investigated to measure the performance map of the installed low-pressure compressor for different engine operating lines. The influence of an inlet swirl distortion with different strengths on the performance map of the compressor was investigated experimentally. It is shown that the performance parameters decrease, and a temperature distortion is generated behind the compressor. Author

A91-34791#
THREE-DIMENSIONAL FLOWFIELDS INSIDE A TRANSONIC COMPRESSOR WITH SWEPT BLADES
C. HAH (GE Research and Development Center, Schenectady, NY) and A. J. WENNERSTROM (USAF, Aero Propulsion and Power Laboratory, Wright-Patterson AFB, OH) ASME, Transactions, Journal of Turbomachinery (ISSN 0889-504X), vol. 113, April 1991, p. 241-250; Discussion, p. 250, 251. refs
(ASME PAPER 90-GT-359) Copyright

The concept of swept blades for a transonic or supersonic compressor was reconsidered by Wennerstorm in the early 1980s. Several transonic rotors designed with swept blades have shown very good aerodynamic efficiency. The improved performance of the rotor is believed to be due to reduced shock strength near the shroud and better distribution of secondary flows. A three-dimensional flowfield inside a transonic rotor with swept blades is analyzed in detail experimentally and numerically. A Reynolds-averaged Navier-Stokes equation is solved for the flow inside the rotor. The numerical solution is based on a high-order upwinding relaxation scheme, and a two-equation turbulence model with a low Reynolds number modification is used for the turbulence modeling. To predict flows near the shroud properly, the tip-clearance flow also must be properly calculated. The numerical results at three different operating conditions agree well with the available experimental data and reveal various interesting aspects of shock structure inside the rotor. Author

A91-34792#
TIP LEAKAGE FLOW IN AXIAL COMPRESSORS
J. A. STORER and N. A. CUMPSTY (Cambridge, University, England) ASME, Transactions, Journal of Turbomachinery (ISSN 0889-504X), vol. 113, April 1991, p. 252-259; Discussion, p. 259. Rolls-Royce, PLC-supported research. refs
(ASME PAPER 90-GT-127) Copyright

Experimental measurements in a linear cascade with tip clearance are complemented by numerical solutions of the three-dimensional Navier-Stokes equations in an investigation of tip leakage flow. Measurements reveal that the clearance flow, which separates near the entry of the tip gap, remains unattached for the majority of the blade chord when the tip clearance is similar to that typical of a machine. The numerical predictions of leakage flow rate agree very well with measurements, and detailed comparisons show that the mechanism of tip leakage is primarily inviscid. It is demonstrated by simple calculation that it is the static pressure field near the end of the blade that controls chordwise distribution of the flow across the tip. Although the presence of a vortex caused by the roll-up of the leakage flow may affect the local pressure field, the overall magnitude of the tip leakage flow remains strongly related to the aerodynamic loading of the blades. Author

A91-34793# Massachusetts Inst. of Tech., Cambridge.
SIMILARITY ANALYSIS OF COMPRESSOR TIP CLEARANCE FLOW STRUCTURE
G. T. CHEN, E. M. GREITZER, C. S. TAN (MIT, Cambridge, MA), and F. E. MARBLE (JPL, Pasadena, CA) ASME, Transactions, Journal of Turbomachinery (ISSN 0889-504X), vol. 113, April 1991, p. 260-269; Discussion, p. 270, 271. Research supported by GE Aircraft Engines. refs
(Contract NSG-3208)
(ASME PAPER 90-GT-153) Copyright

A new approach is presented for analyzing compressor tip clearance flow. The basic idea is that the clearance velocity field can be (approximately) decomposed into independent throughflow and crossflow, since chordwise pressure gradients are much smaller than normal pressure gradients in the clearance region. As in the slender body approximation in external aerodynamics, this description implies that the three-dimensional steady clearance flow can be viewed as a two-dimensional, unsteady flow. Using this approach, a similarity scaling for the crossflow in the clearance region is developed and a generalized description of the clearance vortex is derived. Calculations based on the similarity scaling agree well with a wide range of experimental data in regard to flow features such as crossflow velocity field, static pressure field, and tip clearance vortex trajectory. Author

A91-34794#
COMPRESSOR DRUM AERODYNAMIC EXPERIMENTS AND ANALYSIS WITH COOLANT INJECTED AT SELECTED LOCATIONS
B. V. JOHNSON, W. A. DANIELS (United Technologies Research Center, East Hartford, CT), E. J. KAWECKI (Pratt and Whitney Group, Government Products Div., West Palm Beach, FL), and R. J. MARTIN (USAF, Wright Research and Development Center, Wright-Patterson AFB, OH) ASME, Transactions, Journal of Turbomachinery (ISSN 0889-504X), vol. 113, April 1991, p. 272-280. Research supported by United Technologies Corp. refs
(Contract F33615-83-C-2331)
(ASME PAPER 90-GT-151) Copyright

Experiments were conducted to determine the pressure distributions within a multicavity compressor drum model for two coolant injection locations and a range of flow conditions. Flow as injected through the upstream conical wall or through the cylindrical wall of the rotating model. The coolant flow, the drum rotational rate, and the model pressure were varied to produce a range of tangential and coolant flow Reynolds numbers, typical of large aircraft engine high-pressure compressor drums. The experimental results were used to evaluate analytical procedures for predicting flow characteristics in rotating annular cavities with radially inward flow and for correlating flow characteristics in multiple-rotating annular cavities, which are not currently predicted. Swirling flows, radially inward between compressor disks and within rotating annular cavities with no net flow, were analyzed with a procedure that coupled a viscous solution for the rotating core flow with a momentum integral analysis for the boundary layers on the disks. Constant viscosity and variable turbulent viscosity models were used in the analysis. Results from the analysis and the experiments were used to estimate the tangential velocity distribution in trapped cavities for two coolant injection configurations and a range of flow rates. Author

A91-34795#
DETECTION OF A ROTATING STALL PRECURSOR IN ISOLATED AXIAL FLOW COMPRESSOR ROTORS
M. INOUE, M. KUROUMARU, T. IWAMOTO, and Y. ANDO (Kyushu University, Fukuoka, Japan) ASME, Transactions, Journal of

Turbomachinery (ISSN 0889-504X), vol. 113, April 1991, p. 281-287; Discussion, p. 288, 289. refs
(ASME PAPER 90-GT-157) Copyright

Statistical characteristics of pressure fluctuation on the casing wall of two axial flow compressor rotors have been investigated experimentally to find a precursor of rotating stall. Near stall, the casing wall pressure across a flow passage near the leading edge is characterized by a highly unsteady region where low-momentum fluid accumulates. The periodicity of the pressure fluctuation with blade spacing disappears and an alternative phenomenon comes into existence, which supports the disturbance propagating at a different speed from the rotor revolution. The precursor of rotating stall can be detected by monitoring collapse of the periodicity in the pressure fluctuation. To represent the periodicity qualitatively, a practical detection parameter has been proposed, which is easily obtained from signals of a single pressure sensor installed at an appropriate position on the casing wall during operation of a compressor. Author

A91-34796#
ROTATING WAVES AS A STALL INCEPTION INDICATION IN AXIAL COMPRESSORS
V. H. GARNIER, A. H. EPSTEIN, and E. M. GREITZER (MIT, Cambridge, MA) ASME, Transactions, Journal of Turbomachinery (ISSN 0889-504X), vol. 113, April 1991, p. 290-301; Discussion, p. 301, 302. Research supported by U.S. Navy and USAF. refs
(ASME PAPER 90-GT-156) Copyright

Stall inception has been studied in two low-speed compressors (a single-stage and a three-stage) and in a high-speed three-stage compressor, using temporally and spatially resolved measurements. In all three machines, rotating stall was preceded by a period in which sma;;-amplitude waves were observed traveling around the circumference of the machine at a speed slightly less than the fully developed rotating stall cell speed. The waves evolved smoothly into rotating stall without sharp changes in phase or amplitude, implying that, in the machines tested, the prestall waves and the fully developed rotating stall are two stages of the same phenomenon. The growth rate of these disturbances was in accord with that predicted by current analytical models. The prestall waves were observed both with uniform and with distorted inflow, but were most readily discerned with uniform inflow. Engineering uses and limitations of these waves are discussed. Author

A91-34797#
HIGH-SPEED COMPRESSOR SURGE WITH APPLICATION TO ACTIVE CONTROL
A. M. CARGILL and C. FREEMAN (Rolls-Royce, PLC, Derby, England) ASME, Transactions, Journal of Turbomachinery (ISSN 0889-504X), vol. 113, April 1991, p. 303-311. refs
(ASME PAPER 90-GT-354) Copyright

This paper discusses the mechanics of surge as observed on the high-speed axial compressors of modern aero-engines. It argues that the initial stage of the instability consists of a high-amplitude blast wave that develops nonlinearly from a small-scale disturbance and is thus not correctly described by traditional small perturbation stability theories. It follows from this that active control schemes of the global type may be inappropriate, since to be effective, control would have to be applied in a short time and in a very detailed manner, requiring a large number of transducers and actuators. Active control may, though, be effective in controlling the disturbances that grow into the above blast wave and in the control of other phenomena such as rotating stall, given an adequate number of transducers. Author

A91-34798#
FORCING FUNCTION EFFECTS ON ROTOR PERIODIC AERODYNAMIC RESPONSE
S. R. MANWARING and S. FLEETER (Purdue University, West Lafayette, IN) ASME, Transactions, Journal of Turbomachinery (ISSN 0889-504X), vol. 113, April 1991, p. 312-319. refs
(Contract F49620-88-C-0022)
(ASME PAPER 90-GT-109) Copyright

A series of experiments are performed in an extensively instrumental axial flow research compressor to investigate the effects of different low reduced frequency aerodynamic forcing functions and steady loading level on the gust-generated unsteady aerodynamics of a first-stage rotor blade row. Two different two-per-rev forcing functions are considered: (1) the velocity deficit from the two 90 deg circumferential inlet flow distortions, and (2) the wakes from two upstream obstructions, which are characteristic of airfoil or probe excitations. The data show that the wake-generated rotor row first harmonic response is much greater than that generated by the inlet distortion, with the difference decreasing with increased steady loading. Author

A91-35660
AN APPROXIMATE METHOD FOR DETERMINING FRICTION AND HEAT TRANSFER IN CHEMICALLY NONEQUILIBRIUM FLOW PAST BODIES AT ANGLE OF ATTACK [PRIBLIZHENNYI METOD OPREDELENIIA TRENIIA I TEPLOOBMENA PRI KHIMICHESKI NERAVNOVESNOM OBTEKANII TEL POD UGLOM ATAKI]
I. G. BRYKINA, V. V. RUSAKOV, and V. G. SHCHERBAK (Moskovskii Gosudarstvennyi Universitet, Moscow, USSR) Teplofizika Vysokikh Temperatur (ISSN 0040-3644), vol. 29, Jan.-Feb. 1991, p. 179-182. In Russian. refs
Copyright

An approximate method for calculating heat transfer and friction in the vicinity of the plane of symmetry of three-dimensional bodies in the path of flow of a chemically nonequilibrium viscous gas at angle of attack is proposed which is valid over a wide range of Reynolds numbers. The method is based on similarity relations representing heat flow and the friction coefficient near the spread line in terms of their values for an axisymmetric body. The validity of the approach proposed here is verified numerically for bodies of different shapes entering the earth atmosphere along a gliding trajectory at different angles of attack and for different catalytic activities of the surface. V.L.

A91-35784
INERTIAL AEROSOL PRECIPITATION ON OGIVAL BODIES OF REVOLUTION IN HIGH-VELOCITY FLOW [INERTSIONNOE OSAZHDENIE AEROZOLIA NA OZHIVAL'NYE TELA VRASHCHENIIA V VYSOKOSKOROSTNOM POTOKE]
L. I. DZVONIK and V. A. PAVLOV (Kievskii Gosudarstvennyi Universitet, Kiev, Ukrainian SSR) Vychislitel'naia i Prikladnaia Matematika (ISSN 0321-4117), no. 70, 1990, p. 99-104. In Russian.
Copyright

The problem of inertial aerosol precipitation on obstacles in the shape of ogival bodies of revolution is investigated analytically assuming that solid particles pass through a shock wave and interact with the obstacle without fractionation or coagulation. By using the small perturbation formalism, an asymptotic solution is obtained in the region between a given body surface and the unknown surface of the shock wave. V.L.

A91-35796
CALCULATION OF A COMPRESSIBLE LAMINAR BOUNDARY LAYER ON A TAPERED BODY OF BIELLIPTICAL CROSS SECTION [RASCHET SZHIMAEMOGO LAMINARNOGO POGRANICHNOGO SLOIA NA ZAOSTRENNOM TELE BIELLIPTICHESKOGO SECHENIIA]
V. N. VETLUTSKII PMTF - Zhurnal Prikladnoi Mekhaniki i Tekhnicheskoi Fiziki (ISSN 0044-4626), Jan.-Feb. 1991, p. 55-61. In Russian. refs
Copyright

The problem of a compressible laminar boundary layer on a tapered body is formulated, and computation algorithms are developed. Calculation results are presented for a body of bielliptical cross section at freestream Mach 2 and angles of attack 0-10 deg. The evolution of a three-dimensional boundary layer with the angle of attack is examined. V.L.

A91-35984
EULER ANALYSIS OF TRANSONIC STATOR-ROTOR INTERACTION USING A FINITE VOLUME METHOD
IN-MO KANG and KEUN-SHIK CHANG (Korea Advanced Institute of Science and Technology, Seoul, Republic of Korea) International Journal for Numerical Methods in Fluids (ISSN 0271-2091), vol. 12, April 20, 1991, p. 625-636. Research supported by Korea Science and Engineering Foundation. refs
Copyright

A generalized finite volume method that can solve the Euler equations for the stator and rotor parts of stage flow in similar formulations is presented. The method consists of a new moving grid finite volume formulation applied to the rotor region and the existing fixed grid finite volume method used in the stator region, with the data transfer made by an interpolation procedure at the sliding surface in between. The accuracy of the method has been demonstrated on a simple cascade flow before the time-dependent compressor stage flow is fully investigated. The transonic stator-rotor flow interaction is elucidated within the inviscid and rotational flow limit. Author

A91-35985
COMPUTATIONS FOR A JET IMPINGING OBLIQUELY ON A FLAT SURFACE
SHU-HAO CHUANG and CHING-YUAN WEI (National Chunghsing University, Taichung, Republic of China) International Journal for Numerical Methods in Fluids (ISSN 0271-2091), vol. 12, April 20, 1991, p. 637-653. refs
Copyright

A SIMPLE-C algorithm and Jones-Launder k-epsilon two-equation turbulence model are used to simulate a two-dimensional jet impinging obliquely on a flat surface. Both the continuity and momentum equations for the unsteady state are cast into suitable finite difference equations. The pressure, velocity, turbulent kinetic energy, and turbulent energy dissipation rate distributions are solved and show good agreement with various experimental data. The calculations show that the flow-field structure of the jet impinging obliquely on a flat surface is strongly affected by the oblique impingement angle. The maximum pressure zone of the obliquely impinging jet flow field moves towards the left as the oblique impingement angle is decreased. Author

N91-21060*# National Aeronautics and Space Administration. Lewis Research Center, Cleveland, OH.
COMPRESSIBLE FLOWS WITH PERIODIC VORTICAL DISTURBANCES AROUND LIFTING AIRFOILS Ph.D. Thesis - Notre Dame Univ.
JAMES R. SCOTT Jan. 1991 214 p
(NASA-TM-103742; E-5984; NAS 1.15:103742) Avail: NTIS HC/MF A10 CSCL 01A

A numerical method is developed for solving periodic, three-dimensional, vortical flows around lifting airfoils in subsonic flow. The first-order method that is presented fully accounts for the distortion effects of the nonuniform mean flow on the convected upstream vortical disturbances. The unsteady velocity is split into a vortical component which is a known function of the upstream flow conditions and the Lagrangian coordinates of the mean flow, and an irrotational field whose potential satisfies a non-constant-coefficient, inhomogeneous, convective wave equation. Using an elliptic coordinate transformation, the unsteady boundary value problem is solved in the frequency domain on grids which are determined as a function of the Mach number and reduced frequency. The numerical scheme is validated through extensive comparisons with known solutions to unsteady vortical flow problems. In general, it is seen that the agreement between the numerical and analytical results is very good for reduced frequencies ranging from 0 to 4, and for Mach numbers ranging from .1 to .8. Numerical results are also presented for a wide variety of flow configurations for the purpose of determining the effects of airfoil thickness, angle of attack, camber, and Mach number on the unsteady lift and moment of airfoils subjected to periodic vortical gusts. It is seen that each of these parameters can have a significant effect on the unsteady airfoil response to the incident disturbances, and that the effect depends strongly upon the reduced frequency and the dimensionality of the gust. For a one-dimensional (transverse) or two-dimensional (transverse and longitudinal) gust, the results indicate that airfoil thickness increases the unsteady lift and moment at the low reduced frequencies but decreases it at the high reduced frequencies. The results show that an increase in airfoil Mach number leads to a significant increase in the unsteady lift and moment for the low reduced frequencies, but a significant decrease for the high reduced frequencies. Author

N91-21062*# National Aeronautics and Space Administration. Lewis Research Center, Cleveland, OH.
COMPUTATIONAL FLUID DYNAMICS SYMPOSIUM ON AEROPROPULSION
Washington Jan. 1991 687 p Symposium held in Cleveland, OH, 24-26 Apr. 1990 Supersedes NASA-CP-10045 Original contains color illustrations
(NASA-CP-3078; E-5296; NASA-CP-10045; NAS 1.55:3078)
Avail: NTIS HC/MF A99; 10 functional color pages CSCL 01A

Recognizing the considerable advances that have been made in computational fluid dynamics, the Internal Fluid Mechanics Division of NASA Lewis Research Center sponsored this symposium with the objective of providing a forum for exchanging information regarding recent developments in numerical methods, physical and chemical modeling, and applications. This conference publication is a compilation of 4 invited and 34 contributed papers presented in six sessions: algorithms one and two, turbomachinery, turbulence, components application, and combustors. Topics include numerical methods, grid generation, chemically reacting flows, turbulence modeling, inlets, nozzles, and unsteady flows.

N91-21100*# Virginia Polytechnic Inst. and State Univ., Blacksburg. Dept. of Aerospace and Ocean Engineering.
VELOCITY MEASUREMENTS IN A TURBULENT TRAILING VORTEX AND THEIR APPLICATION TO BWI NOISE PREDICTION Semiannual Report
WILLIAM J. DEVENPORT and STEWART A. L. GLEGG (Florida Atlantic Univ., Boca Raton.) Apr. 1991 32 p
(Contract NAG1-1119)
(NASA-CR-188083; NAS 1.26:188083) Avail: NTIS HC/MF A03 CSCL 01A

The objectives were to observe the turbulence structure and spectral characteristics of the trailing vortex shed by a rectangular NACA 0012 wing over a range of conditions and to incorporate these observations into the blade-wake interaction (BWI) noise-prediction method of Glegg (1989). The following sections are presented: (1) measurements performed during the first year of this two year investigation; (2) presentation and discussion of a representative sample of the results; (3) implications for the BWI noise prediction method; and (4) re-evaluation of work planned for the second year. Author

N91-21101*# Imperial Coll. of Science and Technology, London (England). Dept. of Aeronautics.
FINITE ELEMENT METHODS FOR INTEGRATED AERODYNAMIC HEATING ANALYSIS Report, 1 Oct. 1989 - 30 Sep. 1990
J. PERAIRE 30 Sep. 1990 44 p
(Contract NAGW-1809)
(NASA-CR-188079; NAS 1.26:188079) Avail: NTIS HC/MF A03 CSCL 01A

Over the past few years finite element based procedures for the solution of high speed viscous compressible flows were developed. The objective of this research is to build upon the finite element concepts which have already been demonstrated and to develop these ideas to produce a method which is applicable to the solution of large scale practical problems. The problems of interest range from three dimensional full vehicle Euler simulations to local analysis of three-dimensional viscous laminar flow. Transient Euler flow simulations involving moving bodies are also to be included. An important feature of the research is to be the coupling of the flow solution methods with thermal/structural

modeling techniques to provide an integrated fluid/thermal/structural modeling capability. The progress made towards achieving these goals during the first twelve month period of the research is presented. Author

N91-21102 ESDU International Ltd., London (England).
COMPUTER PROGRAM FOR THE CALCULATION OF NORMAL FORCE AND PITCHING MOMENT OF FOREBODY-CYLINDER COMBINATIONS AT ANGLES OF ATTACK UP TO 90 DEGREES AND MACH NUMBERS UP TO 5, INCLUDING EFFECTS OF CONICAL BOAT-TAILING
Dec. 1990 45 p
(ESDU-90034; ISBN-0-85679-760-X; ISSN-0141-397X) Avail: ESDU

ESDU 90034 gives the Fortran program listing of the prediction method. It uses ESDU 77028 to obtain the required geometric properties of the various axisymmetric forebody shapes, the method of ESDU 89008 for normal-force-curve and pitching-moment-curve slopes at zero angle of attack, and the method of ESDU 89014 for normal force, pitching moment, and center of pressure position at angle of attack modified, if required, by the method of ESDU 87033 to allow for the effects of any boat-tailing. The input data required and the interpretation of the output are described and illustrated with three worked examples. The limitations of the program are those of the original prediction methods on which it is based, and if any of them are exceeded the program stops and provides an appropriate error message. ESDU

N91-21104# Institut Franco-Allemand de Recherches, Saint-Louis (France).
INFRARED THERMOGRAPHY FOR THE QUALITATIVE AERODYNAMIC STUDY OF A SLENDER BODY [THERMOGRAPHIE INFRAROUGE APPLIQUEE A L'AERODYNAMIQUE D'UN CORPS FUSELE. ETUDE QUALITATIVE]
E. CATTIN and F. JAGUSINSKI 18 Sep. 1989 41 p In FRENCH Original contains color illustrations
(ISL-R-122/89; ETN-91-98989) Avail: NTIS HC/MF A03

The flow and the variations of the wall temperature of a slender body are studied in the case of an increase of 50 C in relation to the ambient temperature. Tests were carried out with a model made of insulating material located in a jet to detect the presence of unsticking and resticking areas. To evaluate the accuracy and the reliability of a thermography, a comparison with velocimetry laser measurements was made. An extension of the method to three dimensional phenomena is considered. ESA

N91-21105# Institut Franco-Allemand de Recherches, Saint-Louis (France).
PRACTICAL METHODS TO EVALUATE THE FRICTION DRAG COEFFICIENT OF A PROJECTILE IN FREE FLIGHT [SUR LES METHODES PRATIQUES D'EVALUATION DU COEFFICIENT DE TRAINEE DE FROTTEMENT D'UN PROJECTILE EN VOL LIBRE]
A. D. DUPUIS and M. GIRAUD 1 Sep. 1989 109 p In FRENCH
(ISL-R-123/89; ETN-91-98990) Avail: NTIS HC/MF A06

A comparison between the usual method to calculate the drag coefficients for a free flight motion is presented. The laminar and turbulent boundary layers were studied and the possible shapes of the cylindrical projectile were considered. The influence of the local conditions of the coefficients were taken into account as well as the compressibility coefficients and the wall temperature. A program in FORTRAN for the calculation of the drag and shape coefficients for a projectile of revoltion was proposed. The comparison between theory and experiment shows a good agreement of the results. ESA

N91-21106# Institut Franco-Allemand de Recherches, Saint-Louis (France).
COMPARISON STUDY OF THE AERODYNAMIC COEFFICIENTS MEASURED ON MODELS WITH CIRCULAR OR SQUARED SECTION AND LARGE ELONGATION IN SUPERSONIC FLOW [ETUDE COMPAREE DES COEFFICIENTS AERODYNAMIQUES MESURES SUR DES MAQUETTES DE SECTION CIRCULAIRE OU CARREE DE GRAND ALLONGEMENT EN ECOULEMENT SUPERSONIQUE]
B. GAUTIER, A. KOENEKE, J.-P. DUPEROUX, and E. CATTIN
22 Nov. 1989 43 p In FRENCH
(ISL-R-125/89; ETN-91-98992) Avail: NTIS HC/MF A03

Aerodynamic coefficients of ogives are measured for the Mach numbers 1.7 and 3.02. The Reynolds number was based on the caliber and the maximal incidence was 30 deg. It is shown that the linearized theory is a good approximation for models of circular cross section until an incidence of 20 deg. It is noticed that the transition of a circular section to a squared section produces an increasing of the coefficient for transonic flows. For models with a squared section, the rolling angle has a significant influence and the lift drag ratio is maximum for an angle of 45 deg. ESA

N91-21108# Deutsche Forschungsanstalt fuer Luft- und Raumfahrt, Brunswick (Germany, F.R.). Abt. Mathematische Verfahren und Datentechnik.
FLIGHT PATH RECONSTRUCTION USING EXTENDED KALMAN FILTERING TECHNIQUES
VENKATARAMAN PARAMESWARAN (National Aeronautical Lab., Bangalore, India) and ERMIN PLAETSCHKE Aug. 1990 38 p
(DLR-FB-90-41; ISSN-0171-1342; ETN-91-99036) Avail: NTIS HC/MF A03; DLR, Wissenschaftliches Berichtswesen, VB-PL-DO, Postfach 90 60 58, 5000 Cologne, Fed. Republic of Germany, HC 16 DM

A Flight Path Reconstruction (FPR) algorithm for the estimation of unknown constant bias and scale factor errors in measured data using extended Kalman filter and fixed interval smoother was developed. The models are based on the six degree of freedom kinematic equations relating measured aircraft responses. The technique is demonstrated with the aid of a typical example using flight test data. Also some sensitivity studies on the variation of noise covariance matrices were carried out. The results of flight path reconstruction using extended Kalman filter and maximum likelihood methods are presented. Estimation of aerodynamic parameters is carried out with a simple model using data sets which, on the one hand, were corrected for measurement bias and scale factor errors and, on the other hand, were not corrected. The effect of mesurement errors on the aerodynamic derivatives is demonstrated. ESA

N91-21109# Aeronautical Research Inst. of Sweden, Stockholm. Dept. of Aerodynamics.
LOW SPEED WIND TUNNEL INVESTIGATION OF PROPELLER SLIPSTREAM AERODYNAMIC EFFECTS ON DIFFERENT NACELLE/WING COMBINATIONS. PART 2: PROPELLER SLIPSTREAM FLOW FIELD SURVEYS (VELOCITY COMPONENTS, DYNAMIC, TOTAL AND STATIC PRESSURE DISTRIBUTIONS) AT ZERO ANGLE OF ATTACK AND HIGH POWER
INGEMAR SAMUELSSON Oct. 1990 173 p Sponsored by National Swedish Board for Technical Development, Stockholm
(FFA-TN-1990-24-PT-2; ETN-91-99042) Avail: NTIS HC/MF A08

A low speed wind tunnel investigation of the propeller slipstream flow fields around four wing/nacelle combinations was carried out. The flow fields were surveyed by means of a five hole pressure probe at zero angle of attack. The test was performed at a free stream speed of 50 m/s with a thrust coefficient (0.23) and at advance ratio J = 0.70 corresponding to a rather high power condition. The results (slipstream velocities and pressures) are shown versus radius for at least three different axial survey planes along the nacelle for the four configurations. The experimental data show that there could be large effects on the velocity and pressure distributions within the slipstream from the nacelle shapes and from the presence of the wing in the slipstream. This could

lead to rather large asymmetrical nacelle loads. The results seem to indicate that the wing influence of the propeller inflow is small, at least for the tested wing configurations. The wing has, however, a strong influence on the location of the slipstream boundaries since these boundaries are sheared by the wing. Due to the rotating slipstream there is a certain amount of swirl recovery attributed to the induced flow around the wing leading edges. For the case tested (with J = 0.70) there still remains a large amount of swirl in the slipstream downstream of the wing, so the swirl recovery is far from complete. The investigation also shows the presence of the propeller tip vortices at the slipstream boundary as marked gradients in the pressures and that there is a distinct tip loss of thrust associated with total pressure loss in the viscous tip vortex cores. ESA

N91-21110# Aeronautical Research Inst. of Sweden, Stockholm. Dept. of Aerodynamics.
MATGRID, A PROGRAM FOR GENERATION OF C-H AND C-O TOPOLOGY GRIDS AROUND WING/BODY CONFIGURATIONS: USER'S GUIDE
SVEN G. HEDMAN and LARS G. TYSELL Dec. 1990 63 p Sponsored by National Swedish Board for Technical Development, Stockholm
(FFA-TN-1991-03; ETN-91-99047) Avail: NTIS HC/MF A04

MATGRID is a computer program for generation of C-H or C-O topology grids for the discretization of flow fields around configurations consisting of a wing alone or a wing and a fuselage. It was developed primarily for use together with the full potential flow solver MATRICS. The principles for MATGRID, the files required, some parameters, how to modify the input, and how to run the program are described. An example is included as a test case. ESA

N91-21111# National Aerospace Lab., Tokyo (Japan).
CONING MOTION OF SLENDER BODIES AT HIGH ANGLES OF ATTACK
ATSUSHI TATE, TAKASHI YOSHINAGA, and KENJI INOUE Mar. 1990 39 p In JAPANESE; ENGLISH summary
(NAL-TR-1059; ISSN-0389-4010) Avail: NTIS HC/MF A03

The experimental results are presented for the coming motion of slender bodies such as a cone-cylinder or a cylinder model created by the side force at high angles of attack (45 deg less than or equal to alpha less than or equal to 135 deg). The free rotation motion was utilized to study the coning angular motions of the models. Models were supported free to rotate at their centers of gravity in a low speed wind tunnel. For angles of attack of 45 deg less or equal to alpha less or equal to 90 deg (nose first), a cone-cylinder model shows a steady angular rotation. For the range of 90 deg less than or equal to alpha less than or equal to 135 deg (base first), the model shows alternating rotation where the direction of rotation reverses within a certain period of time. Author

N91-21112# National Aerospace Lab., Tokyo (Japan).
WIND TUNNEL TEST OF A PROPELLER WORKING IN A LOW REYNOLDS NUMBER RANGE
KINGO TAKASAWA, MASATAKA HASHIDATE, and OSAMU NONAKA Jun. 1990 39 p In JAPANESE; ENGLISH summary
(NAL-TR-1071; ISSN-0389-4010) Avail: NTIS HC/MF A03

An optimum propeller design, whose representative Reynolds number is between 1 and 2 x 10(exp 5), was tested in the NAL large low-speed wind tunnel. After removing the wind tunnel interference effects, the test results were compared with predictions by a computer program based on Adkins and Liebeck's theory. Thrust predictions show very good coincidence with test results. Torque predictions show fairly good coincidence. The difference between the theoretical predictions and experimental values are thought to be attributable to the shrinkage of the drag bucket in propeller blade sections, compared with the two-dimensional airfoil data. The aerodynamics design method of propellers working in the low Reynolds number range was established. The computer program is very useful in designing propellers for man-powered airplanes and motor soarers, as well as microwave powered airplanes. Author

N91-21113# National Aerospace Lab., Tokyo (Japan).
AN EXPERIMENTAL STUDY OF A THREE-DIMENSIONAL SWEPT-BACK WING WITH SUCTION LAMINAR-FLOW-CONTROL
YOJI ISHIDA, MASAYOSHI NOGUCHI, SHIGEO KAYABA, OSAMU NONAKA, and HIDEO HOSHINO Jul. 1990 23 p In JAPANESE; ENGLISH summary
(NAL-TR-1072; ISSN-0389-4010) Avail: NTIS HC/MF A03

A wind tunnel test of a three-dimensional swept-back wing with suction laminar flow control (LFC) was executed to investigate the drag reduction effect of the LFC under various test conditions. The wing model has a hybrid suction surface which consists of a porous surface with very fine holes from near the leading edge to 25 percent chord and a slotted surface with a large number of fine slots from 25 to 80 percent chord. Total drag, C(sub DT), which is defined as the sum of the wake drag and the equivalent drag, was measured for various suction quantities. Application of the optimum suction quantities, which were determined so as to delay the natural transition points up to 90 percent chord with the minimum total suction quantity for each test condition, gives a fairly large drag reduction (about 40 percent) compared with the no suction case for Reynolds numbers up to 3.6 x 10(exp 6). A suction applied only in the leading edge region also gives not a little drag reduction, but a suction in the rear part of the wing where the boundary layer flow is already turbulent has no effect on the drag reduction. It was observed that when there is no suction the porous suction surface generates much earlier transitions than does the solid surface. As transition is a very important problem for practical application of LFC, further investigation will be required. Author

N91-21114# National Aerospace Lab., Tokyo (Japan).
BLUNT TRAILING EDGE ANALYSIS OF SUPERCRITICAL AIRFOILS BY A NAVIER-STOKES CODE
NAOKI HIROSE and NOBUHIKO KAMIYA Aug. 1990 26 p Previously announced in IAA as A91-24424
(NAL-TR-1075-T; ISSN-0389-4010) Avail: NTIS HC/MF A03

A preliminary analysis of flow about the blunt trailing edge of the NACA 0012 and supercritical airfoils in transonic speed was made utilizing a 2-D time-averaged Navier-Stokes code with the turbulence model of Baldwin and Lomax. A very fine mesh distribution was focused at the trailing edge region which conventional codes treat as a sharp trailing edge with zero thickness. Computation was made for the NACA 0012 airfoil with three kinds of trailing edge thicknesses, cusp-type sharp, standard and 1 percent thickness and was compared with the result of a conventionally-treated trailing edge. A fifteen percent thickness supercritical airfoil with a trailing edge thickness of 0.5 percent was also analyzed. It was found that a vortex shedding similar to the Karman vortices is formed and surface pressure near the trailing edge shows unsteady oscillation due to the vortices. The magnitude and periodicity of the oscillation is governed by the bluntness. Also, it was shown that the Kutta condition is not necessarily satisfied for the blunt trailing edge. Author

N91-21116*# National Aeronautics and Space Administration. Lewis Research Center, Cleveland, OH.
HOT GAS INGESTION TEST RESULTS OF A TWO-POSTER VECTORED THRUST CONCEPT WITH FLOW VISUALIZATION IN THE NASA LEWIS 9- X 15-FOOT LOW SPEED WIND TUNNEL
ALBERT L. JOHNS, GEORGE NEINER, TIMOTHY J. BENCIC, JOSEPH D. FLOOD, KURT C. AMUEDO, and THOMAS W. STROCK (McDonnell-Douglas Corp., Saint Louis, MO.) Jul. 1990 27 p Presented at the 26th Joint Propulsion Conference, Orlando, FL, 16-18 Jul. 1990; sponsored in part by AIAA, SAE, ASME, and ASEE Original contains color illustrations
(NASA-TM-103258; E-5690; NAS 1.15:103258; AIAA-90-2268)
Avail: NTIS HC/MF A03; 1 functional color page CSCL 01A

A 9.2 percent scale Short Takeoff and Vertical Landing (STOVL)

hot gas ingestion model was designed and built by McDonnell Douglas Corporation (MCAIR) and tested in the Lewis Research Center 9 x 15 foot Low Speed Wind Tunnel (LSWT). Hot gas ingestion, the entrainment of heated engine exhaust into the inlet flow field, is a key development issure for advanced short takeoff and vertical landing aircraft. Flow visualization from the Phase 1 test program, which evaluated the hot ingestion phenomena and control techniques, is covered. The Phase 2 test program evaluated the hot gas ingestion phenomena at higher temperatures and used a laser sheet to investigate the flow field. Hot gas ingestion levels were measured for the several forward nozzle splay configurations and with flow control/life improvement devices (LIDs) which reduced the hot gas ingestion. The model support system had four degrees of freedom - pitch, roll, yaw, and vertical height variation. The model support system also provided heated high-pressure air for nozzle flow and a suction system exhaust for inlet flow. The test was conducted at full scale nozzle pressure ratios and inlet Mach numbers. Test and data analysis results from Phase 2 and flow visualization from both Phase 1 and 2 are documented. A description of the model and facility modifications is also provided. Headwind velocity was varied from 10 to 23 kn. Results are presented over a range of nozzle pressure ratios at a 10 kn headwind velocity. The Phase 2 program was conducted at exhaust nozzle temperatures up to 1460 R and utilized a sheet laser system for flow visualization of the model flow field in and out of ground effects. The results reported are for nozzle exhaust temperatures up to 1160 R. These results will contain the compressor face pressure and temperature distortions, the total pressure recovery, the inlet temperature rise, and the environmental effects of the hot gas. The environmental effects include the ground plane contours, the model airframe heating, and the location of the ground flow separation. Author

N91-21117*# Old Dominion Univ., Norfolk, VA. Dept. of Mechanical Engineering and Mechanics.

INVESTIGATION OF NOSE BLUNTNESS AND ANGLE OF ATTACK EFFECTS ON SLENDER BODIES IN VISCOUS HYPERTENSION FLOWS Progress Report, period ending 30 Apr. 1991

A. K. SEHGAL, S. N. TIWARI, and D. J. SINGH May 1991 124 p

(Contract NCC1-68; NAG1-363)

(NASA-CR-188153; NAS 1.26:188153) Avail: NTIS HC/MF A06 CSCL 01A

Hypersonic flows over cones and straight biconic configurations are calculated for a wide range of free stream conditions in which the gas behind the shock is treated as perfect. Effect of angle of attack and nose bluntness on these slender cones in air is studied extensively. The numerical procedures are based on the solution of complete Navier-Stokes equations at the nose section and parabolized Navier-Stokes equations further downstream. The flow field variables and surface quantities show significant differences when the angle of attack and nose bluntness are varied. The complete flow field is thoroughly analyzed with respect to velocity, temperature, pressure, and entropy profiles. The post shock flow field is studied in detail from the contour plots of Mach number, density, pressure, and temperature. The effect of nose bluntness for slender cones persists as far as 200 nose radii downstream. Author

N91-21118# Air Force Inst. of Tech., Wright-Patterson AFB, OH. School of Engineering.

BIFURCATION ANALYSIS OF THE LONGITUDINAL DYNAMICS OF A SIMPLE POWERED LIFTING HYPERSONIC VEHICLE M.S. Thesis

ERIC E. FOX Dec. 1990 102 p

(AD-A230826; AFIT/GAE/ENY/90D-07) Avail: NTIS HC/MF A06 CSCL 22/3

Bifurcation analysis was used to investigate the nonlinear behavior of a simple powered lifting hypersonic vehicle in circular orbit about a spherical nonrotating earth with gradients in atmospheric density and pressure and an inverse square law for gravity. Vehicle motion is constrained to a vertical plane so only longitudinal dynamics were modeled. Bifurcation analysis was conducted using the AUTO software package. A simple five-state model with three different thrust laws was derived to describe an unaugmented vehicle whose geometric and aerodynamic characteristics follow those of the literature. A parameter representing a body flap deflection was used to conduct one set of bifurcation sweeps for each thrust law. A second set of bifurcation sweeps for each thrust law was obtained using a parameter representing a throttle which scaled the thrust. Secondary parameters representing simple feedback gains were subsequently added. Results were surprising for a simple system with basically linear aerodynamics. Periodic branches arising from the loss of pitch stability or associated with a resonance altitude are routinely found with significant amplitude, and periods on the order of an elliptical orbit's period for a given geocentric radius. Rotational states generally had sub-oscillations of greater frequency. GRA

N91-21119# Air Force Inst. of Tech., Wright-Patterson AFB, OH. School of Engineering.

VORTEX BURSTING OVER A UNIT AREA ASPECT RATIO DELTA WING USING VORTEX PANELING METHODS M.S. Thesis

DONALD A. LOREY Dec. 1990 77 p

(AD-A231028; AFIT/GAE/ENY/90D-14) Avail: NTIS HC/MF A05 CSCL 01/1

A unit aspect ratio delta wing is analyzed to determine if an unsteady vortex panel method can calculate the vortex bursting of the vortex developed along the leading edge. A two-dimensional vortex panel method is used to investigate wake splitting schemes of the vortex cores that comprise the vortex sheet, or wake. The worthier of the splitting methods is later implemented into the three-dimensional wake. The weighting values of the Kutta equations are investigated for the leading edges, and are determined to be problem specific. An alternative approach to management of the wake data is presented and implemented. The delta wing is then analyzed for 20.5 and 30 deg angle of attack. The panel method produced a perturbation and enlargement in the wake at two thirds chord position over the wing at 30 deg angle of attack, indicative of vortex breakdown. However, a qualitative comparison with the results of the 20.5 deg angle of attack calculation negates this conclusion. Vortex bursting was not evident over the wing at 30 deg angle of attack. GRA

N91-21120# Nielsen Engineering and Research, Inc., Mountain View, CA.

PREDICTION OF UNSTEADY TRANSONIC SEPARATED FLOW FOR MISSILE APPLICATIONS Final Report, 1 Jul. 1987 - 15 Oct. 1990

P. REISENTHEL and D. NIXON 20 Nov. 1990 121 p

(Contract DAAL03-87-C-0008)

(AD-A231259; NEAR-TR-418; ARO-24788.7-EG) Avail: NTIS HC/MF A06 CSCL 20/4

A theory was developed to treat flow separation and related vortex effects in unsteady transonic flow around slender bodies. This theory involves the simultaneous solution of a modified Transonic Small Disturbance Equation, a kinematic vector potential equation, and a 3-D transport equation for the streamwise vorticity. In this theory, flow separation is modeled using normal vorticity jets placed along the separation line. The location and strength of the separating vorticity was determined from empirical criteria. A steady version of the theory was implemented using a considerably developed form of the TWING potential code, while the unsteady implementation was performed using an enhanced version of the computational aeroelasticity program (CAP-TSD). A critical result was that a second order correction to the pressure, namely, the inclusion of the rotational streamwise velocity component, is necessary to account for the tilting of vortices away from the body axis. Time-accurate computations of subsonic, transonic, and supersonic flow show that it is possible to compute the flow around realistic angle of attack missile configurations, thus showing considerable potential for aeroelastic computations and unsteady aerodynamics. Results of 2-D Navier-Stokes

calculations indicate that several key aspects characterizing the time-dependent behavior of boundary layer separation may be accurately predicted using indicial theory. These results demonstrate the possibility of significant phase lags and fluctuation overshoots of the normal vorticity flux at separation. GRA

N91-22069*# National Aeronautics and Space Administration. Langley Research Center, Hampton, VA.
AEROPROPULSIVE CHARACTERISTICS OF CANTED TWIN PITCH-VECTORING NOZZLES AT MACH 0.20 TO 1.20
FRANCIS J. CAPONE, MARY L. MASON, and GEORGE T. CARSON, JR. Washington May 1991 257 p
(NASA-TP-3060; L-16823; NAS 1.60:3060) Avail: NTIS HC/MF A12 CSCL 01/1

The multiaxis thrust vectoring capability from canting 2-D convergent-divergent exhaust nozzles installed on a twin jet afterbody model was determined in an investigation conducted in the Langley 16 foot Transonic Tunnel. Pitch vectoring was accomplished by the deflection of the nozzle upper and lower divergent flaps. Several combinations of symmetric and differential pitch deflection angles were tested at nozzle cant angles of 0, 30, and 45 degrees. The effect of varying nozzle divergent flap length was also studied. Mach numbers from 0.20 to 1.20, angles of attack from 0 to 27.5 degrees nozzle pressure ratios up to 8.0, and sideslip angles of 0 to 5 degrees were the variables used. Author

N91-22070*# National Aeronautics and Space Administration. Langley Research Center, Hampton, VA.
NUMERICAL STUDY OF THE AERODYNAMIC EFFECTS OF USING SULFUR HEXAFLUORIDE AS A TEST GAS IN WIND TUNNELS
W. KYLE ANDERSON Washington Jan. 1991 26 p Previously announced in IAA as A90-37958
(NASA-TP-3086; L-16849; NAS 1.60:3086) Avail: NTIS HC/MF A03 CSCL 01/1

A numerical study is presented which investigates effects of using sulfur hexafluoride, SF6, as a substitute for air. Inviscid results for airfoils indicate that for transonic cases the shock location calculated for SF6 is vastly different from that in air and moves progressively forward on the airfoil as the freestream pressure is increased and real gas effects become more pronounced. Application of a simple Mach number scaling procedure results in good correlation between SF6 and air even for pressures at which non-ideal gas effects are significant. Computations for subsonic turbulent flows over a NACA 0012 airfoil show that the maximum angle of attack at which steady lift can be obtained is different between air and SF6. In addition, for SF6, this angle of attack depends greatly on the freestream conditions. Close agreement with air can be achieved by altering the freestream Mach number according to the inviscid scaling procedure. Transonic results show that even with Mach number scaling, the shock location and skin friction values calculated between air and SF6 are in disagreement. This is attributed to the limitations of the scaling procedure and to the thinner boundary layer for SF6. Author

N91-22071*# MCAT Inst., San Jose, CA.
GRID GENERATION ABOUT COMPLEX THREE-DIMENSIONAL AIRCRAFT CONFIGURATIONS Final Report
GOETZ H. KLOPFER Apr. 1991 16 p
(Contract NCC2-616)
(NASA-CR-188097; NAS 1.26:188097; MCAT-91-003) Avail: NTIS HC/MF A03 CSCL 01/1

The problem of obtaining three dimensional grids with sufficient resolution to resolve all the flow or other physical features of interest is addressed. The generation of a computational grid involves a series of compromises to resolve several conflicting requirements. On one hand, one would like the grid to be fine enough and not too skewed to reduce the numerical errors and to adequately resolve the pertinent physical features of the flow field about the aircraft. On the other hand, the capabilities of present or even future supercomputers are finite and the number of mesh points must be limited to a reasonable number: one which is usually much less than desired for numerical accuracy. One technique to overcome this limitation is the 'zonal' grid approach. In this method, the overall field is subdivided into smaller zones or blocks in each of which an independent grid is generated with enough grid density to resolve the flow features in that zone. The zonal boundaries or interfaces require special boundary conditions such that the conservation properties of the governing equations are observed. Much work was done in 3-D zonal approaches with nonconservative zonal interfaces. A 3-D zonal conservative interfacing method that is efficient and easy to implement was developed during the past year. During the course of the work, it became apparent that it would be much more feasible to do the conservative interfacing with cell-centered finite volume codes instead of the originally planned finite difference codes. Accordingly, the CNS code was converted to finite volume form. This new version of the code is named CNSFV. The original multi-zonal interfacing capability of the CNS code was enhanced by generalizing the procedure to allow for completely arbitrarily shaped zones with no mesh continuity between the zones. While this zoning capability works well for most flow situations, it is, however, still nonconservative. The conservative interface algorithm was also implemented but was not completely validated. Author

N91-22074 Cranfield Inst. of Tech., Bedford (England).
APPROXIMATE METHODS FOR PREDICTING THE LIFTING CHARACTERISTICS OF WING-BODY COMBINATIONS Ph.D. Thesis
SAKHER HAMWI 1989 349 p
Avail: Univ. Microfilms Order No. BRDX90890

The development of the theory and program (DBVL), based on two well established analysis tools, the vortex-lattice method and axial distributions of discrete doublets, which were combined in a relatively simple way to study aerodynamic wing/body interference are described. Comparisons, for isolated bodies (blunt or pointed), isolated plate wings and wing/body combinationd, were made with exact solutions, experimental data, and some other available methods, such as the panel method (SPARV). It is concluded that the new method and its associated program are accurate, versatile, and efficient, requiring only 4 to 5 percent of the CPU time employed by SPARV when applied to examples of considerable complexity. An additional feature of these comparisons was the accuracy with which the wing-body interference factors could be predicted, particularly when compared with those based on slender-body theory. Dissert. Abstr.

N91-22077*# National Aeronautics and Space Administration. Ames Research Center, Moffett Field, CA.
FORCES AND PRESSURES INDUCED ON CIRCULAR PLATES BY A SINGLE LIFTING JET IN GROUND EFFECT
DAVID C. BELLAVIA, DOUGLAS A. WARDWELL, VICTOR R. CORSIGLIA, and RICHARD E. KUHN (STO-VL Technology, San Diego, CA.) Mar. 1991 100 p
(NASA-TM-102816; A-90142; NAS 1.15:102816) Avail: NTIS HC/MF A05 CSCL 01/1

NASA Ames is conducting a program to develop improved methods for predicting suckdown and hot-gas ingestion on jet V/STOL aircraft when they are in ground effect. As part of that program a data base is being created that provides a systematic variation of parameters so that current empirical prediction procedures can be modified. The first series of tests in this program is complete. This report is one of three that presents the data obtained from tests conducted at Lockheed Aeronautical Systems - Rye Canyon Facility and the High Bay area of the 40 by 80 foot Wind Tunnel at Ames Research Center. Suckdown on two circular plates is examined. Author

N91-22078*# Lockheed Engineering and Sciences Co., Hampton, VA.
AERODYNAMIC PARAMETER STUDIES AND SENSITIVITY ANALYSIS FOR ROTOR BLADES IN AXIAL FLIGHT
Y. DANNY CHIU and DAVID A. PETERS (Georgia Inst. of Tech., Atlanta.) Mar. 1991 17 p Presented at the International Technical Specialists' Meeting on Rotorcraft Basic Research,

Atlanta, GA, 25-27 Mar. 1991
(Contract NAS1-19000; NAG1-710)
(NASA-CR-187524; NAS 1.26:187524) Avail: NTIS HC/MF A03 CSCL 01/1

The analytical capability is offered for aerodynamic parametric studies and sensitivity analyses of rotary wings in axial flight by using a 3-D undistorted wake model in curved lifting line theory. The governing equations are solved by both the Multhopp Interpolation technique and the Vortex Lattice method. The singularity from the bound vortices is eliminated through the Hadamard's finite part concept. Good numerical agreement between both analytical methods and finite differences methods are found. Parametric studies were made to assess the effects of several shape variables on aerodynamic loads. It is found, e.g., that a rotor blade with out-of-plane and inplane curvature can theoretically increase lift in the inboard and outboard regions respectively without introducing an additional induced drag.
Author

N91-22080*# Arizona State Univ., Tempe. Coll. of Engineering and Applied Sciences.
A REVIEW OF NEAR-WALL REYNOLDS-STRESS
R. M. C. SO, Y. G. LAI, H. S. ZHANG, and B. C. HWANG (David Taylor Research Center, Annapolis, MD.) Washington May 1991 64 p
(Contract NAG1-1080)
(NASA-CR-4369; NAS 1.26:4369) Avail: NTIS HC/MF A04 CSCL 01/1

The advances made in second-order near-wall turbulence closures are summarized. All closures examined are based on some form of high Reynolds number models for the Reynolds stress and the turbulent kinetic energy dissipation rate equations. Consequently, most near-wall closures proposed to data attempt to modify the high Reynolds number models for the dissipation rate equation so that the resultant models are applicable all the way to the wall. The near-wall closures are examined for their asymptotic behavior so that they can be compared with the proper near-wall behavior of the exact equations. A comparison of the closure's performance in the calculation of a low Reynolds number plane channel flow is carried out. In addition, the closures are evaluated for their ability to predict the turbulence statistics and the limiting behavior of the structure parameters compared to direct simulation data.
Author

N91-22081# Naval Postgraduate School, Monterey, CA.
SEPARATING BOUNDARY LAYER RESPONSE TO AN UNSTEADY TURBULENT ENVIRONMENT M.S. Thesis
DAVID J. GWILLIAM, JR. Dec. 1989 43 p
(AD-A231483) Avail: NTIS HC/MF A03 CSCL 01/1

An experimental investigation of the separating boundary layer of a wing subjected to periodic turbulent disturbances was conducted. Turbulence pulses were generated by a non-thrusting spinning rod placed upstream of the test airfoil at the reduced frequencies of .09 and .47. Time-varying velocity measurements were made at various heights above the 70 percent chord location at 12 degrees angle of attack (nearly separated flow) and 22 degrees angle of attack (fully separated flow). Split-film anemometry was used to determine flow speed and direction. The flow responses were compared to the quasi-steady state of undisturbed separated flow. Variation of reduced frequency had a dramatic influence on the effects which the periodic disturbance had on the flow response. At a reduced frequency of .47, the periodic disturbance had no noticeable influence. Imposition of periodic disturbance of the same reduced frequency on attached flow near separation (12 degrees angle of attack) once again caused no apparent destabilizing effects. The lack of sensitivity of the separated boundary layer to the pulses generated at the higher reduced frequency of .47 apparently resulted from its inability to resolve turbulent pulses from one another. Imposition at 22 degrees angle of attack of a pulse at the reduced frequency of .09, however, first stabilized the flow, then greatly intensified the original separation before allowing the flow to return to its undisturbed separated state.
GRA

N91-22082# Virginia Polytechnic Inst. and State Univ., Blacksburg. Dept. of Engineering Science and Mechanics.
THE TRANSIENT DEVELOPMENT OF VORTICES OVER A DELTA WING Final Report, 1 Mar. 1989 - 30 Sep. 1990
DEMETRI P. TELIONIS 23 Dec. 1990 9 p
(Contract AF-AFOSR-0283-89; AF PROJ. 2307)
(AD-A231946; AFOSR-91-0026TR) Avail: NTIS HC/MF A02 CSCL 01/1

The most interesting finding was that for large angles of attack, a delta wing actually sheds vortices alternately, just like bluff bodies do. Also, at high sweep angles, vortex shedding is suddenly initiated at an angle of attack of 37 degrees. In addition, it was found that a seven-hole probe as small in diameter as 2 pct. of the diameter of the vortex can actually precipitate breakdown, but with little effect on the static pressure on the wing suction surface.
GRA

N91-22083*# National Aeronautics and Space Administration. Hugh L. Dryden Flight Research Facility, Edwards, CA.
MULTIAXIS THRUST VECTORING USING AXISYMMETRIC NOZZLES AND POSTEXIT VANES ON AN F/A-18 CONFIGURATION VEHICLE
ALBION H. BOWERS, GREGORY K. NOFFZ, SUE B. GRAFTON, MARY L. MASON, and LEE R. PERON (California Polytechnic State Univ., San Luis Obispo.) Apr. 1991 36 p Presented at the High-Angle-of Attack Technology Conference, Hampton, VA, 30 Oct. - 1 Nov. 1990
(NASA-TM-101741; H-1705; NAS 1.15:101741) Avail: NTIS HC/MF A03 CSCL 01/1

A ground-based investigation was conducted on an operational system of multiaxis thrust vectoring using postexit vanes around an axisymmetric nozzle. This thrust vectoring system will be tested on the NASA F/A-18 High Alpha Research Vehicle (HARV) aircraft. The system provides thrust vectoring capability in both pitch and yaw. Ground based data were gathered from two separate tests at NASA Langley Research Center. The first was a static test in the 16-foot Transonic Tunnel Cold-Jet Facility with a 14.25 percent scale model of the axisymmetric nozzle and the postexit vanes. The second test was conducted in the 30 by 60 foot wind tunnel with a 16 percent F/A-18 complete configuration model. Data from the two sets are being used to develop models of jet plume deflection and thrust loss as a function of vane deflection. In addition, an aerodynamic interaction model based on plume deflection angles will be developed. Results from the scale model nozzle test showed that increased vane deflection caused exhaust plume turning. Aerodynamic interaction effects consisted primarily of favorable interaction of moments and unfavorable interaction of forces caused by the vectored jet plume.
Author

N91-22086# Bristol Univ. (England). Dept. of Aerospace Engineering.
EFFECT OF PLANFORM ON INDUCED DRAG B.S. Thesis
J. P. DARCY and D. A. PARKIN-MOORE Jun. 1990 46 p
(BU-500; ETN-91-99193) Avail: NTIS HC/MF A03

A baseline, elliptical wing with a straight line quarter chord was tested and results compared with a crescent moon shaped planform wing with the same Clark-Y section, chord distribution and aspect ratio of 4.5. The provision of flow visualization photographs assisted in the qualitative assessment of the results and facilitated the analysis of planforms effects on the flow. Induced drag factors of near and below unity were calculated for both wings, which were tested at Reynolds numbers of between 0.40 and 0.55 million. The baseline wing had an induced drag factor of 0.935 compared to the larger induced drag factor of the crescent wing of 0.953.
ESA

N91-22087# Bristol Univ. (England). Dept. of Aerospace Engineering.
A LEADING-EDGE CONTROL SURFACE B.S. Thesis
S. R. B. LEES and U. PERIYATHAMBY Jun. 1990 105 p
(BU-508; ETN-91-99201) Avail: NTIS HC/MF A06

The effects of a simply hinged leading edge control device was investigated with regard to supression of flutter at high angles of attack. At high angles of attack the rotation of the trailing and

leading edge devices independently and simultaneously were studied, using flow visualization to determine the range of deflections in which they can have a beneficial effect on the flow and consequently on changes in lift, drag, etc. These are compared with results from another model with identical section, which has well known pressure distributions and well known aerodynamic coefficients from the integration of these pressure distributions. The investigation shows that at high angles of attack a stalled airflow can be recovered in the static case using the leading edge device. However, it is difficult to predict whether very rapid movement of these surfaces would also produce attractive lift coefficients when the motion itself could cause the airflow to become stalled or at least temporarily separated. ESA

N91-22089# Bristol Univ. (England). Dept. of Aerospace Engineering.
AN INVESTIGATION INTO THE EXTENT AND EFFECTS OF SPANWISE FLOW IN THE BOUNDARY LAYER OF A HELICOPTER ROTOR IN HOVER B.S. Thesis
R. G. TAYLOR-HUNT and J. P. WINTER Jun. 1990 54 p
(BU-519; ETN-91-99212) Avail: NTIS HC/MF A04

Results are presented for an investigation into the spanwise component of flow which is purported to exist in the boundary layer of a helicopter rotor. A model rotor of 1.6 m diameter was tested in the hovering condition, using 'microtufts' and the China clay method in order to study the boundary layer flow. The flow visualization techniques were developed with considerable success, and it was shown that the extent of signficant spanwise flow is small. The spanwise flow which did exist in a separation bubble was prevented by chordwise fences as a control, and numerical results did not measure any stall delaying effects associated with the weak spanwise flow. ESA

N91-22091*# National Aeronautics and Space Administration. Ames Research Center, Moffett Field, CA.
SMALL-SCALE EXPERIMENTS IN STOVL GROUND EFFECTS
VICTOR R. CORSIGLIA, DOUGLAS A. WARDWELL, and RICHARD E. KUHN (Kuhn, Richard E., San Diego, CA) Apr. 1991 16 p Presented at the RAS International Powered Life Conference, London, England, Aug. 1990 Previously announced in IAA as A91-21256
(NASA-TM-102813; A-90137; NAS 1.15:102813) Avail: NTIS HC/MF A03 CSCL 01/1

A series of tests was completed in which suckdown and fountain forces and pressures were measured on circular plates and twin-tandem-jet generic STOVL (short takeoff and vertical landing) configurations. The tests were conducted using a small-scale hover rig, for jet pressure ratios up to 6 and jet temperatures up to 700 F. The measured suckdown force on a circular plate with a central jet was greater than that found with a commonly used empirical prediction method. The present data showed better agreement with other sets of data. The tests of the generic STOVL configurations were conducted to provide force and pressure data with a parametric variation of parameters so that an empirical prediction method could be developed. The effects of jet pressure ratio and temperature were found to be small. Lift improvement devices were shown to substantially reduce the net suckdown forces. Author

N91-22093*# Polytechnic Inst. of New York, Brooklyn. Dept. of Aerospace Engineering.
DEVELOPMENT OF A COMPUTER TECHNIQUE FOR THE PREDICTION OF TRANSPORT AIRCRAFT FLIGHT PROFILE SONIC BOOM SIGNATURES M.S. Thesis
PETER G. COEN Mar. 1991 139 p Sponsored by NASA, Washington
(NASA-CR-188117; NAS 1.26:188117) Avail: NTIS HC/MF A07 CSCL 01/1

A new computer technique for the analysis of transport aircraft sonic boom signature characteristics was developed. This new technique, based on linear theory methods, combines the previously separate equivalent area and F function development with a signature propagation method using a single geometry description. The new technique was implemented in a stand-alone computer program and was incorporated into an aircraft performance analysis program. Through these implementations, both configuration designers and performance analysts are given new capabilities to rapidly analyze an aircraft's sonic boom characteristics throughout the flight envelope. Author

N91-22094# Sandia National Labs., Albuquerque, NM.
AN INTRODUCTION TO TESTING PARACHUTES IN WIND TUNNELS
J. MACHA 1991 11 p Presented at the 11th AIAA Aerodynamic Decelerator Systems Technology Conference, San Diego, 9-11 Apr. 1991
(Contract DE-AC04-76DP-00789)
(DE91-009166; SAND-91-0531C; AIAA-91-0858; CONF-9104171-6) Avail: NTIS HC/MF A03

This paper reviews some of the technical considerations and current practices for testing parachutes in conventional wind tunnels. Special challenges to the experimentalist caused by the fabric construction, flexible geometry, and buff shape of parachutes are discussed. In particular, the topics of measurement technique, similarity considerations, and wall interference are addressed in a summary manner. Many references are cited which provide detailed coverage of the state of the art in testing methods. From the discussions presented, it is obvious that there are some serious problems with state of the art methods, especially in the area of canopy instrumentation and when working with reduced-scale models. But if the experimentalist is informed about the relative importance of the various factors for a specific test objective, it is usually possible to design a test that will yield meaningful results. The lower cost and the more favorable measurement environment of wind tunnels make their use an attractive alternative to flight testing whenever possible. DOE

N91-22095*# Arizona State Univ., Tempe. Dept. of Mechanical and Aerospace Engineering.
NUMERICAL SIMULATION OF SWEPT-WING FLOWS Progress Report
HELEN L. REED Feb. 1991 55 p
(Contract NAG1-1158)
(NASA-CR-188201; NAS 1.26:188201) Avail: NTIS HC/MF A04 CSCL 01/1

The transition process characteristics of flows over swept wings were computationally modelled. The crossflow instability and crossflow/T-S wave interaction are analyzed through the numerical solution of the full three dimensional Navier-Stokes equations including unsteadiness, curvature, and sweep. The leading-edge region of a swept wing is considered in a three-dimensional spatial simulation with random disturbances as the initial conditions. Author

N91-22105# Notre Dame Univ., IN. Dept. of Aerospace and Mechanical Engineering.
UNSTEADY AERODYNAMICS OF SLENDER WINGS
ROBERT C. NELSON *In* AGARD, Special Course on Aircraft Dynamics at High Angles of Attack: Experiments and Modelling 26 p Mar. 1991
Copyright Avail: NTIS HC/MF A07; Non-NATO Nationals requests available only from AGARD/Scientific Publications Executive

A review of unsteady aerodynamics for slender wings undergoing large amplitude motions is presented. Static and unsteady aerodynamics characteristics are discussed, and the relationship between the aerodynamic loads and the leeward structure is investigated. Data is presented showing the influence of the wing motion on the aerodynamic loads. Both large amplitude pitching and rolling motion experimental results are discussed. In the case of large amplitude pitching motions, significant aerodynamic hysteresis is apparent. The hysteresis in the aerodynamic loads is shown to be related to the delay in vortex breakdown on the upstroke and the delay in the re-establishment of the leading edge vortical flow after complete flow separation on the downstroke. A second example of unsteady aerodynamics, namely the phenomenon of wing rock, is examined. Author

N91-22108# National Research Council of Canada, Ottawa (Ontario).
LARGE AMPLITUDE OSCILLATIONS
E. S. HANFF *In* AGARD, Special Course on Aircraft Dynamics at High Angles of Attack: Experiments and Modelling 19 p Mar. 1991
Copyright Avail: NTIS HC/MF A07; Non-NATO Nationals requests available only from AGARD/Scientific Publications Executive

Over the past several years a consensus has been developing that the locally linear analysis technique is inadequate for the prediction of aircraft behavior in the nonlinear regime. This situation arises mainly in flight at high angles of attack, particularly during large-amplitude and high-rate maneuvers, where the flow may be severely separated, vortex dominated, and time dependent. In recognition of this situation, work is currently underway to develop techniques that can provide a better physical understanding and more accurate prediction capabilities of aircraft behavior in this regime. Much of the effort is of a rather theoretical nature, essentially consisting of a attempt to identify and implement a mathematical formalism capable of handling the various types of nonlinearities present under the above conditions. Presented here is a more empirical formulation for the treatment of aerodynamic nonlinearities and time dependence, which is based on a knowledge of the instantaneous values of the pertinent motion variables. A wind tunnel technique and rig used at the Institute for Aeronautical Research (IAR) to obtain the necessary data is described as well as some interesting results. A brief review of work involving large amplitude oscillations being conducted at the Royal Aircraft Establishment (RAE) is also included. Author

N91-22109# Royal Aircraft Establishment, Bedford (England). Aerodynamics Dept.
OSCILLATORY DATA FOR TYPICAL CONFIGURATIONS
C. O. OLEARY *In* AGARD, Special Course on Aircraft Dynamics at High Angles of Attack: Experiments and Modelling 18 p Mar. 1991
Copyright Avail: NTIS HC/MF A07; Non-NATO Nationals requests available only from AGARD/Scientific Publications Executive

Since the early 1950's many aircraft configurations, nearly all military, have been tested on a variety of oscillatory rigs. There is a need for reliable test data on new configurations prior to flight testing and for general research on dynamic flight characteristics of combat aircraft. Examples of published test data on small amplitude oscillatory derivatives from three research centers are presented in order to give some insight into the effects of configuration, model attitude, frequency parameter, etc. on the stability derivatives. Data is given on the effect of a wing planform on a fighter configuration; forced oscillation; the effects of canards, tails, and fuselage strakes on a three-surface configuration; and subsonic roll oscillation tests on the standard dynamics model. Author

03

AIR TRANSPORTATION AND SAFETY

Includes passenger and cargo air transport operations; and aircraft accidents.

A91-33273
THE DELAYED EJECTION DECISION
JESSE JENKINS (USAF, Kelly AFB, TX) SAFE Journal, vol. 21, Spring 1991, p. 13-15.
Copyright

The USAF ejection data covering the years 1977 through 1989 are reviewed. It was found that, in spite of the advanced capabilities of modern ejections seats in the USAF inventory, the ejection survival rates continue at an excessive level. It is shown that the delayed ejection decision has been responsible for more unsuccessful ejections than all other factors combined. Data show that the average survivor of an ejection had two more minutes to decide to eject than did the fatalities. In addition, the survivors had, on the average, an additional 2500 feet separation from the ground when the decision was finally made. It is suggested that the pilot should give himself the maximum time possible by knowing the system, so that he can understand and study a problem faster, and by not delaying the decision. I.S.

A91-33668
THE EFFECT OF THE MICROWAVE LANDING SYSTEM ON AIRPORT CAPACITY
DANIEL J. BERNINGER (Galaxy Scientific Corp., Mays Landing, NJ) IN: IEEE PLANS '90 - Position Location and Navigation Symposium, Las Vegas, NV, Mar. 20-23, 1990, Record. New York, Institute of Electrical and Electronics Engineers, Inc., 1990, p. 650-655. refs
Copyright

An attempt is made to identify how MLS (microwave landing system) will affect airport capacity. It is noted that MLS has the potential to address capacity in many areas, including parallel runways, converging runways, conflicting approaches, incompatible aircraft mix, wake vortex avoidance, curved approaches, and reduced siting restrictions. It is concluded that since the basic technology of MLS has been demonstrated, efforts should focus of developing approaches that will improve its operational feasibility. Fixed-course-MLS is one such approach that will reduce the burden on controllers of coordinating curved approaches and simplify airborne equipment. I.E.

A91-34161
AIR SAFETY REGULATION AND ITS COMMERCIAL IMPACT
RONALD ASHFORD (Civil Aviation Authority, London, England) Aeronautical Journal (ISSN 0001-9240), vol. 95, March 1991, p. 77-87.
Copyright

While the ICAO requires that all aircraft involved in international navigation conform to a detailed and comprehensive code of safety-related practices, the detailed provisions for such practices, and their interpretation, may vary from country to country. The present, comprehensive evaluation of trends in safety regulation of commercial aviation notes that while world-wide accident trends continue to improve, there is substantial scope for improvement in the accident records of business jets, commuter aircraft, and light twins. 'Controlled flight into terrain' remains the largest single cause of accidents. The costs associated with safety improvements can be quite high, so that a uniform system for the cost recovery of safety regulation is desirable in order to minimize competitive penalties. The cost of saving more lives through additional safety improvements increases with the improvement of the general accident rate. O.C.

A91-34250
THE FINAL CALL: WHY AIRLINE DISASTERS CONTINUE TO HAPPEN
STEPHEN BARLAY New York, Pantheon Books, 1991, 469 p. refs
Copyright

Technological, economic, and political issues of commercial airline accidents are examined critically in a book for general readers. Detailed accounts of a large number of recent accidents are given, and the redundant and avoidable nature of most accidents is stressed. It is argued that stronger, more strictly enforced government regulations are needed to assure that cost-cutting measures and shortcuts do not have a negative effect on passenger safety. T.K.

A91-34341
BIODYNAMIC AND OPTIMIZATION ASPECTS OF EMERGENCY EJECTION FROM AN AIRCRAFT [BIODYNAMICZNE I OPTYMALIZACYJNE ASPEKTY W PROCESIE AWARYJNEGO OPUSZCZANIA SAMOLOTU]
STANISLAW SZAJNAR (Wojskowa Akademia Techniczna, Warsaw, Poland) and MIECZYSLAW WOJTKOWIAK (Wojskowy Instytut

Medycyny Lotniczej, Warsaw, Poland) Postepy Astronautyki (ISSN 0373-5982), vol. 23, no. 1-2, 1991, p. 103-118. In Polish. refs
Copyright

Possible ways to reduce the effects of acceleration acting on the pilot during emergency ejection from an aircraft are examined. It is suggested that optimal ejection can be achieved by improving the efficiency of the ejection system and the biodynamic aspects of this procedure. B.J.

A91-34912
HUMAN PERFORMANCE FACTORS IN AIRCRAFT ACCIDENT INVESTIGATION
PHYLLIS KAYTEN (National Transportation Safety Board, Washington, DC) IN: Human error avoidance techniques; Proceedings of the 2nd Conference, Herndon, VA, Sept. 18, 19, 1989. Warrendale, PA, Society of Automotive Engineers, Inc., 1989, p. 49-56. refs
(SAE PAPER 892608) Copyright

The study deals with human performance investigations and the major issues associated with it: who should conduct human performance investigations, what facts should be collected and what should be ignored, how should human-performance data be analyzed, and how is human-factors research utilized. The experience of the National Transportation Safety Board in investigations is analyzed, and it is noted that the investigators still investigate accidents in all modes of transportation. In the data collection area, such factors as experience, equipment design, and crew interaction are outlined. Attention is focused on the policy factor, alcohol and drugs, fatigue, cockpit voice recording, and privacy. V.T.

A91-35107# Massachusetts Inst. of Tech., Cambridge.
MODELING OF SURFACE ROUGHNESS EFFECTS ON GLAZE ICE ACCRETION
R. JOHN HANSMAN, JR., KEIKO YAMAGUCHI (MIT, Cambridge, MA), BRIAN BERKOWITZ (Sverdrup Technology, Inc., Middleburg Heights, OH), and MARK POTAPCZUK (NASA, Lewis Research Center, Cleveland, OH) Journal of Thermophysics and Heat Transfer (ISSN 0887-8722), vol. 5, Jan. 1991, p. 54-60. NSF-supported research. Previously cited in issue 10, p. 1433, Accession no. A89-28451. refs
(Contract NAG3-666; NGL-22-009-640)
Copyright

A91-36011
COPING WITH DRAMATIC AIR TRANSPORT GROWTH
PHILIP J. WIJERS (All Nippon Airways, Tokyo, Japan) ICAO Journal (ISSN 0018-8778), vol. 46, Jan. 1991, p. 10-15.
Copyright

A review is presented of the factors involved in the huge growth of air traffic and attendant infrastructure requirements in Japan. Though this is a small country geographically, it now ranks as the third largest market for domestic air travel in the world. Shortage of ramp spots and takeoff and landing slots, additionally hindered by strict adherence to long curfews has created severe airport congestion problems. Expansion of existing airports is being rushed to handle the continuing demand for more capacity in both the passenger and cargo areas. A completely new major traffic center is being developed in the Bay of Osaka that will be the first fully offshore airport in the world. Regional airports are also being expanded to handle international traffic to relieve some of the over-capacity experienced at the major hubs. R.E.P.

N91-21121*# Battelle Columbus Labs., Mountain View, CA.
NON-AIRBORNE CONFLICTS: THE CAUSES AND EFFECTS OF RUNWAY TRANSGRESSIONS
RICHARD J. TARREL Sep. 1985 86 p
(Contract NAS2-11934)
(NASA-CR-177372; NAS 1.26:177372) Avail: NTIS HC/MF A05 CSCL 01/3

The 1210 ASRS runway transgression reports are studied and expanded to yield descriptive statistics. Additionally, a one of three subset was studied in detail for purposes of evaluating the causes, risks, and consequences behind trangression events. Occurrences are subdivided by enabling factor and flight phase designations. It is concluded that a larger risk of collision is associated with controller enabled departure transgressions over all other categories. The influence of this type is especially evident during the period following the air traffic controllers' strike of 1981. Causal analysis indicates that, coincidentally, controller enabled departure transgressions also, show the strongest correlations between causal factors. It shows that departure errors occur more often when visibility is reduced, and when multiple takeoff runways or intersection takeoffs are employed. In general, runway transgressions attributable to both pilot and controller errors arise from three problem areas: information transfer, awareness, and spatial judgement. Enhanced awareness by controllers will probably reduce controller enabled incidents. Author

N91-21122# Dayton Univ., OH. Structural Integrity Div.
STUDY OF BIRD INGESTIONS INTO SMALL INLET AREA AIRCRAFT TURBINE ENGINES Final Report, May 1987 - Apr. 1989
JOSEPH P. MARTINO, DONALD A. SKINN, and JOSEPH J. WILSON Dec. 1990 93 p
(Contract DTFA03-88-C-00024)
(DOT/FAA/CT-90/13; UDR-TR-90-23) Avail: NTIS HC/MF A05

Summarized here are two years of data collection on the ingestion of birds into small inlet area aircraft turbine engines. A total of 16.1 million engine operations were flown by aircraft equipped with the small inlet area engines (ALF502, TFE731, TPE331, and JT15D) included in this study. This includes 24 months of operations for the first three engines and 12 months of operations for the last engine. A total of 210 engine ingestion events were reported during the two years of data collection. These events were analyzed to determine the degree of probability of ingestion, probability of degree of damage, probability of ingestion by phase of flight, and frequency of ingestion by geographic area. Author

N91-21123# Deutsche Forschungsanstalt fuer Luft- und Raumfahrt, Oberpfaffenhofen (Germany, F.R.). Abt. Wolkenphysik.
ANALYSIS OF THREE ICING TEST FLIGHTS REACHING THE AIRCRAFT-REFERRED ICING DEGREE SEVERE
HANS-EBERHARD HOFFMANN and JOHANN DEMMEL Aug. 1990 118 p In GERMAN; ENGLISH summary Report will also be announced as translation (ESA-TT-1254)
(DLR-FB-90-34; ISSN-0171-1342; ETN-91-99031) Avail: NTIS HC/MF A06; DLR, Wissenschaftliches Berichtswesen, VB-PL-DO, Postfach 90 60 58, 5000 Cologne, Fed. Republic of Germany, HC 45.50 DM

Three test flights in icing conditions where the aircraft referred icing degree severe is reached are discussed. One was in the range of a high pressure area, the others were in the range of warm fronts. In the area of the pneumatic deicing boots, the deicing was totally ineffective or incomplete. The cloud paths in the range of the warm fronts were only 0.1 or 0.3 times the cloud path in the range of a high pressure area, for obtaining the maximum icing characteristics (extension roughness, mass) of the high pressure area because of the considerably higher value of the median volume diameter in the range of the warmfronts. ESA

N91-21124# Naval Environmental Prediction Research Facility, Monterey, CA.
IMPACT OF ICING ON UNMANNED AERIAL VEHICLE (UAV) OPERATIONS
RICHARD A. SIQUIG 1990 8 p
(AD-A231191) Avail: NTIS HC/MF A02 CSCL 01/3

Clouds with supercooled liquid water constitute a significant aviation hazard because of the potential risk of aircraft icing. Icing reduces rate of lift, rate of climb, and fuel efficiency while increasing drag, stalling speed, weight, and power requirements. Indirectly, icing also exacts a penalty because on board icing detection/removal equipment may be required at the expense of other payload and because icing conditions may restrict launch/recovery or possible flight paths. All of these considerations

can be of increased importance for unmanned aerial vehicle (UAV) operations because of the unique design features of some UAVs and because of the extra burden placed on autonomous control systems. Therefore, UAV operations will require strong icing forecast support and remote icing detector systems at the vehicle bases and possibly on the vehicles themselves. High flying long endurance UAVs will be able to fly above icing levels but are at special risk in ascending/descending through icing layers due to the degradation icing causes to the highly optimized wing shape of such vehicles. Low flying short endurance vehicles do not have such sensitive wing shapes but may not be able to fly above all icing layers. The high flyers may be able to ascend/descend over their bases and thus require remote sensors only at the bases, whereas low flyers may require on board sensors when they are out of base sensor range. GRA

N91-22096*# National Aeronautics and Space Administration. Langley Research Center, Hampton, VA.
FLIGHT TEST TO DETERMINE FEASIBILITY OF A PROPOSED AIRBORNE WAKE VORTEX DETECTION CONCEPT Report, Jul. 1989 - Feb. 1990
JAMES R. BRANSTETTER, E. C. HASTINGS, JR., and JAMES C. PATTERSON, JR. (Vigyan Research Associates, Inc., Hampton, VA.) Apr. 1991 41 p Prepared in cooperation with FAA, Washington, DC
(NASA-TM-102672; NAS 1.15:102672; DOT/FAA/CT-TN90/25; ACD-20) Avail: NTIS HC/MF A03 CSCL 01/3

This investigation was conducted to determine the radial extent at which aircraft mounted flow vanes or roll rate gyros can sense the circulatory flow field that exists around the lift induced vortex system generated by an aircraft in flight. The probe aircraft was equipped with wingtip sensors for measuring angle of attack and angle of sideslip, and with a fuselage mounted gyroscope for measuring roll rate. Analysis of flight test data indicated that the vortex was detectable at a lateral distance of about 105 feet (best results) using unsophisticated equipment. Measurements were made from the centerline of the probe aircraft to the center of the nearest vortex with the probe aircraft flying between one half and one and one half miles behind the vortex generating aircraft. Author

N91-22098# Wichita State Univ., KS. National Inst. for Aviation Research.
AIRLINE QUALITY RATING .
BRENT D. BOWEN, DEAN E. HEADLEY, and JACQUELINE R. LUEDTKE Apr. 1991 128 p
(NIAR-91-11) Avail: NTIS HC/MF A07

An Airline Quality Rating (AQR) scale is proposed that assesses the quality of the U.S. major airlines using comparable, objective, quantifiable, periodically published data that addresses customer satisfaction concerns. This data is not consumer opinion based, but has distinct performance characteristics that are specifically attuned to the consumers point of view. The AQR focuses on quantitative factors in order to provide a more reliable and objective result in assessing service quality levels across all major domestic airlines. The combining of quantifiable and readily available data provides an objective starting point for monitoring the quality of service an individual airline might be providing. Author

N91-22099# Advisory Group for Aerospace Research and Development, Neuilly-Sur-Seine (France). Aerospace Medical Panel.
THE HUMAN FACTORS RELATING TO ESCAPE AND SURVIVAL FROM HELICOPTERS DITCHING IN WATER
C. J. BROOKS (Defence and Civil Inst. of Environmental Medicine, Downsview, Ontario) Feb. 1991 125 p In FRENCH English language document was announced as N90-13358
(AGARD-AG-305(F); ISBN-92-835-2116-1) Copyright Avail: NTIS HC/MF A06; Non-NATO Nationals requests available only from AGARD/Scientific Publications Executive

The worldwide incidence of military and civilian over-water helicopter accidents and the problems related to survival are described. Typical accident scenarios are reviewed from the moment the occupant steps onboard a helicopter to the pre-flight briefing through to the accident itself, to the difficulties with escape (commonly from underwater and in darkness), to the rescue and return safely to dry land. Improvements to crashworthiness and life support equipment in current in-servive and future helicopters are proposed. A syllabus for underwater escape training is also discussed. Author

N91-23052*# National Aeronautics and Space Administration. Ames Research Center, Moffett Field, CA.
LIGHTWEIGHT, FIRE-RETARDANT, CRASHWORTHY AIRCRAFT SEAT CUSHIONING
LEONARD A. HASLIM and PAUL T. MCDONOUGH *In* National Aeronautics and Space Administration, Technology 2000, Volume 1 p 254-259 Mar. 1991
Avail: NTIS HC/MF A18 CSCL 01/3

A two page discussion of non-aerospace seating applications and the design of NASA's safety seat cushioning (SSC) is presented. The SSC was designed for both safety and comfort in order to replace polyurethane cushioning which is flammable and produces lethal fumes upon combustion. The SSC is composed of advanced fabric reinforced composites and is lightweight, fire-retardent, and crashworthy. The seat design consists of central elliptical tubular spring supports made of fire-resistant and fatigue-durable composites surrounded by a fire-blocking sheath. The cushioning is made crashworthy by incorporating energy-absorbing, viscoelastic layers between the nested, elliptical-hoop springs. The design is intended to provide comfortable seating that meets aircraft-loading requirements without using the conventional polyurethane materials. The designs of an aircraft seat and structural components of the SSC are also presented. K.S.

04

AIRCRAFT COMMUNICATIONS AND NAVIGATION

Includes digital and voice communication with aircraft; air navigation systems (satellite and ground based); and air traffic control.

A91-33607#
THE LORAN EARLY IMPLEMENTATION PROJECT - GATEWAY FOR GPS
GEORGE H. QUINN (FAA, Washington, DC), FRANKLIN D. MACKENZIE, and IAN G. MCWILLIAMS (DOT, Transportation Systems Center, Cambridge, MA) IN: IEEE PLANS '90 - Position Location and Navigation Symposium, Las Vegas, NV, Mar. 20-23, 1990, Record. New York, Institute of Electrical and Electronics Engineers, Inc., 1990, p. 44-51. refs

The Early Implementation Project (EIP) was the initial step in the process of loran integration into the National Airspace System (NAS). The EIP was designed to give the FAA and the loran user community experience in the operation use of loran. The experience gained in the EIP has helped the FAA make the transition from the limited project to the fully operational system with airports distributed around the country with general users operating with TSO standard receivers. In addition, the EIP serves as a model for the introduction of the Global Positioning System (GPS) into the NAS during the 1990s. It is recommended that the FAA/NASAO Loran Working Group be expanded to include technical expertise from the GPS area. This group would guide a requirements study for a mutually supportive system. The development of a comprehensive plan for the navigation system for the 21st century is also recommended. I.E.

A91-33608
THE COMPRESSED AERONAUTICAL CHART DATABASE - SUPPORT OF NAVAL AIRCRAFT'S DIGITAL MOVING MAP SYSTEMS
MAURA C. LOHRENZ, PERRY B. WISCHOW, HENRY ROSCHE,

III, MICHAEL E. TRENCHARD (U.S. Navy, Naval Oceanographic and Atmospheric Research Laboratory, Bay Saint Louis, MS), and LANCELOT M. RIEDLINGER (Planing Systems, Inc., Slidell, LA) IN: IEEE PLANS '90 - Position Location and Navigation Symposium, Las Vegas, NV, Mar. 20-23, 1990, Record. New York, Institute of Electrical and Electronics Engineers, Inc., 1990, p. 67-73. U.S. Navy-sponsored research. refs
Copyright

Recent movement toward the electronic display of aeronautical charts for mission planning and navigation in military aircraft is discussed. With the installation of the Digital Moving Map System (DMS) in the AV-8B Harrier, the US Navy has taken the first step toward the widespread use of electronic navigational charts in its aircraft. In order to maximize the benefits from these systems, a new map image database has been specifically designed to meet the requirements of the DMS. The Naval Oceanographic Laboratory and Atmospheric Research Laboratory (NOARL) is creating a compressed aeronautical chart database by compressing and transforming scanner chart data into a format that is compatible with the aircraft DMS. Image compression techniques have been chosen to allow rapid decompression and display while maximizing image quality. I.E.

A91-33614
A VEHICLE LOCATION SYSTEM (VLS) SOLUTION APPROACH
J. BROOKS CHADWICK and J. L. BRICKER (Hughes Aircraft Co., Ground Systems Group, Fullerton, CA) IN: IEEE PLANS '90 - Position Location and Navigation Symposium, Las Vegas, NV, Mar. 20-23, 1990, Record. New York, Institute of Electrical and Electronics Engineers, Inc., 1990, p. 127-132.
Copyright

The Hughes vehicle location system (VLS), which locates and tracks one or more asynchronous aperiodic transmitters in either two or three dimensions, is described. It uses a dynamic receiver time-of-arrival (TOA) source selection, a direct hyperbolic position location solution, and an observation noise filter. For tracking a transmitter in two dimensions in an overdetermined system, hyperbolic geometric-dilution-of-precision (GDOP) is used to select an optimum subset of TOA triplets and to form a weighted position estimate. Particular emphasis is placed on the 2-D direct solution approach. The effect of observation noise on position estimation error in 2-D for an overdetermined system is demonstrated, and the derivation of the 2-D direct solution approach is presented. I.E.

A91-33616
STAND-ALONE VS. EMBEDDED GPS USER EQUIPMENT - THE EXPLORATION OF NEW STANDARDS
STAN GOLDSTEIN (ITT Avionics, Nutley, NJ) IN: IEEE PLANS '90 - Position Location and Navigation Symposium, Las Vegas, NV, Mar. 20-23, 1990, Record. New York, Institute of Electrical and Electronics Engineers, Inc., 1990, p. 139-142.
Copyright

Configurations of a stand-alone receiver chassis and embedded receiver module sets to meet the diversity of high-performance GPS (Global Positioning System) applications are addressed. The ITT design approach is shown to meet these applications. Specifically, the current ITT 3/8 ATR short-short (PPS-capable) production receiver is available in a 230-in2 volume to meet stand-alone receiver chassis requirements. An embedded GPS receiver (PPS-capable) consisting of individual modules from 9052 receiver requiring only 82 in3 is also described. Technology insertion is described for the 3/8 ATR stand-alone receiver as a cost reduction and reliability preplanned product improvement. Technology insertion is also described for embedded configurations resulting in a single SEM-E GPS receiver (PPS-capable) module standard requiring only 23 in3. I.E.

A91-33622
ASHTECH XII GPS TECHNOLOGY
JAVAD ASHJAEE (Ashtech, Inc., Sunnyvale, CA) IN: IEEE PLANS '90 - Position Location and Navigation Symposium, Las Vegas, NV, Mar. 20-23, 1990, Record. New York, Institute of Electrical and Electronics Engineers, Inc., 1990, p. 184-190.
Copyright

Several enhancements of GPS (Global Positioning System) technology are presented, including new data processing algorithms, enhanced application techniques, more hardware capabilities, and reduction in size and power consumption. The use of Doppler measurements for instantaneous (every one second) stationary position fixes is introduced. This technique has the potential of reducing the effect of selective availability in static point positioning. It is shown that the combination of Doppler and code phase measurements can provide two-dimensional deterministic static position fixes (and time) with only two satellites. It also can provide three-dimensional position fixes (and time) with three satellites. The proposed techniques expand the usage of GPS in areas with low satellite visibility and in the interim period while the GPS satellite constellation is not complete. The notion of multiple ramp smoothing of code phase with integrated Doppler is introduced. The results of implementation of this technique in Ashtech XII receivers for real-time differential GPS is given. Minimizing the errors in the use of GPS for aerial photogrammetry applications is discussed. A new technique implemented in Ashtech XII GPS is presented. A new generation of GPS receiver (Ashtech M-XII) is introduced. It is capable of performing precision survey, navigation, and time transfer. The new 12-channel receiver uses a higher level of hardware integration. The results of Ashtech XII dual frequency receivers on the FGCC (Federal Geodetic Control Committee) test network are presented. I.E.

A91-33623
COTS GPS C/A-CODE RECEIVERS WITH PSEUDOLITES FOR RANGE PLS APPLICATION
BARRY A. STEIN and WAI L. TSANG (Science Applications International Corp., McLean, VA) IN: IEEE PLANS '90 - Position Location and Navigation Symposium, Las Vegas, NV, Mar. 20-23, 1990, Record. New York, Institute of Electrical and Electronics Engineers, Inc., 1990, p. 191-197. refs
Copyright

The authors evaluate the concept of a GPS-instrumented PLS (position location system) solution using commercial off-the-shelf (COTS) GPS (Global Positioning System) equipment. Benefits of the solution include cost savings, nonexisting security issues, smaller size, reduced weight, and less consumed power. The COTS GPS-instrumented PLS derives its accurate positioning location by employing pseudolites for broadcast of differential corrections to players within their localized coverage areas. The pseudolite also provides for an added source of ranging information to enhance GPS system coverage and availability. Blockage and physical effects are modeled in the evaluation of the connectivity among range players supplemented with pseudolites. It is shown that COTS GPS equipment could meet the PLS size, weight, and power requirements, as well as accurate positioning specifications with differential GPS operation using pseudolites. A cost/performance tradeoff supports the viability and applicability of this solution. I.E.

A91-33624
A FIVE CHANNEL LOW COST GPS RECEIVER
LEE E. ESTES and GILBERT FAIN (Southeastern Massachusetts University, North Dartmouth, MA) IN: IEEE PLANS '90 - Position Location and Navigation Symposium, Las Vegas, NV, Mar. 20-23, 1990, Record. New York, Institute of Electrical and Electronics Engineers, Inc., 1990, p. 198-204. Research supported by Massachusetts Centers of Excellence Corp.
Copyright

A progress report on a program to develop a low-cost GPS (Global Positioning System) receiver for marine applications is presented. The unit described is a highly digital, mostly one bit, software intensive receiver. The unit uses one RF mixer to baseband, a one-bit 2-MHz A/D (analog-to-digital converter), and five digital parallel signal processing channels. An AMLE (approximate maximum likelihood estimator) technique is used to

acquire signals, and low dynamic loops are used for tracking. General principles guiding the design and a description of the receiver are given. I.E.

A91-33626
TEST PROGRAM FOR HONEYWELL/DND HELICOPTER INTEGRATED NAVIGATION SYSTEM (HINS)
JAN ZYWIEL, CHRIS WEBB (Honeywell, Ltd., Advanced Technology Centre, Markham, Canada), and HARVEY RUSSELL (DND, Ottawa, Canada) IN: IEEE PLANS '90 - Position Location and Navigation Symposium, Las Vegas, NV, Mar. 20-23, 1990, Record. New York, Institute of Electrical and Electronics Engineers, Inc., 1990, p. 212-218.
Copyright

The advanced development model (ADM) for the Helicopter Integrated Navigation System (HINS) is being built for the Canadian Department of National Defence and is currently undergoing developmental testing at the Honeywell Advanced Technology Centre (ATC). The system blends the complementary strengths of its components sensors, resulting in fast alignment and optimum navigation accuracy. A failure detection isolation and reconfiguration functionality monitors sensor health, identifies failed components, and automatically reconfigures the system to optimally integrate the remaining components, thus providing a graceful degradation of performance in the event of a sensor failure. Both the test program approach and the test results to date are discussed. The testing has given the HINS team a high degree of confidence in the navigation system design and in the software that implements the sensor blending algorithms in the real-time system. I.E.

A91-33628
INS RESET REMOVAL FOR ENHANCED POST-FLIGHT PERFORMANCE ANALYSIS
JOHN S. A. HEPBURN, JAN Z. ZYWIEL, and D. BLAKE REID (Honeywell, Ltd., Advanced Technology Centre, Markham, Canada) IN: IEEE PLANS '90 - Position Location and Navigation Symposium, Las Vegas, NV, Mar. 20-23, 1990, Record. New York, Institute of Electrical and Electronics Engineers, Inc., 1990, p. 226-230. refs
Copyright

High-performance integrated inertial navigation systems (INSs) use a Kalman filter to compute the optimal navigation solution from the data provided by an INS and various navigation aids such as GPS (Global Positioning System) and Doppler. The error estimates of the Kalman filter are used to reset the INS when the navigation system operates in feedback mode. A reset removal procedure (RRP) has been developed for recovering, during postflight processing, a high-fidelity approximation to the unaided pure inertial navigation solution that would have been produced by the INS had it not been operated in feedback mode. The procedure is of great value in carrying out a performance evaluation of an integrated INS because it effectively broadens the scope and extent of actual physical flight trials. The RRP is described and discussed, and simulation results are presented to illustrate its behavior. The RRP will be applied to real data collected during flight trials of the Helicopter Inertial Navigation System (HINS), which is currently under development for the Canadian Department of National Defence. I.E.

A91-33630
A FAST AND LOW-COST VALIDATION TECHNIQUE FOR ILS AND MLS
P. R. MAHAPATRA (Indian Institute of Science, Bangalore, India) and M. M. POULOSE (Telecommunications Research Centre, Bangalore, India) IN: IEEE PLANS '90 - Position Location and Navigation Symposium, Las Vegas, NV, Mar. 20-23, 1990, Record. New York, Institute of Electrical and Electronics Engineers, Inc., 1990, p. 240-246. refs
Copyright

A feasibility study of evaluating site effects on ILS (instrument landing system) and MLS (microwave landing system) using analytical and computational techniques is presented. The problem of site effect evaluation is divided into three stages: terrain modeling, ray tracing, and field evaluation. Innovative techniques are introduced at each stage to make the model versatile enough to handle most general terrain contours and surface conditions and also reduce computational requirements to a minimum. The result is a scheme that can be used to evaluate most terrain types on a mini/microcomputer. Specifically, it is shown that, using a simple two-dimensional multiwedge model of the terrain (i.e., no variation of terrain height in the third dimension), it is possible to obtain accurate estimates of the glideslope parameters by simulating procedures similar to those specified by ICAO (the International Civil Aviation Organization). The computational results have been visualized by comparison with actual data from flight tests. A summary of results for actual sites is presented. I.E.

A91-33631
EVALUATION OF CONTROLLER TOOLS FOR CONDUCTING MLS CURVED APPROACHES TO NEW YORK'S JFK AIRPORT
A. SMITH, C. SHIVELY, R. TARAKAN, G. DORFMAN, and K. MARKIN (Mitre Corp., McLean, VA) IN: IEEE PLANS '90 - Position Location and Navigation Symposium, Las Vegas, NV, Mar. 20-23, 1990, Record. New York, Institute of Electrical and Electronics Engineers, Inc., 1990, p. 247-254. refs
Copyright

The authors describe the simulation and evaluation of an automation aid for helping air traffic controllers deal with aircraft that might fly MLS (microwave landing system) curved approaches to John F. Kennedy International Airport (JFK) in New York. In the scenario studied, aircraft with appropriate MLS equipment would fly a curved approach to JFK's runway 13R, while other aircraft would fly the currently used straight-in ILS (instrument landing system) approach to parallel runway 13L. To deal with the possible case of an MLS aircraft that blunders toward the ILS path, this scenario requires controllers to maintain an appropriate stagger between aircraft on the two approaches. The automation aid being investigated is a projected image of the controller's display. Controllers from the New York Terminal Radar Approach Control Facility have participated in simulated traffic scenarios to evaluate this aid. This work is currently in progress, and initial observations are given. I.E.

A91-33632#
PROSPECTS FOR REDUCTION OF SEPARATION STANDARDS IN OCEANIC AIRSPACES WITH SATELLITE SERVICES
DALE A. LIVINGSTON (FAA, Technical Center, Washington, DC) IN: IEEE PLANS '90 - Position Location and Navigation Symposium, Las Vegas, NV, Mar. 20-23, 1990, Record. New York, Institute of Electrical and Electronics Engineers, Inc., 1990, p. 255-261.

How satellites will influence the ATC (air traffic control) system of the future is examined from the control system perspective. It is maintained that, in a future environment, where significantly improved safety margins will be required, ADS (automatic dependent surveillance), by itself, will not permit substantial reductions in lateral separation. Likewise, satellite-based navigation systems will not, by themselves, lead to a greatly improved ATC system because if large errors persist at their current rate, improvements in nominal accuracy will not overcome their effect on the overall rate of collisions. It is concluded that only when satellites are integrated into a control system that uses their ability to furnish highly accurate positional data and frequent surveillance updates will they permit anticipated traffic increases while reducing the risk of collision enough to allow separation reductions. I.E.

A91-33633#
APPLYING KINEMATIC GPS TECHNIQUES AT OUR NATION'S AIRPORTS
BENJAMIN REMONDI, W. (NOAA, National Geodetic Survey, Rockville, MD) IN: IEEE PLANS '90 - Position Location and Navigation Symposium, Las Vegas, NV, Mar. 20-23, 1990, Record. New York, Institute of Electrical and Electronics Engineers, Inc., 1990, p. 262-266. refs

The National Geodetic Survey (NGS) began surveying US airports using a mixture of static, kinematic, antenna swap, and

pseudokinematic techniques. The methodologies and the associated theoretical rationale are described. The NGS performed an online operational test of GPS (Global Positioning System) kinematic surveying at several Florida airports, and it was found to be a complete success. All successful processing variations in the Apalachicola example agreed at the 1-cm level. I.E.

A91-33636
AREA NAVIGATION CAPABILITY IN A MINIATURE AIRBORNE GPS RECEIVER
VERLYN MOEN and REDGE BARTHOLOMEW (Rockwell International Corp., Collins Government Avionics Div., Cedar Rapids, IA) IN: IEEE PLANS '90 - Position Location and Navigation Symposium, Las Vegas, NV, Mar. 20-23, 1990, Record. New York, Institute of Electrical and Electronics Engineers, Inc., 1990, p. 293-302. refs
Copyright

The area navigation (RNAV) capabilities of the Collins five-channel miniaturized airborne GPS (Global Positioning System) receiver (less than 3/8 ATR) are discussed. These capabilities include the computation of radial navigation parameters, standard air data retrieval functions, warnings with respect to preplanned flight events, and flight data storage and editing functions. Great circuit routes can be defined, deviation parameters can be computed, and station declinations can be stored (as magvar) with waypoints, allowing pilots to fly VOR/VORTAC radials. The vector approach allows the accuracy of the GPS navigation solution to be propagated into RNAV data. These functional and performance capabilities will provide an approach to compliance with the Federal Radionavigation Plan. I.E.

A91-33644
ULISS G, A FULLY INTEGRATED 'ALL-IN-ONE' AND 'ALL-IN-VIEW' INERTIA-GPS UNIT
L. CAMBERLEIN and B. CAPIT (Societe d'Applications Generales d'Electricite et de Mecanique, Paris, France) IN: IEEE PLANS '90 - Position Location and Navigation Symposium, Las Vegas, NV, Mar. 20-23, 1990, Record. New York, Institute of Electrical and Electronics Engineers, Inc., 1990, p. 399-406. refs
Copyright

An eight-channel GPS (Global Positioning System) receiver (500 cm3, 0.5 kg, 9 W) has been physically embedded into an existing Uliss inertial system, resulting in a small, light, all-in-one, all-in-view unit functionally optimized through tight coupling of GPS and INS (inertial navigation system) for performance and robustness. Flight tests have been conducted on a Mirage III at the French Official Flight Test Center of Bretigny, and excellent performance has been demonstrated. I.E.

A91-33645
FLIGHT TEST RESULTS OF A TIGHTLY INTEGRATED RLG-BASED GLOBAL POSITIONING SYSTEM/INERTIAL NAVIGATION SYSTEM
MICHAEL F. LYNCH and DONALD J. WEBER (Kearfott Guidance and Navigation Corp., Wayne, NJ) IN: IEEE PLANS '90 - Position Location and Navigation Symposium, Las Vegas, NV, Mar. 20-23, 1990, Record. New York, Institute of Electrical and Electronics Engineers, Inc., 1990, p. 421-428.
Copyright

Development of a tightly integrated Global Positioning System/inertial navigation system (GPS/INS) is being pursued following the development of a miniaturized GPS receiver and a compact multiaxis ring laser gyro. The flight test program is reviewed, and the results are discussed in detail. The flight test results showed the excellent performance capabilities of the GPS/INS integrated configuration. In a region of nonoptimum satellite geometry, the unit performed very close to the planned accuracy levels. It is noted that, for both test flights, satellite geometry was, at best, not optimum and the aircraft landed in a period of very poor satellite geometry. However, the terminal performance of the integrated system was not degraded and demonstrated GPS-quality performance, with INS and air data computer providing the altitude information unavailable due to poor satellite geometry. Evaluation of the integrated GPS/INS by independent agencies and further planned enhancements to the system's performance are presented. I.E.

A91-33646
THE DESIGN, SIMULATION AND IMPLEMENTATION OF AN ACCURATE POSITIONING SYSTEM FOR AUTOMATIC FLIGHT INSPECTION
BRUNO M. SCHERZINGER (Honeywell, Ltd., Advanced Technology Centre, Markham, Canada) and CECELIA M. FEIT (LTV Corp., Sierra Research Div., Buffalo, NY) IN: IEEE PLANS '90 - Position Location and Navigation Symposium, Las Vegas, NV, Mar. 20-23, 1990, Record. New York, Institute of Electrical and Electronics Engineers, Inc., 1990, p. 444-451. refs
Copyright

The design and simulation of the integrated navigation algorithms of the C-29A automatic flight inspection system (AFIS) are presented. The automatic flight inspection design problem is one of determining the inspecting aircraft's position with respect to the threshold of the runway independently of the ILS (instrument landing system) beam being inspected. The C-29A design is a unique application of the integrated navigation concept, in which the aircraft position is computed by an aided inertial navigation solution where the primary aiding measurements are the aircraft position at the runway threshold and end, each occurring once per inspection pass. A UD-factorized Kalman filter estimates the navigation errors, and a modified Bryson-Frazier smoother improves these estimates to provide the best estimate of aircraft position for calibration of the ILS beam. Results indicate that the errors occurring in the runway referenced position estimates can be controlled quite well. Moreover, the limited measurements available are sufficient to calibrate some sensor errors. The key component to achieving a specified accuracy (e.g., CAT I, II, or III position error) is the PPS (precision position subsystem), in that the AFIS basically inherits the PPS errors. I.E.

A91-33647
IMPACT OF NAVIGATION ACCURACY ON THE INTERVENTION RATE IN A HIGHLY AUTOMATED AIR TRAFFIC CONTROL SYSTEM
MARK J. ROCKMAN and RONALD BRAFF (Mitre Corp., McLean, VA) IN: IEEE PLANS '90 - Position Location and Navigation Symposium, Las Vegas, NV, Mar. 20-23, 1990, Record. New York, Institute of Electrical and Electronics Engineers, Inc., 1990, p. 452-456.
Copyright

Progress in navigation technology is expected to bring about a lower air traffic control (ATC) intervention rate than the rate that could be expected based upon today's navigation and flight control capabilities. The extent to which this may occur is quantified, and additional possible benefits, such as increasing air traffic throughput and intervening earlier in potential loss of separation between aircraft, are discussed. A prototypic aircraft-aircraft encounter is defined. It includes a simple intervention-decision rule which attempts to capture the prudence practiced by today's air traffic controllers, and which typifies one type of decision rule presently under consideration for use in a future automated ATC system such as AERA 3. This rule is applied to an operational environment where GPS (Global Positioning System) is employed to navigate user-preferred routes. I.E.

A91-33649
ISS - A COMBINED TERRAIN TOPOGRAPHY REFERENCED NAVIGATION SYSTEM
PETER LUX and MAX EIBERT (Dornier Luftfahrt GmbH, Friedrichshafen, Federal Republic of Germany) IN: IEEE PLANS '90 - Position Location and Navigation Symposium, Las Vegas, NV, Mar. 20-23, 1990, Record. New York, Institute of Electrical and Electronics Engineers, Inc., 1990, p. 470-473.
Copyright

The ISS system was developed for navigation update based on knowledge of feature availability and range data constancy. The ISS consists basically of a laser radar sensor, a data processing

unit, and the real-time capability to determine position through comparison of laser radar information with suitable reference information. A Kalman filter provides a link to the inertial navigation system (INS). This filter connects the continually available update information with the INS measurement values to estimate position, speed, and attitude. The ISS development program was initiated with algorithm development, commencing with fundamental investigations on mathematical procedures which led to laboratory computer experiments, via microprocessor realization for helicopter flight trials. Once development and testing are completed, the requirements will have been met for offering this system for the demonstration phase of the Modular Standoff Weapon and also for the planned midlife improvement of Tornado. I.E.

A91-33651
TERRAIN REFERENCED NAVIGATION
NEIL PRIESTLEY (Ferranti International, PLC, Cheadle and Gatley, England) IN: IEEE PLANS '90 - Position Location and Navigation Symposium, Las Vegas, NV, Mar. 20-23, 1990, Record. New York, Institute of Electrical and Electronics Engineers, Inc., 1990, p. 482-489.
Copyright

An attempt is made to provide airframe manufacturers and system integrators with an overview of terrain referenced navigation, with particular emphasis on the principle of operation, the types of sensors, and correlation processes in use. The optimization of the sensors for terrain referenced navigation is discussed, and terrain referenced navigation is compared with the Global Positioning System (GPS). It is noted that applications of terrain referenced navigation in conjunction with the database are perhaps more important than the improved navigation accuracy. How each of these applications is implemented and the hardware implications are detailed. The three-dimensional accurate position and the database can be used for other functions such as terrain following and intelligent ground proximity warning. I.E.

A91-33652
PRECISION AIDED INERTIAL NAVIGATION USING SAR AND DIGITAL MAP DATA
JAMES E. BEVINGTON and CHARLES A. MARTTILA (Honeywell Systems and Research Center, Minneapolis, MN) IN: IEEE PLANS '90 - Position Location and Navigation Symposium, Las Vegas, NV, Mar. 20-23, 1990, Record. New York, Institute of Electrical and Electronics Engineers, Inc., 1990, p. 490-496.
Copyright

The authors describe a novel scheme for obtaining position update information for an inertial navigation system through the use of imagery from a synthetic aperture radar (SAR) sensor and an onboard digital map database. Updated information is obtained through comparison of the locations of terrain features extracted from the SAR imagery with locations predicted using the digital map and current navigation estimates. The authors also discuss the overall system concept along with experimental and analytical results obtained to date. Analytical results include a preliminary error analysis which treats SAR image distortions introduced through navigation errors and the consequent effects on update accuracies. A description of the terrain feature extraction algorithms is presented along with experimental results. I.E.

A91-33653
GLOBAL POSITIONING SYSTEM (GPS) AUTONOMOUS NAVIGATION
M. P. ANANDA, H. BERNSTEIN, K. E. CUNNINGHAM, W. A. FEESS, and E. G. STROUD (Aerospace Corp., El Segundo, CA) IN: IEEE PLANS '90 - Position Location and Navigation Symposium, Las Vegas, NV, Mar. 20-23, 1990, Record. New York, Institute of Electrical and Electronics Engineers, Inc., 1990, p. 497-508. refs
Copyright

A system description, a discussion of design issues, and performance results obtained from the Aerospace Corporation simulation of the GPS autonomous navigation system (ANS) concept are given. Analysis methods, physical models, and pertinent equations are presented. Measurement data are realistically simulated and include the effects of all known environmental and hardware phenomena affecting performance. Performance under nominal and anomalous conditions (satellite failures) and in nuclear environments is described. Unobservable errors which degrade performance are discussed. Preliminary studies show that the full constellation system is measurement rich. A simple scheme such as rejecting low signal-to-noise ratio or high delay measurements will probably be a satisfactory design response to distortion due to scintillation in the enhanced environment. I.E.

A91-33660
IMPROVED LANDING AID AVAILABILITY THROUGH THE USE OF NEW CRITERIA
RICHARD H. MCFARLAND (Ohio University, Athens) IN: IEEE PLANS '90 - Position Location and Navigation Symposium, Las Vegas, NV, Mar. 20-23, 1990, Record. New York, Institute of Electrical and Electronics Engineers, Inc., 1990, p. 574-578. refs
Copyright

A relatively new approach and concept that are being used to qualify the ILS (instrument landing system) glide slope for operational use are presented. It is argued that greater availability of ILS components means a higher level of safety. A proposal is also presented for consideration of a new standard which will also allow for still greater availability. This relates to lateral coverage requirements for glide slopes. It is concluded that, with new criteria, greater availability is present, improved standards are in place, and the public is better served, not only with greater safety, but also with increased reliability of air travel schedules. I.E.

A91-33661
KINEMATIC GPS - RESOLVING INTEGER AMBIGUITIES ON THE FLY
PATRICK Y. C. HWANG (Rockwell International Corp., Avionics Group, Cedar Rapids, IA) IN: IEEE PLANS '90 - Position Location and Navigation Symposium, Las Vegas, NV, Mar. 20-23, 1990, Record. New York, Institute of Electrical and Electronics Engineers, Inc., 1990, p. 579-586.
Copyright

In kinematic GPS (Global Positioning System), the initial integer ambiguity must be resolved either by a static survey over time or by instant calibration with a known baseline or an antenna exchange. It is pointed out that, while these standard methods require maintaining a baseline strategy to an earth-fixed reference frame during the initialization, there are situations when at least one of the receivers may be constantly in motion. Two ideas are proposed for adapting standard kinematic techniques to situations that do not naturally allow for the constraint of a fixed baseline. The first calls for extracting the information needed to resolve the integer ambiguity from the data collected while the kinematic survey is in progress. The second addresses the use of the antenna exchange technique for mobile platforms where the original locations of the antennas are not likely to remain stationary during the physical exchange. Both ideas count on information from additional measurements to augment their respective measurement models. I.E.

A91-33663
TERRAIN AIDED NAVIGATION - CURRENT STATUS, TECHNIQUES FOR FLAT TERRAIN AND REFERENCE DATA REQUIREMENTS
A. J. HENLEY (GEC Avionics, Ltd., Rochester, England) IN: IEEE PLANS '90 - Position Location and Navigation Symposium, Las Vegas, NV, Mar. 20-23, 1990, Record. New York, Institute of Electrical and Electronics Engineers, Inc., 1990, p. 608-615. refs
Copyright

It is pointed out that terrain referenced navigation (TRN) techniques are now well established as effective position-fixing systems suitable for use in manned and unmanned vehicles. The SPARTAN TRN technique, which has been selected for the UK Toronado GR4 update, provides accurate navigation with rapid initial capture without recourse to an initialization mode. An overview of the SPARTAN technique is provided, and techniques for

improving navigation performance over very flat terrain are described. The benefits of the terrain characteristic matching techniques are outlined, and a summary of integrated navigation system performance is given. Terrain-aided systems require appropriate reference databases. The availability of the data and its suitability are discussed. The need for careful consideration of database quality and registration when terrain aided systems are being designed is indicated. I.E.

A91-33664
HELI/SITAN - A TERRAIN REFERENCED NAVIGATION ALGORITHM FOR HELICOPTERS
JEFF HOLLOWELL (Sandia National Laboratories, Albuquerque, NM) IN: IEEE PLANS '90 - Position Location and Navigation Symposium, Las Vegas, NV, Mar. 20-23, 1990, Record. New York, Institute of Electrical and Electronics Engineers, Inc., 1990, p. 616-625. U.S. Army-supported research. Previously announced in STAR as N90-19217. refs
(Contract DE-AC04-76DP-00789)
Copyright

Heli/SITAN is a Terrain Referenced Navigation (TRN) algorithm that utilizes radar altimeter ground clearance measurements in combination with a conventional navigation system and a stored digital terrain elevation map to accurately estimate a helicopter's position. Multiple Model Adaptive Estimation (MMAE) techniques are employed using a bank of single state Kalman filters to ensure that reliable position estimates are obtained even in the face of large initial position errors. A real-time implementation of the algorithm was tested aboard a U.S. Army UH-1 helicopter equipped with a Singer-Kearfott Doppler Velocity Sensor (DVS) and a Litton LR-80 strapdown Attitude and Heading Reference Sensor (AHRS). The median radial error of the position fixes provided in real-time by this implementation was less than 50 m for a variety of mission profiles. Author

A91-33665
OMEGA SIGNAL COVERAGE PREDICTION IN THE 1990'S
R. S. WARREN, P. B. MORRIS, K. A. TENCH, and R. R. GUPTA (Analytic Sciences Corp., Reading, MA) IN: IEEE PLANS '90 - Position Location and Navigation Symposium, Las Vegas, NV, Mar. 20-23, 1990, Record. New York, Institute of Electrical and Electronics Engineers, Inc., 1990, p. 626-633. refs
Copyright

The evolution of Omega signal coverage portrayal is briefly traced from the early compilation of hard copy world maps to the current electronic format with emphasis on the display medium rather than the scientific bases of signal coverage. The outlook for Omega signal coverage displays in the 1990s is examined on the basis of projections of current technology and user requirements. Future coverage displays are expected to do more than indicate the available station signals at a selected geographic location: Omega coverage displays of the 1990s are likely to include increased time resolution, attainable position accuracy, probability of station signal outage (due to station off-air, local noise spikes, or propagation effects), and coverage during anomalous ionospheric events. I.E.

A91-33666
THE MISSING (DATA) LINK IN PILOT NAVIGATION
MALCOLM L. RITCHIE (Midwest Systems Research, Inc., Dayton, OH) IN: IEEE PLANS '90 - Position Location and Navigation Symposium, Las Vegas, NV, Mar. 20-23, 1990, Record. New York, Institute of Electrical and Electronics Engineers, Inc., 1990, p. 634-637. FAA-supported research.
Copyright

It is noted that some aircraft accidents have occurred for lack of vital information which was somewhere in the National Airspace System but not available to the pilots and the air traffic controllers in time and in the right form. It is suggested that the mode S radar has the potential of closing the system loop to allow all parties to have the information needed at the time needed. Most of the required elements are already becoming a part of the system design. The missing link to the system design lies within the data link cockpit interface. It is shown that a smart data link can be achieved by adding to the MOPS for the airborne system (1) data storage and (2) an interface to the aircraft's own systems. I.E.

A91-33667
VLS - A DTOA SYSTEM FOR POSITION LOCATION
W. E. SAGEY and W. R. FRIED (Hughes Aircraft Co., Fullerton, CA) IN: IEEE PLANS '90 - Position Location and Navigation Symposium, Las Vegas, NV, Mar. 20-23, 1990, Record. New York, Institute of Electrical and Electronics Engineers, Inc., 1990, p. 645-649. refs
Copyright

A vehicle location system (VLS) is described. It is a derivative of the military position location and reporting system and offers higher accuracies with the lowest vehicle electronics cost of all comparable systems. The original design concept envisioned a satellite-based implementation in the radio determination satellite service (RDSS) band at 1.6 GHz for the location of surface vehicles on a nationwide basis. A second version of the system has evolved which is suitable for the tracking of aircraft to accuracies of 30 m in areas of interest and achieves those accuracies through the use of auxiliary ground enhancement stations. Most recently, terrestrial adaptations utilizing the cellular telephone infrastructure are in the exploratory phase. Experimental systems suitable for local area coverage, such as military range instrumentation, have reached the field evaluation engineering model stage. Some preliminary field-test results are presented. It is shown that, for VLS applications requiring land vehicle coverage over the entire continental US, a three-geostationary-satellite configuration is clearly preferable. For applications requiring land vehicle coverage in a limited geographic area, excellent accuracy can be obtained without the use of satellites. For applications requiring good 3-D accuracy, such as aircraft surveillance, a configuration using two or more geostationary satellites in combination with suitably placed ground stations is found to be optimum. I.E.

A91-33775
OCEANIC CLEARANCE TRIAL PROVES UTILITY OF DATA LINK COMMUNICATIONS FOR ATC
GRAHAM LAKE (Societe Internationale de Telecommunications Aeronautiques, Paris, France) ICAO Journal (ISSN 0018-8778), vol. 45, Dec. 1990, p. 8-10.
Copyright

Notwithstanding delays in the implementation of the Airborne Communications Addressing and Reporting System (ACARS), nearly 3000 aircraft are currently using VHF data links of ACARS type throughout the world. One aspect of such data links which has been developed more slowly than initially envisioned in 1988 is ACARS avionics implementation by airlines, due primarily to vendor delays in the delivery of onboard software. Nevertheless, all new aircraft are now being delivered with ACARS capability. Current and planned developments in data linkage will achieve transparency between the various media, namely VHF, communications satellites, and Mode S. O.C.

A91-33868
NONLINEAR FILTERING OF A TRAJECTORY MESSAGE [NELINEINAIA FIL'TRATSIIA TRAEKTORNOGO SOOBSHCHENIIA]
A. I. VELICHKIN and A. N. DETKOV Radiotekhnika (ISSN 0033-8486), Sept. 1990, p. 3-7. In Russian. refs
Copyright

The Markov theory of nonlinear filtering is used to synthesize a filter that is optimal according to the minimum rms error of the estimation of the trajectory message of a flight vehicle. The filter is assumed to be digital, and the observation noise is assumed to be colored. B.J.

A91-34011
TRANSMIT/RECEIVE MODULE TECHNOLOGY FOR X-BAND ACTIVE ARRAY RADAR
DAVID N. MCQUIDDY, JR., JAMES S. MASON, JOHN M. BEDINGER (Texas Instruments, Inc., Dallas), RONALD L.

GASSNER, and WILLIAM P. HULL (Texas Instruments, Inc., Plano) IEEE, Proceedings (ISSN 0018-9219), vol. 79, March 1991, p. 308-341. refs
Copyright

Phased array radar system developments using X-band transmit/receive (T/R) module technology are summarized. Requirements are developed from systems concepts for fighter aircraft radar applications. Factors influencing system performance are discussed in terms of the allowable tradeoffs, that must be considered for deployable systems. T/R module architectures are investigated in light of the system derived performance requirements. These module requirements are reduced to the individual circuit function level, and examples of circuits developed to meet these requirements are presented. Critical T/R module technologies are discussed in view of the latest developments in microwave active and control devices, manufacturing assembly processes and equipment, package materials and fabrication processes, and test automation. Module developments during the past 25 years are discussed chronologically and described in terms of the performance characteristics attained. I.E.

A91-35902
THE EFFECTS OF SIMULATED ELECTROMAGNETIC PULSE ON COMMERCIAL AIRCRAFT
RODNEY A. PERALA, JAMES R. ELLIOT, and J. D. CURRY (Electro Magnetic Applications, Inc., Lakewood, CO) IEEE Transactions on Electromagnetic Compatibility (ISSN 0018-9375), vol. 33, May 1991, p. 120-131. Research supported by Electro Magnetic Applications, Inc., Sol Telecommunications Services, Inc., and U.S. Army. refs
Copyright

The susceptibility of commercial aircraft to the SEMP (simulated electromagnetic pulse) hazard is evaluated on the basis of the US Army's AESOP (Army EMP simulator operations) simulator. The following issues are addressed: (1) the AESOP environment at various altitudes, (2) coupling to cables within commercial aircraft, (3) known transient safe levels for commercial aircraft, and (4) determination of threshold levels. Data from commercial aircraft indicate that civil aircraft critical systems should not be adversely affected by SEMP levels up to about 15 kV/m. This is based on a limited number of data points, however. There is a much larger military database, and it is found from this that perhaps a factor-of-two margin should be considered to bring the threshold level down to about 8 kV/m. I.E.

A91-36012
ASTRE IMPROVEMENTS EXPAND USEFULNESS OF SURFACE MOVEMENT RADAR
J.-C. CHEVALLIER (Thomson-CSF, Paris, France) ICAO Journal (ISSN 0018-8778), vol. 46, Jan. 1991, p. 16-18.
Copyright

Safety requirements, along with the need for efficient management of ground traffic, demand installation of reliable, high-performance equipment to assist in the control of aircraft movements on the ground. It is also a means of monitoring other vehicles on aprons, runways, taxiways and parking areas. Airport control towers equipped with airfield surface traffic radar equipment (ASTRE) have available one or more displays for approach control, or several displays devoted to ground control assistance. Further enhancements of this system, such as digital scan conversion, new antenna law and solid-state technology are being developed. The radar's high-resolution in range and azimuth, suitable for detection of very small vehicles, is due to a high operating frequency, small angular aperture and very small pulse width. R.E.P.

N91-22100# Federal Aviation Administration, Atlantic City, NJ.
FLIGHT SERVICE AUTOMATION SYSTEM (FSAS) MODEL 1 FULL CAPACITY (M1FC) OPERATIONAL TEST AND EVALUATION (OT/E)/INTEGRATION TEST REPORT
FRANCES MACKUSE, WILLIAM BENNER, and ROBERT F. HAVEL (Alabama Univ., Huntsville.) Apr. 1991 34 p
(DOT/FAA/CT-TN90/45) Avail: NTIS HC/MF A03

The Operational Test and Evaluation (OT&E)/Integration Test of the Flight Service Automation System (FSAS), Model 1 Full Capacity (M1FC) was conducted at the Federal Aviation Administration Technical Center, July 23-27, 1991. The FSAS M1FC consists of three subsystems: the Aviation Weather Processor (AWP); the Flight Service Data Processing System (FSDPS); and the Automated Flight Service Station (AFSS). The purpose of this testing was to verify National Airspace System (NAS) integration requirements of the subsystems and the operational effectiveness of the M1FC in meeting OT&E/integration test requirements. It was concluded that the M1FC system requires corrections and/or modifications to satisfactorily meet integration and operational requirements for effective performance in the NAS environment. Based on these conclusions, it was recommended that the deficiencies be corrected and the M1FC system be successfully retested prior to deployment. Author

N91-22101# Federal Aviation Administration, Atlantic City, NJ. Concepts Analysis Div.
AIR TRAFFIC CONTROL MEMORY: A FIELD SURVEY
Technical Report, Jan. 1990 - Jan. 1991
EARL S. STEIN Mar. 1991 57 p
(DOT/FAA/CT-TN90/60) Avail: NTIS HC/MF A04

This study had two goals. First was the need to evaluate the Controller Memory Handbook using input from current field controllers. The second goal was to gather data from field facilities concerning the impact of memory on the performance of controllers and how they went about trying to manage their memory resources in daily operations. Controllers agreed that memory was an important element in their work. They were able to rate it independently of their evaluation of the Handbook. The majority of the respondents liked the Handbook and saw it as a positive contribution. Most controllers suggested that effective memory management involved practicing what they were taught and using the tools provided in a consistant and conscientious manner. Author

N91-22102*# National Aeronautics and Space Administration. Langley Research Center, Hampton, VA.
TRAFFIC ALERT AND COLLISION AVOIDANCE SYSTEM (TCAS): COCKPIT DISPLAY OF TRAFFIC INFORMATION (CDTI) INVESTIGATION. PHASE 1: FEASIBILITY STUDY
TCAS-CDTI Report, Feb. - Jun. 1990
MALCOLM BURGESS, DEAN DAVIS, WALTER HOLLISTER, and JOHN A. SORENSEN Apr. 1991 92 p Sponsored in part by AF
(Contract F19628-85-C-0002)
(NASA-TM-104956; NAS 1.15:104956; DOT/FAA/RD-91/8)
Avail: NTIS HC/MF A05 CSCL 17/7

The possibility of the Threat Alert and Collision Avoidance System (TCAS) traffic sensor and display being used for meaningful Cockpit Display of Traffic Information (CDTI) applications has resulted in the Federal Aviation Administration initiating a project to establish the technical and operational requirements to realize this potential. Phase 1 of the project is presented here. Phase 1 was organized to define specific CDTI applications for the terminal area, to determine what has already been learned about CDTI technology relevant to these applications, and to define the engineering required to supply the remaining TCAS-CDTI technology for capacity benefit realization. The CDTI applications examined have been limited to those appropriate to the final approach and departure phases of flight. Author

05

AIRCRAFT DESIGN, TESTING AND PERFORMANCE

Includes aircraft simulation technology.

A91-32455
FIN STRUCTURES OF THE AIRBUS FAMILY EXPERIENCE WITH ADVANCED COMPOSITES
DIETER SCHULZ (MBB GmbH, Munich, Federal Republic of Germany) IN: ICCM-VII; Proceedings of the 7th International Conference on Composite Materials, Guangzhou, People's Republic of China, Nov. 22-24, 1989. Vol. 1. Beijing/Oxford, International Academic Publishers/Pergamon Press, 1989, p. 55-66. refs
Copyright

The design features and the dimensioning principles of the rudder and the fin-box structures, made of carbon fiber composites, which were designed for the wide and the narrow versions of Airbus are discussed. Special consideration is given to the qualification of the chosen designs and the selected materials with respect to the static strength, the fatigue strength, the damage tolerance, and the maintenance requirements. Also discussed are the applied manufacturing and quality asssurance principles reflecting the experience with these structures since 1981. I.S.

A91-32646
AEROELASTIC OPTIMUM DESIGN OF COMPOSITE ROTOR BLADE WITH RETURNING WAKE EFFECT
SEUNG JO KIM, HAE KYUNG LEE, and KYO NAM KOO (Seoul National University, Republic of Korea) IN: ICCM-VII; Proceedings of the 7th International Conference on Composite Materials, Guangzhou, People's Republic of China, Nov. 22-24, 1989. Vol. 3. Beijing/Oxford, International Academic Publishers/Pergamon Press, 1989, p. 371-376. refs
Copyright

The optimum design of a helicopter rotor blade made of graphite/epoxy composite material is reported. The blade is modeled as a laminated plate, and ply angles are used as design variables. Natural frequencies and flutter speeds are calculated for various ply angles. A Rayleigh-Ritz formulation is utilized, and four vibration modes involving two bending modes and two torsion modes are assumed. An unsteady incompressible two-dimensional aerodynamic theory using Lowey's function of the returning shed wake is employed, and the computed speeds are compared with those derived from Theodorsen's function. The necessity of taking into account the effect of the returning shed wake for the flutter analysis of rotary wings is emphasized. V.T.

A91-33323
LANGLEY DEVELOPS THERMAL MANAGEMENT CONCEPT FOR HYPERSONIC AIRCRAFT
EDWARD H. PHILLIPS Aviation Week and Space Technology (ISSN 0005-2175), vol. 134, April 15, 1991, p. 41, 47.
Copyright

NASA-Langley has undertaken the development of structure and powerplant active cooling systems for a projected USN carrier-based, turbojet-and-ramjet-powered aircraft capable of Mach 5 cruise at 90,000 ft, with a 1200-n.mi. range. The two-element system involves a primary cooling system that takes advantage of the chemical heat-sink available from the endothermic fuel methylcyclohexane (MCH), which from a volumetric standpoint possesses about 4 times the combustion capability of LH2. The fuel passes through a two-stage heat exchanger/reactor, where it is endothermically converted to hydrogen and toluene. The secondary cooling system concentrates on ramjet surfaces and nozzle areas, and employs the Syltherm 800 coolant fluid in a closed fuel preheater/reactor-heating cycle. O.C.

A91-33527*# California Univ., Los Angeles.
HELICOPTER VIBRATION REDUCTION USING STRUCTURAL OPTIMIZATION WITH AEROELASTIC/MULTIDISCIPLINARY CONSTRAINTS - A SURVEY
PERETZ P. FRIEDMANN (California, University, Los Angeles) Journal of Aircraft (ISSN 0021-8669), vol. 28, Jan. 1991, p. 8-21. refs
(Contract NAG1-833)
Copyright

This paper presents a survey of the state-of-the-art in the field of structural optimization when applied to vibration reduction of helicopters in forward flight with aeroelastic and multidisciplinary constraints. It emphasizes the application of the modern approach where the optimization is formulated as a mathematical programming problem, the objective function consists of the vibration levels at the hub, and behavior constraints are imposed on the blade frequencies and aeroelastic stability margins, as well as on a number of additional ingredients that can have a significant effect on the overall performance and flight mechanics of the helicopter. It is shown that the integrated multidisciplinary optimization of rotorcraft offers the potential for substantial improvements, which can be achieved by careful preliminary design and analysis without requiring additional hardware such as rotor vibration absorbers of isolation systems. Author

A91-33528*# National Aeronautics and Space Administration. Langley Research Center, Hampton, VA.
INTEGRATED MULTIDISCIPLINARY DESIGN OPTIMIZATION OF ROTORCRAFT
HOWARD M. ADELMAN and WAYNE R. MANTAY (NASA, Langley Research Center, Hampton, VA) Journal of Aircraft (ISSN 0021-8669), vol. 28, Jan. 1991, p. 22-28. Previously cited in issue 21, p. 3268, Accession no. A89-49478. refs
Copyright

A91-33529*# Maryland Univ., College Park.
AEROELASTIC OPTIMIZATION OF A HELICOPTER ROTOR USING AN EFFICIENT SENSITIVITY ANALYSIS
JOON W. LIM and INDERJIT CHOPRA (Maryland, University, College Park) Journal of Aircraft (ISSN 0021-8669), vol. 28, Jan. 1991, p. 29-37. Previously cited in issue 11, p. 1613, Accession no. A90-29237. refs
(Contract NAG1-739)
Copyright

A91-33530#
HELICOPTER ROTOR DYNAMICS OPTIMIZATION WITH EXPERIMENTAL VERIFICATION
MARK W. DAVIS and WILLIAM H. WELLER (United Technologies Research Center, East Hartford, CT) Journal of Aircraft (ISSN 0021-8669), vol. 28, Jan. 1991, p. 38-48. refs
Copyright

Improved helicopter blade structural properties are presently attempted by means of an automated design optimization analysis in which modal optimizatiom criteria are defined by a coupled-mode eigenvalue analysis. Design parameter scaling, algorithm selection, and objective function formulation are found to exert a significant influence on optimizer performance. Two experimental programs were conducted to verify the analysis in which formal optimization techniques are used to modify the structural properties of dynamically scaled models, in order to improve operating characteristics. It is demonstrated that the modal-based analysis can yield significant improvements in aeromechanical stability and rotor vibratory response. O.C.

A91-33531*# Maryland Univ., College Park.
OPTIMUM AEROELASTIC DESIGN OF HELICOPTER ROTORS FOR LONGITUDINAL HANDLING QUALITIES IMPROVEMENT
ROBERTO CELI (Maryland, University, College Park) Journal of Aircraft (ISSN 0021-8669), vol. 28, Jan. 1991, p. 49-57. Previously cited in issue 12, p. 1781, Accession no. A89-30753. refs
(Contract NAG1-739; DAAL03-88-C-002)
Copyright

A91-33532*# Analytical Services and Materials, Inc., Hampton, VA.
INTEGRATED AERODYNAMIC LOAD/DYNAMIC OPTIMIZATION OF HELICOPTER ROTOR BLADES
ADITI CHATTOPADHYAY (Analytical Services and Materials, Inc., Hampton, VA), JOANNE L. WALSH (NASA, Langley Research Center, Hampton, VA), and MICHAEL F. RILEY (Lockheed Engineering and Management Services Co., Inc., Hampton, VA) Journal of Aircraft (ISSN 0021-8669), vol. 28, Jan. 1991, p. 58-65. Previously cited in issue 12, p. 1781, Accession no. A89-30752. refs
Copyright

A91-33533*# Lockheed Engineering and Sciences Co., Hampton, VA.
OPTIMIZATION OF HELICOPTER AIRFRAME STRUCTURES FOR VIBRATION REDUCTION - CONSIDERATIONS, FORMULATIONS, AND APPLICATIONS
T. SREEKANTA MURTHY (Lockheed Engineering and Sciences Co., Hampton, VA) Journal of Aircraft (ISSN 0021-8669), vol. 28, Jan. 1991, p. 66-73. Previously cited in issue 22, p. 3648, Accession no. A88-51942. refs
(Contract NAS1-19000)
Copyright

A91-33534*# Stanford Univ., CA.
AERODYNAMIC AND STRUCTURAL STUDIES OF JOINED-WING AIRCRAFT
ILAN KROO (Stanford University, CA), STEPHEN SMITH (NASA, Ames Research Center, Moffett Field, CA), and JOHN GALLMAN Journal of Aircraft (ISSN 0021-8669), vol. 28, Jan. 1991, p. 74-81. refs
(Contract NCA2-84)
Copyright
A method for rapidly evaluating the structural and aerodynamic characteristics of joined-wing aircraft was developed and used to study the fundamental advantages attributed to this concept. The technique involves a rapid turnaround aerodynamic analysis method for computing minimum trimmed drag combined with a simple structural optimization. A variety of joined-wing designs are compared on the basis of trimmed drag, structural weight, and, finally, trimmed drag with fixed structural weight. The range of joined-wing design parameters resulting in best cruise performance is identified. Structural weight savings and net drag reductions are predicted for certain joined-wing configurations compared with conventional cantilever-wing configurations. Author

A91-34122
STARSHIP - BRIGHT NEWCOMER IN A CONSERVATIVE FIRMAMENT
GORDON SWANBOROUGH Air International (ISSN 0306-5634), vol. 40, April 1991, p. 183-188.
Copyright
An evaluation is made of the design features and performance characteristics of the all-composite, twin-pusher prop canard configuration Beech Starship business aircraft, whose pressurized passenger cabin seats eight. The powerplants are 1200-shp PT6A-67A turboprops. The pilot and copilot are provided with an 'all-glass' cockpit with two electronic flight instrumentation system displays and two airspeed-and-altitude CRTs. The canard configuration, which features a variable-sweep canard, was dictated by the need to combine high cruise speed with good short-field operation capabilities and docile handling. The all-composite, primarily CFRP structure is a response to weight-reduction requirements, and was arrived at via CADAM. O.C.

A91-34144*# Virginia Polytechnic Inst. and State Univ., Blacksburg.
SHAPE SENSITIVITY ANALYSIS OF FLUTTER RESPONSE OF A LAMINATED WING
RAKESH K. KAPANIA, FREDERICK D'OENCH BERGEN, JR. (Virginia Polytechnic Institute and State University, Blacksburg), and JEAN-FRANCOIS M. BARTHELEMY (NASA, Langley Research Center, Hampton, VA) AIAA Journal (ISSN 0001-1452), vol. 29, April 1991, p. 611, 612. Previously cited in issue 12, p. 1781, Accession no. A89-30750. refs
(Contract NAS1-18471)

A91-34164
THE FLYING WING SUPERSONIC TRANSPORT
R. T. JONES Aeronautical Journal (ISSN 0001-9240), vol. 95, March 1991, p. 103-106. refs
Copyright
While anthropogenic artifacts exhibit an irrepressible tendency toward bilateral symmetry, aerodynamic theory displays no such tendency, while retaining a distinct preference for fore-aft symmetry; thus, all known shapes satisfying minimum wave drag requirements possess fore-aft symmetry. An account is presently given of a 'flying wing' SST whose sole component, a passengers-containing elliptical-planform wing, can be obliquely steered to a range of sweep angles in order to adapt to variations in flight Mach number. Attention is given to the results of recent studies of such as SST flight stability, efficiency, and potential operational problems. By limiting the cruise Mach number to twice the speed of subsonic airliners, a fuel efficiency comparable to that of such turbofan-powered aircraft could be achieved (in conjunction with variable-bypass engines). O.C.

A91-34260
HYTEX - DEMONSTRATOR FOR HYPERSONIC FLIGHT UP TO MACH 5 [HYTEX - DEMONSTRATOR FUER HYPERSCHALLFLUEGE BIS MACH 5]
Luft- und Raumfahrt (ISSN 0173-6264), vol. 12, no. 1-2, 1991, p. 26-29. In German.
Copyright
The hypersonic demonstrator HYTEX, which will permit the Saenger spacecraft technologies to be tested, is discussed. The development of HYTEX is reviewed, including the role of supercomputers in developing the HYTEX aerothermodynamics, the role of wind tunnel tests, and the development of the light and heat-resistant structures for the spacecraft. The HYTEX project definition is briefly reviewed. C.D.

A91-34375
X-31 FLIGHT TESTS TO EXPLORE COMBAT AGILITY TO 70 DEG. AOA
MICHAEL A. DORNHEIM Aviation Week and Space Technology (ISSN 0005-2175), vol. 134, March 11, 1991, p. 38-41.
Copyright
A review updating the X-31 research aircraft program is presented with a look at the expanding flight envelope that will explore the use of thrust-vectoring paddles at very high angles of attack. To date the aircraft has climbed to 30,000 ft, attained Mach 0.67, pulled 4g and achieved a maximum angle of attack (AOA) of 20 deg. Principal goals of the program are to demonstrate post-stall controllability and to determine how enhanced maneuverability affects kill ratios. The elevons are the prime roll and pitch control, while the canards are mainly for nose-down recovery and are geared to stay unloaded as AOA changes during cruise. Three thrust-vectoring paddles can deflect engine thrust up to 10 deg off axis to provide yaw and pitch forces. The control stick commands roll about the velocity vector, not about the body axis, which makes little difference in conventional flight, but at higher AOA rolls becoms a combination of body axis roll and yaw, until at 90 deg AOA a velocity vector roll is solely body axis yaw. Various flight simulator maneuvers are described to demonstrate the actual flight tests forthcoming in this program. R.E.P.

A91-35425#
THE N-DIMENSIONAL FIGHTER
LEIF JOHNSON (USAF, Sheppard AFB, TX), BERT SILICH (U.S. Air Force Academy, Colorado Springs, CO), and RIZWAN RIAZ (Pakistan Air Force, Chaklala) AIAA Student Journal (ISSN 0001-1460), vol. 28, Fall 1990, p. 12-19. refs
Copyright

The paper describes the N-Dimensional Fighter (NDF) concept for a fighter that will have all conventional capabilities at long range but that will have the ability to perform coordinated and uncoordinated maneuvers in any direction without providing visual cues to the enemy, and with no adverse physiological effects on the pilot. The NDF concept employs a cockpit that rotates about the longitudinal axis of the aircraft and independent of the wing system trailing behind, using differential canards to place the pilot in the desired direction of pull. The ability of rotating the cockpit with the canards will keep the pilot feeling only positive gravitational acceleration aligned head to toe. Results of wind-tunnel tests with a flying NDF model showed that the NDF idea is viable and that a means of controlling NDF can be defined. I.S.

A91-35427*# National Aeronautics and Space Administration. Lewis Research Center, Cleveland, OH.
ELEVATOR DEFLECTIONS ON THE ICING PROCESS
RANDALL K. BRITTON (NASA, Lewis Research Center, Cleveland, OH) AIAA Student Journal (ISSN 0001-1460), vol. 27, Winter 1989-1990, p. 8-18. refs
Copyright

The effect of elevator deflection of the horizontal stabilizer for certain icing parameters is investigated. Elevator deflection can severely change the lower and upper leading-edge impingement limits, and ice can accrete on the elevator itself. Also, elevator deflection had practically no effect on the maximum local collection efficiency. It is shown that for severe icing conditions (large water droplets), elevator deflections that increase the projected height of the airfoil can significantly increase the total collection efficiency of the airfoil. R.E.P.

N91-21127*# National Aeronautics and Space Administration. Langley Research Center, Hampton, VA.
SPAN REDUCTION EFFECTS ON THE FLUTTER CHARACTERISTICS OF ARROW-WING SUPERSONIC TRANSPORT CONFIGURATIONS
DONALD F. KELLER and ELLEN PARKER BULLOCK 26 Dec. 1990 55 p
(NASA-TP-3077; L-16807; NAS 1.60:3077) Avail: NTIS HC/MF A04 CSCL 01/3

An experimental and analytical investigation was initiated to determine the effect of span reduction on the flutter characteristics of several arrow-wing supersonic transport (SST) configurations. The model was a semispan wing with the experimental flutter results obtained in the Langley Transonic Dynamics Tunnel over a Mach number range from 0.60 to 1.20. Two flow-through nacelles were used to represent wing-mounted engines. A wing fin was mounted either vertically or canted outboard at 45 degrees. Portions of the wingtip were removed in increments parallel to the root chord to provide reductions un wing span of 10, 20, and 30 percent. Reducing the wing span increased the flutter dynamic pressure for all configurations tested. The largest increases in the flutter dynamic pressure were observed for the configurations with nacelles. Although reducing the span had little effect on flutter-speed index for the wing only and the wing with fin configuration, and increase was observed for the configurations with nacelles, particularly in the high transonic region. The flutter analysis, which generally showed the same trends as the experimental results, was consistently more conservative in the low transonic region than in the high transonic region. Author

N91-21129 ESDU International Ltd., London (England).
LIFT AND ROLLING MOMENT DUE TO SPOILERS ON WINGS AT SUBSONIC SPEEDS Abstract Only
Nov. 1990 25 p
(ESDU-90030; ISBN-0-85679-756-1; ISSN-0141-397X) Avail: ESDU

ESDU 90030 considers the flat plate (deflecting in a plane normal to the aerofoil surface) and flap (pivoting about a hinge on the airfoil surface) types of unvented spoilers with or without porosity on the upper surface of a wing with trailing-edge flaps undeployed. It discusses the flow behavior with variation of spoiler chordwise position and deflection and illustrates the effect on wing lift-curve slope and shape. By correlating experimental data drawn from the literature, a method is developed for predicting the lift decrement in two-dimensional flow which is then corrected to three dimensions (by scaling by the wing lift-curve slop predicted using ESDU 70011) and for part span effects by means of an empirically derived factor. The rolling moment is predicted assuming the lift decrement acts at spoiler mid-span and correcting the moment arm for wing taper and for lift carry-over beyond the physical extent of the spoiler at either end. The method allows for any form of porosity (face perforations, hinge-line gaps, spoiler segmentation or edge castellation) up to 0.25 of the spoiler area. Spoiler locations from 0.4 chord to the trailing-edge are covered for spoiler deflections (defined as height as a fraction of chord where height is measured above the aerofoil surface for the plate type or above the pivot for the flap type) from 0.04 to 0.15 where the lower limit is set by the onset of Reynolds number effects. The experimental data that was used covered a wide range of straight-tapered wing planforms with aspect ratio 3 and above, taper ratios from 0.4 to 1 and mid-chord sweep up to 30 degrees for Mach numbers up to 0.7. Behavior is affected by wing angle of attack and limits of applicability for both minimum and maximum incidence are suggested. Sketches show plots of predictions by the method against experimental results; predictions lie within 0.05 for lift coefficient and within 0.007 for rolling moment coefficient for 75 percent of the data. ESDU

N91-21130# Deutsche Forschungsanstalt fuer Luft- und Raumfahrt, Brunswick (Germany, F.R.). Abt. Mathematische Verfahren und Datentechnik.
IDENTIFICATION OF THE AERODYNAMIC MODEL OF THE DLR RESEARCH AIRCRAFT ATTAS FROM FLIGHT TEST DATA
RAVINDRA JATEGAONKAR Aug. 1990 102 p Prepared in cooperation with Technische Univ. Brunswick, Fed. Republic of Germany
(DLR-FB-90-40; ISSN-0171-1342; ETN-91-99035) Avail: NTIS HC/MF A06; DLR, Wissenschaftliches Berichtswesen, VB-PL-DO, Postfach 90 60 58, 5000 Cologne, Fed. Republic of Germany, HC 37 DM

Determination of aerodynamic characteristics of the Advanced Technologies Testing Aircraft System (ATTAS) Aircraft from flight test data is addressed. The details of flight tests carried out for this purpose, together with the results of consistency checking of the onboard recorded data and identification of the aerodynamic model are reported. The data checking is based on the kinematic equations of aircraft motion. The estimation of aerodynamic derivatives is carried out from the coupled equations of aircraft motion pertaining to the longitudinal and lateral directional motion. For both of these purposes the maximum likelihood estimation method is employed. The details of mass characterisrics data, such as position of center of gravity and moments of inertia, are provided along with other aircraft installation dependent data required for parameter estimation. The results of kinematic consistency checking, the aerodynamic derivatives at typical flight conditions, and attempts to derive a combined model valid over a wider range of speed variations are reported. Such an extended aerodynamic model can be incorporated in the ground based simulation of the test aircraft. ESA

N91-21131*# National Aeronautics and Space Administration. Ames Research Center, Moffett Field, CA.
SIMULATION OF NAP-OF-THE-EARTH FLIGHT IN HELICOPTERS
GREGORY W. CONDON Feb. 1991 20 p Presented at the AGARD 50th Symposium on Computer Aided System Design and Simulation, Izmir, Turkey, 22-25 May 1990 Previously announced as N91-15744
(NASA-TM-102830; A-90178; NAS 1.15:102830) Avail: NTIS HC/MF A03 CSCL 01/3

NASA-Ames along with the U.S. Army has conducted extensive simulation studies of rotorcraft in the nap-of-the-Earth (NOE) environment and has developed facility capabilities specifically designed for this flight regime. The experience gained to date in

applying these facilities to the NOE flight regime are reported along with the results of specific experimental studies conducted to understand the influence of both motion and visual scene on the fidelity of NOE simulation. Included are comparisons of results from concurrent piloted simulation and flight research studies. The results of a recent simulation experiment to study simulator sickness in this flight regime is also discussed. Author

N91-21132*# National Aeronautics and Space Administration. Langley Research Center, Hampton, VA.
A SIMPLE, ANALYTICAL, AXISYMMETRIC MICROBURST MODEL FOR DOWNDRAFT ESTIMATION
DAN D. VICROY Feb. 1991 13 p Sponsored in part by FAA
(NASA-TM-104053; NAS 1.15:104053) Avail: NTIS HC/MF A03 CSCL 01/3

A simple analytical microburst model was developed for use in estimating vertical winds from horizontal wind measurements. It is an axisymmetric, steady state model that uses shaping functions to satisfy the mass continuity equation and simulate boundary layer effects. The model is defined through four model variables: the radius and altitude of the maximum horizontal wind, a shaping function variable, and a scale factor. The model closely agrees with a high fidelity analytical model and measured data, particularly in the radial direction and at lower altitudes. At higher altitudes, the model tends to overestimate the wind magnitude relative to the measured data. Author

N91-21133# Army Natick Labs., MA.
EVALUATION OF AN ALTERNATIVE ROTORCRAFT CARGO LOWERING DEVICE FOR THE DELIVERY OF 500-LB AMMUNITION LOADS Final Report, Oct. 1987 - Aug. 1989
GLENN DOUCET Dec. 1990 40 p
(AD-A230995; NATICK/TR-91/010) Avail: NTIS HC/MF A03 CSCL 15/5

The focus of this analysis was to investigate a commercial lowering device called the Sky Genie for rotorcraft delivery of 500-lb ammunition loads. This item, similar to the presently used cargo and personnel rappelling device, uses the friction of rope on metal to control the payload's descent. Reduction in payload descent time, which translates into improved troop and aircraft survivability, was sought. This report describes the functional and operational tests performed on this item. Based on these tests, it was concluded that the Sky Genie represents an effective, predictable means of delivering up to 500-lb payloads from altitudes up to 100 ft with no user input once the load leaves the rotorcraft. GRA

N91-22103*# National Aeronautics and Space Administration. Langley Research Center, Hampton, VA.
COMPUTER PROGRAM FOR ESTIMATING PERFORMANCE OF AIR-BREATHING AIRCRAFT ENGINES
KARL A. GEISELHART, MICHAEL J. CADDY (Naval Air Development Center, Warminster, PA.), and SHELBY J. MORRIS, JR. Washington May 1991 132 p
(NASA-TM-4254; L-16765; NAS 1.15:4254) Avail: NTIS HC/MF A07 CSCL 01/3

QNEP is a reliable, easy to use computer program for predicting the design point and off-design steady state performance for a variety of airbreathing aircraft engines. These include gas turbines with single or multiple spools, multiple flow paths, and multiple exhaust nozzles, as well as, ramjets. QNEP is a modified version of the Navy Engine Performance Computer Program (NEPCOMP). NEPCOMP and its successor, the Navy NASA Engine Program (NNEP), have broad capabilities including optimization and chemical equilibrium gas computers memory requirements. QNEP was developed to be used for conceptual and preliminary design studies where the broad capability, the attendant complexity, and large memory are not necessary. QNEP is small enough to be run on a personal computers with 640 kilobytes of memory. It first sizes the engine for a selected design point where off-design performance data are to be computed. QNEP is shown to reliably compute performance parameters which agree with existing data for a variety of engines. A companion preprocessor program called QDATGEN was developed to aid inexperienced users of QNEP. It is used to interactively generate input files. QDATGEN contains a data base of seven engine configurations from which the user can choose. It includes two unducted turbofans, two ducted turbofans, two turbojets, and a ramjet. The user can also enter a new configuration or modify an existing configuration. The small size of QNEP should appeal to a wide range of users, including small companies or research organizations and especially students. It has the potential to be directly linked to other computer programs (i.e., mission weight, cost, or noise analyses) that require propulsion performance data or aircraft engine thermodynamic cycle data. A detailed description is given of QNEP including its input, accuracy, reliability, and limitations. A description is also presented of QDATGEN, sample calculations, and a user's guide. Author

N91-22104# Advisory Group for Aerospace Research and Development, Neuilly-Sur-Seine (France). Fluid Dynamics Panel.
SPECIAL COURSE ON AIRCRAFT DYNAMICS AT HIGH ANGLES OF ATTACK: EXPERIMENTS AND MODELLING
Mar. 1991 144 p Special course held in Hampton, VA, 8-11 Apr. 1991 and in Rhode-Saint-Genese, Belgium, 22-25 Apr. 1991; sponsored by AGARD and the von Karman Inst.
(AGARD-R-776; ISBN-92-835-0607-3) Copyright Avail: NTIS HC/MF A07; Non-NATO Nationals requests available only from AGARD/Scientific Publications Executive

Lecture notes for an AGARD Fluid Dynamic Panel Special Course on 'Aircraft Dynamics at High Angles of Attack: Experiments and Modelling' are presented. These notes present the latest information on the development and use of dynamic experiments in wind tunnels from several NATO nations. Current oscillatory and rotary test techniques, experimental results for typical configurations, and the use of these data for flight mechanics applications are addressed. Subjects include dynamic lift, wing rock, fluid dynamics of rotary flows, mathematical modelling, nonlinear data representation, vortex manipulation for control enhancement, and correlations of predictions based on rotary and oscillatory wind tunnel and flight test results.

N91-22106*# National Aeronautics and Space Administration. Langley Research Center, Hampton, VA.
DYNAMIC STALL EFFECTS AND APPLICATIONS TO HIGH PERFORMANCE AIRCRAFT
JAY M. BRANDON *In* AGARD, Special Course on Aircraft Dynamics at High Angles of Attack: Experiments and Modelling 15 p Mar. 1991
Copyright Avail: NTIS HC/MF A07; Non-NATO Nationals requests available only from AGARD/Scientific Publications Executive CSCL 01/3

Recent research conducted at the NASA Langley Research Center on the effects of large amplitude pitching motions on the aerodynamic characteristics of modern fighter aircraft configurations is highlighted. Wind tunnel tests were conducted on simple flat-plate wings to gain understanding of the complex flow phenomena during unsteady motions at high angles of attack. Studies then progressed to a representative modern fighter configuration. Using a computer controlled dynamic apparatus, tests were conducted to investigate effects of pitch rate and motion time history and to determine the persistence of unsteady effects. Data were also obtained in sideslip and with control surface deflections to investigate dynamic effects on lateral stability and available control power. Force and moment data were obtained using a 6-component internal strain-gage balance. To aid in the interpretation of the results, flow visualization using a laser light-sheet system was also obtained. Results of these tests are discussed, along with their implications on the maneuverability of future advanced airplanes designed to operate in the highly dynamic, high angle-of-attack environment. Author

N91-22110# Eidetics International, Inc., Torrance, CA.
FOREBODY VORTEX CONTROL
GERALD N. MALCOLM *In* AGARD, Special Course on Aircraft Dynamics at High Angles of Attack: Experiments and Modelling

40 p Mar. 1991
Copyright Avail: NTIS HC/MF A07; Non-NATO Nationals requests available only from AGARD/Scientific Publications Executive

Because conventional fighter aircraft control surfaces (e.g. rudder) become ineffective at high angles of attack, alternate means of providing aerodynamic control are being explored. A prime potential source for improved control power is the vortex flowfield existing on typical fighter aircraft forebodies. Several techniques to manipulate the forebody vortices to produce controlled forces and moments at high angles of attack have been investigated by a number of researchers in the past few years. Some of the research results and the merits of several methods applied directly to the forebody are discussed. These methods include movable strakes, blowing surface jets, blowing and suction through surface slots, suction through surface holes, and miniaturized rotatable tip strakes. All of these were found to be effective over a varying range of angles of attack and sideslip. Most of the methods work on the basis of boundary layer separation control. The presence of closely spaced forebody vortices enhances the effectiveness, since controlling the separation controls the vortices which, in turn, creates large changes in forebody forces. Regardless of which method is employed, the maximum effectiveness is realized if it is applied near the forebody tip. The advantage of one method over another will depend on the configuration and specific performance requirements. Author

N91-22112 Cranfield Inst. of Tech., Bedford (England).
VARIABLE CAMBER WINGS FOR TRANSPORT AIRCRAFT Ph.D. Thesis
A. J. RAO 1989 257 p
Avail: Univ. Microfilms Order No. BRDX90881

A variable camber system was designed which ensured that the airfoil profile remained smooth and continuous throughout the range of camber shapes without requiring the use of flexible surfaces. It was made up of a fixed centre section with modified leading and trailing edge devices designed such that their deployment caused a simultaneous rotational and translational movement. A series of 2D tests were carried out to investigate the characteristics of this variable camber airfoil design. The effect of distribution of variable section camber across the span of a transport aircraft wing was investigated using a 30 deg swept, untapered half-wing model. An initial investigation of incorporating this proposed variable camber design into a medium haul transport aircraft suggested that, even allowing for an increase in the mechanism weight of the variable camber devices themselves, a wing weight saving of 10 percent could be achieved compared with the conventional aircraft design. Dissert. Abstr.

N91-22117*# Sparta, Inc., Laguna Hills, CA.
AUTOMATED FLIGHT TEST MANAGEMENT SYSTEM
M. D. HEWETT, D. M. TARTT, and A. AGARWAL (Integrated Systems, Inc., Santa Clara, CA.) May 1991 40 p
(Contract NAS2-12670)
(NASA-CR-186011; H-1699; NAS 1.26:186011) Avail: NTIS HC/MF A03 CSCL 01/3

The Phase 1 development of an automated flight test management system (ATMS) as a component of a rapid prototyping flight research facility for artificial intelligence (AI) based flight concepts is discussed. The ATMS provides a flight engineer with a set of tools that assist in flight test planning, monitoring, and simulation. The system is also capable of controlling an aircraft during flight test by performing closed loop guidance functions, range management, and maneuver-quality monitoring. The ATMS is being used as a prototypical system to develop a flight research facility for AI based flight systems concepts at NASA Ames Dryden. Author

N91-22118# Messerschmitt-Boelkow-Blohm G.m.b.H., Munich (Germany, F.R.). Theoretical Aerodynamics Dept.
AN ITERATIVE PROCEDURE FOR THE DESIGN OF PRESSURE-SPECIFIED 3-DIMENSIONAL CONFIGURATIONS AT SUBSONIC AND SUPERSONIC SPEEDS BY MEANS OF A HIGHER-ORDER PANEL METHOD
L. FORNASIER 11 Sep. 1989 13 p Presented at 64th Fluid Dynamics Panel Specialists' Meeting on Computational Methods for Aerodynamic Design (Inverse) and Optimization, Loen, Norway, 22-23 May 1989
(Contract BMVG-T/RF41/E0010/E14)
(MBB-FE122/S/PUB/375; ETN-91-99190) Copyright Avail: NTIS HC/MF A03

An advanced panel method employing singularity distributions of high order and based on mixed Dirichlet and Neumann type boundary conditions was recently developed for the potential flow analysis of arbitrary airplane configurations at subsonic and supersonic speeds. Some work is in progress to provide this method with a design option capable of relofting the surface of a given configuration from prescribed pressure distributions. The mathematical background of the herein used inverse algorithm is presented and some examples of application are discussed. ESA

N91-22119# Bristol Univ. (England). Dept. of Aerospace Engineering.
THE PRELIMINARY AERODYNAMIC DESIGN OF LIGHT AIRCRAFT B.S. Thesis
P. J. GRIFFITHS and M. A. STANDEVEN Jun. 1990 111 p
(BU-504; ETN-91-99197) Avail: NTIS HC/MF A06

The development of a computer program to aid the preliminary design of light aeroplanes is described. It is written in Borland TURBO PASCAL for use on an IBM PC or compatible computer; thus, providing the light aircraft designer with an inexpensive desktop design tool. The highly structured nature of TURBO PASCAL is exploited to match the overall aircraft design philosophy, as well as providing a modular framework suitable for future expansion. At the end of the study, the program is capable of calculating both the untrimmed and trimmed cruise performance characteristics, simply from the basic aeroplane geometry. The predictions are presented in either tabular or graphical form. However, there do exist reliability problems within the calculation of the trimmed drag coefficients, which could not be solved within the time scale available. This project produced a sound basis for the development of a comprehensive system capable of reducing the time and cost of a preliminary light aircraft design study. ESA

N91-22120# Bristol Univ. (England). Dept. of Aerospace Engineering.
A QUANTITATIVE INVESTIGATION INTO THE AERODYNAMIC COUPLING EFFECTS IN A COAXIAL CONTRA-ROTATING ROTOR SYSTEM B.S. Thesis
A. SEGAL and M. TOMBLIN Jun. 1990 73 p
(BU-517; ETN-91-99210) Avail: NTIS HC/MF A04

The total lift, lift difference and power supplied for a coaxial contrarotating rotor were measured at various speeds separations and incidences. This included differential pitch on upper and lower rotors. Performance comparisons were made at 800 rpm, between 0.4 and 0.12 m separation and with 1 to 9 degs of positive pitch. Lift and lift per kilowatt (a measure of efficiency) were used as a means of comparison between different configurations. The lower rotor was found to perform very poorly in the wake of the upper rotor, producing only between 14 and 28 pct. of the total lift. The optimum overall efficiency was found when the lower rotor produced minimum lift and the separation was about 10 pct. of the rotor's diameter. ESA

N91-22318*# Lockheed Aeronautical Systems Co., Burbank, CA.
FLEXIBLE BODY DYNAMIC STABILITY FOR HIGH PERFORMANCE AIRCRAFT
E. A. GOFORTH, H. M. YOUSSEF, C. V. APELIAN, and S. C. SCHROEDER *In* NASA. Langley Research Center, Fourth NASA Workshop on Computational Control of Flexible Aerospace Systems, Part 1 p 145-155 Mar. 1991
Avail: NTIS HC/MF A20 CSCL 01/3

Dynamic equations which include the effects of unsteady aerodynamic forces and a flexible body structure were developed

for a free flying high performance fighter aircraft. The linear and angular deformations are assumed to be small in the body reference frame, allowing the equations to be linearized in the deformation variables. Equations for total body dynamics and flexible body dynamics are formulated using the hybrid coordinate method and integrated in a state space format. A detailed finite element model of a generic high performance fighter aircraft is used to generate the mass and stiffness matrices. Unsteady aerodynamics are represented by a rational function approximation of the doublet lattice matrices. The equations simplify for the case of constant angular rate of the body reference frame, allowing the effect of roll rate to be studied by computing the eigenvalues of the system. It is found that the rigid body modes of the aircraft are greatly affected by introducing a constant roll rate, while the effect on the flexible modes is minimal for this configuration. Author

N91-22333*# *National Aeronautics and Space Administration.* Langley Research Center, Hampton, VA.
AEROELASTIC MODELING OF THE ACTIVE FLEXIBLE WING WIND-TUNNEL MODEL
WALTER A. SILVA (Lockheed Engineering and Sciences Co., Hampton, VA.), JENNIFER HEEG, and ROBERT M. BENNETT *In its* Fourth NASA Workshop on Computational Control of Flexible Aerospace Systems, Part 2 p 497-533 Mar. 1991
Avail: NTIS HC/MF A20 CSCL 01/3

The primary issues involved in the generation of linear, state-space equations of motion of a flexible wind tunnel model, the Active Flexible Wing (AFW), are discussed. The codes that were used and their inherent assumptions and limitations are also briefly discussed. The application of the CAP-TSD code to the AFW for determination of the model's transonic flutter boundary is included as well. Author

06

AIRCRAFT INSTRUMENTATION

Includes cockpit and cabin display devices; and flight instruments.

A91-33268
IN-FLIGHT SYSTEM FOR HELICOPTER BLADE INSPECTION
DONALD W. BLINCOW, SAM C. DOMINEY, JOHN J. MAHONEY, and JEROLD H. MCCORMICK (General Nucleonics, Inc., Pomona, CA) Materials Evaluation (ISSN 0025-5327), vol. 49, April 1991, p. 456-458, 460, 461.
Copyright

An in-flight blade inspection system (IBIS) with a radioactive source in the pressure indicator and a radiation detector in the top of the fuselage is described. It uses Sr-90 isotope in conjunction with a Geiger-Muller detector with 100 percent efficiency for beta particles. A warning light in the cockpit is activated at indications of incipient blade failures. IBIS is characterized by a low level of radioactivity and presents no radiation hazard to the crew. Attention is also given to the system's fail-safe design and built-in test features. O.G.

A91-33370
AN AIRWORTHY EXPERIMENTAL SYSTEM FOR MODERN NAVIGATION AND REMOTE-SENSING METHODS - REDUCTION, STORAGE, AND TRANSMISSION OF AERIAL PHOTOGRAPHY SCENES [EIN FLUGFAEHIGES EXPERIMENTALSYSTEM FUER MODERNE NAVIGATIONS- UND AUFKLAERUNGSMETHODEN - LUFTBILDSZENEN REDUZIEREN, SPEICHERN UND UEBERTRAGEN]
PETER SCHULZ (DLR, Institut fuer Flugfuehrung, Brunswick, Federal Republic of Germany) DLR-Nachrichten (ISSN 0937-0420), Feb. 1991, p. 12-14. In German.
Copyright

A91-33615
COMMON INTEGRATED PROCESSING IN MODULAR AVIONICS
THOMAS H. ROBINSON and EDWARD TRUJILLO (Hughes Aircraft Co., El Segundo, CA) IN: IEEE PLANS '90 - Position Location and Navigation Symposium, Las Vegas, NV, Mar. 20-23, 1990, Record. New York, Institute of Electrical and Electronics Engineers, Inc., 1990, p. 133-138.
Copyright

The authors present a review of the current modular avionics concepts and discuss a powerful processing system, the Hughes modular processor, developed to meet the objectives defined from those concepts. They also discuss future trends in avionics into the next century along with how modular avionics will affect the way equipment developers interact. Current modular avionic concepts, as embodied in advanced avionics systems, are reviewed. Initially mandated because of the perceived cost advantages, modular avionics also provide significant performance potential. A key characteristic of modular avionics is the partitioning of the system into highly integrated, common and modular building blocks. The partitioning features are defined, and the rationale for the approach taken is presented. The Hughes modular processor family of imbedded avionics processors has been shown to be a powerful and innovative realization of the application of modular avionics concepts to the core avionics. It is further noted that the US Department of Defense has embarked, through the USAF Pave Pace and Modular Avionics System Architecture (MASA) programs, on defining further extensions of the modular avionics concepts into new aircraft and retrofits. Functions within the aircraft, including navigation, will become more integrated, requiring innovative approaches to the requirements and design phases of specific system applications. I.E.

A91-33625
MOTION COMPENSATION FOR ASTOR LONG RANGE SAR
JOHN S. A. HEPBURN and COLIN P. DOYLE (Honeywell, Ltd., Advanced Technology Centre, Markham, Canada) IN: IEEE PLANS '90 - Position Location and Navigation Symposium, Las Vegas, NV, Mar. 20-23, 1990, Record. New York, Institute of Electrical and Electronics Engineers, Inc., 1990, p. 205-211. refs
Copyright

The United Kingdom Ministry of Defence is conducting a Long Range Synthetic Aperture Radar (SAR) Technology Demonstrator Programme (TDP) in support of their Airborne Stand-Off Radar Programme. A major goal is to develop a high-resolution airborne SAR with both strip map and spotlight modes. To attain the image quality objectives of the project, it is essential that very accurate motion compensation be applied to the radar returns to reduce image degradation, caused by spurious antenna phase center motion, to acceptable levels. The SAR motion compensation system (SARMC) currently under development includes a master inertial navigation system located near the center of mass of the host aircraft and a slaved strapdown inertial measurement unit mounted on the back of the radar antenna, as well as Doppler velocity and barometric and radar altimeters. The performance of the SARMC has been evaluated both by analysis and computer simulation. These evaluations accounted for all major system error sources, including errors associated with sensors, transfer alignment, and computation, with the system operating in an environment of moderate atmospheric turbulence. Results from these evaluations are presented. I.E.

A91-33627
DEMONSTRATION OF A RING LASER GYRO SYSTEM FOR POINTING AND STABILIZATION APPLICATIONS
ROBERT G. MAJURE (Honeywell, Inc., Space Systems Group, Clearwater, FL) IN: IEEE PLANS '90 - Position Location and Navigation Symposium, Las Vegas, NV, Mar. 20-23, 1990, Record. New York, Institute of Electrical and Electronics Engineers, Inc., 1990, p. 219-225.
Copyright

A system specifically designed to meet the requirements of the pointing and stabilization community is presented. Such

applications include synthetic aperture radar (SAR) motion compensation and infrared sensor stabilization. Requirements peculiar to this application are discussed and contrasted with traditional inertial navigation requirements. Pointing and stabilization demand consideration of requirements such as high bandwidth, low noise, minimal data latency, dither effects, reference alignment, minimization of size, near-instantaneous turn-on, and analysis of structural resonances. the GG1320 RLG (ring laser gyro) was chosen for this application since it provided the necessary accuracy and could be contained in a small volume. Test results are presented indicating the performance of the IMU (inertial measurement unit). Testing techniques are also discussed and contrasted with traditional inertial navigation system testing. Results indicate that the GG1320 RLG IAU (inertial attitude unit) is capable of meeting the requirements of the pointing and stabilization community. Current and future development activities are discussed relative to performance enhancement, and further applications and requirements are identified. I.E.

A91-33650
TERRAIN-AIDED ALTITUDE COMPUTATIONS ON THE AFTI/F-16
CHARLES A. BAIRD, FRANKLIN B. SNYDER (Harris Corp., Government Aerospace Systems Div., Melbourne, FL), and MARK BEIERLE (USAF, Wright Research and Development Center, Wright-Patterson AFB, OH) IN: IEEE PLANS '90 - Position Location and Navigation Symposium, Las Vegas, NV, Mar. 20-23, 1990, Record. New York, Institute of Electrical and Electronics Engineers, Inc., 1990, p. 474-481. refs
Copyright

Over the past several years a variety of barometric and inertial-based altitude channel implementations has been flight-tested on the US Air Force's advanced fighter technology integration (AFTI) F-16. Accurate terrain-referenced altitude knowledge on the AFTI aircraft is required to support low-level flight experiments to evaluate and demonstrate close air support functions. Previous mechanizations of the altitude channel had been variations on the standard barometrically damped inertial systems, which had to be manually updated to remove biases due to pressure altitude drift. These mechanizations are briefly reviewed, together with flight test data describing their performance. More recently, a color moving map system with an associated digital terrain elevation database has been added to the AFTI avionics suite and is being integrated into the weapon delivery system. This digital map system includes an implementation of the Sandia inertial terrain-aided navigation (SITAN) algorithm, whose principal outputs are used to update the horizontal position estimates of the inertial navigation system. The design, mechanization, and preliminary flight testing of a new altitude channel implementation are described, referenced primarily to the SITAN altitude estimates. This mechanization automatically corrects for pressure altitude bias and drift, while referencing the altitude estimate to the terrain database which forms the common reference grid for low-level maneuvering flight, targeting, and weapon delivery. I.E.

A91-33655
GG1308 RING LASER GYRO INERTIAL MEASUREMENT SYSTEMS - HONEYWELL'S LOW-COST SOLUTION FOR TACTICAL APPLICATIONS
JOHN M. OELSCHLAEGER and LEROY O. THIELMAN (Honeywell, Inc., Military Avionics Div., Minneapolis, MN) IN: IEEE PLANS '90 - Position Location and Navigation Symposium, Las Vegas, NV, Mar. 20-23, 1990, Record. New York, Institute of Electrical and Electronics Engineers, Inc., 1990, p. 528-536.
Copyright

The GG1308 ring laser gyro (RLG) inertial measurement systems represent the smallest-volume, lightest-weight, and lowest-cost RLG systems. These systems are designed to provide the functions required for inertial guidance, aided or midcourse navigation, and vehicle stabilization and control to a wide variety of tactical missiles, standoff weapons, unmanned aerial vehicles, torpedoes, and manned rotorcraft. GG1308 inertial systems achieve their low cost as a result of several significant development thrusts. Low-cost inertial sensors must be utilized. The GG1308 RLG is a true design-to-cost device with producibility and the cost of parts, materials, assembly labor, and manufacturing automation being the dominant design drivers. Additionally, these GG1308 inertial systems use a commonality design approach. This philosophy has made it possible to develop several generic hardware elements which need only be repackaged to provide an inertial system in the form factor required for specific programs. It also provides the system with an adaptability and intelligence to improve its performance throughout its useful life by making software improvements which do not affect the hardware design or production process. I.E.

A91-33656
THE NEXT FRONTIER FOR STRAPDOWN RLG INERTIAL SYSTEMS - PRECISION NAVIGATION
ROBERT W. UPTON, JR. and WILLIAM G. MILLER (Honeywell, Inc., Military Avionics Div., Clearwater, FL) IN: IEEE PLANS '90 - Position Location and Navigation Symposium, Las Vegas, NV, Mar. 20-23, 1990, Record. New York, Institute of Electrical and Electronics Engineers, Inc., 1990, p. 537-542.
Copyright

Honeywell research and development projects directed at improvements in the design, building, and testing of RLG (ring laser gyro) strapdown systems are reviewed. Some of the performance standards being set with current hardware are discussed, as are a number of the known error sources existing in these systems along with candidate solutions, the analysis and test results upon which precision navigation performance projections are based, and plans to demonstrate the feasibility of a precision pure strapdown RLG system. Based upon current performance, reasonable projections and analysis, and laboratory test data, it is anticipated that strapdown RLG systems can deliver performance consistent with the precision requirements of SNU 84-3 (0.2 nm/h after a precision-extended time-alignment) while retaining the major advantages that the pure strapdown mechanization offers. I.E.

A91-33657
RING LASER GYRO APPLICATIONS FOR TACTICAL MISSILES - THE ARMY TACMS SOLUTION
GEORGE L. CURRAN and DANIEL J. ENGELKEN (Honeywell, Inc., Military Avionics Div., Minneapolis, MN) IN: IEEE PLANS '90 - Position Location and Navigation Symposium, Las Vegas, NV, Mar. 20-23, 1990, Record. New York, Institute of Electrical and Electronics Engineers, Inc., 1990, p. 543-548.
Copyright

The Honeywell H700-3A ring laser gyro missile guidance set (AN/DJW-51) provides navigation, guidance, autopilot, weapons dispensing, and communications functions for the US Army TACMS missile in a low-initial-cost and low-life-cycle-cost package. It is primarily the use of low-cost inertial sensors which make the use of a ring laser gyro navigation system feasible in the tactical missile market. The H700-3A ring laser gyro missile guidance set has proven to be a low-cost, high-accuracy guidance and navigation system for the deep-strike Army missile weapons system. This has been borne out by a highly successful test program of 26 missile flights. The components of the missile guidance set are described in detail. I.E.

A91-35738
OPTIMIZATION OF RADIO-MEASURING DEVICES INCORPORATED IN ONBOARD LASER VELOCIMETERS [OPTIMIZATSIIA RADIOIZMERITEL'NYKH USTROISTV BORTOVYKH LAZERNYKH IZMERITELEI SKOROSTI]
A. A. SOSNOVSKII and S. N. KHAIKIN Radioelektronika (ISSN 0021-3470), vol. 34, Jan. 1991, p. 46-51. In Russian. refs
Copyright

The paper examines aspects of the optimization of radio-measuring channels and devices incorporated in laser Doppler velocimeters. A promising technique of random-noise time selection

for these devices is investigated, and criteria for use in their computer-aided design are proposed. L.M.

A91-35978
KNOWLEDGE-BASED TARGET RECOGNITION SYSTEM EVOLUTION
JOHN F. GILMORE (Georgia Institute of Technology, Atlanta) Optical Engineering (ISSN 0091-3286), vol. 30, May 1991, p. 557-570. refs
Copyright

The implications of artificial intelligence techniques for the target recognition process is discussed. Basic target recognition mission requirements are presented to establish problem constraints in terms of applications, algorithms, and processors, current target recognition algorithms are discussed and their deficiencies are identified. Original knowledge-based target recognition systems are examined in terms of their contributions to automatic target recognizer technology. An architecture for synergistically integrating vision algorithms and knowledge-based systems is presented, and preliminary results from a system being developed using this architecture are presented. C.D.

N91-21134*# National Aeronautics and Space Administration. Ames Research Center, Moffett Field, CA.
SUPPRESSION OF BIODYNAMIC INTERFERENCE IN HEAD-TRACKED TELEOPERATION
S. LIFSHITZ, S. J. MERHAV, A. J. GRUNWALD, G. E. TUCKER, and M. B. TISCHLER (Army Aviation Systems Command, Moffett Field, CA.) Jan. 1991 15 p Presented at the 16th European Rotorcraft Forum, Glasgow, Scotland, 18-20 Sep. 1990
(NASA-TM-103833; A-91058; NAS 1.15:103833; AVSCOM-TR-90-A-005) Avail: NTIS HC/MF A03 CSCL 01/4

The utility of helmet-tracked sights to provide pointing commands for teleoperation of cameras, lasers, or antennas in aircraft is degraded by the presence of uncommanded, involuntary heat motion, referred to as biodynamic interference. This interference limits the achievable precision required in pointing tasks. The noise contributions due to biodynamic interference consists of an additive component which is correlated with aircraft vibration and an uncorrelated, nonadditive component, referred to as remnant. An experimental simulation study is described which investigated the improvements achievable in pointing and tracking precision using dynamic display shifting in the helmet-mounted display. The experiment was conducted in a six degree of freedom motion base simulator with an emulated helmet-mounted display. Highly experienced pilot subjects performed precision head-pointing tasks while manually flying a visual flight-path tracking task. Four schemes using adaptive and low-pass filtering of the head motion were evaluated to determine their effects on task performance and pilot workload in the presence of whole-body vibration characteristic of helicopter flight. The results indicate that, for tracking tasks involving continuously moving targets, improvements of up to 70 percent can be achieved in percent on-target dwelling time and of up to 35 percent in rms tracking error, with the adaptive plus low-pass filter configuration. The results with the same filter configuration for the task of capturing randomly-positioned, stationary targets show an increase of up to 340 percent in the number of targets captured and an improvement of up to 24 percent in the average capture time. The adaptive plus low-pass filter combination was considered to exhibit the best overall display dynamics by each of the subjects. Author

N91-21135*# National Aeronautics and Space Administration. Ames Research Center, Moffett Field, CA.
DIGITAL SIGNAL CONDITIONING FOR FLIGHT TEST INSTRUMENTATION
GLENN A. BEVER Mar. 1991 81 p Sponsored by AGARD Flight Mechanics Panel, Flight Test Techniques Working Group
(NASA-TM-101739; H-1695; NAS 1.15:101739; AGARDOGRAPH-160) Avail: NTIS HC/MF A05 CSCL 01/4

An introduction to digital measurement processes on aircraft is provided. Flight test instrumentation systems are rapidly evolving from analog-intensive to digital intensive systems, including the use of onboard digital computers. The topics include measurements that are digital in origin, as well as sampling, encoding, transmitting, and storing data. Particular emphasis is placed on modern avionic data bus architectures and what to be aware of when extracting data from them. Examples of data extraction techniques are given. Tradeoffs between digital logic families, trends in digital development, and design testing techniques are discussed. An introduction to digital filtering is also covered. Author

N91-21136# General Accounting Office, Washington, DC. Information Management and Technology Div.
EMBEDDED COMPUTERS: NAVY'S APPROACH TO DEVELOPING PATROL AIRCRAFT AVIONICS SYSTEM TOO RISKY
Sep. 1990 15 p
(AD-A230868; GAO/IMTEC-90-79) Avail: NTIS HC/MF A03 CSCL 15/5

The Navy plans to buy complex avionics computer systems, and related communications equipment and sensors, for submarine patrol aircraft. This acquisition, designated the Update IV Program, is intended to provide the Navy with the capability to locate, identify, and attack the expected threat of more quiet submarines. This report reviews the Department of Defense's acquisition of computer systems embedded in weapon systems. Objectives were to determine whether (1) the Navy plans to adequately test the avionics computer systems before buying them and (2) Navy management oversight of these computer systems has occurred. The Navy is taking a high risk approach in acquiring a new complex computer-based avionics system for its patrol aircraft. Although the Navy originally planned to thoroughly test this system before buying more than four, program delays led to the Navy to postpone complete testing. This clearly contrary to (1) Defense policies which, when followed, should be effective in mitigating computer system development risks and (2) the principle of fly before you buy. GRA

07

AIRCRAFT PROPULSION AND POWER

Includes prime propulsion systems and systems components, e.g., gas turbine engines and compressors; and on-board auxiliary power plants for aircraft.

A91-32700*# Texas A&M Univ., College Station.
FINITE-ELEMENT ANALYSIS OF TURBULENT FLOW IN ANNULAR EXHAUST DIFFUSERS OF GAS TURBINE ENGINES
E. A. BASKHARONE (Texas A & M University, College Station) ASME, Transactions, Journal of Fluids Engineering (ISSN 0098-2202), vol. 113, March 1991, p. 104-110. Houston Advanced Research Center-supported research. refs
(Contract NAS8-37821)
Copyright

A modified version of the Petrov-Galerkin weighted residual method coupled with a biquadratic finite element of the Lagrangian type was used to develop a finite-element model of the turbulent flow field in the annular exhaust diffuser of a gas turbine engine. The swirling flow field was analyzed with emphasis on the diffuser off-design operation. A comparison of the numerical results with experimental data shows that the model is applicable to moderately separating flows of the kind that are typically associated with the off-design performance of diffusing passages in gas turbines. I.S.

A91-34111#
SPANNING THE GLOBE WITH JET PROPULSION
B. L. KOFF (Pratt and Whitney Group, West Palm Beach, FL) AIAA, Annual Meeting and Exhibit, Arlington, VA, Apr. 30-May 2, 1991. 18 p.
(AIAA PAPER 91-2987) Copyright

The role of key propulsion system technological advances and their impact on commercial aviation are outlined. Engine cycle evolution is discussed including fuel efficiency trends, engine performance history, engine performance trends, and increasing overall efficiency from the advent of the early De Havilland Comet Ghost 50 turbojet engines, powering the world's first jet powered airliner in 1952, through the high bypass ratio fan engines such as the Advanced Ducted Propulsor with additional core engine improvements which represent the propulsion systems of the future. Improvements for core engine performance are addressed. The contributions of improved computer modelling techniques in developing improved aerodynamic configurations are noted. Various advances in the development of composites and challenges for the immediate future are cited. Progress in emission reductions, improvements in combustion performance and turbine cooling and materials are reviewed. Various engine systems improvements are outlined. L.K.S.

A91-34808#
THEORETICAL BASIS FOR EXTRAPOLATION OF CALIBRATION DATA OF PTC 6 THROAT TAP NOZZLES
J. W. MURDOCK (Drexel University, Philadelphia, PA) and D. R. KEYSER (U.S. Navy, Naval Air Development Center, Warminster, PA) ASME, Transactions, Journal of Engineering for Gas Turbines and Power (ISSN 0022-0825), vol. 113, April 1991, p. 228-232.
(ASME PAPER 90-JPGC/PTC-1) Copyright

Equations for the extrapolation of calibration data for ASME/PTC 6 throat tap nozzles are derived from boundary layer theory. The results match published coefficients with a maximum difference of +0.03 percent. It is also shown that the effects of transition in the boundary layer extend to throat Reynolds numbers in excess of 10,000,000, far beyond the capacity of any known calibration laboratory. The present PTC 6 requirement that calibration data must be in the fully turbulent range cannot be met with current facilities. Author

A91-34809#
A METHOD FOR THE EXTRAPOLATION OF CALIBRATION DATA OF PTC 6 THROAT TAP NOZZLES
J. W. MURDOCK (Drexel University, Philadelphia, PA) and D. R. KEYSER (U.S. Navy, Naval Air Development Center, Warminster, PA) ASME, Transactions, Journal of Engineering for Gas Turbines and Power (ISSN 0022-0825), vol. 113, April 1991, p. 233-239; Discussion, p. 239, 240; Authors' Closure, p. 240, 241. refs
(ASME PAPER 90-JPGC/PTC-2) Copyright

This paper describes a precise method for extrapolating the coefficient of discharge of PTC 6 throat tap nozzles using all or most of the calibration data. Numerical examples are given using actual calibration data to describe this method. Because this method permits the use of all calibration data at or above Reynolds numbers of 1,000,000, it is a clear improvement over the PTC 6-1976 method, which permits only the highest single point. Author

A91-34811#
SERVICE TEMPERATURE ESTIMATION OF TURBINE BLADES BASED ON MICROSTRUCTURAL OBSERVATIONS
J. M. AURRECOECHEA, W. D. BRENTNALL, and J. R. GAST (Solar Turbines, Inc., San Diego, CA) ASME, Transactions, Journal of Engineering for Gas Turbines and Power (ISSN 0022-0825), vol. 113, April 1991, p. 251-260. refs
(ASME PAPER 90-GT-23) Copyright

Optical and electron metallographic (SEM) examination was performed on MAR-M-421 samples subjected to controlled furnace exposures, to quantify the microstructural changes associated with the prolonged high-temperature exposures. Gamma prime size measurements were used to generate a mathematical model, based on diffusion-controlled kinetics, designed to estimate temperatures. This computational technique was utilized to estimate exposure temperatures of turbine blades that had seen service in land-based gas turbine engines. The engines had accumulated from 1200 to more than 98,000 hours, operating under a variety of conditions. The procedure is generally applicable to commonly used gamma prime strengthened nickel-base superalloys. Author

A91-34813#
FAST RESPONSE WALL PRESSURE MEASUREMENT AS A MEANS OF GAS TURBINE BLADE FAULT IDENTIFICATION
K. MATHIOUDAKIS, A. PAPATHANASIOU, E. LOUKIS, and K. PAPAILIOU (Athens, National Technical University, Greece) ASME, Transactions, Journal of Engineering for Gas Turbines and Power (ISSN 0022-0825), vol. 113, April 1991, p. 269-275. Research supported by Hellenic General Secretariat for Research and Technology and EEC. refs
(ASME PAPER 90-GT-341) Copyright

The distortions of the pressure field around rotating blades of turbomachinery components due to alterations of their shape can be utilized for the identification of faults related to the blading. Measurement of the unsteady pressure field near the wall provides information on such flow and pressure distortions and can thus be used for diagnostic purposes. An experimental investigation of the compressor rotating blade pressure field of an industrial gas turbine has been undertaken, in order to demonstrate the feasibility of the abovementioned principle. Various realistic gas turbine blade faults have been examined. Application of the appropriate processing techniques demonstrates that unsteady pressure measurements can be used to identify the occurrence of minor blade faults (not traceable by standard techniques) as well as the kind of fault. The proposed methodology has the potential for being incorporated in a computerized engine health monitoring system. Author

A91-34814#
FAULT DETECTION AND DIAGNOSIS IN GAS TURBINES
G. MERRINGTON (Department of Defence, Aeronautical Research Laboratories, Melbourne, Australia), OH-KYU KWON (Inha University, Inchon, Republic of Korea), G. GOODWIN (Newcastle, University, Australia), and B. CARLSSON (Uppsala University, Sweden) ASME, Transactions, Journal of Engineering for Gas Turbines and Power (ISSN 0022-0825), vol. 113, April 1991, p. 276-282. refs
(ASME PAPER 90-GT-339) Copyright

Analytical redundancy methods have been applied to gas turbine engine transient data with the view to extracting the desired fault information. The basic idea is to use mathematical models to interrelate the measured variables and then monitor the effects of fault conditions on the new estimates of the model parameters. In the technique to be described, a new method of quantifying the effects of changes in the operating conditions is presented when simplified models are employed. The technique accounts for undermodeling effects and errors arising from linearization of an inherently nonlinear system. Results obtained show a marked improvement over those obtained with traditional methods. Author

A91-34815#
DESIGN OF ROBUST CONTROLLERS FOR GAS TURBINE ENGINES
D. E. MOELLENHOFF, S. VITTAL RAO (Missouri-Rolla, University, Rolla), and C. A. SKARVAN (General Motors Corp., Allison Gas Turbine Div., Indianapolis, IN) ASME, Transactions, Journal of Engineering for Gas Turbines and Power (ISSN 0022-0825), vol. 113, April 1991, p. 283-289. refs
(ASME PAPER 90-GT-113) Copyright

This paper describes robust controller design methodologies for gas turbine engines. A linear state variable model for the engine is derived using partial derivatives. The Linear Quadratic Gaussian with Loop Transfer Recovery (LQG/LTR) and the Parameter Robust Linear Quadratic Gaussian (PRLQG) robust controller design methodologies have been used to design a controller for gas turbine engines. A new method is proposed by combining the features of LQG/LTR and PRLQG methods, which yields good robustness properties with respect to both unstructured uncertainties in the frequency domain and structured parameter

variations in the time domain. The new procedure is illustrated with the help of an aircraft gas turbine engine model. Author

A91-35815
METHODS FOR THE OPTIMIZATION OF THE TESTING AND MODELING OF CONTROL SYSTEMS FOR GAS TURBINE ENGINES [METODY OPTIMIZATSII ISPYTANII I MODELIROVANIIA SISTEM UPRAVLENIIA GAZOTURBINNYMI DVIGATELIAMI]
VIKTOR T. DEDESH, VLADIMIR M. GERMAN, VALERII G. AVGUSTINOVICH, G. N. ARKHIPOV, S. V. BEREZNIAKOV et al. Moscow, Izdatel'stvo Mashinostroenie, 1990, 160 p. In Russian. refs
Copyright

Methods for optimizing laboratory, bench, and flight tests are discussed, as are methods for the physical and mathematical modeling of control systems for gas turbine engines. The role of each type of experimental and simulation studies is defined with reference to the use of a complex optimization criterion including the quality, time, and cost of testing. The possibilities afforded by the use of digital computers in testing are demonstrated. V.L.

A91-35822
CONTROL OF THE WORKING CYCLE OF GAS TURBINE ENGINES (2ND REVISED AND ENLARGED EDITION) [UPRAVLENIE RABOCHIM PROTSESSOM GAZOTURBINNYKH DVIGATELEI /2ND REVISED AND ENLARGED EDITION/]
VLADIMIR P. KOLODOCHKIN Moscow, Izdatel'stvo Mashinostroenie, 1990, 144 p. In Russian. refs
Copyright

The efficiency of single-shaft turbojet and bypass turbofan engines is examined. In particular, attention is given to the effect of the working cycle parameters on the engine output characteristics; engine control; operation of the engine compressor; and interrelation between the cycle parameters. The discussion also covers turbine control; optimization of engine throttle characteristics; specific engine parameters under conditions of bench testing; and optimization of the power plants of multiple-purpose aircraft. V.L.

N91-21137*# National Aeronautics and Space Administration. Lewis Research Center, Cleveland, OH.
INTEGRATED FLIGHT/PROPULSION CONTROL SYSTEM DESIGN BASED ON A DECENTRALIZED, HIERARCHICAL APPROACH
DUANE MATTERN, SANJAY GARG (Sverdrup Technology, Inc., Brook Park, OH.), and RANDY BULLARD 1989 41 p Presented at the Guidance, Navigation and Control Conference, Boston, MA, 14-16 Aug. 1989; sponsored by AIAA Previously announced in IAA as A89-53301
(NASA-TM-103678; E-5895; NAS 1.15:103678; AIAA-89-3519) Avail: NTIS HC/MF A03 CSCL 21/5

A sample integrated flight/propulsion control system design is presented for the piloted longitudinal landing task with a modern, statistically unstable fighter aircraft. The design procedure is summarized. The vehicle model used in the sample study is described, and the procedure for partitioning the integrated system is presented along with a description of the subsystems. The high-level airframe performance specifications and control design are presented and the control performance is evaluated. The generation of the low-level (engine) subsystem specifications from the airframe requirements are discussed, and the engine performance specifications are presented along with the subsystem control design. A compensator to accommodate the influence of airframe outputs on the engine subsystem is also considered. Finally, the entire closed loop system performance and stability characteristics are examined. Author

N91-21138*# Sverdrup Technology, Inc., Brook Park, OH.
A MODAL AEROELASTIC ANALYSIS SCHEME FOR TURBOMACHINERY BLADING M.S. Thesis - Case Western Reserve Univ. Final Report
TODD E. SMITH Mar. 1991 132 p
(Contract NAS3-25266)
(NASA-CR-187089; E-6081; NAS 1.26:187089) Avail: NTIS HC/MF A07 CSCL 21/5

An aeroelastic analysis is developed which has general application to all types of axial-flow turbomachinery blades. The approach is based on linear modal analysis, where the blade's dynamic response is represented as a linear combination of contributions from each of its in-vacuum free vibrational modes. A compressible linearized unsteady potential theory is used to model the flow over the oscillating blades. The two-dimensional unsteady flow is evaluated along several stacked axisymmetric strips along the span of the airfoil. The unsteady pressures at the blade surface are integrated to result in the generalized force acting on the blade due to simple harmonic motions. The unsteady aerodynamic forces are coupled to the blade normal modes in the frequency domain using modal analysis. An iterative eigenvalue problem is solved to determine the stability of the blade when the unsteady aerodynamic forces are included in the analysis. The approach is demonstrated by applying it to a high-energy subsonic turbine blade from a rocket engine turbopump power turbine. The results indicate that this turbine could undergo flutter in an edgewise mode of vibration. Author

N91-21139*# Institute for Computer Applications in Science and Engineering, Hampton, VA.
PRELIMINARY CALIBRATION OF A GENERIC SCRAMJET COMBUSTOR Final Interim Report No. 16
P. A. JACOBS, R. G. MORGAN, R. C. ROGERS, M. WENDT, C. BRESCIANINI, A. PAULL, and G. KELLY (Queensland Univ., Saint Lucia, Australia) Mar. 1991 32 p Sponsored by Australian Research Council
(Contract NAS1-18605; NAGW-674)
(NASA-CR-187539; NAS 1.26:187539; ICASE-16) Avail: NTIS HC/MF A03 CSCL 21/5

The results of a preliminary investigation of the combustion of hydrogen fuel at hypersonic flow conditions are provided. The tests were performed in a generic, constant-area combustor model with test gas supplied by a free-piston-driven reflected-shock tunnel. Static pressure measurements along the combustor wall indicated that burning did occur for combustor inlet conditions of P(static) approximately equal to 19kPa, T(static) approximately equal to 1080 K, and U approximately equal to 3630 m/s with a fuel equivalence ratio approximately equal to 0.9. These inlet conditions were obtained by operating the tunnel with stagnation enthalpy approximately equal to 8.1 MJ/kg, stagnation pressure approximately equal to 52 MPa, and a contoured nozzle with a nominal exit Mach number of 5.5. Author

N91-21140*# National Aeronautics and Space Administration. Lewis Research Center, Cleveland, OH.
INTEGRATED FLIGHT/PROPULSION CONTROL DESIGN FOR A STOVL AIRCRAFT USING H-INFINITY CONTROL DESIGN TECHNIQUES
SANJAY GARG and PETER J. OUZTS 1991 33 p Presented at the American Control Conference, Boston, MA, 26-28 Jun. 1991; sponsored in part by the American Automatic Control Council
(NASA-TM-104340; E-6113; NAS 1.15:104340) Avail: NTIS HC/MF A03 CSCL 21/5

Results are presented from an application of H-infinity control design methodology to a centralized integrated flight propulsion control (IFPC) system design for a supersonic Short Takeoff and Vertical Landing (STOVL) fighter aircraft in transition flight. The emphasis is on formulating the H-infinity control design problem such that the resulting controller provides robustness to modeling uncertainties and model parameter variations with flight condition. Experience gained from a preliminary H-infinity based IFPC design study performed earlier is used as the basis to formulate the robust H-infinity control design problem and improve upon the previous design. Detailed evaluation results are presented for a reduced order controller obtained from the improved H-infinity control design showing that the control design meets the specified nominal performance objectives as well as provides stability robustness for variations in plant system dynamics with changes

in aircraft trim speed within the transition flight envelope. A controller scheduling technique which accounts for changes in plant control effectiveness with variation in trim conditions is developed and off design model performance results are presented. Author

N91-21143# Wright Research Development Center, Wright-Patterson AFB, OH.
AN EXPERIMENTAL STUDY OF EXIT FLOW PATTERNS IN A MULTISTAGE COMPRESSOR IN ROTATING STALL Final Technical Report, Jun. 1989 - May 1990
STEVEN E. GORRELL Nov. 1990 146 p
(AD-A231353; WRDC-TR-90-2083) Avail: NTIS HC/MF A07 CSCL 13/7

High-response pressure measurements of a high-speed, 10-stage, axial-flow compressor operating in rotating stall are analyzed. Procedures used to digitize analog voltages and calibrate pressure transducers are presented. From total and static pressures measured at the exit of the test compressor, stall cell Mach number distributions are calculated and used to study the effects of discharge throttle levels and variable vane changes on the 10th-stage rotating stall cells. Results indicate that significant transition zones exist between the reverse flow and peak Mach number of the stall cell cycle. Since the axial Mach numbers of the stall cell cycle are constantly changing, the amount of leading and trailing edge transition zones and fully unstalled flow zones are not easily defined. A method is devised to approximate the different flow zone ranges and correlate them to in-stall pressure characteristic behavior of the 10th stage of the test compressor. Changes in the time-averaged pressure characteristics are found to correlate with changes in the rotating stall flow zones. A lower pressure coefficient appears to correspond to an increase in ratio of trailing to leading edge transition zone size and the average transition zone size. Results also suggest that recovery hysteresis in the test compressor is characterized by reverse flow in the rotating stall cell. GRA

N91-22122 Cranfield Inst. of Tech., Bedford (England).
EXPERIMENTAL STUDY OF RADIATION FROM COATED TURBINE BLADES Ph.D. Thesis
ARKAN KHILKHAL HUSAI AL-TAIE 1990 301 p
Avail: Univ. Microfilms Order No. BRDX90876

The specific power of modern gas turbines is much influenced by the gas temperature at turbine inlet. Ceramic coatings operate as thermal barriers and can allow gas temperature to be increased by 50 to 220 K. There is little experience in measuring surface temperatures of blades coated with ceramic coatings. There is evidence that the radiation signal picked up by the pyrometer will not only depend on the surface temperature but also on a number of optical properties of the coating. Among these are the emissivity of the coating and whether the coating is translucent. Parameters affecting this are coating material, coating surface finish, coating thickness, and whether or not a bond coat is used. These variables are explored in a rig that simulates the conditions within a turbine stage of a gas turbine engine. Six thermal barrier coating systems were tested, including four stabilized zirconia systems and two alumina based systems. Analysis shows that the measured blade surface temperature was within 10 K of that calculated. The use of 0.3 mm of C-YPSZ on air cooled turbine blades caused 250 K surface temperature increase and 270 K metal temperature decrease for turbine entry temperature of 1673 K. Dissert. Abstr.

N91-22124# Naval Postgraduate School, Monterey, CA.
AN EXPERIMENTAL INVESTIGATION INTO NO(X) CONTROL OF A GAS TURBINE COMBUSTOR AND AUGMENTOR TUBE INCORPORATING A CATALYTIC REDUCTION SYSTEM M.S. Thesis
CHRISTOPHER K. BEHRENS Mar. 1990 88 p
(AD-A231427) Avail: NTIS HC/MF A05 CSCL 24/1

An initial experimental investigation was conducted to examine the feasibility of NO(x) emission control using catalytic reduction techniques in the jet engine test cell environment. A modified T-63 gas turbine combustor and an augmentor tube, 21 feet in length and containing a perlite catalyst, were used as a gas generator and catalytic reduction system. Four data runs were made. Three runs were completed without the catalyst installed. Temperature and velocity profile measurements were obtained in order to calculate augmentation ratios for different engine fuel to air ratios. NO(x), CO, and unburned hydrocarbon concentrations in the exhaust were measured to provide a baseline for further tests. A fourth data run was made with the perlite catalyst installed in the augmentor tube. A 64 percent NO(x) reduction was observed, however, the large pressure drop across the catalytic bed deemed the current configuration impractical. Recommendations for alternative configurations are presented. The results of the investigation have proven that further study is warranted. GRA

N91-22125# Marquardt Corp., Van Nuys, CA.
SKIN FRICTION MEASUREMENT TECHNIQUES FOR SCRAMJET APPLICATIONS. PHASE 1: PRELIMINARY DESIGN Final Report, Sep. 1989 - Feb. 1990
R. C. STEELE Aug. 1990 60 p
(Contract F33615-87-C-2755)
(AD-A231899; MR-S-1800-PHASE-1;
WRDC-TR-90-2062-PHASE-1) Avail: NTIS HC/MF A04 CSCL 20/4

The objective of this program was to carry out a preliminary design of a gauge to measure skin friction of a scramjet combustor. Preliminary designs of two skin friction measurement approaches have been completed. The work was accomplished by the Marquardt Company and a subcontracted group from Virginia Polytechnic Institute (VPI). With the recent interest in hypersonic flight the challenge to obtain accurate skin friction measurements has became necessary. For example, at a flight condition of Mach 8, at 100,000 feet altitude the estimated skin friction drag of a scramjet engine is approximately 36 percent of the net thrust. The environment within a scramjet combustor is extremely hostile of any physical object, thus increasing the difficulty of successful measurement of skin friction. The first approach reported is the Cantilever Beam (Design A) design based on the use of a multi-purpose displacement transducer which has the property of being very sensitive while still being stiff. The second or the Thin Film (Design B) approach is a newly established concept by VPI. The design exploits thin film sputtering technology for the purpose of attaching microstrain gauges. GRA

08

AIRCRAFT STABILITY AND CONTROL

Includes aircraft handling qualities; piloting; flight controls; and autopilots.

A91-33535*# National Aeronautics and Space Administration. Ames Research Center, Moffett Field, CA.
REDUCTION OF AERODYNAMIC AUGMENTED STATES IN ACTIVE FLUTTER SUPPRESSION SYSTEMS
E. NISSIM (NASA, Ames Research Center, Moffett Field, CA) Journal of Aircraft (ISSN 0021-8669), vol. 28, Jan. 1991, p. 82-93. Previously cited in issue 23, p. 3618, Accession no. A89-52561. refs
Copyright

A91-33536*# National Aeronautics and Space Administration. Langley Research Center, Hampton, VA.
CONICAL EULER SIMULATION OF WING ROCK FOR A DELTA WING PLANFORM
ELIZABETH M. LEE and JOHN T. BATINA (NASA, Langley Research Center, Hampton, VA) Journal of Aircraft (ISSN 0021-8669), vol. 28, Jan. 1991, p. 94-96. refs
Copyright

Unsteady, vortex-dominated flowfields are presently studied by using the conical Euler equations as an efficient first step toward

investigation of the full three-dimensional problem, under the assumption that the supersonic flow about a delta wing is conical and therefore allows the three-dimensional problem to be reduced to a two-dimensional one. Attention is given to the case of a delta wing undergoing wing-rock motion. The code developed has also been modified to allow treatment of the 'free-to-roll' case. O.C.

A91-33611
THE ADVANTAGES OF VELOCITY VECTOR REFERENCING IN PROPORTIONAL NAVIGATION
PRAVAS R. MAHAPATRA and UDAY S. SHUKLA (Indian Institute of Science, Bangalore, India) IN: IEEE PLANS '90 - Position Location and Navigation Symposium, Las Vegas, NV, Mar. 20-23, 1990, Record. New York, Institute of Electrical and Electronics Engineers, Inc., 1990, p. 102-109. refs
Copyright

Two broad classes of proportional navigation laws are compared with regard to their implementation, analysis, and behavior. The first consists of laws such as the PPN (pure proportional navigation) laws, which are referenced relative to the pursuer velocity vector, and the second consists of line-of-sight (LOS) referenced laws such as TPN (true PN), GTPN (generalized TPN), and GGL (generalized guidance law). It is shown that the latter class has serious drawbacks in terms of implementation and trajectory behavior, which more than offset the limited advantage in analytical treatment exploited hitherto in the literature. Among the major drawbacks are forward acceleration and braking requirements which are difficult to achieve, relative inefficiency in the utilization of control effects, restrictions on initial conditions for intercept, lack of robustness, and the possibility of unbounded acceleration. From a practical point of view, PPN is a superior guidance law to TPN and its generalizations. The only utility of the LOS-reference laws appears to be to serve as approximations to analyze the more practical and efficient PPN law and its variants. I.E.

A91-33639#
FLIGHT EVALUATION OF THE INTEGRATED INERTIAL SENSOR ASSEMBLY (IISA) ON A HELICOPTER
ROBERT E. MACK and JACK J. JANKOVITZ (U.S. Navy, Naval Air Development Center, Warminster, PA) IN: IEEE PLANS '90 - Position Location and Navigation Symposium, Las Vegas, NV, Mar. 20-23, 1990, Record. New York, Institute of Electrical and Electronics Engineers, Inc., 1990, p. 322-329.

After successful flight test evaluation of the Integrated Inertial Sensor Assembly (IISA) on an F-15 aircraft, the system was installed onboard a Blackhawk helicopter at Wilmington Airport in Delaware. An overview of the flight test evaluation conducted on the Blackhawk is presented. It is concluded that all program objectives were successfully demonstrated and proved that the IISA system can be used for helicopter applications. The IISA Helicopter Demonstration Program consisted of two phases. During the first phase, vibration data were obtained to quantify the helicopter's vibration environment. Based on these data, IISA's digital flight control filters were modified for flight control signal quality evaluations during the second phase. During the flight tests, no evidence of body bending modes or local structural vibration degrading IISA's performance was found. The flight test data indicate that IISA's flight control signals have the necessary dynamic range to satisfy future helicopter fly-by-wire flight control systems. IISA's redundancy management software worked flawlessly during the insertion of hardover failures. From the standpoint of flight safety IISA exhibits full QUAD redundancy. I.E.

A91-33640
FAILURE MANAGEMENT IN SPATIO-TEMPORAL REDUNDANT, INTEGRATED NAVIGATION AND FLIGHT CONTROL REFERENCE-SYSTEMS
UWE K. KROGMANN (Bodenseewerk Geraetetechnik GmbH, Ueberlingen, Federal Republic of Germany) IN: IEEE PLANS '90 - Position Location and Navigation Symposium, Las Vegas, NV, Mar. 20-23, 1990, Record. New York, Institute of Electrical and Electronics Engineers, Inc., 1990, p. 330-337.
Copyright

Failure management techniques for highly reliable, fault-tolerant inertial reference systems are described. Cost, weight, and power considerations imply the use of a minimum number of inertial sensors in a skewed geometry. Fault-tolerant hardware performance is obtained by spatially separated channels with a preceptron-type information flow. Data diversity in temporally separated software channels yields software fault tolerance. Advanced vector space procedures for fault detection, localization, masking, and dynamic system reconfiguration permit safe and quick response, yielding minimal data and recovery latency. I.E.

A91-34162
UNSTEADY AERODYNAMIC MODELLING FOR AIRCRAFT LATERAL PARAMETER ESTIMATION
J. SINGH and S. C. RAISINGHANI (Indian Institute of Technology, Kanpur, India) Aeronautical Journal (ISSN 0001-9240), vol. 95, March 1991, p. 88-94. refs
Copyright

A mathematical model of unsteady aerodynamic effects for use in lateral aircraft dynamics has been proposed based on Weissinger's arrangement of trailing vortex system. The suggested model is shown to be suitable for use in parameter extraction algorithm. Simulated flight data of an example airplane has been analyzed through maximum likelihood parameter estimation algorithm in frequency-domain to show the effect of inclusion and omission of unsteady aerodynamics on estimated parameters. Author

A91-34816#
NONLINEAR BEHAVIOR OF A ROTORCRAFT MODEL DURING AIR RESONANCE
G. T. FLOWERS (South Florida, University, Tampa, FL) and B. H. TONGUE (California, University, Berkeley) ASME, Transactions, Journal of Vibration and Acoustics (ISSN 0739-3717), vol. 113, April 1991, p. 141-151. U.S. Army-supported research. refs
Copyright

The term 'air resonance' refers to an instability associated with helicopters in hover. It is characterized by a coupling between motions of the fuselage and the blades and is of primary concern for helicopters having soft in-plane rotors. This paper presents a study of the effects of nonlinearities on the dynamical behavior of a simplified air resonace model. In order to provide a direct comparison between the behavior of the linearized system and the nonlinear one, a linear analysis of the air resonance model is first performed. Then, the system is analyzed for the effect of selected nonlinearities on its steady state dynamical responses. Geometric nonlinearities and cubic lag damping are considered in these analyses. Author

A91-35576
A FREQUENCY DOMAIN MAXIMUM LIKELIHOOD IDENTIFICATION SCHEME WITH APPLICATION TO FLIGHT FLUTTER DATA ANALYSIS
HERMAN VAN DER AUWERAER, JAN LEURIDAN (LMS International, Louvain, Belgium), RIK PINTELON, and JOHAN SCHOUKENS (Brussels, Free University, Belgium) IN: International Modal Analysis Conference, 8th, Kissimmee, FL, Jan. 29-Feb. 1, 1990, Proceedings. Vol. 2. Bethel, CT, Society for Experimental Mechanics, Inc., 1990, p. 1252-1261. refs
Copyright

The paper deals with the application of a frequency domain maximum likelihood estimation method for linear system identification in the field of flutter data analysis. Unlike methods based on least squares error minimization, the proposed method takes into account the disturbing process or measurement noise on as well the input as the output of the device under test. This enables the optimal and unbiased identification of the parameters in the linear system model. A few examples of the identification of the system parameters of a mechanical single-input single-output

system from flutter test data are discussed and compared to more classical linear estimation methods. Author

N91-21144*# National Aeronautics and Space Administration. Langley Research Center, Hampton, VA.
HOT-BENCH SIMULATION OF THE ACTIVE FLEXIBLE WING WIND-TUNNEL MODEL
CAREY S. BUTTRILL and JACOB A. HOUCK Nov. 1990 14 p Presented at the AIAA Flight Simulation Technologies Conference, Dayton, OH, 17-19 Sep. 1990 Previously announced in IAA as A91-16678
(NASA-TM-102758; NAS 1.15:102758; AIAA-90-3121) Avail: NTIS HC/MF A03 CSCL 01/3

Two simulations, one batch and one real-time, of an aeroelastically-scaled wind-tunnel model were developed. The wind-tunnel model was a full-span, free-to-roll model of an advanced fighter concept. The batch simulation was used to generate and verify the real-time simulation and to test candidate control laws prior to implementation. The real-time simulation supported hot-bench testing of a digital controller, which was developed to actively control the elastic deformation of the wind-tunnel model. Time scaling was required for hot-bench testing. The wind-tunnel model, the mathematical models for the simulations, the techniques employed to reduce the hot-bench time-scale factors, and the verification procedures are described. IAA

N91-21149*# Systems Technology, Inc., Mountain View, CA.
FULLY AUTOMATIC GUIDANCE AND CONTROL FOR ROTORCRAFT NAP-OF-THE-EARTH FLIGHT FOLLOWING PLANNED PROFILES. VOLUME 1: REAL-TIME PILOTED SIMULATION
WARREN F. CLEMENT, PETER J. GORDER, and WAYNE F. JEWELL Jan. 1991 145 p
(Contract NAS2-12640)
(NASA-CR-177571-VOL-1; NAS 1.26:177571-VOL-1; STI-TR-1254-1) Avail: NTIS HC/MF A07 CSCL 01/3

Developing a single-pilot, all-weather nap-of-the-earth (NOE) capability requires fully automatic NOE (ANOE) navigation and flight control. Innovative guidance and control concepts are investigated in a four-fold research effort that: (1) organizes the on-board computer-based storage and real-time updating of NOE terrain profiles and obstacles in course-oriented coordinates indexed to the mission flight plan; (2) defines a class of automatic anticipative pursuit guidance algorithms and necessary data preview requirements to follow the vertical, lateral, and longitudinal guidance commands dictated by the updated flight profiles; (3) automates a decision-making process for unexpected obstacle avoidance; and (4) provides several rapid response maneuvers. Acquired knowledge from the sensed environment is correlated with the forehand knowledge of the recorded environment (terrain, cultural features, threats, and targets), which is then used to determine an appropriate evasive maneuver if a nonconformity of the sensed and recorded environments is observed. This four-fold research effort was evaluated in both fixed-based and moving-based real-time piloted simulations, thereby, providing a practical demonstration for evaluating pilot acceptance of the automated concepts, supervisory override, manual operation, and re-engagement of the automatic system. Volume one describes the major components of the guidance and control laws as well as the results of the piloted simulations. Volume two describes the complete mathematical model of the fully automatic guidance system for rotorcraft NOE flight following planned flight profiles. Author

N91-21150*# Systems Technology, Inc., Mountain View, CA.
FULLY AUTOMATIC GUIDANCE AND CONTROL FOR ROTORCRAFT NAP-OF-THE-EARTH FLIGHT FOLLOWING PLANNED PROFILES. VOLUME 2: MATHEMATICAL MODEL
WARREN F. CLEMENT, PETER J. GORDER, and WAYNE F. JEWELL Jan. 1991 468 p
(Contract NAS2-12640)
(NASA-CR-177571-VOL-2; NAS 1.26:177571-VOL-2; STI-TR-1254-2) Avail: NTIS HC/MF A20 CSCL 01/3

Developing a single-pilot, all-weather nap-of-the-earth (NOE) capability requires fully automatic NOE (ANOE) navigation and flight control. Innovative guidance and control concepts are investigated in a four-fold research effort that: (1) organizes the on-board computer-based storage and real-time updating of NOE terrain profiles and obstacles in course-oriented coordinates indexed to the mission flight plan; (2) defines a class of automatic anticipative pursuit guidance algorithms and necessary data preview requirements to follow the vertical, lateral, and longitudinal guidance commands dictated by the updated flight profiles; (3) automates a decision-making process for unexpected obstacle avoidance; and (4) provides several rapid response maneuvers. Acquired knowledge from the sensed environment is correlated with the forehand knowledge of the recorded environment (terrain, cultural features, threats, and targets), which is then used to determine an appropriate evasive maneuver if a nonconformity of the sensed and recorded environments is observed. This four-fold research effort was evaluated in both fixed-base and moving-base real-time piloted simulations; thereby, providing a practical demonstration for evaluating pilot acceptance of the automated concepts, supervisory override, manual operation, and re-engagement of the automatic system. Volume one describes the major components of the guidance and control laws as well as the results of the piloted simulations. Volume two describes the complete mathematical model of the fully automatic guidance system for rotorcraft NOE flight following planned flight profiles. GRA

N91-21151# Institut Franco-Allemand de Recherches, Saint-Louis (France).
POSSIBILITIES OF TRAJECTORY MODIFICATION [MOEGLICHKEITEN ZUR FLUGBAHNBEEINFLUSSUNG]
G. PATZ, G. SMEETS, K. W. NAUMANN, and H. ENDE 23 Jan. 1990 19 p In GERMAN Presented at ONERA, Palaiseau, France, 3 Oct. 1989
(Contract BMVG-T/R-760/K-0007/K-1707)
(ISL-CO-209/90; ETN-91-98983) Avail: NTIS HC/MF A03

The feasibility of some projects for the piloting of flight vehicles by gaseous spoilers and external combustion is studied. Experimental tests were carried out with shock tubes at the flow conditions of self-ignition. A supersonic wind tunnel was used to investigate the formation of combustible mixtures, such as hydrogen/air and acetylene/air, with varied Mach numbers and configurations. Measurements are obtained by Raman diffusion and showed that the mixture formation significantly influences the turbulent flows. ESA

N91-21152# Deutsche Forschungsanstalt fuer Luft- und Raumfahrt, Brunswick (Germany, F.R.). Abt. fuer Drehfluegelflugzeuge.
RESULTS OF THE HHC WIND TUNNEL TESTS, 1986 - 1988
ROLAND KUBE, GERT LEHMANN, and SUSANNE MALKE Jun. 1990 120 p In GERMAN; ENGLISH summary Report will also be announced as translation (ESA-TT-1257)
(DLR-FB-90-42; ISSN-0171-1342; ETN-91-99034) Avail: NTIS HC/MF A06; DLR, Wissenschaftliches Berichtswesen, VB-PL-DO, Postfach 90 60 58, 5000 Cologne, Fed. Republic of Germany, HC 51 DM

The results of two higher harmonic control (HHC) wind tunnel experiments, which included open and closed loop tests, are presented. The rotor test rig, the data acquisition system, the higher harmonic control system, and the calibration method are described, and the achievable accuracy is specified. The illustration of the tests results provides information about the rotor reaction in the case of higher harmonic control inputs and demonstrates the behavior of the implemented controller. ESA

N91-21153# Minnesota Univ., Minneapolis. Dept. of Aerospace Engineering and Mechanics.
EIGENSPACE DESIGN OF HELICOPTER FLIGHT CONTROL SYSTEMS Final Report
WILLIAM L. GARRARD and EICHER LOW Nov. 1990 204 p

(Contract DAAL03-86-K-0056)
(AD-A231588; ARO-23422.9-EL) Avail: NTIS HC/MF A10 CSCL 01/3

An eigenstructure based design methodology for helicopter flight control systems is developed and evaluated. A detailed review is provided of the application of multivariable design techniques to helicopter flight control systems, along with a review of applicable handling quality specifications, a description of the mathematical models used, a presentation of the theory of eigenstructure design, application of the theory to a helicopter design problem, and evaluation of the performance and robustness properties of the resulting control laws. GRA

N91-22127*# Washington Univ., Seattle. Dept. of Aeronautics and Astronautics.
ROBUST INTEGRATED AUTOPILOT/AUTOTHROTTLE DESIGN USING CONSTRAINED PARAMETER OPTIMIZATION Final Report, 16 Sep. 1988 - 16 Sep. 1990
UY-LOI LY, CHRISTOPHER VOTH, and SWAMY SANJAY 1990 203 p
(Contract NAG1-193)
(NASA-CR-188011; NAS 1.26:188011) Avail: NTIS HC/MF A10 CSCL 01/3

A multivariable control design method based on constrained parameter optimization was applied to the design of a multiloop aircraft flight control system. Specifically, the design method is applied to the following: (1) direct synthesis of a multivariable 'inner-loop' feedback control system based on total energy control principles; (2) synthesis of speed/altitude-hold designs as 'outer-loop' feedback/feedforward control systems around the above inner loop; and (3) direct synthesis of a combined 'inner-loop' and 'outer-loop' multivariable control system. The design procedure offers a direct and structured approach for the determination of a set of controller gains that meet design specifications in closed-loop stability, command tracking performance, disturbance rejection, and limits on control activities. The presented approach may be applied to a broader class of multiloop flight control systems. Direct tradeoffs between many real design goals are rendered systematic by this method following careful problem formulation of the design objectives and constraints. Performance characteristics of the optimization design were improved over the current autopilot design on the B737-100 Transport Research Vehicle (TSRV) at the landing approach and cruise flight conditions; particularly in the areas of closed-loop damping, command responses, and control activity in the presence of turbulence. Author

N91-22131*# National Aeronautics and Space Administration. Hugh L. Dryden Flight Research Facility, Edwards, CA.
RESEARCH FLIGHT-CONTROL SYSTEM DEVELOPMENT FOR THE F-18 HIGH ALPHA RESEARCH VEHICLE
JOSEPH W. PAHLE, BRUCE POWERS, VICTORIA REGENIE, VINCE CHACON, STEVE DEGROOTE, and STEVEN MURNYAK (McDonnell Aircraft Co., Saint Louis, MO.) Apr. 1991 25 p Presented at the High-Angle-of-Attack Technology Conference, Hampton, VA, 30 Oct. - 1 Nov. 1990
(NASA-TM-104232; H-1715; NAS 1.15:104232) Avail: NTIS HC/MF A03 CSCL 01/3

The F-18 high alpha research vehicle was recently modified by adding a thrust vectoring control system. A key element in the modification was the development of a research flight control system integrated with the basic F-18 flight control system. Discussed here are design requirements, system development, and research utility of the resulting configuration as an embedded system for flight research in the high angle of attack regime. Particular emphasis is given to control system modifications and control law features required for high angle of attack flight. Simulation results are used to illustrate some of the thrust vectoring control system capabilities and predicted maneuvering improvements. Author

N91-22132# Bristol Univ. (England). Dept. of Aerospace Engineering.
SIGNAL BLENDING IN CONTROL SYSTEMS STRUCTURAL INTERACTIONS B.S. Thesis
R. M. HART and J. C. RUTLER Jun. 1990 63 p
(BU-505; ETN-91-99198) Avail: NTIS HC/MF A04

Flexible modes of vibration must be removed from the feedback control system of an aircraft. A computer model of a rig, which was being used to model an aircraft fuselage as a simple beam, was created in order to calculate the gains required to remove these modes of vibration using signal blending, instead of notch filters with their associated problems. This was achieved successfully, and the effects of variations of stiffness and damping, that occur when an aircraft is in flight, on signal blending were investigated using the computer model. ESA

N91-22133# Bristol Univ. (England). Dept. of Aerospace Engineering.
FLUTTER SUPPRESSION OF AN AIRCRAFT WING USING A CONTROL SURFACE B.S. Thesis
N. P. JACKSON and D. J. TOSTEVIN Jun. 1990 128 p
(BU-506; ETN-91-99199) Avail: NTIS HC/MF A07

A set of techniques was devised to design a control system to suppress the onset of hard and soft flutter to a higher speed. The study was a purely theoretical analysis carried out an two wing models: a tip missile configuration which exhibited hard flutter, and an engine pylon configuration which exhibited soft flutter. The method of flutter control used frequency response data fits around unity radius encirclements of the 1 point on Nyquist plots. These methods were revised and made much more efficient and easy to use giving better results than achieved before. The engine pylon (soft flutter) model was suppressed to 1.37 Vf using the onboard pair of tranducers as defined by BAe (British Aerospace), and the tip missile (hard flutter) model was suprressed to 1.73 Vf using all four BAe transducers as defined by BAe. These control laws gave stability between the original flutter speeds and those as above so gain scheduling against velocity was not required. Using an optical transducer positioning method, the soft flutter model was suppressed further, to 1.46 Vf but the outboard transducers were found to be in the optimal position for the hard flutter model. ESA

N91-22332*# National Aeronautics and Space Administration. Langley Research Center, Hampton, VA.
AN OVERVIEW OF THE ACTIVE FLEXIBLE WING PROGRAM
STANLEY R. COLE, BOYD PERRY, III, and GERALD D. MILLER (Rockwell International Corp., Los Angeles, CA.) *In its* Fourth NASA Workshop on Computational Control of Flexible Aerospace Systems, Part 2 p 459-495 Mar. 1991
Avail: NTIS HC/MF A20 CSCL 01/3

An outline of the Active Flexible Wing (AFW) project that was meant to serve as an introduction to an entire session of the Computational Control Workshop is presented. Following background information on the project is a description of the AFW wind tunnel model and results from the initial wind tunnel test of the AFW model under the current project. Emphasis is on major project accomplishments. The AFW project is an effort to demonstrate aeroelastic control through the application of digital controls technology. Active flutter suppression and active control of maneuver loads during high speed rolling maneuvers are examined. Author

N91-22334*# National Aeronautics and Space Administration. Langley Research Center, Hampton, VA.
DESIGN AND TEST OF THREE ACTIVE FLUTTER SUPPRESSION CONTROLLERS
DAVID M. CHRISTHILF, MARTIN R. WASZAK, WILLIAM M. ADAMS, S. SRINATHKUMAR (National Aeronautical Lab., Bangalore, India), and VIVEK MUKHOPADHYAY *In its* Fourth NASA Workshop on Computational Control of Flexible Aerospace Systems, Part 2 p 535-560 Mar. 1991
Avail: NTIS HC/MF A20 CSCL 01/3

Three flutter suppression control law design techniques are

presented. Each uses multiple control surfaces and/or sensors. The first uses linear combinations of several accelerometer signals together with dynamic compensation to synthesize the modal rate of the critical mode for feedback to distributed control surfaces. The second uses traditional tools (pole/zero loci and Nyquist diagrams) to develop a good understanding of the flutter mechanism and produce a controller with minimal complexity and good robustness to plant uncertainty. The third starts with a minimum energy Linear Quadratic Gaussian controller, applies controller order reduction, and then modifies weight and noise covariance matrices to improve multi-variable robustness. The resulting designs were implemented digitally and tested subsonically on the Active Flexible Wing (AFW) wind tunnel model. Test results presented here include plant characteristics, maximum attained closed-loop dynamic pressure, and Root Mean Square control surface activity. A key result is that simultaneous symmetric and antisymmetric flutter suppression was achieved by the second control law, with a 24 percent increase in attainable dynamic pressure. Author

N91-22335*# Rockwell International Corp., Los Angeles, CA.
ROLL PLUS MANEUVER LOAD ALLEVIATION CONTROL SYSTEM DESIGNS FOR THE ACTIVE FLEXIBLE WING WIND-TUNNEL MODEL
DOUGLAS B. MOORE, GERALD D. MILLER, and MARTIN J. KLEPL *In* NASA, Langley Research Center, Fourth NASA Workshop on Computational Control of Flexible Aerospace Systems, Part 2 p 561-582 Mar. 1991
Avail: NTIS HC/MF A20 CSCL 01/3

Three designs for controlling loads while rolling for the Active Flexible Wing (AFW) are discussed. The goal is to provide good roll control while simultaneously limiting the torsion and bending loads experienced by the wing. The first design uses Linear Quadratic Gaussian/Loop Transfer Recovery (LQG/LTR) modern control methods to control roll rate and torsional loads at four different wing locations. The second design uses a nonlinear surface command function to produce surface position commands as a function of current roll rate and commanded roll rate. The final design is a flutter suppression control system. This system stabilizes both symmetric and axisymmetric flutter modes of the AFW. Author

N91-22337*# National Aeronautics and Space Administration. Langley Research Center, Hampton, VA.
DEVELOPMENT AND TESTING OF CONTROLLER PERFORMANCE EVALUATION METHODOLOGY FOR MULTI-INPUT/MULTI-OUTPUT DIGITAL CONTROL SYSTEMS
ANTHONY POTOTZKY (Lockheed Engineering and Sciences Co., Hampton, VA.), CAROL WIESEMAN, SHERWOOD TIFFANY HOADLEY, and VIVEK MUKHOPADHYAY *In its* Fourth NASA Workshop on Computational Control of Flexible Aerospace Systems, Part 2 p 615-653 Mar. 1991
Avail: NTIS HC/MF A20 CSCL 01/3

Described here is the development and implementation of on-line, near real time controller performance evaluation (CPE) methods capability. Briefly discussed are the structure of data flow, the signal processing methods used to process the data, and the software developed to generate the transfer functions. This methodology is generic in nature and can be used in any type of multi-input/multi-output (MIMO) digital controller application, including digital flight control systems, digitally controlled spacecraft structures, and actively controlled wind tunnel models. Results of applying the CPE methodology to evaluate (in near real time) MIMO digital flutter suppression systems being tested on the Rockwell Active Flexible Wing (AFW) wind tunnel model are presented to demonstrate the CPE capability. Author

N91-23053*# National Aeronautics and Space Administration. Lewis Research Center, Cleveland, OH.
CIVIL AIR TRANSPORT: A FRESH LOOK AT POWER-BY-WIRE AND FLY-BY-LIGHT
GALE R. SUNDBERG *In* National Aeronautics and Space Administration, Technology 2000, Volume 1 p 263-267 Mar. 1991 Previously announced as N90-21283
Avail: NTIS HC/MF A18 CSCL 01/3

Power-by-wire (PBW) is a key element under subsonic transport flight systems technology with potential savings of over 10 percent in operating empty weight and in fuel consumption compared to today's transport aircraft. The PBW technology substitutes electrical actuation in place of centralized hydraulics, uses internal starter-motor/generators and eliminates the need for variable engine bleed air to supply cabin comfort. The application of advanced fiber optics to the electrical power system controls, to built-in-test (BIT) equipment, and to fly-by-light (FBL) flight controls provides additional benefits in lightning and high energy radio frequency (HERF) immunity over existing mechanical or even fly-by-wire controls. The program plan is reviewed and a snapshot is given of the key technologies and their benefits to all future aircraft, both civil and military. Author

09

RESEARCH AND SUPPORT FACILITIES (AIR)

Includes airports, hangars and runways; aircraft repair and overhaul facilities; wind tunnels; shock tube facilities; and engine test blocks.

A91-33371
ROTORS IN THE WIND TUNNEL - DLR HELICOPTER RESEARCH METHODS IN THE GERMAN-DUTCH WIND TUNNEL [ROTOREN IM WINDKANAL - DLR-HUBSCHRAUBER-VERSUCHSTECHNIK IM DNW]
BERND GMELIN, HANS-JUERGEN LANGER, and GUNTER BRAUN (DLR, Institut fuer Flugmechanik, Brunswick, Federal Republic of Germany) DLR-Nachrichten (ISSN 0937-0420), Feb. 1991, p. 19-22. In German. refs
Copyright

The facilities and procedures used by the DLR for wind-tunnel experiments on helicopter rotors are described. Consideration is given to the special rotor test stand ROTEST, the modular rotor model ROTOS, basic research projects, projects aimed at the development and testing of advanced technologies, and measurements performed on a contractual or cooperative basis for NASA, the Dutch aerospace agency NLR, etc. Diagrams, drawings, graphs, and photographs are provided. T.K.

A91-33373
PROCESS CONTROL TO SET MACH NUMBER RATIOS FOR JET-ENGINE INTAKE MEASUREMENTS - DEVELOPMENT OF AN AUTOMATIC MACH-NUMBER REGULATOR [PROZESSSTEUERUNG ZUR EINSTELLUNG VON MACHZAHLVERHAELTNISSEN BEI TRIEBWERKSEINLAUFMESSUNGEN - ENTWICKLUNG EINER AUTOMATISCHEN MACHZAHLREGELUNG]
RUEDIGER SIEBERT (DLR, Brunswick, Federal Republic of Germany) DLR-Nachrichten (ISSN 0937-0420), Feb. 1991, p. 26-28. In German.
Copyright

A91-33919
MODELING OF FLOW PARAMETERS IN A CRYOGENIC WIND TUNNEL [MODELIROVANIE PARAMETROV POTOKA V KRIOGENNOI AERODINAMICHESKOI TRUBE]
V. V. KOZLOV, A. I. OMELAEV, and M. P. RAMAZANOV (AN SSSR, Institut Teoreticheskoi i Prikladnoi Mekhaniki, Novosibirsk, USSR) Akademiia Nauk SSSR, Sibirskoe Otdelenie, Izvestiia, Seriia Tekhnicheskie Nauki (ISSN 0002-3434), June 1990, p. 42-46. In Russian.
Copyright

The use of cryogenic wind tunnels is investigated in an effort to provide for higher Reynolds numbers without a further increase

in the dynamic pressure and wind tunnel size. It is noted that this approach can be used in the subsonic, transonic, and low supersonic velocity ranges only. Specific implementations of cryogenic wind tunnels are examined, and it is shown that, with proper equipment and test procedures, cryogenic regimes do not pose any fundamental obstacles and allow accurate flow modeling at considerably higher Reynolds numbers. V.L.

N91-21155*# Vigyan Research Associates, Inc., Hampton, VA.
DESCRIPTION AND EVALUATION OF AN INTERFERENCE ASSESSMENT FOR A SLOTTED-WALL WIND TUNNEL
WILLIAM B. KEMP, JR. Washington Apr. 1991 53 p
(Contract NAS1-18585)
(NASA-CR-4352; NAS 1.26:4352) Avail: NTIS HC/MF A04
CSCL 14/2

A wind-tunnel interference assessment method applicable to test sections with discrete finite-length wall slots is described. The method is based on high order panel method technology and uses mixed boundary conditions to satisfy both the tunnel geometry and wall pressure distributions measured in the slotted-wall region. Both the test model and its sting support system are represented by distributed singularities. The method yields interference corrections to the model test data as well as surveys through the interference field at arbitrary locations. These results include the equivalent of tunnel Mach calibration, longitudinal pressure gradient, tunnel flow angularity, wall interference, and an inviscid form of sting interference. Alternative results which omit the direct contribution of the sting are also produced. The method was applied to the National Transonic Facility at NASA Langley Research Center for both tunnel calibration tests and tests of two models of subsonic transport configurations. Author

N91-21156# Advisory Group for Aerospace Research and Development, Neuilly-Sur-Seine (France). Fluid Dynamics Panel.
ROTARY-BALANCE TESTING FOR AIRCRAFT DYNAMICS
1991 267 p
(AGARD-AR-265; ISBN-92-835-0597-2) Copyright Avail: NTIS HC/MF A12; Non-NATO Nationals requests available only from AGARD/Scientific Publications Executive

The results of a study on rotary-balance testing for aircraft dynamics are presented. Both the experimental techniques used to obtain rotary-flow aerodynamics data and the procedures involved in using this type of data in the mathematical modeling of the dynamic behavior of a maneuvering fighter aircraft are examined. A special effort was made to summarize experiences involving correlation of dynamic behavior predictions with the observed motions of free-flight models and aircraft in flight. Specific hardware and problems encountered in rotary-balance experiments were addressed for experimental facilities in several countries and advanced applications were noted. Author

N91-21158# Federal Aviation Administration, Washington, DC. Office of Airport Safety and Standards.
A GUIDE TO GROUND VEHICLE OPERATIONS ON THE AIRPORT
Aug. 1990 29 p
(AD-A231077; DOT/FAA/AS-90-3) Avail: NTIS HC/MF A03
CSCL 05/6

Some airport operators, airlines, and fixed base operators have extensive formal training programs for employees whose duties involve operating a ground vehicle on the air operations area. However, many rely solely on informal on-the-job training. In an effort to improve the safety of ground vehicle operations on airports, the FAA developed this guide to ground vehicle operations. The guide provides airport orientation and operational information and would be used as a resource document by the airport operators and other members of the aviation community responsible for training ground vehicle operators. In addition to orientation and operational information, the guide touches on some other areas that a ground vehicle operator may encounter such as foreign object damage, security, and reporting emergencies. GRA

N91-21199*# National Aeronautics and Space Administration. Langley Research Center, Hampton, VA.
A SOLID-STATE CONTROLLABLE POWER SUPPLY FOR A MAGNETIC SUSPENSION WIND TUNNEL
TAUMI S. DANIELS and JOHN S. TRIPP *In its* Aerospace Applications of Magnetic Suspension Technology, Part 1 p 281-302 Mar. 1991
Avail: NTIS HC/MF A17 CSCL 14/2

The NASA Langley 6-inch Magnetic Suspension and Balance System (6-in. MSBS) requires an independently controlled bidirectional dc power source for each of six positioning electromagnets. These electromagnets provide five-degree-of-freedom control over a suspended aerodynamic test model. Existing power equipment, which employs resistance-coupled thyratron-controlled rectifiers as well as ac to dc motor-generator converters, is obsolete, inefficient, and unreliable. A replacement six-phase bidirectional controlled bridge rectifier is proposed, which employs power MOSFET switches sequenced by hybrid analog/digital circuits. Full-load efficiency is 80 percent compared with 25 percent for the resistance-coupled thyratron system. Current feedback provides high control linearity, adjustable current limiting, and current overload protection. A quenching circuit suppresses inductive voltage impulses. It is shown that 20-kHz interference from positioning magnet power into MSBS electromagnetic model position sensors results predominantly from capacitively coupled electric fields. Hence, proper shielding and grounding techniques are necessary. Inductively coupled magnetic interference is negligible. Author

N91-22136# Aeronautical Research Labs., Melbourne (Australia).
AEROTHERMODYNAMIC DESIGN APPRAISAL OF NOISE SUPPRESSORS FOR F/A-18 ENGINE RUN-UP FACILITIES AT RAAF WILLIAMTOWN
S. A. FISHER and A. M. ABDEL-FATTAH Oct. 1990 66 p
(ARL-PROP-R-177; AR-006-126) Copyright Avail: NTIS HC/MF A04

Upgraded facilities for ground running of F404 engines in F/A-18 aircraft at RAAF Williamtown will feature air-cooled exhaust augmentors for noise suppression. Aerothermodynamical aspects of the augmentor designs were appraised in some detail, making use of isothermal scale model tests, ejector theory, and available empirical data. In initial design development, quantitative assessments were made of cooling flow pumping performance. Changes were recommended to improve the aerodynamic characteristics of the exhaust augmentors and eliminate high risk features, and the sizes of the augmentor ducts were significantly reduced. The model tests identified certain geometric features which were important for symmetry of the flow in the augmentor ducts and to pumping performance. Once modified accordingly, the designs displayed satisfactory aerodynamic behavior, which was tolerant to both inlet asymmetries and reasonable levels of engine jet misalignment. The pumping performance was shown to exceed the design requirements. Author

N91-22137# Air Force Inst. of Tech., Wright-Patterson AFB, OH.
STATUS OF PAVER IMPLEMENTATION WITHIN THE US AIR FORCE M.S. Thesis
C. L. EADDY Dec. 1990 164 p
(AD-A231158; AFIT/CI/CIA-90-126) Avail: NTIS HC/MF A08
CSCL 13/2

Regardless of how well conceived a pavement management system (PMS) is, unless well implemented and accepted by the end user its benefits cannot be realized. This paper seeks to estimate the present status of implementation within the U.S. Air Force of the pavement management system, PAVER. This work is based in part on an initial effort by Captain Timothy R. McLean who in 1984 wrote his graduate thesis on improving PAVER implementation. In his research he sought to determine the problems encountered in the field during the implementation of PAVER as well as recommendations from the field for improving or refining PAVER. He identified training, manpower, equipment,

and top management support as key areas requiring attention to improve PAVER implementation. This work seeks to estimate and validate not only the present extent of these pre-identified problem areas, but also the current extent of PAVER's use and application. Example areas which the questionnaire addresses include an estimation of the following: the number of air bases which have partially or fully implemented PAVER; the accuracy of pavement distress and inventory data being used; the application of PAVER to project programming; the ranking of benefits from using PAVER; and preceptions of PAVER as an innovation which have been identified in various literature as factors influencing the diffusion of innovation. GRA

N91-22138# Army Cold Regions Research and Engineering Lab., Hanover, NH.
SNOW ROADS AND RUNWAYS
GUNARS ABELE Nov. 1990 109 p
(AD-A231490; CRREL-90-3) Avail: NTIS HC/MF A06 CSCL 08/12

This monograph presents a complete review of all successful techniques that have been used to construct and maintain snow roads, trails, and aircraft landing fields. The snow properties that must be considered prior to the construction process are identified, and the kinds of apparatus available for the measure of the properties are reviewed and assessed. A discussion of construction techniques is presented and includes the following: (1) types of snow pavements; (2) classification of roads by use; (3) classification of surface and subsurface strength; (4) considerations impacting on site selection; (5) various kinds of equipment that have been developed to construct and maintain the roads; and (6) additives that have been used to construct roads with sufficient bearing strength. The design criteria that have been established are cited. GRA

10

ASTRONAUTICS

Includes astronautics (general); astrodynamics; ground support systems and facilities (space); launch vehicles and space vehicles; space transportation; spacecraft communications, command and tracking; spacecraft design, testing and performance; spacecraft instrumentation; and spacecraft propulsion and power.

A91-33601
IEEE PLANS '90 - POSITION LOCATION AND NAVIGATION SYMPOSIUM, LAS VEGAS, NV, MAR. 20-23, 1990, RECORD
Symposium sponsored by IEEE. New York, Institute of Electrical and Electronics Engineers, Inc., 1990, 667 p. For individual items see A91-33602 to A91-33668.
Copyright

Various papers on position, location, and navigation are presented. The general topics addressed include: space-based navigation systems; inertial sensor development; other radio navigation system technologies; surveying, mapping, and digital electronics technology; positioning, pointing, and stabilization of space systems; inertial systems development and applications; integrated communicaiton/navigration systems and standard avionics; application of statistical filtering to navigation technology; GPS applications and equipment in civil, governmental, and commercial areas. Also discussed are: integrated navigation and targeting systems; civil aviation and marine navigation/traffic control; geodesy, gravity measurement, and earth reference systems; GPS military applications and equipment; integrated aircraft navigation and flight control; land vehicle navigation, positioning, and information systems; differential GPS; GPS/inertial navigation; terrain aided air vehicle navigation. C.D.

A91-33609
INTEGRATED INERTIAL NAVIGATION SYSTEM/GLOBAL POSITIONING SYSTEM (INS/GPS) FOR MANNED RETURN VEHICLE AUTOLAND APPLICATION
KEVIN BRADEN, CLINT BROWNING, HENDRIK GELDERLOOS, FRED SMITH (Honeywell Space Systems Group, Clearwater, FL), CHUCK MARTTILA (Honeywell Systems Research Center, Minneapolis, MN) et al. IN: IEEE PLANS '90 - Position Location and Navigation Symposium, Las Vegas, NV, Mar. 20-23, 1990, Record. New York, Institute of Electrical and Electronics Engineers, Inc., 1990, p. 74-82. refs
Copyright

It is noted that with the development of the International Space Station Freedom, people will permanently live in space and require routine access and an assured crew return capability in case of emergencies in space. The extended duration in space requires a manned return vehicle that is less demanding on the crew and provides an autonomous deorbit, entry, and autoland capability. The authors discuss an autoland capability with an integrated differential GPS/INS that provides the required position and velocity accuracies without the need for tactical aircraft navigation (TACAN) and Microwave Landing System (MLS) navigation aides. Simulation results are used to demonstrate the feasibility of autoland using differential GPS aided with a high-precision altimeter. This concept applies to several manned space applications, such as Assured Crew Return Vehicle (ACRV), Assured Shuttle Availability (ASA), Advanced Manned Launch System (AMLS), and National Aerospace Plane (NASP), and to unmanned return vehicles such as the Propulsion Avionics Module (P/AM). I.E.

N91-21197*# Madison Magnetics, Inc., WI.
MAGNETIC SUSPENSION AND BALANCE SYSTEM ADVANCED STUDY, 1989 DESIGN
ROGER W. BOOM, Y. M. EYSSA, MOUSTAFA K. ABDELSALAM, and GLEN E. MCINTOSH *In* NASA, Langley Research Center, Aerospace Applications of Magnetic Suspension Technology, Part 1 p 225-248 Mar. 1991
Avail: NTIS HC/MF A17 CSCL 22/2

The objectives are to experimentally confirm several advanced design concepts on the Magnetic Suspension and Balance Systems (MSBS). The advanced design concepts were identified as potential improvements by Madison Magnetics, Inc. (MMI) during 1984 and 1985 studies of an MSBS utilizing 14 external superconductive coils and a superconductive solenoid in an airplane test model suspended in a wind tunnel. This study confirmed several advanced design concepts on magnetic suspension and balance systems. The 1989 MSBS redesign is based on the results of these experiments. Savings of up to 30 percent in supporting magnet ampere meters and 50 percent in energy stored over the 1985 design were achieved. Author

N91-21198*# National Aeronautics and Space Administration. Langley Research Center, Hampton, VA.
PROPULSION SIMULATOR FOR MAGNETICALLY-SUSPENDED WIND TUNNEL MODELS
PRAKASH B. JOSHI, C. L. GOLDEY, G. P. SACCO (Physical Sciences, Inc., Andover, MA.), and PIERCE L. LAWING *In its* Aerospace Applications of Magnetic Suspension Technology, Part 1 p 249-280 Mar. 1991
(Contract NAS1-18845)
Avail: NTIS HC/MF A17 CSCL 22/2

The objective of phase two of a current investigation sponsored by NASA Langley Research Center is to demonstrate the measurement of aerodynamic forces/moments, including the effects of exhaust gases, in magnetic suspension and balance system (MSBS) wind tunnels. Two propulsion simulator models are being developed: a small-scale and a large-scale unit, both employing compressed, liquified carbon dioxide as propellant. The small-scale unit was designed, fabricated, and statically-tested at Physical Sciences Inc. (PSI). The large-scale simulator is currently in the preliminary design stage. The small-scale simulator design/development is presented, and the data from its static firing on a thrust stand are discussed. The analysis of this data

provides important information for the design of the large-scale unit. A description of the preliminary design of the device is also presented. Author

N91-21208*# Draper (Charles Stark) Lab., Inc., Cambridge, MA.
DYNAMIC MODELLING AND ANALYSIS OF A MAGNETICALLY SUSPENDED FLEXIBLE ROTOR M.S. Thesis, 1988
DUNCAN C. MCCALLUM *In* NASA, Langley Research Center, Aerospace Applications of Magnetic Suspension Technology, Part 2 p 499-537 Mar. 1991
Avail: NTIS HC/MF A17 CSCL 22/2

A 12-state lumped-element model is presented for a flexible rotor supported by two attractive force electromagnetic journal bearings. The rotor is modeled as a rigid disk with radial mass unbalance mounted on a flexible, massless shaft with internal damping (Jeffcott rotor). The disk is offset axially from the midspan of the shaft. Bearing dynamics in each radial direction are modeled as a parallel combination of a negative (unstable) spring and a linear current-to-force actuator. The model includes translation and rotation of the rigid mass and the first and second bending models of the flexible shaft, and it simultaneously includes internal shaft damping, gyroscopic effects, and the unstable nature of the attractive force magnetic bearings. The model is used to analyze the dependence of the system transmission zeros and open-loop poles on system parameters. The dominant open-loop poles occur in stable/unstable pairs with bandwidth dependent on the ratios of bearing (unstable) stiffnesses to rotor mass and damping dependent on the shaft spin rate. The zeros occur in complex conjugate pairs with bandwidth dependent on the ratios of shaft stiffness to rotor mass and damping dependent on the shaft spin rate. Some of the transmission zeros are non-minimum phase when the spin rate exceeds the shaft critical speed. The transmission zeros and open-loop poles impact the design of magnetic bearing control systems. The minimum loop cross-over frequency of the closed-loop system is the speed of the unstable open-loop poles. For the supercritical shaft spin rates, the presence of non-minimum phase zeros limits the distribution rejection achievable at frequencies near or above the shaft critical speed. Since non-minimum phase transmission zeros can only be changed by changing the system inputs and/or outputs, closed-loop performance is limited for supercritical spin rates unless additional force or torque actuators are added. Author

N91-21209*# Virginia Polytechnic Inst. and State Univ., Blacksburg. Dept. of Mechanical Engineering.
CRITICAL SPEEDS AND FORCED RESPONSE SOLUTIONS FOR ACTIVE MAGNETIC BEARING TURBOMACHINERY, PART 1
J. KEESEE, D. RAWAL, and R. GORDON KIRK *In* NASA, Langley Research Center, Aerospace Applications of Magnetic Suspension Technology, Part 2 p 539-558 Mar. 1991 Sponsored in part by Virginia Center for Innovative Technology; Dresser-Rand Co.; and Magnetic Bearings, Inc.
Avail: NTIS HC/MF A17 CSCL 22/2

The prediction of critical speeds and forced response of active magnetic bearing turbomachinery is of great interest due to the increased use of this new and promising technology. Calculating the system undamped critical speeds and forced response is important to all those who are involved in the design of the active magnetic bearing system. An extended Jeffcott model which was used as an approximate solution to a more accurate transfer matrix procedure is presented. Theory behind a two-degree-of freedom extended Jeffcoat model is presented. Results of the natural frequency calculation are shown followed by the results of the forced response calculation. The system response was predicted for two types of forcing. A constant magnitude excitation with a wide frequency variation was applied at the bearings as one forcing function. The normal unbalance force at the midspan was the second source of excitation. The results of this extended Jeffcott solution gives useful design guidance for the influence of the first and third modes of a symmetric rotor system. Author

N91-21210*# Virginia Polytechnic Inst. and State Univ., Blacksburg. Dept. of Mechanical Engineering.
CRITICAL SPEEDS AND FORCED RESPONSE SOLUTIONS FOR ACTIVE MAGNETIC BEARING TURBOMACHINERY, PART 2
D. RAWAL, J. KEESEE, and R. GORDON KIRK *In* NASA, Langley Research Center, Aerospace Applications of Magnetic Suspension Technology, Part 2 p 559-582 Mar. 1991 Sponsored in part by Virginia Center for Innovative Technology; Dresser-Rand Co.; and Magnetic Bearings, Inc.
Avail: NTIS HC/MF A17 CSCL 22/2

The need for better performance of turbomachinery with active magnetic bearings has necessitated a study of such systems for accurate prediction of their vibrational characteristics. A modification of existing transfer matrix methods for rotor analysis is presented to predict the response of rotor systems with active magnetic bearings. The position of the magnetic bearing sensors is taken into account and the effect of changing sensor position on the vibrational characteristics of the rotor system is studied. The modified algorithm is validated using a simpler Jeffcott model described previously. The effect of changing from a rotating unbalance excitation to a constant excitation in a single plane is also studied. A typical eight stage centrifugal compressor rotor is analyzed using the modified transfer matrix code. The results for a two mass Jeffcott model were presented previously. The results obtained by running this model with the transfer matrix method were compared with the results of the Jeffcott analysis for the purposes of verification. Also included are plots of amplitude versus frequency for the eight stage centrifugal compressor rotor. These plots demonstrate the significant influence that sensor location has on the amplitude and critical frequencies of the rotor system. Author

N91-21238# Federal Aviation Administration, Atlantic City, NJ.
MODEL ROCKETRY HAZARD STUDY
CHARLES C. T. CHEN and CAESAR A. CAIAFA Mar. 1991 23 p
(DOT/FAA/CT-TN90/28) Avail: NTIS HC/MF A03

The potential hazard was evaluated to an approaching or departing aircraft from a collision with a model rocket. Typically, these rockets have a gross weight of 1.5 kg (53 ounces) or less and carry a maximum of 0.125 kg (4.4 ounces) of propellant. The potential damage to jet transports, commuter aircraft, general aviation aircraft, and rotorcraft resulting from an impact with these rockets is determined. Author

N91-22331*# National Aeronautics and Space Administration. Langley Research Center, Hampton, VA.
FOURTH NASA WORKSHOP ON COMPUTATIONAL CONTROL OF FLEXIBLE AEROSPACE SYSTEMS, PART 2
LAWRENCE W. TAYLOR, JR., comp. Mar. 1991 464 p Workshop held in Williamsburg, VA, 11-13 Jul. 1990
(NASA-CP-10065-PT-2; NAS 1.55:10065-PT-2) Avail: NTIS HC/MF A20 CSCL 22/2

A collection of papers presented at the Fourth NASA Workshop on Computational Control of Flexible Aerospace Systems is given. The papers address modeling, systems identification, and control of flexible aircraft, spacecraft and robotic systems.

11

CHEMISTRY AND MATERIALS

Includes chemistry and materials (general); composite materials; inorganic and physical chemistry; metallic materials; nonmetallic materials; and propellants and fuels.

A91-32451
ICCM-VII; PROCEEDINGS OF THE 7TH INTERNATIONAL CONFERENCE ON COMPOSITE MATERIALS, GUANGZHOU, PEOPLE'S REPUBLIC OF CHINA, NOV. 22-24, 1989. VOLS. 1-3
YUNSHU WU, ED., ZHENLONG GU, ED., and RENJIE WU, ED. Conference sponsored by China Association for Science and Technology, American Society for Composites, ASME, et al. Beijing/Oxford, International Academic Publishers/Pergamon Press, 1989, p. Vol. 1, 721 p.; vol. 2, 701 p.; vol. 3, 525 p. For individual items see A91-32452 to A91-32514, A91-32516 to A91-32670.
Copyright

This volume discusses topics on the manufacture of composite materials and on their mechanical characterization, polymer matrices, the metal matrix and ceramic matrix composites, and nondestructive testing. Attention is given to the optimization of aircraft structure in composite materials, the fiber distribution and resin flow in the laminate molding process, optimal cooling for minimum residual stresses, the wear characteristics of continuous-fiber-reinforced composites, the structure-property relationships of composite sandwich panels, and the mechanical behavior of fiber-reinforced thermoplastic composites. Other papers are on high-temperature joining of fiber-reinforced metals, carbon-fiber-reinforced tin superconductor composites, crack-bridging mechanisms in the fiber-reinforced ceramics, a new method for measurement of carbon fiber axial compressive strength and some applications, and analysis of the damage field and the actual stress-strain field in composite plate by moire interferometry. I.S.

A91-32549
THERMAL SPIKES ON CFRP LAMINATES - ASSESSMENT OF MICRODAMAGE AND ITS CONSEQUENCES ON FATIGUE LIFE
ALFREDO GUEMES and WENCESLAO BARRERA (Escuela Tecnica Superior de Ingenieros Aeronauticos, Madrid, Spain) IN: ICCM-VII; Proceedings of the 7th International Conference on Composite Materials, Guangzhou, People's Republic of China, Nov. 22-24, 1989. Vol. 2. Beijing/Oxford, International Academic Publishers/Pergamon Press, 1989, p. 222-225.
Copyright

The fatigue life of (+ or - 45) graphite/epoxy laminates is investigated, with and without previous thermal spiking. A permanent drop of characteristics is found, even in the absence of any observable microscopic damage. The severity of the spike seems to be more important than the number of them; after a certain number of spikes, degradation of material remains stationary. Author

A91-32573
DAMAGE TOLERANCE ASPECTS OF ARALL FUSELAGE SKIN STRUCTURE (PHILOSOPHY AND EXPERIMENTS)
D. CHEN (Delft University of Technology, Netherlands) IN: ICCM-VII; Proceedings of the 7th International Conference on Composite Materials, Guangzhou, People's Republic of China, Nov. 22-24, 1989. Vol. 2. Beijing/Oxford, International Academic Publishers/Pergamon Press, 1989, p. 460-466. refs
Copyright

Information available on the damage tolerance of fuselage skin structures made of ARALL laminates is examined. It is found that, in comparison with monolithic aluminum alloy sheets, ARALL laminates show superior fatigue and static test results under realistic fuselage loading conditions (such as biaxiality, internal pressurization, and curvature). Graphs illustrating results of some tests are presented. I.S.

A91-32576
CUMULATIVE DAMAGE PROBLEM IN PULL-THROUGH FATIGUE OF C.F.R.P. LAMINATE
B. Z. YANG, Y. B. LIU, D. LIU, W. G. GU, and K. D. ZHANG (Northwestern Polytechnical University, Xian, People's Republic of China) IN: ICCM-VII; Proceedings of the 7th International Conference on Composite Materials, Guangzhou, People's Republic of China, Nov. 22-24, 1989. Vol. 2. Beijing/Oxford, International Academic Publishers/Pergamon Press, 1989, p. 477-483. refs
Copyright

A pull-through fatigue test for CFRP laminates was developed using a specially designed testing fixture. The test was used to investigate the development of fatigue damage in specimens made from T300/648 CFRP material with stacking sequence (0/+,-45)s. Special consideration was given to the effect of environmental conditions on the fatigue damage behavior. Results indicate that, under the wet condition, the strength and the stiffness of the laminate decreased significantly. I.S.

A91-33324
AEROSPACE MATERIALS
MICHAEL A. DORNHEIM Aviation Week and Space Technology (ISSN 0005-2175), vol. 134, April 15, 1991, p. 50-52, 55-57, 60 (7 ff.).
Copyright

A comprehensive evaluation is made of the development trends in high performance advanced aerospace structural materials applications. It is noted that the anticipated predominance of thermoplastic composite-matrix polymers in the F-22/F-23 ATF propotypes has not materialized, due both to their high materials and processing costs and the emergence of a more tractable high operating temperature thermoset, BMI, whose toughness characteristics are of the order of those associated with thermoplastics. No more than 15 percent of F-22 weight is thermoplastics; the F-23 use of such resins is nill. Throughout the advanced nonmetallics industry, reduced DOD procurements have come to represent slow growth and the prospect of consolidation. Also, such lightweight Al-based metallics as the Al-Li alloys have posed a major market-share challenge to polymeric composites, as in the case of the C-17 airlifter's 6,269 lbs of such Al-Li alloys as 2090, largely in cargo floor and ramp bulkhead structures. The EFA fighter makes frequent use of SPF-DB Ti alloys in combat damage-critical components. Metal-matrix composites employing titanium aluminide matrices will be extensively used in the X-30 hypersonic aircraft program. O.C.

A91-33725
COST-EFFECTIVE MANUFACTURING OF ADVANCED CERAMICS
LAUREL M. SHEPPARD American Ceramic Society, Bulletin (ISSN 0002-7812), vol. 70, April 1991, p. 692-701.
Copyright

A development status evaluation is presented for representative advanced-applications ceramics-processing methods, involving inexpensive sinterable powder production, continuous fiber production and coating, pressureless consolidation, and near-net-shape fabrication of AlPO4-matrix composites with a range of reinforcements by techniques analogous to those of polymeric-matrix composite production. Attention is given to a hot-wall CVD reactor for coating large-diameter ceramic monofilaments, a comparison of dip-coating, in situ-curing, and reaction-bonding sol-gel methods for coating of ceramic tows, RF-RF plasma-torch production of ultrafine Si3N4 powders, and the highly automated 'Quickset' intelligent-processing system for ceramics preparation, low-temperature molding, and shrinking. O.C.

A91-34287
USE OF RESIN COMPOSITES FOR CRYOGENIC TANKAGE
M. T. CALLAGHAN (McDonnell Douglas Corp., Saint Louis, MO)

(Non-metallic materials and composites at low temperatures; Proceedings of the Conference, Heidelberg, Federal Republic of Germany, May 17, 18, 1990. A91-34276 13-23) Cryogenics (ISSN 0011-2275), vol. 31, April 1991, p. 282-287. refs
Copyright

The resurgence in development of hypersonic vehicles has led to the evaluation of lightweight materials and structures for cryogenic tankage. Over the past 20 years, resin composites have replaced conventional metallic structures in improving aircraft and spacecraft performance. Previous attempts to develop resin matrix composites for cryogenic tankage were unsuccessful, due to the brittle nature of the matrix or the need for metallic liners to prevent permeation. With the development of new tougher resins and improved processing techniques, resin composites are once again being considered. This paper addresses the advancements made in resin composite technology and their potential advantages and drawbacks for use as cryogenic tankage. Author

A91-34841
SUPERPLASTICITY IN A TI3AL-BASE ALLOY STABILIZED BY NB, V AND MO
HONG S. YANG, PAUL JIN, AMIYA K. MUKHERJEE (California, University, Davis), and EDWARD DALDER (Lawrence Livermore National Laboratory, Livermore, CA) Scripta Metallurgica et Materialia (ISSN 0956-716X), vol. 25, May 1991, p. 1223-1228. refs
(Contract NSF DMR-90-13337)
Copyright

The superplastic deformation behavior of Ti-25Al-10Nb-3V-1Mo (in at. pct) alloy, referred to as Super-alpha-2, was investigated in order to optimize the temperature and strain-rate ranges suitable for superplastic forming operations. It was found that Super-alpha-2 exhibits maximum elongation of 570 percent when deformed at 980 C and a strain rate of 0.00015/sec. At a temperature of 1010 C and/or strain rates below 0.00015/sec, the stress-strain curves showed strain hardening, whereas at lower temperatures and/or higher strain rates, the curves revealed strain softening. The predominant mode of failure in the Super-alpha-2 alloy is transgranular fracture. I.S.

A91-35949* National Aeronautics and Space Administration. Lewis Research Center, Cleveland, OH.
RESISTIVITY OF PRISTINE AND INTERCALATED GRAPHITE FIBER EPOXY COMPOSITES
JAMES R. GAIER (NASA, Lewis Research Center, Cleveland, OH), PAUL D. HAMBOURGER, and MELISSA E. SLABE (Cleveland State University, OH) Carbon (ISSN 0008-6223), vol. 29, no. 3, 1991, p. 313-320. Previously announced in STAR as N90-21192. refs
(Contract NCC3-19)
Copyright

Laminar composites were fabricated from pristine and bromine intercalated Amoco P-55, P-75, and P-100 graphite fibers and Hysol-Grafil EAG101-1 film epoxy. The thickness and r.f. eddy current resistivity of several samples were measured at grid points and averaged point by point to obtain final values. Although the values obtained this way have high precision (less than 3 percent deviation), the resistivity values appear to be 20 to 90 percent higher than resistivities measured on high aspect ratio samples using multi-point techniques, and by those predicted by theory. The temperature dependence of the resistivity indicates that the fibers are neither damaged nor deintercalated by the composite fabrication process. The resistivity of the composites is a function of sample thickness (i.e., resin content). Composite resistivity is dominated by fiber resistivity, so lowering the resistivity of the fibers, either through increased graphitization or intercalation, results in a lower composite resistivity. A modification of the simple rule of mixtures model appears to predict the conductivity of high aspect ratio samples measured along a fiber direction, but a directional dependence appears which is not predicted by the theory. The resistivity of these materials is clearly more complex than that of homogeneous materials. Author

N91-22380# Tokyo Univ. (Japan).
PROCEEDINGS OF A FRENCH-JAPANESE SEMINAR ON COMPOSITE MATERIALS: PROCESSING, USE AND DATABASES
1990 126 p Seminar held in Paris, France, 13-14 Mar. 1990 Prepared in cooperation with Aerospatiale, Suresnes (France)
Avail: NTIS HC/MF A07

Topics addressed include: new composite materials; processing and fabrication; data bases; reinforcing fibers; metal matrix composites; fatigue tests; creep properties; and evaluation and fabrication. B.G.

N91-22381 Cranfield Inst. of Tech., Bedford (England).
DAMAGE ACCUMULATION AND DEGRADATION OF COMPOSITE LAMINATES UNDER AIRCRAFT SERVICE LOADING: ASSESSMENT AND PREDICTION, VOLUMES 1 AND 2 Ph.D. Thesis
I. R. FARROW 1989 387 p
Avail: Univ. Microfilms Order BRDX90938

Methods were investigated for load idealization and damage accumulation modeling for life and residual strength prediction of advanced composite materials. A comprehensive test program was performed including static strength and fatigue of continuous carbon fiber epoxy composite specimens. Test control and monitoring systems were developed and the importance of error and frequency optimization and transducer monitoring of composite laminate materials were monitored. Load and displacement data acquisition has provided invaluable information in terms of modulus and creep parameters to illustrate the damage accumulation trends and effective failure states. Three phase damage accumulations, described by wear-in, stable, and wear-out phases of modulus reduction were recorded, statistically processed, and used in subsequent analysis. Spectrum fatigue tests have shown that the high load truncation level should be taken to the once per life design limit level and low load omission should be restricted to cycles with low mean stresses. Two-level programmed block tests have shown a pronounced load sequence effect. Assumptions of available standardized load spectra and the concept of statistical counting were reviewed. Classical and contemporary damage accumulation models were also reviewed. Linear and nonlinear damage accumulation models were developed, based on a modulus reduction damage parameter. The models were applied to predict the fatigue lives of variable amplitude tests performed. Damage accumulation models based on nondestructive measurements are recommended for their potential of damage tolerant support from in-service measurements. An estimation of minimum expected residual strength for a given level of damage parameter was proposed. The development of a nonlinear 'Interactive Parameter Cumulative Damage' model was considered as a fundamental attempt to exploit constant amplitude fatigue data for the prediction of variable amplitude fatigue of advanced composites.
Dissert. Abstr.

N91-22399# Bristol Univ. (England). Dept. of Aerospace Engineering.
THE FLEXURAL STRENGTH OF UNIDIRECTIONAL CARBON FIBRE COMPOSITES B.S. Thesis
B. R. LEWIS and V. W. Y. SHIN Jun. 1990 103 p
(BU-509; ETN-91-99202) Avail: NTIS HC/MF A06

The objective was to study why, when the unidirectional carbon fiber composite specimens were subjected to bending, they failed on the tension side of the material rather than the compressive side. Tests were carried out on unidirectional carbon fiber reinforced plastics (CFRP) using a specifically designed combined compression and bending rig. An automatic data recording system was used in order to record strain and load data efficiently and accurately. This required the writing of a data logging computer program. Results and conclusions are given. ESA

N91-22407# California Inst. of Tech., Pasadena.
INVESTIGATIONS INTO SHOCK-INDUCED ENHANCEMENT OF MIXING AND COMBUSTION IN SUPERSONIC BURNERS Final Report, 1 Oct. 1986 - 30 Sep. 1990

FRANK E. MARBLE 30 Nov. 1990 22 p
(Contract F49620-86-C-0113)
(AD-A231750; AFOSR-91-0012TR) Avail: NTIS HC/MF A03 CSCL 21/5

Experiments were carried out in the GALCIT 17 in. shock tube to investigate the effectiveness of shock enhancement on the mixing rate of a cylinder of helium gas into the surrounding air. Laser induced fluorescence was employed to trace the time development of mixing using byacetal dye to mark the helium. The concentration of helium was reduced below 20 pct. of its initial value over 0.6 of the helium volume within less than one ms by a weak (M=1.1) shock. The results corresponded well to results of computational analysis. Details of the combustion within the vortex were investigated in large vortices, created by a pulsing technique in the Unsteady Combustion Facility. The results of this program were sufficiently promising to encourage the design, construction and test of a scramjet injector using the technique. GRA

N91-22416*# Alabama Univ., Birmingham. Dept. of Materials Science and Engineering.
INFLUENCE OF A MAGNETIC FIELD DURING DIRECTIONAL SOLIDIFICATION OF MAR-M 246 + HF SUPERALLOY Final Technical Report
J. BARRY ANDREWS, WENDY ALTER, and DIANNE SCHMIDT (National Aeronautics and Space Administration. Marshall Space Flight Center, Huntsville, AL.) Jan. 1991 59 p
(Contract NAS8-36461)
(NASA-CR-184114; NAS 1.26:184114) Avail: NTIS HC/MF A04 CSCL 11/6

An area that has been almost totally overlooked in the optimization of properties in directionally solidified superalloys is the control of microstructural features through the application of a magnetic field during solidification. The influence of a magnetic field on the microstructural features of a nickel-base superalloys is investigated. Studies were performed on the dendritic MAR-M 246+Hf alloy, which was solidified under both a 5 K gauss magnetic field and under no-applied-field conditions. The possible influences of the magnetic field on the solidification process were observed by studying variations in microstructural features including volume fraction, surface area, number, and shape of the carbide particles. Stereological factors analyzed also included primary and secondary dendrite arm spacing and the volume fraction of the interdendritic eutectic constituent. Microprobe analysis was performed to determine the chemistry of the carbides, dendrites, and interdendritic constituents, and how it varied between field and no-field solidification samples. Experiments involving periodic application and removal of the magnetic field were also performed in order to permit a comparison with structural variations observed in a MAR-M 246+Hf alloy solidified during KC-135 high-g, low-g maneuvers. Author

N91-22424# Ribbon Technology Corp., Gahanna, OH.
DIRECT CAST TITANIUM ALUMINIDE STRIP Final Report, 24 Jun. - 23 Dec. 1987
T. A. GASPAR and L. E. HACKMAN Jan. 1991 25 p
(Contract F33615-86-C-5139)
(AD-A231906; WL-TR-91-4002) Avail: NTIS HC/MF A03 CSCL 11/6

The purpose of the Phase 1 research project is to demonstrate the feasibility of melting titanium alloys using Duriron's induction slag melting process and casting them into rapidly solidified strip by RIBTEC's melt overflow process. The strip might be used for SiC-Ti metal matrix composites for advanced airframe structures. GRA

N91-23048*# National Aeronautics and Space Administration. Langley Research Center, Hampton, VA.
COST-EFFICIENT MANUFACTURING OF COMPOSITE STRUCTURES
W. TOM FREEMAN, JOHN G. DAVIS, and NORMAN J. JOHNSTON *In* National Aeronautics and Space Administration, Technology 2000, Volume 1 p 221-230 Mar. 1991
Avail: NTIS HC/MF A18 CSCL 11/4

The Advanced Composites Technology (ACT) program is seeking research breakthroughs that will allow structures made of graphite epoxy materials to replace metals in the wings and fuselages of future aircrafts. NASA's goals are to reduce acquisition cost by 20 to 25 percent, structural weight for a resized aircraft by 40 to 50 percent, and the number of parts by half compared to current production aluminum aircraft. The innovative structural concepts, materials, and fabrication techniques emerging from the ACT program are described, and the relationship between aerospace developments and industrial, commercial, and sporting goods applications are discussed. Author

12

ENGINEERING

Includes engineering (general); communications; electronics and electrical engineering; fluid mechanics and heat transfer; instrumentation and photography; lasers and masers; mechanical engineering; quality assurance and reliability; and structural mechanics.

A91-32461
SIGNIFICANCE OF RESIDUAL CURING STRAINS IN COMPOSITE STRUCTURE REPAIR TECHNOLOGY
JERZY P. KOMOROWSKI, M. DONALD RAIZENNE, JAMES B. HEATH, and RONALD W. GOULD (National Aeronautical Establishment, Ottawa, Canada) IN: ICCM-VII; Proceedings of the 7th International Conference on Composite Materials, Guangzhou, People's Republic of China, Nov. 22-24, 1989. Vol. 1. Beijing/Oxford, International Academic Publishers/Pergamon Press, 1989, p. 117-122. refs
Copyright

The Structures and Materials Laboratory is engaged in developing generic technology for the repair of composite aircraft structures. As a preliminary task, a suitable specimen geometry for static and fatigue related testing of graphite/epoxy laminates is being developed. This report describes the use of a photoelastic coating to measure strain patterns surrounding machined holes in laminates. This technique also identified and quantified the residual stresses. These stresses are inherent to the multidirectional laminates and may be partially released during machining operations. Author

A91-32547
TEMPERATURE EFFECT ON THE STRESS CONCENTRATION IN THE COMPOSITE MATERIAL USED BY THE X-29A FORWARD-SWEPT WING AIRCRAFT
HSIEN-YANG YEH (California State University, Long Beach) IN: ICCM-VII; Proceedings of the 7th International Conference on Composite Materials, Guangzhou, People's Republic of China, Nov. 22-24, 1989. Vol. 2. Beijing/Oxford, International Academic Publishers/Pergamon Press, 1989, p. 198-203. refs
Copyright

The anisotropic stress concentration factors of laminated composite plates used by the X-29A (forward-swept wing) research aircraft were evaluated, at three different temperature levels, in the framework of the theory of anisotropic elasticity, using both the mixture-rule approach and the constant-strain approach to calculate stress concentration factors. The analyses showed that the anisotropic stress concentration factor for the composite materials could be greater or less than 3 and that the location of the maximum tangential-stress points could be shifted by changing the fiber orientation with respect to the loading axis. Results predicted by the constant-strain approach (but not by the mixture-rule approach) matched well the experimental data, pointing to the importance of the inplane shear effect on the evaluation of stress concentration factors for the X-29A laminated plates. I.S.

A91-32650
OPTIMAL DESIGN OF METAL AND COMPOSITE THIN-WALLED STRUCTURES WITH FLUTTER CONSTRAINT
C. Q. HUANG and X. QIAO (Nanjing Aeronautical Institute, People's Republic of China) IN: ICCM-VII; Proceedings of the 7th International Conference on Composite Materials, Guangzhou, People's Republic of China, Nov. 22-24, 1989. Vol. 3. Beijing/Oxford, International Academic Publishers/Pergamon Press, 1989, p. 404-410. Chinese Academy of Sciences-supported research. refs
Copyright

The optimal design of metal and composite thin-walled structures with flutter constraint and gauge requirements is discussed. The sequential quadratic dual programming method is applied to the flutter speed constrained optimization problem. The calculating speed for each iteration is very fast. The introduction of the relaxation factor is quite efficient, successfully overcoming the difficulty caused by the high nonlinearity. Due to the rapidity of iteration, this method can be used to modify the original structural design at the first several iterations. Then, the more sophisticated optimization package is used, which has multiconstraint conditions, such as strength, stiffness, and flutter, to continue the design process. L.K.S.

A91-32651
ANALYSIS AND OPTIMAL DESIGN OF COMPOSITE STRUCTURES
HUI-LIANG DING, XIA-SHENG SUN, WEI WANG, and XIAN-XUE SUN (Aircraft Strength Research Institute, Yaoxian, People's Republic of China) IN: ICCM-VII; Proceedings of the 7th International Conference on Composite Materials, Guangzhou, People's Republic of China, Nov. 22-24, 1989. Vol. 3. Beijing/Oxford, International Academic Publishers/Pergamon Press, 1989, p. 411-418. refs
Copyright

A large-scale Composite Structural Analysis and Synthesis System (COMPASS) program targeting the possibility of tailoring composite structures for particular design requirements is overviewed. A prototype reference system YIDOYU-1x supporting the development of COMPASS is considered. This prototype system is based on an aircraft multiconstraint optimal-design system YIDOYU-1. Numerical examples including the structural analysis of a cantilever box wing, swept wing, and delta wing are presented. It is observed that the self-orthotropic behavior and tension-shear, tension-bending, and bending-twisting coupling behaviors of composite laminates can be used to realize aeroelastic tailoring obtainable by adjusting the orientation angles of ply and/or thickness of laminates. V.T.

A91-32961#
AVIONICS ENVIRONMENTAL RELIABILITY USING FINITE ELEMENT ANALYSIS
AMAR BHUNGALIA and ALAN BURKHARD (USAF, Flight Dynamics Laboratory, Wright-Patterson AFB, OH) ASME, Winter Annual Meeting, Dallas, TX, Nov. 25-30, 1990. 9 p. refs
(ASME PAPER 90-WA/TS-1)

Avionics Environmental Reliability (AER) software developed for predicting the fatigue-life expectancy of avionics when subjected to the vibration and thermal environments of military aircraft is presented. Attention is focused on the vibration and thermal stresses in the lead wire and solder joints of electronic components when mounted on a printed circuit board within a line replaceable unit, and their predictions. Detailed finite-element modeling is used for predicting localized induced thermal and vibrational deformation and stress levels. A more extensive evaluation of the AER life-prediction accuracy is recommended in order to identify its full range of applicability. In order to improve the accuracy of the fatigue-life prediction of electronic components, a nonlinear thermal/vibration analysis is suggested to be considered and incorporated into the analytical capability. V.T.

A91-33227#
ANALYSIS OF LAMINAR SEPARATION BUBBLE USING A SIMPLE EDDY-VISCOSITY TURBULENCE MODEL
KENICHI RINOIE and NOBUHIKO KAMIYA Japan Society for Aeronautical and Space Sciences, Journal (ISSN 0021-4663), vol. 39, no. 444, 1991, p. 20-27. In Japanese, with abstract in English. refs

Laminar separation bubbles formed on airfoils were expressed numerically using a simple eddy-viscosity turbulence model. The eddy viscosity constant, epsilon(t), was set to a uniform value inside the turbulent part of the bubble. Overall characteristics of numerical results agreed closely with experimental results. The relation between epsilon(t) and velocity distributions was analyzed by the momentum balance inside the bubble. It was shown that the pressure recovery inside the bubble is proportional to epsilon(t). Finally, the semiempirical parameter which determines epsilon(t) was proposed. Author

A91-33464
ANALYSIS OF BEARING INCIDENTS IN AIRCRAFT GAS TURBINE MAINSHAFT BEARINGS
B. L. AVERBACH (MIT, Cambridge, MA) and E. N. BAMBERGER (GE Aircraft Engines, Cincinnati, OH) (STLE, Annual Meeting, 45th, Denver, CO, May 7-10, 1990) STLE Tribology Transactions (ISSN 0569-8197), vol. 34, April 1991, p. 241-247. USAF-sponsored research. refs
Copyright

An examination of approximately 200 bearing incidents in current aircraft engines has shown that damage in the bearing is initiated at the surface. Twenty-one cases were studied in detail, and five typical incidents are presented here. The initial damage was produced by abrasive particles, dents, grinding scores, skidding, large carbides and corrosion pits. The first phase of the failure mechanism appeared to be by peeling, where microscopic regions about 0.13 mm (0.005 in) were removed from the surface, and the peels eventually developed into spalls. These mechanisms of failure are a consequence of the partial EHD lubrication utilized in these bearings, and the consequent sharing of the load by the asperities and the EHD film. Failures of this type were reproduced in test bearings run under typical engine conditions, and these tests were used to study the peeling mechanism. Techniques for the minimization of surface-initiated fatigue are also discussed. Author

A91-33604
START - A BROAD APPLICATION SPECTRUM GYRO FOR THE 1990'S
D. G. HARRIS (GEC Avionics, Ltd., Rochester, England) IN: IEEE PLANS '90 - Position Location and Navigation Symposium, Las Vegas, NV, Mar. 20-23, 1990, Record. New York, Institute of Electrical and Electronics Engineers, Inc., 1990, p. 21-28.
Copyright

START is an all-solid-state angular rate sensor which began development in the early 1980s for weapons applications. The development phases of the START program are outlined, and the principle of operation is described. The current status and performance achieved to date are described. The areas of application for which START is either used or projected for field tests are given. The expected time scale for moving from prototype to large quantity production is considered. The version of START which is currently being prepared is the first generation of a new rate sensor technology in which the emphasis is on providing a wide performance range with very high shock resistance at the lowest price. I.E.

A91-33674
VORTICAL SOLUTIONS OF THE CONICAL EULER EQUATIONS
KENNETH GRANT POWELL (Michigan, University, Ann Arbor) Wiesbaden, Federal Republic of Germany/Hauppauge, NY, Friedr. Vieweg & Sohn/Ballen Books (Notes on Numerical Fluid Mechanics. Vol. 28), 1990, 294 p. refs
Copyright

Analytical, numerical, and experimental investigations of supersonic flows on delta wings are reported, with a focus on leading-edge vortices. A numerical algorithm employing local mesh refinement is developed to solve the Euler equations for inviscid compressible flow, and a model based on a similarity solution of the axisymmetric Navier-Stokes equations is constructed to treat localized regions of total pressure loss near the vortices. Computational results are compared in extensive graphs with experimental data obtained in the low-Mach-number test section of the Unitary Plan Wind Tunnel at NASA Langley (Miller and Wood, 1985; Powell et al., 1986). Good general agreement is demonstrated, except in the cases with vortex flaps, where hinge-line viscous effects are found. A complete listing of the Euler solution algorithm LEVIS is provided in an appendix. D.G.

A91-34014
METHOD FOR CALCULATING BOUNDARY REGION CORRECTIONS IN MULTISTEP AXIAL TURBOMACHINES [METHODE ZUR BERECHNUNG VON RANDZONENKORREKTUREN IN MEHRSTUFIGEN AXIALEN TURBOMASCHINEN]
KLAUS G. GRAHL (Bochum, Ruhr-Universitaet, Federal Republic of Germany) and MICHAEL SCHWARZ (Mannesmann Demag Verdichter und Druckluftechnik, Duisburg, Federal Republic of Germany) Forschung im Ingenieurwesen (ISSN 0015-7899), vol. 57, March 1991, p. 37-52. In German. refs
Copyright
A proven streamline geometry method is used here, together with a two-dimensional integral sidewall boundary layer theory and an improved secondary flow correlation, to calculate the boundary region-corrected blading in multistep, axial turbomachines. As an example, the determination of optimal flow relationships over a wide range of operation is shown for a three-step mean-pressure compressor. C.D.

A91-34015
WEIGHTLESS TEST BALANCING OF ELASTIC ROTORS WITH THE HELP OF INTERCHANGEABLE LONGITUDINAL BEARING STIFFNESSES [TESTGEWICHTLOSES AUSWUCHTEN ELASTISCHER ROTOREN MIT HILFE UMSCHALTBARER LAGERSTEIFIGKEITEN]
PETER GNIELKA (Schenk-ASG, Darmstadt, Federal Republic of Germany), QIZHOU LIU (Northwestern Polytechnical University, Xian, People's Republic of China), and ROBERT GASCH (Berlin, Technische Universitaet, Federal Republic of Germany) Forschung im Ingenieurwesen (ISSN 0015-7899), vol. 57, March 1991, p. 66-72. In German. Volkswagen-Stiftung-supported research. refs
Copyright
First experimental results are presented of the balancing of elastic rotors using interchangeable bearing stiffnesses. The use of weighting factors and modal balancing elements in this approach is examined. The results are compared with those from other methods. C.D.

A91-34064
AN IMPLICIT PREDICTOR-CORRECTOR RELAXATION METHOD FOR VISCOUS TRANSONIC FLOWS
W. KORDULLA (DLR, Institut fuer theoretische Stroemungsmechanik, Goettingen, Federal Republic of Germany) IN: Finite approximations in fluid mechanics II: DFG priority research programme results 1986-1988. Wiesbaden, Federal Republic of Germany/Hauppauge, NY, Friedr. Vieweg & Sohn/Ballen Books, 1989, p. 230-235. refs
(Contract DFG-KO-956/1-1)
Copyright
An unfactored implicit predictor-corrector scheme for the numerical simulation of transonic flows on airfoils is described and demonstrated. The method combines the MacCormack (1985) finite-volume predictor-corrector technique with an iterative implicit method incorporating upwinding with inherent numerical diffusion which does not falsify the flow physics. Results for an RAE 2822 profile at Mach 0.73, angle of attack 2.79 deg, and Reynolds number 6.5 x 10 to the 6th are presented in graphs and shown to be in good agreement with published experimetal data. D.G.

A91-34125
THE EFFECT OF SHEAR AND ROTARY INERTIA OF A ROTOR AT ITS CRITICAL SPEEDS
R. GRYBOS (Silesian Technical University, Gliwice, Poland) Archive of Applied Mechanics (ISSN 0939-1353), vol. 61, March 1991, p. 104-109. refs
Copyright
This paper deals with the eigenfrequencies of flexural vibration of a homogeneous rotor model which includes shear, rotary inertia and the gyroscopic effect. A formula for the critical speeds of this rotor has also been found. It appears that the effect of these factors is smaller when the critical speed increases and the ratio of slenderness of a rotor decreases. Author

A91-34127#
VELOCITY OF CAVITATION BUBBLES IN UNIFORM FLOWFIELD HIGH AND LOW REYNOLDS NUMBER
MAURO PIERUCCI (San Diego State University, CA) AIAA Journal (ISSN 0001-1452), vol. 29, April 1991, p. 505, 506.
Copyright
A gaseous bubble caused by the tip cavitation of a propeller blade operating in a uniform flowfield environment experiences a drag force in relation to its angular velocity and a thrust force in the axial direction. In this paper, a mathematical model is presented that studies propagation of the gaseous bubble at low and high Reynolds number cases. The temporal and the spatial profile velocity variations are presented. The time constants involved in both regimes are obtained. The velocity variations are shown to be exponential for the low Reynolds number case and algebraic for the high Reynolds number case. Author

A91-34176
GAMM-CONFERENCE ON NUMERICAL METHODS IN FLUID MECHANICS, 8TH, DELFT UNIVERSITY OF TECHNOLOGY, NETHERLANDS, SEPT. 27-29, 1989, PROCEEDINGS
PIETER WESSELING, ED. (Delft University of Technology, Netherlands) Conference supported by Gesellschaft fuer angewandte Mathematik und Mechanik, Royal Academy of Sciences, U.S. Navy, et al. Wiesbaden, Federal Republic of Germany/Hauppauge, NY, Friedr. Vieweg & Sohn/Ballen Books (Notes on Numerical Fluid Mechanics. Vol. 29), 1990, 631 p. For individual items see A91-34177 to A91-34231.
Copyright
Recent advances in computational fluid dynamics are discussed in reviews and reports. Topics addressed include an extension of Roe's approximate Riemann solver to equilibrium and nonequilibrium flows, characteristic boundary conditions for cell-centered Euler flow calculations, a multigrid flux-difference splitting method for the steady incompressible Navier-Stokes equations, and the simulation of glancing-shock/boundary-layer interactions. Consideration is given to interfacial instabilities at high Mach numbers, three-dimensional Euler flows on aircraft, a posteriori error estimators for adaptive spectral-element methods, numerical simulations of the near field of a plane jet, a sparse quasi-Newton method for Navier-Stokes solutions, calculation of a buoyancy-driven three-dimensional cavity flow using a multiprocessor system, and an eigenvalue analysis of finite-difference approximations for hyperbolic initial/boundary-value problems. D.G.

A91-34178
DEVELOPMENT AND VALIDATION OF CHARACTERISTIC BOUNDARY CONDITIONS FOR CELL-CENTERED EULER FLOW CALCULATIONS
J. I. VAN DEN BERG and J. W. BOERSTOEL (National Aerospace Laboratory, Amsterdam, Netherlands) IN: GAMM-Conference on Numerical Methods in Fluid Mechanics, 8th, Delft, Netherlands, Sept. 27-29, 1989, Proceedings. Wiesbaden, Federal Republic of Germany/Hauppauge, NY, Friedr. Vieweg & Sohn/Ballen Books,

1990, p. 11-21. Netherlands Agency for Aerospace Programs-supported research. refs
Copyright

An overview of the development, analysis, and numerical validation of a solid-wall boundary condition for cell-centered Euler-flow calculations is presented. This solid-wall boundary condition is provided by the theory of characteristics, and is based on a central-difference scheme. The boundary condition was developed to investigate the effect of various boundary-condition algorithms on the accuracy of calculation results for three-dimensional Euler flows around delta wings. A mathematical analysis of the boundary condition was performed. The numerical validation consists of a comparison of calculation results with various boundary conditions. Also discretization and convergence errors were investigated. As a test case, the NLR 7301 profile under supercritical, shock-free flow conditions of M = 0.721, alpha = -0.194 deg, were chosen. Author

A91-34181
SOLUTION OF THE 3-D, INCOMPRESSIBLE NAVIER-STOKES EQUATIONS FOR THE SIMULATION OF VORTEX BREAKDOWN

M. BREUER and D. HAENEL (Aachen, Rheinisch-Westfaelische Technische Hochschule, Federal Republic of Germany) IN: GAMM-Conference on Numerical Methods in Fluid Mechanics, 8th, Delft, Netherlands, Sept. 27-29, 1989, Proceedings. Wiesbaden, Federal Republic of Germany/Hauppauge, NY, Friedr. Vieweg & Sohn/Ballen Books, 1990, p. 42-51. refs
Copyright

A method of solution is presented for the three-dimensional, unsteady Navier-Stokes equations of an incompressible fluid. The method is based on the principle of artificial compressibility, extended to time-dependent solutions by the concept of dual time stepping. Higher order upwinding (QUICK interpolation, and Roe-type splitting) is used for the spatial discretization. The properties of the method were tested by means of different validated flow problems. Present computations concern with the unsteady, and three-dimensional problem of the breakdown of an isolated vortex. The temporal evolution and the internal structure of the breakdown bubble is investigated and compared with experimental observations. Author

A91-34439#
INTERACTION BETWEEN TWO JETS EXHAUSTED FROM NOZZLES ARRANGED IN PARALLEL

NATSUO HATTA, HITOSHI FUJIMOTO (Kyoto University, Japan), and JUN-ICHI KOKADO Kyoto University, Faculty of Engineering, Memoirs (ISSN 0023-6063), vol. 53, Jan. 1991, p. 19-48. refs
(Contract MOESC-01550532)

The flow structures of two interacting free jets expanded from uniform sonic nozzles into a stagnant ambient gas region are studied. A two-dimensional Cartesian coordinate system is used for the present simulations. A choked underexpanded supersonic single free jet is investigated in the context of continuum ideal gas dynamics. K.K.

A91-34810#
EVALUATING THERMOGRAPHIC PHOSPHORS IN AN OPERATING TURBINE ENGINE

B. W. NOEL, H. M. BORELLA (Los Alamos National Laboratory, NM), W. LEWIS, W. D. TURLEY (EG & G Energy Measurements, Inc., Goleta, CA), D. L. BESHEARS (Oak Ridge National Laboratory, TN) et al. ASME, Transactions, Journal of Engineering for Gas Turbines and Power (ISSN 0022-0825), vol. 113, April 1991, p. 242-245. USAF-supported research. Previously announced in STAR as N90-22044. refs
(ASME PAPER 90-GT-266) Copyright

The results of a field test in a commercial turbine engine showed that we can remotely measure the temperature of engine components in operating engines using thermographic phosphors. The remote measurement method exploits the temperature dependence of the characteristic decay time of the laser-induced fluorescence of thermographic phosphors. This paper summarizes recent work leading up to and including a successful test of the thermographic-phosphor method in an operating turbine engine. Author

A91-34822#
ROTORDYNAMIC COEFFICIENTS FOR PARTIALLY ROUGHENED PUMP ANNULAR SEALS

J. K. SCHARRER (Rockwell International Corp., Rocketdyne Div., Canoga Park, CA) and C. C. NELSON (Texas A & M University, College Station) ASME, Transactions, Journal of Vibration and Acoustics (ISSN 0739-3717), vol. 113, April 1991, p. 240-244. refs
Copyright

The basic equations are derived for incompressible flow in an annular seal with partially roughened surfaces. The flow is assumed to be completely turbulent in the axial and circumferential directions with no separation, and is modeled by Hirs' turbulent lubrication equations. Linearized zeroth and first-order perturbation equations are developed for small motion about a centered position by an expansion in the eccentricity ratio. The zeroth-order continuity and momentum equations are solved numerically, yielding the axial and circumferential velocity components and the pressure distribution. The first-order equations are reduced to three linear, complex, ordinary, differential equations in the axial coordinate Z. The equations are integrated to satisfy the boundary conditions and yield the perturbated pressure distribution. This resultant pressure distribution is integrated along and around the seal to yield the force developed by the seal from which the corresponding dynamic coefficients are derived. The results of a parametric study on the effect of the rough length/smooth length ratio on the seal leakage and rotordynamic coefficients are presented. Author

A91-35117*# Florida Inst. of Tech., Melbourne.
GREEN'S FUNCTION SOLUTION TO RADIATIVE HEAT TRANSFER BETWEEN LONGITUDINAL GRAY FINS

J. I. FRANKEL (Florida Institute of Technology, Melbourne) and J. J. SILVESTRI Journal of Thermophysics and Heat Transfer (ISSN 0887-8722), vol. 5, Jan. 1991, p. 120-122. Research supported by Space Research Institute. refs
(Contract NAG8-109)
Copyright

A demonstration is presented of the applicability and versatility of a pure integral formulation for radiative-conductive heat-transfer problems. Preliminary results have been obtained which indicate that this formulation allows an accurate, fast, and stable computation procedure to be implemented. Attention is given to the accessory problem defining Green's function. O.C.

A91-35498
DYNAMIC ANALYSIS TECHNIQUE OF CENTRIFUGAL IMPELLOR WITH SPLIT BLADES

JIN ZHANG (Beijing University of Aeronautics and Astronautics, People's Republic of China), XIANG-JUN CHEN (Wuxi Institute of Aeroengine Design, People's Republic of China), and WEN-LIANG WANG (Fudan University, Shanghai, People's Republic of China) IN: International Modal Analysis Conference, 8th, Kissimmee, FL, Jan. 29-Feb. 1, 1990, Proceedings. Vol. 1. Bethel, CT, Society for Experimental Mechanics, Inc., 1990, p. 229-233. refs
Copyright

The paper presents a dynamic analysis technique for application to a gas-turbine centrifugal impeller with split blades. The Hermite generalized mass and stiffness matrices under reduced coordinates are found by utilizing Benfield mode substitution transformation combined with group transformation. The natural frequencies of the system are found, and transformation is employed to discover the corresponding modal shapes. Analysis results are compared with other methods and experimental data on a test model. The method is shown to be reliable and practical, as the modal shapes are confirmed, the maximum relative error is less than 1 percent, and computation time is reduced. The possibility of multicomponent partition is confirmed in the repetitive sector of the centrifugal impeller. The method may be combined with the substructure

simultaneous iteration method to be used directly in creating a rotational state dynamic analysis of a real centrifugal impeller with split blades. C.C.S.

A91-35516
EXPERIMENTAL AND ANALYTICAL STUDY OF SHAFT CRACKING RESPONSE IN ROTATORY MACHINES
LUIS SAN JUAN (*Universidad del Bio-Bio, Concepcion, Chile*) and PEDRO SAAVEDRA (Concepcion, Universidad, Chile) IN: International Modal Analysis Conference, 8th, Kissimmee, FL, Jan. 29-Feb. 1, 1990, Proceedings. Vol. 1. Bethel, CT, Society for Experimental Mechanics, Inc., 1990, p. 445-450. Fondo Nacional de Desarrollo Cientifico y Tecnologico-supported research. refs
Copyright

The effects of a transverse crack on the dynamics of a rotor system have been studied. The crack has been simulated by a localized reduction in shaft diameter at the crack position. An analytical model of a rotor mounted on bearing and containing a traverse crack is used for simulating its dynamical response under different rotation speeds, size, and location of the crack. The effect of the out-of-balance distribution and the ratio of dynamical to steady loads on the shaft vibrational behavior is also studied. The theoretical results-orbits, amplitude specters, phase specters, ratio of nonsynchronic to synchronic spectral amplitudes, and vibration modes prove that the 1x and 2x spectral components present the principal changes. Author

A91-35529
APPLICATION OF SENSITIVITY METHODS FOR ERROR LOCALIZATION IN FINITE ELEMENT SYSTEMS
WOLFGANG LUBER and ALBERT LOTZE (MBB GmbH, Munich, Federal Republic of Germany) IN: International Modal Analysis Conference, 8th, Kissimmee, FL, Jan. 29-Feb. 1, 1990, Proceedings. Vol. 1. Bethel, CT, Society for Experimental Mechanics, Inc., 1990, p. 598-604. refs
Copyright

A principal objective of modal updating is to improve the finite element model of a test structure which then can be used to predict the system dynamics. During the past decade mathematical optimization methods have been developed. The sensitivity analysis gives information about the areas of potential errors and can therefore be used to localize these errors, causing the discrepancies between analytical and experimental normal modes. This paper presents sensitivity procedures used for error localization as well as the results of updated stiffness and mass values of an aircraft structure. Author

A91-35536* Ohio State Univ., Columbus.
LINEAR AND NON-LINEAR DYNAMIC MODELS OF A GEARED ROTOR-BEARING SYSTEM
AHMET KAHRAMAN and RAJENDRA SINGH (Ohio State University, Columbus) IN: International Modal Analysis Conference, 8th, Kissimmee, FL, Jan. 29-Feb. 1, 1990, Proceedings. Vol. 1. Bethel, CT, Society for Experimental Mechanics, Inc., 1990, p. 697-703. NASA-supported research. refs
Copyright

A three degree of freedom non-linear model of a geared rotor-bearing system with gear backlash and radial clearances in rolling element bearings is proposed here. This reduced order model can be used to describe the transverse-torsional motion of the system. It is justified by comparing the eigen solutions yielded by corresponding linear model with the finite element method results. Nature of nonlinearities in bearings is examined and two approximate nonlinear stiffness functions are proposed. These approximate bearing models are verified by comparing their frequency responses with the results given by the exact form of nonlinearity. The proposed nonlinear dynamic model of the geared rotor-bearing system can be used to investigate the dynamic behavior and chaos. Author

A91-35537* Ohio State Univ., Columbus.
FORCE AND MOMENT TRANSMISSIBILITIES THROUGH ROLLING ELEMENT BEARINGS IN A SINGLE-STAGE ROTOR SYSTEM
TEIK CHIN LIM and RAJENDRA SINGH (Ohio State University, Columbus) IN: International Modal Analysis Conference, 8th, Kissimmee, FL, Jan. 29-Feb. 1, 1990, Proceedings. Vol. 1. Bethel, CT, Society for Experimental Mechanics, Inc., 1990, p. 704-710. NASA-supported research. refs
Copyright

A lumped parameter model of a single-stage rotor system is developed which includes a new mathematical model for precision rolling element bearings to clarify this issue quantitatively and qualitatively. A comprehensive bearing stiffness matrix of dimension six is proposed which clearly demonstrates the coupling between the rotating shaft and casing motion. An eigensolution and the forced harmonic solution are obtained numerically. The natural frequencies predicted are found to be in excellent agreement with a finite element model. Author

A91-35539
VORTEX ELEMENT METHODS FOR FLUID DYNAMIC ANALYSIS OF ENGINEERING SYSTEMS
REGINALD IVAN LEWIS (Newcastle-upon-Tyne, University, England) Cambridge, England and New York, Cambridge University Press (Cambridge Engine Technology Series. Vol. 1), 1991, 587 p. refs
Copyright

The surface-vorticity method of computational fluid mechanics is described, with an emphasis on turbomachinery applications, in an introduction for engineers. Chapters are devoted to surface singularity modeling; lifting bodies, two-dimensional airfoils, and cascades; mixed-flow and radial cascades; bodies of revolution, ducts, and annuli; ducted propellers and fans; three-dimensional and meridional flows in turbomachines; free vorticity shear layers and inverse methods; vortex dynamics in inviscid flows; the simulation of viscous diffusion in discrete vortex modeling; vortex-cloud modeling by the boundary-integral method; vortex-cloud models for lifting bodies and cascades; and grid systems for vortex dynamics and meridional flows. Diagrams, graphs, and the listings for a set of computer programs are provided. T.K.

A91-35742
USING A LOCALLY ONE-DIMENSIONAL METHOD FOR SOLVING THE HEAT CONDUCTIVITY EQUATION TO DETERMINE THE THERMAL STATE OF COOLED ROTOR DISKS [PRIMENENIE LOKAL'NO-ODNOMERNOGO METODA RESHENIIA URAVNENIIA TEPLOPROVODNOSTI DLIA OPREDELENIIA TEPLOVOGO SOSTOIANIIA OKHLAZHDAEMYKH DISKOV ROTOROV]
B. D. BILEKA and V. IA. KABKOV (AN USSR, Institut Tekhnicheskoi Teplofiziki, Kiev, Ukrainian SSR) Promyshlennaia Teplotekhnika (ISSN 0204-3602), vol. 13, no. 1, 1991, p. 37-43. In Russian. refs
Copyright

A locally one-dimensional method is used for calculating the steady-state thermal condition of rotor disks by consecutively solving the axisymmetric and three-dimensional problems and coordinating the solutions over the reference radius. Unsteady state calculations are also carried out for a disk using a two-dimensional formulation for the part of the disk located below the reference radius. Results of calculations for a series of gas turbine engine disks are presented and compared with experimental data. V.L.

A91-35743
CALCULATION OF THE COOLING SYSTEM OF SMALL-SIZE BLADES OF HIGH-TEMPERATURE GAS TURBINE ENGINES [RASCHET SISTEMY OKHLAZHDENIIA MALORAZMERNYKH LOPATOK VYSOKOTEMPERATURNYKH GTD]
V. M. KLIMENKO and I. M. CHIGAREV (AN USSR, Institut Tekhnicheskoi Teplofiziki, Kiev, Ukrainian SSR) Promyshlennaia

Teplotekhnika (ISSN 0204-3602), vol. 13, no. 1, 1991, p. 88-91. In Russian.
Copyright

A small-channel cooling system for small-size gas turbine blades is considered, and a method for calculating such a system is proposed. The method is based on representing small-channel cooling as an equivalent of the internal ribbing of the heat transfer surfaces. The calculation results are compared with calculations based on the electrothermal analogy approach. V.L.

A91-35785
STATE STABILITY OF A SYSTEM OF INTEGRO-DIFFERENTIAL EQUATIONS OF NONSTATIONARY AEROELASTICITY [OB USTOICHIVOSTI PO SOSTOIANIIU SISTEMY INTEGRO-DIFFERENTSIAL'NYKH URAVNENII NESTATSIONARNOI AEROUPRUGOSTI]
A. I. EGOROV and P. I. KOGUT (Dnepropetrovskii Institut Inzhenerov Zheleznodorozhnogo Transporta, Dnepropetrovsk, Ukrainian SSR) Vychislitel'naia i Prikladnaia Matematika (ISSN 0321-4117), no. 70, 1990, p. 112-121. In Russian. refs
Copyright

The paper is concerned with nonstationary aeroelasticity described by a system of integro-differential equations that are unresolved with respect to a derivative. The necessary and sufficient conditions for the exponential stability of such a system in the metrics of infinite-dimensional Gilbert space are formulated in terms of Liapunov functionals. The analysis is illustrated by an example. V.L.

A91-35787
AN APPROACH TO THE NUMERICAL SOLUTION OF TWO-DIMENSIONAL NAVIER-STOKES EQUATIONS BY A FINITE DIFFERENCE METHOD [OB ODNOM PODKHODE K CHISLENNOMU RESHENIIU DVUMERNYKH URAVNENII NAV'E-STOKSA METODOM SKVOZNOGO SCHETA]
I. V. EGOROV and O. L. ZAITSEV Zhurnal Vychislitel'noi Matematiki i Matematicheskoi Fiziki (ISSN 0044-4669), vol. 31, Feb. 1991, p. 286-299. In Russian. refs
Copyright

A finite difference method based on an implicit second-order conservative scheme is used to obtain a numerical solution for the Navier-Stokes equations. The convective terms of the Navier-Stokes equations are approximated by using a monotonic scheme; the diffusion terms are approximated by using a central difference scheme. The problem of steady-state supersonic flow of a gas past a cylinder is examined as an example. V.L.

A91-35986
SIMULATION OF TWO- AND THREE-DIMENSIONAL INTERNAL SUBSONIC FLOWS USING A FINITE ELEMENT METHOD
MARC BUFFAT (Lyon, Ecole Centrale, Ecully, France) International Journal for Numerical Methods in Fluids (ISSN 0271-2091), vol. 12, April 20, 1991, p. 683-704. refs
Copyright

In this paper a finite element method is presented to predict internal subsonic flows. Using a low-Mach-number approximation, the pressure is decomposed into a mean thermodynamic contribution and a dynamic fluctuation to deal with the complex role of the pressure in internal aerodynamics. A semi-implicit time integration and a finite element method with a moving mesh are described to take into account complex geometries and moving boundaries. An Uzawa algorithm accelerated by a preconditioned residual method is introduced to solve the coupled nonsymmetric linear system for the velocity components and the pressure. An efficient conjugate gradient method combined with an incomplete LU preconditioning is used to solve the nonsymmetric linear systems arising from the discretization. The implementation of the numerical scheme on parallel supercomputers is also discussed. Efficient algorithms for the finite element assembly phase and for the solution of linear system are described which take advantage of the parallel architecture of the new generation of supercomputers. With this technique a global speed-up of 10 is achieved on a supercomputer with eight processors. To illustrate the capabilities of the numerical method, two- and three-dimensional simulations of flows in the combustion chamber of a reciprocating engine and around the combustor dome of a gas turbine engine are presented. Author

N91-21067*# National Aeronautics and Space Administration. Lewis Research Center, Cleveland, OH.
A FINITE-DIFFERENCE, FREQUENCY-DOMAIN NUMERICAL SCHEME FOR THE SOLUTION OF THE LINEARIZED UNSTEADY EULER EQUATIONS
JAMES R. SCOTT and HAFIZ M. ATASSI (Notre Dame Univ., IN.) *In its* Computational Fluid Dynamics Symposium on Aeropropulsion p 55-104 Jan. 1991
Avail: NTIS HC/MF A99; 10 functional color pages CSCL 20D

A numerical method is developed for solving periodic, three-dimensional, vortical flows around lifting airfoils in subsonic flow. The first-order method, that is presented, fully accounts for the distortion effects of the nonuniform mean flow on the convected upstream vortical disturbances. The unsteady velocity is split into a vortical component which is a known function of the upstream flow conditions and the Lagrangian coordinates of the mean flow, and an irrotational field whose potential satisfies a nonconstant-coefficient, inhomogeneous, convective wave equation. Using an elliptic coordinate transformation, the unsteady boundary value problem is solved in the frequency domain on grids which are determined as a function of the Mach number and reduced frequency. Extensive comparisons are made with known solutions to unsteady vortical flow problems, and it is seen that the agreement is generally very good for reduced frequencies ranging from 0 up to 4. Author

N91-21068*# Cincinnati Univ., OH.
A PRESSURE FLUX-SPLIT TECHNIQUE FOR COMPUTATION OF INLET FLOW BEHAVIOR
H. S. PORDAL, P. K. KHOSLA, and S. G. RUBIN *In* NASA, Lewis Research Center, Computational Fluid Dynamics Symposium on Aeropropulsion p 105-117 Jan. 1991
(Contract NAG3-716; F49620-85-C-0027)
Avail: NTIS HC/MF A99; 10 functional color pages CSCL 20D

A method for calculating the flow field in aircraft engine inlets is presented. The phenomena of inlet unstart and restart are investigated. Solutions of the reduced Navier-Stokes (RNS) equations are obtained with a time consistent direct sparse matrix solver that computes the transient flow field both internal and external to the inlet. Time varying shocks and time varying recirculation regions can be efficiently analyzed. The code is quite general and is suitable for the computation of flow for a wide variety of geometries and over a wide range of Mach and Reynolds numbers. Author

N91-21070*# Rockwell International Corp., Canoga Park, CA. Rocketdyne Div.
NUMERICAL SOLUTIONS OF 2-D MULTI-STAGE ROTOR/STATOR UNSTEADY FLOW INTERACTIONS
R.-J. YANG and S.-J. LIN *In* NASA, Lewis Research Center, Computational Fluid Dynamics Symposium on Aeropropulsion p 127-142 Jan. 1991 Original contains color illustrations
(Contract NAS8-40000)
Avail: NTIS HC/MF A99; 10 functional color pages CSCL 20D

The Rai method of single-stage rotor/stator flow interaction is extended to handle multistage configurations. In this study, a two-dimensional Navier-Stokes multi-zone approach was used to investigate unsteady flow interactions within two multistage axial turbines. The governing equations are solved by an iterative, factored, implicit finite-difference, upwind algorithm. Numerical accuracy is checked by investigating the effect of time step size, the effect of subiteration in the Newton-Raphson technique, and the effect of full viscous versus thin-layer approximation. Computer results compared well with experimental data. Unsteady flow interactions, wake cutting, and the associated evolution of vortical entities are discussed. Author

N91-21071*# National Aeronautics and Space Administration. Lewis Research Center, Cleveland, OH.
TRANSONIC CASCADE FLOW CALCULATIONS USING NON-PERIODIC C-TYPE GRIDS
ANDREA ARNONE, MENG-SING LIOU, and LOUIS A. POVINELLI *In its* Computational Fluid Dynamics Symposium on Aeropropulsion p 143-162 Jan. 1991
(Contract NASA ORDER C-99066-G)
Avail: NTIS HC/MF A99; 10 functional color pages CSCL 20D

A new kind of C-type grid is proposed for turbomachinery flow calculations. This grid is nonperiodic on the wake and results in minimum skewness for cascades with high turning and large camber. Euler and Reynolds averaged Navier-Stokes equations are discretized on this type of grid using a finite volume approach. The Baldwin-Lomax eddy-viscosity model is used for turbulence closure. Jameson's explicit Runge-Kutta scheme is adopted for the integration in time, and computational efficiency is achieved through accelerating strategies such as multigriding and residual smoothing. A detailed numerical study was performed for a turbine rotor and for a vane. A grid dependence analysis is presented and the effect of artificial dissipation is also investigated. Comparison of calculations with experiments clearly demonstrates the advantage of the proposed grid. Author

N91-21072*# Pennsylvania State Univ., University Park. Dept. of Aerospace Engineering.
COMPUTATION OF SUPERSONIC AND LOW SUBSONIC CASCADE FLOWS USING AN EXPLICIT NAVIER-STOKES TECHNIQUE AND THE KAPPA-EPSILON TURBULENCE MODEL
R. F. KUNZ and B. LAKSHMINARAYANA *In* NASA, Lewis Research Center, Computational Fluid Dynamics Symposium on Aeropropulsion p 163-201 Jan. 1991
(Contract DAAL03-86-G-0044)
Avail: NTIS HC/MF A99; 10 functional color pages CSCL 20D

A fully explicit two-dimensional flow solver, based on a four-stage Runge-Kutta scheme, was developed and utilized to predict two-dimensional viscous flow through turbomachinery cascades for which experimental data is available. The formulation is applied to the density averaged Navier-Stokes equations. Several features of the technique improve the ability of the code to predict high Reynolds number flows on highly stretched grids. These include a low Reynolds number compressible form of the k-epsilon turbulence model, anisotropic scaling of artificial dissipation terms and locally varying timestep evaluation based on hyperbolic and parabolic stability considerations. Comparisons between computation and experiment are presented for both a supersonic and a low-subsonic compressor cascade. These results indicate that the code is capable of predicting steady two-dimensional viscous cascade flows over a wide range of Mach numbers in reasonable computational times. Author

N91-21089*# Analytical Services and Materials, Inc., Hampton, VA.
ZONAL ANALYSIS OF TWO HIGH-SPEED INLETS
A. D. DILLEY, G. F. SWITZER, and W. M. EPPARD *In* NASA, Lewis Research Center, Computational Fluid Dynamics Symposium on Aeropropulsion p 507-519 Jan. 1991
(Contract NAS1-18599)
Avail: NTIS HC/MF A99; 10 functional color pages CSCL 20D

Using a zonal technique, thin layer Navier-Stokes solutions for two high speed inlet geometries are presented and compared with experimental data. The first configuration consists of a 3-D inlet preceded by a sharp flat plate. Results with two different grids demonstrate the importance of adequate grid refinement in high speed internal flow computations. The fine grid solution has reasonably good agreement with experimental heat transfer and pressure values inside the inlet. The other configuration consists of a 3-D inlet mounted on a research hypersonic forebody. Numerical results for this configuration have good agreement with experimental pressure data along the forebody, but not inside the inlet. A more refined grid calculation is currently being done to better predict the flowfield in the inlet. Author

N91-21098*# National Aeronautics and Space Administration. Langley Research Center, Hampton, VA.
A HIGHLY EFFICIENT ENGINEERING TOOL FOR THREE-DIMENSIONAL SCRAMJET FLOWFIELD AND HEAT TRANSFER COMPUTATIONS
PRADEEP S. KAMATH, RICHARD W. HAWKINS, NATHANIEL R. BAKER (Lockheed Engineering and Sciences Co., Hampton, VA.), and CHARLES R. MCCLINTON *In* NASA, Lewis Research Center, Computational Fluid Dynamics Symposium on Aeropropulsion p 669-681 Jan. 1991
Avail: NTIS HC/MF A99; 10 functional color pages CSCL 20D

The SIMPLE-based parabolic flow code, SHIP3D, was under development for use as a parametric design and analysis tool for scramjets. Some capabilities and applications of the code are demonstrated, and a report on its current status is given. The focus is on the combustor for which the code was mostly used. Recently, it was also applied to nozzle flows. Code validation results are presented for combustor unit problems involving film cooling, transverse fuel injection, and nozzle test. A parametric study of a film cooled or transpiration cooled Mach 16 combustor is also conducted to illustrate the application of the code to a design problem. Author

N91-21379# National Aerospace Lab., Tokyo (Japan).
PROCEEDINGS OF THE 8TH NAL SYMPOSIUM ON AIRCRAFT COMPUTATIONAL AERODYNAMICS: PROSPECTS OF COMPUTATIONAL FLUID DYNAMICS AND SUPER COMPUTERS IN AEROSPACE SCIENCE AND TECHNOLOGY
Sep. 1990 118 p In ENGLISH and JAPANESE Symposium held in Tokyo, Japan, 25-27 Jun. 1990
(NAL-SP-13; ISSN-0289-260X) Avail: NTIS HC/MF A06

The papers presented at the symposium are given. Some representative titles are as follows: Computer requirements for further CFD development; Present and future of CFD on the Aero-Engine development in IHI; CFD research and systems in Kawasaki Heavy Industries and its future prospects; The CFD analysis related aerospace in Fuji Heavy Industries, Ltd.; and Parallelization techniques for a supercomputer with Hierarchical Memory Architecture.

N91-21381# Ishikawajima-Harima Heavy Industries Co. Ltd., Tokyo (Japan).
PRESENT AND FUTURE OF CFD ON THE AERO-ENGINE DEVELOPMENT IN IHI
ATSUSHIGE TANAKA *In* National Aerospace Lab., Proceedings of the 8th NAL Symposium on Aircraft Computational Aerodynamics: Prospects of Computational Fluid Dynamics and Super Computers in Aerospace Science and Technology p 27-46 Sep. 1990 In JAPANESE; ENGLISH summary
Avail: NTIS HC/MF A06

Advances in aircraft engine performance and economy are achieved by a fusion of many individual advances in technology. Especially striking advances in the evolution of aerodynamic technology have appeared in the development and utilization of computational fluid dynamics (CFD). CFD already may have attained the level and continues to demonstrate extraordinarily valuable possibilities, in which it is an essential complement to testing and experimentation. A brief review is presented of the current status and the future of CFD on aircraft engine development in IHI. Author

N91-21382# Kawasaki Heavy Industries Ltd., Gifu (Japan). Aircraft Research Lab.
CFD RESEARCH AND SYSTEMS IN KAWASAKI HEAVY INDUSTRIES AND ITS FUTURE PROSPECTS
KOICHI HIRAOKA *In* National Aerospace Lab., Proceedings of the 8th NAL Symposium on Aircraft Computational Aerodynamics: Prospects of Computational Fluid Dynamics and Super Computers in Aerospace Science and Technology p 47-55 Sep. 1990 In JAPANESE; ENGLISH summary
Avail: NTIS HC/MF A06

KHI Computational Fluid Dynamics (CFD) system is composed of VP100 computer and 2-D and 3-D Euler and/or Navier-Stokes

(NS) analysis softwares. For KHI, this system has become a very powerful aerodynamic tool together with the Kawasaki 1 m Transonic Wind Tunnel. The 2-D Euler/NS software, developed in-house, is fully automated, requires no special skill, and was successfully applied to the design of YXX high lift devices and SST supersonic inlet, etc. The 3-D Euler/NS software, developed under joint research with NAL, has an interactively operated Multi-Block type grid generator and can effectively generate grids around complex airplane shapes. Due to the main memory size limitation, 3-D analysis of relatively simple shape, such as SST wing-body, was computed in-house on VP100, otherwise, such as detailed 3-D analyses of ASUKA and HOPE, were computed on NAL VP400, which is 10 times more powerful than VP100, under KHI-NAL joint research. These analysis results have very good correlation with experimental results. However, the present CFD system is less productive than wind tunnel and has applicability limitations. Author

N91-21383# Fuji Heavy Industries Ltd., Utsunomiya (Japan).
THE CFD ANALYSIS RELATED AEROSPACE IN FUJI HEAVY INDUSTRIES, LTD.
KOHEI TANAKA, HIDEHIRO HIROSE, and YASUHIRO KOSHIOKA *In* National Aerospace Lab., Proceedings of the 8th NAL Symposium on Aircraft Computational Aerodynamics: Prospects of Computational Fluid Dynamics and Super Computers in Aerospace Science and Technology p 57-67 Sep. 1990 In JAPANESE; ENGLISH summary
Avail: NTIS HC/MF A06

The relationships of Computational Fluid Dynamics (CFD) with design processes are discussed. CFD activities in FHI, Ltd. are introduced. To obtain full merit of CFD in design, the interactive manner of use is very important. Much more high computing speed is needed, also, more flexible in-out systems, too. In FHI, 2D/3D Euler, 2D/3D N-S codes were developed and in operation for several years. Also, many codes of panel method, potential method, and Newtonian flow method, are in use. These CFD tools are very effective in design. FHI is still making efforts to get more refined and quicker systems. CFD is very high technology, so efforts from aircraft makers have some limitations. Author

N91-21384# Mitsubishi Heavy-Industries Ltd., Nagoya (Japan). Engineering Research Dept.
STATUS AND OUTLOOK OF CFD TECHNOLOGY AT MITSUBISHI HEAVY INDUSTRIES, NAGOYA
TADAYUKI TANIOKA *In* National Aerospace Lab., Proceedings of the 8th NAL Symposium on Aircraft Computational Aerodynamics: Prospects of Computational Fluid Dynamics and Super Computers in Aerospace Science and Technology p 69-81 Sep. 1990 In JAPANESE; ENGLISH summary
Avail: NTIS HC/MF A06

Computational Fluid Dynamics (CFD) technology has made tremendous progress in the last several years. It has matured to become a practical simulation tool in aircraft industries. In MHI, CFD has become an indispensible tool for aerodynamic design aerospace vehicles. The present status is described of this advanced technology at MHI. Also mentioned are some future advances of the fast growing technology as well as associated hardware requirements. Author

N91-21407# Lawrence Livermore National Lab., CA.
THE SINGLE ANTENNA INTERFEROMETER
J. P. FITCH 15 Jan. 1990 6 p Presented at the 1991 Institute of Electrical and Electronics Engineers (IEEE) International Conference on Acoustics, Speech and Signal Processing, Toronto, Ontario, 14-17 May 1991
(Contract W-7405-ENG-48)
(DE91-007128; UCRL-JC-105984; CONF-9105122-1) Avail: NTIS HC/MF A02

Air and spaceborne platforms using synthetic aperture radars (SAR) have made interferometric measurement by using either two physical antennas mounted on one airframe or two passes of one antenna over a scene. A new interferometric technique using one pass of a single-antenna SAR system is proposed and demonstrated on data collected by the NASA-JPL AirSAR. Remotely sensed L-band microwave data are used to show the sensitivity of this technique to ocean surface features as well as a baseline for comparison with work by others using two-antenna system. DOE

N91-21410# Air Force Inst. of Tech., Wright-Patterson AFB, OH. School of Engineering.
SPEECH RECOGNITION USING KOHONEN NEURAL NETWORKS, DYNAMIC PROGRAMMING, AND MULTI-FEATURE FUSION M.S. Thesis
FRANCIS S. STOWE Dec. 1990 311 p
(AD-A230951; AFIT/GE/ENG/90D-59) Avail: NTIS HC/MF A14 CSCL 25/4

The purpose of this thesis was to develop and evaluate the performance of a three-feature speech recognition system. The three features used were LPC spectrum, formants (F1/F2), and cepstrum. The system uses Kohonen neural networks, dynamic programming, and a rule-based, feature-fusion process which integrates the three input features into one output result. The first half of this research involved evaluating the system in a speaker-dependent atmosphere. For this, the 70 word F-16 cockpit command vocabulary was used and both isolated and connected speech was tested. Results obtained are compared to a two-feature system with the same system configuration. Isolated-speech testing yielded 98.7 percent accuracy. Connected-speech testing yielded 75/0 percent accuracy. The three-feature system performed an average of 1.7 percent better than the two-feature system for isolated-speech. The second half of this research was concerned with the speaker-independent performance of the system. First, cross-speaker testing was performed using an updated 86 word library. In general, this testing yielded less than 50 percent accuracy. Then, testing was performed using averaged templates. This testing yielded an overall average in-template recognition rate of approximately 90 percent and an out-of-template recognition rate of approximately 75 percent. GRA

N91-21446*# National Aeronautics and Space Administration. Hugh L. Dryden Flight Research Facility, Edwards, CA.
A PRELIMINARY EVALUATION OF AN F100 ENGINE PARAMETER ESTIMATION PROCESS USING FLIGHT DATA
TRINDEL A. MAINE, GLENN B. GILYARD, and HEATHER H. LAMBERT Washington Aug. 1990 32 p Presented at the 26th AIAA Joint Propulsion Conference, Orlando, FL, 16-18 Jul. 1990 Previously announced in IAA as A90-40559
(NASA-TM-4216; H-1602; NAS 1.15:4216) Avail: NTIS HC/MF A03 CSCL 20/4

The parameter estimation algorithm developed for the F100 engine is described. The algorithm is a two-step process. The first step consists of a Kalman filter estimation of five deterioration parameters, which model the off-nominal behavior of the engine during flight. The second step is based on a simplified steady-state model of the compact engine model (CEM). In this step, the control vector in the CEM is augmented by the deterioration parameters estimated in the first step. The results of an evaluation made using flight data from the F-15 aircraft are presented, indicating that the algorithm can provide reasonable estimates of engine variables for an advanced propulsion control law development. Author

N91-21447*# National Aeronautics and Space Administration. Lewis Research Center, Cleveland, OH.
CFD FOR HYPERSONIC PROPULSION
LOUIS A. POVINELLI 1990 17 p Presented at the Workshop on Hypersonic Flow, Antibes, France, 22-25 Jan. 1990; cosponsored by National Research Inst. for Information and Automation and Group for Advancement of Numerical Engineering Methods
(NASA-TM-103791; E-5689; NAS 1.15:103791) Avail: NTIS HC/MF A03 CSCL 20/4

An overview is given of research activity on the application of computational fluid dynamics (CDF) for hypersonic propulsion systems. After the initial consideration of the highly integrated

nature of air-breathing hypersonic engines and airframe, attention is directed toward computations carried out for the components of the engine. A generic inlet configuration is considered in order to demonstrate the highly three dimensional viscous flow behavior occurring within rectangular inlets. Reacting flow computations for simple jet injection as well as for more complex combustion chambers are then discussed in order to show the capability of viscous finite rate chemical reaction computer simulations. Finally, the nozzle flow fields are demonstrated, showing the existence of complex shear layers and shock structure in the exhaust plume. The general issues associated with code validation as well as the specific issue associated with the use of CFD for design are discussed. A prognosis for the success of CFD in the design of future propulsion systems is offered. Author

N91-21458*# National Aeronautics and Space Administration. Lewis Research Center, Cleveland, OH.
APPLICATION OF COMPUTATIONAL FLUID DYNAMICS IN HIGH SPEED AEROPROPULSION
LOUIS A. POVINELLI 1991 5 p Proposed for presentation at the 13th IMACS World Congress on Computation and Applied Mathematics, Dublin, Ireland, 22-26 Jul. 1991; cosponsored by International Federation for Automatic Control, International Federation for Information Processing International Federation for of Operational Research Societies, and International Measurement Confederation
(NASA-TM-103780; E-6053; NAS 1.15:103780) Avail: NTIS HC/MF A01 CSCL 20/4

The application is described of computational fluid dynamics (CFD) to a hypersonic propulsion system. An overview of the problems associated with a propulsion system of this type is presented, highlighting the special role that CFD plays in the design of said systems. Author

N91-21464# Advisory Group for Aerospace Research and Development, Neuilly-Sur-Seine (France). Fluid Dynamics Panel.
APPLICATION OF MESH GENERATION TO COMPLEX 3-D CONFIGURATIONS
JOSEPH L. STEGER and W. SCHMIDT, ed. (Messerschmitt-Boelkow-Blohm G.m.b.H., Munich, Germany, F.R.) 1991 18 p Presented at the AGARD Fluid Dynamics Panel Specialists Meeting, Loen, Norway, 24-25 May 1989
(AGARD-AR-268; ISBN-92-835-0608-1) Copyright Avail: NTIS HC/MF A03; Non-NATO Nationals requests available only from AGARD/Scientific Publications Executive

The papers presented at the AGARD Fluid Dynamics Panel Specialists' Meeting are summarized and evaluated. Some general comments regarding progress in mesh generation are provided and the important role of grid generation in providing accurate aerodynamic simulations is underscored. Recommendations and opinions are offered regarding the use of both structured and unstructured grids for CFD applications. Author

N91-21466# Deutsche Forschungsanstalt fuer Luft- und Raumfahrt, Brunswick (Germany, F.R.). Abt. Zellenaerodynamik.
FLOW VISUALIZATION ION HELICOPTER BLADES USING ACENAPHTHEN
CLAAS-HINRIK ROHARDT Jul. 1990 42 p In GERMAN; ENGLISH summary Report will also be announced as translation (ESA-TT-1255)
(DLR-FB-90-37; ISSN-0171-1342; ETN-91-99032) Avail: NTIS HC/MF A03; DLR, Wissenschaftliches Berichtswesen, VB-PL-DO, Postfach 90 60 58, 5000 Cologne, Fed. Republic of Germany, HC 11.50 DM

An experiment for flow visualization of boundary layer character on a helicopter blade under operational conditions is carried out. Comparisons with two dimensional computations were discussed to determine transition locations. The flow visualization with acenaphthene was chosen because of its speed and ease in evaluating the laminar turbulent transition. It is shown that considerably longer laminar flow are possible. ESA

N91-21469# Aeronautical Research Inst. of Sweden, Stockholm. Dept. of Aerodynamics.
SOME TREATMENTS ON BOUNDARY CONDITIONS FOR QUASI ONE-DIMENSIONAL EULER EQUATIONS
HU JIASEN Sep. 1990 20 p Sponsored by National Swedish Board for Technical Development, Stockholm
(FFA-TN-1990-36; ETN-91-99045) Avail: NTIS HC/MF A03

Three different methods to specify the boundary conditions for quasi one-dimensional Euler equations are presented. A Euler solver with the methods for the isenthalpic one-dimensional nozzle flow was developed. The code is designed to predict all typical flow regimes and was applied to seven model problems. The results obtained are compared with analytical solutions and good agreements are achieved. ESA

N91-21472* National Aeronautics and Space Administration. Langley Research Center, Hampton, VA.
METHOD AND APPARATUS FOR DETECTING LAMINAR FLOW SEPARATION AND REATTACHMENT Patent
JOHN P. STACK, inventor (to NASA) and SIVARAMAKRISHNAN M. MANGALAM, inventor (to NASA) (Analytical Services and Materials, Inc., Hampton, VA.) 26 Jun. 1990 11 p Filed 4 May 1989 Division of US-Patent-Appl-SN-203178, filed 7 Jun. 1988
(NASA-CASE-LAR-13952-2-SB; US-PATENT-4,936,146; US-PATENT-APPL-SN-348223; US-PATENT-APPL-SN-203178; US-PATENT-CLASS-73-432.1; INT-PATENT-CLASS-G01F-1/00) Avail: US Patent and Trademark Office CSCL 20/4

The invention is a method and apparatus for simultaneously detecting laminar separation and reattachment of a fluid stream such as an airstream from and to the upper surface of an airfoil by simultaneously sensing and comparing a plurality of output signals. Each signal represents the dynamic shear stress at one of an equal number of sensors spaced along a straight line on the surface of the airfoil that extends parallel to the airstream. The output signals are simultaneously compared to detect the sensors across which a reversal in phase of said output signal occurs, said detected sensors being in the region of laminar separation or reattachment.
Official Gazette of the U.S. Patent and Trademark Office

N91-21485*# Nebraska Univ., Lincoln.
COMPARISON OF UNL LASER IMAGING AND SIZING SYSTEM AND A PHASE DOPPLER SYSTEM FOR ANALYZING SPRAYS FROM A NASA NOZZLE Final Report
DENNIS R. ALEXANDER Mar. 1990 134 p
(Contract NAG3-634)
(NASA-CR-185239; NAS 1.26:185239) Avail: NTIS HC/MF A07 CSCL 14/2

Research was conducted on characteristics of aerosol sprays using a P/DPA and a laser imaging/video processing system on a NASA MOD-1 air assist nozzle being evaluated for use in aircraft icing research. Benchmark tests were performed on monodispersed particles and on the NASA MOD-1 nozzle under identical lab operating conditions. The laser imaging/video processing system and the P/DPA showed agreement on a calibration tests in monodispersed aerosol sprays of + or - 2.6 micron with a standard deviation of + or - 2.6 micron. Benchmark tests were performed on the NASA MOD-1 nozzle on the centerline and radially at 0.5 inch increments to the outer edge of the spray plume at a distance 2 ft downstream from the exit nozzle. Comparative results at two operation conditions of the nozzle are presented for the two instruments. For the 1st case studied, the deviation in arithmetic mean diameters determined by the two instruments was in a range of 0.1 to 2.8 micron, and the deviation in Sauter mean diameters varied from 0 to 2.2 micron. Severe operating conditions in the 2nd case resulted in the arithmetic mean diameter deviating from 1.4 to 7.1 micron and the deviation in the Sauter mean diameters ranging from 0.4 to 6.7 micron. Author

N91-21531*# National Aeronautics and Space Administration. Lewis Research Center, Cleveland, OH.
ADVANCED ROTORCRAFT TRANSMISSION PROGRAM

ROBERT C. BILL 1990 18 p Presented at the 46th Annual American Helicopter Society Forum, Washington, DC, 21 May 1990 Previously announced in IAA as A91-17214 Prepared in cooperation with Army Aviation Systems Command, Cleveland, OH
(Contract DA PROJ. 1L1-62211-A-47-A)
(NASA-TM-103276; E-5722; NAS 1.15:103276;
AVSCOM-TR-90-C-015) Avail: NTIS HC/MF A03 CSCL 13/9

The Advanced Rotorcraft Transmission (ART) program is an Army-funded, joint Army/NASA program to develop and demonstrate lightweight, quiet, durable drivetrain systems for next generation rotorcraft. ART addresses the drivetrain requirements of two distinct next generation aircraft classes: Future Air Attack Vehicle, a 10,000 to 20,000 lb. aircraft capable of undertaking tactical support and air-to-air missions; and Advanced Cargo Aircraft, a 60,000 to 80,000 lb. aircraft capable of heavy life field support operations. Both tiltrotor and more conventional helicopter configurations are included in the ART program. Specific objectives of ART include reduction of drivetrain weight by 25 percent compared to baseline state-of-the-art drive systems configured and sized for the next generation aircraft, reduction of noise level at the transmission source by 10 dB relative to a suitably sized and configured baseline, and attainment of at least a 5000 hr mean-time-between-removal. The technical approach for achieving the ART goals includes application of the latest available component, material, and lubrication technology to advanced concept drivetrains that utilize new ideas in gear configuration, transmission layout, and airframe/drivetrain integration. To date, candidate drivetrain systems were carried to a conceptual design stage, and tradeoff studies were conducted resulting in selection of an ART transmission configuration for each of the four contractors. The final selection was based on comparative weight, noise, and reliability studies. A description of each of the selected ART designs is included. Preliminary design of each of the four selected ART transmission was completed, as have mission impact studies wherein comparisons of aircraft mission performance and life cycle costs are undertaken for the next generation aircraft with ART and with the baseline transmission. Author

N91-21534*# National Aeronautics and Space Administration. Lewis Research Center, Cleveland, OH.
EFFECTS OF GEAR BOX VIBRATION AND MASS IMBALANCE ON THE DYNAMICS OF MULTI-STAGE GEAR TRANSMISSIONS
FRED K. CHOY, YU K. TU (Akron Univ., OH.), JAMES J. ZAKRAJSEK, and DENNIS P. TOWNSEND Mar. 1991 33 p Prepared in cooperation with Army Aviation Systems Command, Cleveland, OH
(Contract DA PROJ. 1L1-62211-A-47-A)
(NASA-TM-103695; E-5916; NAS 1.15:103695;
AVSCOM-TR-90-C-022) Avail: NTIS HC/MF A03 CSCL 13/9

The dynamic behavior of multistage gear transmission system, with the effects of gear-box-induced vibrations and rotor mass-imbalances is analyzed. The model method, using undamped frequencies and planar mode shapes, is used to reduce the degree-of-freedom of the system. The various rotor-bearing stages as well as lateral and torsional vibrations of each individual stage are coupled through localized gear-mesh-tooth interactions. Gear-box vibrations are coupled to the gear stage dynamics through bearing support forces. Transient and steady state dynamics of lateral and torsional vibrations of the geared system are examined in both time and frequency domain. A typical three-staged geared system is used as an example. Effects of mass-imbalance and gear box vibrations on the system dynamic behavior are presented in terms of modal excitation functions for both lateral and torsional vibrations. Operational characteristics and conclusions are drawn from the results presented. Author

N91-21568# Aeronautical Research Inst. of Sweden, Stockholm. Dept. of Structures.
STABILITY ANALYSIS OF A FUSELAGE SIDE
ROLF JARLAAS and ADAM ZDUNEK Dec. 1990 42 p Sponsored by Defence Material Administration, Stockholm, Sweden
(FFA-TN-1990-32; ETN-91-99043) Avail: NTIS HC/MF A03

The structural response of a fuselage side of the civil aircraft SAAB 340A was investigated as a part of the certification program for the aircraft. The purpose was according to the test report to verify the stability of the fuselage frames and the window frames as well as the buckling behavior in the representing area. The structure was later analyzed with the finite element method. A comparison between experimental data and compared data showed unacceptably large discrepancies. The experimental situation as well as the finite element analysis are examined in an attempt to point the major causes for the discrepancies. Boundary conditions, discretization errors and modeling errors are discussed. No single effect was found which on its own explain the discrepancy between experimental and computed data. Significant discretization errors are shown to be present in the model used. It is also shown that the test-rig used in the experiments can not be considered as very stiff, making a non negligable contribution to the discrepancy. There are additional modeling errors such as neglection of thickness steps in the skin, and modeling of stringer fuselage intersections which were not considered in the present analyses. The p-version of the finite element method is introduced for the first time in the analysis of a real aircraft shell type structure. Results analyzed with both the linear and the newly developed nonlinear version of the program STRIPE are presented. ESA

N91-21587*# National Aeronautics and Space Administration. Hugh L. Dryden Flight Research Facility, Edwards, CA.
STARS: AN INTEGRATED GENERAL-PURPOSE FINITE ELEMENT STRUCTURAL, AEROELASTIC, AND AEROSERVOELASTIC ANALYSIS COMPUTER PROGRAM
KAJAL K. GUPTA Jan. 1991 181 p Revised
(NASA-TM-101709-REV; H-1582-REV; NAS 1.15:101709-REV)
Copyright Avail: NTIS HC/MF A09 CSCL 20/11

The details of an integrated general-purpose finite element structural analysis computer program which is also capable of solving complex multidisciplinary problems is presented. Thus, the SOLIDS module of the program possesses an extensive finite element library suitable for modeling most practical problems and is capable of solving statics, vibration, buckling, and dynamic response problems of complex structures, including spinning ones. The aerodynamic module, AERO, enables computation of unsteady aerodynamic forces for both subsonic and supersonic flow for subsequent flutter and divergence analysis of the structure. The associated aeroservoelastic analysis module, ASE, effects aero-structural-control stability analysis yielding frequency responses as well as damping characteristics of the structure. The program is written in standard FORTRAN to run on a wide variety of computers. Extensive graphics, preprocessing, and postprocessing routines are also available pertaining to a number of terminals. Author

N91-22047# Max-Planck-Inst. fuer Radioastronomie, Bonn (Germany, F.R.).
AIRBORNE HETERODYNE RECEIVER FOR THE RANGE 600 GHZ TO 3,000 GHZ
HANS PETER ROESER, JOHANNES SCHMID-BURGK, GERHARD W. SCHWAAB, and RUTH U. TITZ *In* ESA, From Ground-Based to Space-Borne Sub-mm Astronomy p 369-373 Dec. 1990
Copyright Avail: NTIS HC/MF A17; EPD, ESTEC, Noordwijk, Netherlands, HC 80 Dutch guilders

The heterodyne receiver system used aboard the Kuiper Airborne Observatory is described. High resolution detections of CO(J = 7-6, 9-8, 11-10, 12-11 and 14-13), are presented. The down converted signal is amplified by low noise amplifiers and decomposed by an acousto-optical spectrometer. The spectrometer has a maximum bandwidth of 1200 MHz with a resolution of 1.8 MHz. At 3000 GHz, this yields an instantaneous velocity range of 150 km/sec with a resolution of 0.2 km/sec. ESA

N91-22475*# Stanford Univ., CA. Dept. of Psychology.
ANALYSIS OF ROUTINE COMMUNICATION IN THE AIR TRAFFIC CONTROL SYSTEM Final Report, Sep. 1989 - Aug. 1990
HERBERT H. CLARK, DANIEL MORROW, and MICHELLE RODVOID Aug. 1990 12 p
(Contract NCC2-622)
(NASA-CR-188116; NAS 1.26:188116) Avail: NTIS HC/MF A03 CSCL 17/2

The present project has three related goals. The first is to describe the organization of routine controller-pilot communication. This includes identifying the basic units of communication and how they are organized into discourse, how controllers and pilots use language to achieve their goals, and what topics they discuss. The second goal is to identify the type and frequency of problems that interrupt routine information transfer and prompt pilots and controllers to focus on the communication itself. The authors analyze the costs of these problems in terms of communication efficiency, and the techniques used to resolve these problems. Third, the authors hope to identify factors associated with communication problems, such as deviations from conventional air traffic control procedures. Author

N91-22480# Army Engineer Topographic Labs., Fort Belvoir, VA.
AUTOMATED EXTRACTION OF AIRPORT RUNWAY PATTERNS FROM RADAR IMAGERY Research Note, Jun. 1985 - Mar. 1989
RICHARD A. HEVENOR and PI-FUAY CHEN Jun. 1990 41 p
(AD-A231809; ETL-0567) Avail: NTIS HC/MF A03 CSCL 17/9

A method is presented to extract linear terrain features from Synthetic Aperture Radar imagery. An input radar image is smoothed with an edge-preserving smoothing operation. Edge detection is performed using a Sobel operator, and both the magnitude and directional images are computed. The edges are then strengthened using several iterations of a relaxation operation in which both the magnitude image and the directional image are updated with each iteration. The output of the relaxation operation is a binary edge image, which is then thinned. A connected components routine is then run in which two passes through the image are used to provide a unique label for each connected component. The connected components related only to the runaway pattern are then extracted by computing certain properties of each component. A border-following algorithm is then used to follow only the outermost borders and give each of the pixels on an outermost border a maximum brightness value. A tracking algorithm is used to change the binary image array into a set of Freeman chain codes, which serve as the input to a line-forming routine that uses a standard polygon approximation algorithm. Experimental results on a real synthetic aperture radar image are presented. GRA

N91-22511# Aeronautical Research Labs., Melbourne (Australia).
WATER TUNNEL FLOW VISUALISATION OF VORTEX BREAKDOWN OVER THE F/A-18
D. H. THOMPSON Dec. 1990 64 p
(ARL-FLIGHT-MECH-R-179; AR-005-607) Copyright Avail: NTIS HC/MF A04

Vortex flow patterns over models of the F/A-18 aircraft were visualized using dye and hydrogen bubble techniques in a water tunnel. The axial position of vortex breakdown in the leading-edge extension (LEX) vortices was measured, and was found to be insensitive to Reynolds number, to flap setting, and to small variations in model cross-section shape. Engine inlet flow did alter the vortex breakdown position, at flow rates that might be encountered under flight conditions. The fitting of fences on the LEX upper surface did not affect the axial position of vortex breakdown, but did alter the vortex structure. These alterations were examined in some detail. Author

N91-22520# National Aerospace Lab., Tokyo (Japan).
ANALYSIS OF LAMINAR SEPARATION BUBBLES USING A SIMPLE EDDY-VISCOSITY TURBULENCE MODEI
KENICHI RINOIE and NOBUHIKO KAMIYA Sep. 1990 19 p In JAPANESE; ENGLISH summary
(NAL-TR-1079; ISSN-0389-4010) Avail: NTIS HC/MF A03

Laminar separation bubbles formed on airfoils are expressed numerically using a simple eddy-viscosity turbulence model which satisfies the basic characteristics of the short bubble. The eddy viscosity constant was set to a uniform value inside the turbulent part of the bubble. Overall, characteristics of numerical results agreed closely with experimental results. The relation between the eddy viscosity constant and velocity distributions was analyzed by the momentum balance inside the bubble. It was shown that the pressure recovery inside the bubble is proportional to the eddy viscosity constant. Finally, the eddy viscosity constant is related to the non-dimensional parameter which represents the flow inside the bubble. Author

N91-22528# Bristol Univ. (England). Dept. of Aerospace Engineering.
FLOW INVESTIGATION OF A GROUND EFFECT VEHICLE B.S. Thesis
C. C. V. SALMON and S. G. THOMPSON Jun. 1990 48 p
(BU-516; ETN-91-99209) Avail: NTIS HC/MF A03

Quantitative and qualitative tests were performed on a proposed tricycle lifting jet configured delta aircraft, operating in ground effect, to determine the flow characteristics, jet stability and pressure forces on the underside of the vehicle. For jet speeds of 200 ft/s and 300 ft/s, and a range of forward speeds, the jet stability at heights above the ground plane ranging from 0.14 S to 0.51 S were investigated, where S is the span of the model. Instability of the jet system occurred where the jets tucked under the model, and this was recorded as a critical forward speed. In addition, the effects of both positive and negative incidence changes and forward inclination of the front jet, were investigated. Plots of the ratio critical forward speed/jet speed with height were produced, along with lift performance curves, for the above flight variables. At zero forward speed, clear peaks were noted in lift performance at a vehicle height of approximately 0.35 S, for both jet speeds. This was modified by incidence and jet inclination, the maximum lift decreasing in both cases. Pressure distributions and wool tuft flow visualization on the underside of the model led to the determination of local flow pattern characteristics. Normal pressure forces and pitch stability for hovering and transitional flight were investigated. Regions of jet impingement from the reflected 'lifting jets' and jet entrainment, were clearly seen and monitored for varying flight conditions. ESA

N91-22529# Bristol Univ. (England). Dept. of Aerospace Engineering.
THE USE OF AXISYMMETRIC FLOW FOR INVESTIGATION OF SHOCK WAVE-BOUNDARY LAYER INTERACTIONS B.S. Thesis
C. K. TUNBRIDGE and A. C. YOUNGS Jun. 1990 39 p
(BU-520; ETN-91-99213) Avail: NTIS HC/MF A03

An experimental rig was designed and manufactured to enable the study of one particular situation of shock wave boundary layer interaction. The concept of axisymmetry was used to create a pseudo 2-D flow situation, thus alleviating the problem of side wall effects. Important design parameters were: a Mach number of 2; Reynolds number range of 250,000 to 450,000; working section diameter of 80 mm (approx). The required supersonic nozzle was obtained by scaling from an existing design. Detailed information regarding this method is included. Time constaints restricted testing to rig calibration and the implementation of associated instrumentation. Further specialized instrumentation was designed and manufactured, but not tested. Uniform Mach 2 supersonic flow was achieved but with slight concession to some of the design specifications. This was due to problems with maintaining a sufficiently low downstream pressure while running the rig. The success of the project is reviewed, and

recommendations for further work required for the full operation of the tunnel are made. ESA

N91-22540*# National Aeronautics and Space Administration. Langley Research Center, Hampton, VA.
A SYNCHRONOUS STROBED LASER LIGHT SHEET FOR ROTOR FLOW VISUALIZATION
BRADLEY D. LEIGHTY, DAVID B. RHODES, JOHN M. FRANKE, and STEPHEN B. JONES Washington May 1991 19 p Presented at the 36th International Instrumentation Symposium, Denver, CO, 6 May 1990 Previously announced in IAA as A91-24979
(NASA-TM-4266; L-16877; NAS 1.15:4266) Avail: NTIS HC/MF A03 CSCL 14/2

A synchronous strobed laser light sheet generator was designed and used for flow visualization of a helicopter rotor model. The laser light sheet strobe circuit was designed to allow selectable blade position viewing, strobe duration, and multiple pulses per revolution for rotors having 2 to 9 blades. A slip-sync mode permits slow motion visualization of the flow field over complete rotations of the rotor. The design was tested at NASA Langley Research Center's 14 by 22 foot subsonic tunnel where the flow was seeded with propylene glycol smoke. Between runs, a calibration grid board was placed in the plane of the laser sheet and recorded with the video camera at the position used to record the flow field. The system was used to make 2-dimensional flow field cuts of a four-bladed rotor operating at wind tunnel speeds up to 79.25 meters per second (260 feet per second). Author

N91-22550# Spectron Development Labs., Inc., Costa Mesa, CA.
DEVELOPMENT OF AN OPTICAL VOLUMETRIC FLOWMETER Final Report, Apr. 1985 - Mar. 1989
MEDHAT AZZAZY Sep. 1990 231 p
(Contract GRI-5084-271-0987)
(PB91-136481; SDL-89-2532-13; GRI-89/0201) Avail: NTIS HC/MF A11 CSCL 14/2

The feasibility of determing the volumetric flow rate with high degree accuracy by integrating the optically measured velocity profile over the pipe cross sectional area was performed. The velocity was measured using the laser transit anemometry technique. The comparison results, of a laboratory otpical flowmeter with a Roots meter installed in series, showed that the optical flowmeter could yield highly accurate volumeteric flow rates. A 'handmade' optical volumetric flowmeter prototype based on the concept of laser transit anemometry was design and fabricated. The accuracy and precision of the prototype were tested in a laboratory wind tunnel and compared to a well-calibrated vortex meter connected in series. The accuracy of the prototype relative to the vortex meters was within + or - 0.29 percent. The center line flow velocity repeatability measured by the prototype was within + or - 0.46 percent. Field measurements of particle size and particle arrival rate in a gas pipeline were conducted. The results showed that the average particle size was 3.3 micrometers and the particle arrival rate to the prototype probe volume was few hundreds per second which is sufficient for the operation of the optical flowmeter. Optical access to the pipeline is imperative to an optical flowmeter, therefore, a field experiment to determine the rate of deposition of contaminants on the window was performed. The results show no significant deposition over 6 months. GRA

N91-22564# Dynamet Technology, Inc., Burlington, MA.
FEASIBILITY STUDY FOR THE QUALIFICATION OF AN ECONOMICALLY ADVANTAGEOUS TI-6AL-4V BEARING HOUSING FOR GAS TURBINE ENGINE APPLICATION BY POWDER METAL MANUFACTURING TECHNOLOGY Final Report, Nov. 1988 - Apr. 1989
STANLEY ABKOWITZ Jan. 1991 21 p
(Contract F33615-88-C-5504)
(AD-A231666; WRDC-TR-90-4140) Avail: NTIS HC/MF A03 CSCL 11/6

This Small Business Innovative Research (SBIR) Phase I program has demonstrated that titanium alloy aircraft engine components can be manufactured to near-net shape by an economical advanced powder metallurgy (P/M) process without compromising the structural performance and reliability of the component. In the program Ti-6A1-4V alloys test bar materials were made by the Dynamet CHIP process. Two types of alloy test material were evaluated, one utilizing standard low cost titanium powder containing 1500 ppm of chloride impurity and a second premium priced titanium powder with extra low levels of chloride. Tensile properties of the former material were near specified minimums for the forgings currently used in turbine engine components. For the extra low chloride material, however, tensile strength and ductility were far in excess of the specified minimums. GRA

N91-22567*# National Aeronautics and Space Administration. Lewis Research Center, Cleveland, OH.
HIGH TEMPERATURE PERFORMANCE EVALUATION OF A HYPERSONIC ENGINE CERAMIC WAFER SEAL
BRUCE M. STEINETZ Apr. 1991 23 p
(NASA-TM-103737; E-5942; NAS 1.15:103737) Avail: NTIS HC/MF A03 CSCL 13/1

Leakage rates of an innovative hypersonic engine seal were measured using a specially developed static high temperature seal test fixture at NASA Lewis Research Center. The three foot long structural panel-edge seal is designed to minimize leakage of high temperature, high pressure gases past the movable panels of advanced ramjet/scramjet engines. The seal is made of a stack of precision machined ceramic wafer pieces that are inserted into a closely conforming seal channel in the movable engine panel. The wafer seal accommodates the significant distortions in the adjacent engine walls through relative sliding between adjacent wafers. Seal leakage rates are presented for engine simulated air temperatures up to 1350 F and for engine pressures up to 100 psi. Leakage rates are also presented for the seal, sealing both a flat wall condition, and an engine simulated distorted wall condition in which the distortion was 0.15 in. in only an 18 in. span. Seal leakage rates were low, meeting an industry-established tentative leakage limit for all combinations of temperature, pressure, and wall conditions considered. Comparisons are made between the measured leakage rates and leakage rates predicted using a seal leakage model developed from externally-pressurized gas film bearing theory. Author

N91-22576*# National Aeronautics and Space Administration. Langley Research Center, Hampton, VA.
COMPUTATIONAL METHODS FOR FRICTIONLESS CONTACT WITH APPLICATION TO SPACE SHUTTLE ORBITER NOSE-GEAR TIRES
KYUN O. KIM, JOHN A. TANNER, AHMED K. NOOR (Virginia Univ., Charlottesville.), and MARTHA P. ROBINSON Washington May 1991 36 p Original contains color illustrations
(NASA-TP-3073; L-16750; NAS 1.60:3073) Avail: NTIS HC/MF A03; 2 functional color pages CSCL 20/11

A computational procedure is presented for the solution of frictionless contact problems of aircraft tires. The Space Shuttle nose-gear tire is modeled using 2-D laminated anisotropic shell theory with the effects of variation in material and geometric parameters, transverse shear deformation, and geometric nonlinearities included. The contact conditions are incorporated into the formulation by using a perturbed Lagrangian approach with the fundamental unknowns consisting of the stress resultants, the generalized displacements, and the Lagrange multipliers associated with the contact conditions. The elemental arrays are obtained by using a modified two-field, mixed variational principle. Numerical results are presented for the Space Shuttle nose-gear tire when subjected to inflation pressure and pressed against a flat plate. Comparison is made with experiments conducted at NASA-Langley. The detailed information presented assists in gaining physical insight about the structural response of the tire. The numerical studies have demonstrated the high accuracy of the mixed formulation models and the effectiveness of the

computational procedure which combines both the geometrically nonlinear terms and the contact conditions in one iteration loop. Author

N91-22578*# National Aeronautics and Space Administration. Langley Research Center, Hampton, VA.
SENSITIVITY-BASED SCALING FOR CORRELATING STRUCTURAL RESPONSE FROM DIFFERENT ANALYTICAL MODELS
KWAN J. CHANG, RAPHAEL T. HAFTKA, GARY L. GILES, and PI-JEN KAO (Analytical Services and Materials, Inc., Hampton, VA.) Feb. 1991 11 p
(Contract NAG1-224)
(NASA-TM-104042; NAS 1.15:104042) Avail: NTIS HC/MF A03 CSCL 20/11

A sensitivity-based linearly varying scale factor is described used to reconcile results from refined models for analysis of the same structure. The improved accuracy of the linear scale factor compared to a constant scale factor as well as the commonly used tangent approximation is demonstrated. A wing box structure is used as an example, with displacements, stresses, and frequencies correlated. The linear scale factor could permit the use of a simplified model in an optimization procedure during preliminary design to approximate the response given by a refined model over a considerable range of design changes. Author

N91-22583 Brown Univ., Providence, RI.
MICROMECHANISMS OF QUASI-STATIC AND FATIGUE CRACK GROWTH IN TITANIUM-ALUMINIDES Ph.D. Thesis
PRANESH BELGOD ASWATH 1990 217 p
Avail: Univ. Microfilms Order No. DA9101728

The rapid development of advanced aerospace technology has put an increasing demand on the development of a new generation of structural materials for aircraft engines. Intermetallic materials with low densities and improved fracture toughness at elevated temperature show promise for replacing widely used Ni-base superalloys. TiAl and Ti3Al, ordered intermetallic compounds of Ti and Al, have been the subject of increasing research activity in the recent past because of their light weight and high strength. An understanding of the resistance to quasi-static and cyclic load fracture in these intermetallics at both ambient and elevated temperatures is of paramount importance for damage-tolerant, fatigue-critical structural applications for which the intermetallics are candidate materials. The effects of microstructure, microstructural stability, mechanical variables (such as load ratio and fatigue frequency), and temperature on the the quasi-static and fatigue crack growth characteristics of Ti-Al and Ti-Al-Nb alloys. With the aid of controlled heat treatments, duplex microstructures comprising either alpha(sub 2) and beta or alpha(sub 2) and gamma phases as well as predominantly alpha(sub 2) phase microstructures are produced. The fatigue crack growth characteristics are monitered over a range of delta K values from threshold to final failure. The effects of controlled microstructures on the overall fatigue and fracture resistance are examined in light of transmission electron microscopy (TEM) observations of crack tip damage, scanning auger spectroscopy of fracture surface oxidation, and scanning electron fractography. The stability of these microstructures are examined in light of their response to both fatigue crack growth and fracture toughness. Microstructural features which lead to a betterment of fatigue crack growth and fracture toughness are discussed in context of the present experimental results. Author

N91-22589*# National Aeronautics and Space Administration. Langley Research Center, Hampton, VA.
STRUCTURAL INTEGRITY OF WIND TUNNEL WOODEN FAN BLADES
CLARENCE P. YOUNG, JR., ROBERT T. WINGATE, JAMES R. ROOKER, KENNETH W. MORT (National Aeronautics and Space Administration. Ames Research Center, Moffett Field, CA.), and HAROLD E. ZAGER Apr. 1991 75 p
(NASA-TM-104059; NAS 1.15:104059) Avail: NTIS HC/MF A04 CSCL 20/11

Information is presented which was compiled by the NASA Inter-Center Committee on Structural Integrity of Wooden Fan Blades and is intended for use as a guide in design, fabrication, evaluation, and assurance of fan systems using wooden blades. A risk assessment approach for existing NASA wind tunnels with wooden fan blades is provided. Also, state of the art information is provided for wooden fan blade design, drive system considerations, inspection and monitoring methods, and fan blade repair. Proposed research and development activities are discussed, and recommendations are provided which are aimed at future wooden fan blade design activities and safely maintaining existing NASA wind tunnel fan blades. Information is presented that will be of value to wooden fan blade designers, fabricators, inspectors, and wind tunnel operations personnel. Author

13

GEOSCIENCES

Includes geosciences (general); earth resources; energy production and conversion; environment pollution; geophysics; meteorology and climatology; and oceanography.

A91-33634
AIRBORNE GRAVIMETRY AND THE GLOBAL POSITIONING SYSTEM
ALFRED KLEUSBERG, DERRICK PEYTON, and DAVID WELLS (New Brunswick, University, Fredericton, Canada) IN: IEEE PLANS '90 - Position Location and Navigation Symposium, Las Vegas, NV, Mar. 20-23, 1990, Record. New York, Institute of Electrical and Electronics Engineers, Inc., 1990, p. 273-278. Research supported by NSERC and Department of Energy, Mines and Resources. refs
Copyright

The capabilities of using precise range and range rate measurements to satellites of the Global Positioning System (GPS) for the determination of the platform position and its time derivatives are explored. The accuracy requirements for airborne gravimetry are reviewed, and different schemes for correcting the gravimeter measurements are presented. It is shown that the separation of gravitational and inertial accelerations in the measurements imposes the most stringent requirements on the GPS measurement accuracy and the GPS data processing. The results of GPS data reduction show that currently available GPS receivers allow fixed-wing-aircraft gravity data reduction at the milligal accuracy level for a spatial gravity field resolution of five kilometers. I.E.

A91-33648
MODERN AVIATION WEATHER SYSTEMS FOR EFFICIENT FLIGHT MANAGEMENT
PRAVAS R. MAHAPATRA and DUSAN S. ZRNIC (NOAA, National Severe Storms Laboratory, Norman, OK) IN: IEEE PLANS '90 - Position Location and Navigation Symposium, Las Vegas, NV, Mar. 20-23, 1990, Record. New York, Institute of Electrical and Electronics Engineers, Inc., 1990, p. 457-463. Research supported by National Research Council. refs
Copyright

Weather effects on aviation are summarized, and aviation-significant atmospheric processes are briefly discussed. In situ sensing of surface wind shear is reviewed. The role of Doppler weather radars as aviation weather sensors is discussed, and three currently evolving Doppler radar systems-NEXRAD, TDWR, and ASR-9-are briefly described with regard to their role in flight management. The uses of each system are outlined. Emphasis is placed on automated generation of high-level products and displays. The influence of these instrument systems on flight management is discussed. I.E.

N91-22653# National Center for Atmospheric Research, Boulder, CO.
AIR MOTION MEASUREMENTS: PAST AND FUTURE
DONALD H. LENSCHOW *In* DLR, International Workshop on the Airborne Measurement of Wind, Turbulence and Position: Workshop Report p 22-28 23 Jun. 1990
Avail: NTIS HC/MF A05; DLR, Wissenschaftliches Berichtswesen, VB-PL-DO, Postfach 90 60 58, 5000 Cologne, Fed. Republic of Germany, HC 25 Deutsche marks

The concept of using aircraft for air motion measurements is introduced. Their prime advantage is their mobility, however this mobility and their response to turbulence adds to the difficulty in obtaining accurate measurements. The latter is discussed and ways of overcoming these problems are presented. An historical survey of the use of airplanes as qualitative indicators of atmospheric motions is given and the measurement techniques, including vanes, pressure sensing probes and the inertial navigation system are presented. Based on the current status of aircraft instrumentation and the limits discussed, the needs for improved air motion sensing capabilities are summarized and a variety of possible technological solutions to these needs are given. ESA

N91-22654# Deutsche Forschungsanstalt fuer Luft- und Raumfahrt, Oberpfaffenhofen (Germany, F.R.). Abt. Meteorologische Flugmesssysteme.
AIR MOTION MEASUREMENT UNCERTAINTIES: THEIR IMPACT ON ATMOSPHERIC STUDIES
DARREL BAUMGARDNER (National Center for Atmospheric Research, Boulder, CO.) *In its* International Workshop on the Airborne Measurement of Wind, Turbulence and Position: Workshop Report p 29-35 23 Jun. 1990
Avail: NTIS HC/MF A05; DLR, Wissenschaftliches Berichtswesen, VB-PL-DO, Postfach 90 60 58, 5000 Cologne, Fed. Republic of Germany, HC 25 Deutsche marks

The effect of the uncertainties in the measurement of primary quantities (such as pressure or temperature) on the secondary quantities that are derived from them must be evaluated by propagating these uncertainties from the equations that relate the primary and secondary quantities. The process for derivation of errors in wind measurement is described and the possible magnitudes of the error are illustrated. Error propagation techniques provide a means of assessing the quality of measurements and guidance in data interpolation. The results showed that the accuracy in calculated winds would be improved by making only small improvements in the measurement of attack, sideslip, and heading angles. ESA

N91-22655# Flinders Univ., Bedford Park (Australia). Flinders Inst. for Atmospheric and Marine Science.
THE FIAMS RESEARCH AIRCRAFT OR SMALL IS BEAUTIFUL
JOERG M. HACKER *In* DLR, International Workshop on the Airborne Measurement of Wind, Turbulence and Position: Workshop Report p 36-41 23 Jun. 1990
Avail: NTIS HC/MF A05; DLR, Wissenschaftliches Berichtswesen, VB-PL-DO, Postfach 90 60 58, 5000 Cologne, Fed. Republic of Germany, HC 25 Deutsche marks

The GROB G109B, a small research aircraft used in atmospheric boundary layer research projects, is presented. This aircraft was designed to measure basic meteorological parameters with a high degree of accuracy. A list of the sensors and scientific systems fitted to the aircraft is given and the onboard data system is summarized. Since becoming operational in 1985 the aircraft was used in a wide variety of research projects all over Australia. As typical examples, some results from two observational studies are presented. These included investigation into the fine structure of a sea breeze front, and others into the vertical energy fluxes over a desert lake area. ESA

N91-22656# Centre d'Essais en Vol, Bretigny-sur-Orge (France).
TECHNICAL PRESENTATION OF THE MERLIN'S RADOME: CALIBRATION AND DATA PROCESSING
MICHEL ANDRE and MARIE PIERRE LEPIPEC *In* DLR, International Workshop on the Airborne Measurement of Wind, Turbulence and Position: Workshop Report p 42-46 23 Jun. 1990
Avail: NTIS HC/MF A05; DLR, Wissenschaftliches Berichtswesen, VB-PL-DO, Postfach 90 60 58, 5000 Cologne, Fed. Republic of Germany, HC 25 Deutsche marks

The status of the French meteorological research center's work on dynamic data is presented. The Merlin 4 is used for meteorological measurements. The different dynamic measurement points on the aircraft, radome, boom, Inertial Navigation System (INS), and Doppler radar, are illustrated. The radome data and inertial data are discussed. In the latter, angle data coding and pendular movement of the INS are given attention. It is concluded that the INS should be coupled with a reference. This is either the Doppler radar (though it is noisy), or the Ground Positioning System (GPS) which should be available within a few years. The Merlin's INS is already equipped with a GPS output, so this could be easily done. ESA

N91-22657# Deutsche Forschungsanstalt fuer Luft- und Raumfahrt, Oberpfaffenhofen (Germany, F.R.).
THE IMPROVEMENT OF THE INSTALLATION OF THE DLR RESEARCH AIRCRAFT FALCON: DESCRIPTION AND FIRST RESULTS
ROBERT BAUMANN, H. G. CHRISTNER, HANS P. FIMPEL, and G. WILKE *In its* International Workshop on the Airborne Measurement of Wind, Turbulence and Position: Workshop Report p 47-50 23 Jun. 1990
Avail: NTIS HC/MF A05; DLR, Wissenschaftliches Berichtswesen, VB-PL-DO, Postfach 90 60 58, 5000 Cologne, Fed. Republic of Germany, HC 25 Deutsche marks

The upgrading of the DLR research aircraft is discussed. The new modern Electronic Flight Information System (EFIS) is described along with its sources of information: the Inertial Reference System (IRS), the weather radar, and the Flight Management Computer (FMC). Results of comparisons between the new INS, the replaced INS, and the new FMC are given. The new data aquisition system is also described. It is concluded that the efficiency of flight management and the acccuracy of navigation data will be improved as a result of the modernization. ESA

N91-22658# National Aeronautics and Space Administration. Ames Research Center, Moffett Field, CA.
THE NASA-ER2 METEOROLOGICAL MEASUREMENT SYSTEM: INSTRUMENTAION, CALIBRATION AND INTERCOMPARISON RESULTS
K. ROLAND CHAN, STUART W. BOWEN (San Jose State Univ., CA.), STAN G. SCOTT, and T. PAUL BUI *In* DLR, International Workshop on the Airborne Measurement of Wind, Turbulence and Position: Workshop Report p 51-55 23 Jun. 1990
Avail: NTIS HC/MF A05; DLR, Wissenschaftliches Berichtswesen, VB-PL-DO, Postfach 90 60 58, 5000 Cologne, Fed. Republic of Germany, HC 25 Deutsche marks

The NASA ER-2 aircraft is used as a platform for high altitude atmospheric missions. The Meteorological Measurement System (MMS) was designed specifically for atmospheric research to provide accurate, fast response, in situ measurements of pressure, temperature, and the three dimensional wind vector. The MMS consists of three subsystems: an air motion sensing system to measure the velocity of the air with respect to the aircraft, a high resolution Inertial Navigation System (INS) to measure the velocity of the aircraft with respect to the Earth, and a Data Acquisition System, to sample, process and record the measured quantities. Details of each of these systems are given. The location of the MMS instrumentation is illustrated. The calibration of the MMS is discussed and results on an intercomparison of MMS measurements, Vaisala radiosonde observation and radar tracking data are given. An illustration of the MMS measurement of vertical wind is given. ESA

N91-22659# Deutsche Airbus G.m.b.H., Bremen (Germany, F.R.).
FAST RESPONSE GUST MEASUREMENT DEVICE

MEINHARD SCHUMUECKER and GEORG LEMONIS *In* DLR, International Workshop on the Airborne Measurement of Wind, Turbulence and Position: Workshop Report p 56-60 23 Jun. 1990
Avail: NTIS HC/MF A05; DLR, Wissenschaftliches Berichtswesen, VB-PL-DO, Postfach 90 60 58, 5000 Cologne, Fed. Republic of Germany, HC 25 Deutsche marks

A fast response gust measurement device for on line wind and turbulence measurement from the aircraft is described. The requirements of the gust measurement system are given and the five hole probe, the pressure transducers and the transfer function of the pneumatic lines are described. Flight test results are given. The gust sensor design bases on the connection of a Rosemount five hole probe to an isolated, temperature controlled pressure transducer unit by extremely short pneumatic lines. This arrangement results in an advantageous pneumatic frequency response of the system, with very high resonance frequencies and negligible response errors in the low frequency range. ESA

N91-22661# Eidgenoessische Technische Hochschule, Zurich (Switzerland). Atmospheric Physics.
SUMMARY OF AIRCRAFT MEASURING ACTIVITIES AT LAPETH
BRUNO NEININGER and HANS RICHNER *In* DLR, International Workshop on the Airborne Measurement of Wind, Turbulence and Position: Workshop Report p 66-67 23 Jun. 1990
Avail: NTIS HC/MF A05; DLR, Wissenschaftliches Berichtswesen, VB-PL-DO, Postfach 90 60 58, 5000 Cologne, Fed. Republic of Germany, HC 25 Deutsche marks

Two completely different types and sizes of aircraft used in atmospheric research, instrumented motorgliders, and wide bodied airliners with Aircraft Integrated Monitoring Systems (AIMS) are presented. The instrumentation for dedicated research flights, on specially equipped aircraft is listed and details of the post flight software and the measuring platforms used are given. The missions which have been flown and the data evaluated are given. Details of the AIMS equipped aircraft and in airline services are given. The outlook for a new dedicated measuring platform is presented. ESA

N91-22663# Deutsche Forschungsanstalt fuer Luft- und Raumfahrt, Oberpfaffenhofen (Germany, F.R.). Abt. Meteorologische Flugmesssysteme.
TURBULENCE PROFILING IN THE ATMOSPHERIC BOUNDARY LAYER USING THREE POWERED GLIDERS
ANNE M. JOACHUM *In its* International Workshop on the Airborne Measurement of Wind, Turbulence and Position: Workshop Report p 74-77 23 Jun. 1990
Avail: NTIS HC/MF A05; DLR, Wissenschaftliches Berichtswesen, VB-PL-DO, Postfach 90 60 58, 5000 Cologne, Fed. Republic of Germany, HC 25 Deutsche marks

Three instrumented ASK 16 powered gliders are being operated as meteorological research aircraft. A low flight speed enabling the resolution of very small scales and a high degree of flexibility makes them the ideal research platform even for complex terrain studies. Due to their limited altitude range and payload they are primarily used in the atmospheric boundary layer. The investigation of the atmospheric boundary layer requires high spacetime resolution, and this is achieved by the utilization of three identically equipped aircraft. The main objectives in developing such a system, and thus its basic advantages are summarized. The main characteristics of the basic measurement system are presented, and the quality of the measurements are discussed. ESA

N91-22670# National Oceanic and Atmospheric Administration, Boulder, CO. Wave Propagation Lab.
REMOTE SENSOR OBSER'/ATIONS DURING WISP90: THE USE OF MICROWAVE RADIOMETERS, RASS, AND CEILOMETERS FOR DETECTION OF AIRCRAFT ICING CONDITIONS
B. B. STANKOV, E. R. WESTWATER, J. B. SNIDER, and R. L. WEBER Nov. 1990 83 p
(PB91-131839; NOAA-TM-ERL-WPL-187) Avail: NTIS HC/MF A05 CSCL 04/2

During Feb. and Mar. 1990, the National Center for Atmospheric Research, the National Oceanic and Atmospheric Administration (NOAA) Wave Propagation Laboratory, and the NOAA Forecast Systems Laboratory conducted the Winter Icing and Storms Project (WISP). One of the principal objectives was to determine the utility of unattended microwave radiometers in detecting atmospheric liquid water and providing input to forecasts of aircraft icing. Arrays of microwave radiometers, infrared radiometers, lidar ceilometers, and radio-acoustic sounding systems were used to determine spatial and temporal distribution of supercooled liquid water. Results are presented from four representative cases to demonstrate that the integrated system, which comprises a microwave water substance radiometer, a radio-acoustic sounding system, and a ceilometer, can identify supercooled liquid water. Occasional outages because of environmental effects on the radiometer antenna were encountered, and quality control procedures were employed to detect erroneous data. GRA

15

MATHEMATICAL AND COMPUTER SCIENCES

Includes mathematical and computer sciences (general); computer operations and hardware; computer programming and software; computer systems; cybernetics; numerical analysis; statistics and probability; systems analysis; and theoretical mathematics.

A91-33056* AS&M, Inc., Hampton, VA.
DOMAIN DECOMPOSITION METHODS IN AERODYNAMICS
V. VENKATAKRISHNAN (AS&M, Inc., Hampton, VA) and JOEL SALTZ (NASA, Langley Research Center; ICASE, Hampton, VA) IN: SIAM Conference on Parallel Processing for Scientific Computing, 4th, Chicago, IL, Dec. 11-13, 1989, Proceedings. Philadelphia, PA, Society for Industrial and Applied Mathematics, 1990, p. 278-284. *refs*
Copyright

Compressible Euler equations are solved for two-dimensional problems by a preconditioned conjugate gradient-like technique. An approximate Riemann solver is used to compute the numerical fluxes to second order accuracy in space. Two ways to achieve parallelism are tested, one which makes use of parallelism inherent in triangular solves and the other which employs domain decomposition techniques. The vectorization/parallelism in triangular solves is realized by the use of a recording technique called wavefront ordering. This process involves the interpretation of the triangular matrix as a directed graph and the analysis of the data dependencies. It is noted that the factorization can also be done in parallel with the wave front ordering. The performances of two ways of partitioning the domain, strips and slabs, are compared. Results on Cray YMP are reported for an inviscid transonic test case. The performances of linear algebra kernels are also reported. L.K.S.

A91-33932
ACTIVE VIBRATION CONTROL USING FIXED ORDER DYNAMIC COMPENSATION WITH FREQUENCY SHAPED COST FUNCTIONALS
J. V. R. PRASAD, ANTHONY J. CALISE, and EDWARD V. BYRNS, JR. (Georgia Institute of Technology, Atlanta) IEEE Control Systems Magazine (ISSN 0272-1708), vol. 11, April 1991, p. 71-78. refs
Copyright

An approach for the design of controllers for active suppression of helicopter vibration that combines recent developments in the design of fixed-order dynamic compensators with the frequency-shaped cost functional approach is presented. A robust compensator that provides loop shaping at the plant input is used in conjunction with frequency-shaped cost functionals to arrive at

a controller for vibration reduction. The effectiveness of this technique is demonstrated by a detailed case study for the design of an active vibration controller. I.E.

A91-34230
DEVELOPMENT OF A GENERAL MULTIBLOCK FLOW SOLVER FOR COMPLEX CONFIGURATIONS
N. J. YU, H. C. CHEN, T. Y. SU, and T. J. KAO (Boeing Commercial Airplanes, Seattle, WA) IN: GAMM-Conference on Numerical Methods in Fluid Mechanics, 8th, Delft, Netherlands, Sept. 27-29, 1989, Proceedings. Wiesbaden, Federal Republic of Germany/Hauppauge, NY, Friedr. Vieweg & Sohn/Ballen Books, 1990, p. 603-612. refs
Copyright

A configuration- and grid topology-independent flow solver has been developed for the analysis of complex flow fields over geometrically complex configurations. The approach used in the present study is based on a multiblock method where the complete flow field is divided into a number of topologically simple blocks, such that within each block, surface-fitted grids and efficient flow solution algorithms can easily be constructed. In the present study, the field grid is generated using a combination of algebraic and elliptic methods. The flow solver utilizes an explicit time-stepping scheme to solve the Euler equations. A multiblock version of the multigrid method is implemented to improve the convergence of the calculations. The generality of the present method is demonstrated through the analysis of a number of complex configurations at various flow conditions. Results are checked against available data for code validation. Author

A91-35100
GENERALIZED HEURISTICS FOR THE GATE ASSIGNMENT PROBLEM
ROBERT P. BRAZILE and KATHLEEN M. SWIGGER (North Texas, University, Denton, TX) Control and Computers (ISSN 0315-8934), vol. 19, no. 1, 1991, p. 27-32. refs
Copyright

In an effort to reduce the amount of time necessary to prepare an airline operations gate schedule, a gate allocation and tracking expert system (GATES) was developed to create the monthly and daily gate assignment schedule. GATES is a constraint satisfaction expert system using production rules to guide its search, running on a 386-based machine making specific gate assignments, producing an audit trail of its rules, and performing 'what if' analyses. It also includes an elaborate user interface that permits ground controllers to change gate assignments, question the main database, and adjust the tolerance levels on individual rules. As GATES is linked directly to the airline's mainframe computer, the new gate assignments can be transmitted immediately to other parts of the system, including the airport monitors that display gate information to passengers. R.E.P.

A91-35241
A MODEL-BASED METHOD FOR OBJECT RECOGNITION
HORMOZ SHARIAT (Lockheed Artificial Intelligence Center, Palo Alto, CA) IN: 1990 IEEE International Conference on Robotics and Automation, Cincinnati, OH, May 13-18, 1990, Proceedings. Vol. 3. Los Alamitos, CA, IEEE Computer Society Press, 1990, p. 1846-1851. refs
Copyright

A method is presented for using the high-level descriptions of objects (i.e., their models) to recognize them in an image. A complex object is viewed as a congregation of a set of component parts with simple shapes. The model of an object, therefore, describes the shapes of its component parts and states the geometrical relationships among those parts. This method also includes a recognition strategy which is a simple high-level description of how that object must be recognized. The shape descriptions of the parts are first used to extract a set of candidates for each part from the image. An object candidate is formed whenever a group of part candidates satisfy the model's geometrical relationships. A model-based prediction and verification scheme is used to verify (or refute) the existence of the object candidates with low certainty. The scheme not only substantially increases the accuracy of recognition, but also makes it possible to detect and recognize partially occluded and camouflaged objects. Another advantage of the approach is that to recognize a new object, one only needs to define its model, and thus no programming is required. The user's task is further simplified by the fact that each newly defined model is sufficient for recognizing a new category of objects. I.E.

N91-21735# Frontier Technology, Inc., Beavercreek, OH.
METHODOLOGY DEVELOPMENT FOR THE VERIFICATION AND VALIDATION OF FLIGHT CRITICAL SYSTEMS SOFTWARE, PHASE 1 Final Report, Dec. 1989 - Aug. 1990
RONALD L. BRAET Oct. 1990 107 p
(Contract F33615-89-C-3610)
(AD-A229932; FTI-9042-001-PHASE-1;
WRDC-TR-90-3067-PHASE-1) Avail: NTIS HC/MF A06 CSCL 12/5

The results of this conceptual design study have that there is a growing need to develop a methodology by which flight critical systems (FCS) software can be verified and validated for performance and safety impacts. The nature of the evolving technology and its application to FCS Software verification an validation requirements has current V and V methods lagging behind design methods and tools. It is recognized throughout government and industry that FCS software V and V requires knowledgeable and skilled individuals utilizing proper tools and techniques to successfully complete the V and V effort in a timely manner. This report provides an overview of the development process of flight critical systems and the roles of verification an validation which go hand-in-hand with the development process. It provides a conceptual design for a computer aided environment to perform FCS software verification and validation. Current trends in applications of advanced control and integration technologies are bringing about the development of on-board systems that are designed to enhance combat effectiveness and survivability in ever increasing hostile combat environments. Flight critical systems (including integrated flight vehicle sensors) are being controlled and integrated in software. GRA

N91-22313*# Illinois Univ., Chicago. Lab. for Advanced Computing.
SUPERCOMPUTER OPTIMIZATIONS FOR STOCHASTIC OPTIMAL CONTROL APPLICATIONS
SIU-LEUNG CHUNG, FLOYD B. HANSON, and HUIHUANG XU *In* NASA. Langley Research Center, Fourth NASA Workshop on Computational Control of Flexible Aerospace Systems, Part 1 p 57-70 Mar. 1991 Sponsored in part by ANL
(Contract NSF DMS-88-06099)
Avail: NTIS HC/MF A20 CSCL 09/2

Supercomputer optimizations for a computational method of solving stochastic, multibody, dynamic programming problems are presented. The computational method is valid for a general class of optimal control problems that are nonlinear, multibody dynamical systems, perturbed by general Markov noise in continuous time, i.e., nonsmooth Gaussian as well as jump Poisson random white noise. Optimization techniques for vector multiprocessors or vectorizing supercomputers include advanced data structures, loop restructuring, loop collapsing, blocking, and compiler directives. These advanced computing techniques and superconducting hardware help alleviate Bellman's curse of dimensionality in dynamic programming computations, by permitting the solution of large multibody problems. Possible applications include lumped flight dynamics models for uncertain environments, such as large scale and background random aerospace fluctuations. Author

N91-22728*# Houston Univ., Clear Lake, TX. Research Inst. for Computing and Information Systems.
RICIS SOFTWARE ENGINEERING 90 SYMPOSIUM: AEROSPACE APPLICATIONS AND RESEARCH DIRECTIONS PROCEEDINGS APPENDICES
1990 136 p Symposium held in Houston, TX, 7-8 Nov. 1990

(Contract NCC9-16)
(NASA-CR-187994; NAS 1.26:187994) Avail: NTIS HC/MF A07 CSCL 09/2

Papers presented at RICIS Software Engineering Symposium are compiled. The following subject areas are covered: flight critical software; management of real-time Ada; software reuse; megaprogramming software; Ada net; POSIX and Ada integration in the Space Station Freedom Program; and assessment of formal methods for trustworthy computer systems.

N91-22729*# Boeing Co., Seattle, WA.
SOFTWARE: WHERE WE ARE AND WHAT IS REQUIRED IN THE FUTURE
JERRY COHEN *In* Houston Univ., RICIS Software Engineering 90 Symposium: Aerospace Applications and Research Directions Proceedings Appendices 27 p 1990
Avail: NTIS HC/MF A07 CSCL 09/2

The current status and future direction of flight critical software are presented in the form of view-graphs. The following subject areas are covered: the programmers environment; Saab Grippen Flight test program; present day tools; analysis tools (reverse engineering); automatic code generators; and future plans.
Author

N91-22734# Dayton Univ., OH.
CREW CHIEF CAD SYSTEM INTERFACE GUIDE (VERSION 2 - SI) Technical Report, May 1988 - Nov. 1989
P. J. KRAUSKOPF, J. W. QUINN, M. W. JONES, and W. J. STUMP Mar. 1990 190 p
(Contract F33615-84-C-0519)
(AD-A231433; UDR-TR-90-15; AAMRL-TR-90-015) Avail: NTIS HC/MF A09 CSCL 12/5

This report describes the procedures to interface the CREW CHIEF programs with a user's computer aided design system through the Common Users Interface (CUI). The CUI was developed as the vehicle to pass information between the CREW CHIEF core programs and data bases and the user's CAD system. A set of interface subroutines pass input, output, and diagnostic parameters, in that order. Each passed variable is named according to FORTRAN variable type defaults, with identical parameter entities always represented by identical parameter names. CADAM and Computervision CV4001 and CADDStation are commercial CAD systems, used during the development of CREW CHIEF and CREW CHIEF interfaces. Their use, and reference to them, does not constitute an endorsement by the United States Air Force or the University of Dayton. GRA

N91-22792*# College of William and Mary, Williamsburg, VA. Dept. of Computer Science.
DESIGN OF AN INTELLIGENT INFORMATION SYSTEM FOR IN-FLIGHT EMERGENCY ASSISTANCE
STEFAN FEYOCK and STAMOS KARAMOUZIS *In* NASA. Goddard Space Flight Center, The 1991 Goddard Conference on Space Applications of Artificial Intelligence p 295-306 May 1991
Avail: NTIS HC/MF A16 CSCL 09/2

The present research has as its goal the development of AI tools to help flight crews cope with in-flight malfunctions. The relevant tasks in such situations include diagnosis, prognosis, and recovery plan generation. Investigation of the information requirements of these tasks has shown that the determination of paths figures largely: what components or systems are connected to what others, how are they connected, whether connections satisfying certain criteria exist, and a number of related queries. The formulation of such queries frequently requires capabilities of the second-order predicate calculus. An information system is described that features second-order logic capabilities, and is oriented toward efficient formulation and execution of such queries. Author

N91-22794*# National Aeronautics and Space Administration. Lyndon B. Johnson Space Center, Houston, TX.
METAMORPHOSES OF ONAV CONSOLE OPERATIONS: FROM PROTOTYPE TO REAL TIME APPLICATION
MALISE MILLIS and LUI WANG *In* NASA. Goddard Space Flight Center, The 1991 Goddard Conference on Space Applications of Artificial Intelligence p 317-326 May 1991
Avail: NTIS HC/MF A16 CSCL 09/2

The ONAV (Onboard Navigation) Expert System is being developed as a real time console assistant to the ONAV flight controller for use in the Mission Control Center at the Johnson Space Center. Currently the entry and rendezvous systems are in verification, and the ascent is being prototyped. To arrive at this stage, from a prototype to real world application, the ONAV project has had to deal with not only AI issues but operating environment issues. The AI issues included the maturity of AI languages and the debugging tools, what is verification, and availability, stability, and the size of the expert pool. The environmental issues included real time data acquisition, hardware stability, and how to achieve acceptance by users and management. Author

N91-22805*# Grumman Aerospace Corp., Bethpage, NY.
ADDENDUM TO THE DYCAST USER'S MANUAL DESCRIBING THE CURVED, WARP BEAM FINITE ELEMENT Final Report
L. M. KUTT and A. B. PIFKO Washington NASA May 1991 51 p Prepared for LMSC, Palo Alto, CA
(Contract NAS1-18444)
(NASA-CR-4362; NAS 1.26:4362; RE-780) Avail: NTIS HC/MF A04 CSCL 12/1

DYCAST is a finite element computer program for the nonlinear transient dynamic analysis of structures. As part of the Computational Structural Mechanics (CSM) research program of NASA, the Grumman CRC is developing capabilities in its DYCAST software system for the analysis of aerospace structures made of composite materials. One result of this development effort is that a curved, linear, thin walled beam element was incorporated into the DYCAST library of finite elements. The formulation of this new element, called the WARP element, includes both shear deformations and nonuniform torsion (restrained warping). The basic concepts, the input data, and several example problems essential to the DYCAST analyst for the successful use the WARP element are described. Author

16

PHYSICS

Includes physics (general); acoustics; atomic and molecular physics; nuclear and high-energy physics; optics; plasma physics; solid-state physics; and thermodynamics and statistical physics.

A91-32707
EXPERIMENTAL PERFORMANCE OF A BINARY PHASE-ONLY OPTICAL CORRELATOR USING VISUAL AND INFRARED IMAGERY
S. P. KOZAITIS (Florida Institute of Technology, Melbourne), S. HALBY, and W. FOOR (USAF, Photonics Laboratory, Griffiss AFB, NY) IN: Advances in optical information processing IV; Proceedings of the Meeting, Orlando, FL, Apr. 18-20, 1990. Bellingham, WA, Society of Photo-Optical Instrumentation Engineers, 1990, p. 140-151. refs
Copyright

Experimental results of an optical binary phase-only correlator using both visual and IR imagery are presented. The inputs to the correlator originate from actual aerial imagery containing aircraft and a variety of distortions. Filters used as a database for the system are derived from models of aircraft. Digital image processing techniques are used on images before being input into the optical correlator to enhance the performance of the system. Both noise removing and segmentation techniques are investigated. Input

images to the correlator are displayed on a 128 x 128 magnetooptic spatial light modulator (SLM). Experimental results are presented which show that the system performs well with images which are easily segmented from the background. Author

A91-33368
THE LOCATION OF ACOUSTIC BLADE-VORTEX INTERACTION - A FURTHER STEP TOWARD AN UNDERSTANDING OF HELICOPTER NOISE [ORTUNG DER AKUSTISCHEN BLATT-/WIRBELINTERAKTIONSQUELLEN - EIN WEITERER SCHRITT ZUM VERSTAENDNIS DES HUBSCHRAUBERLAERMS]
HANNO HELLER, WOLF SPLETTSTOESSER, and KLAUS J. SCHULTZ (DLR, Institut fuer Entwurfsaerodynamik, Brunswick, Federal Republic of Germany) DLR-Nachrichten (ISSN 0937-0420), Feb. 1991, p. 2-6. In German.
Copyright

An ongoing DLR program to determine the sites of helicopter-rotor blade-vortex interactions (BVIs) by means of wind-tunnel experiments is described, and typical results are presented in graphs. A 40-percent-scale model of the BO-105 main rotor is mounted in the main test section of the German-Dutch Wind Tunnel so as to permit undisturbed measurements of the downward-directed acoustic field with a microphone array, and a novel iterative procedure is used to estimate the BVI source regions. This procedure has been validated by comparing the predicted source regions with (1) direct measurements using a rotor model equipped with pressure sensors and (2) the predictions of a three-dimensional aerodynamic blade-tip-vortex wake model. T.K.

A91-35791
MHD DRAG AND HEAT TRANSFER OF A SPHERE IN SUPERSONIC FLOW OF A PARTIALLY IONIZED GAS [MGD-TORMOZHENIE I TEPLOOBMEN SFERY V SVERKHZVUKOVOM POTOKE CHASTICHNO IONIZOVANNOGO GAZA]
V. V. GUBIN and V. A. SHUVALOV PMTF - Zhurnal Prikladnoi Mekhaniki i Tekhnicheskoi Fiziki (ISSN 0044-4626), Jan.-Feb. 1991, p. 15-19. In Russian. refs
Copyright

Results of an experimental study of the MHD drag and heat transfer characteristics of a body are reported for the case where the orientation of the intensity vector of the body's own magnetic field changes relative to that of the incoming flow velocity vector. The possibility of the MHD control of the aerodynamic quality of the sphere and its convective heat transfer characteristics through the rotation of the sphere's magnetic field relative to the velocity vector of the rarefied plasma flow is demonstrated. V.L.

N91-21828*# National Aeronautics and Space Administration. Ames Research Center, Moffett Field, CA.
ACOUSTIC AND AERODYNAMIC STUDY OF A PUSHER-PROPELLER AIRCRAFT MODEL
PAUL T. SODERMAN and W. CLIFTON HORNE Washington Sep. 1990 67 p
(NASA-TP-3040; A-89038; NAS 1.60:3040) Avail: NTIS HC/MF A04 CSCL 20/1

An aerodynamic and acoustic study was made of a pusher-propeller aircraft model in the NASA-Ames 7 x 10 ft Wind Tunnel. The test section was changed to operate as an open jet. The 591 mm diameter unswept propeller was operated alone and in the wake of three empennages: an I tail, Y tail, and a V tail. The radiated noise and detailed wake properties were measured. Results indicate that the unsteady blade loading caused by the blade interactions with the wake mean velocity distribution had a strong effect on the harmonics of blade passage noise. The blade passage harmonics above the first were substantially increased in all horizontal directions by the empennage/propeller interaction. Directivity in the plane of the propeller was maximum perpendicular to the blade surface. Increasing the tail loading caused the propeller harmonics to increase 3 to 5 dB for an empennage/propeller spacing of 0.38 mean empennage chords. The interaction noise became weak as empennage propeller spacing was increased beyond 1.0 mean empennage chord lengths. Unlike the mean wake deficit, the wake turbulence had only a small effect on the propeller noise, that effect being a small increase in the broadband noise. Author

N91-21829*# Cornell Univ., Ithaca, NY. School of Mechanical and Aerospace Engineering.
A STUDY OF ROTOR BROADBAND NOISE MECHANISMS AND HELICOPTER TAIL ROTOR NOISE
SHAU-TAK RUDY CHOU Aug. 1990 188 p
(Contract NAG2-379)
(NASA-CR-177565; A-90269; NAS 1.26:177565) Avail: NTIS HC/MF A09 CSCL 20/1

The rotor broadband noise mechanisms considered are the following: (1) lift fluctuation due to turbulence ingestion; (2) boundary layer/trailing edge interaction; (3) tip vortex formation; and (4) turbulent vortex shedding from blunt trailing edge. Predictions show good agreement with available experimental data. The study shows that inflow turbulence is the most important broadband noise source for typical helicopters' main rotors at low- and mid-frequencies. Due to the size difference, isolated helicopter tail rotor broadband noise is not important compared to the much louder main rotor broadband noise. However, the inflow turbulence noise from a tail rotor can be very significant because it is operating in a highly turbulent environment, ingesting wakes from upstream components of the helicopter. The study indicates that the main rotor turbulent wake is the most important source of tail rotor broadband noise. The harmonic noise due to ingestion of main rotor tip vortices is studied. Author

N91-21830# Institut Franco-Allemand de Recherches, Saint-Louis (France).
PROPAGATION OF HELICOPTER NOISE IN THE LOW ATMOSPHERE LAYERS [PROPAGATION DU BRUIT DES HELICOPTERES DANS LES BASSES COUCHES DE L'ATMOSPHERE]
P. NAZ and G. PARMENTIER 23 May 1990 10 p In FRENCH Presented at the 1st Congres Francais d'Acoustique, Lyon, France, 10-13 Apr. 1990
(ISL-CO-203/90; ETN-91-98981) Avail: NTIS HC/MF A02

The acoustic signatures of several different helicopters, are recorded. For some helicopters, it was observed that noise levels of the characteristic frequencies of the main and back rotor show different attenuations according to the distance between the helicopter and the microphone. The experimental signals show that the acoustic propagation is influenced by the meteorological parameters and their variations. Numerical propagation models based on the wave method are used to simulate the effects of atmospheric fluctuations on the sound trajectories, which were taken into account with statistic evaluations from random methods. ESA

N91-21831# Institut Franco-Allemand de Recherches, Saint-Louis (France).
CALCULATION OF THICKNESS AND CHARGE NOISE RADIATED BY A ROTOR IN FORWARD FLIGHT [CALCUL DU BRUIT D'EPAISSEUR ET DU BRUIT DE CHARGE RAYONNES PAR UN ROTOR EN VOL D'AVANCEMENT]
J. HAERTIG and P. GNEMMI 25 Sep. 1989 57 p In FRENCH
(Contract DRET-88/214)
(ISL-R-119/89; ETN-91-98987) Avail: NTIS HC/MF A04

The noise radiated by moving bodies is investigated by establishing the wave equation in a moving area with solid surfaces. By solving this equation, the acoustic pressure radiated in a far field is obtained. The blade vortex interaction noise is calculated by means of aerodynamic data supplied by a three dimensional extension of a two dimensional numerical code of profile/vortex interaction. The calculated acoustic signatures are shown to be in a good agreement with the flow around the rotor. ESA

N91-21832# Institut Franco-Allemand de Recherches, Saint-Louis (France).
BLADE-WAKE INTERACTION ON A TWO BLADE ROTOR WITH PREDICTION OF THE RADIATED NOISE STATIONARY AND FORWARD FLIGHT, COMPARISON BETWEEN CALCULATION, AND EXPERIMENT [INTERACTION PALE/SILLAGE SUR UN ROTOR BIPALE AVEC PREVISION DU BRUIT RAYONNE (VOL STATIONNAIRE ET VOL D'AVANCEMMENT, COMPARAISON CALCUL/EXPERIENCE)]
M. SCHAFFAR, J. HAERTIG, and F. GNEMMI 23 Oct. 1989 34 p In FRENCH Original contains color illustrations
(ISL-R-120/89; ETN-91-98988) Avail: NTIS HC/MF A03

The method of the vortex networks is applied to the calculation of the flow around a two blade rotor. The obtained results were compared to measured results with a good agreement for the stationary flight. The charges obtained for the forward flight were used to calculate the radiated noise by the Ffowcs-Williams and Hawkings equation. It is concluded that the radiated noise is greatly influenced by the flight conditions and the parameters of the calculation method, such as the coefficients of the Biot and Savert law. ESA

N91-21833# Federal Aviation Administration, Atlantic City, NJ.
COMPARISON OF 14 DECIBELS VERSUS 20 DECIBELS DESIRED TO UNDESIRED SIGNAL PROTECTION RATIOS
MARTIN BADINELLI, ARTHUR CUSHMAN, and PHILIP RANDAZZO Apr. 1991 14 p
(DOT/FAA/CT-TN89/69) Avail: NTIS HC/MF A03

Due to a shortage of very high frequency (VHF) communications frequencies, the FAA must use the same frequencies in different airspaces across the country. The geographical separation between ground transmitters is engineered to provide a desired signal that is at least 14 decibel (dB) above any co-channel signal the receiver may receive. The International Civil Aviation Organization (ICAO) recommends a greater 20-dB separation. This difference between the two signals is known as the desired to undesired (D/U) ratio. Tests performed on eight avionics receivers at the FAA Technical Center to compare receiver performance when exposed to 14- and 20-dB co-channel interference are described. It was concluded that at both D/U ratios, the receiver was able to reproduce clear, audible, and intelligible speech at both D/U ratios. Author

N91-22830*# Tech-U-Fit Corp., Alexandria, VA.
DESIGN METHODOLOGY FOR A COMMUNITY RESPONSE QUESTIONNAIRE ON SONIC BOOM EXPOSURE Final Report
JOHN E. FARBRY, JR., JAMES M. FIELDS, JOHN A. MOLINO, and GWENDOLYN A. DEMIRANDA May 1991 86 p Prepared in cooperation with Wyle Labs., Inc., Hampton, VA; and Douglas Aircraft Co., Inc., St. Louis, MO
(Contract NAS1-19060)
(NASA-CR-187503; NAS 1.26:187503; TUF-90-07) Avail: NTIS HC/MF A05 CSCL 20/1

A preliminary draft questionnaire concerning community response to sonic booms was developed. Interviews were conducted in two communities that had experienced supersonic overflights of the SR-71 airplane for several years. Even though the overflights had ceased about 6 months prior to the interviews, people clearly remembered hearing sonic booms. A total of 22 people living in central Utah and 23 people living along Idaho/Washington state border took part in these interviews. The draft questionnaire was constantly modified during the study in order to evaluate different versions. Questions were developed which related to annoyance, startle, sleep disturbance, building vibration, and building damage. Based on the data collected, a proposed community response survey response instrument was developed for application in a full-scale sonic boom study. Author

17

SOCIAL SCIENCES

Includes social sciences (general); administration and management; documentation and information science; economics and cost analysis; law and political science; and urban technology and transportation.

A91-35121
A PRACTICAL APPROACH TO RULE 26(C) PROTECTIVE ORDERS IN AVIATION LITIGATION
WILTON J. SMITH (Gilman, Olson, and Pangia, Washington, DC) Journal of Air Law and Commerce (ISSN 0021-8642), vol. 56, Spring 1991, p. 765-801. refs
Copyright

Steps that have been taken over the past few years to improve the implementation of Rule 26(c) of the Federal Rules of Civil Procedure are reviewed. Rule 26(c) authorizes a courts's issuance of orders protecting information upon the motion of a party. The basic principles that courts have crafted to determine whether trade secret information deserves protection are summarized. Court decisions concerning such trade secrets protective practices are presented. The procedures developed for handling protective order issues in product liability and terrorist actions are discussed. C.D.

A91-35122
AIRPORT RESTRICTIONS - A DILEMMA OF FEDERAL PREEMPTION AND PROPRIETARY CONTROL
WILLIAM PENNINGTON Journal of Air Law and Commerce (ISSN 0021-8642), vol. 56, Spring 1991, p. 805-845. refs
Copyright

The extent to which airport proprietors may regulate their facilities in the face of federal statutes is demonstrated. The principal statutes concerned with federal preemption of airport regulation are reviewed, and the development of proprietary control, beginning with the recognition that noise regulation is a legitimate area of proprietary interest, is discussed. The reasonable and nondiscriminatory limitations imposed on any airport restrictions, and the application of these limitations on proprietary restrictions are considered. C.D.

A91-35123
GENERAL AVIATION ACCIDENT LIABILITY STANDARDS - WHY THE FUSS?
GREGORY P. WELLS Journal of Air Law and Commerce (ISSN 0021-8642), vol. 56, Spring 1991, p. 895-935. refs
Copyright

In an effort to alleviate the increase in the cost of accident liability insurance, both houses of Congress introduced bills in the 101st Congress to provide uniform liability standards for general aviation accidents. Here, the impact the House Bill will have on existing law in the area of general aviation accidents is analyzed and discussed. C.D.

19

GENERAL

N91-22066*# National Aeronautics and Space Administration. Ames Research Center, Moffett Field, CA.
NASA AMES AEROSPACE SYSTEMS DIRECTORATE RESEARCH
JAMES A. ALBERS Mar. 1991 55 p
(NASA-TM-103844; A-91088; NAS 1.15:103844) Avail: NTIS HC/MF A04 CSCL 05/4

The Aerospace Systems Directorate is one of four research directorates at the NASA Ames Research Center. The Directorate conducts research and technology development for advanced aircraft and aircraft systems in intelligent computational systems and human-machine systems for aeronautics and space. The Directorate manages research and aircraft technology development projects, and operates and maintains major wind tunnels and flight simulation facilities. The Aerospace Systems Directorate's research and technology as it relates to NASA agency goals and specific strategic thrusts are discussed. Author

N91-23020# Wichita State Univ., KS. Inst. for Aviation Research.

BUSINESS PLANS FOR THE INSTITUTE FOR AVIATION RESEARCH, FY 1990 - FY 1995 Annual Report, FY 1989

Sep. 1989 113 p Sponsored by Kansas Technology Enterprise Corp.

(IAR-89-15) Avail: NTIS HC/MF A06

The design, development, and production of commercial and military aircraft is a significant industry. The Institute for Aviation Research was established to transfer technology and conduct research, educational, and service programs directed toward meeting the challenges of the American aviation industry. Key accomplishments are highlighted. The Center for Basic and Applied Research (the Aerodynamic, Propulsion, Flight Simulation, Structures, and Advanced Materials Laboratory); the Center for Aviation Safety Research; and the Center for Productivity Enhancement (CAS/CAM Laboratory, Composites Laboratory) objectives, goals, and accomplishments are described. B.G.

Typical Subject Index Listing

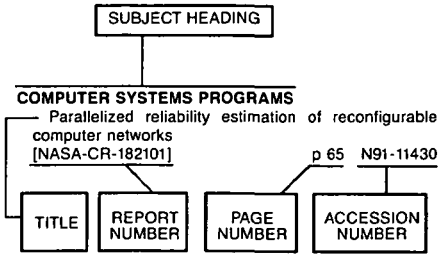

The subject heading is a key to the subject content of the document. The title is used to provide a description of the subject matter. When the title is insufficiently descriptive of document content, a title extension is added, separated from the title by three hyphens. The accession number and the page number are included in each entry to assist the user in locating the abstract in the abstract section. If applicable, a report number is also included as an aid in identifying the document. Under any one subject heading, the accession numbers are arranged in sequence.

A

ACCELERATION STRESSES (PHYSIOLOGY)
Biodynamic and optimization aspects of emergency ejection from an aircraft p 561 A91-34341

ACCELEROMETERS
Airborne gravimetry and the Global Positioning System p 602 A91-33634

ACCIDENT PREVENTION
The final call: Why airline disasters continue to happen --- Book p 561 A91-34250

ACOUSTIC PROPAGATION
Propagation of helicopter noise in the low atmosphere layers
[ISL-CO-203/90] p 607 N91-21830

ACOUSTO-OPTICS
Airborne heterodyne receiver for the range 600 GHz to 3,000 GHz p 599 N91-22047

ACTIVE CONTROL
Active vibration control using fixed order dynamic compensation with frequency shaped cost functionals p 604 A91-33932
High-speed compressor surge with application to active control
[ASME PAPER 90-GT-354] p 553 A91-34797
Hot-bench simulation of the active flexible wing wind-tunnel model
[NASA-TM-102758] p 582 N91-21144
A leading-edge control surface
[BU-508] p 559 N91-22087
An overview of the active flexible wing program p 583 N91-22332
Design and test of three active flutter suppression controllers p 583 N91-22334
Development and testing of controller performance evaluation methodology for multi-input/multi-output digital control systems p 584 N91-22337

AERIAL PHOTOGRAPHY
An airworthy experimental system for modern navigation and remote-sensing methods - Reduction, storage, and transmission of aerial photography scenes p 575 A91-33370

AERIAL RECONNAISSANCE
Flight test to determine feasibility of a proposed airborne wake vortex detection concept
[NASA-TM-102672] p 563 N91-22096

AEROACOUSTICS
Acoustic and aerodynamic study of a pusher-propeller aircraft model
[NASA-TP-3040] p 607 N91-21828

AERODYNAMIC CHARACTERISTICS
Analysis of laminar separation bubble using a simple eddy-viscosity turbulence model p 591 A91-33227
Aerodynamic and structural studies of joined-wing aircraft p 571 A91-33534
Interference-free measurements of the subsonic aerodynamics of slanted-base ogive cylinders p 547 A91-34130
Infrared thermography for the qualitative aerodynamic study of a slender body
[ISL-R-122/89] p 555 N91-21104
Bifurcation analysis of the longitudinal dynamics of a simple powered lifting hypersonic vehicle
[AD-A230826] p 557 N91-21118
Identification of the aerodynamic model of the DLR research aircraft ATTAS from flight test data
[DLR-FB-90-40] p 572 N91-21130
Rotary-balance testing for aircraft dynamics
[AGARD-AR-265] p 585 N91-21156
Multiaxis thrust vectoring using axisymmetric nozzles and postexit vanes on an F/A-18 configuration vehicle
[NASA-TM-101741] p 559 N91-22083
Special Course on Aircraft Dynamics at High Angles of Attack: Experiments and Modelling
[AGARD-R-776] p 573 N91-22104
Dynamic stall effects and applications to high performance aircraft p 573 N91-22106
A quantitative investigation into the aerodynamic coupling effects in a coaxial contra-rotating rotor system
[BU-517] p 574 N91-22120

AERODYNAMIC COEFFICIENTS
Comparison study of the aerodynamic coefficients measured on models with circular or squared section and large elongation in supersonic flow
[ISL-R-125/89] p 555 N91-21106

AERODYNAMIC CONFIGURATIONS
Low speed wind tunnel investigation of propeller slipstream aerodynamic effects on different nacelle/wing combinations. Part 2: Propeller slipstream flow field surveys (velocity components, dynamic, total and static pressure distributions) at zero angle of attack and high power
[FFA-TN-1990-24-PT-2] p 555 N91-21109
Application of mesh generation to complex 3-D configurations
[AGARD-AR-268] p 598 N91-21464
Advanced rotorcraft transmission program
[NASA-TM-103276] p 598 N91-21531
Effect of planform on induced drag
[BU-500] p 559 N91-22086
Special Course on Aircraft Dynamics at High Angles of Attack: Experiments and Modelling
[AGARD-R-776] p 573 N91-22104
An iterative procedure for the design of pressure-specified 3-dimensional configurations at subsonic and supersonic speeds by means of a higher-order panel method
[MBB-FE122/S/PUB/375] p 574 N91-22118

AERODYNAMIC DRAG
Progress in the prediction of the laminar-turbulent transition for laminar wings - The profile and wing geometries determine the friction drag of an aircraft p 544 A91-33369
A method to calculate the influence of vortex roll-up on the induced drag of wings p 546 A91-34055
MHD drag and heat transfer of a sphere in supersonic flow of a partially ionized gas p 607 A91-35791
Practical methods to evaluate the friction drag coefficient of a projectile in free flight
[ISL-R-123/89] p 555 N91-21105
Forces and pressures induced on circular plates by a single lifting jet in ground effect
[NASA-TM-102816] p 558 N91-22077

AERODYNAMIC FORCES
Reduction of aerodynamic augmented states in active flutter suppression systems p 580 A91-33535
Effects of heat transfer on aerodynamics and possible implications for wind tunnel tests p 545 A91-33802
Forcing function effects on rotor periodic aerodynamic response
[ASME PAPER 90-GT-109] p 553 A91-34798
A modal aeroelastic analysis scheme for turbomachinery blading
[NASA-CR-187089] p 579 N91-21138
STARS: An integrated general-purpose finite element structural, aeroelastic, and aeroservoelastic analysis computer program
[NASA-TM-101709-REV] p 599 N91-21587

AERODYNAMIC HEAT TRANSFER
Flowfield and vehicle parameter influence on results of engineering aerothermal methods p 544 A91-33378

AERODYNAMIC HEATING
Finite element methods for integrated aerodynamic heating analysis
[NASA-CR-188079] p 554 N91-21101

AERODYNAMIC INTERFERENCE
Description and evaluation of an interference assessment for a slotted-wall wind tunnel
[NASA-CR-4352] p 585 N91-21155
Approximate methods for predicting the lifting characteristics of wing-body combinations p 558 N91-22074

AERODYNAMIC LOADS
Integrated multidisciplinary design optimization of rotorcraft p 570 A91-33528
Integrated aerodynamic load/dynamic optimization of helicopter rotor blades p 571 A91-33532
Forces and pressures induced on circular plates by a single lifting jet in ground effect
[NASA-TM-102816] p 558 N91-22077
Aerodynamic parameter studies and sensitivity analysis for rotor blades in axial flight
[NASA-CR-187524] p 558 N91-22078
Unsteady aerodynamics of slender wings p 560 N91-22105
Large amplitude oscillations p 561 N91-22108

AERODYNAMIC NOISE
A study of rotor broadband noise mechanisms and helicopter tail rotor noise
[NASA-CR-177565] p 607 N91-21829
Propagation of helicopter noise in the low atmosphere layers
[ISL-CO-203/90] p 607 N91-21830

AERODYNAMIC STABILITY
Prediction of slender body coning characteristics p 544 A91-33382
A leading-edge control surface
[BU-508] p 559 N91-22087
Flutter suppression of an aircraft wing using a control surface
[BU-506] p 583 N91-22133

AERODYNAMIC STALLING
Dynamic stall effects and applications to high performance aircraft p 573 N91-22106

AERODYNAMICS
Aerodynamic and structural studies of joined-wing aircraft p 571 A91-33534
Low speed wind tunnel investigation of propeller slipstream aerodynamic effects on different nacelle/wing combinations. Part 2: Propeller slipstream flow field surveys (velocity components, dynamic, total and static pressure distributions) at zero angle of attack and high power
[FFA-TN-1990-24-PT-2] p 555 N91-21109
Possibilities of trajectory modification
[ISL-CO-209/90] p 582 N91-21151
Aerodynamic parameter studies and sensitivity analysis for rotor blades in axial flight
[NASA-CR-187524] p 558 N91-22078
Multiaxis thrust vectoring using axisymmetric nozzles and postexit vanes on an F/A-18 configuration vehicle
[NASA-TM-101741] p 559 N91-22083

Special Course on Aircraft Dynamics at High Angles of Attack: Experiments and Modelling
[AGARD-R-776] p 573 N91-22104
Large amplitude oscillations p 561 N91-22108
Forebody vortex control p 573 N91-22110

AEROELASTIC RESEARCH WINGS
Shape sensitivity analysis of flutter response of a laminated wing p 571 A91-34144

AEROELASTICITY
Aeroelastic optimum design of composite rotor blade with returning wake effect p 570 A91-32646
Helicopter vibration reduction using structural optimization with aeroelastic/multidisciplinary constraints - A survey p 570 A91-33527
Aeroelastic optimization of a helicopter rotor using an efficient sensitivity analysis p 570 A91-33529
Optimum aeroelastic design of helicopter rotors for longitudinal handling qualities improvement p 570 A91-33531
Optimization of helicopter airframe structures for vibration reduction - Considerations, formulations, and applications p 571 A91-33533
State stability of a system of integro-differential equations of nonstationary aeroelasticity p 595 A91-35785
Prediction of unsteady transonic separated flow for missile applications
[AD-A231259] p 557 N91-21120
A modal aeroelastic analysis scheme for turbomachinery blading
[NASA-CR-187089] p 579 N91-21138
STARS: An integrated general-purpose finite element structural, aeroelastic, and aeroservoelastic analysis computer program
[NASA-TM-101709-REV] p 599 N91-21587
An overview of the active flexible wing program p 583 N91-22332
Aeroelastic modeling of the active flexible wing wind-tunnel model p 575 N91-22333

AERONAUTICS
A practical approach to Rule 26(c) protective orders in aviation litigation p 608 A91-35121

AEROSOLS
Inertial aerosol precipitation on ogival bodies of revolution in high-velocity flow p 553 A91-35784
Comparison of UNL laser imaging and sizing system and a phase Doppler system for analyzing sprays from a NASA nozzle
[NASA-CR-185239] p 598 N91-21485

AEROSPACE ENGINEERING
NASA Ames aerospace systems directorate research
[NASA-TM-103844] p 608 N91-22066
RICIS Software Engineering 90 Symposium: Aerospace Applications and Research Directions Proceedings Appendices
[NASA-CR-187994] p 605 N91-22728

AEROSPACE SCIENCES
Interdisciplinary cooperative aerospace research - Examples of scientific cooperation with Braunschweig Technical University p 543 A91-33372

AEROSPACE SYSTEMS
NASA Ames aerospace systems directorate research
[NASA-TM-103844] p 608 N91-22066
Fourth NASA Workshop on Computational Control of Flexible Aerospace Systems, part 2
[NASA-CP-10065-PT-2] p 587 N91-22331

AEROTHERMOCHEMISTRY
Fully coupled implicit method for thermochemical nonequilibrium air at suborbital flight speeds p 544 A91-33380

AEROTHERMODYNAMICS
Aerothermodynamic design appraisal of noise suppressors for F/A-18 engine run-up facilities at RAAF Williamtown
[ARL-PROP-R-177] p 585 N91-22136

AH-1G HELICOPTER
Optimization of helicopter airframe structures for vibration reduction - Considerations, formulations, and applications p 571 A91-33533

AIR BREATHING ENGINES
CFD for hypersonic propulsion
[NASA-TM-103791] p 597 N91-21447
Computer program for estimating performance of air-breathing aircraft engines
[NASA-TM-4254] p 573 N91-22103

AIR CARGO
Evaluation of an alternative rotorcraft cargo lowering device for the delivery of 500-lb ammunition loads
[AD-A230995] p 573 N91-21133

AIR COOLING
Aerothermodynamic design appraisal of noise suppressors for F/A-18 engine run-up facilities at RAAF Williamtown
[ARL-PROP-R-177] p 585 N91-22136

AIR FLOW
Air motion measurements: Past and future p 603 N91-22653
Air motion measurement uncertainties: Their impact on atmospheric studies p 603 N91-22654

AIR INTAKES
Process control to set Mach number ratios for jet-engine intake measurements - Development of an automatic Mach-number regulator p 584 A91-33373

AIR NAVIGATION
An airworthy experimental system for modern navigation and remote-sensing methods - Reduction, storage, and transmission of aerial photography scenes p 575 A91-33370
Test program for Honeywell/DND Helicopter Integrated Navigation System (HINS) p 565 A91-33626
The missing (data) link in pilot navigation p 568 A91-33666

AIR TRAFFIC
Coping with dramatic air transport growth p 562 A91-36011

AIR TRAFFIC CONTROL
Evaluation of controller tools for conducting MLS curved approaches to New York's JFK Airport p 565 A91-33631
Prospects for reduction of separation standards in oceanic airspaces with satellite services p 565 A91-33632
Impact of navigation accuracy on the intervention rate in a highly automated air traffic control system p 566 A91-33647
The missing (data) link in pilot navigation p 568 A91-33666
Oceanic clearance trial proves utility of data link communications for ATC p 568 A91-33775
ASTRE improvements expand usefulness of surface movement radar p 569 A91-36012
Flight Service Automation System (FSAS) Model 1 Full Capacity (M1FC) Operational Test and Evaluation (OT/E)/integration test report
[DOT/FAA/CT-TN90/45] p 569 N91-22100
Air traffic control memory: A field survey
[DOT/FAA/CT-TN90/60] p 569 N91-22101
Traffic Alert and Collision Avoidance System (TCAS): Cockpit Display of Traffic Information (CDTI) investigation. Phase 1: Feasibility study
[NASA-TM-104956] p 569 N91-22102
Analysis of routine communication in the air traffic control system
[NASA-CR-188116] p 600 N91-22475

AIR TRAFFIC CONTROLLERS (PERSONNEL)
Air traffic control memory: A field survey
[DOT/FAA/CT-TN90/60] p 569 N91-22101
Analysis of routine communication in the air traffic control system
[NASA-CR-188116] p 600 N91-22475

AIR TRANSPORTATION
Coping with dramatic air transport growth p 562 A91-36011
FAA aviation forecasts: Fiscal years 1991-2002
[AD-A231721] p 543 N91-22068

AIRBORNE EQUIPMENT
Airborne gravimetry and the Global Positioning System p 602 A91-33634
Area navigation capability in a miniature airborne GPS receiver p 566 A91-33636
Air motion measurements: Past and future p 603 N91-22653
Air motion measurement uncertainties: Their impact on atmospheric studies p 603 N91-22654
The FIAMS research aircraft or small is beautiful p 603 N91-22655
Technical presentation of the Merlin's radome: Calibration and data processing p 603 N91-22656
The improvement of the installation of the DLR research aircraft Falcon: Description and first results p 603 N91-22657
The NASA-ER2 meteorological measurement system: Instrumentaion, calibration and intercomparison results p 603 N91-22658
Fast response gust measurement device p 603 N91-22659
Summary of aircraft measuring activities at LAPETH p 604 N91-22661
Turbulence profiling in the atmospheric boundary layer using three powered gliders p 604 N91-22663

AIRBORNE LASERS
Optimization of radio-measuring devices incorporated in onboard laser velocimeters p 576 A91-35738

AIRBORNE/SPACEBORNE COMPUTERS
Digital signal conditioning for flight test instrumentation
[NASA-TM-101739] p 577 N91-21135
Methodology development for the verification and validation of flight critical systems software, phase 1
[AD-A229932] p 605 N91-21735

AIRCRAFT ACCIDENT INVESTIGATION
The final call: Why airline disasters continue to happen --- Book p 561 A91-34250
Human performance factors in aircraft accident investigation
[SAE PAPER 892608] p 562 A91-34912

AIRCRAFT ACCIDENTS
Impact of navigation accuracy on the intervention rate in a highly automated air traffic control system p 566 A91-33647
Air safety regulation and its commercial impact p 561 A91-34161
The final call: Why airline disasters continue to happen --- Book p 561 A91-34250
General aviation accident liability standards - Why the fuss? p 608 A91-35123
The human factors relating to escape and survival from helicopters ditching in water
[AGARD-AG-305(F)] p 563 N91-22099

AIRCRAFT COMMUNICATION
Oceanic clearance trial proves utility of data link communications for ATC p 568 A91-33775

AIRCRAFT CONFIGURATIONS
Solution adaptive local rectangular grid refinement for transonic aerodynamic flow problems p 547 A91-34179
3D Euler flows around modern airplanes p 549 A91-34201
The N-Dimensional Fighter p 571 A91-35425
Span reduction effects on the flutter characteristics of arrow-wing supersonic transport configurations
[NASA-TP-3077] p 572 N91-21127
Advanced rotorcraft transmission program
[NASA-TM-103276] p 598 N91-21531
Grid generation about complex three-dimensional aircraft configurations
[NASA-CR-188097] p 558 N91-22071
Dynamic stall effects and applications to high performance aircraft p 573 N91-22106
Oscillatory data for typical configurations p 561 N91-22109

AIRCRAFT CONSTRUCTION MATERIALS
Damage tolerance aspects of ARALL fuselage skin structure (philosophy and experiments) p 588 A91-32573
Advanced composite technology of West German general aviation aircraft p 543 A91-32648
Aerospace materials p 588 A91-33324

AIRCRAFT CONTROL
Conical Euler simulation of wing rock for a delta wing planform p 580 A91-33536
Impact of icing on Unmanned Aerial Vehicle (UAV) operations
[AD-A231191] p 562 N91-21124
A leading-edge control surface
[BU-508] p 559 N91-22087
Special Course on Aircraft Dynamics at High Angles of Attack: Experiments and Modelling
[AGARD-R-776] p 573 N91-22104
Forebody vortex control p 573 N91-22110
Automated flight test management system
[NASA-CR-186011] p 574 N91-22117
Signal blending in control systems structural interactions
[BU-505] p 583 N91-22132
Flutter suppression of an aircraft wing using a control surface
[BU-506] p 583 N91-22133
Fourth NASA Workshop on Computational Control of Flexible Aerospace Systems, part 2
[NASA-CP-10065-PT-2] p 587 N91-22331

AIRCRAFT DESIGN
Integrated multidisciplinary design optimization of rotorcraft p 570 A91-33528
Aerodynamic and structural studies of joined-wing aircraft p 571 A91-33534
Solution adaptive local rectangular grid refinement for transonic aerodynamic flow problems p 547 A91-34179
Biodynamic and optimization aspects of emergency ejection from an aircraft p 561 A91-34341
The N-Dimensional Fighter p 571 A91-35425
CFD research and systems in Kawasaki Heavy Industries and its future prospects p 596 N91-21382
The CFD analysis related aerospace in Fuji Heavy Industries, Ltd. p 597 N91-21383
Status and outlook of CFD technology at Mitsubishi Heavy Industries, Nagoya p 597 N91-21384
NASA Ames aerospace systems directorate research
[NASA-TM-103844] p 608 N91-22066
Variable camber wings for transport aircraft p 574 N91-22112

An iterative procedure for the design of pressure-specified 3-dimensional configurations at subsonic and supersonic speeds by means of a higher-order panel method
[MBB-FE122/S/PUB/375] p 574 N91-22118
The preliminary aerodynamic design of light aircraft
[BU-504] p 574 N91-22119

AIRCRAFT DETECTION
VLS - A DTOA system for position location
p 568 A91-33667
Knowledge-based target recognition system evolution
p 577 A91-35978

AIRCRAFT ENGINES
Process control to set Mach number ratios for jet-engine intake measurements - Development of an automatic Mach-number regulator p 584 A91-33373
Analysis of bearing incidents in aircraft gas turbine mainshaft bearings p 591 A91-33464
Theoretical basis for extrapolation of calibration data of PTC 6 throat tap nozzles
[ASME PAPER 90-JPGC/PTC-1] p 578 A91-34808
A method for the extrapolation of calibration data of PTC 6 throat tap nozzles
[ASME PAPER 90-JPGC/PTC-2] p 578 A91-34809
Fault detection and diagnosis in gas turbines
[ASME PAPER 90-GT-339] p 578 A91-34814
Design of robust controllers for gas turbine engines
[ASME PAPER 90-GT-113] p 578 A91-34815
Control of the working cycle of gas turbine engines (2nd revised and enlarged edition) --- Russian book
p 579 A91-35822
A pressure flux-split technique for computation of inlet flow behavior p 595 N91-21068
Study of bird ingestions into small inlet area aircraft turbine engines
[DOT/FAA/CT-90/13] p 562 N91-21122
Present and future of CFD on the aero-engine development in IHI p 596 N91-21381
Application of computational fluid dynamics in high speed aeropropulsion
[NASA-TM-103780] p 598 N91-21458
Aerothermodynamic design appraisal of noise suppressors for F/A-18 engine run-up facilities at RAAF Williamtown
[ARL-PROP-R-177] p 585 N91-22136

AIRCRAFT GUIDANCE
Evaluation of controller tools for conducting MLS curved approaches to New York's JFK Airport
p 565 A91-33631
Fully automatic guidance and control for rotorcraft nap-of-the-Earth flight following planned profiles. Volume 1: Real-time piloted simulation
[NASA-CR-177571-VOL-1] p 582 N91-21149
Fully automatic guidance and control for rotorcraft nap-of-the-Earth flight following planned profiles. Volume 2: Mathematical model
[NASA-CR-177571-VOL-2] p 582 N91-21150

AIRCRAFT HAZARDS
The human factors relating to escape and survival from helicopters ditching in water
[AGARD-AG-305(F)] p 563 N91-22099

AIRCRAFT INDUSTRY
Advanced composite technology of West German general aviation aircraft p 543 A91-32648

AIRCRAFT INSTRUMENTS
Airborne heterodyne receiver for the range 600 GHz to 3,000 GHz p 599 N91-22047
Technical presentation of the Merlin's radome: Calibration and data processing p 603 N91-22656
The improvement of the installation of the DLR research aircraft Falcon: Description and first results
p 603 N91-22657
The NASA-ER2 meteorological measurement system: Instrumentaion, calibration and intercomparison results
p 603 N91-22658
Fast response gust measurement device
p 603 N91-22659
Summary of aircraft measuring activities at LAPETH
p 604 N91-22661

AIRCRAFT LANDING
The effect of the microwave landing system on airport capacity p 561 A91-33668
Integrated flight/propulsion control system design based on a decentralized, hierarchical approach
[NASA-TM-103678] p 579 N91-21137

AIRCRAFT MAINTENANCE
Crew chief CAD system interface guide (version 2 - SI)
[AD-A231433] p 606 N91-22734

AIRCRAFT MANEUVERS
Roll plus maneuver load alleviation control system designs for the active flexible wing wind-tunnel model
p 584 N91-22335

AIRCRAFT MODELS
Unsteady aerodynamic modelling for aircraft lateral parameter estimation p 581 A91-34162
Identification of the aerodynamic model of the DLR research aircraft ATTAS from flight test data
[DLR-FB-90-40] p 572 N91-21130
Acoustic and aerodynamic study of a pusher-propeller aircraft model
[NASA-TP-3040] p 607 N91-21828
Water tunnel flow visualisation of vortex breakdown over the F/A-18
[ARL-FLIGHT-MECH-R-179] p 600 N91-22511

AIRCRAFT NOISE
The location of acoustic blade-vortex interaction - A further step toward an understanding of helicopter noise
p 607 A91-33368
A study of rotor broadband noise mechanisms and helicopter tail rotor noise
[NASA-CR-177565] p 607 N91-21829

AIRCRAFT PERFORMANCE
X-31 flight tests to explore combat agility to 70 deg. AOA p 571 A91-34375

AIRCRAFT PILOTS
Suppression of biodynamic interference in head-tracked teleoperation
[NASA-TM-103833] p 577 N91-21134
Analysis of routine communication in the air traffic control system
[NASA-CR-188116] p 600 N91-22475

AIRCRAFT POWER SUPPLIES
Civil air transport: A fresh look at power-by-wire and fly-by-light p 584 N91-23053

AIRCRAFT RELIABILITY
An airworthy experimental system for modern navigation and remote-sensing methods - Reduction, storage, and transmission of aerial photography scenes
p 575 A91-33370

AIRCRAFT SAFETY
Evaluation of controller tools for conducting MLS curved approaches to New York's JFK Airport
p 565 A91-33631
Air safety regulation and its commercial impact
p 561 A91-34161
The final call: Why airline disasters continue to happen --- Book p 561 A91-34250
Non-airborne conflicts: The causes and effects of runway transgressions
[NASA-CR-177372] p 562 N91-21121
A simple, analytical, axisymmetric microburst model for downdraft estimation
[NASA-TM-104053] p 573 N91-21132
Model rocketry hazard study
[DOT/FAA/CT-TN90/28] p 587 N91-21238
The human factors relating to escape and survival from helicopters ditching in water
[AGARD-AG-305(F)] p 563 N91-22099

AIRCRAFT STABILITY
Flow investigation of a ground effect vehicle
[BU-516] p 600 N91-22528

AIRCRAFT STRUCTURES
Application of sensitivity methods for error localization in finite element systems p 594 A91-35529
Proceedings of a French-Japanese Seminar on Composite Materials: Processing, Use and Databases
p 589 N91-22380
Damage accumulation and degradation of composite laminates under aircraft service loading: Assessment and prediction, volumes 1 and 2 p 589 N91-22381

AIRCRAFT TIRES
Computational methods for frictionless contact with application to Space Shuttle Orbiter nose-gear tires
[NASA-TP-3073] p 601 N91-22576

AIRCRAFT WAKES
A method to calculate the influence of vortex roll-up on the induced drag of wings p 546 A91-34055
Velocity measurements in a turbulent trailing vortex and their application to BWI noise prediction
[NASA-CR-188083] p 554 N91-21100
Acoustic and aerodynamic study of a pusher-propeller aircraft model
[NASA-TP-3040] p 607 N91-21828

AIRFIELD SURFACE MOVEMENTS
The effect of the microwave landing system on airport capacity p 561 A91-33668
ASTRE improvements expand usefulness of surface movement radar p 569 A91-36012
Non-airborne conflicts: The causes and effects of runway transgressions
[NASA-CR-177372] p 562 N91-21121

AIRFOIL OSCILLATIONS
Numerical calculation of the unsteady separating flow on oscillating airfoils (dynamic stall) p 546 A91-34057

AIRFOIL PROFILES
Computation of unsteady incompressible viscous flow around airfoils p 546 A91-34074
Cell-vertex, multigrid Euler scheme for use with multiblock grids p 547 A91-34128
Compressible flows with periodic vortical disturbances around lifting airfoils
[NASA-TM-103742] p 554 N91-21060
Variable camber wings for transport aircraft
p 574 N91-22112

AIRFOILS
Airfoils in two- and three-dimensional gust fields
p 546 A91-34073
Numerical simulation of turbulent flows around airfoil and wing p 549 A91-34203
Elevator deflections on the icing process
p 572 A91-35427
Compressible flows with periodic vortical disturbances around lifting airfoils
[NASA-TM-103742] p 554 N91-21060
A finite-difference, frequency-domain numerical scheme for the solution of the linearized unsteady Euler equations p 595 N91-21067
Numerical study of the aerodynamic effects of using sulfur hexafluoride as a test gas in wind tunnels
[NASA-TP-3086] p 558 N91-22070
Separating boundary layer response to an unsteady turbulent environment
[AD-A231483] p 559 N91-22081
Analysis of laminar separation bubbles using a simple eddy-viscosity turbulence model
[NAL-TR-1079] p 600 N91-22520

AIRFRAMES
Optimization of helicopter airframe structures for vibration reduction - Considerations, formulations, and applications p 571 A91-33533
A flexible robotic work cell for the assembly of airframe components p 543 A91-35193
CFD for hypersonic propulsion
[NASA-TM-103791] p 597 N91-21447

AIRLINE OPERATIONS
A guide to ground vehicle operations on the airport
[AD-A231077] p 585 N91-21158
Airline quality rating
[NIAR-91-11] p 563 N91-22098

AIRPORT PLANNING
FAA aviation forecasts: Fiscal years 1991-2002
[AD-A231721] p 543 N91-22068

AIRPORTS
Evaluation of controller tools for conducting MLS curved approaches to New York's JFK Airport
p 565 A91-33631
Applying kinematic GPS techniques at our nation's airports p 565 A91-33633
The effect of the microwave landing system on airport capacity p 561 A91-33668
Airport restrictions - A dilemma of federal preemption and proprietary control p 608 A91-35122
A guide to ground vehicle operations on the airport
[AD-A231077] p 585 N91-21158
Automated extraction of airport runway patterns from radar imagery
[AD-A231809] p 600 N91-22480

ALGORITHMS
Heli/SITAN - A terrain referenced navigation algorithm for helicopters p 568 A91-33664
Critical speeds and forced response solutions for active magnetic bearing turbomachinery, part 2
p 587 N91-21210
Grid generation about complex three-dimensional aircraft configurations
[NASA-CR-188097] p 558 N91-22071
Automated extraction of airport runway patterns from radar imagery
[AD-A231809] p 600 N91-22480

ALTITUDE CONTROL
Terrain-aided altitude computations on the AFTI/F-16
p 576 A91-33650

ALUMINIDES
Direct cast titanium aluminide strip
[AD-A231906] p 590 N91-22424

ALUMINUM ALLOYS
Superplasticity in a Ti3Al-base alloy stabilized by Nb, V and Mo p 589 A91-34841
Feasibility study for the qualification of an economically advantageous Ti-6Al-4V bearing housing for gas turbine engine application by powder metal manufacturing technology
[AD-A231666] p 601 N91-22564
Micromechanisms of quasi-static and fatigue crack growth in titanium-aluminides p 602 N91-22583

AMPLITUDES
Large amplitude oscillations p 561 N91-22108

ANGLE OF ATTACK
Numerical calculation of the unsteady separating flow on oscillating airfoils (dynamic stall) p 546 A91-34057
Vorticity equation solutions for slender wings at high incidence p 547 A91-34126
Effect of geometrical disturbance on vortex asymmetry
p 547 A91-34136

Unsteady flowfield behind a vortex generator rapidly pitched to angle of attack p 547 A91-34139
A streamwise upwind algorithm applied to vortical flow over a delta wing p 548 A91-34192
An approximate method for determining friction and heat transfer in chemically nonequilibrium flow past bodies at angle of attack p 553 A91-35660
Computer program for the calculation of normal force and pitching moment of forebody-cylinder combinations at angles of attack up to 90 degrees and Mach numbers up to 5, including effects of conical boat-tailing
[ESDU-90034] p 555 N91-21102
Coning motion of slender bodies at high angles of attack
[NAL-TR-1059] p 556 N91-21111
Investigation of nose bluntness and angle of attack *effects on slender bodies in viscous hypertension flows*
[NASA-CR-188153] p 557 N91-21117
Separating boundary layer response to an unsteady turbulent environment
[AD-A231483] p 559 N91-22081
The transient development of vortices over a delta wing
[AD-A231946] p 559 N91-22082
Special Course on Aircraft Dynamics at High Angles of Attack: Experiments and Modelling
[AGARD-R-776] p 573 N91-22104

ANNULAR FLOW
Experimental and numerical investigation of three-dimensional viscous flows and vortex motion inside an annular compressor blade row
[ASME PAPER 90-GT-155] p 551 A91-34787
Compressor drum aerodynamic experiments and analysis with coolant injected at selected locations
[ASME PAPER 90-GT-151] p 552 A91-34794

ANNULI
Rotordynamic coefficients for partially roughened pump annular seals p 593 A91-34822

APPLICATIONS PROGRAMS (COMPUTERS)
Computer program for the calculation of normal force and pitching moment of forebody-cylinder combinations at angles of attack up to 90 degrees and Mach numbers up to 5, including effects of conical boat-tailing
[ESDU-90034] p 555 N91-21102
Methodology development for the verification and validation of flight critical systems software, phase 1
[AD-A229932] p 605 N91-21735
RICIS Software Engineering 90 Symposium: Aerospace Applications and Research Directions Proceedings Appendices
[NASA-CR-187994] p 605 N91-22728
Software: Where we are and what is required in the future p 606 N91-22729

APPROXIMATION
Critical speeds and forced response solutions for active magnetic bearing turbomachinery, part 1
p 587 N91-21209
Approximate methods for predicting the lifting characteristics of wing-body combinations
p 558 N91-22074
Sensitivity-based scaling for correlating structural response from different analytical models
[NASA-TM-104042] p 602 N91-22578

ARCHITECTURE (COMPUTERS)
Proceedings of the 8th NAL Symposium on Aircraft Computational Aerodynamics: Prospects of Computational Fluid Dynamics and Super Computers in Aerospace Science and Technology
[NAL-SP-13] p 596 N91-21379
The CFD analysis related aerospace in Fuji Heavy Industries, Ltd. p 597 N91-21383

AREA NAVIGATION
Area navigation capability in a miniature airborne GPS receiver p 566 A91-33636

ARROW WINGS
Span reduction effects on the flutter characteristics of arrow-wing supersonic transport configurations
[NASA-TP-3077] p 572 N91-21127

ARTIFICIAL INTELLIGENCE
Automated flight test management system
[NASA-CR-186011] p 574 N91-22117
Design of an intelligent information system for in-flight emergency assistance p 606 N91-22792
Metamorphoses of ONAV console operations: From prototype to real time application p 606 N91-22794

ASPECT RATIO
Vortex bursting over a unit area aspect ratio delta wing using vortex paneling methods
[AD-A231028] p 557 N91-21119

ASSEMBLING
A flexible robotic work cell for the assembly of airframe components p 543 A91-35193

ASYMPTOTIC METHODS
Inertial aerosol precipitation on ogival bodies of revolution in high-velocity flow p 553 A91-35784
A review of near-wall Reynolds-stress
[NASA-CR-4369] p 559 N91-22080

ATMOSPHERIC BOUNDARY LAYER
The FIAMS research aircraft or small is beautiful
p 603 N91-22655
Turbulence profiling in the atmospheric boundary layer using three powered gliders p 604 N91-22663

ATMOSPHERIC CIRCULATION
Air motion measurements: Past and future
p 603 N91-22653
Air motion measurement uncertainties: Their impact on atmospheric studies p 603 N91-22654

ATMOSPHERIC ENTRY
Flowfield and vehicle parameter influence on results of engineering aerothermal methods p 544 A91-33378

ATMOSPHERIC TURBULENCE
Fast response gust measurement device
p 603 N91-22659
Summary of aircraft measuring activities at LAPETH
p 604 N91-22661
Turbulence profiling in the atmospheric boundary layer using three powered gliders p 604 N91-22663

ATTACK AIRCRAFT
Oscillatory data for typical configurations
p 561 N91-22109

ATTITUDE GYROS
Demonstration of a ring laser gyro system for pointing and stabilization applications p 575 A91-33627

ATTITUDE STABILITY
Demonstration of a ring laser gyro system for pointing and stabilization applications p 575 A91-33627

AUTOMATIC CONTROL
Process control to set Mach number ratios for jet-engine intake measurements - Development of an automatic Mach-number regulator p 584 A91-33373
Impact of navigation accuracy on the intervention rate in a highly automated air traffic control system
p 566 A91-33647
Automated flight test management system
[NASA-CR-186011] p 574 N91-22117
Software: Where we are and what is required in the future p 606 N91-22729

AUTOMATIC FLIGHT CONTROL
Fully automatic guidance and control for rotorcraft nap-of-the-Earth flight following planned profiles. Volume 1: Real-time piloted simulation
[NASA-CR-177571-VOL-1] p 582 N91-21149
Fully automatic guidance and control for rotorcraft nap-of-the-Earth flight following planned profiles. Volume 2: Mathematical model
[NASA-CR-177571-VOL-2] p 582 N91-21150
Flight Service Automation System (FSAS) Model 1 Full Capacity (M1FC) Operational Test and Evaluation (OT/E)/integration test report
[DOT/FAA/CT-TN90/45] p 569 N91-22100
Robust integrated autopilot/autothrottle design using constrained parameter optimization
[NASA-CR-188011] p 583 N91-22127

AUTOMATIC LANDING CONTROL
Integrated inertial navigation system/Global Positioning System (INS/GPS) for manned return vehicle autoland application p 586 A91-33609

AUTOMATIC PILOTS
Fully automatic guidance and control for rotorcraft nap-of-the-Earth flight following planned profiles. Volume 1: Real-time piloted simulation
[NASA-CR-177571-VOL-1] p 582 N91-21149
Robust integrated autopilot/autothrottle design using constrained parameter optimization
[NASA-CR-188011] p 583 N91-22127

AUTONOMOUS NAVIGATION
Global Positioning System (GPS) autonomous navigation p 567 A91-33653
Fully automatic guidance and control for rotorcraft nap-of-the-Earth flight following planned profiles. Volume 1: Real-time piloted simulation
[NASA-CR-177571-VOL-1] p 582 N91-21149
Fully automatic guidance and control for rotorcraft nap-of-the-Earth flight following planned profiles. Volume 2: Mathematical model
[NASA-CR-177571-VOL-2] p 582 N91-21150

AVIATION METEOROLOGY
Flight Service Automation System (FSAS) Model 1 Full Capacity (M1FC) Operational Test and Evaluation (OT/E)/integration test report
[DOT/FAA/CT-TN90/45] p 569 N91-22100

AVIONICS
Avionics Environmental Reliability using finite element analysis
[ASME PAPER 90-WA/TS-1] p 591 A91-32961
START - A broad application spectrum gyro for the 1990's p 591 A91-33604
Common integrated processing in modular avionics
p 575 A91-33615
Transmit/receive module technology for X-band active *array radar* p 568 A91-34011
Embedded computers: Navy's approach to developing patrol aircraft avionics system too risky
[AD-A230868] p 577 N91-21136

AXIAL FLOW
A modal aeroelastic analysis scheme for turbomachinery blading
[NASA-CR-187089] p 579 N91-21138

AXISYMMETRIC FLOW
Numerical simulation of laminar hypersonic flow past blunt bodies including high temperature effects
p 547 A91-34180
The use of axisymmetric flow for investigation of shock wave-boundary layer interactions
[BU-520] p 600 N91-22529

B

BALANCE
Magnetic suspension and balance system advanced study, 1989 design p 586 N91-21197

BALANCING
Weightless test balancing of elastic rotors with the help of interchangeable longitudinal bearing stiffnesses
p 592 A91-34015

BALL BEARINGS
Force and moment transmissibilities through rolling element bearings in a single-stage rotor system
p 594 A91-35537

BEARINGLESS ROTORS
Helicopter rotor dynamics optimization with experimental verification p 570 A91-33530

BEARINGS
Analysis of bearing incidents in aircraft gas turbine mainshaft bearings p 591 A91-33464
Weightless test balancing of elastic rotors with the help of interchangeable longitudinal bearing stiffnesses
p 592 A91-34015

BEECHCRAFT AIRCRAFT
Starship - Bright newcomer in a conservative firmament p 571 A91-34122

BEND TESTS
The flexural strength of unidirectional carbon fibre composites
[BU-509] p 589 N91-22399

BENDING VIBRATION
The effect of shear and rotary inertia of a rotor at its critical speeds p 592 A91-34125

BIODYNAMICS
Biodynamic and optimization aspects of emergency ejection from an aircraft p 561 A91-34341
Suppression of biodynamic interference in head-tracked teleoperation
[NASA-TM-103833] p 577 N91-21134

BIRD-AIRCRAFT COLLISIONS
Study of bird ingestions into small inlet area aircraft turbine engines
[DOT/FAA/CT-90/13] p 562 N91-21122

BISMALEIMIDE
Aerospace materials p 588 A91-33324

BLADE SLAP NOISE
Velocity measurements in a turbulent trailing vortex and their application to BWI noise prediction
[NASA-CR-188083] p 554 N91-21100
Blade-wake interaction on a two blade rotor with prediction of the radiated noise stationary and forward flight, comparison between calculation, and experiment
[ISL-R-120/89] p 608 N91-21832

BLADE TIPS
Tip leakage flow in axial compressors
[ASME PAPER 90-GT-127] p 552 A91-34792
Similarity analysis of compressor tip clearance flow structure
[ASME PAPER 90-GT-153] p 552 A91-34793

BLADE-VORTEX INTERACTION
Three-dimensional flow near the blade/endwall junction of a gas turbine - Visualization in a large-scale cascade *simulator*
[ASME PAPER 90-WA/HT-4] p 544 A91-32958
The location of acoustic blade-vortex interaction - A further step toward an understanding of helicopter noise
p 607 A91-33368
Tip leakage flow in axial compressors
[ASME PAPER 90-GT-127] p 552 A91-34792
Similarity analysis of compressor tip clearance flow structure
[ASME PAPER 90-GT-153] p 552 A91-34793
Velocity measurements in a turbulent trailing vortex and their application to BWI noise prediction
[NASA-CR-188083] p 554 N91-21100
Calculation of thickness and charge noise radiated by a rotor in forward flight
[ISL-R-119/89] p 607 N91-21831

Blade-wake interaction on a two blade rotor with prediction of the radiated noise stationary and forward flight, comparison between calculation, and experiment
[ISL-R-120/89] p 608 N91-21832
BLUFF BODIES
Some aspects of the numerical simulation of compressible viscous flow around bluff bodies at low Ma-number p 550 A91-34220
BLUNT BODIES
Hypersonic flow simulation for blunt bodies at incidence p 546 A91-34070
Numerical simulation of laminar hypersonic flow past blunt bodies including high temperature effects p 547 A91-34180
A numerical study of hypersonic stagnation heat transfer predictions at a coordinate singularity p 548 A91-34193
Investigation of nose bluntness and angle of attack effects on slender bodies in viscous hypertension flows
[NASA-CR-188153] p 557 N91-21117
BLUNT TRAILING EDGES
Blunt trailing edge analysis of supercritical airfoils by a Navier-Stokes code
[NAL-TR-1075-T] p 556 N91-21114
BODY-WING AND TAIL CONFIGURATIONS
MATGRID, a program for generation of C-H and C-O topology grids around wing/body configurations: User's guide
[FFA-TN-1991-03] p 556 N91-21110
BODY-WING CONFIGURATIONS
Approximate methods for predicting the lifting characteristics of wing-body combinations p 558 N91-22074
BOEING 737 AIRCRAFT
Robust integrated autopilot/autothrottle design using constrained parameter optimization
[NASA-CR-188011] p 583 N91-22127
BOUNDARY CONDITIONS
Method for calculating boundary region corrections in multistep axial turbomachines p 592 A91-34014
Development and validation of characteristic boundary conditions for cell-centered Euler flow calculations p 592 A91-34178
Rotordynamic coefficients for partially roughened pump annular seals p 593 A91-34822
Description and evaluation of an interference assessment for a slotted-wall wind tunnel
[NASA-CR-4352] p 585 N91-21155
Some treatments on boundary conditions for quasi one-dimensional Euler equations
[FFA-TN-1990-36] p 598 N91-21469
BOUNDARY LAYER CONTROL
An experimental study of a three-dimensional swept-back wing with suction laminar-flow-control
[NAL-TR-1072] p 556 N91-21113
BOUNDARY LAYER EQUATIONS
Closed-coupled zonal solution for viscous flow problems p 546 A91-34063
BOUNDARY LAYER FLOW
Numerical calculation of the unsteady separating flow on oscillating airfoils (dynamic stall) p 546 A91-34057
A method for the extrapolation of calibration data of PTC 6 throat tap nozzles
[ASME PAPER 90-JPGC/PTC-2] p 578 A91-34809
An experimental study of a three-dimensional swept-back wing with suction laminar-flow-control
[NAL-TR-1072] p 556 N91-21113
An investigation into the extent and effects of spanwise flow in the boundary layer of a helicopter rotor in hover
[BU-519] p 560 N91-22089
The use of axisymmetric flow for investigation of shock wave-boundary layer interactions
[BU-520] p 600 N91-22529
BOUNDARY LAYER SEPARATION
Simulation of glancing shock wave and boundary layer interaction p 548 A91-34195
Prediction of unsteady transonic separated flow for missile applications
[AD-A231259] p 557 N91-21120
Separating boundary layer response to an unsteady turbulent environment
[AD-A231483] p 559 N91-22081
Unsteady aerodynamics of slender wings p 560 N91-22105
Forebody vortex control p 573 N91-22110
BOUNDARY LAYER TRANSITION
Effect of a single three-dimensional surface roughness on the transition in a supersonic boundary layer p 545 A91-33920
Theoretical basis for extrapolation of calibration data of PTC 6 throat tap nozzles
[ASME PAPER 90-JPGC/PTC-1] p 578 A91-34808
BOUNDARY LAYERS
A simple, analytical, axisymmetric microburst model for downdraft estimation
[NASA-TM-104053] p 573 N91-21132
BOUNDARY VALUE PROBLEMS
Compressible flows with periodic vortical disturbances around lifting airfoils
[NASA-TM-103742] p 554 N91-21060
Some treatments on boundary conditions for quasi one-dimensional Euler equations
[FFA-TN-1990-36] p 598 N91-21469
BOW WAVES
Hypersonic leeside flow computations using centered schemes for Euler equations p 548 A91-34187
Inviscid flow about a double ellipse p 549 A91-34210
BROADBAND
A study of rotor broadband noise mechanisms and helicopter tail rotor noise
[NASA-CR-177565] p 607 N91-21829
BUBBLES
Analysis of laminar separation bubble using a simple eddy-viscosity turbulence model p 591 A91-33227
Analysis of laminar separation bubbles using a simple eddy-viscosity turbulence model
[NAL-TR-1079] p 600 N91-22520
BUCKLING
Stability analysis of a fuselage side
[FFA-TN-1990-32] p 599 N91-21568
BURNERS
Investigations into shock-induced enhancement of mixing and combustion in supersonic burners
[AD-A231750] p 589 N91-22407

C

CALIBRATING
Preliminary calibration of a generic scramjet combustor
[NASA-CR-187539] p 579 N91-21139
Description and evaluation of an interference assessment for a slotted-wall wind tunnel
[NASA-CR-4352] p 585 N91-21155
Technical presentation of the Merlin's radome: Calibration and data processing p 603 N91-22656
The NASA-ER2 meteorological measurement system: Instrumentaion, calibration and intercomparison results p 603 N91-22658
CAMBER
Variable camber wings for transport aircraft p 574 N91-22112
CANARD CONFIGURATIONS
Starship - Bright newcomer in a conservative firmament p 571 A91-34122
CAPACITY
The effect of the microwave landing system on airport capacity p 561 A91-33668
CARBON FIBER REINFORCED PLASTICS
Thermal spikes on CFRP laminates - Assessment of microdamage and its consequences on fatigue life p 588 A91-32549
Cumulative damage problem in pull-through fatigue of C.F.R.P. laminate p 588 A91-32576
The flexural strength of unidirectional carbon fibre composites
[BU-509] p 589 N91-22399
CARBON FIBERS
Fin structures of the Airbus family experience with advanced composites p 570 A91-32455
CARBON-CARBON COMPOSITES
Fin structures of the Airbus family experience with advanced composites p 570 A91-32455
CARGO AIRCRAFT
Evaluation of an alternative rotorcraft cargo lowering device for the delivery of 500-lb ammunition loads
[AD-A230995] p 573 N91-21133
CASCADE FLOW
Three-dimensional flow near the blade/endwall junction of a gas turbine - Visualization in a large-scale cascade simulator
[ASME PAPER 90-WA/HT-4] p 544 A91-32958
Three-dimensional wake decay inside of a compressor cascade and its influence on the downstream unsteady flow field. I - Wake decay characteristics in the flow passage. II - Unsteady flow field downstream of the stator
[ASME PAPER 90-GT-21] p 551 A91-34786
Experimental and numerical investigation of three-dimensional viscous flows and vortex motion inside an annular compressor blade row
[ASME PAPER 90-GT-155] p 551 A91-34787
Transonic cascade flow calculations using non-periodic C-type grids p 596 N91-21071
Computation of supersonic and low subsonic cascade flows using an explicit Navier-Stokes technique and the kappa-epsilon turbulence model p 596 N91-21072
CASTING
Direct cast titanium aluminide strip
[AD-A231906] p 590 N91-22424
CAVITATION FLOW
Velocity of cavitation bubbles in uniform flowfield high and low Reynolds number p 592 A91-34127
Compressor drum aerodynamic experiments and analysis with coolant injected at selected locations
[ASME PAPER 90-GT-151] p 552 A91-34794
CERAMIC COATINGS
Experimental study of radiation from coated turbine blades p 580 N91-22122
CERAMIC MATRIX COMPOSITES
Cost-effective manufacturing of advanced ceramics p 588 A91-33725
CERAMICS
High temperature performance evaluation of a hypersonic engine ceramic wafer seal
[NASA-TM-103737] p 601 N91-22567
CHANNEL FLOW
Numerical investigation of three dimensional laminar flows in a channel with a built-in circular cylinder and wing-type vortex generators p 550 A91-34218
A review of near-wall Reynolds-stress
[NASA-CR-4369] p 559 N91-22080
CIRCULAR CYLINDERS
Numerical investigation of three dimensional laminar flows in a channel with a built-in circular cylinder and wing-type vortex generators p 550 A91-34218
CIRCULAR PLATES
Forces and pressures induced on circular plates by a single lifting jet in ground effect
[NASA-TM-102816] p 558 N91-22077
CIVIL AVIATION
Civil air transport: A fresh look at power-by-wire and fly-by-light p 584 N91-23053
CLEARANCES
Similarity analysis of compressor tip clearance flow structure
[ASME PAPER 90-GT-153] p 552 A91-34793
CLOSURES
A review of near-wall Reynolds-stress
[NASA-CR-4369] p 559 N91-22080
COCKPITS
Traffic Alert and Collision Avoidance System (TCAS): Cockpit Display of Traffic Information (CDTI) investigation. Phase 1: Feasibility study
[NASA-TM-104956] p 569 N91-22102
COEFFICIENT OF FRICTION
An approximate method for determining friction and heat transfer in chemically nonequilibrium flow past bodies at angle of attack p 553 A91-35660
Practical methods to evaluate the friction drag coefficient of a projectile in free flight
[ISL-R-123/89] p 555 N91-21105
COLLISION AVOIDANCE
Traffic Alert and Collision Avoidance System (TCAS): Cockpit Display of Traffic Information (CDTI) investigation. Phase 1: Feasibility study
[NASA-TM-104956] p 569 N91-22102
COLLISIONS
Non-airborne conflicts: The causes and effects of runway transgressions
[NASA-CR-177372] p 562 N91-21121
COMBUSTIBLE FLOW
Computation of flowfields for projectiles in hypersonic chemically reacting flows p 544 A91-33379
Computational Fluid Dynamics Symposium on Aeropropulsion
[NASA-CP-3078] p 554 N91-21062
COMBUSTION
Possibilities of trajectory modification
[ISL-CO-209/90] p 582 N91-21151
Investigations into shock-induced enhancement of mixing and combustion in supersonic burners
[AD-A231750] p 589 N91-22407
COMBUSTION CHAMBERS
Computational Fluid Dynamics Symposium on Aeropropulsion
[NASA-CP-3078] p 554 N91-21062
A highly efficient engineering tool for three-dimensional scramjet flowfield and heat transfer computations p 596 N91-21098
Preliminary calibration of a generic scramjet combustor
[NASA-CR-187539] p 579 N91-21139
An experimental investigation into NO(x) control of a gas turbine combustor and augmentor tube incorporating a catalytic reduction system
[AD-A231427] p 580 N91-22124
COMMERCE
Economic impact of aviation in Pennsylvania
[PB91-128264] p 543 N91-22067
Business plans for the Institute for Aviation Research, FY 1990 - FY 1995
[IAR-89-15] p 609 N91-23020
COMMERCIAL AIRCRAFT
Air safety regulation and its commercial impact p 561 A91-34161

The effects of simulated electromagnetic pulse on commercial aircraft p 569 A91-35902
COMMUNICATION THEORY
Analysis of routine communication in the air traffic control system
[NASA-CR-188116] p 600 N91-22475
COMMUNITIES
Design methodology for a community response questionnaire on sonic boom exposure
[NASA-CR-187503] p 608 N91-22830
COMPOSITE MATERIALS
ICCM-VII; Proceedings of the 7th International Conference on Composite Materials, Guangzhou, People's Republic of China, Nov. 22-24, 1989. Vols. 1-3
p 588 A91-32451
Temperature effect on the stress concentration in the composite material used by the X-29A forward-swept wing aircraft p 590 A91-32547
Advanced composite technology of West German general aviation aircraft p 543 A91-32648
Aerospace materials p 588 A91-33324
Addendum to the DYCAST user's manual describing the curved, warp beam finite element
[NASA-CR-4362] p 606 N91-22805
Cost-efficient manufacturing of composite structures
p 590 N91-23048
Lightweight, fire-retardant, crashworthy aircraft seat cushioning p 563 N91-23052
COMPOSITE STRUCTURES
Advanced composite technology of West German general aviation aircraft p 543 A91-32648
Optimal design of metal and composite thin-walled structures with flutter constraint p 591 A91-32650
Analysis and optimal design of composite structures
p 591 A91-32651
Aerospace materials p 588 A91-33324
Damage accumulation and degradation of composite laminates under aircraft service loading: Assessment and prediction, volumes 1 and 2 p 589 N91-22381
Cost-efficient manufacturing of composite structures
p 590 N91-23048
Lightweight, fire-retardant, crashworthy aircraft seat cushioning p 563 N91-23052
COMPRESSIBLE BOUNDARY LAYER
Calculation of a compressible laminar boundary layer on a tapered body of bielliptical cross section
p 553 A91-35796
COMPRESSIBLE FLOW
Domain decomposition methods in aerodynamics
p 604 A91-33056
Numerical simulation of compressible Euler flows --- Book p 544 A91-33675
Comparison of upwind and central finite-difference methods for the compressible Navier-Stokes equations
p 545 A91-34034
Airfoils in two- and three-dimensional gust fields
p 546 A91-34073
Numerical simulation of turbulent flows around airfoil and wing p 549 A91-34203
On the relation between TVD and mesh adaption and application to Navier-Stokes calculations
p 550 A91-34215
Some aspects of the numerical simulation of compressible viscous flow around bluff bodies at low Ma-number p 550 A91-34220
Finite element methods for integrated aerodynamic heating analysis
[NASA-CR-188079] p 554 N91-21101
COMPRESSION TESTS
The flexural strength of unidirectional carbon fibre composites
[BU-509] p 589 N91-22399
COMPRESSOR BLADES
Experimental and numerical investigation of three-dimensional viscous flows and vortex motion inside an annular compressor blade row
[ASME PAPER 90-GT-155] p 551 A91-34787
Three-dimensional flowfields inside a transonic compressor with swept blades
[ASME PAPER 90-GT-359] p 552 A91-34791
Tip leakage flow in axial compressors
[ASME PAPER 90-GT-127] p 552 A91-34792
Similarity analysis of compressor tip clearance flow structure
[ASME PAPER 90-GT-153] p 552 A91-34793
Forcing function effects on rotor periodic aerodynamic response
[ASME PAPER 90-GT-109] p 553 A91-34798
COMPRESSOR ROTORS
Unsteady radial transport in a transonic compressor stage
[ASME PAPER 90-GT-133] p 551 A91-34788
Three-dimensional flowfields inside a transonic compressor with swept blades
[ASME PAPER 90-GT-359] p 552 A91-34791
Similarity analysis of compressor tip clearance flow structure
[ASME PAPER 90-GT-153] p 552 A91-34793
Detection of a rotating stall precursor in isolated axial flow compressor rotors
[ASME PAPER 90-GT-157] p 552 A91-34795
Critical speeds and forced response solutions for active magnetic bearing turbomachinery, part 2
p 587 N91-21210
COMPRESSORS
Three-dimensional wake decay inside of a compressor cascade and its influence on the downstream unsteady flow field. I - Wake decay characteristics in the flow passage. II - Unsteady flow field downstream of the stator
[ASME PAPER 90-GT-21] p 551 A91-34786
Compressor drum aerodynamic experiments and analysis with coolant injected at selected locations
[ASME PAPER 90-GT-151] p 552 A91-34794
An experimental study of exit flow patterns in a multistage compressor in rotating stall
[AD-A231353] p 580 N91-21143
COMPUTATION
Computational methods for frictionless contact with application to Space Shuttle Orbiter nose-gear tires
[NASA-TP-3073] p 601 N91-22576
COMPUTATIONAL FLUID DYNAMICS
Computation of flowfields for projectiles in hypersonic chemically reacting flows p 544 A91-33379
Fully coupled implicit method for thermochemical nonequilibrium air at suborbital flight speeds
p 544 A91-33380
Vortical solutions of the conical Euler equations --- Book p 591 A91-33674
Numerical simulation of compressible Euler flows --- Book p 544 A91-33675
Method for calculating boundary region corrections in multistep axial turbomachines p 592 A91-34014
Laminar shock/boundary-layer interaction - A numerical test problem p 545 A91-34033
A vortex-lattice method for the calculation of vortex sheet roll-up and wing-vortex interaction p 546 A91-34052
Numerical calculation of the unsteady separating flow on oscillating airfoils (dynamic stall) p 546 A91-34057
Closed-coupled zonal solution for viscous flow problems p 546 A91-34063
An implicit predictor-corrector relaxation method for viscous transonic flows p 592 A91-34064
Hypersonic flow simulation for blunt bodies at incidence p 546 A91-34070
Computation of unsteady incompressible viscous flow around airfoils p 546 A91-34074
Velocity of cavitation bubbles in uniform flowfield high and low Reynolds number p 592 A91-34127
Cell-vertex, multigrid Euler scheme for use with multiblock grids p 547 A91-34128
Role of artificial viscosity in Euler and Navier-Stokes solvers p 547 A91-34135
Effect of geometrical disturbance on vortex asymmetry
p 547 A91-34136
GAMM-Conference on Numerical Methods in Fluid Mechanics, 8th, Delft University of Technology, Netherlands, Sept. 27-29, 1989, Proceedings
p 592 A91-34176
Development and validation of characteristic boundary conditions for cell-centered Euler flow calculations
p 592 A91-34178
Solution adaptive local rectangular grid refinement for transonic aerodynamic flow problems
p 547 A91-34179
Numerical simulation of laminar hypersonic flow past blunt bodies including high temperature effects
p 547 A91-34180
Solution of the 3-D, incompressible Navier-Stokes equations for the simulation of vortex breakdown
p 593 A91-34181
Solution method for viscous flows at all speeds in complex domains p 548 A91-34185
Viscous, hypersonic flows over compression ramps
p 548 A91-34194
Simulation of glancing shock wave and boundary layer interaction p 548 A91-34195
Aspects of the application of an Euler-equation method to the simulation of leading-edge vortex flow
p 549 A91-34196
A numerical study of interfacial instabilities at high Mach numbers p 549 A91-34198
3D Euler flows around modern airplanes
p 549 A91-34201
Numerical simulation of turbulent flows around airfoil and wing p 549 A91-34203
Split-matrix marching methods for three-dimensional viscous and inviscid hypersonic flows
p 549 A91-34206
On the relation between TVD and mesh adaption and application to Navier-Stokes calculations
p 550 A91-34215
Numerical investigation of three dimensional laminar flows in a channel with a built-in circular cylinder and wing-type vortex generators p 550 A91-34218
Interaction between two jets exhausted from nozzles arranged in parallel p 593 A91-34439
Mixing in axial-flow compressors - Conclusions drawn from three-dimensional Navier-Stokes analyses and experiments
[ASME PAPER 90-GT-352] p 551 A91-34783
Experimental and numerical investigation of three-dimensional viscous flows and vortex motion inside an annular compressor blade row
[ASME PAPER 90-GT-155] p 551 A91-34787
Temporally and spatially resolved flow in a two-stage axial compressor. I - Experiment
[ASME PAPER 90-GT-259] p 551 A91-34789
Three-dimensional flowfields inside a transonic compressor with swept blades
[ASME PAPER 90-GT-359] p 552 A91-34791
Vortex element methods for fluid dynamic analysis of engineering systems --- Book p 594 A91-35539
An approach to the numerical solution of two-dimensional Navier-Stokes equations by a finite difference method p 595 A91-35787
Computations for a jet impinging obliquely on a flat surface p 554 A91-35985
Simulation of two- and three-dimensional internal subsonic flows using a finite element method
p 595 A91-35986
Compressible flows with periodic vortical disturbances around lifting airfoils
[NASA-TM-103742] p 554 N91-21060
Computational Fluid Dynamics Symposium on Aeropropulsion
[NASA-CP-3078] p 554 N91-21062
Numerical solutions of 2-D multi-stage rotor/stator unsteady flow interactions p 595 N91-21070
Transonic cascade flow calculations using non-periodic C-type grids p 596 N91-21071
Computation of supersonic and low subsonic cascade flows using an explicit Navier-Stokes technique and the kappa-epsilon turbulence model p 596 N91-21072
Blunt trailing edge analysis of supercritical airfoils by a Navier-Stokes code
[NAL-TR-1075-T] p 556 N91-21114
A modal aeroelastic analysis scheme for turbomachinery blading
[NASA-CR-187089] p 579 N91-21138
Proceedings of the 8th NAL Symposium on Aircraft Computational Aerodynamics: Prospects of Computational Fluid Dynamics and Super Computers in Aerospace Science and Technology
[NAL-SP-13] p 596 N91-21379
Present and future of CFD on the aero-engine development in IHI p 596 N91-21381
CFD research and systems in Kawasaki Heavy Industries and its future prospects p 596 N91-21382
The CFD analysis related aerospace in Fuji Heavy Industries, Ltd. p 597 N91-21383
Status and outlook of CFD technology at Mitsubishi Heavy Industries, Nagoya p 597 N91-21384
CFD for hypersonic propulsion
[NASA-TM-103791] p 597 N91-21447
Application of computational fluid dynamics in high speed aeropropulsion
[NASA-TM-103780] p 598 N91-21458
Application of mesh generation to complex 3-D configurations
[AGARD-AR-268] p 598 N91-21464
Calculation of thickness and charge noise radiated by a rotor in forward flight
[ISL-R-119/89] p 607 N91-21831
COMPUTATIONAL GRIDS
Solution adaptive local rectangular grid refinement for transonic aerodynamic flow problems
p 547 A91-34179
A numerical study of hypersonic stagnation heat transfer predictions at a coordinate singularity
p 548 A91-34193
On the relation between TVD and mesh adaption and application to Navier-Stokes calculations
p 550 A91-34215
Computation of the viscous flow past a prolate spheroid at incidence p 550 A91-34216
Development of a general multiblock flow solver for complex configurations p 605 A91-34230
Resistivity of pristine and intercalated graphite fiber epoxy composites p 589 A91-35949
Numerical solutions of 2-D multi-stage rotor/stator unsteady flow interactions p 595 N91-21070
Transonic cascade flow calculations using non-periodic C-type grids p 596 N91-21071

Application of mesh generation to complex 3-D configurations
[AGARD-AR-268] p 598 N91-21464
Grid generation about complex three-dimensional aircraft configurations
[NASA-CR-188097] p 558 N91-22071

COMPUTER AIDED DESIGN
A flexible robotic work cell for the assembly of airframe components p 543 A91-35193
Optimization of radio-measuring devices incorporated in onboard laser velocimeters p 576 A91-35738
Wind tunnel test of a propeller working in a low Reynolds number range
[NAL-TR-1071] p 556 N91-21112
Present and future of CFD on the aero-engine development in IHI p 596 N91-21381
CFD research and systems in Kawasaki Heavy Industries and its future prospects p 596 N91-21382
The CFD analysis related aerospace in Fuji Heavy Industries, Ltd. p 597 N91-21383
Status and outlook of CFD technology at Mitsubishi Heavy Industries, Nagoya p 597 N91-21384
Computer program for estimating performance of air-breathing aircraft engines
[NASA-TM-4254] p 573 N91-22103
The preliminary aerodynamic design of light aircraft
[BU-504] p 574 N91-22119
Crew chief CAD system interface guide (version 2 - SI)
[AD-A231433] p 606 N91-22734

COMPUTER AIDED MANUFACTURING
Cost-effective manufacturing of advanced ceramics p 588 A91-33725
Crew chief CAD system interface guide (version 2 - SI)
[AD-A231433] p 606 N91-22734

COMPUTER AIDED MAPPING
The compressed aeronautical chart database - Support of naval aircraft's digital moving map systems p 563 A91-33608
Precision aided inertial navigation using SAR and digital map data p 567 A91-33652

COMPUTER GRAPHICS
The compressed aeronautical chart database - Support of naval aircraft's digital moving map systems p 563 A91-33608

COMPUTER PROGRAMS
MATGRID, a program for generation of C-H and C-O topology grids around wing/body configurations: User's guide
[FFA-TN-1991-03] p 556 N91-21110
Wind tunnel test of a propeller working in a low Reynolds number range
[NAL-TR-1071] p 556 N91-21112
CFD research and systems in Kawasaki Heavy Industries and its future prospects p 596 N91-21382
STARS: An integrated general-purpose finite element structural, aeroelastic, and aeroservoelastic analysis computer program
[NASA-TM-101709-REV] p 599 N91-21587
Methodology development for the verification and validation of flight critical systems software, phase 1
[AD-A229932] p 605 N91-21735
Approximate methods for predicting the lifting characteristics of wing-body combinations p 558 N91-22074
Computer program for estimating performance of air-breathing aircraft engines
[NASA-TM-4254] p 573 N91-22103
Signal blending in control systems structural interactions
[BU-505] p 583 N91-22132
Addendum to the DYCAST user's manual describing the curved, warp beam finite element
[NASA-CR-4362] p 606 N91-22805

COMPUTER SYSTEMS PERFORMANCE
The CFD analysis related aerospace in Fuji Heavy Industries, Ltd. p 597 N91-21383

COMPUTER TECHNIQUES
Embedded computers: Navy's approach to developing patrol aircraft avionics system too risky
[AD-A230868] p 577 N91-21136
Development of a computer technique for the prediction of transport aircraft flight profile sonic boom signatures
[NASA-CR-188117] p 560 N91-22093
RICIS Software Engineering 90 Symposium: Aerospace Applications and Research Directions Proceedings Appendices
[NASA-CR-187994] p 605 N91-22728

COMPUTER VISION
A model-based method for object recognition p 605 A91-35241
Knowledge-based target recognition system evolution p 577 A91-35978

COMPUTERIZED SIMULATION
A vehicle location system (VLS) solution approach p 564 A91-33614
Test program for Honeywell/DND Helicopter Integrated Navigation System (HINS) p 565 A91-33626
INS reset removal for enhanced post-flight performance analysis p 565 A91-33628
Evaluation of controller tools for conducting MLS curved approaches to New York's JFK Airport p 565 A91-33631
The design, simulation and implementation of an accurate positioning system for automatic flight inspection p 566 A91-33646
Numerical simulation of compressible Euler flows --- Book p 544 A91-33675
Numerical simulation of laminar hypersonic flow past blunt bodies including high temperature effects p 547 A91-34180
Simulation of glancing shock wave and boundary layer interaction p 548 A91-34195
Aspects of the application of an Euler-equation method to the simulation of leading-edge vortex flow p 549 A91-34196
A numerical study of interfacial instabilities at high Mach numbers p 549 A91-34198
3D Euler flows around modern airplanes p 549 A91-34201
Numerical simulation of turbulent flows around airfoil and wing p 549 A91-34203
Numerical simulation of vortices motion in presence of solid boundaries p 549 A91-34213
Simulation of two- and three-dimensional internal subsonic flows using a finite element method p 595 A91-35986
Simulation of nap-of-the-Earth flight in helicopters
[NASA-TM-102830] p 572 N91-21131
Status and outlook of CFD technology at Mitsubishi Heavy Industries, Nagoya p 597 N91-21384
Application of mesh generation to complex 3-D configurations
[AGARD-AR-268] p 598 N91-21464
Stability analysis of a fuselage side
[FFA-TN-1990-32] p 599 N91-21568
Numerical simulation of swept-wing flows
[NASA-CR-188201] p 560 N91-22095

CONDUCTIVE HEAT TRANSFER
Using a locally one-dimensional method for solving the heat conductivity equation to determine the thermal state of cooled rotor disks p 594 A91-35742

CONFERENCES
ICCM-VII; Proceedings of the 7th International Conference on Composite Materials, Guangzhou, People's Republic of China, Nov. 22-24, 1989. Vols. 1-3 p 588 A91-32451
IEEE PLANS '90 - Position Location and Navigation Symposium, Las Vegas, NV, Mar. 20-23, 1990, Record p 586 A91-33601
GAMM-Conference on Numerical Methods in Fluid Mechanics, 8th, Delft University of Technology, Netherlands, Sept. 27-29, 1989, Proceedings p 592 A91-34176
Computational Fluid Dynamics Symposium on Aeropropulsion
[NASA-CP-3078] p 554 N91-21062
Proceedings of the 8th NAL Symposium on Aircraft Computational Aerodynamics: Prospects of Computational Fluid Dynamics and Super Computers in Aerospace Science and Technology
[NAL-SP-13] p 596 N91-21379
Fourth NASA Workshop on Computational Control of Flexible Aerospace Systems, part 2
[NASA-CP-10065-PT-2] p 587 N91-22331
Proceedings of a French-Japanese Seminar on Composite Materials: Processing, Use and Databases p 589 N91-22380

CONICAL BODIES
Coning motion of slender bodies at high angles of attack
[NAL-TR-1059] p 556 N91-21111

CONICAL FLOW
Conical Euler simulation of wing rock for a delta wing planform p 580 A91-33536
Vortical solutions of the conical Euler equations --- Book p 591 A91-33674
A streamwise upwind algorithm applied to vortical flow over a delta wing p 548 A91-34192

CONSOLES
Metamorphoses of ONAV console operations: From prototype to real time application p 606 N91-22794

CONSTRUCTION
Snow roads and runways
[AD-A231490] p 586 N91-22138

CONTRAROTATING PROPELLERS
A quantitative investigation into the aerodynamic coupling effects in a coaxial contra-rotating rotor system
[BU-517] p 574 N91-22120

CONTROL STABILITY
Integrated flight/propulsion control design for a STOVL aircraft using H-infinity control design techniques
[NASA-TM-104340] p 579 N91-21140
STARS: An integrated general-purpose finite element structural, aeroelastic, and aeroservoelastic analysis computer program
[NASA-TM-101709-REV] p 599 N91-21587

CONTROL SURFACES
A leading-edge control surface
[BU-508] p 559 N91-22087
Flutter suppression of an aircraft wing using a control surface
[BU-506] p 583 N91-22133
Design and test of three active flutter suppression controllers p 583 N91-22334

CONTROL SYSTEMS DESIGN
Reduction of aerodynamic augmented states in active flutter suppression systems p 580 A91-33535
Active vibration control using fixed order dynamic compensation with frequency shaped cost functionals p 604 A91-33932
Design of robust controllers for gas turbine engines
[ASME PAPER 90-GT-113] p 578 A91-34815
Methods for the optimization of the testing and modeling of control systems for gas turbine engines --- Russian book p 579 A91-35815
Hot gas ingestion test results of a two-poster vectored thrust concept with flow visualization in the NASA Lewis 9- x 15-foot low speed wind tunnel
[NASA-TM-103258] p 556 N91-21116
Integrated flight/propulsion control system design based on a decentralized, hierarchical approach
[NASA-TM-103678] p 579 N91-21137
Integrated flight/propulsion control design for a STOVL aircraft using H-infinity control design techniques
[NASA-TM-104340] p 579 N91-21140
Eigenspace design of helicopter flight control systems
[AD-A231588] p 582 N91-21153
A solid-state controllable power supply for a magnetic suspension wind tunnel p 585 N91-21199
A preliminary evaluation of an F100 engine parameter estimation process using flight data
[NASA-TM-4216] p 597 N91-21446
Robust integrated autopilot/autothrottle design using constrained parameter optimization
[NASA-CR-188011] p 583 N91-22127
Flutter suppression of an aircraft wing using a control surface
[BU-506] p 583 N91-22133
Supercomputer optimizations for stochastic optimal control applications p 605 N91-22313
Design and test of three active flutter suppression controllers p 583 N91-22334

CONTROL THEORY
Reduction of aerodynamic augmented states in active flutter suppression systems p 580 A91-33535
On management and control of turbulent shear flows p 545 A91-33803
Research flight-control system development for the F-18 high alpha research vehicle
[NASA-TM-104232] p 583 N91-22131
Design and test of three active flutter suppression controllers p 583 N91-22334

CONTROLLERS
Design and test of three active flutter suppression controllers p 583 N91-22334
Development and testing of controller performance evaluation methodology for multi-input/multi-output digital control systems p 584 N91-22337

CONVECTIVE FLOW
A review of predictive efforts for transport phenomena in axial flow compressors p 551 A91-34785

CONVECTIVE HEAT TRANSFER
MHD drag and heat transfer of a sphere in supersonic flow of a partially ionized gas p 607 A91-35791

CONVERGENT-DIVERGENT NOZZLES
Some treatments on boundary conditions for quasi one-dimensional Euler equations
[FFA-TN-1990-36] p 598 N91-21469
Aeropropulsive characteristics of canted twin pitch-vectoring nozzles at Mach 0.20 to 1.20
[NASA-TP-3060] p 558 N91-22069

CONVEXITY
Correlation measurements and structure angles in a turbulent boundary layer recovering from convex curvature p 545 A91-33747

COOLANTS
Compressor drum aerodynamic experiments and analysis with coolant injected at selected locations
[ASME PAPER 90-GT-151] p 552 A91-34794

COOLING SYSTEMS
Langley develops thermal management concept for hypersonic aircraft p 570 A91-33323

Calculation of the cooling system of small-size blades of high-temperature gas turbine engines
p 594 A91-35743

COORDINATE TRANSFORMATIONS
Compressible flows with periodic vortical disturbances around lifting airfoils
[NASA-TM-103742] p 554 N91-21060

CORNER FLOW
Correlation measurements and structure angles in a turbulent boundary layer recovering from convex curvature p 545 A91-33747

CORRELATION
Sensitivity-based scaling for correlating structural response from different analytical models
[NASA-TM-104042] p 602 N91-22578

COST ANALYSIS
Advanced composite technology of West German general aviation aircraft p 543 A91-32648
Air safety regulation and its commercial impact
p 561 A91-34161

COST EFFECTIVENESS
Cost-effective manufacturing of advanced ceramics
p 588 A91-33725
Cost-efficient manufacturing of composite structures
p 590 N91-23048

COST REDUCTION
Ashtech XII GPS technology p 564 A91-33622
Cost-effective manufacturing of advanced ceramics
p 588 A91-33725

COSTS
FAA aviation forecasts: Fiscal years 1991-2002
[AD-A231721] p 543 N91-22068

COUPLING
A quantitative investigation into the aerodynamic coupling effects in a coaxial contra-rotating rotor system
[BU-517] p 574 N91-22120

COVARIANCE
Design and test of three active flutter suppression controllers p 583 N91-22334

CRACK GEOMETRY
Experimental and analytical study of shaft cracking response in rotatory machines p 594 A91-35516

CRACK PROPAGATION
Experimental and analytical study of shaft cracking response in rotatory machines p 594 A91-35516
Micromechanisms of quasi-static and fatigue crack growth in titanium-aluminides p 602 N91-22583

CRASHWORTHINESS
Lightweight, fire-retardant, crashworthy aircraft seat cushioning p 563 N91-23052

CRITICAL VELOCITY
The effect of shear and rotary inertia of a rotor at its critical speeds p 592 A91-34125
Critical speeds and forced response solutions for active magnetic bearing turbomachinery, part 1
p 587 N91-21209
Critical speeds and forced response solutions for active magnetic bearing turbomachinery, part 2
p 587 N91-21210

CROSS FLOW
Similarity analysis of compressor tip clearance flow structure
[ASME PAPER 90-GT-153] p 552 A91-34793
Numerical simulation of swept-wing flows
[NASA-CR-188201] p 560 N91-22095

CRYOGENIC FLUID STORAGE
Use of resin composites for cryogenic tankage
p 588 A91-34287

CRYOGENIC WIND TUNNELS
Modeling of flow parameters in a cryogenic wind tunnel p 584 A91-33919

CUMULATIVE DAMAGE
Cumulative damage problem in pull-through fatigue of C.F.R.P. laminate p 588 A91-32576
Damage accumulation and degradation of composite laminates under aircraft service loading: Assessment and prediction, volumes 1 and 2 p 589 N91-22381

CURVED BEAMS
Addendum to the DYCAST user's manual describing the curved, warp beam finite element
[NASA-CR-4362] p 606 N91-22805

CUSHIONS
Lightweight, fire-retardant, crashworthy aircraft seat cushioning p 563 N91-23052

CYLINDERS
Computer program for the calculation of normal force and pitching moment of forebody-cylinder combinations at angles of attack up to 90 degrees and Mach numbers up to 5, including effects of conical boat-tailing
[ESDU-90034] p 555 N91-21102

CYLINDRICAL BODIES
Interference-free measurements of the subsonic aerodynamics of slanted-base ogive cylinders
p 547 A91-34130
Coning motion of slender bodies at high angles of attack
[NAL-TR-1059] p 556 N91-21111

D

DAMAGE ASSESSMENT
Thermal spikes on CFRP laminates - Assessment of microdamage and its consequences on fatigue life
p 588 A91-32549
Model rocketry hazard study
[DOT/FAA/CT-TN90/28] p 587 N91-21238

DATA ACQUISITION
Study of bird ingestions into small inlet area aircraft turbine engines
[DOT/FAA/CT-90/13] p 562 N91-21122
Technical presentation of the Merlin's radome: Calibration and data processing p 603 N91-22656
The improvement of the installation of the DLR research aircraft Falcon: Description and first results
p 603 N91-22657

DATA BASE MANAGEMENT SYSTEMS
Crew chief CAD system interface guide (version 2 - SI)
[AD-A231433] p 606 N91-22734

DATA BASES
The compressed aeronautical chart database - Support of naval aircraft's digital moving map systems
p 563 A91-33608
Forces and pressures induced on circular plates by a single lifting jet in ground effect
[NASA-TM-102816] p 558 N91-22077
Proceedings of a French-Japanese Seminar on Composite Materials: Processing, Use and Databases
p 589 N91-22380

DATA LINKS
The missing (data) link in pilot navigation
p 568 A91-33666
Oceanic clearance trial proves utility of data link communications for ATC p 568 A91-33775

DATA PROCESSING
Technical presentation of the Merlin's radome: Calibration and data processing p 603 N91-22656

DATA SAMPLING
Digital signal conditioning for flight test instrumentation
[NASA-TM-101739] p 577 N91-21135

DATA STORAGE
Digital signal conditioning for flight test instrumentation
[NASA-TM-101739] p 577 N91-21135

DATA SYSTEMS
Flight Service Automation System (FSAS) Model 1 Full Capacity (M1FC) Operational Test and Evaluation (OT/E)/integration test report
[DOT/FAA/CT-TN90/45] p 569 N91-22100

DATA TRANSMISSION
Oceanic clearance trial proves utility of data link communications for ATC p 568 A91-33775
Digital signal conditioning for flight test instrumentation
[NASA-TM-101739] p 577 N91-21135

DECISION MAKING
The delayed ejection decision p 561 A91-33273

DEFLECTION
Bifurcation analysis of the longitudinal dynamics of a simple powered lifting hypersonic vehicle
[AD-A230826] p 557 N91-21118
Multiaxis thrust vectoring using axisymmetric nozzles and postexit vanes on an F/A-18 configuration vehicle
[NASA-TM-101741] p 559 N91-22083

DEFORMATION
Flexible body dynamic stability for high performance aircraft p 574 N91-22318

DEGRADATION
Impact of icing on Unmanned Aerial Vehicle (UAV) operations
[AD-A231191] p 562 N91-21124
Damage accumulation and degradation of composite laminates under aircraft service loading: Assessment and prediction, volumes 1 and 2 p 589 N91-22381

DELIVERY
Evaluation of an alternative rotorcraft cargo lowering device for the delivery of 500-lb ammunition loads
[AD-A230995] p 573 N91-21133

DELTA WINGS
Analysis and optimal design of composite structures
p 591 A91-32651
Conical Euler simulation of wing rock for a delta wing planform p 580 A91-33536
Vortical solutions of the conical Euler equations --- Book p 591 A91-33674
Vorticity equation solutions for slender wings at high incidence p 547 A91-34126
Development and validation of characteristic boundary conditions for cell-centered Euler flow calculations
p 592 A91-34178
Solution of the 3-D, incompressible Navier-Stokes equations for the simulation of vortex breakdown
p 593 A91-34181
A streamwise upwind algorithm applied to vortical flow over a delta wing p 548 A91-34192
Aspects of the application of an Euler-equation method to the simulation of leading-edge vortex flow
p 549 A91-34196
Vortex bursting over a unit area aspect ratio delta wing using vortex paneling methods
[AD-A231028] p 557 N91-21119
The transient development of vortices over a delta wing
[AD-A231946] p 559 N91-22082
Large amplitude oscillations p 561 N91-22108

DESIGN ANALYSIS
Integrated multidisciplinary design optimization of rotorcraft p 570 A91-33528
Helicopter rotor dynamics optimization with experimental verification p 570 A91-33530
A highly efficient engineering tool for three-dimensional scramjet flowfield and heat transfer computations
p 596 N91-21098
Magnetic suspension and balance system advanced study, 1989 design p 586 N91-21197

DETONATION WAVES
High-speed compressor surge with application to active control
[ASME PAPER 90-GT-354] p 553 A91-34797

DIFFERENTIAL EQUATIONS
State stability of a system of integro-differential equations of nonstationary aeroelasticity
p 595 A91-35785

DIGITAL COMPUTERS
Digital signal conditioning for flight test instrumentation
[NASA-TM-101739] p 577 N91-21135

DIGITAL SIMULATION
Some aspects of the numerical simulation of compressible viscous flow around bluff bodies at low Ma-number p 550 A91-34220

DIGITAL SYSTEMS
A preliminary evaluation of an F100 engine parameter estimation process using flight data
[NASA-TM-4216] p 597 N91-21446
Development and testing of controller performance evaluation methodology for multi-input/multi-output digital control systems p 584 N91-22337

DIGITAL TECHNIQUES
Experimental performance of a binary phase-only optical correlator using visual and infrared imagery
p 606 A91-32707
The compressed aeronautical chart database - Support of naval aircraft's digital moving map systems
p 563 A91-33608
A five channel low cost GPS receiver
p 564 A91-33624
Digital signal conditioning for flight test instrumentation
[NASA-TM-101739] p 577 N91-21135

DIRECT LIFT CONTROLS
Impact of icing on Unmanned Aerial Vehicle (UAV) operations
[AD-A231191] p 562 N91-21124

DIRECTIONAL CONTROL
Dynamic modelling and analysis of a magnetically suspended flexible rotor p 587 N91-21208

DIRECTIONAL SOLIDIFICATION (CRYSTALS)
Influence of a magnetic field during directional solidification of MAR-M 246 + Hf superalloy
[NASA-CR-184114] p 590 N91-22416

DISPLACEMENT MEASUREMENT
Skin friction measurement techniques for scramjet applications. Phase 1: Preliminary design
[AD-A231899] p 580 N91-22125

DISPLAY DEVICES
The compressed aeronautical chart database - Support of naval aircraft's digital moving map systems
p 563 A91-33608
Starship - Bright newcomer in a conservative firmament p 571 A91-34122
Traffic Alert and Collision Avoidance System (TCAS): Cockpit Display of Traffic Information (CDTI) investigation. Phase 1: Feasibility study
[NASA-TM-104956] p 569 N91-22102

DISTORTION
Compressible flows with periodic vortical disturbances around lifting airfoils
[NASA-TM-103742] p 554 N91-21060

DITCHING (LANDING)
The human factors relating to escape and survival from helicopters ditching in water
[AGARD-AG-305(F)] p 563 N91-22099

DIVERGENT NOZZLES
Some treatments on boundary conditions for quasi one-dimensional Euler equations
[FFA-TN-1990-36] p 598 N91-21469

DOPPLER EFFECT
Ashtech XII GPS technology p 564 A91-33622
DOPPLER RADAR
Modern aviation weather systems for efficient flight management p 602 A91-33648
DRAG
Impact of icing on Unmanned Aerial Vehicle (UAV) operations
[AD-A231191] p 562 N91-21124
Effect of planform on induced drag
[BU-500] p 559 N91-22086
DRAG MEASUREMENT
Skin friction measurement techniques for scramjet applications. Phase 1: Preliminary design
[AD-A231899] p 580 N91-22125
DRAG REDUCTION
Aerodynamic and structural studies of joined-wing aircraft p 571 A91-33534
DRONE AIRCRAFT
Impact of icing on Unmanned Aerial Vehicle (UAV) operations
[AD-A231191] p 562 N91-21124
DROP SIZE
Comparison of UNL laser imaging and sizing system and a phase Doppler system for analyzing sprays from a NASA nozzle
[NASA-CR-185239] p 598 N91-21485
DYNAMIC CHARACTERISTICS
Rotary-balance testing for aircraft dynamics
[AGARD-AR-265] p 585 N91-21156
Effects of gear box vibration and mass imbalance on the dynamics of multi-stage gear transmissions
[NASA-TM-103695] p 599 N91-21534
Oscillatory data for typical configurations p 561 N91-22109
DYNAMIC LOADS
Method and apparatus for detecting laminar flow separation and reattachment
[NASA-CASE-LAR-13952-2-SB] p 598 N91-21472
DYNAMIC MODELS
Linear and non-linear dynamic models of a geared rotor-bearing system p 594 A91-35536
Dynamic modelling and analysis of a magnetically suspended flexible rotor p 587 N91-21208
DYNAMIC PRESSURE
Span reduction effects on the flutter characteristics of arrow-wing supersonic transport configurations
[NASA-TP-3077] p 572 N91-21127
DYNAMIC PROGRAMMING
Speech recognition using Kohonen neural networks, dynamic programming, and multi-feature fusion
[AD-A230951] p 597 N91-21410
Supercomputer optimizations for stochastic optimal control applications p 605 N91-22313
DYNAMIC RESPONSE
A modal aeroelastic analysis scheme for turbomachinery blading
[NASA-CR-187089] p 579 N91-21138
DYNAMIC STABILITY
Bifurcation analysis of the longitudinal dynamics of a simple powered lifting hypersonic vehicle
[AD-A230826] p 557 N91-21118
DYNAMIC STRUCTURAL ANALYSIS
Aeroelastic optimum design of composite rotor blade with returning wake effect p 570 A91-32646
Dynamic analysis technique of centrifugal impellor with split blades p 593 A91-35498
Force and moment transmissibilities through rolling element bearings in a single-stage rotor system p 594 A91-35537
Fourth NASA Workshop on Computational Control of Flexible Aerospace Systems, part 2
[NASA-CP-10065-PT-2] p 587 N91-22331
Addendum to the DYCAST user's manual describing the curved, warp beam finite element
[NASA-CR-4362] p 606 N91-22805

E

EARTH GRAVITATION
Airborne gravimetry and the Global Positioning System p 602 A91-33634
ECONOMIC IMPACT
Air safety regulation and its commercial impact p 561 A91-34161
Economic impact of aviation in Pennsylvania
[PB91-128264] p 543 N91-22067
ECONOMICS
Economic impact of aviation in Pennsylvania
[PB91-128264] p 543 N91-22067
FAA aviation forecasts: Fiscal years 1991-2002
[AD-A231721] p 543 N91-22068
EDDY VISCOSITY
Analysis of laminar separation bubble using a simple eddy-viscosity turbulence model p 591 A91-33227
Transonic cascade flow calculations using non-periodic C-type grids p 596 N91-21071
Analysis of laminar separation bubbles using a simple eddy-viscosity turbulence model
[NAL-TR-1079] p 600 N91-22520
EDGE DETECTION
Automated extraction of airport runway patterns from radar imagery
[AD-A231809] p 600 N91-22480
EDUCATION
A guide to ground vehicle operations on the airport
[AD-A231077] p 585 N91-21158
Business plans for the Institute for Aviation Research, FY 1990 - FY 1995
[IAR-89-15] p 609 N91-23020
EIGENVALUES
The effect of shear and rotary inertia of a rotor at its critical speeds p 592 A91-34125
EJECTION INJURIES
The delayed ejection decision p 561 A91-33273
Biodynamic and optimization aspects of emergency ejection from an aircraft p 561 A91-34341
EJECTION TRAINING
The delayed ejection decision p 561 A91-33273
ELASTIC BODIES
Weightless test balancing of elastic rotors with the help of interchangeable longitudinal bearing stiffnesses p 592 A91-34015
ELASTIC DEFORMATION
Stability analysis of a fuselage side
[FFA-TN-1990-32] p 599 N91-21568
ELASTOHYDRODYNAMICS
Analysis of bearing incidents in aircraft gas turbine mainshaft bearings p 591 A91-33464
ELECTRICAL RESISTIVITY
Resistivity of pristine and intercalated graphite fiber *epoxy composites* p 589 A91-35949
ELECTROMAGNETIC INTERFERENCE
A fast and low-cost validation technique for ILS and MLS p 565 A91-33630
ELECTROMAGNETIC MEASUREMENT
The effects of simulated electromagnetic pulse on commercial aircraft p 569 A91-35902
ELECTROMAGNETIC PULSES
The effects of simulated electromagnetic pulse on commercial aircraft p 569 A91-35902
ELECTROMAGNETS
A solid-state controllable power supply for a magnetic suspension wind tunnel p 585 N91-21199
ELECTRONIC EQUIPMENT
A five channel low cost GPS receiver p 564 A91-33624
ELECTRONIC MODULES
Stand-alone vs. embedded GPS user equipment - The exploration of new standards p 564 A91-33616
ELEVATORS (CONTROL SURFACES)
Elevator deflections on the icing process p 572 A91-35427
ELLIPSES
Inviscid flow about a double ellipse p 549 A91-34210
EMBEDDED COMPUTER SYSTEMS
Embedded computers: Navy's approach to developing patrol aircraft avionics system too risky
[AD-A230868] p 577 N91-21136
EMERGENCIES
Biodynamic and optimization aspects of emergency ejection from an aircraft p 561 A91-34341
Design of an intelligent information system for in-flight emergency assistance p 606 N91-22792
EMISSIVITY
Experimental study of radiation from coated turbine blades p 580 N91-22122
END EFFECTORS
A flexible robotic work cell for the assembly of airframe components p 543 A91-35193
ENGINE CONTROL
Methods for the optimization of the testing and modeling of control systems for gas turbine engines --- Russian book p 579 A91-35815
Control of the working cycle of gas turbine engines (2nd revised and enlarged edition) --- Russian book p 579 A91-35822
Integrated flight/propulsion control system design based on a decentralized, hierarchical approach
[NASA-TM-103678] p 579 N91-21137
A preliminary evaluation of an F100 engine parameter estimation process using flight data
[NASA-TM-4216] p 597 N91-21446
ENGINE DESIGN
Spanning the globe with jet propulsion
[AIAA PAPER 91-2987] p 577 A91-34111
Present and future of CFD on the aero-engine development in IHI p 596 N91-21381
Computer program for estimating performance of air-breathing aircraft engines
[NASA-TM-4254] p 573 N91-22103
ENGINE FAILURE
Fast response wall pressure measurement as a means of gas turbine blade fault identification
[ASME PAPER 90-GT-341] p 578 A91-34813
Fault detection and diagnosis in gas turbines
[ASME PAPER 90-GT-339] p 578 A91-34814
ENGINE INLETS
A pressure flux-split technique for computation of inlet flow behavior p 595 N91-21068
Zonal analysis of two high-speed inlets p 596 N91-21089
ENGINE PARTS
Fast response wall pressure measurement as a means of gas turbine blade fault identification
[ASME PAPER 90-GT-341] p 578 A91-34813
Feasibility study for the qualification of an economically advantageous Ti-6Al-4V bearing housing for gas turbine engine application by powder metal manufacturing technology
[AD-A231666] p 601 N91-22564
High temperature performance evaluation of a hypersonic engine ceramic wafer seal
[NASA-TM-103737] p 601 N91-22567
ENGINE TESTS
Methods for the optimization of the testing and modeling of control systems for gas turbine engines --- Russian book p 579 A91-35815
Aerothermodynamic design appraisal of noise suppressors for F/A-18 engine run-up facilities at RAAF Williamtown
[ARL-PROP-R-177] p 585 N91-22136
High temperature performance evaluation of a hypersonic engine ceramic wafer seal
[NASA-TM-103737] p 601 N91-22567
ENVIRONMENTAL TESTS
Avionics Environmental Reliability using finite element analysis
[ASME PAPER 90-WA/TS-1] p 591 A91-32961
EPOXY MATRIX COMPOSITES
Resistivity of pristine and intercalated graphite fiber epoxy composites p 589 A91-35949
EPOXY RESINS
Use of resin composites for cryogenic tankage p 588 A91-34287
ERROR ANALYSIS
INS reset removal for enhanced post-flight performance analysis p 565 A91-33628
The design, simulation and implementation of an accurate positioning system for automatic flight inspection p 566 A91-33646
Global Positioning System (GPS) autonomous navigation p 567 A91-33653
Application of sensitivity methods for error localization in finite element systems p 594 A91-35529
Air motion measurement uncertainties: Their impact on atmospheric studies p 603 N91-22654
ESCAPE (ABANDONMENT)
The human factors relating to escape and survival from helicopters ditching in water
[AGARD-AG-305(F)] p 563 N91-22099
EULER EQUATIONS OF MOTION
Domain decomposition methods in aerodynamics p 604 A91-33056
Conical Euler simulation of wing rock for a delta wing planform p 580 A91-33536
Vortical solutions of the conical Euler equations --- Book p 591 A91-33674
Numerical simulation of compressible Euler flows --- Book p 544 A91-33675
Closed-coupled zonal solution for viscous flow problems p 546 A91-34063
Cell-vertex, multigrid Euler scheme for use with multiblock grids p 547 A91-34128
Role of artificial viscosity in Euler and Navier-Stokes solvers p 547 A91-34135
Development and validation of characteristic boundary conditions for cell-centered Euler flow calculations p 592 A91-34178
Hypersonic leeside flow computations using centered *schemes for Euler equations* p 548 A91-34187
Aspects of the application of an Euler-equation method to the simulation of leading-edge vortex flow p 549 A91-34196
Inviscid flow about a double ellipse p 549 A91-34210
Development of a general multiblock flow solver for complex configurations p 605 A91-34230
A finite-difference, frequency-domain numerical scheme for the solution of the linearized unsteady Euler *equations* p 595 N91-21067
Some treatments on boundary conditions for quasi one-dimensional Euler equations
[FFA-TN-1990-36] p 598 N91-21469

EUROPEAN AIRBUS
Fin structures of the Airbus family experience with advanced composites p 570 A91-32455
EVALUATION
Development and testing of controller performance evaluation methodology for multi-input/multi-output digital control systems p 584 N91-22337
EXHAUST DIFFUSERS
Finite-element analysis of turbulent flow in annular exhaust diffusers of gas turbine engines p 577 A91-32700
EXHAUST GASES
Interaction between two jets exhausted from nozzles arranged in parallel p 593 A91-34439
Multiaxis thrust vectoring using axisymmetric nozzles and postexit vanes on an F/A-18 configuration vehicle [NASA-TM-101741] p 559 N91-22083
An experimental investigation into NO(x) control of a gas turbine combustor and augmentor tube incorporating a catalytic reduction system [AD-A231427] p 580 N91-22124
EXHAUST NOZZLES
Hot gas ingestion test results of a two-poster vectored thrust concept with flow visualization in the NASA Lewis 9- x 15-foot low speed wind tunnel [NASA-TM-103258] p 556 N91-21116
Multiaxis thrust vectoring using axisymmetric nozzles and postexit vanes on an F/A-18 configuration vehicle [NASA-TM-101741] p 559 N91-22083
EXPERT SYSTEMS
Generalized heuristics for the gate assignment problem p 605 A91-35100
Design of an intelligent information system for in-flight emergency assistance p 606 N91-22792
Metamorphoses of ONAV console operations: From prototype to real time application p 606 N91-22794
EXPOSURE
Design methodology for a community response questionnaire on sonic boom exposure [NASA-CR-187503] p 608 N91-22830

F

F-15 AIRCRAFT
A preliminary evaluation of an F100 engine parameter estimation process using flight data [NASA-TM-4216] p 597 N91-21446
F-16 AIRCRAFT
Terrain-aided altitude computations on the AFTI/F-16 p 576 A91-33650
F-18 AIRCRAFT
Research flight-control system development for the F-18 high alpha research vehicle [NASA-TM-104232] p 583 N91-22131
Aerothermodynamic design appraisal of noise suppressors for F/A-18 engine run-up facilities at RAAF Williamtown [ARL-PROP-R-177] p 585 N91-22136
Water tunnel flow visualisation of vortex breakdown over the F/A-18 [ARL-FLIGHT-MECH-R-179] p 600 N91-22511
FABRICATION
Proceedings of a French-Japanese Seminar on Composite Materials: Processing, Use and Databases p 589 N91-22380
Development of an optical volumetric flowmeter [PB91-136481] p 601 N91-22550
Cost-efficient manufacturing of composite structures p 590 N91-23048
FABRICS
Lightweight, fire-retardant, crashworthy aircraft seat cushioning p 563 N91-23052
FAILURE ANALYSIS
In-flight system for helicopter blade inspection p 575 A91-33268
Failure management in spatio-temporal redundant, integrated navigation and flight control reference-systems p 581 A91-33640
Damage accumulation and degradation of composite laminates under aircraft service loading: Assessment and prediction, volumes 1 and 2 p 589 N91-22381
The flexural strength of unidirectional carbon fibre composites [BU-509] p 589 N91-22399
FAN BLADES
Structural integrity of wind tunnel wooden fan blades [NASA-TM-104059] p 602 N91-22589
FATIGUE (MATERIALS)
Cumulative damage problem in pull-through fatigue of C.F.R.P. laminate p 588 A91-32576
Micromechanisms of quasi-static and fatigue crack growth in titanium-aluminides p 602 N91-22583
FATIGUE LIFE
Thermal spikes on CFRP laminates - Assessment of microdamage and its consequences on fatigue life p 588 A91-32549
Advanced composite technology of West German general aviation aircraft p 543 A91-32648
FATIGUE TESTS
Significance of residual curing strains in composite structure repair technology p 590 A91-32461
Damage tolerance aspects of ARALL fuselage skin structure (philosophy and experiments) p 588 A91-32573
Cumulative damage problem in pull-through fatigue of C.F.R.P. laminate p 588 A91-32576
FAULT TOLERANCE
Failure management in spatio-temporal redundant, integrated navigation and flight control reference-systems p 581 A91-33640
FEASIBILITY ANALYSIS
Feasibility study for the qualification of an economically advantageous Ti-6Al-4V bearing housing for gas turbine engine application by powder metal manufacturing technology [AD-A231666] p 601 N91-22564
FEEDBACK CONTROL
Integrated flight/propulsion control system design based on a decentralized, hierarchical approach [NASA-TM-103678] p 579 N91-21137
Results of the HHC wind tunnel tests, 1986 - 1988 [DLR-FB-90-42] p 582 N91-21152
Automated flight test management system [NASA-CR-186011] p 574 N91-22117
Robust integrated autopilot/autothrottle design using constrained parameter optimization [NASA-CR-188011] p 583 N91-22127
Signal blending in control systems structural interactions [BU-505] p 583 N91-22132
Flutter suppression of an aircraft wing using a control surface [BU-506] p 583 N91-22133
Roll plus maneuver load alleviation control system designs for the active flexible wing wind-tunnel model p 584 N91-22335
FEEDFORWARD CONTROL
Robust integrated autopilot/autothrottle design using constrained parameter optimization [NASA-CR-188011] p 583 N91-22127
FIBER COMPOSITES
Damage accumulation and degradation of composite laminates under aircraft service loading: Assessment and prediction, volumes 1 and 2 p 589 N91-22381
FIBER OPTICS
Civil air transport: A fresh look at power-by-wire and fly-by-light p 584 N91-23053
FIBER ORIENTATION
Resistivity of pristine and intercalated graphite fiber epoxy composites p 589 A91-35949
FIELD EFFECT TRANSISTORS
A solid-state controllable power supply for a magnetic suspension wind tunnel p 585 N91-21199
FIGHTER AIRCRAFT
Aerospace materials p 588 A91-33324
Prediction of slender body coning characteristics p 544 A91-33382
The N-Dimensional Fighter p 571 A91-35425
Integrated flight/propulsion control system design based on a decentralized, hierarchical approach [NASA-TM-103678] p 579 N91-21137
Rotary-balance testing for aircraft dynamics [AGARD-AR-265] p 585 N91-21156
Dynamic stall effects and applications to high performance aircraft p 573 N91-22106
Forebody vortex control p 573 N91-22110
An overview of the active flexible wing program p 583 N91-22332
FINITE DIFFERENCE THEORY
Comparison of upwind and central finite-difference methods for the compressible Navier-Stokes equations p 545 A91-34034
An inverse boundary layer procedure with application to 3-D wing flow p 550 A91-34229
An approach to the numerical solution of two-dimensional Navier-Stokes equations by a finite difference method p 595 A91-35787
A finite-difference, frequency-domain numerical scheme for the solution of the linearized unsteady Euler equations p 595 N91-21067
FINITE ELEMENT METHOD
Finite-element analysis of turbulent flow in annular exhaust diffusers of gas turbine engines p 577 A91-32700
Avionics Environmental Reliability using finite element analysis [ASME PAPER 90-WA/TS-1] p 591 A91-32961
Non-equilibrium hypersonic flow computations by implicit second-order upwind finite-elements p 548 A91-34191
Application of sensitivity methods for error localization in finite element systems p 594 A91-35529
Simulation of two- and three-dimensional internal subsonic flows using a finite element method p 595 A91-35986
Finite element methods for integrated aerodynamic heating analysis [NASA-CR-188079] p 554 N91-21101
STARS: An integrated general-purpose finite element structural, aeroelastic, and aeroservoelastic analysis computer program [NASA-TM-101709-REV] p 599 N91-21587
Flexible body dynamic stability for high performance aircraft p 574 N91-22318
Computational methods for frictionless contact with application to Space Shuttle Orbiter nose-gear tires [NASA-TP-3073] p 601 N91-22576
Addendum to the DYCAST user's manual describing the curved, warp beam finite element [NASA-CR-4362] p 606 N91-22805
FINITE VOLUME METHOD
Cell-vertex, multigrid Euler scheme for use with multiblock grids p 547 A91-34128
Hypersonic leeside flow computations using centered schemes for Euler equations p 548 A91-34187
Euler analysis of transonic stator-rotor interaction using a finite volume method p 554 A91-35984
Grid generation about complex three-dimensional aircraft configurations [NASA-CR-188097] p 558 N91-22071
FINS
Simulation of glancing shock wave and boundary layer interaction p 548 A91-34195
Green's function solution to radiative heat transfer between longitudinal gray fins p 593 A91-35117
FLAME RETARDANTS
Lightweight, fire-retardant, crashworthy aircraft seat cushioning p 563 N91-23052
FLAPS (CONTROL SURFACES)
Aeropropulsive characteristics of canted twin pitch-vectoring nozzles at Mach 0.20 to 1.20 [NASA-TP-3060] p 558 N91-22069
FLAT PLATES
Theoretical basis for extrapolation of calibration data of PTC 6 throat tap nozzles [ASME PAPER 90-JPGC/PTC-1] p 578 A91-34808
FLAT SURFACES
Computations for a jet impinging obliquely on a flat surface p 554 A91-35985
FLEXIBLE BODIES
Flexible body dynamic stability for high performance aircraft p 574 N91-22318
FLEXIBLE SPACECRAFT
Fourth NASA Workshop on Computational Control of Flexible Aerospace Systems, part 2 [NASA-CP-10065-PT-2] p 587 N91-22331
FLEXIBLE WINGS
Hot-bench simulation of the active flexible wing wind-tunnel model [NASA-TM-102758] p 582 N91-21144
Fourth NASA Workshop on Computational Control of Flexible Aerospace Systems, part 2 [NASA-CP-10065-PT-2] p 587 N91-22331
An overview of the active flexible wing program p 583 N91-22332
Aeroelastic modeling of the active flexible wing wind-tunnel model p 575 N91-22333
Design and test of three active flutter suppression controllers p 583 N91-22334
Roll plus maneuver load alleviation control system designs for the active flexible wing wind-tunnel model p 584 N91-22335
Development and testing of controller performance evaluation methodology for multi-input/multi-output digital control systems p 584 N91-22337
FLEXING
The flexural strength of unidirectional carbon fibre composites [BU-509] p 589 N91-22399
FLIGHT ALTITUDE
Terrain-aided altitude computations on the AFTI/F-16 p 576 A91-33650
FLIGHT CHARACTERISTICS
Rotary-balance testing for aircraft dynamics [AGARD-AR-265] p 585 N91-21156
Special Course on Aircraft Dynamics at High Angles of Attack: Experiments and Modelling [AGARD-R-776] p 573 N91-22104
Oscillatory data for typical configurations p 561 N91-22109
Flow investigation of a ground effect vehicle [BU-516] p 600 N91-22528

FLIGHT CONDITIONS
Water tunnel flow visualisation of vortex breakdown over the F/A-18
[ARL-FLIGHT-MECH-R-179] p 600 N91-22511
FLIGHT CONTROL
Flight evaluation of the Integrated Inertial Sensor Assembly (IISA) on a helicopter p 581 A91-33639
Failure management in spatio-temporal redundant, integrated navigation and flight control reference-systems p 581 A91-33640
Integrated flight/propulsion control system design based on a decentralized, hierarchical approach
[NASA-TM-103678] p 579 N91-21137
Integrated flight/propulsion control design for a STOVL aircraft using H-infinity control design techniques
[NASA-TM-104340] p 579 N91-21140
Eigenspace design of helicopter flight control systems
[AD-A231588] p 582 N91-21153
Methodology development for the verification and validation of flight critical systems software, phase 1
[AD-A229932] p 605 N91-21735
Special Course on Aircraft Dynamics at High Angles of Attack: Experiments and Modelling
[AGARD-R-776] p 573 N91-22104
Signal blending in control systems structural interactions
[BU-505] p 583 N91-22132
Development and testing of controller performance evaluation methodology for multi-input/multi-output digital control systems p 584 N91-22337
Software: Where we are and what is required in the future p 606 N91-22729
Metamorphoses of ONAV console operations: From prototype to real time application p 606 N91-22794
Civil air transport: A fresh look at power-by-wire and fly-by-light p 584 N91-23053
FLIGHT ENVELOPES
Development of a computer technique for the prediction of transport aircraft flight profile sonic boom signatures
[NASA-CR-188117] p 560 N91-22093
FLIGHT HAZARDS
Impact of icing on Unmanned Aerial Vehicle (UAV) operations
[AD-A231191] p 562 N91-21124
FLIGHT MANAGEMENT SYSTEMS
Modern aviation weather systems for efficient flight management p 602 A91-33648
The improvement of the installation of the DLR research aircraft Falcon: Description and first results p 603 N91-22657
FLIGHT MECHANICS
Special Course on Aircraft Dynamics at High Angles of Attack: Experiments and Modelling
[AGARD-R-776] p 573 N91-22104
Large amplitude oscillations p 561 N91-22108
FLIGHT PATHS
Flight path reconstruction using extended Kalman filtering techniques
[DLR-FB-90-41] p 555 N91-21108
Impact of icing on Unmanned Aerial Vehicle (UAV) operations
[AD-A231191] p 562 N91-21124
FLIGHT RULES
Airport restrictions - A dilemma of federal preemption and proprietary control p 608 A91-35122
FLIGHT SAFETY
The final call: Why airline disasters continue to happen --- Book p 561 A91-34250
The effects of simulated electromagnetic pulse on commercial aircraft p 569 A91-35902
FLIGHT SIMULATION
Simulation of nap-of-the-Earth flight in helicopters
[NASA-TM-102830] p 572 N91-21131
NASA Ames aerospace systems directorate research
[NASA-TM-103844] p 608 N91-22066
FLIGHT TEST INSTRUMENTS
Digital signal conditioning for flight test instrumentation
[NASA-TM-101739] p 577 N91-21135
FLIGHT TESTS
Flowfield and vehicle parameter influence on results of engineering aerothermal methods p 544 A91-33378
Test program for Honeywell/DND Helicopter Integrated Navigation System (HINS) p 565 A91-33626
Flight evaluation of the Integrated Inertial Sensor Assembly (IISA) on a helicopter p 581 A91-33639
Flight test results of a tightly integrated RLG-based Global Positioning System/inertial navigation system p 566 A91-33645
Terrain-aided altitude computations on the AFTI/F-16 p 576 A91-33650
X-31 flight tests to explore combat agility to 70 deg. AOA p 571 A91-34375
Analysis of three icing test flights reaching the aircraft-referred icing degree severe
[DLR-FB-90-34] p 562 N91-21123
Identification of the aerodynamic model of the DLR research aircraft ATTAS from flight test data
[DLR-FB-90-40] p 572 N91-21130
Flight test to determine feasibility of a proposed airborne wake vortex detection concept
[NASA-TM-102672] p 563 N91-22096
Automated flight test management system
[NASA-CR-186011] p 574 N91-22117
FLIGHT VEHICLES
Nonlinear filtering of a trajectory message p 568 A91-33868
FLOW CHARACTERISTICS
Modeling of flow parameters in a cryogenic wind tunnel p 584 A91-33919
Calculation of a compressible laminar boundary layer on a tapered body of bielliptical cross section p 553 A91-35796
Numerical solutions of 2-D multi-stage rotor/stator unsteady flow interactions p 595 N91-21070
Numerical simulation of swept-wing flows
[NASA-CR-188201] p 560 N91-22095
FLOW DISTORTION
Effect of geometrical disturbance on vortex asymmetry p 547 A91-34136
The influence of inlet swirl distortions on the performance of a jet propulsion two-stage axial compressor
[ASME PAPER 90-GT-147] p 552 A91-34790
Rotating waves as a stall inception indication in axial compressors
[ASME PAPER 90-GT-156] p 553 A91-34796
FLOW DISTRIBUTION
Computation of flowfields for projectiles in hypersonic chemically reacting flows p 544 A91-33379
The dynamic behavior of a shock-wave/turbulent boundary layer interaction p 544 A91-33735
Correlation measurements and structure angles in a turbulent boundary layer recovering from convex curvature p 545 A91-33747
Method for calculating boundary region corrections in multistep axial turbomachines p 592 A91-34014
A vortex-lattice method for the calculation of vortex sheet roll-up and wing-vortex interaction p 546 A91-34052
Velocity of cavitation bubbles in uniform flowfield high and low Reynolds number p 592 A91-34127
Effect of geometrical disturbance on vortex asymmetry p 547 A91-34136
Hypersonic leeside flow computations using centered schemes for Euler equations p 548 A91-34187
Inviscid flow about a double ellipse p 549 A91-34210
Numerical simulation of vortices motion in presence of solid boundaries p 549 A91-34213
Temporally and spatially resolved flow in a two-stage axial compressor. I - Experiment
[ASME PAPER 90-GT-259] p 551 A91-34789
Three-dimensional flowfields inside a transonic compressor with swept blades
[ASME PAPER 90-GT-359] p 552 A91-34791
Similarity analysis of compressor tip clearance flow structure
[ASME PAPER 90-GT-153] p 552 A91-34793
Computations for a jet impinging obliquely on a flat surface p 554 A91-35985
A pressure flux-split technique for computation of inlet flow behavior p 595 N91-21068
Zonal analysis of two high-speed inlets p 596 N91-21089
A highly efficient engineering tool for three-dimensional scramjet flowfield and heat transfer computations p 596 N91-21098
Infrared thermography for the qualitative aerodynamic study of a slender body
[ISL-R-122/89] p 555 N91-21104
Low speed wind tunnel investigation of propeller slipstream aerodynamic effects on different nacelle/wing combinations. Part 2: Propeller slipstream flow field surveys (velocity components, dynamic, total and static pressure distributions) at zero angle of attack and high power
[FFA-TN-1990-24-PT-2] p 555 N91-21109
Hot gas ingestion test results of a two-poster vectored thrust concept with flow visualization in the NASA Lewis 9- x 15-foot low speed wind tunnel
[NASA-TM-103258] p 556 N91-21116
Investigation of nose bluntness and angle of attack effects on slender bodies in viscous hypertension flows
[NASA-CR-188153] p 557 N91-21117
Prediction of unsteady transonic separated flow for missile applications
[AD-A231259] p 557 N91-21120
Lift and rolling moment due to spoilers on wings at subsonic speeds
[ESDU-90030] p 572 N91-21129
An experimental study of exit flow patterns in a multistage compressor in rotating stall
[AD-A231353] p 580 N91-21143
CFD research and systems in Kawasaki Heavy Industries and its future prospects p 596 N91-21382
CFD for hypersonic propulsion
[NASA-TM-103791] p 597 N91-21447
Application of computational fluid dynamics in high speed aeropropulsion
[NASA-TM-103780] p 598 N91-21458
Method and apparatus for detecting laminar flow separation and reattachment
[NASA-CASE-LAR-13952-2-SB] p 598 N91-21472
Aeropropulsive characteristics of canted twin pitch-vectoring nozzles at Mach 0.20 to 1.20
[NASA-TP-3060] p 558 N91-22069
Grid generation about complex three-dimensional aircraft configurations
[NASA-CR-188097] p 558 N91-22071
An investigation into the extent and effects of spanwise flow in the boundary layer of a helicopter rotor in hover
[BU-519] p 560 N91-22089
Flight test to determine feasibility of a proposed airborne wake vortex detection concept
[NASA-TM-102672] p 563 N91-22096
Forebody vortex control p 573 N91-22110
Water tunnel flow visualisation of vortex breakdown over the F/A-18
[ARL-FLIGHT-MECH-R-179] p 600 N91-22511
FLOW GEOMETRY
Development of a general multiblock flow solver for complex configurations p 605 A91-34230
Zonal analysis of two high-speed inlets p 596 N91-21089
FLOW STABILITY
A numerical study of interfacial instabilities at high Mach numbers p 549 A91-34198
Computation of supersonic and low subsonic cascade flows using an explicit Navier-Stokes technique and the kappa-epsilon turbulence model p 596 N91-21072
Numerical simulation of swept-wing flows
[NASA-CR-188201] p 560 N91-22095
FLOW VELOCITY
Velocity of cavitation bubbles in uniform flowfield high and low Reynolds number p 592 A91-34127
Solution method for viscous flows at all speeds in complex domains p 548 A91-34185
Three-dimensional wake decay inside of a compressor cascade and its influence on the downstream unsteady flow field. I - Wake decay characteristics in the flow passage. II - Unsteady flow field downstream of the stator
[ASME PAPER 90-GT-21] p 551 A91-34786
Temporally and spatially resolved flow in a two-stage axial compressor. I - Experiment
[ASME PAPER 90-GT-259] p 551 A91-34789
Detection of a rotating stall precursor in isolated axial flow compressor rotors
[ASME PAPER 90-GT-157] p 552 A91-34795
Separating boundary layer response to an unsteady turbulent environment
[AD-A231483] p 559 N91-22081
Flight test to determine feasibility of a proposed airborne wake vortex detection concept
[NASA-TM-102672] p 563 N91-22096
Development of an optical volumetric flowmeter
[PB91-136481] p 601 N91-22550
FLOW VISUALIZATION
Three-dimensional flow near the blade/endwall junction of a gas turbine - Visualization in a large-scale cascade simulator
[ASME PAPER 90-WA/HT-4] p 544 A91-32958
Hot gas ingestion test results of a two-poster vectored thrust concept with flow visualization in the NASA Lewis 9- x 15-foot low speed wind tunnel
[NASA-TM-103258] p 556 N91-21116
Flow visualization ion helicopter blades using Acenaphthen
[DLR-FB-90-37] p 598 N91-21466
Effect of planform on induced drag
[BU-500] p 559 N91-22086
Water tunnel flow visualisation of vortex breakdown over the F/A-18
[ARL-FLIGHT-MECH-R-179] p 600 N91-22511
A synchronous strobed laser light sheet for rotor flow visualization
[NASA-TM-4266] p 601 N91-22540
FLOWMETERS
Development of an optical volumetric flowmeter
[PB91-136481] p 601 N91-22550
FLUID DYNAMICS
Oscillatory data for typical configurations p 561 N91-22109
FLUID INJECTION
Compressor drum aerodynamic experiments and analysis with coolant injected at selected locations
[ASME PAPER 90-GT-151] p 552 A91-34794

FLUID MECHANICS
GAMM-Conference on Numerical Methods in Fluid Mechanics, 8th, Delft University of Technology, Netherlands, Sept. 27-29, 1989, Proceedings p 592 A91-34176

FLUTTER
Optimal design of metal and composite thin-walled structures with flutter constraint p 591 A91-32650
Reduction of aerodynamic augmented states in active flutter suppression systems p 580 A91-33535
A leading-edge control surface
[BU-508] p 559 N91-22087
Flutter suppression of an aircraft wing using a control surface
[BU-506] p 583 N91-22133
Fourth NASA Workshop on Computational Control of Flexible Aerospace Systems, part 2
[NASA-CP-10065-PT-2] p 587 N91-22331
An overview of the active flexible wing program p 583 N91-22332
Design and test of three active flutter suppression controllers p 583 N91-22334
Roll plus maneuver load alleviation control system designs for the active flexible wing wind-tunnel model p 584 N91-22335

FLUTTER ANALYSIS
Shape sensitivity analysis of flutter response of a *laminated wing* *p 571 A91-34144*
A frequency domain maximum likelihood identification scheme with application to flight flutter data analysis p 581 A91-35576
Span reduction effects on the flutter characteristics of arrow-wing supersonic transport configurations
[NASA-TP-3077] p 572 N91-21127
Flutter suppression of an aircraft wing using a control surface
[BU-506] p 583 N91-22133

FLY BY WIRE CONTROL
Civil air transport: A fresh look at power-by-wire and fly-by-light p 584 N91-23053

FLYING PLATFORMS
Airborne gravimetry and the Global Positioning System p 602 A91-33634

FOKKER AIRCRAFT
3D Euler flows around modern airplanes p 549 A91-34201

FORCE DISTRIBUTION
Computer program for the calculation of normal force and pitching moment of forebody-cylinder combinations at angles of attack up to 90 degrees and Mach numbers up to 5, including effects of conical boat-tailing
[ESDU-90034] p 555 N91-21102

FORCED VIBRATION
Large amplitude oscillations p 561 N91-22108
Oscillatory data for typical configurations p 561 N91-22109

FOREBODIES
Computer program for the calculation of normal force and pitching moment of forebody-cylinder combinations at angles of attack up to 90 degrees and Mach numbers up to 5, including effects of conical boat-tailing
[ESDU-90034] p 555 N91-21102
Forebody vortex control p 573 N91-22110

FORECASTING
FAA aviation forecasts: Fiscal years 1991-2002
[AD-A231721] p 543 N91-22068
Remote sensor observations during WISP90: The use of microwave radiometers, RASS, and ceilometers for detection of aircraft icing conditions
[PB91-131839] p 604 N91-22670

FRACTURE MECHANICS
Fault detection and diagnosis in gas turbines
[ASME PAPER 90-GT-339] p 578 A91-34814
Proceedings of a French-Japanese Seminar on Composite Materials: Processing, Use and Databases p 589 N91-22380
Micromechanisms of quasi-static and fatigue crack *growth in titanium-aluminides* *p 602 N91-22583*

FRACTURE STRENGTH
The flexural strength of unidirectional carbon fibre composites
[BU-509] p 589 N91-22399
Micromechanisms of quasi-static and fatigue crack growth in titanium-aluminides p 602 N91-22583

FREE FLIGHT
Practical methods to evaluate the friction drag coefficient of a projectile in free flight
[ISL-R-123/89] p 555 N91-21105

FREE FLOW
Inviscid flow about a double ellipse p 549 A91-34210

FREE JETS
Interaction between two jets exhausted from nozzles arranged in parallel p 593 A91-34439

FREQUENCY CONTROL
Comparison of 14 decibels versus 20 decibels desired to undesired signal protection ratios
[DOT/FAA/CT-TN89/69] p 608 N91-21833

FREQUENCY RANGES
Comparison of 14 decibels versus 20 decibels desired to undesired signal protection ratios
[DOT/FAA/CT-TN89/69] p 608 N91-21833

FREQUENCY STANDARDS
Comparison of 14 decibels versus 20 decibels desired to undesired signal protection ratios
[DOT/FAA/CT-TN89/69] p 608 N91-21833

FRICTION DRAG
Progress in the prediction of the laminar-turbulent transition for laminar wings - The profile and wing geometries determine the friction drag of an aircraft p 544 A91-33369
Practical methods to evaluate the friction drag coefficient of a projectile in free flight
[ISL-R-123/89] p 555 N91-21105

FRICTION MEASUREMENT
Skin friction measurement techniques for scramjet applications. Phase 1: Preliminary design
[AD-A231899] p 580 N91-22125

FRICTIONLESS ENVIRONMENTS
Computational methods for frictionless contact with application to Space Shuttle Orbiter nose-gear tires
[NASA-TP-3073] p 601 N91-22576

FUEL COMBUSTION
Preliminary calibration of a generic scramjet combustor
[NASA-CR-187539] p 579 N91-21139

FUEL CONSUMPTION
Spanning the globe with jet propulsion
[AIAA PAPER 91-2987] p 577 A91-34111

FUEL TANKS
Use of resin composites for cryogenic tankage p 588 A91-34287

FUEL-AIR RATIO
An experimental investigation into NO(x) control of a gas turbine combustor and augmentor tube incorporating a catalytic reduction system
[AD-A231427] p 580 N91-22124

FUNCTIONAL DESIGN SPECIFICATIONS
Integrated flight/propulsion control system design based on a decentralized, hierarchical approach
[NASA-TM-103678] p 579 N91-21137

FUSELAGES
Stability analysis of a fuselage side
[FFA-TN-1990-32] p 599 N91-21568

G

GALLIUM ARSENIDES
Stand-alone vs. embedded GPS user equipment - The exploration of new standards p 564 A91-33616

GAS DYNAMICS
Interaction between two jets exhausted from nozzles arranged in parallel p 593 A91-34439

GAS GENERATORS
An experimental investigation into NO(x) control of a gas turbine combustor and augmentor tube incorporating a catalytic reduction system
[AD-A231427] p 580 N91-22124

GAS TURBINE ENGINES
Finite-element analysis of turbulent flow in annular exhaust diffusers of gas turbine engines p 577 A91-32700
Analysis of bearing incidents in aircraft gas turbine mainshaft bearings p 591 A91-33464
Evaluating thermographic phosphors in an operating turbine engine
[ASME PAPER 90-GT-266] p 593 A91-34810
Fast response wall pressure measurement as a means of gas turbine blade fault identification
[ASME PAPER 90-GT-341] p 578 A91-34813
Fault detection and diagnosis in gas turbines
[ASME PAPER 90-GT-339] p 578 A91-34814
Design of robust controllers for gas turbine engines
[ASME PAPER 90-GT-113] p 578 A91-34815
Using a locally one-dimensional method for solving the *heat conductivity equation to determine the thermal state* of cooled rotor disks p 594 A91-35742
Calculation of the cooling system of small-size blades of high-temperature gas turbine engines p 594 A91-35743
Methods for the optimization of the testing and modeling of control systems for gas turbine engines --- Russian book p 579 A91-35815
Control of the working cycle of gas turbine engines (2nd revised and enlarged edition) --- Russian book p 579 A91-35822
Computer program for estimating performance of air-breathing aircraft engines
[NASA-TM-4254] p 573 N91-22103
Experimental study of radiation from coated turbine blades p 580 N91-22122
An experimental investigation into NO(x) control of a gas turbine combustor and augmentor tube incorporating a catalytic reduction system
[AD-A231427] p 580 N91-22124
Feasibility study for the qualification of an economically advantageous Ti-6Al-4V bearing housing for gas turbine engine application by powder metal manufacturing technology
[AD-A231666] p 601 N91-22564

GAS TURBINES
Three-dimensional flow near the blade/endwall junction of a gas turbine - Visualization in a large-scale cascade simulator
[ASME PAPER 90-WA/HT-4] p 544 A91-32958
Dynamic analysis technique of centrifugal impellor with split blades p 593 A91-35498

GEARS
Linear and non-linear dynamic models of a geared rotor-bearing system p 594 A91-35536

GENERAL AVIATION AIRCRAFT
Starship - Bright newcomer in a conservative firmament p 571 A91-34122

GEODESY
Bifurcation analysis of the longitudinal dynamics of a simple powered lifting hypersonic vehicle
[AD-A230826] *p 557 N91-21118*

GEODETIC SURVEYS
Applying kinematic GPS techniques at our nation's airports p 565 A91-33633

GLAZES
Modeling of surface roughness effects on glaze ice accretion p 562 A91-35107

GLIDE LANDINGS
Improved landing aid availability through the use of new criteria p 567 A91-33660

GLIDE PATHS
A fast and low-cost validation technique for ILS and MLS p 565 A91-33630
Improved landing aid availability through the use of new criteria p 567 A91-33660
The effect of the microwave landing system on airport capacity p 561 A91-33668

GLOBAL POSITIONING SYSTEM
The Loran Early Implementation Project - Gateway for GPS p 563 A91-33607
Integrated inertial navigation system/Global Positioning System (INS/GPS) for manned return vehicle autoland application p 586 A91-33609
Stand-alone vs. embedded GPS user equipment - The exploration of new standards p 564 A91-33616
Ashtech XII GPS technology p 564 A91-33622
COTS GPS C/A-code receivers with pseudolites for range PLS application --- Commercial Off-The-Shelf receivers for Position Location System p 564 A91-33623
A five channel low cost GPS receiver p 564 A91-33624
Applying kinematic GPS techniques at our nation's airports p 565 A91-33633
Airborne gravimetry and the Global Positioning System p 602 A91-33634
Area navigation capability in a miniature airborne GPS receiver p 566 A91-33636
Uliss G, a fully integrated 'all-in-one' and 'all-in-view' inertia-GPS unit p 566 A91-33644
Flight test results of a tightly integrated RLG-based Global Positioning System/inertial navigation system p 566 A91-33645
Impact of navigation accuracy on the intervention rate in a highly automated air traffic control system p 566 A91-33647
ISS - A combined terrain topography referenced navigation system p 566 A91-33649
Terrain referenced navigation p 567 A91-33651
Global Positioning System (GPS) autonomous navigation p 567 A91-33653
Kinematic GPS - Resolving integer ambiguities on the fly p 567 A91-33661

GRAPHITE
Resistivity of pristine and intercalated graphite fiber epoxy composites p 589 A91-35949

GRAPHITE-EPOXY COMPOSITES
Significance of residual curing strains in composite structure repair technology p 590 A91-32461
Thermal spikes on CFRP laminates - Assessment of *microdamage and its consequences on fatigue life* p 588 A91-32549
Aeroelastic optimum design of composite rotor blade with returning wake effect p 570 A91-32646
Cost-efficient manufacturing of composite structures p 590 N91-23048

GRAVIMETRY
Airborne gravimetry and the Global Positioning System p 602 A91-33634

GREEN'S FUNCTIONS
Green's function solution to radiative heat transfer between longitudinal gray fins p 593 A91-35117
GRID GENERATION (MATHEMATICS)
Computational Fluid Dynamics Symposium on Aeropropulsion
[NASA-CP-3078] p 554 N91-21062
Finite element methods for integrated aerodynamic heating analysis
[NASA-CR-188079] p 554 N91-21101
MATGRID, a program for generation of C-H and C-O topology grids around wing/body configurations: User's guide
[FFA-TN-1991-03] p 556 N91-21110
Application of mesh generation to complex 3-D configurations
[AGARD-AR-268] p 598 N91-21464
Grid generation about complex three-dimensional aircraft configurations
[NASA-CR-188097] p 558 N91-22071
GROUND EFFECT (AERODYNAMICS)
Forces and pressures induced on circular plates by a single lifting jet in ground effect
[NASA-TM-102816] p 558 N91-22077
Small-scale experiments in STOVL ground effects
[NASA-TM-102813] p 560 N91-22091
Flow investigation of a ground effect vehicle
[BU-516] p 600 N91-22528
GROUND SUPPORT EQUIPMENT
A guide to ground vehicle operations on the airport
[AD-A231077] p 585 N91-21158
Snow roads and runways
[AD-A231490] p 586 N91-22138
GROUND TESTS
Flowfield and vehicle parameter influence on results of engineering aerothermal methods p 544 A91-33378
Aerothermodynamic design appraisal of noise suppressors for F/A-18 engine run-up facilities at RAAF Williamtown
[ARL-PROP-R-177] p 585 N91-22136
GUIDANCE (MOTION)
The advantages of velocity vector referencing in proportional navigation p 581 A91-33611
GUST LOADS
Airfoils in two- and three-dimensional gust fields p 546 A91-34073
GUSTS
Fast response gust measurement device p 603 N91-22659
GYROSCOPES
START - A broad application spectrum gyro for the 1990's p 591 A91-33604
Flight test results of a tightly integrated RLG-based Global Positioning System/inertial navigation system p 566 A91-33645
GG1308 Ring Laser Gyro Inertial Measurement Systems - Honeywell's low-cost solution for tactical applications p 576 A91-33655
The next frontier for strapdown RLG inertial systems - Precision navigation p 576 A91-33656
Ring laser gyro applications for tactical missiles - The Army TACMS solution p 576 A91-33657
Flight test to determine feasibility of a proposed airborne wake vortex detection concept
[NASA-TM-102672] p 563 N91-22096

H

H-60 HELICOPTER
Flight evaluation of the Integrated Inertial Sensor Assembly (IISA) on a helicopter p 581 A91-33639
HANDBOOKS
Air traffic control memory: A field survey
[DOT/FAA/CT-TN90/60] p 569 N91-22101
HARMONIC CONTROL
Results of the HHC wind tunnel tests, 1986 - 1988
[DLR-FB-90-42] p 582 N91-21152
HARMONICS
Large amplitude oscillations p 561 N91-22108
HARRIER AIRCRAFT
The compressed aeronautical chart database - Support of naval aircraft's digital moving map systems p 563 A91-33608
HAZARDS
Model rocketry hazard study
[DOT/FAA/CT-TN90/28] p 587 N91-21238
HEAT RESISTANT ALLOYS
Service temperature estimation of turbine blades based on microstructural observations
[ASME PAPER 90-GT-23] p 578 A91-34811
Influence of a magnetic field during directional solidification of MAR-M 246 + Hf superalloy
[NASA-CR-184114] p 590 N91-22416
HEAT TRANSFER
Effects of heat transfer on aerodynamics and possible implications for wind tunnel tests p 545 A91-33802
A numerical study of hypersonic stagnation heat transfer predictions at a coordinate singularity p 548 A91-34193
An approximate method for determining friction and heat transfer in chemically nonequilibrium flow past bodies at angle of attack p 553 A91-35660
Calculation of the cooling system of small-size blades of high-temperature gas turbine engines p 594 A91-35743
Zonal analysis of two high-speed inlets p 596 N91-21089
A highly efficient engineering tool for three-dimensional scramjet flowfield and heat transfer computations p 596 N91-21098
HELICOPTER CONTROL
Results of the HHC wind tunnel tests, 1986 - 1988
[DLR-FB-90-42] p 582 N91-21152
Eigenspace design of helicopter flight control systems
[AD-A231588] p 582 N91-21153
HELICOPTER DESIGN
Aeroelastic optimum design of composite rotor blade with returning wake effect p 570 A91-32646
Rotors in the wind tunnel - DLR helicopter research methods in the German-Dutch Wind Tunnel p 584 A91-33371
Helicopter vibration reduction using structural optimization with aeroelastic/multidisciplinary constraints - A survey p 570 A91-33527
Integrated multidisciplinary design optimization of rotorcraft p 570 A91-33528
Optimum aeroelastic design of helicopter rotors for longitudinal handling qualities improvement p 570 A91-33531
Integrated aerodynamic load/dynamic optimization of helicopter rotor blades p 571 A91-33532
Optimization of helicopter airframe structures for vibration reduction - Considerations, formulations, and applications p 571 A91-33533
Advanced rotorcraft transmission program
[NASA-TM-103276] p 598 N91-21531
HELICOPTER PERFORMANCE
Simulation of nap-of-the-Earth flight in helicopters
[NASA-TM-102830] p 572 N91-21131
Eigenspace design of helicopter flight control systems
[AD-A231588] p 582 N91-21153
HELICOPTER PROPELLER DRIVE
Advanced rotorcraft transmission program
[NASA-TM-103276] p 598 N91-21531
HELICOPTER TAIL ROTORS
A study of rotor broadband noise mechanisms and helicopter tail rotor noise
[NASA-CR-177565] p 607 N91-21829
HELICOPTER WAKES
The location of acoustic blade-vortex interaction - A further step toward an understanding of helicopter noise p 607 A91-33368
Aerodynamic parameter studies and sensitivity analysis for rotor blades in axial flight
[NASA-CR-187524] p 558 N91-22078
HELICOPTERS
Helicopter rotor dynamics optimization with experimental verification p 570 A91-33530
Test program for Honeywell/DND Helicopter Integrated Navigation System (HINS) p 565 A91-33626
Heli/SITAN - A terrain referenced navigation algorithm for helicopters p 568 A91-33664
Active vibration control using fixed order dynamic compensation with frequency shaped cost functionals p 604 A91-33932
A study of rotor broadband noise mechanisms and helicopter tail rotor noise
[NASA-CR-177565] p 607 N91-21829
Propagation of helicopter noise in the low atmosphere layers
[ISL-CO-203/90] p 607 N91-21830
The human factors relating to escape and survival from helicopters ditching in water
[AGARD-AG-305(F)] p 563 N91-22099
A synchronous strobed laser light sheet for rotor flow visualization
[NASA-TM-4266] p 601 N91-22540
HELIUM
Investigations into shock-induced enhancement of mixing and combustion in supersonic burners
[AD-A231750] p 589 N91-22407
HELMET MOUNTED DISPLAYS
Suppression of biodynamic interference in head-tracked teleoperation
[NASA-TM-103833] p 577 N91-21134
HEURISTIC METHODS
Generalized heuristics for the gate assignment problem p 605 A91-35100
HIGH ASPECT RATIO
The flying wing supersonic transport p 571 A91-34164
HIGH REYNOLDS NUMBER
A review of near-wall Reynolds-stress
[NASA-CR-4369] p 559 N91-22080
HIGH STRENGTH ALLOYS
Service temperature estimation of turbine blades based on microstructural observations
[ASME PAPER 90-GT-23] p 578 A91-34811
HIGH TEMPERATURE GASES
Hot gas ingestion test results of a two-poster vectored thrust concept with flow visualization in the NASA Lewis 9- x 15-foot low speed wind tunnel
[NASA-TM-103258] p 556 N91-21116
HILBERT SPACE
State stability of a system of integro-differential equations of nonstationary aeroelasticity p 595 A91-35785
HOVERING
An investigation into the extent and effects of spanwise flow in the boundary layer of a helicopter rotor in hover
[BU-519] p 560 N91-22089
HOVERING STABILITY
Nonlinear behavior of a rotorcraft model during air resonance p 581 A91-34816
HUMAN BEHAVIOR
Human performance factors in aircraft accident investigation
[SAE PAPER 892608] p 562 A91-34912
HUMAN FACTORS ENGINEERING
The human factors relating to escape and survival from helicopters ditching in water
[AGARD-AG-305(F)] p 563 N91-22099
Design of an intelligent information system for in-flight emergency assistance p 606 N91-22792
HUMAN PERFORMANCE
Human performance factors in aircraft accident investigation
[SAE PAPER 892608] p 562 A91-34912
HUMAN REACTIONS
Design methodology for a community response questionnaire on sonic boom exposure
[NASA-CR-187503] p 608 N91-22830
HYBRID NAVIGATION SYSTEMS
Uliss G, a fully integrated 'all-in-one' and 'all-in-view' inertia-GPS unit p 566 A91-33644
HYDRAULIC TEST TUNNELS
Water tunnel flow visualisation of vortex breakdown over the F/A-18
[ARL-FLIGHT-MECH-R-179] p 600 N91-22511
HYDROCARBONS
Flow visualization ion helicopter blades using Acenaphthen
[DLR-FB-90-37] p 598 N91-21466
HYDROGEN FUELS
Preliminary calibration of a generic scramjet combustor
[NASA-CR-187539] p 579 N91-21139
HYPERBOLIC SYSTEMS
Airfoils in two- and three-dimensional gust fields p 546 A91-34073
HYPERSONIC AIRCRAFT
Langley develops thermal management concept for hypersonic aircraft p 570 A91-33323
HYTEX - Demonstrator for hypersonic flight up to Mach 5 p 571 A91-34260
Automated flight test management system
[NASA-CR-186011] p 574 N91-22117
HYPERSONIC FLIGHT
Fully coupled implicit method for thermochemical nonequilibrium air at suborbital flight speeds p 544 A91-33380
CFD for hypersonic propulsion
[NASA-TM-103791] p 597 N91-21447
Application of computational fluid dynamics in high speed aeropropulsion
[NASA-TM-103780] p 598 N91-21458
Skin friction measurement techniques for scramjet applications. Phase 1: Preliminary design
[AD-A231899] p 580 N91-22125
HYPERSONIC FLOW
Computation of flowfields for projectiles in hypersonic chemically reacting flows p 544 A91-33379
Hypersonic flow simulation for blunt bodies at incidence p 546 A91-34070
Numerical simulation of laminar hypersonic flow past blunt bodies including high temperature effects p 547 A91-34180
Hypersonic leeside flow computations using centered schemes for Euler equations p 548 A91-34187
Non-equilibrium hypersonic flow computations by implicit second-order upwind finite-elements p 548 A91-34191

A numerical study of hypersonic stagnation heat transfer predictions at a coordinate singularity p 548 A91-34193
Viscous, hypersonic flows over compression ramps p 548 A91-34194
Split-matrix marching methods for three-dimensional viscous and inviscid hypersonic flows p 549 A91-34206
Inertial aerosol precipitation on ogival bodies of revolution in high-velocity flow p 553 A91-35784
Investigation of nose bluntness and angle of attack effects on slender bodies in viscous hypertension flows [NASA-CR-188153] p 557 N91-21117
Preliminary calibration of a generic scramjet combustor [NASA-CR-187539] p 579 N91-21139

HYPERSONIC VEHICLES
Use of resin composites for cryogenic tankage p 588 A91-34287
Bifurcation analysis of the longitudinal dynamics of a simple powered lifting hypersonic vehicle [AD-A230826] p 557 N91-21118

HYPERSONICS
CFD for hypersonic propulsion [NASA-TM-103791] p 597 N91-21447

HYSTERESIS
Unsteady aerodynamics of slender wings p 560 N91-22105

I

ICE FORMATION
Modeling of surface roughness effects on glaze ice accretion p 562 A91-35107
Elevator deflections on the icing process p 572 A91-35427
Analysis of three icing test flights reaching the aircraft-referred icing degree severe [DLR-FB-90-34] p 562 N91-21123
Impact of icing on Unmanned Aerial Vehicle (UAV) operations [AD-A231191] p 562 N91-21124
Remote sensor observations during WISP90: The use of microwave radiometers, RASS, and ceilometers for detection of aircraft icing conditions [PB91-131839] p 604 N91-22670

IMAGE MOTION COMPENSATION
Motion compensation for ASTOR long range SAR p 575 A91-33625

IMAGE PROCESSING
A model-based method for object recognition p 605 A91-35241
Automated extraction of airport runway patterns from radar imagery [AD-A231809] p 600 N91-22480

IMAGING TECHNIQUES
Comparison of UNL laser imaging and sizing system and a phase Doppler system for analyzing sprays from a NASA nozzle [NASA-CR-185239] p 598 N91-21485

IMPELLERS
Dynamic analysis technique of centrifugal impellor with split blades p 593 A91-35498

IN-FLIGHT MONITORING
In-flight system for helicopter blade inspection p 575 A91-33268
Fault detection and diagnosis in gas turbines [ASME PAPER 90-GT-339] p 578 A91-34814

INCIDENCE
Hypersonic flow simulation for blunt bodies at incidence p 546 A91-34070

INCOMPRESSIBLE FLOW
Computation of unsteady incompressible viscous flow around airfoils p 546 A91-34074
Vorticity equation solutions for slender wings at high incidence p 547 A91-34126
Solution of the 3-D, incompressible Navier-Stokes equations for the simulation of vortex breakdown p 593 A91-34181
Rotordynamic coefficients for partially roughened pump annular seals p 593 A91-34822

INDUSTRIES
Business plans for the Institute for Aviation Research, FY 1990 - FY 1995 [IAR-89-15] p 609 N91-23020

INERTIA
The effect of shear and rotary inertia of a rotor at its critical speeds p 592 A91-34125

INERTIAL GUIDANCE
GG1308 Ring Laser Gyro Inertial Measurement Systems - Honeywell's low-cost solution for tactical applications p 576 A91-33655

INERTIAL NAVIGATION
Integrated inertial navigation system/Global Positioning System (INS/GPS) for manned return vehicle autoland application p 586 A91-33609
Demonstration of a ring laser gyro system for pointing and stabilization applications p 575 A91-33627
INS reset removal for enhanced post-flight performance analysis p 565 A91-33628
Flight evaluation of the Integrated Inertial Sensor Assembly (IISA) on a helicopter p 581 A91-33639
Uliss G, a fully integrated 'all-in-one' and 'all-in-view' inertia-GPS unit p 566 A91-33644
Flight test results of a tightly integrated RLG-based Global Positioning System/inertial navigation system p 566 A91-33645
ISS - A combined terrain topography referenced navigation system p 566 A91-33649
Terrain referenced navigation p 567 A91-33651
Precision aided inertial navigation using SAR and digital map data p 567 A91-33652
GG1308 Ring Laser Gyro Inertial Measurement Systems - Honeywell's low-cost solution for tactical applications p 576 A91-33655
The next frontier for strapdown RLG inertial systems - Precision navigation p 576 A91-33656

INERTIAL PLATFORMS
GG1308 Ring Laser Gyro Inertial Measurement Systems - Honeywell's low-cost solution for tactical applications p 576 A91-33655

INERTIAL REFERENCE SYSTEMS
Failure management in spatio-temporal redundant, integrated navigation and flight control reference-systems p 581 A91-33640

INFORMATION FLOW
Development and testing of controller performance evaluation methodology for multi-input/multi-output digital control systems p 584 N91-22337

INFORMATION RETRIEVAL
Design of an intelligent information system for in-flight emergency assistance p 606 N91-22792

INFORMATION SYSTEMS
Design of an intelligent information system for in-flight emergency assistance p 606 N91-22792

INFORMATION TRANSFER
Analysis of routine communication in the air traffic control system [NASA-CR-188116] p 600 N91-22475

INFRARED IMAGERY
Experimental performance of a binary phase-only optical correlator using visual and infrared imagery p 606 A91-32707
Terrain referenced navigation p 567 A91-33651
Terrain Aided Navigation - Current status, techniques for flat terrain and reference data requirements p 567 A91-33663
Infrared thermography for the qualitative aerodynamic study of a slender body [ISL-R-122/89] p 555 N91-21104

INJECTORS
Investigations into shock-induced enhancement of mixing and combustion in supersonic burners [AD-A231750] p 589 N91-22407

INLET FLOW
The influence of inlet swirl distortions on the performance of a jet propulsion two-stage axial compressor [ASME PAPER 90-GT-147] p 552 A91-34790
Forcing function effects on rotor periodic aerodynamic response [ASME PAPER 90-GT-109] p 553 A91-34798
A pressure flux-split technique for computation of inlet flow behavior p 595 N91-21068
Zonal analysis of two high-speed inlets p 596 N91-21089
Hot gas ingestion test results of a two-poster vectored thrust concept with flow visualization in the NASA Lewis 9- x 15-foot low speed wind tunnel [NASA-TM-103258] p 556 N91-21116

INSTRUMENT LANDING SYSTEMS
A fast and low-cost validation technique for ILS and MLS p 565 A91-33630
The design, simulation and implementation of an accurate positioning system for automatic flight inspection p 566 A91-33646
Improved landing aid availability through the use of new criteria p 567 A91-33660

INTAKE SYSTEMS
Direct cast titanium aluminide strip [AD-A231906] p 590 N91-22424

INTEGRAL EQUATIONS
State stability of a system of integro-differential equations of nonstationary aeroelasticity p 595 A91-35785

INTERACTIONAL AERODYNAMICS
Conical Euler simulation of wing rock for a delta wing planform p 580 A91-33536
Laminar shock/boundary-layer interaction - A numerical test problem p 545 A91-34033
Interference-free measurements of the subsonic aerodynamics of slanted-base ogive cylinders p 547 A91-34130
Temporally and spatially resolved flow in a two-stage axial compressor. I - Experiment [ASME PAPER 90-GT-259] p 551 A91-34789
Acoustic and aerodynamic study of a pusher-propeller aircraft model [NASA-TP-3040] p 607 N91-21828
Approximate methods for predicting the lifting characteristics of wing-body combinations p 558 N91-22074
Signal blending in control systems structural interactions [BU-505] p 583 N91-22132
The use of axisymmetric flow for investigation of shock wave-boundary layer interactions [BU-520] p 600 N91-22529

INTERCALATION
Resistivity of pristine and intercalated graphite fiber epoxy composites p 589 A91-35949

INTERCEPTION
The advantages of velocity vector referencing in proportional navigation p 581 A91-33611

INTERFEROMETERS
The single antenna interferometer [DE91-007128] p 597 N91-21407

INTERFEROMETRY
The single antenna interferometer [DE91-007128] p 597 N91-21407

INTERMETALLICS
Superplasticity in a Ti3Al-base alloy stabilized by Nb, V and Mo p 589 A91-34841

INVISCID FLOW
Airfoils in two- and three-dimensional gust fields p 546 A91-34073
Non-equilibrium hypersonic flow computations by implicit second-order upwind finite-elements p 548 A91-34191
Split-matrix marching methods for three-dimensional viscous and inviscid hypersonic flows p 549 A91-34206
Inviscid flow about a double ellipse p 549 A91-34210
Vortex element methods for fluid dynamic analysis of engineering systems --- Book p 594 A91-35539
Euler analysis of transonic stator-rotor interaction using a finite volume method p 554 A91-35984
Numerical study of the aerodynamic effects of using sulfur hexafluoride as a test gas in wind tunnels [NASA-TP-3086] p 558 N91-22070

IONIZED GASES
MHD drag and heat transfer of a sphere in supersonic flow of a partially ionized gas p 607 A91-35791

ITERATIVE SOLUTION
Computation of the viscous flow past a prolate spheroid at incidence p 550 A91-34216
A functional method for the approximate solution of a transonic problem p 550 A91-34398

J

JET AIRCRAFT
Flow investigation of a ground effect vehicle [BU-516] p 600 N91-22528

JET ENGINE FUELS
Langley develops thermal management concept for hypersonic aircraft p 570 A91-33323

JET ENGINES
Process control to set Mach number ratios for jet-engine intake measurements - Development of an automatic Mach-number regulator p 584 A91-33373

JET FLOW
Infrared thermography for the qualitative aerodynamic study of a slender body [ISL-R-122/89] p 555 N91-21104

JET IMPINGEMENT
Computations for a jet impinging obliquely on a flat surface p 554 A91-35985

JET PROPULSION
Spanning the globe with jet propulsion [AIAA PAPER 91-2987] p 577 A91-34111
The influence of inlet swirl distortions on the performance of a jet propulsion two-stage axial compressor [ASME PAPER 90-GT-147] p 552 A91-34790

JOINED WINGS
Aerodynamic and structural studies of joined-wing aircraft p 571 A91-33534

JOURNAL BEARINGS
Dynamic modelling and analysis of a magnetically suspended flexible rotor p 587 N91-21208

K

K-EPSILON TURBULENCE MODEL
Computations for a jet impinging obliquely on a flat surface p 554 A91-35985
Computation of supersonic and low subsonic cascade flows using an explicit Navier-Stokes technique and the kappa-epsilon turbulence model p 596 N91-21072
KALMAN FILTERS
Motion compensation for ASTOR long range SAR p 575 A91-33625
INS reset removal for enhanced post-flight performance analysis p 565 A91-33628
Uliss G, a fully integrated 'all-in-one' and 'all-in-view' inertia-GPS unit p 566 A91-33644
Terrain referenced navigation p 567 A91-33651
Kinematic GPS - Resolving integer ambiguities on the fly p 567 A91-33661
Terrain Aided Navigation - Current status, techniques for flat terrain and reference data requirements p 567 A91-33663
Flight path reconstruction using extended Kalman filtering techniques
[DLR-FB-90-41] p 555 N91-21108
A preliminary evaluation of an F100 engine parameter estimation process using flight data
[NASA-TM-4216] p 597 N91-21446
KINEMATICS
Applying kinematic GPS techniques at our nation's airports p 565 A91-33633
Kinematic GPS - Resolving integer ambiguities on the fly p 567 A91-33661
KNOWLEDGE BASES (ARTIFICIAL INTELLIGENCE)
Knowledge-based target recognition system evolution p 577 A91-35978
KUTTA-JOUKOWSKI CONDITION
A functional method for the approximate solution of a transonic problem p 550 A91-34398
Blunt trailing edge analysis of supercritical airfoils by a Navier-Stokes code
[NAL-TR-1075-T] p 556 N91-21114

L

LAMINAR BOUNDARY LAYER
Effects of heat transfer on aerodynamics and possible implications for wind tunnel tests p 545 A91-33802
Laminar shock/boundary-layer interaction - A numerical test problem p 545 A91-34033
Calculation of a compressible laminar boundary layer on a tapered body of bielliptical cross section p 553 A91-35796
Practical methods to evaluate the friction drag coefficient of a projectile in free flight
[ISL-R-123/89] p 555 N91-21105
An experimental study of a three-dimensional swept-back wing with suction laminar-flow-control
[NAL-TR-1072] p 556 N91-21113
LAMINAR FLOW
Numerical simulation of laminar hypersonic flow past blunt bodies including high temperature effects p 547 A91-34180
A streamwise upwind algorithm applied to vortical flow over a delta wing p 548 A91-34192
Numerical investigation of three dimensional laminar flows in a channel with a built-in circular cylinder and wing-type vortex generators p 550 A91-34218
Finite element methods for integrated aerodynamic heating analysis
[NASA-CR-188079] p 554 N91-21101
Method and apparatus for detecting laminar flow separation and reattachment
[NASA-CASE-LAR-13952-2-SB] p 598 N91-21472
LAMINAR FLOW AIRFOILS
Analysis of laminar separation bubble using a simple eddy-viscosity turbulence model p 591 A91-33227
Progress in the prediction of the laminar-turbulent transition for laminar wings - The profile and wing geometries determine the friction drag of an aircraft p 544 A91-33369
LAMINATES
Significance of residual curing strains in composite structure repair technology p 590 A91-32461
Thermal spikes on CFRP laminates - Assessment of microdamage and its consequences on fatigue life p 588 A91-32549
Damage tolerance aspects of ARALL fuselage skin structure (philosophy and experiments) p 588 A91-32573
Cumulative damage problem in pull-through fatigue of C.F.R.P. laminate p 588 A91-32576
Shape sensitivity analysis of flutter response of a laminated wing p 571 A91-34144
LANDING GEAR
Computational methods for frictionless contact with application to Space Shuttle Orbiter nose-gear tires
[NASA-TP-3073] p 601 N91-22576
LANDING SITES
Snow roads and runways
[AD-A231490] p 586 N91-22138
LARGE SPACE STRUCTURES
Fourth NASA Workshop on Computational Control of Flexible Aerospace Systems, part 2
[NASA-CP-10065-PT-2] p 587 N91-22331
LASER ANEMOMETERS
Comparison of UNL laser imaging and sizing system and a phase Doppler system for analyzing sprays from a NASA nozzle
[NASA-CR-185239] p 598 N91-21485
Development of an optical volumetric flowmeter
[PB91-136481] p 601 N91-22550
LASER APPLICATIONS
Hot gas ingestion test results of a two-poster vectored thrust concept with flow visualization in the NASA Lewis 9- x 15-foot low speed wind tunnel
[NASA-TM-103258] p 556 N91-21116
A synchronous strobed laser light sheet for rotor flow visualization
[NASA-TM-4266] p 601 N91-22540
LASER DOPPLER VELOCIMETERS
Temporally and spatially resolved flow in a two-stage axial compressor. I - Experiment
[ASME PAPER 90-GT-259] p 551 A91-34789
Optimization of radio-measuring devices incorporated in onboard laser velocimeters p 576 A91-35738
Comparison of UNL laser imaging and sizing system and a phase Doppler system for analyzing sprays from a NASA nozzle
[NASA-CR-185239] p 598 N91-21485
LASER INDUCED FLUORESCENCE
Evaluating thermographic phosphors in an operating turbine engine
[ASME PAPER 90-GT-266] p 593 A91-34810
LASER SPECTROSCOPY
Evaluating thermographic phosphors in an operating turbine engine
[ASME PAPER 90-GT-266] p 593 A91-34810
LATERAL CONTROL
Roll plus maneuver load alleviation control system designs for the active flexible wing wind-tunnel model p 584 N91-22335
LATERAL STABILITY
Unsteady aerodynamic modelling for aircraft lateral parameter estimation p 581 A91-34162
LAW (JURISPRUDENCE)
A practical approach to Rule 26(c) protective orders in aviation litigation p 608 A91-35121
Airport restrictions - A dilemma of federal preemption and proprietary control p 608 A91-35122
LEADING EDGES
Aspects of the application of an Euler-equation method to the simulation of leading-edge vortex flow p 549 A91-34196
A leading-edge control surface
[BU-508] p 559 N91-22087
Water tunnel flow visualisation of vortex breakdown over the F/A-18
[ARL-FLIGHT-MECH-R-179] p 600 N91-22511
LEAKAGE
Tip leakage flow in axial compressors
[ASME PAPER 90-GT-127] p 552 A91-34792
High temperature performance evaluation of a hypersonic engine ceramic wafer seal
[NASA-TM-103737] p 601 N91-22567
LEGAL LIABILITY
A practical approach to Rule 26(c) protective orders in aviation litigation p 608 A91-35121
General aviation accident liability standards - Why the fuss? p 608 A91-35123
LIAPUNOV FUNCTIONS
State stability of a system of integro-differential equations of nonstationary aeroelasticity p 595 A91-35785
LIFE (DURABILITY)
Damage accumulation and degradation of composite laminates under aircraft service loading: Assessment and prediction, volumes 1 and 2 p 589 N91-22381
LIFE CYCLE COSTS
Stand-alone vs. embedded GPS user equipment - The exploration of new standards p 564 A91-33616
Ring laser gyro applications for tactical missiles - The Army TACMS solution p 576 A91-33657
LIFE SUPPORT SYSTEMS
The human factors relating to escape and survival from helicopters ditching in water
[AGARD-AG-305(F)] p 563 N91-22099
LIFT
A method to calculate the influence of vortex roll-up on the induced drag of wings p 546 A91-34055
Lift and rolling moment due to spoilers on wings at subsonic speeds
[ESDU-90030] p 572 N91-21129
Forces and pressures induced on circular plates by a single lifting jet in ground effect
[NASA-TM-102816] p 558 N91-22077
Aerodynamic parameter studies and sensitivity analysis for rotor blades in axial flight
[NASA-CR-187524] p 558 N91-22078
A quantitative investigation into the aerodynamic coupling effects in a coaxial contra-rotating rotor system
[BU-517] p 574 N91-22120
Flow investigation of a ground effect vehicle
[BU-516] p 600 N91-22528
LIFTING BODIES
A finite-difference, frequency-domain numerical scheme for the solution of the linearized unsteady Euler equations p 595 N91-21067
Bifurcation analysis of the longitudinal dynamics of a simple powered lifting hypersonic vehicle
[AD-A230826] p 557 N91-21118
LIGHT AIRCRAFT
The preliminary aerodynamic design of light aircraft
[BU-504] p 574 N91-22119
LINEAR QUADRATIC GAUSSIAN CONTROL
Design of robust controllers for gas turbine engines
[ASME PAPER 90-GT-113] p 578 A91-34815
Design and test of three active flutter suppression controllers p 583 N91-22334
Roll plus maneuver load alleviation control system designs for the active flexible wing wind-tunnel model p 584 N91-22335
LINEAR SYSTEMS
A frequency domain maximum likelihood identification scheme with application to flight flutter data analysis p 581 A91-35576
LOADS (FORCES)
Roll plus maneuver load alleviation control system designs for the active flexible wing wind-tunnel model p 584 N91-22335
Damage accumulation and degradation of composite laminates under aircraft service loading: Assessment and prediction, volumes 1 and 2 p 589 N91-22381
LORAN
The Loran Early Implementation Project - Gateway for GPS p 563 A91-33607
LOW COST
A five channel low cost GPS receiver p 564 A91-33624
GG1308 Ring Laser Gyro Inertial Measurement Systems - Honeywell's low-cost solution for tactical applications p 576 A91-33655
LOW REYNOLDS NUMBER
Theoretical basis for extrapolation of calibration data of PTC 6 throat tap nozzles
[ASME PAPER 90-JPGC/PTC-1] p 578 A91-34808
Wind tunnel test of a propeller working in a low Reynolds number range
[NAL-TR-1071] p 556 N91-21112
LUBRICATION
Analysis of bearing incidents in aircraft gas turbine mainshaft bearings p 591 A91-33464
LUMPED PARAMETER SYSTEMS
Force and moment transmissibilities through rolling element bearings in a single-stage rotor system p 594 A91-35537

M

MACH NUMBER
Process control to set Mach number ratios for jet-engine intake measurements - Development of an automatic Mach-number regulator p 584 A91-33373
The flying wing supersonic transport p 571 A91-34164
A numerical study of interfacial instabilities at high Mach numbers p 549 A91-34198
Some aspects of the numerical simulation of compressible viscous flow around bluff bodies at low Ma-number p 550 A91-34220
HYTEX - Demonstrator for hypersonic flight up to Mach 5 p 571 A91-34260
Computer program for the calculation of normal force and pitching moment of forebody-cylinder combinations at angles of attack up to 90 degrees and Mach numbers up to 5, including effects of conical boat-tailing
[ESDU-90034] p 555 N91-21102
MAGNETIC BEARINGS
Critical speeds and forced response solutions for active magnetic bearing turbomachinery, part 1 p 587 N91-21209
Critical speeds and forced response solutions for active magnetic bearing turbomachinery, part 2 p 587 N91-21210

MAGNETIC EFFECTS
Influence of a magnetic field during directional solidification of MAR-M 246 + Hf superalloy
[NASA-CR-184114] p 590 N91-22416
MAGNETIC FIELDS
Influence of a magnetic field during directional solidification of MAR-M 246 + Hf superalloy
[NASA-CR-184114] p 590 N91-22416
MAGNETIC SUSPENSION
Magnetic suspension and balance system advanced study, 1989 design p 586 N91-21197
Propulsion simulator for magnetically-suspended wind tunnel models p 586 N91-21198
A solid-state controllable power supply for a magnetic suspension wind tunnel p 585 N91-21199
Dynamic modelling and analysis of a magnetically suspended flexible rotor p 587 N91-21208
MAGNETOHYDRODYNAMIC FLOW
MHD drag and heat transfer of a sphere in supersonic flow of a partially ionized gas p 607 A91-35791
MAINTENANCE
Status of PAVER implementation within the US Air Force
[AD-A231158] p 585 N91-22137
Snow roads and runways
[AD-A231490] p 586 N91-22138
MALFUNCTIONS
Design of an intelligent information system for in-flight emergency assistance p 606 N91-22792
MANAGEMENT SYSTEMS
Automated flight test management system
[NASA-CR-186011] p 574 N91-22117
Status of PAVER implementation within the US Air Force
[AD-A231158] p 585 N91-22137
MANNED REENTRY
Integrated inertial navigation system/Global Positioning System (INS/GPS) for manned return vehicle autoland application p 586 A91-33609
MANUALS
A guide to ground vehicle operations on the airport
[AD-A231077] p 585 N91-21158
Crew chief CAD system interface guide (version 2 - SI)
[AD-A231433] p 606 N91-22734
MANUFACTURING
Feasibility study for the qualification of an economically advantageous Ti-6Al-4V bearing housing for gas turbine engine application by powder metal manufacturing technology
[AD-A231666] p 601 N91-22564
MARINE TECHNOLOGY
A five channel low cost GPS receiver
p 564 A91-33624
MARKOV PROCESSES
Nonlinear filtering of a trajectory message
p 568 A91-33868
MASS BALANCE
Effects of gear box vibration and mass imbalance on the dynamics of multi-stage gear transmissions
[NASA-TM-103695] p 599 N91-21534
MATHEMATICAL MODELS
Flight path reconstruction using extended Kalman filtering techniques
[DLR-FB-90-41] p 555 N91-21108
Vortex bursting over a unit area aspect ratio delta wing using vortex paneling methods
[AD-A231028] p 557 N91-21119
Prediction of unsteady transonic separated flow for missile applications
[AD-A231259] p 557 N91-21120
A simple, analytical, axisymmetric microburst model for downdraft estimation
[NASA-TM-104053] p 573 N91-21132
Fully automatic guidance and control for rotorcraft nap-of-the-Earth flight following planned profiles. Volume 2: Mathematical model
[NASA-CR-177571-VOL-2] p 582 N91-21150
Description and evaluation of an interference assessment for a slotted-wall wind tunnel
[NASA-CR-4352] p 585 N91-21155
Rotary-balance testing for aircraft dynamics
[AGARD-AR-265] p 585 N91-21156
Critical speeds and forced response solutions for active magnetic bearing turbomachinery, part 1
p 587 N91-21209
Critical speeds and forced response solutions for active magnetic bearing turbomachinery, part 2
p 587 N91-21210
Effects of gear box vibration and mass imbalance on the dynamics of multi-stage gear transmissions
[NASA-TM-103695] p 599 N91-21534
Flexible body dynamic stability for high performance aircraft p 574 N91-22318
Sensitivity-based scaling for correlating structural response from different analytical models
[NASA-TM-104042] p 602 N91-22578
MATRIX METHODS
Critical speeds and forced response solutions for active magnetic bearing turbomachinery, part 2
p 587 N91-21210
MAXIMUM LIKELIHOOD ESTIMATES
A frequency domain maximum likelihood identification scheme with application to flight flutter data analysis
p 581 A91-35576
MEASURING INSTRUMENTS
START - A broad application spectrum gyro for the 1990's p 591 A91-33604
Air motion measurements: Past and future
p 603 N91-22653
Air motion measurement uncertainties: Their impact on atmospheric studies p 603 N91-22654
The FIAMS research aircraft or small is beautiful
p 603 N91-22655
Technical presentation of the Merlin's radome: Calibration and data processing p 603 N91-22656
The NASA-ER2 meteorological measurement system: Instrumentaion, calibration and intercomparison results
p 603 N91-22658
Fast response gust measurement device
p 603 N91-22659
Summary of aircraft measuring activities at LAPETH
p 604 N91-22661
MECHANICAL DRIVES
Advanced rotorcraft transmission program
[NASA-TM-103276] p 598 N91-21531
MECHANICAL PROPERTIES
Damage tolerance aspects of ARALL fuselage skin structure (philosophy and experiments)
p 588 A91-32573
MELTING
Direct cast titanium aluminide strip
[AD-A231906] p 590 N91-22424
MEMORY
Air traffic control memory: A field survey
[DOT/FAA/CT-TN90/60] p 569 N91-22101
MEMORY (COMPUTERS)
Proceedings of the 8th NAL Symposium on Aircraft Computational Aerodynamics: Prospects of Computational Fluid Dynamics and Super Computers in Aerospace Science and Technology
[NAL-SP-13] p 596 N91-21379
METAL MATRIX COMPOSITES
Direct cast titanium aluminide strip
[AD-A231906] p 590 N91-22424
METAL STRIPS
Direct cast titanium aluminide strip
[AD-A231906] p 590 N91-22424
METEOROLOGICAL PARAMETERS
Propagation of helicopter noise in the low atmosphere layers
[ISL-CO-203/90] p 607 N91-21830
The FIAMS research aircraft or small is beautiful
p 603 N91-22655
METEOROLOGICAL RADAR
Modern aviation weather systems for efficient flight management p 602 A91-33648
METEOROLOGICAL RESEARCH AIRCRAFT
The FIAMS research aircraft or small is beautiful
p 603 N91-22655
The improvement of the installation of the DLR research aircraft Falcon: Description and first results
p 603 N91-22657
Turbulence profiling in the atmospheric boundary layer using three powered gliders p 604 N91-22663
METEOROLOGICAL SERVICES
Flight Service Automation System (FSAS) Model 1 Full Capacity (M1FC) Operational Test and Evaluation (OT/E)/integration test report
[DOT/FAA/CT-TN90/45] p 569 N91-22100
METEOROLOGY
Air motion measurement uncertainties: Their impact on atmospheric studies p 603 N91-22654
Technical presentation of the Merlin's radome: Calibration and data processing p 603 N91-22656
The NASA-ER2 meteorological measurement system: Instrumentaion, calibration and intercomparison results
p 603 N91-22658
MICROBURSTS (METEOROLOGY)
A simple, analytical, axisymmetric microburst model for downdraft estimation
[NASA-TM-104053] p 573 N91-21132
MICROMECHANICS
Micromechanisms of quasi-static and fatigue crack growth in titanium-aluminides p 602 N91-22583
MICROSTRUCTURE
Service temperature estimation of turbine blades based on microstructural observations
[ASME PAPER 90-GT-23] p 578 A91-34811
Influence of a magnetic field during directional solidification of MAR-M 246 + Hf superalloy
[NASA-CR-184114] p 590 N91-22416
Micromechanisms of quasi-static and fatigue crack growth in titanium-aluminides p 602 N91-22583
MICROWAVE LANDING SYSTEMS
A fast and low-cost validation technique for ILS and MLS p 565 A91-33630
Evaluation of controller tools for conducting MLS curved approaches to New York's JFK Airport
p 565 A91-33631
The effect of the microwave landing system on airport capacity p 561 A91-33668
MICROWAVE RADIOMETERS
Remote sensor observations during WISP90: The use of microwave radiometers, RASS, and ceilometers for detection of aircraft icing conditions
[PB91-131839] p 604 N91-22670
MIDAIR COLLISIONS
Impact of navigation accuracy on the intervention rate in a highly automated air traffic control system
p 566 A91-33647
Model rocketry hazard study
[DOT/FAA/CT-TN90/28] p 587 N91-21238
MILITARY AIR FACILITIES
Status of PAVER implementation within the US Air Force
[AD-A231158] p 585 N91-22137
MISSILE CONFIGURATIONS
Prediction of unsteady transonic separated flow for missile applications
[AD-A231259] p 557 N91-21120
MISSILE CONTROL
Ring laser gyro applications for tactical missiles - The Army TACMS solution p 576 A91-33657
MIXING
Mixing in axial-flow compressors - Conclusions drawn from three-dimensional Navier-Stokes analyses and experiments
[ASME PAPER 90-GT-352] p 551 A91-34783
Mixing in axial flow compressors. I - Test facilities and measurements in a four-stage compressor. II - Measurements in a single-stage compressor and a duct
[ASME PAPER 90-GT-38] p 551 A91-34784
Investigations into shock-induced enhancement of mixing and combustion in supersonic burners
[AD-A231750] p 589 N91-22407
MODELS
Model rocketry hazard study
[DOT/FAA/CT-TN90/28] p 587 N91-21238
Aeroelastic modeling of the active flexible wing wind-tunnel model p 575 N91-22333
MODULARITY
Common integrated processing in modular avionics
p 575 A91-33615
MONITORS
Automated flight test management system
[NASA-CR-186011] p 574 N91-22117
MOTION SIMULATORS
Suppression of biodynamic interference in head-tracked teleoperation
[NASA-TM-103833] p 577 N91-21134
MOTION STABILITY
Bifurcation analysis of the longitudinal dynamics of a simple powered lifting hypersonic vehicle
[AD-A230826] p 557 N91-21118
MRCA AIRCRAFT
Terrain Aided Navigation - Current status, techniques for flat terrain and reference data requirements
p 567 A91-33663
MULTIGRID METHODS
Cell-vertex, multigrid Euler scheme for use with multiblock grids p 547 A91-34128
MULTIPROCESSING (COMPUTERS)
Supercomputer optimizations for stochastic optimal control applications p 605 N91-22313

N

NAP-OF-THE-EARTH NAVIGATION
Simulation of nap-of-the-Earth flight in helicopters
[NASA-TM-102830] p 572 N91-21131
Fully automatic guidance and control for rotorcraft nap-of-the-Earth flight following planned profiles. Volume 1: Real-time piloted simulation
[NASA-CR-177571-VOL-1] p 582 N91-21149
Fully automatic guidance and control for rotorcraft nap-of-the-Earth flight following planned profiles. Volume 2: Mathematical model
[NASA-CR-177571-VOL-2] p 582 N91-21150
NAPHTHENES
Flow visualization ion helicopter blades using Acenaphthen
[DLR-FB-90-37] p 598 N91-21466

NASA PROGRAMS
The NASA-ER2 meteorological measurement system: Instrumentaion, calibration and intercomparison results p 603 N91-22658
Cost-efficient manufacturing of composite structures p 590 N91-23048
NATIONAL AIRSPACE SYSTEM
The Loran Early Implementation Project - Gateway for GPS p 563 A91-33607
Flight Service Automation System (FSAS) Model 1 Full Capacity (M1FC) Operational Test and Evaluation (OT/E)/integration test report
[DOT/FAA/CT-TN90/45] p 569 N91-22100
NAVIER-STOKES EQUATION
Laminar shock/boundary-layer interaction - A numerical test problem p 545 A91-34033
Comparison of upwind and central finite-difference methods for the compressible Navier-Stokes equations p 545 A91-34034
Closed-coupled zonal solution for viscous flow problems p 546 A91-34063
Hypersonic flow simulation for blunt bodies at incidence p 546 A91-34070
Vorticity equation solutions for slender wings at high incidence p 547 A91-34126
Role of artificial viscosity in Euler and Navier-Stokes solvers p 547 A91-34135
Solution of the 3-D, incompressible Navier-Stokes equations for the simulation of vortex breakdown p 593 A91-34181
A streamwise upwind algorithm applied to vortical flow over a delta wing p 548 A91-34192
Numerical simulation of vortices motion in presence of solid boundaries p 549 A91-34213
On the relation between TVD and mesh adaption and application to Navier-Stokes calculations p 550 A91-34215
Computation of the viscous flow past a prolate spheroid at incidence p 550 A91-34216
An approach to the numerical solution of two-dimensional Navier-Stokes equations by a finite difference method p 595 A91-35787
A pressure flux-split technique for computation of inlet flow behavior p 595 N91-21068
Numerical solutions of 2-D multi-stage rotor/stator unsteady flow interactions p 595 N91-21070
Transonic cascade flow calculations using non-periodic C-type grids p 596 N91-21071
Computation of supersonic and low subsonic cascade flows using an explicit Navier-Stokes technique and the kappa-epsilon turbulence model p 596 N91-21072
Blunt trailing edge analysis of supercritical airfoils by a Navier-Stokes code
[NAL-TR-1075-T] p 556 N91-21114
NAVIGATION
The advantages of velocity vector referencing in proportional navigation p 581 A91-33611
Heli/SITAN - A terrain referenced navigation algorithm for helicopters p 568 A91-33664
NAVIGATION AIDS
IEEE PLANS '90 - Position Location and Navigation Symposium, Las Vegas, NV, Mar. 20-23, 1990, Record p 586 A91-33601
Impact of navigation accuracy on the intervention rate *in a highly automated air traffic control system* p 566 A91-33647
Terrain-aided altitude computations on the AFTI/F-16 p 576 A91-33650
Metamorphoses of ONAV console operations: From prototype to real time application p 606 N91-22794
NAVY
Embedded computers: Navy's approach to developing patrol aircraft avionics system too risky
[AD-A230868] p 577 N91-21136
NEURAL NETS
Speech recognition using Kohonen neural networks, dynamic programming, and multi-feature fusion
[AD-A230951] p 597 N91-21410
NEWTONIAN FLUIDS
Hypersonic flow simulation for blunt bodies at incidence p 546 A91-34070
NITROGEN OXIDES
An experimental investigation into NO(x) control of a gas turbine combustor and augmentor tube incorporating a catalytic reduction system
[AD-A231427] p 580 N91-22124
NOISE (SOUND)
Calculation of thickness and charge noise radiated by a rotor in forward flight
[ISL-R-119/89] p 607 N91-21831
NOISE GENERATORS
A study of rotor broadband noise mechanisms and helicopter tail rotor noise
[NASA-CR-177565] p 607 N91-21829
NOISE POLLUTION
Design methodology for a community response questionnaire on sonic boom exposure
[NASA-CR-187503] p 608 N91-22830
NOISE PREDICTION (AIRCRAFT)
Velocity measurements in a turbulent trailing vortex and their application to BWI noise prediction
[NASA-CR-188083] p 554 N91-21100
NOISE PROPAGATION
Blade-wake interaction on a two blade rotor with prediction of the radiated noise stationary and forward flight, comparison between calculation, and experiment
[ISL-R-120/89] p 608 N91-21832
NOISE REDUCTION
Advanced rotorcraft transmission program
[NASA-TM-103276] p 598 N91-21531
Aerothermodynamic design appraisal of noise suppressors for F/A-18 engine run-up facilities at RAAF Williamtown
[ARL-PROP-R-177] p 585 N91-22136
NOISE SPECTRA
A vehicle location system (VLS) solution approach p 564 A91-33614
NONDESTRUCTIVE TESTS
In-flight system for helicopter blade inspection p 575 A91-33268
NONEQUILIBRIUM FLOW
Non-equilibrium hypersonic flow computations by implicit second-order upwind finite-elements p 548 A91-34191
An approximate method for determining friction and heat transfer in chemically nonequilibrium flow past bodies at angle of attack p 553 A91-35660
NONLINEAR FEEDBACK
Bifurcation analysis of the longitudinal dynamics of a simple powered lifting hypersonic vehicle
[AD-A230826] p 557 N91-21118
NONLINEAR FILTERS
Nonlinear filtering of a trajectory message p 568 A91-33868
NONLINEARITY
Nonlinear behavior of a rotorcraft model during air resonance p 581 A91-34816
Large amplitude oscillations p 561 N91-22108
NOSE CONES
Investigation of nose bluntness and angle of attack effects on slender bodies in viscous hypertension flows
[NASA-CR-188153] p 557 N91-21117
NOZZLE FLOW
Hot gas ingestion test results of a two-poster vectored thrust concept with flow visualization in the NASA Lewis 9- x 15-foot low speed wind tunnel
[NASA-TM-103258] p 556 N91-21116
CFD for hypersonic propulsion
[NASA-TM-103791] p 597 N91-21447
Some treatments on boundary conditions for quasi one-dimensional Euler equations
[FFA-TN-1990-36] p 598 N91-21469
NOZZLE GEOMETRY
Theoretical basis for extrapolation of calibration data of PTC 6 throat tap nozzles
[ASME PAPER 90-JPGC/PTC-1] p 578 A91-34808
A method for the extrapolation of calibration data of PTC 6 throat tap nozzles
[ASME PAPER 90-JPGC/PTC-2] p 578 A91-34809
Comparison of UNL laser imaging and sizing system *and a phase Doppler system for analyzing sprays from a* NASA nozzle
[NASA-CR-185239] p 598 N91-21485
Aeropropulsive characteristics of canted twin pitch-vectoring nozzles at Mach 0.20 to 1.20
[NASA-TP-3060] p 558 N91-22069

O

OBSTACLE AVOIDANCE
Fully automatic guidance and control for rotorcraft nap-of-the-Earth flight following planned profiles. Volume 1: Real-time piloted simulation
[NASA-CR-177571-VOL-1] p 582 N91-21149
OGIVES
Interference-free measurements of the subsonic aerodynamics of slanted-base ogive cylinders p 547 A91-34130
Comparison study of the aerodynamic coefficients measured on models with circular or squared section and large elongation in supersonic flow
[ISL-R-125/89] p 555 N91-21106
OMEGA NAVIGATION SYSTEM
Omega signal coverage prediction in the 1990's p 568 A91-33665
ON-LINE SYSTEMS
Development and testing of controller performance evaluation methodology for multi-input/multi-output digital control systems p 584 N91-22337
ONBOARD EQUIPMENT
Global Positioning System (GPS) autonomous navigation p 567 A91-33653
Methodology development for the verification and validation of flight critical systems software, phase 1
[AD-A229932] p 605 N91-21735
ONE DIMENSIONAL FLOW
Some treatments on boundary conditions for quasi one-dimensional Euler equations
[FFA-TN-1990-36] p 598 N91-21469
OPERATING TEMPERATURE
Service temperature estimation of turbine blades based on microstructural observations
[ASME PAPER 90-GT-23] p 578 A91-34811
OPTICAL BISTABILITY
Experimental performance of a binary phase-only optical correlator using visual and infrared imagery p 606 A91-32707
OPTICAL CORRELATORS
Experimental performance of a binary phase-only optical correlator using visual and infrared imagery p 606 A91-32707
OPTICAL RADAR
ISS - A combined terrain topography referenced navigation system p 566 A91-33649
OPTICAL TRACKING
Suppression of biodynamic interference in head-tracked teleoperation
[NASA-TM-103833] p 577 N91-21134
OPTIMAL CONTROL
Reduction of aerodynamic augmented states in active flutter suppression systems p 580 A91-33535
Supercomputer optimizations for stochastic optimal control applications p 605 N91-22313
Fourth NASA Workshop on Computational Control of Flexible Aerospace Systems, part 2
[NASA-CP-10065-PT-2] p 587 N91-22331
OPTIMIZATION
Optimal design of metal and composite thin-walled structures with flutter constraint p 591 A91-32650
Analysis and optimal design of composite structures p 591 A91-32651
Helicopter vibration reduction using structural optimization with aeroelastic/multidisciplinary constraints - A survey p 570 A91-33527
Integrated multidisciplinary design optimization of rotorcraft p 570 A91-33528
Aeroelastic optimization of a helicopter rotor using an efficient sensitivity analysis p 570 A91-33529
Integrated aerodynamic load/dynamic optimization of helicopter rotor blades p 571 A91-33532
Optimization of helicopter airframe structures for vibration reduction - Considerations, formulations, and applications p 571 A91-33533
Application of sensitivity methods for error localization in finite element systems p 594 A91-35529
Optimization of radio-measuring devices incorporated in onboard laser velocimeters p 576 A91-35738
Methods for the optimization of the testing and modeling *of control systems for gas turbine engines --- Russian* book p 579 A91-35815
Supercomputer optimizations for stochastic optimal control applications p 605 N91-22313
Influence of a magnetic field during directional solidification of MAR-M 246 + Hf superalloy
[NASA-CR-184114] p 590 N91-22416
OSCILLATIONS
Special Course on Aircraft Dynamics at High Angles of Attack: Experiments and Modelling
[AGARD-R-776] p 573 N91-22104
Large amplitude oscillations p 561 N91-22108
Oscillatory data for typical configurations p 561 N91-22109

P

PANEL METHOD (FLUID DYNAMICS)
A method to calculate the influence of vortex roll-up on the induced drag of wings p 546 A91-34055
Vortex bursting over a unit area aspect ratio delta wing using vortex paneling methods
[AD-A231028] p 557 N91-21119
Description and evaluation of an interference assessment for a slotted-wall wind tunnel
[NASA-CR-4352] p 585 N91-21155
An iterative procedure for the design of *pressure-specified 3-dimensional configurations* at subsonic and supersonic speeds by means of a higher-order panel method
[MBB-FE122/S/PUB/375] p 574 N91-22118
PARACHUTES
An introduction to testing parachutes in wind tunnels
[DE91-009166] p 560 N91-22094

PARALLEL PROCESSING (COMPUTERS)
Domain decomposition methods in aerodynamics p 604 A91-33056
PARAMETER IDENTIFICATION
Unsteady aerodynamic modelling for aircraft lateral parameter estimation p 581 A91-34162
A frequency domain maximum likelihood identification scheme with application to flight flutter data analysis p 581 A91-35576
Aerodynamic parameter studies and sensitivity analysis for rotor blades in axial flight
[NASA-CR-187524] p 558 N91-22078
PARTICLE PRECIPITATION
Inertial aerosol precipitation on ogival bodies of revolution in high-velocity flow p 553 A91-35784
PASSENGER AIRCRAFT
The flying wing supersonic transport p 571 A91-34164
The final call: Why airline disasters continue to happen --- Book p 561 A91-34250
Coping with dramatic air transport growth p 562 A91-36011
PATTERN RECOGNITION
A model-based method for object recognition p 605 A91-35241
PAVEMENTS
Status of PAVER implementation within the US Air Force
[AD-A231158] p 585 N91-22137
PENNSYLVANIA
Economic impact of aviation in Pennsylvania
[PB91-128264] p 543 N91-22067
PERFORMANCE PREDICTION
Critical speeds and forced response solutions for active magnetic bearing turbomachinery, part 2 p 587 N91-21210
Approximate methods for predicting the lifting characteristics of wing-body combinations p 558 N91-22074
Computer program for estimating performance of air-breathing aircraft engines
[NASA-TM-4254] p 573 N91-22103
PERFORMANCE TESTS
Precision aided inertial navigation using SAR and digital map data p 567 A91-33652
Global Positioning System (GPS) autonomous navigation p 567 A91-33653
Evaluation of an alternative rotorcraft cargo lowering device for the delivery of 500-lb ammunition loads
[AD-A230995] p 573 N91-21133
An experimental study of exit flow patterns in a multistage compressor in rotating stall
[AD-A231353] p 580 N91-21143
Development and testing of controller performance evaluation methodology for multi-input/multi-output digital control systems p 584 N91-22337
PERSONNEL DEVELOPMENT
A guide to ground vehicle operations on the airport
[AD-A231077] p 585 N91-21158
PHASED ARRAYS
Transmit/receive module technology for X-band active array radar p 568 A91-34011
PHOSPHORS
Evaluating thermographic phosphors in an operating turbine engine
[ASME PAPER 90-GT-266] p 593 A91-34810
PHOTOACOUSTIC SPECTROSCOPY
Airborne heterodyne receiver for the range 600 GHz to 3,000 GHz p 599 N91-22047
PHOTOGRAMMETRY
Ashtech XII GPS technology p 564 A91-33622
PHYSIOLOGICAL EFFECTS
Design methodology for a community response questionnaire on sonic boom exposure
[NASA-CR-187503] p 608 N91-22830
PILOT ERROR
Human performance factors in aircraft accident investigation
[SAE PAPER 892608] p 562 A91-34912
PILOT PERFORMANCE
The missing (data) link in pilot navigation p 568 A91-33666
PIPELINES
Development of an optical volumetric flowmeter
[PB91-136481] p 601 N91-22550
PITCHING MOMENTS
Computer program for the calculation of normal force and pitching moment of forebody-cylinder combinations at angles of attack up to 90 degrees and Mach numbers up to 5, including effects of conical boat-tailing
[ESDU-90034] p 555 N91-21102
Dynamic stall effects and applications to high performance aircraft p 573 N91-22106
Forebody vortex control p 573 N91-22110
PLUMES
Multiaxis thrust vectoring using axisymmetric nozzles and postexit vanes on an F/A-18 configuration vehicle
[NASA-TM-101741] p 559 N91-22083
POINTING CONTROL SYSTEMS
Demonstration of a ring laser gyro system for pointing and stabilization applications p 575 A91-33627
POLLUTION CONTROL
An experimental investigation into NO(x) control of a gas turbine combustor and augmentor tube incorporating a catalytic reduction system
[AD-A231427] p 580 N91-22124
POROSITY
Lift and rolling moment due to spoilers on wings at subsonic speeds
[ESDU-90030] p 572 N91-21129
POSITION (LOCATION)
A vehicle location system (VLS) solution approach p 564 A91-33614
The design, simulation and implementation of an accurate positioning system for automatic flight inspection p 566 A91-33646
VLS - A DTOA system for position location p 568 A91-33667
POSITION INDICATORS
IEEE PLANS '90 - Position Location and Navigation Symposium, Las Vegas, NV, Mar. 20-23, 1990, Record p 586 A91-33601
POSITION SENSING
Heli/SITAN - A terrain referenced navigation algorithm for helicopters p 568 A91-33664
POWDER METALLURGY
Feasibility study for the qualification of an economically advantageous Ti-6Al-4V bearing housing for gas turbine engine application by powder metal manufacturing technology
[AD-A231666] p 601 N91-22564
POWER SUPPLY CIRCUITS
A solid-state controllable power supply for a magnetic suspension wind tunnel p 585 N91-21199
PREDICTION ANALYSIS TECHNIQUES
A highly efficient engineering tool for three-dimensional scramjet flowfield and heat transfer computations p 596 N91-21098
Computer program for the calculation of normal force and pitching moment of forebody-cylinder combinations at angles of attack up to 90 degrees and Mach numbers up to 5, including effects of conical boat-tailing
[ESDU-90034] p 555 N91-21102
Wind tunnel test of a propeller working in a low Reynolds number range
[NAL-TR-1071] p 556 N91-21112
Lift and rolling moment due to spoilers on wings at subsonic speeds
[ESDU-90030] p 572 N91-21129
Forces and pressures induced on circular plates by a single lifting jet in ground effect
[NASA-TM-102816] p 558 N91-22077
Small-scale experiments in STOVL ground effects
[NASA-TM-102813] p 560 N91-22091
PREDICTOR-CORRECTOR METHODS
An implicit predictor-corrector relaxation method for viscous transonic flows p 592 A91-34064
PRESSURE DISTRIBUTION
Compressor drum aerodynamic experiments and analysis with coolant injected at selected locations
[ASME PAPER 90-GT-151] p 552 A91-34794
Flow investigation of a ground effect vehicle
[BU-516] p 600 N91-22528
PRESSURE EFFECTS
Zonal analysis of two high-speed inlets p 596 N91-21089
Forces and pressures induced on circular plates by a single lifting jet in ground effect
[NASA-TM-102816] p 558 N91-22077
Small-scale experiments in STOVL ground effects
[NASA-TM-102813] p 560 N91-22091
PRESSURE MEASUREMENT
Fast response wall pressure measurement as a means of gas turbine blade fault identification
[ASME PAPER 90-GT-341] p 578 A91-34813
PRESSURE RATIO
An experimental study of exit flow patterns in a multistage compressor in rotating stall
[AD-A231353] p 580 N91-21143
PRESSURE SENSORS
Air motion measurements: Past and future p 603 N91-22653
PROBABILITY THEORY
Study of bird ingestions into small inlet area aircraft turbine engines
[DOT/FAA/CT-90/13] p 562 N91-21122
PROCEDURES
An introduction to testing parachutes in wind tunnels
[DE91-009166] p 560 N91-22094
Analysis of routine communication in the air traffic control system
[NASA-CR-188116] p 600 N91-22475
PROGRAM VERIFICATION (COMPUTERS)
Methodology development for the verification and validation of flight critical systems software, phase 1
[AD-A229932] p 605 N91-21735
PROJECT PLANNING
Civil air transport: A fresh look at power-by-wire and fly-by-light p 584 N91-23053
PROJECTILES
Computation of flowfields for projectiles in hypersonic chemically reacting flows p 544 A91-33379
Practical methods to evaluate the friction drag coefficient of a projectile in free flight
[ISL-R-123/89] p 555 N91-21105
PROLATE SPHEROIDS
Computation of the viscous flow past a prolate spheroid at incidence p 550 A91-34216
PROLOG (PROGRAMMING LANGUAGE)
Generalized heuristics for the gate assignment problem p 605 A91-35100
PROPELLER BLADES
Velocity of cavitation bubbles in uniform flowfield high and low Reynolds number p 592 A91-34127
Wind tunnel test of a propeller working in a low Reynolds number range
[NAL-TR-1071] p 556 N91-21112
Acoustic and aerodynamic study of a pusher-propeller aircraft model
[NASA-TP-3040] p 607 N91-21828
PROPELLER NOISE
Acoustic and aerodynamic study of a pusher-propeller aircraft model
[NASA-TP-3040] p 607 N91-21828
PROPELLER SLIPSTREAMS
Low speed wind tunnel investigation of propeller slipstream aerodynamic effects on different nacelle/wing combinations. Part 2: Propeller slipstream flow field surveys (velocity components, dynamic, total and static pressure distributions) at zero angle of attack and high power
[FFA-TN-1990-24-PT-2] p 555 N91-21109
PROPELLERS
Wind tunnel test of a propeller working in a low Reynolds number range
[NAL-TR-1071] p 556 N91-21112
PROPULSION SYSTEM CONFIGURATIONS
Spanning the globe with jet propulsion
[AIAA PAPER 91-2987] p 577 A91-34111
CFD for hypersonic propulsion
[NASA-TM-103791] p 597 N91-21447
PROPULSION SYSTEM PERFORMANCE
Computational Fluid Dynamics Symposium on Aeropropulsion
[NASA-CP-3078] p 554 N91-21062
A highly efficient engineering tool for three-dimensional scramjet flowfield and heat transfer computations p 596 N91-21098
Propulsion simulator for magnetically-suspended wind tunnel models p 586 N91-21198
A preliminary evaluation of an F100 engine parameter estimation process using flight data
[NASA-TM-4216] p 597 N91-21446
CFD for hypersonic propulsion
[NASA-TM-103791] p 597 N91-21447
Application of computational fluid dynamics in high speed aeropropulsion
[NASA-TM-103780] p 598 N91-21458
PROPULSIVE EFFICIENCY
Application of computational fluid dynamics in high speed aeropropulsion
[NASA-TM-103780] p 598 N91-21458
Aeropropulsive characteristics of canted twin pitch-vectoring nozzles at Mach 0.20 to 1.20
[NASA-TP-3060] p 558 N91-22069
PROTOTYPES
Development of an optical volumetric flowmeter
[PB91-136481] p 601 N91-22550
Metamorphoses of ONAV console operations: From prototype to real time application p 606 N91-22794
PROVING
A fast and low-cost validation technique for ILS and MLS p 565 A91-33630
PUMP SEALS
Rotordynamic coefficients for partially roughened pump annular seals p 593 A91-34822
PURSUIT TRACKING
The advantages of velocity vector referencing in proportional navigation p 581 A91-33611

Q

QUADRATIC PROGRAMMING
Optimal design of metal and composite thin-walled structures with flutter constraint p 591 A91-32650

QUALITY
Airline quality rating
[NIAR-91-11] p 563 N91-22098
QUALITY CONTROL
Remote sensor observations during WISP90: The use of microwave radiometers, RASS, and ceilometers for detection of aircraft icing conditions
[PB91-131839] p 604 N91-22670

R

RADAR ANTENNAS
Motion compensation for ASTOR long range SAR p 575 A91-33625
RADAR DETECTION
The missing (data) link in pilot navigation p 568 A91-33666
RADAR EQUIPMENT
Heli/SITAN - A terrain referenced navigation algorithm for helicopters p 568 A91-33664
Transmit/receive module technology for X-band active array radar p 568 A91-34011
RADAR IMAGERY
Motion compensation for ASTOR long range SAR p 575 A91-33625
Precision aided inertial navigation using SAR and digital map data p 567 A91-33652
Automated extraction of airport runway patterns from radar imagery
[AD-A231809] p 600 N91-22480
RADIAL FLOW
A review of predictive efforts for transport phenomena in axial flow compressors p 551 A91-34785
RADIATION HARDENING
The effects of simulated electromagnetic pulse on commercial aircraft p 569 A91-35902
RADIATIVE HEAT TRANSFER
Green's function solution to radiative heat transfer between longitudinal gray fins p 593 A91-35117
RADIO ALTIMETERS
Heli/SITAN - A terrain referenced navigation algorithm for helicopters p 568 A91-33664
RADIO ANTENNAS
A five channel low cost GPS receiver p 564 A91-33624
Applying kinematic GPS techniques at our nation's airports p 565 A91-33633
Kinematic GPS - Resolving integer ambiguities on the fly p 567 A91-33661
RADIO FREQUENCIES
Comparison of 14 decibels versus 20 decibels desired to undesired signal protection ratios
[DOT/FAA/CT-TN89/69] p 608 N91-21833
RADIO NAVIGATION
COTS GPS C/A-code receivers with pseudolites for range PLS application --- Commercial Off-The-Shelf receivers for Position Location System p 564 A91-33623
RADIO RECEIVERS
COTS GPS C/A-code receivers with pseudolites for range PLS application --- Commercial Off-The-Shelf receivers for Position Location System p 564 A91-33623
Area navigation capability in a miniature airborne GPS receiver p 566 A91-33636
Uliss G, a fully integrated 'all-in-one' and 'all-in-view' inertia-GPS unit p 566 A91-33644
RADIO SIGNALS
Comparison of 14 decibels versus 20 decibels desired to undesired signal protection ratios
[DOT/FAA/CT-TN89/69] p 608 N91-21833
RADOMES
Technical presentation of the Merlin's radome: Calibration and data processing p 603 N91-22656
RAMJET ENGINES
Computer program for estimating performance of air-breathing aircraft engines
[NASA-TM-4254] p 573 N91-22103
High temperature performance evaluation of a hypersonic engine ceramic wafer seal
[NASA-TM-103737] p 601 N91-22567
RANDOM NOISE
Optimization of radio-measuring devices incorporated in onboard laser velocimeters p 576 A91-35738
RAREFIED PLASMAS
MHD drag and heat transfer of a sphere in supersonic flow of a partially ionized gas p 607 A91-35791
RATINGS
Airline quality rating
[NIAR-91-11] p 563 N91-22098
REACTION KINETICS
Non-equilibrium hypersonic flow computations by implicit second-order upwind finite-elements p 548 A91-34191
REAL TIME OPERATION
Fully automatic guidance and control for rotorcraft nap-of-the-Earth flight following planned profiles. Volume 1: Real-time piloted simulation
[NASA-CR-177571-VOL-1] p 582 N91-21149
Fully automatic guidance and control for rotorcraft nap-of-the-Earth flight following planned profiles. Volume 2: Mathematical model
[NASA-CR-177571-VOL-2] p 582 N91-21150
Development and testing of controller performance evaluation methodology for multi-input/multi-output digital control systems p 584 N91-22337
Metamorphoses of ONAV console operations: From prototype to real time application p 606 N91-22794
REATTACHED FLOW
A vortex-lattice method for the calculation of vortex sheet roll-up and wing-vortex interaction p 546 A91-34052
Method and apparatus for detecting laminar flow separation and reattachment
[NASA-CASE-LAR-13952-2-SB] p 598 N91-21472
RECONNAISSANCE AIRCRAFT
Embedded computers: Navy's approach to developing patrol aircraft avionics system too risky
[AD-A230868] p 577 N91-21136
RECTANGULAR WINGS
Velocity measurements in a turbulent trailing vortex and their application to BWI noise prediction
[NASA-CR-188083] p 554 N91-21100
REINFORCING FIBERS
Fin structures of the Airbus family experience with advanced composites p 570 A91-32455
RELAXATION METHOD (MATHEMATICS)
An implicit predictor-corrector relaxation method for viscous transonic flows p 592 A91-34064
RELIABILITY ANALYSIS
Avionics Environmental Reliability using finite element analysis
[ASME PAPER 90-WA/TS-1] p 591 A91-32961
REMOTE SENSING
An airworthy experimental system for modern navigation and remote-sensing methods - Reduction, storage, and transmission of aerial photography scenes p 575 A91-33370
REMOTE SENSORS
Remote sensor observations during WISP90: The use of microwave radiometers, RASS, and ceilometers for detection of aircraft icing conditions
[PB91-131839] p 604 N91-22670
RENDEZVOUS
The advantages of velocity vector referencing in proportional navigation p 581 A91-33611
REQUIREMENTS
Impact of icing on Unmanned Aerial Vehicle (UAV) operations
[AD-A231191] p 562 N91-21124
Methodology development for the verification and validation of flight critical systems software, phase 1
[AD-A229932] p 605 N91-21735
RESEARCH AIRCRAFT
Interdisciplinary cooperative aerospace research - Examples of scientific cooperation with Braunschweig Technical University p 543 A91-33372
X-31 flight tests to explore combat agility to 70 deg. AOA p 571 A91-34375
Identification of the aerodynamic model of the DLR research aircraft ATTAS from flight test data
[DLR-FB-90-40] p 572 N91-21130
The FIAMS research aircraft or small is beautiful p 603 N91-22655
Summary of aircraft measuring activities at LAPETH p 604 N91-22661
RESEARCH AND DEVELOPMENT
Proceedings of a French-Japanese Seminar on Composite Materials: Processing, Use and Databases p 589 N91-22380
RESEARCH FACILITIES
NASA Ames aerospace systems directorate research
[NASA-TM-103844] p 608 N91-22066
Business plans for the Institute for Aviation Research, FY 1990 - FY 1995
[IAR-89-15] p 609 N91-23020
RESEARCH PROJECTS
Rotors in the wind tunnel - DLR helicopter research methods in the German-Dutch Wind Tunnel p 584 A91-33371
RESEARCH VEHICLES
Multiaxis thrust vectoring using axisymmetric nozzles and postexit vanes on an F/A-18 configuration vehicle
[NASA-TM-101741] p 559 N91-22083
RESIDUAL STRENGTH
Damage accumulation and degradation of composite laminates under aircraft service loading: Assessment and prediction, volumes 1 and 2 p 589 N91-22381
RESIN MATRIX COMPOSITES
Use of resin composites for cryogenic tankage p 588 A91-34287
RESONANT FREQUENCIES
Signal blending in control systems structural interactions
[BU-505] p 583 N91-22132
REYNOLDS NUMBER
Effects of heat transfer on aerodynamics and possible implications for wind tunnel tests p 545 A91-33802
Velocity of cavitation bubbles in uniform flowfield high and low Reynolds number p 592 A91-34127
Computation of the viscous flow past a prolate spheroid at incidence p 550 A91-34216
A method for the extrapolation of calibration data of PTC 6 throat tap nozzles
[ASME PAPER 90-JPGC/PTC-2] p 578 A91-34809
REYNOLDS STRESS
A review of near-wall Reynolds-stress
[NASA-CR-4369] p 559 N91-22080
RIGID ROTORS
Aeroelastic optimization of a helicopter rotor using an efficient sensitivity analysis p 570 A91-33529
Optimum aeroelastic design of helicopter rotors for longitudinal handling qualities improvement p 570 A91-33531
RING LASERS
Demonstration of a ring laser gyro system for pointing and stabilization applications p 575 A91-33627
Flight test results of a tightly integrated RLG-based Global Positioning System/inertial navigation system p 566 A91-33645
GG1308 Ring Laser Gyro Inertial Measurement Systems - Honeywell's low-cost solution for tactical applications p 576 A91-33655
The next frontier for strapdown RLG inertial systems - Precision navigation p 576 A91-33656
Ring laser gyro applications for tactical missiles - The Army TACMS solution p 576 A91-33657
RISK
Impact of icing on Unmanned Aerial Vehicle (UAV) operations
[AD-A231191] p 562 N91-21124
ROADS
Snow roads and runways
[AD-A231490] p 586 N91-22138
ROBOT ARMS
A flexible robotic work cell for the assembly of airframe components p 543 A91-35193
ROBOT DYNAMICS
A flexible robotic work cell for the assembly of airframe components p 543 A91-35193
ROBOTICS
Fourth NASA Workshop on Computational Control of Flexible Aerospace Systems, part 2
[NASA-CP-10065-PT-2] p 587 N91-22331
ROBUSTNESS (MATHEMATICS)
Design of robust controllers for gas turbine engines
[ASME PAPER 90-GT-113] p 578 A91-34815
Integrated flight/propulsion control design for a STOVL aircraft using H-infinity control design techniques
[NASA-TM-104340] p 579 N91-21140
Robust integrated autopilot/autothrottle design using constrained parameter optimization
[NASA-CR-188011] p 583 N91-22127
ROCKET NOSE CONES
Computational methods for frictionless contact with application to Space Shuttle Orbiter nose-gear tires
[NASA-TP-3073] p 601 N91-22576
ROCKETS
Model rocketry hazard study
[DOT/FAA/CT-TN90/28] p 587 N91-21238
ROLL
Unsteady aerodynamics of slender wings p 560 N91-22105
Roll plus maneuver load alleviation control system designs for the active flexible wing wind-tunnel model p 584 N91-22335
ROLLER BEARINGS
Linear and non-linear dynamic models of a geared rotor-bearing system p 594 A91-35536
ROLLING CONTACT LOADS
Computational methods for frictionless contact with application to Space Shuttle Orbiter nose-gear tires
[NASA-TP-3073] p 601 N91-22576
ROLLING MOMENTS
Lift and rolling moment due to spoilers on wings at subsonic speeds
[ESDU-90030] p 572 N91-21129
Forebody vortex control p 573 N91-22110
ROOT-MEAN-SQUARE ERRORS
Nonlinear filtering of a trajectory message p 568 A91-33868
ROTARY WING AIRCRAFT
Nonlinear behavior of a rotorcraft model during air resonance p 581 A91-34816
Evaluation of an alternative rotorcraft cargo lowering device for the delivery of 500-lb ammunition loads
[AD-A230995] p 573 N91-21133

Fully automatic guidance and control for rotorcraft nap-of-the-Earth flight following planned profiles. Volume 1: Real-time piloted simulation
[NASA-CR-177571-VOL-1] p 582 N91-21149
Fully automatic guidance and control for rotorcraft nap-of-the-Earth flight following planned profiles. Volume 2: Mathematical model
[NASA-CR-177571-VOL-2] p 582 N91-21150
Advanced rotorcraft transmission program
[NASA-TM-103276] p 598 N91-21531

ROTARY WINGS
Aeroelastic optimum design of composite rotor blade with returning wake effect p 570 A91-32646
In-flight system for helicopter blade inspection p 575 A91-33268
The location of acoustic blade-vortex interaction - A further step toward an understanding of helicopter noise p 607 A91-33368
Rotors in the wind tunnel - DLR helicopter research methods in the German-Dutch Wind Tunnel p 584 A91-33371
Aeroelastic optimization of a helicopter rotor using an efficient sensitivity analysis p 570 A91-33529
Helicopter rotor dynamics optimization with experimental verification p 570 A91-33530
Optimum aeroelastic design of helicopter rotors for longitudinal handling qualities improvement p 570 A91-33531
Integrated aerodynamic load/dynamic optimization of helicopter rotor blades p 571 A91-33532
Nonlinear behavior of a rotorcraft model during air resonance p 581 A91-34816
Flow visualization ion helicopter blades using Acenaphthen
[DLR-FB-90-37] p 598 N91-21466
A study of rotor broadband noise mechanisms and helicopter tail rotor noise
[NASA-CR-177565] p 607 N91-21829
Aerodynamic parameter studies and sensitivity analysis for rotor blades in axial flight
[NASA-CR-187524] p 558 N91-22078
An investigation into the extent and effects of spanwise flow in the boundary layer of a helicopter rotor in hover
[BU-519] p 560 N91-22089
The flexural strength of unidirectional carbon fibre composites
[BU-509] p 589 N91-22399
A synchronous strobed laser light sheet for rotor flow visualization
[NASA-TM-4266] p 601 N91-22540

ROTATING CYLINDERS
Prediction of slender body coning characteristics p 544 A91-33382

ROTATING SHAFTS
Experimental and analytical study of shaft cracking response in rotatory machines p 594 A91-35516
Force and moment transmissibilities through rolling element bearings in a single-stage rotor system p 594 A91-35537

ROTATING STALLS
Detection of a rotating stall precursor in isolated axial flow compressor rotors
[ASME PAPER 90-GT-157] p 552 A91-34795
Rotating waves as a stall inception indication in axial compressors
[ASME PAPER 90-GT-156] p 553 A91-34796
An experimental study of exit flow patterns in a multistage compressor in rotating stall
[AD-A231353] p 580 N91-21143

ROTATION
Coning motion of slender bodies at high angles of attack
[NAL-TR-1059] p 556 N91-21111
An experimental study of exit flow patterns in a multistage compressor in rotating stall
[AD-A231353] p 580 N91-21143
Rotary-balance testing for aircraft dynamics
[AGARD-AR-265] p 585 N91-21156

ROTOR AERODYNAMICS
Helicopter rotor dynamics optimization with experimental verification p 570 A91-33530
Optimum aeroelastic design of helicopter rotors for longitudinal handling qualities improvement p 570 A91-33531
Integrated aerodynamic load/dynamic optimization of helicopter rotor blades p 571 A91-33532
Rotordynamic coefficients for partially roughened pump annular seals p 593 A91-34822
A study of rotor broadband noise mechanisms and helicopter tail rotor noise
[NASA-CR-177565] p 607 N91-21829
A quantitative investigation into the aerodynamic coupling effects in a coaxial contra-rotating rotor system
[BU-517] p 574 N91-22120
A synchronous strobed laser light sheet for rotor flow visualization
[NASA-TM-4266] p 601 N91-22540

ROTOR BLADES
Integrated aerodynamic load/dynamic optimization of helicopter rotor blades p 571 A91-33532
Euler analysis of transonic stator-rotor interaction using a finite volume method p 554 A91-35984

ROTOR BLADES (TURBOMACHINERY)
Dynamic analysis technique of centrifugal impellor with split blades p 593 A91-35498
A modal aeroelastic analysis scheme for turbomachinery blading
[NASA-CR-187089] p 579 N91-21138

ROTOR BODY INTERACTIONS
Nonlinear behavior of a rotorcraft model during air resonance p 581 A91-34816

ROTORCRAFT AIRCRAFT
Integrated multidisciplinary design optimization of rotorcraft p 570 A91-33528

ROTORS
Weightless test balancing of elastic rotors with the help of interchangeable longitudinal bearing stiffnesses p 592 A91-34015
The effect of shear and rotary inertia of a rotor at its critical speeds p 592 A91-34125
Experimental and analytical study of shaft cracking response in rotatory machines p 594 A91-35516
Linear and non-linear dynamic models of a geared rotor-bearing system p 594 A91-35536
Force and moment transmissibilities through rolling element bearings in a single-stage rotor system p 594 A91-35537
Numerical solutions of 2-D multi-stage rotor/stator unsteady flow interactions *p 595 N91-21070*
Dynamic modelling and analysis of a magnetically suspended flexible rotor p 587 N91-21208
Critical speeds and forced response solutions for active magnetic bearing turbomachinery, part 1 p 587 N91-21209
Calculation of thickness and charge noise radiated by a rotor in forward flight
[ISL-R-119/89] *p 607 N91-21831*

RUNWAYS
Non-airborne conflicts: The causes and effects of runway transgressions
[NASA-CR-177372] p 562 N91-21121
Status of PAVER implementation within the US Air Force
[AD-A231158] p 585 N91-22137
Snow roads and runways
[AD-A231490] p 586 N91-22138
Automated extraction of airport runway patterns from radar imagery
[AD-A231809] p 600 N91-22480

S

SAFETY
Lightweight, fire-retardant, crashworthy aircraft seat cushioning p 563 N91-23052

SAFETY FACTORS
ASTRE improvements expand usefulness of surface movement radar p 569 A91-36012

SATELLITE COMMUNICATION
VLS - A DTOA system for position location *p 568 A91-33667*

SATELLITE NAVIGATION SYSTEMS
Prospects for reduction of separation standards in oceanic airspaces with satellite services p 565 A91-33632

SATELLITE TRACKING
Stand-alone vs. embedded GPS user equipment - The exploration of new standards p 564 A91-33616
Ashtech XII GPS technology p 564 A91-33622

SCALE EFFECT
Sensitivity-based scaling for correlating structural response from different analytical models
[NASA-TM-104042] p 602 N91-22578

SCHEDULING
Generalized heuristics for the gate assignment problem p 605 A91-35100

SEALS (STOPPERS)
High temperature performance evaluation of a hypersonic engine ceramic wafer seal
[NASA-TM-103737] p 601 N91-22567

SEATS
Lightweight, fire-retardant, crashworthy aircraft seat cushioning p 563 N91-23052

SECONDARY FLOW
Method for calculating boundary region corrections in multistep axial turbomachines p 592 A91-34014
Mixing in axial-flow compressors - Conclusions drawn from three-dimensional Navier-Stokes analyses and experiments
[ASME PAPER 90-GT-352] p 551 A91-34783
Mixing in axial flow compressors. I - Test facilities and measurements in a four-stage compressor. II - Measurements in a single-stage compressor and a duct
[ASME PAPER 90-GT-38] p 551 A91-34784
A review of predictive efforts for transport phenomena in axial flow compressors p 551 A91-34785

SELF TESTS
The design, simulation and implementation of an accurate positioning system for automatic flight inspection p 566 A91-33646

SENSITIVITY
Aeroelastic optimization of a helicopter rotor using an efficient sensitivity analysis p 570 A91-33529
Application of sensitivity methods for error localization in finite element systems p 594 A91-35529

SEPARATED FLOW
Prediction of slender body coning characteristics p 544 A91-33382
Correlation measurements and structure angles in a turbulent boundary layer recovering from convex curvature p 545 A91-33747
Effects of heat transfer on aerodynamics and possible implications for wind tunnel tests p 545 A91-33802
On management and control of turbulent shear flows p 545 A91-33803
A vortex-lattice method for the calculation of vortex sheet roll-up and wing-vortex interaction p 546 A91-34052
Numerical calculation of the unsteady separating flow on oscillating airfoils (dynamic stall) p 546 A91-34057
Method and apparatus for detecting laminar flow separation and reattachment
[NASA-CASE-LAR-13952-2-SB] p 598 N91-21472
Separating boundary layer response to an unsteady turbulent environment
[AD-A231483] p 559 N91-22081

SERVICE LIFE
Avionics Environmental Reliability using finite element analysis
[ASME PAPER 90-WA/TS-1] p 591 A91-32961

SHAFTS (MACHINE ELEMENTS)
Dynamic modelling and analysis of a magnetically suspended flexible rotor p 587 N91-21208

SHAPE CONTROL
Shape sensitivity analysis of flutter response of a laminated wing p 571 A91-34144

SHAPES
Water tunnel flow visualisation of vortex breakdown over the F/A-18
[ARL-FLIGHT-MECH-R-179] p 600 N91-22511

SHEAR FLOW
On management and control of turbulent shear flows p 545 A91-33803
A numerical study of interfacial instabilities at high Mach numbers p 549 A91-34198

SHEAR LAYERS
Effects of heat transfer on aerodynamics and possible implications for wind tunnel tests p 545 A91-33802
Vortex element methods for fluid dynamic analysis of engineering systems --- Book p 594 A91-35539

SHEAR PROPERTIES
The effect of shear and rotary inertia of a rotor at its critical speeds p 592 A91-34125

SHELL STABILITY
Stability analysis of a fuselage side
[FFA-TN-1990-32] p 599 N91-21568

SHOCK TUBES
Possibilities of trajectory modification
[ISL-CO-209/90] p 582 N91-21151
Investigations into shock-induced enhancement of mixing and combustion in supersonic burners
[AD-A231750] p 589 N91-22407

SHOCK WAVE INTERACTION
The dynamic behavior of a shock-wave/turbulent boundary layer interaction p 544 A91-33735
Laminar shock/boundary-layer interaction - A numerical test problem p 545 A91-34033
The use of axisymmetric flow for investigation of shock wave-boundary layer interactions
[BU-520] p 600 N91-22529

SHOCK WAVES
Hypersonic leeside flow computations using centered schemes for Euler equations p 548 A91-34187
Simulation of glancing shock wave and boundary layer interaction p 548 A91-34195

SIGNAL PROCESSING
Digital signal conditioning for flight test instrumentation
[NASA-TM-101739] p 577 N91-21135
Development and testing of controller performance evaluation methodology for multi-input/multi-output digital control systems p 584 N91-22337

SIGNAL RECEPTION
Comparison of 14 decibels versus 20 decibels desired to undesired signal protection ratios
[DOT/FAA/CT-TN89/69] p 608 N91-21833
SIGNAL TO NOISE RATIOS
Comparison of 14 decibels versus 20 decibels desired to undesired signal protection ratios
[DOT/FAA/CT-TN89/69] p 608 N91-21833
SIGNAL TRANSMISSION
Omega signal coverage prediction in the 1990's p 568 A91-33665
SIGNATURES
Development of a computer technique for the prediction of transport aircraft flight profile sonic boom signatures
[NASA-CR-188117] p 560 N91-22093
SILICON CARBIDES
Cost-effective manufacturing of advanced ceramics p 588 A91-33725
SIMPLE HARMONIC MOTION
A modal aeroelastic analysis scheme for turbomachinery blading
[NASA-CR-187089] p 579 N91-21138
SIMULATION
A simple, analytical, axisymmetric microburst model for downdraft estimation
[NASA-TM-104053] p 573 N91-21132
SIMULATORS
Propulsion simulator for magnetically-suspended wind tunnel models p 586 N91-21198
SINGLE-PHASE FLOW
Interaction between two jets exhausted from nozzles arranged in parallel p 593 A91-34439
SINGULARITY (MATHEMATICS)
Description and evaluation of an interference assessment for a slotted-wall wind tunnel
[NASA-CR-4352] p 585 N91-21155
An iterative procedure for the design of pressure-specified 3-dimensional configurations at subsonic and supersonic speeds by means of a higher-order panel method
[MBB-FE122/S/PUB/375] p 574 N91-22118
SKIN (STRUCTURAL MEMBER)
Damage tolerance aspects of ARALL fuselage skin structure (philosophy and experiments) p 588 A91-32573
SKIN FRICTION
Viscous, hypersonic flows over compression ramps p 548 A91-34194
Skin friction measurement techniques for scramjet applications. Phase 1: Preliminary design
[AD-A231899] p 580 N91-22125
SLENDER BODIES
Prediction of slender body coning characteristics p 544 A91-33382
Infrared thermography for the qualitative aerodynamic study of a slender body
[ISL-R-122/89] p 555 N91-21104
Coning motion of slender bodies at high angles of attack
[NAL-TR-1059] p 556 N91-21111
SLENDER CONES
Investigation of nose bluntness and angle of attack effects on slender bodies in viscous hypertension flows
[NASA-CR-188153] p 557 N91-21117
SLENDER WINGS
Vorticity equation solutions for slender wings at high incidence p 547 A91-34126
Unsteady aerodynamics of slender wings p 560 N91-22105
SLOTS
Description and evaluation of an interference assessment for a slotted-wall wind tunnel
[NASA-CR-4352] p 585 N91-21155
SNOW
Snow roads and runways
[AD-A231490] p 586 N91-22138
SNOW COVER
Snow roads and runways
[AD-A231490] p 586 N91-22138
SOCIOLOGY
Design methodology for a community response questionnaire on sonic boom exposure
[NASA-CR-187503] p 608 N91-22830
SOFTWARE ENGINEERING
The next frontier for strapdown RLG inertial systems - Precision navigation p 576 A91-33656
RICIS Software Engineering 90 Symposium: Aerospace Applications and Research Directions Proceedings Appendices
[NASA-CR-187994] p 605 N91-22728
SOFTWARE TOOLS
Motion compensation for ASTOR long range SAR p 575 A91-33625
Uliss G, a fully integrated 'all-in-one' and 'all-in-view' inertia-GPS unit p 566 A91-33644
SOLAR ACTIVITY EFFECTS
Ashtech XII GPS technology p 564 A91-33622
SOLENOIDS
Magnetic suspension and balance system advanced study, 1989 design p 586 N91-21197
SOLID STATE DEVICES
START - A broad application spectrum gyro for the 1990's p 591 A91-33604
A solid-state controllable power supply for a magnetic suspension wind tunnel p 585 N91-21199
SONIC BOOMS
Development of a computer technique for the prediction of transport aircraft flight profile sonic boom signatures
[NASA-CR-188117] p 560 N91-22093
Design methodology for a community response questionnaire on sonic boom exposure
[NASA-CR-187503] p 608 N91-22830
SONIC NOZZLES
Interaction between two jets exhausted from nozzles arranged in parallel p 593 A91-34439
SPACE PLATFORMS
The single antenna interferometer
[DE91-007128] p 597 N91-21407
SPACE SHUTTLE ORBITERS
Computational methods for frictionless contact with application to Space Shuttle Orbiter nose-gear tires
[NASA-TP-3073] p 601 N91-22576
SPACE STATIONS
Integrated inertial navigation system/Global Positioning System (INS/GPS) for manned return vehicle autoland application p 586 A91-33609
SPACE TRANSPORTATION SYSTEM
HYTEX - Demonstrator for hypersonic flight up to Mach 5 p 571 A91-34260
SPACECRAFT CONSTRUCTION MATERIALS
HYTEX - Demonstrator for hypersonic flight up to Mach 5 p 571 A91-34260
SPACECRAFT DESIGN
HYTEX - Demonstrator for hypersonic flight up to Mach 5 p 571 A91-34260
SPANWISE BLOWING
An investigation into the extent and effects of spanwise flow in the boundary layer of a helicopter rotor in hover
[BU-519] p 560 N91-22089
SPATIAL DISTRIBUTION
Remote sensor observations during WISP90: The use of microwave,radiometers, RASS, and ceilometers for detection of aircraft icing conditions
[PB91-131839] p 604 N91-22670
SPATIAL MARCHING
Split-matrix marching methods for three-dimensional viscous and inviscid hypersonic flows p 549 A91-34206
SPECIMEN GEOMETRY
Significance of residual curing strains in composite structure repair technology p 590 A91-32461
SPEECH
Speech recognition using Kohonen neural networks, dynamic programming, and multi-feature fusion
[AD-A230951] p 597 N91-21410
SPEECH RECOGNITION
Speech recognition using Kohonen neural networks, dynamic programming, and multi-feature fusion
[AD-A230951] p 597 N91-21410
SPOILERS
Lift and rolling moment due to spoilers on wings at subsonic speeds
[ESDU-90030] p 572 N91-21129
SPRAY CHARACTERISTICS
Comparison of UNL laser imaging and sizing system and a phase Doppler system for analyzing sprays from a NASA nozzle
[NASA-CR-185239] p 598 N91-21485
STABILITY DERIVATIVES
Oscillatory data for typical configurations p 561 N91-22109
STABILITY TESTS
Rotary-balance testing for aircraft dynamics
[AGARD-AR-265] p 585 N91-21156
STAGNATION POINT
A numerical study of hypersonic stagnation heat transfer predictions at a coordinate singularity p 548 A91-34193
STATE ESTIMATION
Flight path reconstruction using extended Kalman filtering techniques
[DLR-FB-90-41] p 555 N91-21108
STATIC CHARACTERISTICS
Unsteady aerodynamics of slender wings p 560 N91-22105
STATIC PRESSURE
An experimental study of exit flow patterns in a multistage compressor in rotating stall
[AD-A231353] p 580 N91-21143
STATIC TESTS
Significance of residual curing strains in composite structure repair technology p 590 A91-32461
STATISTICAL ANALYSIS
Study of bird ingestions into small inlet area aircraft turbine engines
[DOT/FAA/CT-90/13] p 562 N91-21122
STATISTICAL CORRELATION
Non-airborne conflicts: The causes and effects of runway transgressions
[NASA-CR-177372] p 562 N91-21121
STATOR BLADES
Euler analysis of transonic stator-rotor interaction using a finite volume method p 554 A91-35984
STATORS
Numerical solutions of 2-D multi-stage rotor/stator unsteady flow interactions p 595 N91-21070
STEADY FLOW
Non-equilibrium hypersonic flow computations by implicit second-order upwind finite-elements p 548 A91-34191
Viscous, hypersonic flows over compression ramps p 548 A91-34194
STIFFNESS
Weightless test balancing of elastic rotors with the help of interchangeable longitudinal bearing stiffnesses p 592 A91-34015
Dynamic modelling and analysis of a magnetically suspended flexible rotor p 587 N91-21208
STRAIN MEASUREMENT
The flexural strength of unidirectional carbon fibre composites
[BU-509] p 589 N91-22399
STRAPDOWN INERTIAL GUIDANCE
The next frontier for strapdown RLG inertial systems - Precision navigation p 576 A91-33656
STRESS CONCENTRATION
Temperature effect on the stress concentration in the composite material used by the X-29A forward-swept wing aircraft p 590 A91-32547
STROBOSCOPES
A synchronous strobed laser light sheet for rotor flow visualization
[NASA-TM-4266] p 601 N91-22540
STRUCTURAL ANALYSIS
Analysis and optimal design of composite structures p 591 A91-32651
Aerodynamic and structural studies of joined-wing aircraft p 571 A91-33534
Application of mesh generation to complex 3-D configurations
[AGARD-AR-268] p 598 N91-21464
Stability analysis of a fuselage side
[FFA-TN-1990-32] p 599 N91-21568
STARS: An integrated general-purpose finite element structural, aeroelastic, and aeroservoelastic analysis computer program
[NASA-TM-101709-REV] p 599 N91-21587
Sensitivity-based scaling for correlating structural response from different analytical models
[NASA-TM-104042] p 602 N91-22578
Structural integrity of wind tunnel wooden fan blades
[NASA-TM-104059] p 602 N91-22589
STRUCTURAL DESIGN
Analysis and optimal design of composite structures p 591 A91-32651
Helicopter vibration reduction using structural optimization with aeroelastic/multidisciplinary constraints - A survey p 570 A91-33527
Structural integrity of wind tunnel wooden fan blades
[NASA-TM-104059] p 602 N91-22589
STRUCTURAL DESIGN CRITERIA
Aeroelastic optimization of a helicopter rotor using an efficient sensitivity analysis p 570 A91-33529
STRUCTURAL STABILITY
State stability of a system of integro-differential equations of nonstationary aeroelasticity p 595 A91-35785
STRUCTURAL VIBRATION
Flight evaluation of the Integrated Inertial Sensor Assembly (IISA) on a helicopter p 581 A91-33639
Active vibration control using fixed order dynamic compensation with frequency shaped cost functionals p 604 A91-33932
SUBMILLIMETER WAVES
Airborne heterodyne receiver for the range 600 GHz to 3,000 GHz p 599 N91-22047
SUBSONIC FLOW
Interference-free measurements of the subsonic aerodynamics of slanted-base ogive cylinders p 547 A91-34130
Solution method for viscous flows at all speeds in complex domains p 548 A91-34185
Simulation of two- and three-dimensional internal subsonic flows using a finite element method p 595 A91-35986

A finite-difference, frequency-domain numerical scheme for the solution of the linearized unsteady Euler equations p 595 N91-21067
Computation of supersonic and low subsonic cascade flows using an explicit Navier-Stokes technique and the kappa-epsilon turbulence model p 596 N91-21072
STARS: An integrated general-purpose finite element structural, aeroelastic, and aeroservoelastic analysis computer program
[NASA-TM-101709-REV] p 599 N91-21587
Numerical study of the aerodynamic effects of using sulfur hexafluoride as a test gas in wind tunnels
[NASA-TP-3086] p 558 N91-22070

SUBSONIC SPEED
Lift and rolling moment due to spoilers on wings at subsonic speeds
[ESDU-90030] p 572 N91-21129
An iterative procedure for the design of pressure-specified 3-dimensional configurations at subsonic and supersonic speeds by means of a higher-order panel method
[MBB-FE122/S/PUB/375] p 574 N91-22118

SUCTION
An experimental study of a three-dimensional swept-back wing with suction laminar-flow-control
[NAL-TR-1072] p 556 N91-21113

SULFUR FLUORIDES
Numerical study of the aerodynamic effects of using sulfur hexafluoride as a test gas in wind tunnels
[NASA-TP-3086] p 558 N91-22070

SUPERCOMPUTERS
Proceedings of the 8th NAL Symposium on Aircraft Computational Aerodynamics: Prospects of Computational Fluid Dynamics and Super Computers in Aerospace Science and Technology
[NAL-SP-13] p 596 N91-21379
Supercomputer optimizations for stochastic optimal control applications p 605 N91-22313

SUPERCRITICAL AIRFOILS
Blunt trailing edge analysis of supercritical airfoils by a Navier-Stokes code
[NAL-TR-1075-T] p 556 N91-21114

SUPERHETERODYNE RECEIVERS
Airborne heterodyne receiver for the range 600 GHz to 3,000 GHz p 599 N91-22047

SUPERHIGH FREQUENCIES
Transmit/receive module technology for X-band active array radar p 568 A91-34011

SUPERPLASTICITY
Superplasticity in a Ti3Al-base alloy stabilized by Nb, V and Mo p 589 A91-34841

SUPERSONIC AIRCRAFT
Application of sensitivity methods for error localization in finite element systems p 594 A91-35529
Dynamic stall effects and applications to high performance aircraft p 573 N91-22106

SUPERSONIC BOUNDARY LAYERS
Effect of a single three-dimensional surface roughness on the transition in a supersonic boundary layer p 545 A91-33920

SUPERSONIC COMBUSTION
Preliminary calibration of a generic scramjet combustor
[NASA-CR-187539] p 579 N91-21139

SUPERSONIC COMBUSTION RAMJET ENGINES
A highly efficient engineering tool for three-dimensional scramjet flowfield and heat transfer computations p 596 N91-21098
Preliminary calibration of a generic scramjet combustor
[NASA-CR-187539] p 579 N91-21139
Skin friction measurement techniques for scramjet applications. Phase 1: Preliminary design
[AD-A231899] p 580 N91-22125
Investigations into shock-induced enhancement of mixing and combustion in supersonic burners
[AD-A231750] p 589 N91-22407
High temperature performance evaluation of a hypersonic engine ceramic wafer seal
[NASA-TM-103737] p 601 N91-22567

SUPERSONIC FLOW
Vortical solutions of the conical Euler equations --- Book p 591 A91-33674
Solution method for viscous flows at all speeds in complex domains p 548 A91-34185
An approach to the numerical solution of two-dimensional Navier-Stokes equations by a finite difference method p 595 A91-35787
MHD drag and heat transfer of a sphere in supersonic flow of a partially ionized gas p 607 A91-35791
Calculation of a compressible laminar boundary layer on a tapered body of bielliptical cross section p 553 A91-35796
Computation of supersonic and low subsonic cascade flows using an explicit Navier-Stokes technique and the kappa-epsilon turbulence model p 596 N91-21072
Finite element methods for integrated aerodynamic heating analysis
[NASA-CR-188079] p 554 N91-21101
Comparison study of the aerodynamic coefficients measured on models with circular or squared section and large elongation in supersonic flow
[ISL-R-125/89] p 555 N91-21106
STARS: An integrated general-purpose finite element structural, aeroelastic, and aeroservoelastic analysis computer program
[NASA-TM-101709-REV] p 599 N91-21587

SUPERSONIC JET FLOW
A numerical study of interfacial instabilities at high Mach numbers p 549 A91-34198
Interaction between two jets exhausted from nozzles arranged in parallel p 593 A91-34439

SUPERSONIC SPEED
An iterative procedure for the design of pressure-specified 3-dimensional configurations at subsonic and supersonic speeds by means of a higher-order panel method
[MBB-FE122/S/PUB/375] p 574 N91-22118

SUPERSONIC TEST APPARATUS
The use of axisymmetric flow for investigation of shock wave-boundary layer interactions
[BU-520] p 600 N91-22529

SUPERSONIC TRANSPORTS
The flying wing supersonic transport p 571 A91-34164
Span reduction effects on the flutter characteristics of arrow-wing supersonic transport configurations
[NASA-TP-3077] p 572 N91-21127

SUPPORT SYSTEMS
Hot gas ingestion test results of a two-poster vectored thrust concept with flow visualization in the NASA Lewis 9- x 15-foot low speed wind tunnel
[NASA-TM-103258] p 556 N91-21116

SURFACE FINISHING
Experimental study of radiation from coated turbine blades p 580 N91-22122

SURFACE ROUGHNESS EFFECTS
A fast and low-cost validation technique for ILS and MLS p 565 A91-33630
Effect of a single three-dimensional surface roughness on the transition in a supersonic boundary layer p 545 A91-33920
Rotordynamic coefficients for partially roughened pump annular seals p 593 A91-34822
Modeling of surface roughness effects on glaze ice accretion p 562 A91-35107

SURFACE TEMPERATURE
Experimental study of radiation from coated turbine blades p 580 N91-22122

SURFACE VEHICLES
VLS - A DTOA system for position location p 568 A91-33667
A guide to ground vehicle operations on the airport
[AD-A231077] p 585 N91-21158

SURGES
High-speed compressor surge with application to active control
[ASME PAPER 90-GT-354] p 553 A91-34797

SURVEILLANCE RADAR
Modern aviation weather systems for efficient flight management p 602 A91-33648
ASTRE improvements expand usefulness of surface movement radar p 569 A91-36012

SURVEYS
Air traffic control memory: A field survey
[DOT/FAA/CT-TN90/60] p 569 N91-22101
Design methodology for a community response questionnaire on sonic boom exposure
[NASA-CR-187503] p 608 N91-22830

SURVIVAL
The human factors relating to escape and survival from helicopters ditching in water
[AGARD-AG-305(F)] p 563 N91-22099

SWEPT FORWARD WINGS
Temperature effect on the stress concentration in the composite material used by the X-29A forward-swept wing aircraft p 590 A91-32547

SWEPT WINGS
Analysis and optimal design of composite structures p 591 A91-32651
Numerical simulation of swept-wing flows
[NASA-CR-188201] p 560 N91-22095
Variable camber wings for transport aircraft p 574 N91-22112

SWEPTBACK WINGS
An experimental study of a three-dimensional swept-back wing with suction laminar-flow-control
[NAL-TR-1072] p 556 N91-21113

SWIRLING
The influence of inlet swirl distortions on the performance of a jet propulsion two-stage axial compressor
[ASME PAPER 90-GT-147] p 552 A91-34790

SWITCHING CIRCUITS
A solid-state controllable power supply for a magnetic suspension wind tunnel p 585 N91-21199

SYNCHRONISM
A synchronous strobed laser light sheet for rotor flow visualization
[NASA-TM-4266] p 601 N91-22540

SYNCHRONOUS SATELLITES
VLS - A DTOA system for position location p 568 A91-33667

SYNTHETIC APERTURE RADAR
Motion compensation for ASTOR long range SAR p 575 A91-33625
Demonstration of a ring laser gyro system for pointing and stabilization applications p 575 A91-33627
Precision aided inertial navigation using SAR and digital map data p 567 A91-33652
The single antenna interferometer
[DE91-007128] p 597 N91-21407
Automated extraction of airport runway patterns from radar imagery
[AD-A231809] p 600 N91-22480

SYSTEM FAILURES
Test program for Honeywell/DND Helicopter Integrated Navigation System (HINS) p 565 A91-33626

SYSTEM IDENTIFICATION
A frequency domain maximum likelihood identification scheme with application to flight flutter data analysis p 581 A91-35576

SYSTEMS ENGINEERING
The design, simulation and implementation of an accurate positioning system for automatic flight inspection p 566 A91-33646
VLS - A DTOA system for position location p 568 A91-33667
An experimental study of exit flow patterns in a multistage compressor in rotating stall
[AD-A231353] p 580 N91-21143
Research flight-control system development for the F-18 high alpha research vehicle
[NASA-TM-104232] p 583 N91-22131

SYSTEMS INTEGRATION
Integrated inertial navigation system/Global Positioning System (INS/GPS) for manned return vehicle autoland application p 586 A91-33609
Common integrated processing in modular avionics p 575 A91-33615
Test program for Honeywell/DND Helicopter Integrated Navigation System (HINS) p 565 A91-33626
INS reset removal for enhanced post-flight performance analysis p 565 A91-33628
Flight evaluation of the Integrated Inertial Sensor Assembly (IISA) on a helicopter p 581 A91-33639
Failure management in spatio-temporal redundant, integrated navigation and flight control reference-systems p 581 A91-33640
Flight test results of a tightly integrated RLG-based Global Positioning System/inertial navigation system p 566 A91-33645
Terrain referenced navigation p 567 A91-33651
Terrain Aided Navigation - Current status, techniques for flat terrain and reference data requirements p 567 A91-33663
Integrated flight/propulsion control system design based on a decentralized, hierarchical approach
[NASA-TM-103678] p 579 N91-21137
Flight Service Automation System (FSAS) Model 1 Full Capacity (M1FC) Operational Test and Evaluation (OT/E)/integration test report
[DOT/FAA/CT-TN90/45] p 569 N91-22100

SYSTEMS MANAGEMENT
Failure management in spatio-temporal redundant, integrated navigation and flight control reference-systems p 581 A91-33640

T

TAILLESS AIRCRAFT
Starship - Bright newcomer in a conservative firmament p 571 A91-34122
The flying wing supersonic transport p 571 A91-34164

TARGET ACQUISITION
The advantages of velocity vector referencing in proportional navigation p 581 A91-33611

TARGET RECOGNITION
Knowledge-based target recognition system evolution p 577 A91-35978

TASKS
Suppression of biodynamic interference in head-tracked teleoperation
[NASA-TM-103833] p 577 N91-21134

TECHNOLOGY TRANSFER
Business plans for the Institute for Aviation Research, FY 1990 - FY 1995
[IAR-89-15] p 609 N91-23020
TELEOPERATORS
Suppression of biodynamic interference in head-tracked teleoperation
[NASA-TM-103833] p 577 N91-21134
TEMPERATURE CONTROL
Langley develops thermal management concept for hypersonic aircraft p 570 A91-33323
TEMPERATURE DEPENDENCE
Evaluating thermographic phosphors in an operating turbine engine
[ASME PAPER 90-GT-266] p 593 A91-34810
TEMPERATURE EFFECTS
Temperature effect on the stress concentration in the composite material used by the X-29A forward-swept wing aircraft p 590 A91-32547
TEMPORAL DISTRIBUTION
Remote sensor observations during WISP90: The use of microwave radiometers, RASS, and ceilometers for detection of aircraft icing conditions
[PB91-131839] p 604 N91-22670
TERRAIN
ISS - A combined terrain topography referenced navigation system p 566 A91-33649
Heli/SITAN - A terrain referenced navigation algorithm for helicopters p 568 A91-33664
TERRAIN FOLLOWING AIRCRAFT
Terrain-aided altitude computations on the AFTI/F-16 p 576 A91-33650
Terrain referenced navigation p 567 A91-33651
Terrain Aided Navigation - Current status, techniques for flat terrain and reference data requirements p 567 A91-33663
TEST FACILITIES
Simulation of nap-of-the-Earth flight in helicopters
[NASA-TM-102830] p 572 N91-21131
THERMAL CONTROL COATINGS
Experimental study of radiation from coated turbine blades p 580 N91-22122
THERMAL STRESSES
Thermal spikes on CFRP laminates - Assessment of microdamage and its consequences on fatigue life p 588 A91-32549
Avionics Environmental Reliability using finite element analysis
[ASME PAPER 90-WA/TS-1] p 591 A91-32961
THERMOGRAPHY
Evaluating thermographic phosphors in an operating turbine engine
[ASME PAPER 90-GT-266] p 593 A91-34810
Infrared thermography for the qualitative aerodynamic study of a slender body
[ISL-R-122/89] p 555 N91-21104
THREE DIMENSIONAL BODIES
Three-dimensional flow near the blade/endwall junction of a gas turbine - Visualization in a large-scale cascade simulator
[ASME PAPER 90-WA/HT-4] p 544 A91-32958
A numerical study of hypersonic stagnation heat transfer predictions at a coordinate singularity p 548 A91-34193
An approximate method for determining friction and heat transfer in chemically nonequilibrium flow past bodies at angle of attack p 553 A91-35660
Grid generation about complex three-dimensional aircraft configurations
[NASA-CR-188097] p 558 N91-22071
THREE DIMENSIONAL BOUNDARY LAYER
Effect of a single three-dimensional surface roughness on the transition in a supersonic boundary layer p 545 A91-33920
An inverse boundary layer procedure with application to 3-D wing flow p 550 A91-34229
Calculation of a compressible laminar boundary layer on a tapered body of bielliptical cross section p 553 A91-35796
THREE DIMENSIONAL FLOW
An implicit predictor-corrector relaxation method for viscous transonic flows p 592 A91-34064
Development and validation of characteristic boundary conditions for cell-centered Euler flow calculations p 592 A91-34178
Solution adaptive local rectangular grid refinement for transonic aerodynamic flow problems p 547 A91-34179
Solution of the 3-D, incompressible Navier-Stokes equations for the simulation of vortex breakdown p 593 A91-34181
Simulation of glancing shock wave and boundary layer interaction p 548 A91-34195
3D Euler flows around modern airplanes p 549 A91-34201
Split-matrix marching methods for three-dimensional viscous and inviscid hypersonic flows p 549 A91-34206
Numerical investigation of three dimensional laminar flows in a channel with a built-in circular cylinder and wing-type vortex generators p 550 A91-34218
An inverse boundary layer procedure with application to 3-D wing flow p 550 A91-34229
Development of a general multiblock flow solver for complex configurations p 605 A91-34230
Mixing in axial-flow compressors - Conclusions drawn from three-dimensional Navier-Stokes analyses and experiments
[ASME PAPER 90-GT-352] p 551 A91-34783
Three-dimensional wake decay inside of a compressor cascade and its influence on the downstream unsteady flow field. I - Wake decay characteristics in the flow passage. II - Unsteady flow field downstream of the stator
[ASME PAPER 90-GT-21] p 551 A91-34786
Experimental and numerical investigation of three-dimensional viscous flows and vortex motion inside an annular compressor blade row
[ASME PAPER 90-GT-155] p 551 A91-34787
Three-dimensional flowfields inside a transonic compressor with swept blades
[ASME PAPER 90-GT-359] p 552 A91-34791
Tip leakage flow in axial compressors
[ASME PAPER 90-GT-127] p 552 A91-34792
Simulation of two- and three-dimensional internal subsonic flows using a finite element method p 595 A91-35986
Compressible flows with periodic vortical disturbances around lifting airfoils
[NASA-TM-103742] p 554 N91-21060
A finite-difference, frequency-domain numerical scheme for the solution of the linearized unsteady Euler equations p 595 N91-21067
Finite element methods for integrated aerodynamic heating analysis
[NASA-CR-188079] p 554 N91-21101
CFD for hypersonic propulsion
[NASA-TM-103791] p 597 N91-21447
THREE DIMENSIONAL MODELS
Numerical simulation of swept-wing flows
[NASA-CR-188201] p 560 N91-22095
An iterative procedure for the design of pressure-specified 3-dimensional configurations at subsonic and supersonic speeds by means of a higher-order panel method
[MBB-FE122/S/PUB/375] p 574 N91-22118
THROTTLING
Robust integrated autopilot/autothrottle design using constrained parameter optimization
[NASA-CR-188011] p 583 N91-22127
THRUST
Multiaxis thrust vectoring using axisymmetric nozzles and postexit vanes on an F/A-18 configuration vehicle
[NASA-TM-101741] p 559 N91-22083
THRUST MEASUREMENT
Skin friction measurement techniques for scramjet applications. Phase 1: Preliminary design
[AD-A231899] p 580 N91-22125
THRUST VECTOR CONTROL
Hot gas ingestion test results of a two-poster vectored thrust concept with flow visualization in the NASA Lewis 9- x 15-foot low speed wind tunnel
[NASA-TM-103258] p 556 N91-21116
Aeropropulsive characteristics of canted twin pitch-vectoring nozzles at Mach 0.20 to 1.20
[NASA-TP-3060] p 558 N91-22069
Multiaxis thrust vectoring using axisymmetric nozzles and postexit vanes on an F/A-18 configuration vehicle
[NASA-TM-101741] p 559 N91-22083
Research flight-control system development for the F-18 high alpha research vehicle
[NASA-TM-104232] p 583 N91-22131
TIME LAG
The delayed ejection decision p 561 A91-33273
TIME MARCHING
Split-matrix marching methods for three-dimensional viscous and inviscid hypersonic flows p 549 A91-34206
TITANIUM
Direct cast titanium aluminide strip
[AD-A231906] p 590 N91-22424
TITANIUM ALLOYS
Superplasticity in a Ti3Al-base alloy stabilized by Nb, V and Mo p 589 A91-34841
Feasibility study for the qualification of an economically advantageous Ti-6Al-4V bearing housing for gas turbine engine application by powder metal manufacturing technology
[AD-A231666] p 601 N91-22564
Micromechanisms of quasi-static and fatigue crack growth in titanium-aluminides p 602 N91-22583
TOLERANCES (MECHANICS)
Damage tolerance aspects of ARALL fuselage skin structure (philosophy and experiments) p 588 A91-32573
TOPOGRAPHY
ISS - A combined terrain topography referenced navigation system p 566 A91-33649
TRACKING (POSITION)
Suppression of biodynamic interference in head-tracked teleoperation
[NASA-TM-103833] p 577 N91-21134
TRAFFIC CONTROL
Non-airborne conflicts: The causes and effects of runway transgressions
[NASA-CR-177372] p 562 N91-21121
TRAILING EDGES
A method to calculate the influence of vortex roll-up on the induced drag of wings p 546 A91-34055
A leading-edge control surface
[BU-508] p 559 N91-22087
TRAJECTORY ANALYSIS
Nonlinear filtering of a trajectory message p 568 A91-33868
Possibilities of trajectory modification
[ISL-CO-209/90] p 582 N91-21151
TRANSFER FUNCTIONS
Development and testing of controller performance evaluation methodology for multi-input/multi-output digital control systems p 584 N91-22337
TRANSITION FLOW
Progress in the prediction of the laminar-turbulent transition for laminar wings - The profile and wing geometries determine the friction drag of an aircraft p 544 A91-33369
Separating boundary layer response to an unsteady turbulent environment
[AD-A231483] p 559 N91-22081
TRANSLUCENCE
Experimental study of radiation from coated turbine blades p 580 N91-22122
TRANSMISSIONS (MACHINE ELEMENTS)
Linear and non-linear dynamic models of a geared rotor-bearing system p 594 A91-35536
Advanced rotorcraft transmission program
[NASA-TM-103276] p 598 N91-21531
Effects of gear box vibration and mass imbalance on the dynamics of multi-stage gear transmissions
[NASA-TM-103695] p 599 N91-21534
TRANSMITTER RECEIVERS
Transmit/receive module technology for X-band active array radar p 568 A91-34011
TRANSOCEANIC COMMUNICATION
Oceanic clearance trial proves utility of data link communications for ATC p 568 A91-33775
TRANSOCEANIC FLIGHT
Prospects for reduction of separation standards in oceanic airspaces with satellite services p 565 A91-33632
TRANSONIC COMPRESSORS
Unsteady radial transport in a transonic compressor stage
[ASME PAPER 90-GT-133] p 551 A91-34788
The influence of inlet swirl distortions on the performance of a jet propulsion two-stage axial compressor
[ASME PAPER 90-GT-147] p 552 A91-34790
Three-dimensional flowfields inside a transonic compressor with swept blades
[ASME PAPER 90-GT-359] p 552 A91-34791
Euler analysis of transonic stator-rotor interaction using a finite volume method p 554 A91-35984
TRANSONIC FLOW
Domain decomposition methods in aerodynamics p 604 A91-33056
An implicit predictor-corrector relaxation method for viscous transonic flows p 592 A91-34064
Solution adaptive local rectangular grid refinement for transonic aerodynamic flow problems p 547 A91-34179
A functional method for the approximate solution of a transonic problem p 550 A91-34398
Transonic cascade flow calculations using non-periodic C-type grids p 596 N91-21071
Comparison study of the aerodynamic coefficients measured on models with circular or squared section and large elongation in supersonic flow
[ISL-R-125/89] p 555 N91-21106
Prediction of unsteady transonic separated flow for missile applications
[AD-A231259] p 557 N91-21120
Numerical study of the aerodynamic effects of using sulfur hexafluoride as a test gas in wind tunnels
[NASA-TP-3086] p 558 N91-22070
TRANSONIC FLUTTER
Span reduction effects on the flutter characteristics of arrow-wing supersonic transport configurations
[NASA-TP-3077] p 572 N91-21127

Aeroelastic modeling of the active flexible wing wind-tunnel model p 575 N91-22333
TRANSONIC SPEED
Blunt trailing edge analysis of supercritical airfoils by a Navier-Stokes code
[NAL-TR-1075-T] p 556 N91-21114
TRANSONIC WIND TUNNELS
Description and evaluation of an interference assessment for a slotted-wall wind tunnel
[NASA-CR-4352] p 585 N91-21155
TRANSPORT AIRCRAFT
Development of a computer technique for the prediction of transport aircraft flight profile sonic boom signatures
[NASA-CR-188117] p 560 N91-22093
Variable camber wings for transport aircraft
p 574 N91-22112
Civil air transport: A fresh look at power-by-wire and fly-by-light p 584 N91-23053
TRANSPORT PROPERTIES
A review of predictive efforts for transport phenomena in axial flow compressors p 551 A91-34785
Unsteady radial transport in a transonic compressor stage
[ASME PAPER 90-GT-133] p 551 A91-34788
TRAVELING WAVES
Rotating waves as a stall inception indication in axial compressors
[ASME PAPER 90-GT-156] p 553 A91-34796
TURBINE BLADES
Three-dimensional flow near the blade/endwall junction of a gas turbine - Visualization in a large-scale cascade simulator
[ASME PAPER 90-WA/HT-4] p 544 A91-32958
Service temperature estimation of turbine blades based on microstructural observations
[ASME PAPER 90-GT-23] p 578 A91-34811
Fast response wall pressure measurement as a means of gas turbine blade fault identification
[ASME PAPER 90-GT-341] p 578 A91-34813
Calculation of the cooling system of small-size blades of high-temperature gas turbine engines
p 594 A91-35743
TURBINE WHEELS
Using a locally one-dimensional method for solving the heat conductivity equation to determine the thermal state of cooled rotor disks p 594 A91-35742
TURBOCOMPRESSORS
Method for calculating boundary region corrections in multistep axial turbomachines p 592 A91-34014
Mixing in axial-flow compressors - Conclusions drawn from three-dimensional Navier-Stokes analyses and experiments
[ASME PAPER 90-GT-352] p 551 A91-34783
Mixing in axial flow compressors. I - Test facilities and measurements in a four-stage compressor. II - Measurements in a single-stage compressor and a duct
[ASME PAPER 90-GT-38] p 551 A91-34784
A review of predictive efforts for transport phenomena in axial flow compressors p 551 A91-34785
Temporally and spatially resolved flow in a two-stage axial compressor. I - Experiment
[ASME PAPER 90-GT-259] p 551 A91-34789
The influence of inlet swirl distortions on the performance of a jet propulsion two-stage axial compressor
[ASME PAPER 90-GT-147] p 552 A91-34790
Tip leakage flow in axial compressors
[ASME PAPER 90-GT-127] p 552 A91-34792
Detection of a rotating stall precursor in isolated axial flow compressor rotors
[ASME PAPER 90-GT-157] p 552 A91-34795
Rotating waves as a stall inception indication in axial compressors
[ASME PAPER 90-GT-156] p 553 A91-34796
High-speed compressor surge with application to active control
[ASME PAPER 90-GT-354] p 553 A91-34797
Forcing function effects on rotor periodic aerodynamic response
[ASME PAPER 90-GT-109] p 553 A91-34798
An experimental study of exit flow patterns in a multistage compressor in rotating stall
[AD-A231353] p 580 N91-21143
TURBOFAN ENGINES
Control of the working cycle of gas turbine engines (2nd revised and enlarged edition) --- Russian book
p 579 A91-35822
Study of bird ingestions into small inlet area aircraft turbine engines
[DOT/FAA/CT-90/13] p 562 N91-21122
A preliminary evaluation of an F100 engine parameter estimation process using flight data
[NASA-TM-4216] p 597 N91-21446
TURBOFANS
Computer program for estimating performance of air-breathing aircraft engines
[NASA-TM-4254] p 573 N91-22103
TURBOJET ENGINES
Spanning the globe with jet propulsion
[AIAA PAPER 91-2987] p 577 A91-34111
The influence of inlet swirl distortions on the performance of a jet propulsion two-stage axial compressor
[ASME PAPER 90-GT-147] p 552 A91-34790
TURBOMACHINERY
Computational Fluid Dynamics Symposium on Aeropropulsion
[NASA-CP-3078] p 554 N91-21062
Transonic cascade flow calculations using non-periodic C-type grids p 596 N91-21071
Computation of supersonic and low subsonic cascade flows using an explicit Navier-Stokes technique and the kappa-epsilon turbulence model p 596 N91-21072
A modal aeroelastic analysis scheme for turbomachinery blading
[NASA-CR-187089] p 579 N91-21138
Critical speeds and forced response solutions for active magnetic bearing turbomachinery, part 1
p 587 N91-21209
Critical speeds and forced response solutions for active magnetic bearing turbomachinery, part 2
p 587 N91-21210
TURBOSHAFTS
Analysis of bearing incidents in aircraft gas turbine mainshaft bearings p 591 A91-33464
TURBULENCE
Transonic cascade flow calculations using non-periodic C-type grids p 596 N91-21071
An experimental study of a three-dimensional swept-back wing with suction laminar-flow-control
[NAL-TR-1072] p 556 N91-21113
A review of near-wall Reynolds-stress
[NASA-CR-4369] p 559 N91-22080
TURBULENCE MODELS
Analysis of laminar separation bubble using a simple eddy-viscosity turbulence model p 591 A91-33227
Computational Fluid Dynamics Symposium on Aeropropulsion
[NASA-CP-3078] p 554 N91-21062
Blunt trailing edge analysis of supercritical airfoils by a Navier-Stokes code
[NAL-TR-1075-T] p 556 N91-21114
Analysis of laminar separation bubbles using a simple eddy-viscosity turbulence model
[NAL-TR-1079] p 600 N91-22520
TURBULENT BOUNDARY LAYER
The dynamic behavior of a shock-wave/turbulent boundary layer interaction p 544 A91-33735
Correlation measurements and structure angles in a turbulent boundary layer recovering from convex curvature p 545 A91-33747
Unsteady flowfield behind a vortex generator rapidly pitched to angle of attack p 547 A91-34139
A method for the extrapolation of calibration data of PTC 6 throat tap nozzles
[ASME PAPER 90-JPGC/PTC-2] p 578 A91-34809
Practical methods to evaluate the friction drag coefficient of a projectile in free flight
[ISL-R-123/89] p 555 N91-21105
TURBULENT DIFFUSION
Mixing in axial-flow compressors - Conclusions drawn from three-dimensional Navier-Stokes analyses and experiments
[ASME PAPER 90-GT-352] p 551 A91-34783
Mixing in axial flow compressors. I - Test facilities and measurements in a four-stage compressor. II - Measurements in a single-stage compressor and a duct
[ASME PAPER 90-GT-38] p 551 A91-34784
TURBULENT FLOW
Finite-element analysis of turbulent flow in annular exhaust diffusers of gas turbine engines
p 577 A91-32700
Progress in the prediction of the laminar-turbulent transition for laminar wings - The profile and wing geometries determine the friction drag of an aircraft
p 544 A91-33369
On management and control of turbulent shear flows
p 545 A91-33803
Solution method for viscous flows at all speeds in complex domains p 548 A91-34185
Numerical simulation of turbulent flows around airfoil and wing p 549 A91-34203
Numerical simulation of vortices motion in presence of solid boundaries p 549 A91-34213
An inverse boundary layer procedure with application to 3-D wing flow p 550 A91-34229
Three-dimensional wake decay inside of a compressor cascade and its influence on the downstream unsteady flow field. I - Wake decay characteristics in the flow passage. II - Unsteady flow field downstream of the stator
[ASME PAPER 90-GT-21] p 551 A91-34786
Velocity measurements in a turbulent trailing vortex and their application to BWI noise prediction
[NASA-CR-188083] p 554 N91-21100
Numerical study of the aerodynamic effects of using sulfur hexafluoride as a test gas in wind tunnels
[NASA-TP-3086] p 558 N91-22070
Separating boundary layer response to an unsteady turbulent environment
[AD-A231483] p 559 N91-22081
Analysis of laminar separation bubbles using a simple eddy-viscosity turbulence model
[NAL-TR-1079] p 600 N91-22520
TURBULENT WAKES
Three-dimensional wake decay inside of a compressor cascade and its influence on the downstream unsteady flow field. I - Wake decay characteristics in the flow passage. II - Unsteady flow field downstream of the stator
[ASME PAPER 90-GT-21] p 551 A91-34786
TVD SCHEMES
On the relation between TVD and mesh adaption and application to Navier-Stokes calculations
p 550 A91-34215
TWO DIMENSIONAL BOUNDARY LAYER
The dynamic behavior of a shock-wave/turbulent boundary layer interaction p 544 A91-33735
TWO DIMENSIONAL FLOW
Viscous, hypersonic flows over compression ramps
p 548 A91-34194
Some aspects of the numerical simulation of compressible viscous flow around bluff bodies at low Ma-number p 550 A91-34220
Development of a general multiblock flow solver for complex configurations p 605 A91-34230
Simulation of two- and three-dimensional internal subsonic flows using a finite element method
p 595 A91-35986
TWO DIMENSIONAL JETS
Computations for a jet impinging obliquely on a flat surface p 554 A91-35985
TWO DIMENSIONAL MODELS
Numerical simulation of vortices motion in presence of solid boundaries p 549 A91-34213

U

UNSTEADY AERODYNAMICS
Optimal design of metal and composite thin-walled structures with flutter constraint p 591 A91-32650
Role of artificial viscosity in Euler and Navier-Stokes solvers p 547 A91-34135
Effect of geometrical disturbance on vortex asymmetry
p 547 A91-34136
Unsteady flowfield behind a vortex generator rapidly pitched to angle of attack p 547 A91-34139
Unsteady aerodynamic modelling for aircraft lateral parameter estimation p 581 A91-34162
Forcing function effects on rotor periodic aerodynamic response
[ASME PAPER 90-GT-109] p 553 A91-34798
A modal aeroelastic analysis scheme for turbomachinery blading
[NASA-CR-187089] p 579 N91-21138
STARS: An integrated general-purpose finite element structural, aeroelastic, and aeroservoelastic analysis computer program
[NASA-TM-101709-REV] p 599 N91-21587
Unsteady aerodynamics of slender wings
p 560 N91-22105
Dynamic stall effects and applications to high performance aircraft p 573 N91-22106
Flexible body dynamic stability for high performance aircraft p 574 N91-22318
Aeroelastic modeling of the active flexible wing wind-tunnel model p 575 N91-22333
UNSTEADY FLOW
Numerical calculation of the unsteady separating flow on oscillating airfoils (dynamic stall) p 546 A91-34057
Airfoils in two- and three-dimensional gust fields
p 546 A91-34073
Computation of unsteady incompressible viscous flow around airfoils p 546 A91-34074
Three-dimensional wake decay inside of a compressor cascade and its influence on the downstream unsteady flow field. I - Wake decay characteristics in the flow passage. II - Unsteady flow field downstream of the stator
[ASME PAPER 90-GT-21] p 551 A91-34786
Unsteady radial transport in a transonic compressor stage
[ASME PAPER 90-GT-133] p 551 A91-34788
Compressible flows with periodic vortical disturbances around lifting airfoils
[NASA-TM-103742] p 554 N91-21060

Numerical solutions of 2-D multi-stage rotor/stator unsteady flow interactions p 595 N91-21070
Prediction of unsteady transonic separated flow for missile applications
[AD-A231259] p 557 N91-21120
A modal aeroelastic analysis scheme for turbomachinery blading
[NASA-CR-187089] p 579 N91-21138
Separating boundary layer response to an unsteady turbulent environment
[AD-A231483] p 559 N91-22081

UPPER SURFACE BLOWING
Method and apparatus for detecting laminar flow separation and reattachment
[NASA-CASE-LAR-13952-2-SB] p 598 N91-21472

USER MANUALS (COMPUTER PROGRAMS)
MATGRID, a program for generation of C-H and C-O topology grids around wing/body configurations: User's guide
[FFA-TN-1991-03] p 556 N91-21110
Addendum to the DYCAST user's manual describing the curved, warp beam finite element
[NASA-CR-4362] p 606 N91-22805

USER REQUIREMENTS
Omega signal coverage prediction in the 1990's p 568 A91-33665
Design of an intelligent information system for in-flight emergency assistance p 606 N91-22792

V

V/STOL AIRCRAFT
Integrated flight/propulsion control design for a STOVL aircraft using H-infinity control design techniques
[NASA-TM-104340] p 579 N91-21140
Small-scale experiments in STOVL ground effects
[NASA-TM-102813] p 560 N91-22091

VANADIUM ALLOYS
Feasibility study for the qualification of an economically advantageous Ti-6Al-4V bearing housing for gas turbine engine application by powder metal manufacturing technology
[AD-A231666] p 601 N91-22564

VANES
Multiaxis thrust vectoring using axisymmetric nozzles and postexit vanes on an F/A-18 configuration vehicle
[NASA-TM-101741] p 559 N91-22083
Flight test to determine feasibility of a proposed airborne wake vortex detection concept
[NASA-TM-102672] p 563 N91-22096

VARIATIONAL PRINCIPLES
Computational methods for frictionless contact with application to Space Shuttle Orbiter nose-gear tires
[NASA-TP-3073] p 601 N91-22576

VEHICLES
A vehicle location system (VLS) solution approach p 564 A91-33614

VELOCITY DISTRIBUTION
A functional method for the approximate solution of a transonic problem p 550 A91-34398
Development of an optical volumetric flowmeter
[PB91-136481] p 601 N91-22550

VELOCITY MEASUREMENT
Velocity measurements in a turbulent trailing vortex and their application to BWI noise prediction
[NASA-CR-188083] p 554 N91-21100

VERBAL COMMUNICATION
Analysis of routine communication in the air traffic control system
[NASA-CR-188116] p 600 N91-22475

VERY HIGH FREQUENCIES
Comparison of 14 decibels versus 20 decibels desired to undesired signal protection ratios
[DOT/FAA/CT-TN89/69] p 608 N91-21833

VERY LARGE SCALE INTEGRATION
Stand-alone vs. embedded GPS user equipment - The exploration of new standards p 564 A91-33616

VIBRATION
A modal aeroelastic analysis scheme for turbomachinery blading.
[NASA-CR-187089] p 579 N91-21138
Critical speeds and forced response solutions for active magnetic bearing turbomachinery, part 2 p 587 N91-21210

VIBRATION DAMPING
Helicopter vibration reduction using structural optimization with aeroelastic/multidisciplinary constraints - A survey p 570 A91-33527
Helicopter rotor dynamics optimization with experimental verification p 570 A91-33530
Optimization of helicopter airframe structures for vibration reduction - Considerations, formulations, and applications p 571 A91-33533
Reduction of aerodynamic augmented states in active flutter suppression systems p 580 A91-33535
Active vibration control using fixed order dynamic compensation with frequency shaped cost functionals p 604 A91-33932
Shape sensitivity analysis of flutter response of a laminated wing p 571 A91-34144
Signal blending in control systems structural interactions
[BU-505] p 583 N91-22132
Fourth NASA Workshop on Computational Control of Flexible Aerospace Systems, part 2
[NASA-CP-10065-PT-2] p 587 N91-22331
An overview of the active flexible wing program p 583 N91-22332
Design and test of three active flutter suppression controllers p 583 N91-22334
Development and testing of controller performance evaluation methodology for multi-input/multi-output digital control systems p 584 N91-22337

VIBRATION EFFECTS
Effects of gear box vibration and mass imbalance on the dynamics of multi-stage gear transmissions
[NASA-TM-103695] p 599 N91-21534

VIBRATION MODE
Aeroelastic optimum design of composite rotor blade with returning wake effect p 570 A91-32646
Effects of gear box vibration and mass imbalance on the dynamics of multi-stage gear transmissions
[NASA-TM-103695] p 599 N91-21534
Signal blending in control systems structural interactions
[BU-505] p 583 N91-22132

VIBRATION TESTS
Avionics Environmental Reliability using finite element analysis
[ASME PAPER 90-WA/TS-1] p 591 A91-32961

VISCOUS FLOW
Closed-coupled zonal solution for viscous flow problems p 546 A91-34063
An implicit predictor-corrector relaxation method for viscous transonic flows p 592 A91-34064
Computation of unsteady incompressible viscous flow around airfoils p 546 A91-34074
Role of artificial viscosity in Euler and Navier-Stokes solvers p 547 A91-34135
Solution method for viscous flows at all speeds in complex domains p 548 A91-34185
Viscous, hypersonic flows over compression ramps p 548 A91-34194
Split-matrix marching methods for three-dimensional viscous and inviscid hypersonic flows p 549 A91-34206
Computation of the viscous flow past a prolate spheroid at incidence p 550 A91-34216
Some aspects of the numerical simulation of compressible viscous flow around bluff bodies at low Ma-number p 550 A91-34220
Experimental and numerical investigation of three-dimensional viscous flows and vortex motion inside an annular compressor blade row
[ASME PAPER 90-GT-155] p 551 A91-34787
Finite element methods for integrated aerodynamic heating analysis
[NASA-CR-188079] p 554 N91-21101
Investigation of nose bluntness and angle of attack effects on slender bodies in viscous hypertension flows
[NASA-CR-188153] p 557 N91-21117
CFD for hypersonic propulsion
[NASA-TM-103791] p 597 N91-21447

VORTEX BREAKDOWN
Solution of the 3-D, incompressible Navier-Stokes equations for the simulation of vortex breakdown p 593 A91-34181
Vortex bursting over a unit area aspect ratio delta wing using vortex paneling methods
[AD-A231028] p 557 N91-21119
Unsteady aerodynamics of slender wings p 560 N91-22105
Water tunnel flow visualisation of vortex breakdown over the F/A-18
[ARL-FLIGHT-MECH-R-179] p 600 N91-22511

VORTEX GENERATORS
Unsteady flowfield behind a vortex generator rapidly pitched to angle of attack p 547 A91-34139
Numerical investigation of three dimensional laminar flows in a channel with a built-in circular cylinder and wing-type vortex generators p 550 A91-34218

VORTEX SHEDDING
Computation of unsteady incompressible viscous flow around airfoils p 546 A91-34074
Unsteady radial transport in a transonic compressor stage
[ASME PAPER 90-GT-133] p 551 A91-34788
Velocity measurements in a turbulent trailing vortex and their application to BWI noise prediction
[NASA-CR-188083] p 554 N91-21100
The transient development of vortices over a delta wing
[AD-A231946] p 559 N91-22082

VORTEX SHEETS
A vortex-lattice method for the calculation of vortex sheet roll-up and wing-vortex interaction p 546 A91-34052
A method to calculate the influence of vortex roll-up on the induced drag of wings p 546 A91-34055
Vortex bursting over a unit area aspect ratio delta wing using vortex paneling methods
[AD-A231028] p 557 N91-21119

VORTICES
Vortical solutions of the conical Euler equations --- Book p 591 A91-33674
Effect of geometrical disturbance on vortex asymmetry p 547 A91-34136
A streamwise upwind algorithm applied to vortical flow over a delta wing p 548 A91-34192
Aspects of the application of an Euler-equation method to the simulation of leading-edge vortex flow p 549 A91-34196
Experimental and numerical investigation of three-dimensional viscous flows and vortex motion inside an annular compressor blade row
[ASME PAPER 90-GT-155] p 551 A91-34787
Vortex element methods for fluid dynamic analysis of engineering systems --- Book p 594 A91-35539
Euler analysis of transonic stator-rotor interaction using a finite volume method p 554 A91-35984
Compressible flows with periodic vortical disturbances around lifting airfoils
[NASA-TM-103742] p 554 N91-21060
A finite-difference, frequency-domain numerical scheme for the solution of the linearized unsteady Euler equations p 595 N91-21067
Vortex bursting over a unit area aspect ratio delta wing using vortex paneling methods
[AD-A231028] p 557 N91-21119
The transient development of vortices over a delta wing
[AD-A231946] p 559 N91-22082
Flight test to determine feasibility of a proposed airborne wake vortex detection concept
[NASA-TM-102672] p 563 N91-22096
Large amplitude oscillations p 561 N91-22108
Forebody vortex control p 573 N91-22110
Variable camber wings for transport aircraft p 574 N91-22112

VORTICITY
Numerical simulation of vortices motion in presence of solid boundaries p 549 A91-34213
Vortex element methods for fluid dynamic analysis of engineering systems --- Book p 594 A91-35539

VORTICITY EQUATIONS
Vorticity equation solutions for slender wings at high incidence p 547 A91-34126

VULNERABILITY
Methodology development for the verification and validation of flight critical systems software, phase 1
[AD-A229932] p 605 N91-21735

W

WAFERS
High temperature performance evaluation of a hypersonic engine ceramic wafer seal
[NASA-TM-103737] p 601 N91-22567

WAKES
Unsteady radial transport in a transonic compressor stage
[ASME PAPER 90-GT-133] p 551 A91-34788
Numerical solutions of 2-D multi-stage rotor/stator unsteady flow interactions p 595 N91-21070
Vortex bursting over a unit area aspect ratio delta wing using vortex paneling methods
[AD-A231028] p 557 N91-21119
Flight test to determine feasibility of a proposed airborne wake vortex detection concept
[NASA-TM-102672] p 563 N91-22096

WALL FLOW
On management and control of turbulent shear flows p 545 A91-33803
Development and validation of characteristic boundary conditions for cell-centered Euler flow calculations p 592 A91-34178

WALL PRESSURE
Fast response wall pressure measurement as a means of gas turbine blade fault identification
[ASME PAPER 90-GT-341] p 578 A91-34813

WALL TEMPERATURE
Infrared thermography for the qualitative aerodynamic study of a slender body
[ISL-R-122/89] p 555 N91-21104

WALLS
Description and evaluation of an interference assessment for a slotted-wall wind tunnel
[NASA-CR-4352] p 585 N91-21155
WARM FRONTS
Analysis of three icing test flights reaching the aircraft-referred icing degree severe
[DLR-FB-90-34] p 562 N91-21123
WARNING SYSTEMS
Traffic Alert and Collision Avoidance System (TCAS): Cockpit Display of Traffic Information (CDTI) investigation. Phase 1: Feasibility study
[NASA-TM-104956] p 569 N91-22102
WAVE EQUATIONS
Compressible flows with periodic vortical disturbances around lifting airfoils
[NASA-TM-103742] p 554 N91-21060
Calculation of thickness and charge noise radiated by a rotor in forward flight
[ISL-R-119/89] p 607 N91-21831
WAVE PROPAGATION
High-speed compressor surge with application to active control
[ASME PAPER 90-GT-354] p 553 A91-34797
WEAPON SYSTEMS
START - A broad application spectrum gyro for the 1990's p 591 A91-33604
Ring laser gyro applications for tactical missiles - The Army TACMS solution p 576 A91-33657
WEATHER FORECASTING
Modern aviation weather systems for efficient flight management p 602 A91-33648
WEIGHT REDUCTION
Fin structures of the Airbus family experience with advanced composites p 570 A91-32455
WEIGHTLESSNESS
Weightless test balancing of elastic rotors with the help of interchangeable longitudinal bearing stiffnesses p 592 A91-34015
WIND MEASUREMENT
A simple, analytical, axisymmetric microburst model for downdraft estimation
[NASA-TM-104053] p 573 N91-21132
Air motion measurement uncertainties: Their impact on atmospheric studies p 603 N91-22654
Fast response gust measurement device p 603 N91-22659
WIND PROFILES
A simple, analytical, axisymmetric microburst model for downdraft estimation
[NASA-TM-104053] p 573 N91-21132
WIND SHEAR
Modern aviation weather systems for efficient flight management p 602 A91-33648
A simple, analytical, axisymmetric microburst model for downdraft estimation
[NASA-TM-104053] p 573 N91-21132
WIND TUNNEL APPARATUS
Propulsion simulator for magnetically-suspended wind tunnel models p 586 N91-21198
A solid-state controllable power supply for a magnetic suspension wind tunnel p 585 N91-21199
WIND TUNNEL DRIVES
Structural integrity of wind tunnel wooden fan blades
[NASA-TM-104059] p 602 N91-22589
WIND TUNNEL MODELS
Modeling of flow parameters in a cryogenic wind tunnel p 584 A91-33919
Hot-bench simulation of the active flexible wing wind-tunnel model
[NASA-TM-102758] p 582 N91-21144
Propulsion simulator for magnetically-suspended wind tunnel models p 586 N91-21198
An overview of the active flexible wing program p 583 N91-22332
Aeroelastic modeling of the active flexible wing wind-tunnel model p 575 N91-22333
Roll plus maneuver load alleviation control system designs for the active flexible wing wind-tunnel model p 584 N91-22335
WIND TUNNEL TESTS
The location of acoustic blade-vortex interaction - A further step toward an understanding of helicopter noise p 607 A91-33368
Rotors in the wind tunnel - DLR helicopter research methods in the German-Dutch Wind Tunnel p 584 A91-33371
Interdisciplinary cooperative aerospace research - Examples of scientific cooperation with Braunschweig Technical University p 543 A91-33372
Effects of heat transfer on aerodynamics and possible implications for wind tunnel tests p 545 A91-33802
HYTEX - Demonstrator for hypersonic flight up to Mach 5 p 571 A91-34260
Modeling of surface roughness effects on glaze ice accretion p 562 A91-35107
Low speed wind tunnel investigation of propeller slipstream aerodynamic effects on different nacelle/wing combinations. Part 2: Propeller slipstream flow field surveys (velocity components, dynamic, total and static pressure distributions) at zero angle of attack and high power
[FFA-TN-1990-24-PT-2] p 555 N91-21109
Wind tunnel test of a propeller working in a low Reynolds number range
[NAL-TR-1071] p 556 N91-21112
An experimental study of a three-dimensional swept-back wing with suction laminar-flow-control
[NAL-TR-1072] p 556 N91-21113
Span reduction effects on the flutter characteristics of arrow-wing supersonic transport configurations
[NASA-TP-3077] p 572 N91-21127
Hot-bench simulation of the active flexible wing wind-tunnel model
[NASA-TM-102758] p 582 N91-21144
Possibilities of trajectory modification
[ISL-CO-209/90] p 582 N91-21151
Results of the HHC wind tunnel tests, 1986 - 1988
[DLR-FB-90-42] p 582 N91-21152
Description and evaluation of an interference assessment for a slotted-wall wind tunnel
[NASA-CR-4352] p 585 N91-21155
Propulsion simulator for magnetically-suspended wind tunnel models p 586 N91-21198
CFD research and systems in Kawasaki Heavy Industries and its future prospects p 596 N91-21382
Numerical study of the aerodynamic effects of using sulfur hexafluoride as a test gas in wind tunnels
[NASA-TP-3086] p 558 N91-22070
Small-scale experiments in STOVL ground effects
[NASA-TM-102813] p 560 N91-22091
An introduction to testing parachutes in wind tunnels
[DE91-009166] p 560 N91-22094
Oscillatory data for typical configurations p 561 N91-22109
An overview of the active flexible wing program p 583 N91-22332
Aeroelastic modeling of the active flexible wing wind-tunnel model p 575 N91-22333
Design and test of three active flutter suppression controllers p 583 N91-22334
WIND TUNNEL WALLS
A review of near-wall Reynolds-stress
[NASA-CR-4369] p 559 N91-22080
WIND TUNNELS
Propulsion simulator for magnetically-suspended wind tunnel models p 586 N91-21198
NASA Ames aerospace systems directorate research
[NASA-TM-103844] p 608 N91-22066
WIND VANES
Air motion measurements: Past and future p 603 N91-22653
WING OSCILLATIONS
Optimal design of metal and composite thin-walled structures with flutter constraint p 591 A91-32650
Shape sensitivity analysis of flutter response of a laminated wing p 571 A91-34144
WING PLANFORMS
Conical Euler simulation of wing rock for a delta wing planform p 580 A91-33536
A vortex-lattice method for the calculation of vortex sheet roll-up and wing-vortex interaction p 546 A91-34052
Effect of planform on induced drag
[BU-500] p 559 N91-22086
WING PROFILES
Progress in the prediction of the laminar-turbulent transition for laminar wings - The profile and wing geometries determine the friction drag of an aircraft p 544 A91-33369
An inverse boundary layer procedure with application to 3-D wing flow p 550 A91-34229
WING SPAN
Span reduction effects on the flutter characteristics of arrow-wing supersonic transport configurations
[NASA-TP-3077] p 572 N91-21127
WING TIPS
Flight test to determine feasibility of a proposed airborne wake vortex detection concept
[NASA-TM-102672] p 563 N91-22096
WINGS
Lift and rolling moment due to spoilers on wings at subsonic speeds
[ESDU-90030] p 572 N91-21129
Flutter suppression of an aircraft wing using a control surface
[BU-506] p 583 N91-22133
Design and test of three active flutter suppression controllers p 583 N91-22334
WOODEN STRUCTURES
Structural integrity of wind tunnel wooden fan blades
[NASA-TM-104059] p 602 N91-22589
WORKLOADS (PSYCHOPHYSIOLOGY)
Suppression of biodynamic interference in head-tracked teleoperation
[NASA-TM-103833] p 577 N91-21134

X

X-29 AIRCRAFT
Temperature effect on the stress concentration in the composite material used by the X-29A forward-swept wing aircraft p 590 A91-32547

Y

YAWING MOMENTS
Forebody vortex control p 573 N91-22110

Typical Personal Author Index Listing

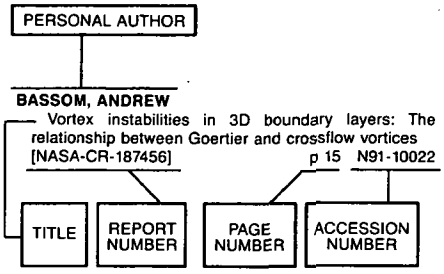

Listings in this index are arranged alphabetically by personal author. The title of the document provides the user with a brief description of the subject matter. The report number helps to indicate the type of document listed (e.g., NASA report, translation, NASA contractor report). The page and accession numbers are located beneath and to the right of the title. Under any one author's name the accession numbers are arranged in sequence.

A

ABDEL-FATTAH, A. M.
Aerothermodynamic design appraisal of noise suppressors for F/A-18 engine run-up facilities at RAAF Williamtown
[ARL-PROP-R-177] p 585 N91-22136

ABDELSALAM, MOUSTAFA K.
Magnetic suspension and balance system advanced study, 1989 design p 586 N91-21197

ABELE, GUNARS
Snow roads and runways
[AD-A231490] p 586 N91-22138

ABKOWITZ, STANLEY
Feasibility study for the qualification of an economically advantageous Ti-6Al-4V bearing housing for gas turbine engine application by powder metal manufacturing technology
[AD-A231666] p 601 N91-22564

ADAMS, WILLIAM M.
Design and test of three active flutter suppression controllers p 583 N91-22334

ADELMAN, HOWARD M.
Integrated multidisciplinary design optimization of rotorcraft p 570 A91-33528

AGARWAL, A.
Automated flight test management system
[NASA-CR-186011] p 574 N91-22117

AL-TAIE, ARKAN KHILKHAL HUSAIN
Experimental study of radiation from coated turbine blades p 580 N91-22122

ALBERS, JAMES A.
NASA Ames aerospace systems directorate research
[NASA-TM-103844] p 608 N91-22066

ALCORN, CHARLES W.
Interference-free measurements of the subsonic aerodynamics of slanted-base ogive cylinders p 547 A91-34130

ALEXANDER, DENNIS R.
Comparison of UNL laser imaging and sizing system and a phase Doppler system for analyzing sprays from a NASA nozzle
[NASA-CR-185239] p 598 N91-21485

ALMOSNINO, D.
Vorticity equation solutions for slender wings at high incidence p 547 A91-34126

ALTER, WENDY
Influence of a magnetic field during directional solidification of MAR-M 246 + Hf superalloy
[NASA-CR-184114] p 590 N91-22416

ALVING, AMY E.
Correlation measurements and structure angles in a turbulent boundary layer recovering from convex curvature p 545 A91-33747

AMUEDO, KURT C.
Hot gas ingestion test results of a two-poster vectored thrust concept with flow visualization in the NASA Lewis 9- x 15-foot low speed wind tunnel
[NASA-TM-103258] p 556 N91-21116

ANANDA, M. P.
Global Positioning System (GPS) autonomous navigation p 567 A91-33653

ANDERSON, J. M.
Cell-vertex, multigrid Euler scheme for use with multiblock grids p 547 A91-34128

ANDERSON, W. KYLE
Numerical study of the aerodynamic effects of using sulfur hexafluoride as a test gas in wind tunnels
[NASA-TP-3086] p 558 N91-22070

ANDO, Y.
Detection of a rotating stall precursor in isolated axial flow compressor rotors
[ASME PAPER 90-GT-157] p 552 A91-34795

ANDRE, MICHEL
Technical presentation of the Merlin's radome: Calibration and data processing p 603 N91-22656

ANDREWS, J. BARRY
Influence of a magnetic field during directional solidification of MAR-M 246 + Hf superalloy
[NASA-CR-184114] p 590 N91-22416

APELIAN, C. V.
Flexible body dynamic stability for high performance aircraft p 574 N91-22318

ARKHIPOV, G. N.
Methods for the optimization of the testing and modeling of control systems for gas turbine engines p 579 A91-35815

ARNONE, ANDREA
Transonic cascade flow calculations using non-periodic C-type grids p 596 N91-21071

ARTHUR, M. T.
Cell-vertex, multigrid Euler scheme for use with multiblock grids p 547 A91-34128

ASHFORD, RONALD
Air safety regulation and its commercial impact p 561 A91-34161

ASHJAEE, JAVAD
Ashtech XII GPS technology p 564 A91-33622

ASWATH, PRANESH BELGOD
Micromechanisms of quasi-static and fatigue crack growth in titanium-aluminides p 602 N91-22583

ATASSI, HAFIZ M.
A finite-difference, frequency-domain numerical scheme for the solution of the linearized unsteady Euler equations p 595 N91-21067

AURRECOECHEA, J. M.
Service temperature estimation of turbine blades based on microstructural observations
[ASME PAPER 90-GT-23] p 578 A91-34811

AVERBACH, B. L.
Analysis of bearing incidents in aircraft gas turbine mainshaft bearings p 591 A91-33464

AVGUSTINOVICH, VALERII G.
Methods for the optimization of the testing and modeling of control systems for gas turbine engines p 579 A91-35815

AZZAZY, MEDHAT
Development of an optical volumetric flowmeter
[PB91-136481] p 601 N91-22550

B

BADINELLI, MARTIN
Comparison of 14 decibels versus 20 decibels desired to undesired signal protection ratios
[DOT/FAA/CT-TN89/69] p 608 N91-21833

BAIRD, CHARLES A.
Terrain-aided altitude computations on the AFTI/F-16 p 576 A91-33650

BAKER, NATHANIEL R.
A highly efficient engineering tool for three-dimensional scramjet flowfield and heat transfer computations p 596 N91-21098

BALLMANN, J.
Airfoils in two- and three-dimensional gust fields p 546 A91-34073

BAMBERGER, E. N.
Analysis of bearing incidents in aircraft gas turbine mainshaft bearings p 591 A91-33464

BARLAY, STEPHEN
The final call: Why airline disasters continue to happen p 561 A91-34250

BARRERA, WENCESLAO
Thermal spikes on CFRP laminates - Assessment of microdamage and its consequences on fatigue life p 588 A91-32549

BARTHELEMY, JEAN-FRANCOIS M.
Shape sensitivity analysis of flutter response of a laminated wing p 571 A91-34144

BARTHOLOMEW, REDGE
Area navigation capability in a miniature airborne GPS receiver p 566 A91-33636

BASKHARONE, E. A.
Finite-element analysis of turbulent flow in annular exhaust diffusers of gas turbine engines p 577 A91-32700

BATINA, JOHN T.
Conical Euler simulation of wing rock for a delta wing planform p 580 A91-33536

BAUMANN, ROBERT
The improvement of the installation of the DLR research aircraft Falcon: Description and first results p 603 N91-22657

BAUMGARDNER, DARREL
Air motion measurement uncertainties: Their impact on atmospheric studies p 603 N91-22654

BEDINGER, JOHN M.
Transmit/receive module technology for X-band active array radar p 568 A91-34011

BEHR, R.
A vortex-lattice method for the calculation of vortex sheet roll-up and wing-vortex interaction p 546 A91-34052

BEHRENS, CHRISTOPHER K.
An experimental investigation into NO(x) control of a gas turbine combustor and augmentor tube incorporating a catalytic reduction system
[AD-A231427] p 580 N91-22124

BEIERLE, MARK
Terrain-aided altitude computations on the AFTI/F-16 p 576 A91-33650

BELLAVIA, DAVID C.
Forces and pressures induced on circular plates by a single lifting jet in ground effect
[NASA-TM-102816] p 558 N91-22077

BENCIC, TIMOTHY J.
Hot gas ingestion test results of a two-poster vectored thrust concept with flow visualization in the NASA Lewis 9- x 15-foot low speed wind tunnel
[NASA-TM-103258] p 556 N91-21116

BENNER, WILLIAM
Flight Service Automation System (FSAS) Model 1 Full Capacity (M1FC) Operational Test and Evaluation (OT/E)/integration test report
[DOT/FAA/CT-TN90/45] p 569 N91-22100

BENNETT, ROBERT M.
Aeroelastic modeling of the active flexible wing wind-tunnel model p 575 N91-22333

BEREZNIAKOV, S. V.
Methods for the optimization of the testing and modeling of control systems for gas turbine engines p 579 A91-35815

BERGEN, FREDERICK D'OENCH, JR.
Shape sensitivity analysis of flutter response of a laminated wing p 571 A91-34144

BERKOWITZ, BRIAN
Modeling of surface roughness effects on glaze ice accretion p 562 A91-35107

BERNINGER, DANIEL J.
The effect of the microwave landing system on airport capacity p 561 A91-33668
BERNSTEIN, H.
Global Positioning System (GPS) autonomous navigation p 567 A91-33653
BESHEARS, D. L.
Evaluating thermographic phosphors in an operating turbine engine
[ASME PAPER 90-GT-266] p 593 A91-34810
BEVER, GLENN A.
Digital signal conditioning for flight test instrumentation
[NASA-TM-101739] p 577 N91-21135
BEVINGTON, JAMES E.
Precision aided inertial navigation using SAR and digital map data p 567 A91-33652
BHUNGALIA, AMAR
Avionics Environmental Reliability using finite element analysis
[ASME PAPER 90-WA/TS-1] p 591 A91-32961
BIETERMAN, MICHAEL B.
Solution adaptive local rectangular grid refinement for transonic aerodynamic flow problems
p 547 A91-34179
BILEKA, B. D.
Using a locally one-dimensional method for solving the *heat conductivity equation to determine the thermal state* of cooled rotor disks p 594 A91-35742
BILL, ROBERT C.
Advanced rotorcraft transmission program
[NASA-TM-103276] p 598 N91-21531
BLAYLOCK, T. A.
Cell-vertex, multigrid Euler scheme for use with multiblock grids p 547 A91-34128
BLINCOW, DONALD W.
In-flight system for helicopter blade inspection
p 575 A91-33268
BLISS, DONALD B.
Role of artificial viscosity in Euler and Navier-Stokes solvers p 547 A91-34135
BOERSTOEL, J. W.
Development and validation of characteristic boundary conditions for cell-centered Euler flow calculations
p 592 A91-34178
3D Euler flows around modern airplanes
p 549 A91-34201
BOOM, ROGER W.
Magnetic suspension and balance system advanced *study, 1989 design* p 586 N91-21197
BORELLA, H. M.
Evaluating thermographic phosphors in an operating turbine engine
[ASME PAPER 90-GT-266] p 593 A91-34810
BOWEN, BRENT D.
Airline quality rating
[NIAR-91-11] p 563 N91-22098
BOWEN, STUART W.
The NASA-ER2 meteorological measurement system: Instrumentaion, calibration and intercomparison results
p 603 N91-22658
BOWERS, ALBION H.
Multiaxis thrust vectoring using axisymmetric nozzles and postexit vanes on an F/A-18 configuration vehicle
[NASA-TM-101741] p 559 N91-22083
BRADEN, KEVIN
Integrated inertial navigation system/Global Positioning System (INS/GPS) for manned return vehicle autoland application p 586 A91-33609
BRAET, RONALD L.
Methodology development for the verification and validation of flight critical systems software, phase 1
[AD-A229932] p 605 N91-21735
BRAFF, RONALD
Impact of navigation accuracy on the intervention rate in a highly automated air traffic control system
p 566 A91-33647
BRANDON, JAY M.
Dynamic stall effects and applications to high performance aircraft p 573 N91-22106
BRANSTETTER, JAMES R.
Flight test to determine feasibility of a proposed airborne wake vortex detection concept
[NASA-TM-102672] p 563 N91-22096
BRAUN, GUNTER
Rotors in the wind tunnel - DLR helicopter research methods in the German-Dutch Wind Tunnel
p 584 A91-33371
BRAZILE, ROBERT P.
Generalized heuristics for the gate assignment problem p 605 A91-35100
BRENNER, G.
Numerical simulation of laminar hypersonic flow past blunt bodies including high temperature effects
p 547 A91-34180
BRENTNALL, W. D.
Service temperature estimation of turbine blades based on microstructural observations
[ASME PAPER 90-GT-23] p 578 A91-34811
BRESCIANINI, C.
Preliminary calibration of a generic scramjet combustor
[NASA-CR-187539] p 579 N91-21139
BREUER, M.
Solution of the 3-D, incompressible Navier-Stokes equations for the simulation of vortex breakdown
p 593 A91-34181
BRICKER, J. L.
A vehicle location system (VLS) solution approach
p 564 A91-33614
BRITCHER, COLIN P.
Interference-free measurements of the subsonic aerodynamics of slanted-base ogive cylinders
p 547 A91-34130
BRITTON, RANDALL K.
Elevator deflections on the icing process
p 572 A91-35427
BROOKS, C. J.
The human factors relating to escape and survival from helicopters ditching in water
[AGARD-AG-305(F)] p 563 N91-22099
BROWNING, CLINT
Integrated inertial navigation system/Global Positioning System (INS/GPS) for manned return vehicle autoland application p 586 A91-33609
BRYKINA, I. G.
An approximate method for determining friction and heat transfer in chemically nonequilibrium flow past bodies at angle of attack p 553 A91-35660
BUFFAT, MARC
Simulation of two- and three-dimensional internal subsonic flows using a finite element method
p 595 A91-35986
BUI, T. PAUL
The NASA-ER2 meteorological measurement system: Instrumentaion, calibration and intercomparison results
p 603 N91-22658
BULLARD, RANDY
Integrated flight/propulsion control system design based on a decentralized, hierarchical approach
[NASA-TM-103678] p 579 N91-21137
BULLOCK, ELLEN PARKER
Span reduction effects on the flutter characteristics of arrow-wing supersonic transport configurations
[NASA-TP-3077] p 572 N91-21127
BURGESS, MALCOLM
Traffic Alert and Collision Avoidance System (TCAS): Cockpit Display of Traffic Information (CDTI) investigation. Phase 1: Feasibility study
[NASA-TM-104956] p 569 N91-22102
BURKHARD, ALAN
Avionics Environmental Reliability using finite element analysis
[ASME PAPER 90-WA/TS-1] p 591 A91-32961
BUSSOLETTI, JOHN E.
Solution adaptive local rectangular grid refinement for transonic aerodynamic flow problems
p 547 A91-34179
BUTTRILL, CAREY S.
Hot-bench simulation of the active flexible wing wind-tunnel model
[NASA-TM-102758] p 582 N91-21144
BYRNS, EDWARD V., JR.
Active vibration control using fixed order dynamic compensation with frequency shaped cost functionals
p 604 A91-33932

C

CADDY, MICHAEL J.
Computer program for estimating performance of air-breathing aircraft engines
[NASA-TM-4254] p 573 N91-22103
CAIAFA, CAESAR A.
Model rocketry hazard study
[DOT/FAA/CT-TN90/28] p 587 N91-21238
CALISE, ANTHONY J.
Active vibration control using fixed order dynamic compensation with frequency shaped cost functionals
p 604 A91-33932
CALLAGHAN, M. T.
Use of resin composites for cryogenic tankage
p 588 A91-34287
CAMBERLEIN, L.
Uliss G, a fully integrated 'all-in-one' and 'all-in-view' inertia-GPS unit p 566 A91-33644
CAPIT, B.
Uliss G, a fully integrated 'all-in-one' and 'all-in-view' inertia-GPS unit p 566 A91-33644
CAPONE, FRANCIS J.
Aeropropulsive characteristics of canted twin pitch-vectoring nozzles at Mach 0.20 to 1.20
[NASA-TP-3060] p 558 N91-22069
CARGILL, A. M.
High-speed compressor surge with application to active control
[ASME PAPER 90-GT-354] p 553 A91-34797
CARLSSON, B.
Fault detection and diagnosis in gas turbines
[ASME PAPER 90-GT-339] p 578 A91-34814
CARSON, GEORGE T., JR.
Aeropropulsive characteristics of canted twin pitch-vectoring nozzles at Mach 0.20 to 1.20
[NASA-TP-3060] p 558 N91-22069
CARTA, F. O.
Temporally and spatially resolved flow in a two-stage axial compressor. I - Experiment
[ASME PAPER 90-GT-259] p 551 A91-34789
CATTIN, E.
Infrared thermography for the qualitative aerodynamic study of a slender body
[ISL-R-122/89] p 555 N91-21104
Comparison study of the aerodynamic coefficients measured on models with circular or squared section and large elongation in supersonic flow
[ISL-R-125/89] p 555 N91-21106
CELI, ROBERTO
Optimum aeroelastic design of helicopter rotors for longitudinal handling qualities improvement
p 570 A91-33531
CHACON, VINCE
Research flight-control system development for the F-18 high alpha research vehicle
[NASA-TM-104232] p 583 N91-22131
CHADWICK, J. BROOKS
A vehicle location system (VLS) solution approach
p 564 A91-33614
CHAN, K. ROLAND
The NASA-ER2 meteorological measurement system: Instrumentaion, calibration and intercomparison results
p 603 N91-22658
CHANG, KEUN-SHIK
Euler analysis of transonic stator-rotor interaction using a finite volume method p 554 A91-35984
CHANG, KWAN J.
Sensitivity-based scaling for correlating structural response from different analytical models
[NASA-TM-104042] p 602 N91-22578
CHATTOPADHYAY, ADITI
Integrated aerodynamic load/dynamic optimization of helicopter rotor blades p 571 A91-33532
CHEN, CHARLES C. T.
Model rocketry hazard study
[DOT/FAA/CT-TN90/28] p 587 N91-21238
CHEN, D.
Damage tolerance aspects of ARALL fuselage skin structure (philosophy and experiments)
p 588 A91-32573
CHEN, G. T.
Similarity analysis of compressor tip clearance flow structure
[ASME PAPER 90-GT-153] p 552 A91-34793
CHEN, H. C.
Development of a general multiblock flow solver for complex configurations p 605 A91-34230
CHEN, PI-FUAY
Automated extraction of airport runway patterns from radar imagery
[AD-A231809] p 600 N91-22480
CHEN, XIANG-JUN
Dynamic analysis technique of centrifugal impellor with split blades p 593 A91-35498
CHEVALLIER, J.-C.
ASTRE improvements expand usefulness of surface movement radar p 569 A91-36012
CHIANG, TING-LUNG
Computation of flowfields for projectiles in hypersonic chemically reacting flows p 544 A91-33379
CHIGAREV, I. M.
Calculation of the cooling system of small-size blades of high-temperature gas turbine engines
p 594 A91-35743
CHIU, Y. DANNY
Aerodynamic parameter studies and sensitivity analysis for rotor blades in axial flight
[NASA-CR-187524] p 558 N91-22078
CHOPRA, INDERJIT
Aeroelastic optimization of a helicopter rotor using an efficient sensitivity analysis p 570 A91-33529
CHOU, SHAU-TAK RUDY
A study of rotor broadband noise mechanisms and helicopter tail rotor noise
[NASA-CR-177565] p 607 N91-21829

CHOY, FRED K.
Effects of gear box vibration and mass imbalance on the dynamics of multi-stage gear transmissions
[NASA-TM-103695] p 599 N91-21534
CHRISTHILF, DAVID M.
Design and test of three active flutter suppression controllers p 583 N91-22334
CHRISTNER, H. G.
The improvement of the installation of the DLR research aircraft Falcon: Description and first results
p 603 N91-22657
CHUANG, SHU-HAO
Computations for a jet impinging obliquely on a flat surface p 554 A91-35985
CHUNG, J. T.
Three-dimensional flow near the blade/endwall junction of a gas turbine - Visualization in a large-scale cascade simulator
[ASME PAPER 90-WA/HT-4] p 544 A91-32958
CHUNG, SIU-LEUNG
Supercomputer optimizations for stochastic optimal control applications p 605 N91-22313
CICCOLI, M. C.
Non-equilibrium hypersonic flow computations by implicit second-order upwind finite-elements
p 548 A91-34191
CLARK, HERBERT H.
Analysis of routine communication in the air traffic control system
[NASA-CR-188116] p 600 N91-22475
CLEMENT, WARREN F.
Fully automatic guidance and control for rotorcraft nap-of-the-Earth flight following planned profiles. Volume 1: Real-time piloted simulation
[NASA-CR-177571-VOL-1] p 582 N91-21149
Fully automatic guidance and control for rotorcraft nap-of-the-Earth flight following planned profiles. Volume 2: Mathematical model
[NASA-CR-177571-VOL-2] p 582 N91-21150
COEN, PETER G.
Development of a computer technique for the prediction of transport aircraft flight profile sonic boom signatures
[NASA-CR-188117] p 560 N91-22093
COHEN, JERRY
Software: Where we are and what is required in the future p 606 N91-22729
COLE, STANLEY R.
An overview of the active flexible wing program
p 583 N91-22332
CONDON, GREGORY W.
Simulation of nap-of-the-Earth flight in helicopters
[NASA-TM-102830] p 572 N91-21131
CORSIGLIA, VICTOR R.
Forces and pressures induced on circular plates by a single lifting jet in ground effect
[NASA-TM-102816] p 558 N91-22077
Small-scale experiments in STOVL ground effects
[NASA-TM-102813] p 560 N91-22091
CUMPSTY, N. A.
Mixing in axial flow compressors. I - Test facilities and measurements in a four-stage compressor. II - Measurements in a single-stage compressor and a duct
[ASME PAPER 90-GT-38] p 551 A91-34784
Tip leakage flow in axial compressors
[ASME PAPER 90-GT-127] p 552 A91-34792
CUNNINGHAM, K. E.
Global Positioning System (GPS) autonomous navigation p 567 A91-33653
CURRAN, GEORGE L.
Ring laser gyro applications for tactical missiles - The Army TACMS solution p 576 A91-33657
CURRY, J. D.
The effects of simulated electromagnetic pulse on commercial aircraft p 569 A91-35902
CUSHMAN, ARTHUR
Comparison of 14 decibels versus 20 decibels desired to undesired signal protection ratios
[DOT/FAA/CT-TN89/69] p 608 N91-21833

D

DAGAN, A.
Vorticity equation solutions for slender wings at high incidence p 547 A91-34126
DALDER, EDWARD
Superplasticity in a Ti3Al-base alloy stabilized by Nb, V and Mo p 589 A91-34841
DALLMANN, U.
Some aspects of the numerical simulation of compressible viscous flow around bluff bodies at low Ma-number p 550 A91-34220
DANIELS, TAUMI S.
A solid-state controllable power supply for a magnetic suspension wind tunnel p 585 N91-21199
DANIELS, W. A.
Compressor drum aerodynamic experiments and analysis with coolant injected at selected locations
[ASME PAPER 90-GT-151] p 552 A91-34794
DARCY, J. P.
Effect of planform on induced drag
[BU-500] p 559 N91-22086
DAVIS, DEAN
Traffic Alert and Collision Avoidance System (TCAS): Cockpit Display of Traffic Information (CDTI) investigation. Phase 1: Feasibility study
[NASA-TM-104956] p 569 N91-22102
DAVIS, JOHN G.
Cost-efficient manufacturing of composite structures
p 590 N91-23048
DAVIS, MARK W.
Helicopter rotor dynamics optimization with experimental verification p 570 A91-33530
DEDESH, VIKTOR T.
Methods for the optimization of the testing and modeling of control systems for gas turbine engines
p 579 A91-35815
DEGANI, DAVID
Effect of geometrical disturbance on vortex asymmetry
p 547 A91-34136
DEGROOTE, STEVE
Research flight-control system development for the F-18 high alpha research vehicle
[NASA-TM-104232] p 583 N91-22131
DEMIRANDA, GWENDOLYN A.
Design methodology for a community response questionnaire on sonic boom exposure
[NASA-CR-187503] p 608 N91-22830
DEMIRDZIC, I.
Solution method for viscous flows at all speeds in complex domains p 548 A91-34185
DEMMEL, JOHANN
Analysis of three icing test flights reaching the aircraft-referred icing degree severe
[DLR-FB-90-34] p 562 N91-21123
DERVIEUX, A.
On the relation between TVD and mesh adaption and application to Navier-Stokes calculations
p 550 A91-34215
DERVIEUX, ALAIN
Numerical simulation of compressible Euler flows
p 544 A91-33675
DESIDERI, J.-A.
Non-equilibrium hypersonic flow computations by implicit second-order upwind finite-elements
p 548 A91-34191
DETKOV, A. N.
Nonlinear filtering of a trajectory message
p 568 A91-33868
DEVENPORT, WILLIAM J.
Velocity measurements in a turbulent trailing vortex and their application to BWI noise prediction
[NASA-CR-188083] p 554 N91-21100
DILLEY, A. D.
Zonal analysis of two high-speed inlets
p 596 N91-21089
DING, HUI-LIANG
Analysis and optimal design of composite structures
p 591 A91-32651
DOHERR, KARL-FRIEDRICH
Interdisciplinary cooperative aerospace research - Examples of scientific cooperation with Braunschweig Technical University p 543 A91-33372
DOMINEY, SAM C.
In-flight system for helicopter blade inspection
p 575 A91-33268
DORFMAN, G.
Evaluation of controller tools for conducting MLS curved approaches to New York's JFK Airport
p 565 A91-33631
DORNHEIM, MICHAEL A.
Aerospace materials p 588 A91-33324
X-31 flight tests to explore combat agility to 70 deg. AOA p 571 A91-34375
DOUCET, GLENN
Evaluation of an alternative rotorcraft cargo lowering device for the delivery of 500-lb ammunition loads
[AD-A230995] p 573 N91-21133
DOWELL, EARL H.
Role of artificial viscosity in Euler and Navier-Stokes solvers p 547 A91-34135
DOYLE, COLIN P.
Motion compensation for ASTOR long range SAR
p 575 A91-33625
DRING, R. P.
Temporally and spatially resolved flow in a two-stage axial compressor. I - Experiment
[ASME PAPER 90-GT-259] p 551 A91-34789
DUPEROUX, J.-P.
Comparison study of the aerodynamic coefficients measured on models with circular or squared section and large elongation in supersonic flow
[ISL-R-125/89] p 555 N91-21106
DUPUIS, A. D.
Practical methods to evaluate the friction drag coefficient of a projectile in free flight
[ISL-R-123/89] p 555 N91-21105
DZVONIK, L. I.
Inertial aerosol precipitation on ogival bodies of revolution in high-velocity flow p 553 A91-35784

E

EADDY, C. L.
Status of PAVER implementation within the US Air Force
[AD-A231158] p 585 N91-22137
EATON, JOHN K.
Unsteady flowfield behind a vortex generator rapidly pitched to angle of attack p 547 A91-34139
EGOROV, A. I.
State stability of a system of integro-differential equations of nonstationary aeroelasticity
p 595 A91-35785
EGOROV, I. V.
An approach to the numerical solution of two-dimensional Navier-Stokes equations by a finite difference method p 595 A91-35787
EIBERT, MAX
ISS - A combined terrain topography referenced navigation system p 566 A91-33649
ELIASSON, PETER
Hypersonic leeside flow computations using centered schemes for Euler equations p 548 A91-34187
ELLIOT, JAMES R.
The effects of simulated electromagnetic pulse on commercial aircraft p 569 A91-35902
ENDE, H.
Possibilities of trajectory modification
[ISL-CO-209/90] p 582 N91-21151
ENGELKEN, DANIEL J.
Ring laser gyro applications for tactical missiles - The Army TACMS solution p 576 A91-33657
EPPARD, W. M.
Zonal analysis of two high-speed inlets
p 596 N91-21089
EPPLER, R.
A method to calculate the influence of vortex roll-up on the induced drag of wings p 546 A91-34055
EPSTEIN, A. H.
Unsteady radial transport in a transonic compressor stage
[ASME PAPER 90-GT-133] p 551 A91-34788
Rotating waves as a stall inception indication in axial compressors
[ASME PAPER 90-GT-156] p 553 A91-34796
ERICSSON, L. E.
Prediction of slender body coning characteristics
p 544 A91-33382
ESTES, LEE E.
A five channel low cost GPS receiver
p 564 A91-33624
EYSSA, Y. M.
Magnetic suspension and balance system advanced study, 1989 design p 586 N91-21197

F

FAIN, GILBERT
A five channel low cost GPS receiver
p 564 A91-33624
FARBRY, JOHN E., JR.
Design methodology for a community response questionnaire on sonic boom exposure
[NASA-CR-187503] p 608 N91-22830
FARROW, I. R.
Damage accumulation and degradation of composite laminates under aircraft service loading: Assessment and prediction, volumes 1 and 2 p 589 N91-22381
FEESS, W. A.
Global Positioning System (GPS) autonomous navigation p 567 A91-33653
FEIT, CECELIA M.
The design, simulation and implementation of an accurate positioning system for automatic flight inspection p 566 A91-33646
FERNHOLZ, H.-H.
On management and control of turbulent shear flows
p 545 A91-33803
FEYOCK, STEFAN
Design of an intelligent information system for in-flight emergency assistance p 606 N91-22792

FEZOUI, L.
Non-equilibrium hypersonic flow computations by implicit second-order upwind finite-elements
p 548 A91-34191

FIEBIG, M.
Numerical investigation of three dimensional laminar flows in a channel with a built-in circular cylinder and wing-type vortex generators p 550 A91-34218

FIEDLER, H. E.
On management and control of turbulent shear flows
p 545 A91-33803

FIELDS, JAMES M.
Design methodology for a community response questionnaire on sonic boom exposure
[NASA-CR-187503] p 608 N91-22830

FIMPEL, HANS P.
The improvement of the installation of the DLR research aircraft Falcon: Description and first results
p 603 N91-22657

FISHER, S. A.
Aerothermodynamic design appraisal of noise suppressors for F/A-18 engine run-up facilities at RAAF Williamtown
[ARL-PROP-R-177] p 585 N91-22136

FITCH, J. P.
The single antenna interferometer
[DE91-007128] p 597 N91-21407

FLEETER, S.
Forcing function effects on rotor periodic aerodynamic response
[ASME PAPER 90-GT-109] p 553 A91-34798

FLOOD, JOSEPH D.
Hot gas ingestion test results of a two-poster vectored thrust concept with flow visualization in the NASA Lewis 9- x 15-foot low speed wind tunnel
[NASA-TM-103258] p 556 N91-21116

FLOWERS, G. T.
Nonlinear behavior of a rotorcraft model during air resonance p 581 A91-34816

FOOR, W.
Experimental performance of a binary phase-only optical correlator using visual and infrared imagery
p 606 A91-32707

FORNASIER, L.
An iterative procedure for the design of pressure-specified 3-dimensional configurations at subsonic and supersonic speeds by means of a higher-order panel method
[MBB-FE122/S/PUB/375] p 574 N91-22118

FOTTNER, L.
The influence of inlet swirl distortions on the performance of a jet propulsion two-stage axial compressor
[ASME PAPER 90-GT-147] p 552 A91-34790

FOX, ERIC E.
Bifurcation analysis of the longitudinal dynamics of a simple powered lifting hypersonic vehicle
[AD-A230826] p 557 N91-21118

FRANKE, JOHN M.
A synchronous strobed laser light sheet for rotor flow visualization
[NASA-TM-4266] p 601 N91-22540

FRANKEL, J. I.
Green's function solution to radiative heat transfer between longitudinal gray fins p 593 A91-35117

FREEMAN, C.
High-speed compressor surge with application to active control
[ASME PAPER 90-GT-354] p 553 A91-34797

FREEMAN, W. TOM
Cost-efficient manufacturing of composite structures
p 590 N91-23048

FRIED, W. R.
VLS - A DTOA system for position location
p 568 A91-33667

FRIEDMANN, PERETZ P.
Helicopter vibration reduction using structural optimization with aeroelastic/multidisciplinary constraints - A survey p 570 A91-33527

FUJIMOTO, HITOSHI
Interaction between two jets exhausted from nozzles arranged in parallel p 593 A91-34439

G

GAIER, JAMES R.
Resistivity of pristine and intercalated graphite fiber epoxy composites p 589 A91-35949

GALLMAN, JOHN
Aerodynamic and structural studies of joined-wing aircraft p 571 A91-33534

GALLUS, H. E.
Three-dimensional wake decay inside of a compressor cascade and its influence on the downstream unsteady flow field. I - Wake decay characteristics in the flow passage. II - Unsteady flow field downstream of the stator
[ASME PAPER 90-GT-21] p 551 A91-34786
Experimental and numerical investigation of three-dimensional viscous flows and vortex motion inside an annular compressor blade row
[ASME PAPER 90-GT-155] p 551 A91-34787

GARG, SANJAY
Integrated flight/propulsion control system design based on a decentralized, hierarchical approach
[NASA-TM-103678] p 579 N91-21137
Integrated flight/propulsion control design for a STOVL aircraft using H-infinity control design techniques
[NASA-TM-104340] p 579 N91-21140

GARNIER, V. H.
Rotating waves as a stall inception indication in axial compressors
[ASME PAPER 90-GT-156] p 553 A91-34796

GARRARD, WILLIAM L.
Eigenspace design of helicopter flight control systems
[AD-A231588] p 582 N91-21153

GASCH, ROBERT
Weightless test balancing of elastic rotors with the help of interchangeable longitudinal bearing stiffnesses
p 592 A91-34015

GASPAR, T. A.
Direct cast titanium aluminide strip
[AD-A231906] p 590 N91-22424

GASSNER, RONALD L.
Transmit/receive module technology for X-band active array radar p 568 A91-34011

GAST, J. R.
Service temperature estimation of turbine blades based on microstructural observations
[ASME PAPER 90-GT-23] p 578 A91-34811

GAUTIER, B.
Comparison study of the aerodynamic coefficients measured on models with circular or squared section and large elongation in supersonic flow
[ISL-R-125/89] p 555 N91-21106

GEISELHART, KARL A.
Computer program for estimating performance of air-breathing aircraft engines
[NASA-TM-4254] p 573 N91-22103

GEISSLER, W.
Numerical calculation of the unsteady separating flow on oscillating airfoils (dynamic stall) p 546 A91-34057

GELDERLOOS, HENDRIK
Integrated inertial navigation system/Global Positioning System (INS/GPS) for manned return vehicle autoland application p 586 A91-33609

GERMAN, VLADIMIR M.
Methods for the optimization of the testing and modeling of control systems for gas turbine engines
p 579 A91-35815

GILES, GARY L.
Sensitivity-based scaling for correlating structural response from different analytical models
[NASA-TM-104042] p 602 N91-22578

GILMORE, JOHN F.
Knowledge-based target recognition system evolution
p 577 A91-35978

GILYARD, GLENN B.
A preliminary evaluation of an F100 engine parameter estimation process using flight data
[NASA-TM-4216] p 597 N91-21446

GIRAUD, M.
Practical methods to evaluate the friction drag coefficient of a projectile in free flight
[ISL-R-123/89] p 555 N91-21105

GLEGG, STEWART A. L.
Velocity measurements in a turbulent trailing vortex and their application to BWI noise prediction
[NASA-CR-188083] p 554 N91-21100

GLINSKY, N.
Non-equilibrium hypersonic flow computations by implicit second-order upwind finite-elements
p 548 A91-34191

GMELIN, BERND
Rotors in the wind tunnel - DLR helicopter research methods in the German-Dutch Wind Tunnel
p 584 A91-33371
Interdisciplinary cooperative aerospace research - Examples of scientific cooperation with Braunschweig Technical University p 543 A91-33372

GNEMMI, F.
Blade-wake interaction on a two blade rotor with prediction of the radiated noise stationary and forward flight, comparison between calculation, and experiment
[ISL-R-120/89] p 608 N91-21832

GNEMMI, P.
Calculation of thickness and charge noise radiated by a rotor in forward flight
[ISL-R-119/89] p 607 N91-21831

GNIELKA, PETER
Weightless test balancing of elastic rotors with the help of interchangeable longitudinal bearing stiffnesses
p 592 A91-34015

GNOFFO, PETER A.
A numerical study of hypersonic stagnation heat transfer predictions at a coordinate singularity
p 548 A91-34193

GOFORTH, E. A.
Flexible body dynamic stability for high performance aircraft p 574 N91-22318

GOLDEY, C. L.
Propulsion simulator for magnetically-suspended wind tunnel models p 586 N91-21198

GOLDSTEIN, STAN
Stand-alone vs. embedded GPS user equipment - The exploration of new standards p 564 A91-33616

GOODWIN, G.
Fault detection and diagnosis in gas turbines
[ASME PAPER 90-GT-339] p 578 A91-34814

GOORJIAN, PETER M.
A streamwise upwind algorithm applied to vortical flow over a delta wing p 548 A91-34192

GORDER, PETER J.
Fully automatic guidance and control for rotorcraft nap-of-the-Earth flight following planned profiles. Volume 1: Real-time piloted simulation
[NASA-CR-177571-VOL-1] p 582 N91-21149
Fully automatic guidance and control for rotorcraft nap-of-the-Earth flight following planned profiles. Volume 2: Mathematical model
[NASA-CR-177571-VOL-2] p 582 N91-21150

GORRELL, STEVEN E.
An experimental study of exit flow patterns in a multistage compressor in rotating stall
[AD-A231353] p 580 N91-21143

GOULD, RONALD W.
Significance of residual curing strains in composite *structure repair technology* p 590 A91-32461

GRAFTON, SUE B.
Multiaxis thrust vectoring using axisymmetric nozzles and postexit vanes on an F/A-18 configuration vehicle
[NASA-TM-101741] p 559 N91-22083

GRAHL, KLAUS G.
Method for calculating boundary region corrections in multistep axial turbomachines p 592 A91-34014

GRASSO, FRANCESCO
A numerical study of hypersonic stagnation heat transfer predictions at a coordinate singularity
p 548 A91-34193

GREITZER, E. M.
Similarity analysis of compressor tip clearance flow structure
[ASME PAPER 90-GT-153] p 552 A91-34793
Rotating waves as a stall inception indication in axial compressors
[ASME PAPER 90-GT-156] p 553 A91-34796

GRIFFITHS, P. J.
The preliminary aerodynamic design of light aircraft
[BU-504] p 574 N91-22119

GRUNWALD, A. J.
Suppression of biodynamic interference in head-tracked teleoperation
[NASA-TM-103833] p 577 N91-21134

GRYBOS, R.
The effect of shear and rotary inertia of a rotor at its critical speeds p 592 A91-34125

GU, W. G.
Cumulative damage problem in pull-through fatigue of C.F.R.P. laminate p 588 A91-32576

GU, ZHENLONG
ICCM-VII; Proceedings of the 7th International *Conference on Composite Materials, Guangzhou, People's* Republic of China, Nov. 22-24, 1989. Vols. 1-3
p 588 A91-32451

GUBIN, V. V.
MHD drag and heat transfer of a sphere in supersonic flow of a partially ionized gas p 607 A91-35791

GUEMES, ALFREDO
Thermal spikes on CFRP laminates - Assessment of microdamage and its consequences on fatigue life
p 588 A91-32549

GUPTA, KAJAL K.
STARS: An integrated general-purpose finite element structural, aeroelastic, and aeroservoelastic analysis computer program
[NASA-TM-101709-REV] p 599 N91-21587

GUPTA, R. R.
Omega signal coverage prediction in the 1990's
p 568 A91-33665

GWILLIAM, DAVID J., JR.
Separating boundary layer response to an unsteady turbulent environment
[AD-A231483] p 559 N91-22081

H

HAASE, WERNER
Viscous, hypersonic flows over compression ramps p 548 A91-34194
HACKER, JOERG M.
The FIAMS research aircraft or small is beautiful p 603 N91-22655
HACKMAN, L. E.
Direct cast titanium aluminide strip
[AD-A231906] p 590 N91-22424
HAENEL, D.
Solution of the 3-D, incompressible Navier-Stokes equations for the simulation of vortex breakdown p 593 A91-34181
HAERTIG, J.
Calculation of thickness and charge noise radiated by a rotor in forward flight
[ISL-R-119/89] p 607 N91-21831
Blade-wake interaction on a two blade rotor with prediction of the radiated noise stationary and forward flight, comparison between calculation, and experiment
[ISL-R-120/89] p 608 N91-21832
HAFTKA, RAPHAEL T.
Sensitivity-based scaling for correlating structural *response from different analytical models*
[NASA-TM-104042] p 602 N91-22578
HAH, C.
Experimental and numerical investigation of three-dimensional viscous flows and vortex motion inside an annular compressor blade row
[ASME PAPER 90-GT-155] p 551 A91-34787
Three-dimensional flowfields inside a transonic compressor with swept blades
[ASME PAPER 90-GT-359] p 552 A91-34791
HALBY, S.
Experimental performance of a binary phase-only optical correlator using visual and infrared imagery p 606 A91-32707
HAMBOURGER, PAUL D.
Resistivity of pristine and intercalated graphite fiber epoxy composites p 589 A91-35949
HAMEL, PETER
Interdisciplinary cooperative aerospace research - Examples of scientific cooperation with Braunschweig Technical University p 543 A91-33372
HAMWI, SAKHER
Approximate methods for predicting the lifting characteristics of wing-body combinations p 558 N91-22074
HANFF, E. S.
Large amplitude oscillations p 561 N91-22108
HANSMAN, R. JOHN, JR.
Modeling of surface roughness effects on glaze ice accretion p 562 A91-35107
HANSON, FLOYD B.
Supercomputer optimizations for stochastic optimal control applications p 605 N91-22313
HARRIS, D. G.
START - A broad application spectrum gyro for the 1990's p 591 A91-33604
HART, R. M.
Signal blending in control systems structural *interactions*
[BU-505] p 583 N91-22132
HASHIDATE, MASATAKA
Wind tunnel test of a propeller working in a low Reynolds number range
[NAL-TR-1071] p 556 N91-21112
HASLIM, LEONARD A.
Lightweight, fire-retardant, crashworthy aircraft seat cushioning p 563 N91-23052
HASTINGS, E. C., JR.
Flight test to determine feasibility of a proposed airborne wake vortex detection concept
[NASA-TM-102672] p 563 N91-22096
HATTA, NATSUO
Interaction between two jets exhausted from nozzles arranged in parallel p 593 A91-34439
HAVEL, ROBERT F.
Flight Service Automation System (FSAS) Model 1 Full Capacity (M1FC) Operational Test and Evaluation (OT/E)/integration test report
[DOT/FAA/CT-TN90/45] p 569 N91-22100
HAWKINS, RICHARD W.
A highly efficient engineering tool for three-dimensional scramjet flowfield and heat transfer computations p 596 N91-21098
HEADLEY, DEAN E.
Airline quality rating
[NIAR-91-11] p 563 N91-22098
HEATH, JAMES B.
Significance of residual curing strains in composite structure repair technology p 590 A91-32461
HEDMAN, SVEN G.
MATGRID, a program for generation of C-H and C-O topology grids around wing/body configurations: User's guide
[FFA-TN-1991-03] p 556 N91-21110
HEEG, JENNIFER
Aeroelastic modeling of the active flexible wing wind-tunnel model p 575 N91-22333
HELLER, HANNO
The location of acoustic blade-vortex interaction - A further step toward an understanding of helicopter noise p 607 A91-33368
HENLEY, A. J.
Terrain Aided Navigation - Current status, techniques for flat terrain and reference data requirements p 567 A91-33663
HEPBURN, JOHN S. A.
Motion compensation for ASTOR long range SAR p 575 A91-33625
INS reset removal for enhanced post-flight performance analysis p 565 A91-33628
HEVENOR, RICHARD A.
Automated extraction of airport runway patterns from radar imagery
[AD-A231809] p 600 N91-22480
HEWETT, M. D.
Automated flight test management system
[NASA-CR-186011] p 574 N91-22117
HILMES, CRAIG L.
Solution adaptive local rectangular grid refinement for transonic aerodynamic flow problems p 547 A91-34179
HIRAOKA, KOICHI
CFD research and systems in Kawasaki Heavy Industries and its future prospects p 596 N91-21382
HIROSE, HIDEHIRO
The CFD analysis related aerospace in Fuji Heavy Industries, Ltd. p 597 N91-21383
HIROSE, NAOKI
Blunt trailing edge analysis of supercritical airfoils by a Navier-Stokes code
[NAL-TR-1075-T] p 556 N91-21114
HIRSCHEL, ERNST HEINRICH
Closed-coupled zonal solution for viscous flow problems p 546 A91-34063
HOADLEY, SHERWOOD TIFFANY
Development and testing of controller performance evaluation methodology for multi-input/multi-output digital control systems p 584 N91-22337
HOEIJMAKERS, H. W. M.
Aspects of the application of an Euler-equation method to the simulation of leading-edge vortex flow p 549 A91-34196
HOFFMANN, HANS-EBERHARD
Analysis of three icing test flights reaching the aircraft-referred icing degree severe
[DLR-FB-90-34] p 562 N91-21123
HOFFMANN, KLAUS A.
Computation of flowfields for projectiles in hypersonic chemically reacting flows p 544 A91-33379
HOLLISTER, WALTER
Traffic Alert and Collision Avoidance System (TCAS): Cockpit Display of Traffic Information (CDTI) investigation. Phase 1: Feasibility study
[NASA-TM-104956] p 569 N91-22102
HOLLOWELL, JEFF
Heli/SITAN - A terrain referenced navigation algorithm for helicopters p 568 A91-33664
HORNE, W. CLIFTON
Acoustic and aerodynamic study of a pusher-propeller aircraft model
[NASA-TP-3040] p 607 N91-21828
HORSTMANN, KARL H.
Progress in the prediction of the laminar-turbulent transition for laminar wings - The profile and wing geometries determine the friction drag of an aircraft p 544 A91-33369
HOSHINO, HIDEO
An experimental study of a three-dimensional swept-back wing with suction laminar-flow-control
[NAL-TR-1072] p 556 N91-21113
HOUCK, JACOB A.
Hot-bench simulation of the active flexible wing wind-tunnel model
[NASA-TM-102758] p 582 N91-21144
HUANG, C. Q.
Optimal design of metal and composite thin-walled structures with flutter constraint p 591 A91-32650
HULL, WILLIAM P.
Transmit/receive module technology for X-band active array radar p 568 A91-34011
HUNG, CHING-MAO
Simulation of glancing shock wave and boundary layer interaction p 548 A91-34195
HWANG, B. C.
A review of near-wall Reynolds-stress
[NASA-CR-4369] p 559 N91-22080
HWANG, PATRICK Y. C.
Kinematic GPS - Resolving integer ambiguities on the fly p 567 A91-33661

I

INOUE, KENJI
Coning motion of slender bodies at high angles of attack
[NAL-TR-1059] p 556 N91-21111
INOUE, M.
Detection of a rotating stall precursor in isolated axial flow compressor rotors
[ASME PAPER 90-GT-157] p 552 A91-34795
ISHIDA, YOJI
An experimental study of a three-dimensional swept-back wing with suction laminar-flow-control
[NAL-TR-1072] p 556 N91-21113
ISSA, R. I.
Solution method for viscous flows at all speeds in complex domains p 548 A91-34185
IWAMOTO, T.
Detection of a rotating stall precursor in isolated axial flow compressor rotors
[ASME PAPER 90-GT-157] p 552 A91-34795

J

JACKSON, N. P.
Flutter suppression of an aircraft wing using a control surface
[BU-506] p 583 N91-22133
JACOBS, J. M. J. W.
Aspects of the application of an Euler-equation method to the simulation of leading-edge vortex flow p 549 A91-34196
JACOBS, P. A.
Preliminary calibration of a generic scramjet combustor
[NASA-CR-187539] p 579 N91-21139
JAGUSINSKI, F.
Infrared thermography for the qualitative aerodynamic study of a slender body
[ISL-R-122/89] p 555 N91-21104
JANKOVITZ, JACK J.
Flight evaluation of the Integrated Inertial Sensor Assembly (IISA) on a helicopter p 581 A91-33639
JARLAAS, ROLF
Stability analysis of a fuselage side
[FFA-TN-1990-32] p 599 N91-21568
JATEGAONKAR, RAVINDRA
Identification of the aerodynamic model of the DLR research aircraft ATTAS from flight test data
[DLR-FB-90-40] p 572 N91-21130
JENKINS, JESSE
The delayed ejection decision p 561 A91-33273
JEWELL, WAYNE F.
Fully automatic guidance and control for rotorcraft nap-of-the-Earth flight following planned profiles. Volume 1: Real-time piloted simulation
[NASA-CR-177571-VOL-1] p 582 N91-21149
Fully automatic guidance and control for rotorcraft nap-of-the-Earth flight following planned profiles. Volume 2: Mathematical model
[NASA-CR-177571-VOL-2] p 582 N91-21150
JIASEN, HU
Some treatments on boundary conditions for quasi one-dimensional Euler equations
[FFA-TN-1990-36] p 598 N91-21469
JIN, PAUL
Superplasticity in a Ti3Al-base alloy stabilized by Nb, V and Mo p 589 A91-34841
JOACHUM, ANNE M.
Turbulence profiling in the atmospheric boundary layer using three powered gliders p 604 N91-22663
JOHNS, ALBERT L.
Hot gas ingestion test results of a two-poster vectored thrust concept with flow visualization in the NASA Lewis 9- x 15-foot low speed wind tunnel
[NASA-TM-103258] p 556 N91-21116
JOHNSON, B. V.
Compressor drum aerodynamic experiments and analysis with coolant injected at selected locations
[ASME PAPER 90-GT-151] p 552 A91-34794

JOHNSON, FORRESTER T.
Solution adaptive local rectangular grid refinement for transonic aerodynamic flow problems p 547 A91-34179
JOHNSON, LEIF
The N-Dimensional Fighter p 571 A91-35425
JOHNSTON, NORMAN J.
Cost-efficient manufacturing of composite structures p 590 N91-23048
JONES, M. W.
Crew chief CAD system interface guide (version 2 - SI)
[AD-A231433] p 606 N91-22734
JONES, R. T.
The flying wing supersonic transport p 571 A91-34164
JONES, STEPHEN B.
A synchronous strobed laser light sheet for rotor flow visualization
[NASA-TM-4266] p 601 N91-22540
JOSHI, PRAKASH B.
Propulsion simulator for magnetically-suspended wind tunnel models p 586 N91-21198

K

KABKOV, V. IA.
Using a locally one-dimensional method for solving the heat conductivity equation to determine the thermal state of cooled rotor disks p 594 A91-35742
KAHRAMAN, AHMET
Linear and non-linear dynamic models of a geared rotor-bearing system p 594 A91-35536
KAMATH, PRADEEP S.
A highly efficient engineering tool for three-dimensional scramjet flowfield and heat transfer computations p 596 N91-21098
KAMIYA, NOBUHIKO
Analysis of laminar separation bubble using a simple eddy-viscosity turbulence model p 591 A91-33227
Blunt trailing edge analysis of supercritical airfoils by a Navier-Stokes code
[NAL-TR-1075-T] p 556 N91-21114
Analysis of laminar separation bubbles using a simple eddy-viscosity turbulence model
[NAL-TR-1079] p 600 N91-22520
KANG, IN-MO
Euler analysis of transonic stator-rotor interaction using a finite volume method p 554 A91-35984
KAO, PI-JEN
Sensitivity-based scaling for correlating structural response from different analytical models
[NASA-TM-104042] p 602 N91-22578
KAO, T. J.
Development of a general multiblock flow solver for complex configurations p 605 A91-34230
KAPANIA, RAKESH K.
Shape sensitivity analysis of flutter response of a laminated wing p 571 A91-34144
KARAMOUZIS, STAMOS
Design of an intelligent information system for in-flight emergency assistance p 606 N91-22792
KATZER, E.
Laminar shock/boundary-layer interaction - A numerical test problem p 545 A91-34033
KAWECKI, E. J.
Compressor drum aerodynamic experiments and analysis with coolant injected at selected locations
[ASME PAPER 90-GT-151] p 552 A91-34794
KAYABA, SHIGEO
An experimental study of a three-dimensional swept-back wing with suction laminar-flow-control
[NAL-TR-1072] p 556 N91-21113
KAYTEN, PHYLLIS
Human performance factors in aircraft accident investigation
[SAE PAPER 892608] p 562 A91-34912
KEESEE, J.
Critical speeds and forced response solutions for active magnetic bearing turbomachinery, part 1 p 587 N91-21209
Critical speeds and forced response solutions for active magnetic bearing turbomachinery, part 2 p 587 N91-21210
KELLER, DONALD F.
Span reduction effects on the flutter characteristics of arrow-wing supersonic transport configurations
[NASA-TP-3077] p 572 N91-21127
KELLY, G.
Preliminary calibration of a generic scramjet combustor
[NASA-CR-187539] p 579 N91-21139
KEMP, WILLIAM B., JR.
Description and evaluation of an interference assessment for a slotted-wall wind tunnel
[NASA-CR-4352] p 585 N91-21155
KEYSER, D. R.
Theoretical basis for extrapolation of calibration data of PTC 6 throat tap nozzles
[ASME PAPER 90-JPGC/PTC-1] p 578 A91-34808
A method for the extrapolation of calibration data of PTC 6 throat tap nozzles
[ASME PAPER 90-JPGC/PTC-2] p 578 A91-34809
KHAIKIN, S. N.
Optimization of radio-measuring devices incorporated in onboard laser velocimeters p 576 A91-35738
KHOSLA, P. K.
A pressure flux-split technique for computation of inlet flow behavior p 595 N91-21068
KIM, KYUN O.
Computational methods for frictionless contact with application to Space Shuttle Orbiter nose-gear tires
[NASA-TP-3073] p 601 N91-22576
KIM, SEUNG JO
Aeroelastic optimum design of composite rotor blade with returning wake effect p 570 A91-32646
KIRK, R. GORDON
Critical speeds and forced response solutions for active magnetic bearing turbomachinery, part 1 p 587 N91-21209
Critical speeds and forced response solutions for active magnetic bearing turbomachinery, part 2 p 587 N91-21210
KLEIN, R.
A numerical study of interfacial instabilities at high Mach numbers p 549 A91-34198
KLEPL, MARTIN J.
Roll plus maneuver load alleviation control system designs for the active flexible wing wind-tunnel model p 584 N91-22335
KLEUSBERG, ALFRED
Airborne gravimetry and the Global Positioning System p 602 A91-33634
KLIMENKO, V. M.
Calculation of the cooling system of small-size blades of high-temperature gas turbine engines p 594 A91-35743
KLOPFER, GOETZ H.
Grid generation about complex three-dimensional aircraft configurations
[NASA-CR-188097] p 558 N91-22071
KOENEKE, A.
Comparison study of the aerodynamic coefficients measured on models with circular or squared section and large elongation in supersonic flow
[ISL-R-125/89] p 555 N91-21106
KOFF, B. L.
Spanning the globe with jet propulsion
[AIAA PAPER 91-2987] p 577 A91-34111
KOGUT, P. I.
State stability of a system of integro-differential equations of nonstationary aeroelasticity p 595 A91-35785
KOKADO, JUN-ICHI
Interaction between two jets exhausted from nozzles arranged in parallel p 593 A91-34439
KOLODOCHKIN, VLADIMIR P.
Control of the working cycle of gas turbine engines (2nd revised and enlarged edition) p 579 A91-35822
KOMOROWSKI, JERZY P.
Significance of residual curing strains in composite structure repair technology p 590 A91-32461
KOO, KYO NAM
Aeroelastic optimum design of composite rotor blade with returning wake effect p 570 A91-32646
KORDULLA, W.
An implicit predictor-corrector relaxation method for viscous transonic flows p 592 A91-34064
KOSHIOKA, YASUHIRO
The CFD analysis related aerospace in Fuji Heavy Industries, Ltd. p 597 N91-21383
KOTIDIS, P. A.
Unsteady radial transport in a transonic compressor stage
[ASME PAPER 90-GT-133] p 551 A91-34788
KOZAITIS, S. P.
Experimental performance of a binary phase-only optical correlator using visual and infrared imagery p 606 A91-32707
KOZLOV, V. V.
Modeling of flow parameters in a cryogenic wind tunnel p 584 A91-33919
KRAG, BERND
Interdisciplinary cooperative aerospace research - Examples of scientific cooperation with Braunschweig Technical University p 543 A91-33372
KRAUSKOPF, P. J.
Crew chief CAD system interface guide (version 2 - SI)
[AD-A231433] p 606 N91-22734
KROGMANN, UWE K.
Failure management in spatio-temporal redundant, integrated navigation and flight control reference-systems p 581 A91-33640
KROO, ILAN
Aerodynamic and structural studies of joined-wing aircraft p 571 A91-33534
KUBE, ROLAND
Results of the HHC wind tunnel tests, 1986 - 1988
[DLR-FB-90-42] p 582 N91-21152
KUHN, RICHARD E.
Forces and pressures induced on circular plates by a single lifting jet in ground effect
[NASA-TM-102816] p 558 N91-22077
Small-scale experiments in STOVL ground effects
[NASA-TM-102813] p 560 N91-22091
KUNZ, R. F.
Computation of supersonic and low subsonic cascade flows using an explicit Navier-Stokes technique and the kappa-epsilon turbulence model p 596 N91-21072
KUROUMARU, M.
Detection of a rotating stall precursor in isolated axial flow compressor rotors
[ASME PAPER 90-GT-157] p 552 A91-34795
KUTT, L. M.
Addendum to the DYCAST user's manual describing the curved, warp beam finite element
[NASA-CR-4362] p 606 N91-22805
KUYVENHOVEN, J. L.
3D Euler flows around modern airplanes p 549 A91-34201
KWON, OH-KYU
Fault detection and diagnosis in gas turbines
[ASME PAPER 90-GT-339] p 578 A91-34814

L

LAI, Y. G.
A review of near-wall Reynolds-stress
[NASA-CR-4369] p 559 N91-22080
LAKE, GRAHAM
Oceanic clearance trial proves utility of data link communications for ATC p 568 A91-33775
LAKSHMINARAYANA, B.
Computation of supersonic and low subsonic cascade flows using an explicit Navier-Stokes technique and the kappa-epsilon turbulence model p 596 N91-21072
LAMBERT, HEATHER H.
A preliminary evaluation of an F100 engine parameter estimation process using flight data
[NASA-TM-4216] p 597 N91-21446
LANGER, HANS-JUERGEN
Rotors in the wind tunnel - DLR helicopter research methods in the German-Dutch Wind Tunnel p 584 A91-33371
LAWING, PIERCE L.
Propulsion simulator for magnetically-suspended wind tunnel models p 586 N91-21198
LEE, ELIZABETH M.
Conical Euler simulation of wing rock for a delta wing planform p 580 A91-33536
LEE, HAE KYUNG
Aeroelastic optimum design of composite rotor blade with returning wake effect p 570 A91-32646
LEES, S. R. B.
A leading-edge control surface
[BU-508] p 559 N91-22087
LEHMANN, GERT
Results of the HHC wind tunnel tests, 1986 - 1988
[DLR-FB-90-42] p 582 N91-21152
LEIGHTY, BRADLEY D.
A synchronous strobed laser light sheet for rotor flow visualization
[NASA-TM-4266] p 601 N91-22540
LEMONIS, GEORG
Fast response gust measurement device p 603 N91-22659
LENSCHOW, DONALD H.
Air motion measurements: Past and future p 603 N91-22653
LEPIPEC, MARIE PIERRE
Technical presentation of the Merlin's radome: Calibration and data processing p 603 N91-22656
LEURIDAN, JAN
A frequency domain maximum likelihood identification scheme with application to flight flutter data analysis p 581 A91-35576
LEWIS, B. R.
The flexural strength of unidirectional carbon fibre composites
[BU-509] p 589 N91-22399

LEWIS, REGINALD IVAN
Vortex element methods for fluid dynamic analysis of engineering systems p 594 A91-35539
LEWIS, W.
Evaluating thermographic phosphors in an operating turbine engine
[ASME PAPER 90-GT-266] p 593 A91-34810
LEYLEK, J. H.
Mixing in axial-flow compressors - Conclusions drawn from three-dimensional Navier-Stokes analyses and experiments
[ASME PAPER 90-GT-352] p 551 A91-34783
LI, Y. S.
Mixing in axial flow compressors. I - Test facilities and measurements in a four-stage compressor. II - Measurements in a single-stage compressor and a duct
[ASME PAPER 90-GT-38] p 551 A91-34784
LIFSHITZ, S.
Suppression of biodynamic interference in head-tracked teleoperation
[NASA-TM-103833] p 577 N91-21134
LILEK, Z.
Solution method for viscous flows at all speeds in complex domains p 548 A91-34185
LIM, JOON W.
Aeroelastic optimization of a helicopter rotor using an efficient sensitivity analysis p 570 A91-33529
LIM, TEIK CHIN
Force and moment transmissibilities through rolling element bearings in a single-stage rotor system p 594 A91-35537
LIN, S.-J.
Numerical solutions of 2-D multi-stage rotor/stator unsteady flow interactions p 595 N91-21070
LIOU, MENG-SING
Transonic cascade flow calculations using non-periodic C-type grids p 596 N91-21071
LITTELL, HOWARD S.
Unsteady flowfield behind a vortex generator rapidly pitched to angle of attack p 547 A91-34139
LIU, D.
Cumulative damage problem in pull-through fatigue of C.F.R.P. laminate p 588 A91-32576
LIU, QIZHOU
Weightless test balancing of elastic rotors with the help of interchangeable longitudinal bearing stiffnesses p 592 A91-34015
LIU, Y. B.
Cumulative damage problem in pull-through fatigue of C.F.R.P. laminate p 588 A91-32576
LIVINGSTON, DALE A.
Prospects for reduction of separation standards in oceanic airspaces with satellite services p 565 A91-33632
LOHRENZ, MAURA C.
The compressed aeronautical chart database - Support of naval aircraft's digital moving map systems p 563 A91-33608
LOREY, DONALD A.
Vortex bursting over a unit area aspect ratio delta wing using vortex paneling methods
[AD-A231028] p 557 N91-21119
LOTZE, ALBERT
Application of sensitivity methods for error localization in finite element systems p 594 A91-35529
LOUKIS, E.
Fast response wall pressure measurement as a means of gas turbine blade fault identification
[ASME PAPER 90-GT-341] p 578 A91-34813
LOW, EICHER
Eigenspace design of helicopter flight control systems
[AD-A231588] p 582 N91-21153
LUBER, WOLFGANG
Application of sensitivity methods for error localization in finite element systems p 594 A91-35529
LUEDTKE, JACQUELINE R.
Airline quality rating
[NIAR-91-11] p 563 N91-22098
LUX, PETER
ISS - A combined terrain topography referenced navigation system p 566 A91-33649
LY, UY-LOI
Robust integrated autopilot/autothrottle design using constrained parameter optimization
[NASA-CR-188011] p 583 N91-22127
LYNCH, MICHAEL F.
Flight test results of a tightly integrated RLG-based Global Positioning System/inertial navigation system p 566 A91-33645

M

MABEY, D. G.
Effects of heat transfer on aerodynamics and possible implications for wind tunnel tests p 545 A91-33802
MACHA, J.
An introduction to testing parachutes in wind tunnels
[DE91-009166] p 560 N91-22094
MACK, ROBERT E.
Flight evaluation of the Integrated Inertial Sensor Assembly (IISA) on a helicopter p 581 A91-33639
MACKENZIE, FRANKLIN D.
The Loran Early Implementation Project - Gateway for GPS p 563 A91-33607
MACKUSE, FRANCES
Flight Service Automation System (FSAS) Model 1 Full Capacity (M1FC) Operational Test and Evaluation (OT/E)/integration test report
[DOT/FAA/CT-TN90/45] p 569 N91-22100
MAHAJAN, APARAJIT J.
Role of artificial viscosity in Euler and Navier-Stokes solvers p 547 A91-34135
MAHAPATRA, P. R.
A fast and low-cost validation technique for ILS and MLS p 565 A91-33630
MAHAPATRA, PRAVAS R.
The advantages of velocity vector referencing in proportional navigation p 581 A91-33611
Modern aviation weather systems for efficient flight management p 602 A91-33648
MAHONEY, JOHN J.
In-flight system for helicopter blade inspection p 575 A91-33268
MAINE, TRINDEL A.
A preliminary evaluation of an F100 engine parameter estimation process using flight data
[NASA-TM-4216] p 597 N91-21446
MAJURE, ROBERT G.
Demonstration of a ring laser gyro system for pointing and stabilization applications p 575 A91-33627
MALCOLM, GERALD N.
Forebody vortex control p 573 N91-22110
MALKE, SUSANNE
Results of the HHC wind tunnel tests, 1986 - 1988
[DLR-FB-90-42] p 582 N91-21152
MANGALAM, SIVARAMAKRISHNAN M.
Method and apparatus for detecting laminar flow separation and reattachment
[NASA-CASE-LAR-13952-2-SB] p 598 N91-21472
MANTAY, WAYNE R.
Integrated multidisciplinary design optimization of rotorcraft p 570 A91-33528
MANWARING, S. R.
Forcing function effects on rotor periodic aerodynamic response
[ASME PAPER 90-GT-109] p 553 A91-34798
MARBLE, F. E.
Similarity analysis of compressor tip clearance flow structure
[ASME PAPER 90-GT-153] p 552 A91-34793
MARBLE, FRANK E.
Investigations into shock-induced enhancement of mixing and combustion in supersonic burners
[AD-A231750] p 589 N91-22407
MARKIN, K.
Evaluation of controller tools for conducting MLS curved approaches to New York's JFK Airport p 565 A91-33631
MARTIN, R. J.
Compressor drum aerodynamic experiments and analysis with coolant injected at selected locations
[ASME PAPER 90-GT-151] p 552 A91-34794
MARTINO, JOSEPH P.
Study of bird ingestions into small inlet area aircraft turbine engines
[DOT/FAA/CT-90/13] p 562 N91-21122
MARTTILA, CHARLES A.
Precision aided inertial navigation using SAR and digital map data p 567 A91-33652
MARTTILA, CHUCK
Integrated inertial navigation system/Global Positioning System (INS/GPS) for manned return vehicle autoland application p 586 A91-33609
MARX, YVES P.
Numerical simulation of turbulent flows around airfoil and wing p 549 A91-34203
MASLOV, A. A.
Effect of a single three-dimensional surface roughness on the transition in a supersonic boundary layer p 545 A91-33920
MASON, JAMES S.
Transmit/receive module technology for X-band active array radar p 568 A91-34011
MASON, MARY L.
Aeropropulsive characteristics of canted twin pitch-vectoring nozzles at Mach 0.20 to 1.20
[NASA-TP-3060] p 558 N91-22069
Multiaxis thrust vectoring using axisymmetric nozzles and postexit vanes on an F/A-18 configuration vehicle
[NASA-TM-101741] p 559 N91-22083
MATHIOUDAKIS, K.
Fast response wall pressure measurement as a means of gas turbine blade fault identification
[ASME PAPER 90-GT-341] p 578 A91-34813
MATTERN, DUANE
Integrated flight/propulsion control system design based on a decentralized, hierarchical approach
[NASA-TM-103678] p 579 N91-21137
MCCALLUM, DUNCAN C.
Dynamic modelling and analysis of a magnetically suspended flexible rotor p 587 N91-21208
MCCLINTON, CHARLES R.
A highly efficient engineering tool for three-dimensional scramjet flowfield and heat transfer computations p 596 N91-21098
MCCORMICK, JEROLD H.
In-flight system for helicopter blade inspection p 575 A91-33268
MCDONOUGH, PAUL T.
Lightweight, fire-retardant, crashworthy aircraft seat cushioning p 563 N91-23052
MCFARLAND, RICHARD H.
Improved landing aid availability through the use of new criteria p 567 A91-33660
MCINTOSH, GLEN E.
Magnetic suspension and balance system advanced study, 1989 design p 586 N91-21197
MCQUIDDY, DAVID N., JR.
Transmit/receive module technology for X-band active array radar p 568 A91-34011
MCWILLIAMS, IAN G.
The Loran Early Implementation Project - Gateway for GPS p 563 A91-33607
MELVIN, ROBIN G.
Solution adaptive local rectangular grid refinement for transonic aerodynamic flow problems p 547 A91-34179
MENNE, S.
Split-matrix marching methods for three-dimensional viscous and inviscid hypersonic flows p 549 A91-34206
MERHAV, S. J.
Suppression of biodynamic interference in head-tracked teleoperation
[NASA-TM-103833] p 577 N91-21134
MERRINGTON, G.
Fault detection and diagnosis in gas turbines
[ASME PAPER 90-GT-339] p 578 A91-34814
MILLER, GERALD D.
An overview of the active flexible wing program p 583 N91-22332
Roll plus maneuver load alleviation control system designs for the active flexible wing wind-tunnel model p 584 N91-22335
MILLER, WILLIAM G.
The next frontier for strapdown RLG inertial systems - Precision navigation p 576 A91-33656
MILLIS, MALISE
Metamorphoses of ONAV console operations: From prototype to real time application p 606 N91-22794
MOELLENHOFF, D. E.
Design of robust controllers for gas turbine engines
[ASME PAPER 90-GT-113] p 578 A91-34815
MOEN, VERLYN
Area navigation capability in a miniature airborne GPS receiver p 566 A91-33636
MOLINO, JOHN A.
Design methodology for a community response questionnaire on sonic boom exposure
[NASA-CR-187503] p 608 N91-22830
MOORE, DOUGLAS B.
Roll plus maneuver load alleviation control system designs for the active flexible wing wind-tunnel model p 584 N91-22335
MORETTI, GINO
Inviscid flow about a double ellipse p 549 A91-34210
MORGAN, R. G.
Preliminary calibration of a generic scramjet combustor
[NASA-CR-187539] p 579 N91-21139
MORRIS, P. B.
Omega signal coverage prediction in the 1990's p 568 A91-33665
MORRIS, SHELBY J., JR.
Computer program for estimating performance of air-breathing aircraft engines
[NASA-TM-4254] p 573 N91-22103
MORROW, DANIEL
Analysis of routine communication in the air traffic control system
[NASA-CR-188116] p 600 N91-22475
MORT, KENNETH W.
Structural integrity of wind tunnel wooden fan blades
[NASA-TM-104059] p 602 N91-22589

MUELLER, B.
Comparison of upwind and central finite-difference methods for the compressible Navier-Stokes equations p 545 A91-34034
Hypersonic flow simulation for blunt bodies at incidence p 546 A91-34070
Numerical simulation of laminar hypersonic flow past blunt bodies including high temperature effects p 547 A91-34180
Some aspects of the numerical simulation of compressible viscous flow around bluff bodies at low Ma-number p 550 A91-34220
MUKHERJEE, AMIYA K.
Superplasticity in a Ti3Al-base alloy stabilized by Nb, V and Mo p 589 A91-34841
MUKHOPADHYAY, VIVEK
Design and test of three active flutter suppression controllers p 583 N91-22334
Development and testing of controller performance evaluation methodology for multi-input/multi-output digital control systems p 584 N91-22337
MUNZ, C. D.
A numerical study of interfacial instabilities at high Mach numbers p 549 A91-34198
MURDOCK, J. W.
Theoretical basis for extrapolation of calibration data of PTC 6 throat tap nozzles
[ASME PAPER 90-JPGC/PTC-1] p 578 A91-34808
A method for the extrapolation of calibration data of PTC 6 throat tap nozzles
[ASME PAPER 90-JPGC/PTC-2] p 578 A91-34809
MURNYAK, STEVEN
Research flight-control system development for the F-18 high alpha research vehicle
[NASA-TM-104232] p 583 N91-22131

N

NAUMANN, K. W.
Possibilities of trajectory modification
[ISL-CO-209/90] p 582 N91-21151
NAZ, P.
Propagation of helicopter noise in the low atmosphere layers
[ISL-CO-203/90] p 607 N91-21830
NEINER, GEORGE
Hot gas ingestion test results of a two-poster vectored thrust concept with flow visualization in the NASA Lewis 9- x 15-foot low speed wind tunnel
[NASA-TM-103258] p 556 N91-21116
NEININGER, BRUNO
Summary of aircraft measuring activities at LAPETH p 604 N91-22661
NELSON, C. C.
Rotordynamic coefficients for partially roughened pump annular seals p 593 A91-34822
NELSON, ROBERT C.
Unsteady aerodynamics of slender wings p 560 N91-22105
NISSIM, E.
Reduction of aerodynamic augmented states in active flutter suppression systems p 580 A91-33535
NITRA, N. K.
Numerical investigation of three dimensional laminar flows in a channel with a built-in circular cylinder and wing-type vortex generators p 550 A91-34218
NIXON, D.
Prediction of unsteady transonic separated flow for missile applications
[AD-A231259] p 557 N91-21120
NOEL, B. W.
Evaluating thermographic phosphors in an operating turbine engine
[ASME PAPER 90-GT-266] p 593 A91-34810
NOFFZ, GREGORY K.
Multiaxis thrust vectoring using axisymmetric nozzles and postexit vanes on an F/A-18 configuration vehicle
[NASA-TM-101741] p 559 N91-22083
NOGUCHI, MASAYOSHI
An experimental study of a three-dimensional swept-back wing with suction laminar-flow-control
[NAL-TR-1072] p 556 N91-21113
NONAKA, OSAMU
Wind tunnel test of a propeller working in a low Reynolds number range
[NAL-TR-1071] p 556 N91-21112
An experimental study of a three-dimensional swept-back wing with suction laminar-flow-control
[NAL-TR-1072] p 556 N91-21113
NOOR, AHMED K.
Computational methods for frictionless contact with application to Space Shuttle Orbiter nose-gear tires
[NASA-TP-3073] p 601 N91-22576
NOVIKOV, V. E.
Effect of a single three-dimensional surface roughness on the transition in a supersonic boundary layer p 545 A91-33920

O

OBAYASHI, SHIGERU
A streamwise upwind algorithm applied to vortical flow over a delta wing p 548 A91-34192
OELSCHLAEGER, JOHN M.
GG1308 Ring Laser Gyro Inertial Measurement Systems - Honeywell's low-cost solution for tactical applications p 576 A91-33655
OLEARY, C. O.
Oscillatory data for typical configurations p 561 N91-22109
OLIVIER, C.
On the relation between TVD and mesh adaption and application to Navier-Stokes calculations p 550 A91-34215
OLSEN, HOWARD B.
A flexible robotic work cell for the assembly of airframe components p 543 A91-35193
OMELAEV, A. I.
Modeling of flow parameters in a cryogenic wind tunnel p 584 A91-33919
ORLANDI, PAOLO
Numerical simulation of vortices motion in presence of solid boundaries p 549 A91-34213
OUZTS, PETER J.
Integrated flight/propulsion control design for a STOVL aircraft using H-infinity control design techniques
[NASA-TM-104340] p 579 N91-21140

P

PAHLE, JOSEPH W.
Research flight-control system development for the F-18 high alpha research vehicle
[NASA-TM-104232] p 583 N91-22131
PALMERIO, B.
On the relation between TVD and mesh adaption and application to Navier-Stokes calculations p 550 A91-34215
PAPAILIOU, K.
Fast response wall pressure measurement as a means of gas turbine blade fault identification
[ASME PAPER 90-GT-341] p 578 A91-34813
PAPATHANASIOU, A.
Fast response wall pressure measurement as a means of gas turbine blade fault identification
[ASME PAPER 90-GT-341] p 578 A91-34813
PARAMESWARAN, VENKATARAMAN
Flight path reconstruction using extended Kalman filtering techniques
[DLR-FB-90-41] p 555 N91-21108
PARK, CHUL
Fully coupled implicit method for thermochemical nonequilibrium air at suborbital flight speeds p 544 A91-33380
PARKIN-MOORE, D. A.
Effect of planform on induced drag
[BU-500] p 559 N91-22086
PARMENTIER, G.
Propagation of helicopter noise in the low atmosphere layers
[ISL-CO-203/90] p 607 N91-21830
PATTERSON, JAMES C., JR.
Flight test to determine feasibility of a proposed airborne wake vortex detection concept
[NASA-TM-102672] p 563 N91-22096
PATZ, G.
Possibilities of trajectory modification
[ISL-CO-209/90] p 582 N91-21151
PAULL, A.
Preliminary calibration of a generic scramjet combustor
[NASA-CR-187539] p 579 N91-21139
PAVLOV, V. A.
Inertial aerosol precipitation on ogival bodies of revolution in high-velocity flow p 553 A91-35784
PAZUR, W.
The influence of inlet swirl distortions on the performance of a jet propulsion two-stage axial compressor
[ASME PAPER 90-GT-147] p 552 A91-34790
PENNINGTON, WILLIAM
Airport restrictions - A dilemma of federal preemption and proprietary control p 608 A91-35122
PERAIRE, J.
Finite element methods for integrated aerodynamic heating analysis
[NASA-CR-188079] p 554 N91-21101
PERALA, RODNEY A.
The effects of simulated electromagnetic pulse on commercial aircraft p 569 A91-35902
PERIAUX, JACQUES
Numerical simulation of compressible Euler flows p 544 A91-33675
PERIYATHAMBY, U.
A leading-edge control surface
[BU-508] p 559 N91-22087
PERON, LEE R.
Multiaxis thrust vectoring using axisymmetric nozzles and postexit vanes on an F/A-18 configuration vehicle
[NASA-TM-101741] p 559 N91-22083
PERRY, BOYD, III
An overview of the active flexible wing program p 583 N91-22332
PETERS, DAVID A.
Aerodynamic parameter studies and sensitivity analysis for rotor blades in axial flight
[NASA-CR-187524] p 558 N91-22078
PEYTON, DERRICK
Airborne gravimetry and the Global Positioning System p 602 A91-33634
PHILLIPS, EDWARD H.
Langley develops thermal management concept for hypersonic aircraft p 570 A91-33323
PIERUCCI, MAURO
Velocity of cavitation bubbles in uniform flowfield high and low Reynolds number p 592 A91-34127
PIFKO, A. B.
Addendum to the DYCAST user's manual describing the curved, warp beam finite element
[NASA-CR-4362] p 606 N91-22805
PINTELON, RIK
A frequency domain maximum likelihood identification scheme with application to flight flutter data analysis p 581 A91-35576
PIQUET, JEAN
Computation of the viscous flow past a prolate spheroid at incidence p 550 A91-34216
PLAETSCHKE, ERMIN
Flight path reconstruction using extended Kalman filtering techniques
[DLR-FB-90-41] p 555 N91-21108
POENSGEN, C.
Three-dimensional wake decay inside of a compressor cascade and its influence on the downstream unsteady flow field. I - Wake decay characteristics in the flow passage. II - Unsteady flow field downstream of the stator
[ASME PAPER 90-GT-21] p 551 A91-34786
POGU, MARC
A functional method for the approximate solution of a transonic problem p 550 A91-34398
PORDAL, H. S.
A pressure flux-split technique for computation of inlet flow behavior p 595 N91-21068
POTAPCZUK, MARK
Modeling of surface roughness effects on glaze ice accretion p 562 A91-35107
POTOTZKY, ANTHONY
Development and testing of controller performance evaluation methodology for multi-input/multi-output digital control systems p 584 N91-22337
POULOSE, M. M.
A fast and low-cost validation technique for ILS and MLS p 565 A91-33630
POVINELLI, LOUIS A.
Transonic cascade flow calculations using non-periodic C-type grids p 596 N91-21071
CFD for hypersonic propulsion
[NASA-TM-103791] p 597 N91-21447
Application of computational fluid dynamics in high speed aeropropulsion
[NASA-TM-103780] p 598 N91-21458
POWELL, KENNETH GRANT
Vortical solutions of the conical Euler equations p 591 A91-33674
POWERS, BRUCE
Research flight-control system development for the F-18 high alpha research vehicle
[NASA-TM-104232] p 583 N91-22131
PRASAD, J. V. R.
Active vibration control using fixed order dynamic compensation with frequency shaped cost functionals p 604 A91-33932
PRIESTLEY, NEIL
Terrain referenced navigation p 567 A91-33651

Q

QIAO, X.
Optimal design of metal and composite thin-walled structures with flutter constraint p 591 A91-32650

QUEUTEY, PATRICK
Computation of the viscous flow past a prolate spheroid at incidence p 550 A91-34216
QUINN, GEORGE H.
The Loran Early Implementation Project - Gateway for GPS p 563 A91-33607
QUINN, J. W.
Crew chief CAD system interface guide (version 2 - SI)
[AD-A231433] p 606 N91-22734

R

RAISINGHANI, S. C.
Unsteady aerodynamic modelling for aircraft lateral parameter estimation p 581 A91-34162
RAIZENNE, M. DONALD
Significance of residual curing strains in composite structure repair technology p 590 A91-32461
RAMAZANOV, M. P.
Modeling of flow parameters in a cryogenic wind tunnel p 584 A91-33919
RANDAZZO, PHILIP
Comparison of 14 decibels versus 20 decibels desired to undesired signal protection ratios
[DOT/FAA/CT-TN89/69] p 608 N91-21833
RAO, A. J.
Variable camber wings for transport aircraft
p 574 N91-22112
RAO, S. VITTAL
Design of robust controllers for gas turbine engines
[ASME PAPER 90-GT-113] p 578 A91-34815
RAWAL, D.
Critical speeds and forced response solutions for active magnetic bearing turbomachinery, part 1
p 587 N91-21209
Critical speeds and forced response solutions for active magnetic bearing turbomachinery, part 2
p 587 N91-21210
REDEKER, GUENTER
Progress in the prediction of the laminar-turbulent transition for laminar wings - The profile and wing geometries determine the friction drag of an aircraft
p 544 A91-33369
REED, HELEN L.
Numerical simulation of swept-wing flows
[NASA-CR-188201] p 560 N91-22095
REGENIE, VICTORIA
Research flight-control system development for the F-18 high alpha research vehicle
[NASA-TM-104232] p 583 N91-22131
REID, D. BLAKE
INS reset removal for enhanced post-flight performance analysis p 565 A91-33628
REISENTHEL, P.
Prediction of unsteady transonic separated flow for missile applications
[AD-A231259] p 557 N91-21120
REMONDI, BENJAMIN, W.
Applying kinematic GPS techniques at our nation's airports p 565 A91-33633
RHODES, DAVID B.
A synchronous strobed laser light sheet for rotor flow visualization
[NASA-TM-4266] p 601 N91-22540
RIAZ, RIZWAN
The N-Dimensional Fighter p 571 A91-35425
RICHNER, HANS
Summary of aircraft measuring activities at LAPETH
p 604 N91-22661
RIEDELBAUCH, S.
Hypersonic flow simulation for blunt bodies at incidence p 546 A91-34070
Numerical simulation of laminar hypersonic flow past blunt bodies including high temperature effects
p 547 A91-34180
RIEDLINGER, LANCELOT M.
The compressed aeronautical chart database - Support of naval aircraft's digital moving map systems
p 563 A91-33608
RILEY, MICHAEL F.
Integrated aerodynamic load/dynamic optimization of helicopter rotor blades p 571 A91-33532
RINOIE, KENICHI
Analysis of laminar separation bubble using a simple eddy-viscosity turbulence model p 591 A91-33227
Analysis of laminar separation bubbles using a simple eddy-viscosity turbulence model
[NAL-TR-1079] p 600 N91-22520
RITCHIE, MALCOLM L.
The missing (data) link in pilot navigation
p 568 A91-33666
RIZZI, ARTHUR
Numerical simulation of compressible Euler flows
p 544 A91-33675
Hypersonic leeside flow computations using centered schemes for Euler equations p 548 A91-34187
ROBINSON, MARTHA P.
Computational methods for frictionless contact with application to Space Shuttle Orbiter nose-gear tires
[NASA-TP-3073] p 601 N91-22576
ROBINSON, THOMAS H.
Common integrated processing in modular avionics
p 575 A91-33615
ROCKMAN, MARK J.
Impact of navigation accuracy on the intervention rate in a highly automated air traffic control system
p 566 A91-33647
RODVOID, MICHELLE
Analysis of routine communication in the air traffic control system
[NASA-CR-188116] p 600 N91-22475
ROESER, HANS PETER
Airborne heterodyne receiver for the range 600 GHz to 3,000 GHz p 599 N91-22047
ROGERS, R. C.
Preliminary calibration of a generic scramjet combustor
[NASA-CR-187539] p 579 N91-21139
ROHARDT, CLAAS-HINRIK
Flow visualization ion helicopter blades using Acenaphthen
[DLR-FB-90-37] p 598 N91-21466
ROOKER, JAMES R.
Structural integrity of wind tunnel wooden fan blades
[NASA-TM-104059] p 602 N91-22589
ROSCHE, HENRY, III
The compressed aeronautical chart database - Support of naval aircraft's digital moving map systems
p 563 A91-33608
RUBIN, S. G.
A pressure flux-split technique for computation of inlet flow behavior p 595 N91-21068
RUES, D.
Hypersonic flow simulation for blunt bodies at incidence p 546 A91-34070
RUSAKOV, V. V.
An approximate method for determining friction and heat transfer in chemically nonequilibrium flow past bodies at angle of attack p 553 A91-35660
RUSSELL, HARVEY
Test program for Honeywell/DND Helicopter Integrated Navigation System (HINS) p 565 A91-33626
RUTLEDGE, WALTER H.
Computation of flowfields for projectiles in hypersonic chemically reacting flows p 544 A91-33379
RUTLER, J. C.
Signal blending in control systems structural interactions
[BU-505] p 583 N91-22132

S

SAAVEDRA, PEDRO
Experimental and analytical study of shaft cracking response in rotatory machines p 594 A91-35516
SACCO, G. P.
Propulsion simulator for magnetically-suspended wind tunnel models p 586 N91-21198
SAGEY, W. E.
VLS - A DTOA system for position location
p 568 A91-33667
SALMON, C. C. V.
Flow investigation of a ground effect vehicle
[BU-516] p 600 N91-22528
SALTZ, JOEL
Domain decomposition methods in aerodynamics
p 604 A91-33056
SAMUELSSON, INGEMAR
Low speed wind tunnel investigation of propeller slipstream aerodynamic effects on different nacelle/wing combinations. Part 2: Propeller slipstream flow field surveys (velocity components, dynamic, total and static pressure distributions) at zero angle of attack and high power
[FFA-TN-1990-24-PT-2] p 555 N91-21109
SAN JUAN, LUIS
Experimental and analytical study of shaft cracking response in rotatory machines p 594 A91-35516
SANCHEZ, M.
Numerical investigation of three dimensional laminar flows in a channel with a built-in circular cylinder and wing-type vortex generators p 550 A91-34218
SANJAY, SWAMY
Robust integrated autopilot/autothrottle design using constrained parameter optimization
[NASA-CR-188011] p 583 N91-22127
SCHAFFAR, M.
Blade-wake interaction on a two blade rotor with prediction of the radiated noise stationary and forward flight, comparison between calculation, and experiment
[ISL-R-120/89] p 608 N91-21832
SCHARRER, J. K.
Rotordynamic coefficients for partially roughened pump annular seals p 593 A91-34822
SCHERZINGER, BRUNO M.
The design, simulation and implementation of an accurate positioning system for automatic flight inspection p 566 A91-33646
SCHLECHTRIEM, S.
Airfoils in two- and three-dimensional gust fields
p 546 A91-34073
SCHMID-BURGK, JOHANNES
Airborne heterodyne receiver for the range 600 GHz to 3,000 GHz p 599 N91-22047
SCHMID-GOELLER, S.
A method to calculate the influence of vortex roll-up on the induced drag of wings p 546 A91-34055
SCHMIDT, DIANNE
Influence of a magnetic field during directional solidification of MAR-M 246 + Hf superalloy
[NASA-CR-184114] p 590 N91-22416
SCHMIDT, L.
A numerical study of interfacial instabilities at high Mach numbers p 549 A91-34198
SCHMIDT, W.
Application of mesh generation to complex 3-D configurations
[AGARD-AR-268] p 598 N91-21464
SCHOUKENS, JOHAN
A frequency domain maximum likelihood identification scheme with application to flight flutter data analysis
p 581 A91-35576
SCHROEDER, S. C.
Flexible body dynamic stability for high performance aircraft p 574 N91-22318
SCHUETZ, H.
Computation of unsteady incompressible viscous flow around airfoils p 546 A91-34074
SCHULTE-WERNING, B.
Some aspects of the numerical simulation of compressible viscous flow around bluff bodies at low Ma-number p 550 A91-34220
SCHULTZ, KLAUS J.
The location of acoustic blade-vortex interaction - A further step toward an understanding of helicopter noise
p 607 A91-33368
SCHULZ, DIETER
Fin structures of the Airbus family experience with advanced composites p 570 A91-32455
SCHULZ, H. D.
Experimental and numerical investigation of three-dimensional viscous flows and vortex motion inside an annular compressor blade row
[ASME PAPER 90-GT-155] p 551 A91-34787
SCHULZ, PETER
An airworthy experimental system for modern navigation and remote-sensing methods - Reduction, storage, and transmission of aerial photography scenes
p 575 A91-33370
SCHUMUECKER, MEINHARD
Fast response gust measurement device
p 603 N91-22659
SCHWAAB, GERHARD W.
Airborne heterodyne receiver for the range 600 GHz to 3,000 GHz p 599 N91-22047
SCHWARZ, MICHAEL
Method for calculating boundary region corrections in multistep axial turbomachines p 592 A91-34014
SCOTT, JAMES R.
Compressible flows with periodic vortical disturbances around lifting airfoils
[NASA-TM-103742] p 554 N91-21060
A finite-difference, frequency-domain numerical scheme for the solution of the linearized unsteady Euler equations p 595 N91-21067
SCOTT, STAN G.
The NASA-ER2 meteorological measurement system: Instrumentaion, calibration and intercomparison results
p 603 N91-22658
SEGAL, A.
A quantitative investigation into the aerodynamic coupling effects in a coaxial contra-rotating rotor system
[BU-517] p 574 N91-22120
SEHGAL, A. K.
Investigation of nose bluntness and angle of attack effects on slender bodies in viscous hypertension flows
[NASA-CR-188153] p 557 N91-21117
SELIG, MICHAEL S.
The dynamic behavior of a shock-wave/turbulent boundary layer interaction p 544 A91-33735

SHARIAT, HORMOZ
A model-based method for object recognition
p 605 A91-35241
SHCHERBAK, V. G.
An approximate method for determining friction and heat transfer in chemically nonequilibrium flow past bodies at angle of attack p 553 A91-35660
SHEPPARD, LAUREL M.
Cost-effective manufacturing of advanced ceramics
p 588 A91-33725
SHEVEL'KOV, S. G.
Effect of a single three-dimensional surface roughness on the transition in a supersonic boundary layer
p 545 A91-33920
SHIN, V. W. Y.
The flexural strength of unidirectional carbon fibre composites
[BU-509] p 589 N91-22399
SHIVELY, C.
Evaluation of controller tools for conducting MLS curved approaches to New York's JFK Airport
p 565 A91-33631
SHUKLA, UDAY S.
The advantages of velocity vector referencing in proportional navigation p 581 A91-33611
SHUVALOV, V. A.
MHD drag and heat transfer of a sphere in supersonic flow of a partially ionized gas p 607 A91-35791
SIEBERT, RUEDIGER
Process control to set Mach number ratios for jet-engine intake measurements - Development of an automatic Mach-number regulator p 584 A91-33373
SILICH, BERT
The N-Dimensional Fighter p 571 A91-35425
SILVA, WALTER A.
Aeroelastic modeling of the active flexible wing wind-tunnel model p 575 N91-22333
SILVESTRI, J. J.
Green's function solution to radiative heat transfer between longitudinal gray fins p 593 A91-35117
SIMON, T. W.
Three-dimensional flow near the blade/endwall junction of a gas turbine - Visualization in a large-scale cascade simulator
[ASME PAPER 90-WA/HT-4] p 544 A91-32958
SINGH, D. J.
Investigation of nose bluntness and angle of attack effects on slender bodies in viscous hypertension flows
[NASA-CR-188153] p 557 N91-21117
SINGH, J.
Unsteady aerodynamic modelling for aircraft lateral parameter estimation p 581 A91-34162
SINGH, RAJENDRA
Linear and non-linear dynamic models of a geared rotor-bearing system p 594 A91-35536
Force and moment transmissibilities through rolling element bearings in a single-stage rotor system
p 594 A91-35537
SIQUIG, RICHARD A.
Impact of icing on Unmanned Aerial Vehicle (UAV) operations
[AD-A231191] p 562 N91-21124
SKARVAN, C. A.
Design of robust controllers for gas turbine engines
[ASME PAPER 90-GT-113] p 578 A91-34815
SKINN, DONALD A.
Study of bird ingestions into small inlet area aircraft turbine engines
[DOT/FAA/CT-90/13] p 562 N91-21122
SLABE, MELISSA E.
Resistivity of pristine and intercalated graphite fiber epoxy composites p 589 A91-35949
SMEETS, G.
Possibilities of trajectory modification
[ISL-CO-209/90] p 582 N91-21151
SMITH, A.
Evaluation of controller tools for conducting MLS curved approaches to New York's JFK Airport
p 565 A91-33631
SMITH, FRED
Integrated inertial navigation system/Global Positioning System (INS/GPS) for manned return vehicle autoland application p 586 A91-33609
SMITH, STEPHEN
Aerodynamic and structural studies of joined-wing aircraft p 571 A91-33534
SMITH, TODD E.
A modal aeroelastic analysis scheme for turbomachinery blading
[NASA-CR-187089] p 579 N91-21138
SMITH, WILTON J.
A practical approach to Rule 26(c) protective orders in aviation litigation p 608 A91-35121
SMITS, ALEXANDER J.
The dynamic behavior of a shock-wave/turbulent boundary layer interaction p 544 A91-33735
Correlation measurements and structure angles in a turbulent boundary layer recovering from convex curvature p 545 A91-33747
SNIDER, J. B.
Remote sensor observations during WISP90: The use of microwave radiometers, RASS, and ceilometers for detection of aircraft icing conditions
[PB91-131839] p 604 N91-22670
SNYDER, FRANKLIN B.
Terrain-aided altitude computations on the AFTI/F-16
p 576 A91-33650
SO, R. M. C.
A review of near-wall Reynolds-stress
[NASA-CR-4369] p 559 N91-22080
SODERMAN, PAUL T.
Acoustic and aerodynamic study of a pusher-propeller aircraft model
[NASA-TP-3040] p 607 N91-21828
SORENSEN, JOHN A.
Traffic Alert and Collision Avoidance System (TCAS): Cockpit Display of Traffic Information (CDTI) investigation. Phase 1: Feasibility study
[NASA-TM-104956] p 569 N91-22102
SOSNOVSKII, A. A.
Optimization of radio-measuring devices incorporated in onboard laser velocimeters p 576 A91-35738
SPLETTSTOESSER, WOLF
The location of acoustic blade-vortex interaction - A further step toward an understanding of helicopter noise
p 607 A91-33368
SREEKANTA MURTHY, T.
Optimization of helicopter airframe structures for vibration reduction - Considerations, formulations, and applications p 571 A91-33533
SRINATHKUMAR, S.
Design and test of three active flutter suppression controllers p 583 N91-22334
STACK, JOHN P.
Method and apparatus for detecting laminar flow separation and reattachment
[NASA-CASE-LAR-13952-2-SB] p 598 N91-21472
STANDEVEN, M. A.
The preliminary aerodynamic design of light aircraft
[BU-504] p 574 N91-22119
STANKOV, B. B.
Remote sensor observations during WISP90: The use of microwave radiometers, RASS, and ceilometers for detection of aircraft icing conditions
[PB91-131839] p 604 N91-22670
STAUTER, R. C.
Temporally and spatially resolved flow in a two-stage axial compressor. I - Experiment
[ASME PAPER 90-GT-259] p 551 A91-34789
STEELE, R. C.
Skin friction measurement techniques for scramjet applications. Phase 1: Preliminary design
[AD-A231899] p 580 N91-22125
STEGER, JOSEPH L.
Application of mesh generation to complex 3-D configurations
[AGARD-AR-268] p 598 N91-21464
STEIN, BARRY A.
COTS GPS C/A-code receivers with pseudolites for range PLS application p 564 A91-33623
STEIN, EARL S.
Air traffic control memory: A field survey
[DOT/FAA/CT-TN90/60] p 569 N91-22101
STEINETZ, BRUCE M.
High temperature performance evaluation of a hypersonic engine ceramic wafer seal
[NASA-TM-103737] p 601 N91-22567
STORER, J. A.
Tip leakage flow in axial compressors
[ASME PAPER 90-GT-127] p 552 A91-34792
STOWE, FRANCIS S.
Speech recognition using Kohonen neural networks, dynamic programming, and multi-feature fusion
[AD-A230951] p 597 N91-21410
STROCK, THOMAS W.
Hot gas ingestion test results of a two-poster vectored thrust concept with flow visualization in the NASA Lewis 9- x 15-foot low speed wind tunnel
[NASA-TM-103258] p 556 N91-21116
STROUD, E. G.
Global Positioning System (GPS) autonomous navigation p 567 A91-33653
STUMP, W. J.
Crew chief CAD system interface guide (version 2 - SI)
[AD-A231433] p 606 N91-22734
SU, T. Y.
Development of a general multiblock flow solver for complex configurations p 605 A91-34230
SUN, XIA-SHENG
Analysis and optimal design of composite structures
p 591 A91-32651
SUN, XIAN-XUE
Analysis and optimal design of composite structures
p 591 A91-32651
SUNDBERG, GALE R.
Civil air transport: A fresh look at power-by-wire and fly-by-light p 584 N91-23053
SWANBOROUGH, GORDON
Starship - Bright newcomer in a conservative firmament p 571 A91-34122
SWIGGER, KATHLEEN M.
Generalized heuristics for the gate assignment problem p 605 A91-35100
SWITZER, G. F.
Zonal analysis of two high-speed inlets
p 596 N91-21089
SZAJNAR, STANISLAW
Biodynamic and optimization aspects of emergency ejection from an aircraft p 561 A91-34341

T

TAKASAWA, KINGO
Wind tunnel test of a propeller working in a low Reynolds number range
[NAL-TR-1071] p 556 N91-21112
TAN, C. S.
Similarity analysis of compressor tip clearance flow structure
[ASME PAPER 90-GT-153] p 552 A91-34793
TANAKA, ATSUSHIGE
Present and future of CFD on the aero-engine development in IHI p 596 N91-21381
TANAKA, KOHEI
The CFD analysis related aerospace in Fuji Heavy Industries, Ltd. p 597 N91-21383
TANIOKA, TADAYUKI
Status and outlook of CFD technology at Mitsubishi Heavy Industries, Nagoya p 597 N91-21384
TANNER, JOHN A.
Computational methods for frictionless contact with application to Space Shuttle Orbiter nose-gear tires
[NASA-TP-3073] p 601 N91-22576
TARAKAN, R.
Evaluation of controller tools for conducting MLS curved approaches to New York's JFK Airport
p 565 A91-33631
TARREL, RICHARD J.
Non-airborne conflicts: The causes and effects of runway transgressions
[NASA-CR-177372] p 562 N91-21121
TARTT, D. M.
Automated flight test management system
[NASA-CR-186011] p 574 N91-22117
TATE, ATSUSHI
Coning motion of slender bodies at high angles of attack
[NAL-TR-1059] p 556 N91-21111
TAYLOR-HUNT, R. G.
An investigation into the extent and effects of spanwise flow in the boundary layer of a helicopter rotor in hover
[BU-519] p 560 N91-22089
TAYLOR, LAWRENCE W., JR.
Fourth NASA Workshop on Computational Control of Flexible Aerospace Systems, part 2
[NASA-CP-10065-PT-2] p 587 N91-22331
TELIONIS, DEMETRI P.
The transient development of vortices over a delta wing
[AD-A231946] p 559 N91-22082
TENCH, K. A.
Omega signal coverage prediction in the 1990's
p 568 A91-33665
THIELE, F.
Computation of unsteady incompressible viscous flow around airfoils p 546 A91-34074
An inverse boundary layer procedure with application to 3-D wing flow p 550 A91-34229
THIELMAN, LEROY O.
GG1308 Ring Laser Gyro Inertial Measurement Systems - Honeywell's low-cost solution for tactical applications
p 576 A91-33655
THOMPSON, D. H.
Water tunnel flow visualisation of vortex breakdown over the F/A-18
[ARL-FLIGHT-MECH-R-179] p 600 N91-22511
THOMPSON, RICHARD A.
Flowfield and vehicle parameter influence on results of engineering aerothermal methods p 544 A91-33378
THOMPSON, S. G.
Flow investigation of a ground effect vehicle
[BU-516] p 600 N91-22528
TISCHLER, M. B.
Suppression of biodynamic interference in head-tracked teleoperation
[NASA-TM-103833] p 577 N91-21134

TITZ, RUTH U.
Airborne heterodyne receiver for the range 600 GHz to 3,000 GHz p 599 N91-22047
TIWARI, S. N.
Investigation of nose bluntness and angle of attack effects on slender bodies in viscous hypertension flows [NASA-CR-188153] p 557 N91-21117
TOMBLIN, M.
A quantitative investigation into the aerodynamic coupling effects in a coaxial contra-rotating rotor system [BU-517] p 574 N91-22120
TONGUE, B. H.
Nonlinear behavior of a rotorcraft model during air resonance p 581 A91-34816
TOSTEVIN, D. J.
Flutter suppression of an aircraft wing using a control surface [BU-506] p 583 N91-22133
TOURNEMINE, GEORGES
A functional method for the approximate solution of a transonic problem p 550 A91-34398
TOWNSEND, DENNIS P.
Effects of gear box vibration and mass imbalance on the dynamics of multi-stage gear transmissions [NASA-TM-103695] p 599 N91-21534
TRENCHARD, MICHAEL E.
The compressed aeronautical chart database - Support of naval aircraft's digital moving map systems p 563 A91-33608
TRIPP, JOHN S.
A solid-state controllable power supply for a magnetic suspension wind tunnel p 585 N91-21199
TRUJILLO, EDWARD
Common integrated processing in modular avionics p 575 A91-33615
TSANG, WAI L.
COTS GPS C/A-code receivers with pseudolites for range PLS application p 564 A91-33623
TU, YU K.
Effects of gear box vibration and mass imbalance on the dynamics of multi-stage gear transmissions [NASA-TM-103695] p 599 N91-21534
TUCKER, G. E.
Suppression of biodynamic interference in head-tracked teleoperation [NASA-TM-103833] p 577 N91-21134
TUNBRIDGE, C. K.
The use of axisymmetric flow for investigation of shock wave-boundary layer interactions [BU-520] p 600 N91-22529
TURLEY, W. D.
Evaluating thermographic phosphors in an operating turbine engine [ASME PAPER 90-GT-266] p 593 A91-34810
TYSELL, LARS G.
MATGRID, a program for generation of C-H and C-O topology grids around wing/body configurations: User's guide [FFA-TN-1991-03] p 556 N91-21110

U

UPTON, ROBERT W., JR.
The next frontier for strapdown RLG inertial systems - Precision navigation p 576 A91-33656

V

VALORANI, MAURO
Inviscid flow about a double ellipse p 549 A91-34210
VAN DEN BERG, J. I.
Development and validation of characteristic boundary conditions for cell-centered Euler flow calculations p 592 A91-34178
VAN DER AUWERAER, HERMAN
A frequency domain maximum likelihood identification scheme with application to flight flutter data analysis p 581 A91-35576
VAN LEER, BRAM
Numerical simulation of compressible Euler flows p 544 A91-33675
VELICHKIN, A. I.
Nonlinear filtering of a trajectory message p 568 A91-33868
VENKATAKRISHNAN, V.
Domain decomposition methods in aerodynamics p 604 A91-33056
VETLUTSKII, V. N.
Calculation of a compressible laminar boundary layer on a tapered body of bielliptical cross section p 553 A91-35796
VICROY, DAN D.
A simple, analytical, axisymmetric microburst model for downdraft estimation [NASA-TM-104053] p 573 N91-21132
VOTH, CHRISTOPHER
Robust integrated autopilot/autothrottle design using constrained parameter optimization [NASA-CR-188011] p 583 N91-22127

W

WAGNER, S.
A vortex-lattice method for the calculation of vortex sheet roll-up and wing-vortex interaction p 546 A91-34052
WALSH, JOANNE L.
Integrated aerodynamic load/dynamic optimization of helicopter rotor blades p 571 A91-33532
WANG, LUI
Metamorphoses of ONAV console operations: From prototype to real time application p 606 N91-22794
WANG, WEI
Analysis and optimal design of composite structures p 591 A91-32651
WANG, WEN-LIANG
Dynamic analysis technique of centrifugal impellor with split blades p 593 A91-35498
WANIE, K. M.
Closed-coupled zonal solution for viscous flow problems p 546 A91-34063
WARDWELL, DOUGLAS A.
Forces and pressures induced on circular plates by a single lifting jet in ground effect [NASA-TM-102816] p 558 N91-22077
Small-scale experiments in STOVL ground effects [NASA-TM-102813] p 560 N91-22091
WARREN, R. S.
Omega signal coverage prediction in the 1990's p 568 A91-33665
WASZAK, MARTIN R.
Design and test of three active flutter suppression controllers p 583 N91-22334
WEBB, CHRIS
Test program for Honeywell/DND Helicopter Integrated Navigation System (HINS) p 565 A91-33626
WEBER, DONALD J.
Flight test results of a tightly integrated RLG-based Global Positioning System/inertial navigation system p 566 A91-33645
WEBER, R. L.
Remote sensor observations during WISP90: The use of microwave radiometers, RASS, and ceilometers for detection of aircraft icing conditions [PB91-131839] p 604 N91-22670
WEI, CHING-YUAN
Computations for a jet impinging obliquely on a flat surface p 554 A91-35985
WEILAND, C.
Split-matrix marching methods for three-dimensional viscous and inviscid hypersonic flows p 549 A91-34206
WELLER, WILLIAM H.
Helicopter rotor dynamics optimization with experimental verification p 570 A91-33530
WELLS, DAVID
Airborne gravimetry and the Global Positioning System p 602 A91-33634
WELLS, GREGORY P.
General aviation accident liability standards - Why the fuss? p 608 A91-35123
WENDT, M.
Preliminary calibration of a generic scramjet combustor [NASA-CR-187539] p 579 N91-21139
WENNERSTROM, A. J.
A review of predictive efforts for transport phenomena in axial flow compressors p 551 A91-34785
Three-dimensional flowfields inside a transonic compressor with swept blades [ASME PAPER 90-GT-359] p 552 A91-34791
WESSELING, PIETER
GAMM-Conference on Numerical Methods in Fluid Mechanics, 8th, Delft University of Technology, Netherlands, Sept. 27-29, 1989, Proceedings p 592 A91-34176
WESTWATER, E. R.
Remote sensor observations during WISP90: The use of microwave radiometers, RASS, and ceilometers for detection of aircraft icing conditions [PB91-131839] p 604 N91-22670
WIESEMAN, CAROL
Development and testing of controller performance evaluation methodology for multi-input/multi-output digital control systems p 584 N91-22337
WIJERS, PHILIP J.
Coping with dramatic air transport growth p 562 A91-36011
WILKE, G.
The improvement of the installation of the DLR research aircraft Falcon: Description and first results p 603 N91-22657
WILSON, JOSEPH J.
Study of bird ingestions into small inlet area aircraft turbine engines [DOT/FAA/CT-90/13] p 562 N91-21122
WINGATE, ROBERT T.
Structural integrity of wind tunnel wooden fan blades [NASA-TM-104059] p 602 N91-22589
WINTER, J. P.
An investigation into the extent and effects of spanwise flow in the boundary layer of a helicopter rotor in hover [BU-519] p 560 N91-22089
WISCHOW, PERRY B.
The compressed aeronautical chart database - Support of naval aircraft's digital moving map systems p 563 A91-33608
WISLER, D. C.
Mixing in axial-flow compressors - Conclusions drawn from three-dimensional Navier-Stokes analyses and experiments [ASME PAPER 90-GT-352] p 551 A91-34783
WOITHE, KLAUS
Advanced composite technology of West German general aviation aircraft p 543 A91-32648
WOJTKOWIAK, MIECZYSLAW
Biodynamic and optimization aspects of emergency ejection from an aircraft p 561 A91-34341
WU, RENJIE
ICCM-VII; Proceedings of the 7th International Conference on Composite Materials, Guangzhou, People's Republic of China, Nov. 22-24, 1989. Vols. 1-3 p 588 A91-32451
WU, YUNSHU
ICCM-VII; Proceedings of the 7th International Conference on Composite Materials, Guangzhou, People's Republic of China, Nov. 22-24, 1989. Vols. 1-3 p 588 A91-32451
WURSTER, KATHRYN E.
Flowfield and vehicle parameter influence on results of engineering aerothermal methods p 544 A91-33378

X

XU, HUIHUANG
Supercomputer optimizations for stochastic optimal control applications p 605 N91-22313
XUE, L.
An inverse boundary layer procedure with application to 3-D wing flow p 550 A91-34229

Y

YAMAGUCHI, KEIKO
Modeling of surface roughness effects on glaze ice accretion p 562 A91-35107
YANG, B. Z.
Cumulative damage problem in pull-through fatigue of C.F.R.P. laminate p 588 A91-32576
YANG, HONG S.
Superplasticity in a Ti3Al-base alloy stabilized by Nb, V and Mo p 589 A91-34841
YANG, R.-J.
Numerical solutions of 2-D multi-stage rotor/stator unsteady flow interactions p 595 N91-21070
YEH, HSIEN-YANG
Temperature effect on the stress concentration in the composite material used by the X-29A forward-swept wing aircraft p 590 A91-32547
YOON, SEOKKWAN
Fully coupled implicit method for thermochemical nonequilibrium air at suborbital flight speeds p 544 A91-33380
YOSHINAGA, TAKASHI
Coning motion of slender bodies at high angles of attack [NAL-TR-1059] p 556 N91-21111
YOUNG, CLARENCE P., JR.
Structural integrity of wind tunnel wooden fan blades [NASA-TM-104059] p 602 N91-22589
YOUNGS, A. C.
The use of axisymmetric flow for investigation of shock wave-boundary layer interactions [BU-520] p 600 N91-22529
YOUSSEF, H. M.
Flexible body dynamic stability for high performance aircraft p 574 N91-22318

YU, N. J.
Development of a general multiblock flow solver for complex configurations p 605 A91-34230

Z

ZAGER, HAROLD E.
Structural integrity of wind tunnel wooden fan blades [NASA-TM-104059] p 602 N91-22589
ZAITSEV, O. L.
An approach to the numerical solution of two-dimensional Navier-Stokes equations by a finite difference method p 595 A91-35787
ZAKRAJSEK, JAMES J.
Effects of gear box vibration and mass imbalance on the dynamics of multi-stage gear transmissions [NASA-TM-103695] p 599 N91-21534
ZDUNEK, ADAM
Stability analysis of a fuselage side [FFA-TN-1990-32] p 599 N91-21568
ZHANG, H. S.
A review of near-wall Reynolds-stress [NASA-CR-4369] p 559 N91-22080
ZHANG, JIN
Dynamic analysis technique of centrifugal impellor with split blades p 593 A91-35498
ZHANG, K. D.
Cumulative damage problem in pull-through fatigue of C.F.R.P. laminate p 588 A91-32576
ZININ, O. I.
Effect of a single three-dimensional surface roughness on the transition in a supersonic boundary layer p 545 A91-33920
ZOBY, E. VINCENT
Flowfield and vehicle parameter influence on results of engineering aerothermal methods p 544 A91-33378
ZRNIC, DUSAN S.
Modern aviation weather systems for efficient flight management p 602 A91-33648
ZYWIEL, JAN
Test program for Honeywell/DND Helicopter Integrated Navigation System (HINS) p 565 A91-33626
ZYWIEL, JAN Z.
INS reset removal for enhanced post-flight performance analysis p 565 A91-33628

Typical Corporate Source Index Listing

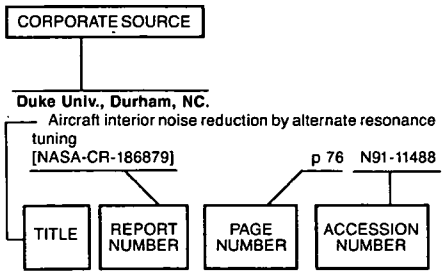

Listings in this index are arranged alphabetically by corporate source. The title of the document is used to provide a brief description of the subject matter. The page number and the accession number are included in each entry to assist the user in locating the abstract in the abstract section. If applicable, a report number is also included as an aid in identifying the document.

A

Advisory Group for Aerospace Research and Development, Neuilly-Sur-Seine (France).
Rotary-balance testing for aircraft dynamics
[AGARD-AR-265] p 585 N91-21156
Application of mesh generation to complex 3-D configurations
[AGARD-AR-268] p 598 N91-21464
The human factors relating to escape and survival from helicopters ditching in water
[AGARD-AG-305(F)] p 563 N91-22099
Special Course on Aircraft Dynamics at High Angles of Attack: Experiments and Modelling
[AGARD-R-776] p 573 N91-22104

Aeronautical Research Inst. of Sweden, Stockholm.
Low speed wind tunnel investigation of propeller slipstream aerodynamic effects on different nacelle/wing combinations. Part 2: Propeller slipstream flow field surveys (velocity components, dynamic, total and static pressure distributions) at zero angle of attack and high power
[FFA-TN-1990-24-PT-2] p 555 N91-21109
MATGRID, a program for generation of C-H and C-O topology grids around wing/body configurations: User's guide
[FFA-TN-1991-03] p 556 N91-21110
Some treatments on boundary conditions for quasi one-dimensional Euler equations
[FFA-TN-1990-36] p 598 N91-21469
Stability analysis of a fuselage side
[FFA-TN-1990-32] p 599 N91-21568

Aeronautical Research Labs., Melbourne (Australia).
Aerothermodynamic design appraisal of noise suppressors for F/A-18 engine run-up facilities at RAAF Williamtown
[ARL-PROP-R-177] p 585 N91-22136
Water tunnel flow visualisation of vortex breakdown over the F/A-18
[ARL-FLIGHT-MECH-R-179] p 600 N91-22511

Aerospatiale, Suresnes (France).
Proceedings of a French-Japanese Seminar on Composite Materials: Processing, Use and Databases
p 589 N91-22380

Air Force Inst. of Tech., Wright-Patterson AFB, OH.
Bifurcation analysis of the longitudinal dynamics of a simple powered lifting hypersonic vehicle
[AD-A230826] p 557 N91-21118
Vortex bursting over a unit area aspect ratio delta wing using vortex paneling methods
[AD-A231028] p 557 N91-21119
Speech recognition using Kohonen neural networks, dynamic programming, and multi-feature fusion
[AD-A230951] p 597 N91-21410
Status of PAVER implementation within the US Air Force
[AD-A231158] p 585 N91-22137

Alabama Univ., Birmingham.
Influence of a magnetic field during directional solidification of MAR-M 246 + Hf superalloy
[NASA-CR-184114] p 590 N91-22416

Analytical Services and Materials, Inc., Hampton, VA.
Integrated aerodynamic load/dynamic optimization of helicopter rotor blades p 571 A91-33532
Zonal analysis of two high-speed inlets
p 596 N91-21089

Arizona State Univ., Tempe.
A review of near-wall Reynolds-stress
[NASA-CR-4369] p 559 N91-22080
Numerical simulation of swept-wing flows
[NASA-CR-188201] p 560 N91-22095

Army Aviation Systems Command, Cleveland, OH.
Advanced rotorcraft transmission program
[NASA-TM-103276] p 598 N91-21531
Effects of gear box vibration and mass imbalance on the dynamics of multi-stage gear transmissions
[NASA-TM-103695] p 599 N91-21534

Army Cold Regions Research and Engineering Lab., Hanover, NH.
Snow roads and runways
[AD-A231490] p 586 N91-22138

Army Engineer Topographic Labs., Fort Belvoir, VA.
Automated extraction of airport runway patterns from radar imagery
[AD-A231809] p 600 N91-22480

Army Natick Labs., MA.
Evaluation of an alternative rotorcraft cargo lowering device for the delivery of 500-lb ammunition loads
[AD-A230995] p 573 N91-21133

AS&M, Inc., Hampton, VA.
Domain decomposition methods in aerodynamics
p 604 A91-33056

Aviation Planning Associates, Inc., Cincinnati, OH.
Economic impact of aviation in Pennsylvania
[PB91-128264] p 543 N91-22067

B

Battelle Columbus Labs., Mountain View, CA.
Non-airborne conflicts: The causes and effects of runway transgressions
[NASA-CR-177372] p 562 N91-21121

Boeing Co., Seattle, WA.
Solution adaptive local rectangular grid refinement for transonic aerodynamic flow problems
p 547 A91-34179
Software: Where we are and what is required in the future p 606 N91-22729

Bristol Univ. (England).
Effect of planform on induced drag
[BU-500] p 559 N91-22086
A leading-edge control surface
[BU-508] p 559 N91-22087
An investigation into the extent and effects of spanwise flow in the boundary layer of a helicopter rotor in hover
[BU-519] p 560 N91-22089
The preliminary aerodynamic design of light aircraft
[BU-504] p 574 N91-22119
A quantitative investigation into the aerodynamic coupling effects in a coaxial contra-rotating rotor system
[BU-517] p 574 N91-22120
Signal blending in control systems structural interactions
[BU-505] p 583 N91-22132
Flutter suppression of an aircraft wing using a control surface
[BU-506] p 583 N91-22133
The flexural strength of unidirectional carbon fibre composites
[BU-509] p 589 N91-22399
Flow investigation of a ground effect vehicle
[BU-516] p 600 N91-22528
The use of axisymmetric flow for investigation of shock wave-boundary layer interactions
[BU-520] p 600 N91-22529

Brown Univ., Providence, RI.
Micromechanisms of quasi-static and fatigue crack growth in titanium-aluminides p 602 N91-22583

C

California Inst. of Tech., Pasadena.
Investigations into shock-induced enhancement of mixing and combustion in supersonic burners
[AD-A231750] p 589 N91-22407

California Univ., Los Angeles.
Helicopter vibration reduction using structural optimization with aeroelastic/multidisciplinary constraints - A survey p 570 A91-33527

Centre d'Essais en Vol, Bretigny-sur-Orge (France).
Technical presentation of the Merlin's radome: Calibration and data processing p 603 N91-22656

Cincinnati Univ., OH.
A pressure flux-split technique for computation of inlet flow behavior p 595 N91-21068

Cleveland State Univ., OH.
Resistivity of pristine and intercalated graphite fiber epoxy composites p 589 A91-35949

College of William and Mary, Williamsburg, VA.
Design of an intelligent information system for in-flight emergency assistance p 606 N91-22792

Cornell Univ., Ithaca, NY.
A study of rotor broadband noise mechanisms and helicopter tail rotor noise
[NASA-CR-177565] p 607 N91-21829

Cranfield Inst. of Tech., Bedford (England).
Approximate methods for predicting the lifting characteristics of wing-body combinations
p 558 N91-22074
Variable camber wings for transport aircraft
p 574 N91-22112
Experimental study of radiation from coated turbine blades p 580 N91-22122
Damage accumulation and degradation of composite laminates under aircraft service loading: Assessment and prediction, volumes 1 and 2 p 589 N91-22381

D

Dayton Univ., OH.
Study of bird ingestions into small inlet area aircraft turbine engines
[DOT/FAA/CT-90/13] p 562 N91-21122
Crew chief CAD system interface guide (version 2 - SI)
[AD-A231433] p 606 N91-22734

Deutsche Airbus G.m.b.H., Bremen (Germany, F.R.).
Fast response gust measurement device
p 603 N91-22659

Deutsche Forschungsanstalt fuer Luft- und Raumfahrt, Brunswick (Germany, F.R.).
Flight path reconstruction using extended Kalman filtering techniques
[DLR-FB-90-41] p 555 N91-21108
Identification of the aerodynamic model of the DLR research aircraft ATTAS from flight test data
[DLR-FB-90-40] p 572 N91-21130
Results of the HHC wind tunnel tests, 1986 - 1988
[DLR-FB-90-42] p 582 N91-21152
Flow visualization ion helicopter blades using Acenaphthen
[DLR-FB-90-37] p 598 N91-21466

SOURCE

Deutsche Forschungsanstalt fuer Luft- und Raumfahrt, Oberpfaffenhofen (Germany, F.R.).
Analysis of three icing test flights reaching the aircraft-referred icing degree severe
[DLR-FB-90-34] p 562 N91-21123
Air motion measurement uncertainties: Their impact on atmospheric studies p 603 N91-22654
The improvement of the installation of the DLR research aircraft Falcon: Description and first results p 603 N91-22657
Turbulence profiling in the atmospheric boundary layer using three powered gliders p 604 N91-22663

Douglas Aircraft Co., Inc., Saint Louis, MO.
Design methodology for a community response questionnaire on sonic boom exposure
[NASA-CR-187503] p 608 N91-22830

Draper (Charles Stark) Lab., Inc., Cambridge, MA.
Dynamic modelling and analysis of a magnetically suspended flexible rotor p 587 N91-21208

Duke Univ., Durham, NC.
Role of artificial viscosity in Euler and Navier-Stokes solvers p 547 A91-34135

Dynamet Technology, Inc., Burlington, MA.
Feasibility study for the qualification of an economically advantageous Ti-6Al-4V bearing housing for gas turbine engine application by powder metal manufacturing technology
[AD-A231666] p 601 N91-22564

E

Eidetics International, Inc., Torrance, CA.
Forebody vortex control p 573 N91-22110

Eidgenoessische Technische Hochschule, Zurich (Switzerland).
Summary of aircraft measuring activities at LAPETH p 604 N91-22661

ESDU International Ltd., London (England).
Computer program for the calculation of normal force and pitching moment of forebody-cylinder combinations at angles of attack up to 90 degrees and Mach numbers up to 5, including effects of conical boat-tailing
[ESDU-90034] *p 555 N91-21102*
Lift and rolling moment due to spoilers on wings at subsonic speeds
[ESDU-90030] p 572 N91-21129

F

Federal Aviation Administration, Atlantic City, NJ.
Model rocketry hazard study
[DOT/FAA/CT-TN90/28] p 587 N91-21238
Comparison of 14 decibels versus 20 decibels desired to undesired signal protection ratios
[DOT/FAA/CT-TN89/69] p 608 N91-21833
Flight Service Automation System (FSAS) Model 1 Full Capacity (M1FC) Operational Test and Evaluation (OT/E)/integration test report
[DOT/FAA/CT-TN90/45] p 569 N91-22100
Air traffic control memory: A field survey
[DOT/FAA/CT-TN90/60] p 569 N91-22101

Federal Aviation Administration, Washington, DC.
A guide to ground vehicle operations on the airport
[AD-A231077] p 585 N91-21158
FAA aviation forecasts: Fiscal years 1991-2002
[AD-A231721] p 543 N91-22068
Flight test to determine feasibility of a proposed airborne wake vortex detection concept
[NASA-TM-102672] p 563 N91-22096

Flinders Univ., Bedford Park (Australia).
The FIAMS research aircraft or small is beautiful p 603 N91-22655

Florida Inst. of Tech., Melbourne.
Green's function solution to radiative heat transfer between longitudinal gray fins p 593 A91-35117

Frontier Technology, Inc., Beavercreek, OH.
Methodology development for the verification and validation of flight critical systems software, phase 1
[AD-A229932] p 605 N91-21735

Fuji Heavy Industries Ltd., Utsunomiya (Japan).
The CFD analysis related aerospace in Fuji Heavy Industries, Ltd. p 597 N91-21383

G

General Accounting Office, Washington, DC.
Embedded computers: Navy's approach to developing patrol aircraft avionics system too risky
[AD-A230868] p 577 N91-21136

Grumman Aerospace Corp., Bethpage, NY.
Addendum to the DYCAST user's manual describing the curved, warp beam finite element
[NASA-CR-4362] p 606 N91-22805

H

Houston Univ., Clear Lake, TX.
RICIS Software Engineering 90 Symposium: Aerospace Applications and Research Directions Proceedings Appendices
[NASA-CR-187994] p 605 N91-22728

I

Illinois Univ., Chicago.
Supercomputer optimizations for stochastic optimal control applications p 605 N91-22313

Imperial Coll. of Science and Technology, London (England).
Finite element methods for integrated aerodynamic heating analysis
[NASA-CR-188079] p 554 N91-21101

Institut Franco-Allemand de Recherches, Saint-Louis (France).
Infrared thermography for the qualitative aerodynamic study of a slender body
[ISL-R-122/89] p 555 N91-21104
Practical methods to evaluate the friction drag coefficient of a projectile in free flight
[ISL-R-123/89] p 555 N91-21105
Comparison study of the aerodynamic coefficients measured on models with circular or squared section and large elongation in supersonic flow
[ISL-R-125/89] p 555 N91-21106
Possibilities of trajectory modification
[ISL-CO-209/90] p 582 N91-21151
Propagation of helicopter noise in the low atmosphere layers
[ISL-CO-203/90] p 607 N91-21830
Calculation of thickness and charge noise radiated by a rotor in forward flight
[ISL-R-119/89] p 607 N91-21831
Blade-wake interaction on a two blade rotor with prediction of the radiated noise stationary and forward flight, comparison between calculation, and experiment
[ISL-R-120/89] p 608 N91-21832

Institute for Computer Applications in Science and Engineering, Hampton, VA.
Domain decomposition methods in aerodynamics p 604 A91-33056
Preliminary calibration of a generic scramjet combustor
[NASA-CR-187539] p 579 N91-21139

Ishikawajima-Harima Heavy Industries Co. Ltd., Tokyo (Japan).
Present and future of CFD on the aero-engine development in IHI p 596 N91-21381

J

Jet Propulsion Lab., California Inst. of Tech., Pasadena.
Similarity analysis of compressor tip clearance flow structure
[ASME PAPER 90-GT-153] p 552 A91-34793

K

Kawasaki Heavy Industries Ltd., Gifu (Japan).
CFD research and systems in Kawasaki Heavy Industries and its future prospects p 596 N91-21382

L

Lawrence Livermore National Lab., CA.
The single antenna interferometer
[DE91-007128] p 597 N91-21407

Lockheed Aeronautical Systems Co., Burbank, CA.
Flexible body dynamic stability for high performance aircraft p 574 N91-22318

Lockheed Engineering and Sciences Co., Hampton, VA.
Optimization of helicopter airframe structures for vibration reduction - Considerations, formulations, and applications p 571 A91-33533
Aerodynamic parameter studies and sensitivity analysis for rotor blades in axial flight
[NASA-CR-187524] p 558 N91-22078

Lockheed Missiles and Space Co., Palo Alto, CA.
Addendum to the DYCAST user's manual describing the curved, warp beam finite element
[NASA-CR-4362] p 606 N91-22805

M

Madison Magnetics, Inc., WI.
Magnetic suspension and balance system advanced study, 1989 design p 586 N91-21197

Marquardt Corp., Van Nuys, CA.
Skin friction measurement techniques for scramjet applications. Phase 1: Preliminary design
[AD-A231899] *p 580 N91-22125*

Maryland Univ., College Park.
Aeroelastic optimization of a helicopter rotor using an efficient sensitivity analysis p 570 A91-33529
Optimum aeroelastic design of helicopter rotors for longitudinal handling qualities improvement p 570 A91-33531

Massachusetts Inst. of Tech., Cambridge.
Similarity analysis of compressor tip clearance flow structure
[ASME PAPER 90-GT-153] p 552 A91-34793
Modeling of surface roughness effects on glaze ice accretion p 562 A91-35107

Max-Planck-Inst. fuer Radioastronomie, Bonn (Germany, F.R.).
Airborne heterodyne receiver for the range 600 GHz to 3,000 GHz p 599 N91-22047

MCAT Inst., Moffett Field, CA.
Fully coupled implicit method for thermochemical nonequilibrium air at suborbital flight speeds p 544 A91-33380

MCAT Inst., San Jose, CA.
Grid generation about complex three-dimensional aircraft configurations
[NASA-CR-188097] p 558 N91-22071

Messerschmitt-Boelkow-Blohm G.m.b.H., Munich (Germany, F.R.).
An iterative procedure for the design of pressure-specified 3-dimensional configurations at subsonic and supersonic speeds by means of a higher-order panel method
[MBB-FE122/S/PUB/375] p 574 N91-22118

Minnesota Univ., Minneapolis.
Eigenspace design of helicopter flight control systems
[AD-A231588] p 582 N91-21153

Mitsubishi Heavy Industries Ltd., Nagoya (Japan).
Status and outlook of CFD technology at Mitsubishi Heavy Industries, Nagoya p 597 N91-21384

N

National Aeronautics and Space Administration. Ames Research Center, Moffett Field, CA.
Fully coupled implicit method for thermochemical nonequilibrium air at suborbital flight speeds p 544 A91-33380
Aerodynamic and structural studies of joined-wing aircraft p 571 A91-33534
Reduction of aerodynamic augmented states in active flutter suppression systems p 580 A91-33535
Effect of geometrical disturbance on vortex asymmetry p 547 A91-34136
A streamwise upwind algorithm applied to vortical flow over a delta wing p 548 A91-34192
Simulation of glancing shock wave and boundary layer interaction p 548 A91-34195
Simulation of nap-of-the-Earth flight in helicopters
[NASA-TM-102830] p 572 N91-21131
Suppression of biodynamic interference in head-tracked teleoperation
[NASA-TM-103833] p 577 N91-21134
Digital signal conditioning for flight test instrumentation
[NASA-TM-101739] p 577 N91-21135
Acoustic and aerodynamic study of a pusher-propeller aircraft model
[NASA-TP-3040] p 607 N91-21828
NASA Ames aerospace systems directorate research
[NASA-TM-103844] p 608 N91-22066
Forces and pressures induced on circular plates by a single lifting jet in ground effect
[NASA-TM-102816] p 558 N91-22077
Small-scale experiments in STOVL ground effects
[NASA-TM-102813] p 560 N91-22091
The NASA-ER2 meteorological measurement system: Instrumentaion, calibration and intercomparison results p 603 N91-22658
Lightweight, fire-retardant, crashworthy aircraft seat cushioning p 563 N91-23052

National Aeronautics and Space Administration. Hugh L. Dryden Flight Research Facility, Edwards, CA.
A preliminary evaluation of an F100 engine parameter estimation process using flight data
[NASA-TM-4216] p 597 N91-21446
STARS: An integrated general-purpose finite element structural, aeroelastic, and aeroservoelastic analysis computer program
[NASA-TM-101709-REV] p 599 N91-21587

Multiaxis thrust vectoring using axisymmetric nozzles and postexit vanes on an F/A-18 configuration vehicle
[NASA-TM-101741] p 559 N91-22083
Research flight-control system development for the F-18 high alpha research vehicle
[NASA-TM-104232] p 583 N91-22131

National Aeronautics and Space Administration. Lyndon B. Johnson Space Center, Houston, TX.
Metamorphoses of ONAV console operations: From prototype to real time application p 606 N91-22794

National Aeronautics and Space Administration. Langley Research Center, Hampton, VA.
Domain decomposition methods in aerodynamics p 604 A91-33056
Flowfield and vehicle parameter influence on results of engineering aerothermal methods p 544 A91-33378
Integrated multidisciplinary design optimization of rotorcraft p 570 A91-33528
Integrated aerodynamic load/dynamic optimization of helicopter rotor blades p 571 A91-33532
Conical Euler simulation of wing rock for a delta wing planform p 580 A91-33536
Shape sensitivity analysis of flutter response of a laminated wing p 571 A91-34144
A numerical study of hypersonic stagnation heat transfer predictions at a coordinate singularity p 548 A91-34193
Numerical simulation of turbulent flows around airfoil and wing p 549 A91-34203
A highly efficient engineering tool for three-dimensional scramjet flowfield and heat transfer computations p 596 N91-21098
Span reduction effects on the flutter characteristics of arrow-wing supersonic transport configurations
[NASA-TP-3077] p 572 N91-21127
A simple, analytical, axisymmetric microburst model for downdraft estimation
[NASA-TM-104053] p 573 N91-21132
Hot-bench simulation of the active flexible wing wind-tunnel model
[NASA-TM-102758] p 582 N91-21144
Propulsion simulator for magnetically-suspended wind tunnel models p 586 N91-21198
A solid-state controllable power supply for a magnetic suspension wind tunnel p 585 N91-21199
Method and apparatus for detecting laminar flow separation and reattachment
[NASA-CASE-LAR-13952-2-SB] p 598 N91-21472
Aeropropulsive characteristics of canted twin pitch-vectoring nozzles at Mach 0.20 to 1.20
[NASA-TP-3060] p 558 N91-22069
Numerical study of the aerodynamic effects of using sulfur hexafluoride as a test gas in wind tunnels
[NASA-TP-3086] p 558 N91-22070
Flight test to determine feasibility of a proposed airborne wake vortex detection concept
[NASA-TM-102672] p 563 N91-22096
Traffic Alert and Collision Avoidance System (TCAS): Cockpit Display of Traffic Information (CDTI) investigation. Phase 1: Feasibility study
[NASA-TM-104956] p 569 N91-22102
Computer program for estimating performance of air-breathing aircraft engines
[NASA-TM-4254] p 573 N91-22103
Dynamic stall effects and applications to high performance aircraft p 573 N91-22106
Fourth NASA Workshop on Computational Control of Flexible Aerospace Systems, part 2
[NASA-CP-10065-PT-2] p 587 N91-22331
An overview of the active flexible wing program p 583 N91-22332
Aeroelastic modeling of the active flexible wing wind-tunnel model p 575 N91-22333
Design and test of three active flutter suppression controllers p 583 N91-22334
Development and testing of controller performance evaluation methodology for multi-input/multi-output digital control systems p 584 N91-22337
A synchronous strobed laser light sheet for rotor flow visualization
[NASA-TM-4266] p 601 N91-22540
Computational methods for frictionless contact with application to Space Shuttle Orbiter nose-gear tires
[NASA-TP-3073] p 601 N91-22576
Sensitivity-based scaling for correlating structural response from different analytical models
[NASA-TM-104042] p 602 N91-22578
Structural integrity of wind tunnel wooden fan blades
[NASA-TM-104059] p 602 N91-22589
Cost-efficient manufacturing of composite structures p 590 N91-23048

National Aeronautics and Space Administration. Lewis Research Center, Cleveland, OH.
Role of artificial viscosity in Euler and Navier-Stokes solvers p 547 A91-34135
Modeling of surface roughness effects on glaze ice accretion p 562 A91-35107
Elevator deflections on the icing process p 572 A91-35427
Resistivity of pristine and intercalated graphite fiber epoxy composites p 589 A91-35949
Compressible flows with periodic vortical disturbances around lifting airfoils
[NASA-TM-103742] p 554 N91-21060
Computational Fluid Dynamics Symposium on Aeropropulsion
[NASA-CP-3078] p 554 N91-21062
A finite-difference, frequency-domain numerical scheme for the solution of the linearized unsteady Euler equations p 595 N91-21067
Transonic cascade flow calculations using non-periodic C-type grids p 596 N91-21071
Hot gas ingestion test results of a two-poster vectored thrust concept with flow visualization in the NASA Lewis 9- x 15-foot low speed wind tunnel
[NASA-TM-103258] p 556 N91-21116
Integrated flight/propulsion control system design based on a decentralized, hierarchical approach
[NASA-TM-103678] p 579 N91-21137
Integrated flight/propulsion control design for a STOVL aircraft using H-infinity control design techniques
[NASA-TM-104340] p 579 N91-21140
CFD for hypersonic propulsion
[NASA-TM-103791] p 597 N91-21447
Application of computational fluid dynamics in high speed aeropropulsion
[NASA-TM-103780] p 598 N91-21458
Advanced rotorcraft transmission program
[NASA-TM-103276] p 598 N91-21531
Effects of gear box vibration and mass imbalance on the dynamics of multi-stage gear transmissions
[NASA-TM-103695] p 599 N91-21534
High temperature performance evaluation of a hypersonic engine ceramic wafer seal
[NASA-TM-103737] p 601 N91-22567
Civil air transport: A fresh look at power-by-wire and fly-by-light p 584 N91-23053

National Aerospace Lab., Tokyo (Japan).
Coning motion of slender bodies at high angles of attack
[NAL-TR-1059] p 556 N91-21111
Wind tunnel test of a propeller working in a low Reynolds number range
[NAL-TR-1071] p 556 N91-21112
An experimental study of a three-dimensional swept-back wing with suction laminar-flow-control
[NAL-TR-1072] p 556 N91-21113
Blunt trailing edge analysis of supercritical airfoils by a Navier-Stokes code
[NAL-TR-1075-T] p 556 N91-21114
Proceedings of the 8th NAL Symposium on Aircraft Computational Aerodynamics: Prospects of Computational Fluid Dynamics and Super Computers in Aerospace Science and Technology
[NAL-SP-13] p 596 N91-21379
Analysis of laminar separation bubbles using a simple eddy-viscosity turbulence model
[NAL-TR-1079] p 600 N91-22520

National Center for Atmospheric Research, Boulder, CO.
Air motion measurements: Past and future p 603 N91-22653

National Oceanic and Atmospheric Administration, Boulder, CO.
Remote sensor observations during WISP90: The use of microwave radiometers, RASS, and ceilometers for detection of aircraft icing conditions
[PB91-131839] p 604 N91-22670

National Research Council of Canada, Ottawa (Ontario).
Large amplitude oscillations p 561 N91-22108

Naval Environmental Prediction Research Facility, Monterey, CA.
Impact of icing on Unmanned Aerial Vehicle (UAV) operations
[AD-A231191] p 562 N91-21124

Naval Postgraduate School, Monterey, CA.
Separating boundary layer response to an unsteady turbulent environment
[AD-A231483] p 559 N91-22081
An experimental investigation into NO(x) control of a gas turbine combustor and augmentor tube incorporating a catalytic reduction system
[AD-A231427] p 580 N91-22124

Nebraska Univ., Lincoln.
Comparison of UNL laser imaging and sizing system and a phase Doppler system for analyzing sprays from a NASA nozzle
[NASA-CR-185239] p 598 N91-21485

Nielsen Engineering and Research, Inc., Mountain View, CA.
Prediction of unsteady transonic separated flow for missile applications
[AD-A231259] p 557 N91-21120

Notre Dame Univ., IN.
Unsteady aerodynamics of slender wings p 560 N91-22105

O

Ohio State Univ., Columbus.
Linear and non-linear dynamic models of a geared rotor-bearing system p 594 A91-35536
Force and moment transmissibilities through rolling element bearings in a single-stage rotor system p 594 A91-35537

Old Dominion Univ., Norfolk, VA.
Interference-free measurements of the subsonic aerodynamics of slanted-base ogive cylinders p 547 A91-34130
Investigation of nose bluntness and angle of attack effects on slender bodies in viscous hypertension flows
[NASA-CR-188153] p 557 N91-21117

P

Pennsylvania State Univ., University Park.
Computation of supersonic and low subsonic cascade flows using an explicit Navier-Stokes technique and the kappa-epsilon turbulence model p 596 N91-21072

Polytechnic Inst. of New York, Brooklyn.
Development of a computer technique for the prediction of transport aircraft flight profile sonic boom signatures
[NASA-CR-188117] p 560 N91-22093

R

Ribbon Technology Corp., Gahanna, OH.
Direct cast titanium aluminide strip
[AD-A231906] p 590 N91-22424

Rockwell International Corp., Canoga Park, CA.
Numerical solutions of 2-D multi-stage rotor/stator unsteady flow interactions p 595 N91-21070

Rockwell International Corp., Los Angeles, CA.
Roll plus maneuver load alleviation control system designs for the active flexible wing wind-tunnel model p 584 N91-22335

Rome Univ. (Italy).
A numerical study of hypersonic stagnation heat transfer predictions at a coordinate singularity p 548 A91-34193

Royal Aircraft Establishment, Bedford (England).
Oscillatory data for typical configurations p 561 N91-22109

S

Sandia National Labs., Albuquerque, NM.
An introduction to testing parachutes in wind tunnels
[DE91-009166] p 560 N91-22094

Sparta, Inc., Laguna Hills, CA.
Automated flight test management system
[NASA-CR-186011] p 574 N91-22117

Spectron Development Labs., Inc., Costa Mesa, CA.
Development of an optical volumetric flowmeter
[PB91-136481] p 601 N91-22550

Stanford Univ., CA.
Aerodynamic and structural studies of joined-wing aircraft p 571 A91-33534
Analysis of routine communication in the air traffic control system
[NASA-CR-188116] p 600 N91-22475

Sverdrup Technology, Inc., Brook Park, OH.
A modal aeroelastic analysis scheme for turbomachinery blading
[NASA-CR-187089] p 579 N91-21138

Sverdrup Technology, Inc., Middleburg Heights, OH.
Modeling of surface roughness effects on glaze ice accretion p 562 A91-35107

Systems Technology, Inc., Mountain View, CA.
Fully automatic guidance and control for rotorcraft nap-of-the-Earth flight following planned profiles. Volume 1: Real-time piloted simulation
[NASA-CR-177571-VOL-1] p 582 N91-21149
Fully automatic guidance and control for rotorcraft nap-of-the-Earth flight following planned profiles. Volume 2: Mathematical model
[NASA-CR-177571-VOL-2] p 582 N91-21150

T

Tech-U-Fit Corp., Alexandria, VA.
Design methodology for a community response questionnaire on sonic boom exposure
[NASA-CR-187503] p 608 N91-22830
Technische Univ., Brunswick (Germany, F.R.).
Identification of the aerodynamic model of the DLR research aircraft ATTAS from flight test data
[DLR-FB-90-40] p 572 N91-21130
Texas A&M Univ., College Station.
Finite-element analysis of turbulent flow in annular exhaust diffusers of gas turbine engines
p 577 A91-32700
Tokyo Univ. (Japan).
Proceedings of a French-Japanese Seminar on Composite Materials: Processing, Use and Databases
p 589 N91-22380

V

Vigyan Research Associates, Inc., Hampton, VA.
Description and evaluation of an interference assessment for a slotted-wall wind tunnel
[NASA-CR-4352] p 585 N91-21155
Virginia Polytechnic Inst. and State Univ., Blacksburg.
Shape sensitivity analysis of flutter response of a laminated wing p 571 A91-34144
Velocity measurements in a turbulent trailing vortex and their application to BWI noise prediction
[NASA-CR-188083] p 554 N91-21100
Critical speeds and forced response solutions for active magnetic bearing turbomachinery, part 1
p 587 N91-21209
Critical speeds and forced response solutions for active magnetic bearing turbomachinery, part 2
p 587 N91-21210
The transient development of vortices over a delta wing
[AD-A231946] p 559 N91-22082

W

Washington Univ., Seattle.
Robust integrated autopilot/autothrottle design using constrained parameter optimization
[NASA-CR-188011] p 583 N91-22127
Wichita State Univ., KS.
Airline quality rating
[NIAR-91-11] p 563 N91-22098
Business plans for the Institute for Aviation Research, FY 1990 - FY 1995
[IAR-89-15] p 609 N91-23020
Wright Research Development Center, Wright-Patterson AFB, OH.
An experimental study of exit flow patterns in a multistage compressor in rotating stall
[AD-A231353] p 580 N91-21143
Wyle Labs., Inc., Hampton, VA.
Design methodology for a community response questionnaire on sonic boom exposure
[NASA-CR-187503] p 608 N91-22830

Typical Foreign Technology Index Listing

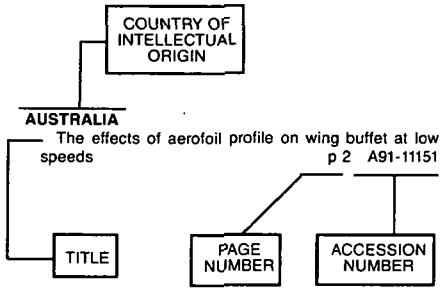

Listings in this index are arranged alphabetically by country of intellectual origin. The title of the document is used to provide a brief description of the subject matter. The page number and the accession number are included in each entry to assist the user in locating the citation in the abstract section. If applicable, a report number is also included as an aid in identifying the document.

A

AUSTRALIA
Fault detection and diagnosis in gas turbines [ASME PAPER 90-GT-339] p 578 A91-34814
Aerothermodynamic design appraisal of noise suppressors for F/A-18 engine run-up facilities at RAAF Williamtown [ARL-PROP-R-177] p 585 N91-22136
Water tunnel flow visualisation of vortex breakdown over the F/A-18 [ARL-FLIGHT-MECH-R-179] p 600 N91-22511
The FIAMS research aircraft or small is beautiful p 603 N91-22655

B

BELGIUM
A frequency domain maximum likelihood identification scheme with application to flight flutter data analysis p 581 A91-35576

C

CANADA
Significance of residual curing strains in composite structure repair technology p 590 A91-32461
Motion compensation for ASTOR long range SAR p 575 A91-33625
Test program for Honeywell/DND Helicopter Integrated Navigation System (HINS) p 565 A91-33626
INS reset removal for enhanced post-flight performance analysis p 565 A91-33628
Airborne gravimetry and the Global Positioning System p 602 A91-33634
The design, simulation and implementation of an accurate positioning system for automatic flight inspection p 566 A91-33646
Large amplitude oscillations p 561 N91-22108

CHILE
Experimental and analytical study of shaft cracking response in rotatory machines p 594 A91-35516

CHINA, PEOPLE'S REPUBLIC OF
ICCM-VII; Proceedings of the 7th International Conference on Composite Materials, Guangzhou, People's Republic of China, Nov. 22-24, 1989. Vols. 1-3 p 588 A91-32451
Cumulative damage problem in pull-through fatigue of C.F.R.P. laminate p 588 A91-32576
Optimal design of metal and composite thin-walled structures with flutter constraint p 591 A91-32650
Analysis and optimal design of composite structures p 591 A91-32651
Dynamic analysis technique of centrifugal impellor with split blades p 593 A91-35498

F

FRANCE
Uliss G, a fully integrated 'all-in-one' and 'all-in-view' inertia-GPS unit p 566 A91-33644
Numerical simulation of compressible Euler flows p 544 A91-33675
Oceanic clearance trial proves utility of data link communications for ATC p 568 A91-33775
Non-equilibrium hypersonic flow computations by implicit second-order upwind finite-elements p 548 A91-34191
On the relation between TVD and mesh adaption and application to Navier-Stokes calculations p 550 A91-34215
Computation of the viscous flow past a prolate spheroid at incidence p 550 A91-34216
A functional method for the approximate solution of a transonic problem p 550 A91-34398
Simulation of two- and three-dimensional internal subsonic flows using a finite element method p 595 A91-35986
ASTRE improvements expand usefulness of surface movement radar p 569 A91-36012
Infrared thermography for the qualitative aerodynamic study of a slender body [ISL-R-122/89] p 555 N91-21104
Practical methods to evaluate the friction drag coefficient of a projectile in free flight [ISL-R-123/89] p 555 N91-21105
Comparison study of the aerodynamic coefficients measured on models with circular or squared section and large elongation in supersonic flow [ISL-R-125/89] p 555 N91-21106
Possibilities of trajectory modification [ISL-CO-209/90] p 582 N91-21151
Rotary-balance testing for aircraft dynamics [AGARD-AR-265] p 585 N91-21156
Propagation of helicopter noise in the low atmosphere layers [ISL-CO-203/90] p 607 N91-21830
Calculation of thickness and charge noise radiated by a rotor in forward flight [ISL-R-119/89] p 607 N91-21831
Blade-wake interaction on a two blade rotor with prediction of the radiated noise stationary and forward flight, comparison between calculation, and experiment [ISL-R-120/89] p 608 N91-21832
The human factors relating to escape and survival from helicopters ditching in water [AGARD-AG-305(F)] p 563 N91-22099
Special Course on Aircraft Dynamics at High Angles of Attack: Experiments and Modelling [AGARD-R-776] p 573 N91-22104
Technical presentation of the Merlin's radome: Calibration and data processing p 603 N91-22656

G

GERMANY,FEDERAL REPUBLIC OF
Fin structures of the Airbus family experience with advanced composites p 570 A91-32455
Advanced composite technology of West German general aviation aircraft p 543 A91-32648
The location of acoustic blade-vortex interaction - A further step toward an understanding of helicopter noise p 607 A91-33368
Progress in the prediction of the laminar-turbulent transition for laminar wings - The profile and wing geometries determine the friction drag of an aircraft p 544 A91-33369
An airworthy experimental system for modern navigation and remote-sensing methods - Reduction, storage, and transmission of aerial photography scenes p 575 A91-33370
Rotors in the wind tunnel - DLR helicopter research methods in the German-Dutch Wind Tunnel p 584 A91-33371
Interdisciplinary cooperative aerospace research - Examples of scientific cooperation with Braunschweig Technical University p 543 A91-33372
Process control to set Mach number ratios for jet-engine intake measurements - Development of an automatic Mach-number regulator p 584 A91-33373
Failure management in spatio-temporal redundant, integrated navigation and flight control reference-systems p 581 A91-33640
ISS - A combined terrain topography referenced navigation system p 566 A91-33649
On management and control of turbulent shear flows p 545 A91-33803
Method for calculating boundary region corrections in multistep axial turbomachines p 592 A91-34014
Weightless test balancing of elastic rotors with the help of interchangeable longitudinal bearing stiffnesses p 592 A91-34015
Laminar shock/boundary-layer interaction - A numerical test problem p 545 A91-34033
Comparison of upwind and central finite-difference methods for the compressible Navier-Stokes equations p 545 A91-34034
A vortex-lattice method for the calculation of vortex sheet roll-up and wing-vortex interaction p 546 A91-34052
A method to calculate the influence of vortex roll-up on the induced drag of wings p 546 A91-34055
Numerical calculation of the unsteady separating flow on oscillating airfoils (dynamic stall) p 546 A91-34057
Closed-coupled zonal solution for viscous flow problems p 546 A91-34063
An implicit predictor-corrector relaxation method for viscous transonic flows p 592 A91-34064
Hypersonic flow simulation for blunt bodies at incidence p 546 A91-34070
Airfoils in two- and three-dimensional gust fields p 546 A91-34073
Computation of unsteady incompressible viscous flow around airfoils p 546 A91-34074
Numerical simulation of laminar hypersonic flow past blunt bodies including high temperature effects p 547 A91-34180
Solution of the 3-D, incompressible Navier-Stokes equations for the simulation of vortex breakdown p 593 A91-34181
Viscous, hypersonic flows over compression ramps p 548 A91-34194
Split-matrix marching methods for three-dimensional viscous and inviscid hypersonic flows p 549 A91-34206
Numerical investigation of three dimensional laminar flows in a channel with a built-in circular cylinder and wing-type vortex generators p 550 A91-34218
Some aspects of the numerical simulation of compressible viscous flow around bluff bodies at low Ma-number p 550 A91-34220
An inverse boundary layer procedure with application to 3-D wing flow p 550 A91-34229
HYTEX - Demonstrator for hypersonic flight up to Mach 5 p 571 A91-34260
Three-dimensional wake decay inside of a compressor cascade and its influence on the downstream unsteady flow field. I - Wake decay characteristics in the flow passage. II - Unsteady flow field downstream of the stator [ASME PAPER 90-GT-21] p 551 A91-34786

Experimental and numerical investigation of three-dimensional viscous flows and vertex motion inside an annular compressor blade row
[ASME PAPER 90-GT-155] p 551 A91-34787
The influence of inlet swirl distortions on the performance of a jet propulsion two-stage axial compressor
[ASME PAPER 90-GT-147] p 552 A91-34790
Application of sensitivity methods for error localization in finite element systems p 594 A91-35529
Flight path reconstruction using extended Kalman filtering techniques
[DLR-FB-90-41] p 555 N91-21108
Analysis of three icing test flights reaching the aircraft-referred icing degree severe
[DLR-FB-90-34] p 562 N91-21123
Identification of the aerodynamic model of the DLR research aircraft ATTAS from flight test data
[DLR-FB-90-40] p 572 N91-21130
Results of the HHC wind tunnel tests, 1986 - 1988
[DLR-FB-90-42] p 582 N91-21152
Flow visualization ion helicopter blades using Acenaphthen
[DLR-FB-90-37] p 598 N91-21466
Airborne heterodyne receiver for the range 600 GHz to 3,000 GHz p 599 N91-22047
An iterative procedure for the design of pressure-specified 3-dimensional configurations at subsonic and supersonic speeds by means of a higher-order panel method
[MBB-FE122/S/PUB/375] p 574 N91-22118
Air motion measurement uncertainties: Their impact on atmospheric studies p 603 N91-22654
The improvement of the installation of the DLR research aircraft Falcon: Description and first results
p 603 N91-22657
Fast response gust measurement device
p 603 N91-22659
Turbulence profiling in the atmospheric boundary layer using three powered gliders p 604 N91-22663

GREECE

Fast response wall pressure measurement as a means of gas turbine blade fault identification
[ASME PAPER 90-GT-341] p 578 A91-34813

I

INDIA

The advantages of velocity vector referencing in proportional navigation p 581 A91-33611
A fast and low-cost validation technique for ILS and MLS p 565 A91-33630
Unsteady aerodynamic modelling for aircraft lateral parameter estimation p 581 A91-34162

ISRAEL

Vorticity equation solutions for slender wings at high incidence p 547 A91-34126

ITALY

A numerical study of hypersonic stagnation heat transfer predictions at a coordinate singularity
p 548 A91-34193
Numerical simulation of vortices motion in presence of solid boundaries p 549 A91-34213

J

JAPAN

Analysis of laminar separation bubble using a simple eddy-viscosity turbulence model p 591 A91-33227
Interaction between two jets exhausted from nozzles arranged in parallel p 593 A91-34439
Detection of a rotating stall precursor in isolated axial flow compressor rotors
[ASME PAPER 90-GT-157] p 552 A91-34795
Coping with dramatic air transport growth
p 562 A91-36011
Coning motion of slender bodies at high angles of attack
[NAL-TR-1059] p 556 N91-21111
Wind tunnel test of a propeller working in a low Reynolds number range
[NAL-TR-1071] p 556 N91-21112
An experimental study of a three-dimensional swept-back wing with suction laminar-flow-control
[NAL-TR-1072] p 556 N91-21113
Blunt trailing edge analysis of supercritical airfoils by a Navier-Stokes code
[NAL-TR-1075-T] p 553 N91-21114
Proceedings of the 8th NAL Symposium on Aircraft Computational Aerodynamics: Prospects of Computational Fluid Dynamics and Super Computers in Aerospace Science and Technology
[NAL-SP-13] p 596 N91-21379
Present and future of CFD on the aero-engine development in IHI p 596 N91-21381
CFD research and systems in Kawasaki Heavy Industries and its future prospects p 596 N91-21382
The CFD analysis related aerospace in Fuji Heavy Industries, Ltd. p 597 N91-21383
Status and outlook of CFD technology at Mitsubishi Heavy Industries, Nagoya p 597 N91-21384
Proceedings of a French-Japanese Seminar on Composite Materials: Processing, Use and Databases
p 589 N91-22380
Analysis of laminar separation bubbles using a simple eddy-viscosity turbulence model
[NAL-TR-1079] p 600 N91-22520

K

KOREA(SOUTH)

Aeroelastic optimum design of composite rotor blade with returning wake effect p 570 A91-32646
Euler analysis of transonic stator-rotor interaction using a finite volume method p 554 A91-35984

N

NETHERLANDS

Damage tolerance aspects of ARALL fuselage skin structure (philosophy and experiments)
p 588 A91-32573
GAMM-Conference on Numerical Methods in Fluid Mechanics, 8th, Delft University of Technology, Netherlands, Sept. 27-29, 1989, Proceedings
p 592 A91-34176
Development and validation of characteristic boundary conditions for cell-centered Euler flow calculations
p 592 A91-34178
Aspects of the application of an Euler-equation method to the simulation of leading-edge vortex flow
p 549 A91-34196
3D Euler flows around modern airplanes
p 549 A91-34201

P

POLAND

The effect of shear and rotary inertia of a rotor at its critical speeds p 592 A91-34125
Biodynamic and optimization aspects of emergency ejection from an aircraft p 561 A91-34341

S

SPAIN

Thermal spikes on CFRP laminates - Assessment of microdamage and its consequences on fatigue life
p 588 A91-32549

SWEDEN

Hypersonic leeside flow computations using centered schemes for Euler equations p 548 A91-34187
Low speed wind tunnel investigation of propeller slipstream aerodynamic effects on different nacelle/wing combinations. Part 2: Propeller slipstream flow field surveys (velocity components, dynamic, total and static pressure distributions) at zero angle of attack and high power
[FFA-TN-1990-24-PT-2] p 555 N91-21109
MATGRID, a program for generation of C-H and C-O topology grids around wing/body configurations: User's guide
[FFA-TN-1991-03] p 556 N91-21110
Some treatments on boundary conditions for quasi one-dimensional Euler equations
[FFA-TN-1990-36] p 598 N91-21469
Stability analysis of a fuselage side
[FFA-TN-1990-32] p 599 N91-21568

SWITZERLAND

Summary of aircraft measuring activities at LAPETH
p 604 N91-22661

T

TAIWAN

Computations for a jet impinging obliquely on a flat surface p 554 A91-35985

U

U.S.S.R.

Nonlinear filtering of a trajectory message
p 568 A91-33868
Modeling of flow parameters in a cryogenic wind tunnel p 584 A91-33919
Effect of a single three-dimensional surface roughness on the transition in a supersonic boundary layer
p 545 A91-33920
An approximate method for determining friction and heat transfer in chemically nonequilibrium flow past bodies at angle of attack p 553 A91-35660
Optimization of radio-measuring devices incorporated in onboard laser velocimeters p 576 A91-35738
Using a locally one-dimensional method for solving the heat conductivity equation to determine the thermal state of cooled rotor disks p 594 A91-35742
Calculation of the cooling system of small-size blades of high-temperature gas turbine engines
p 594 A91-35743
Inertial aerosol precipitation on ogival bodies of revolution in high-velocity flow p 553 A91-35784
State stability of a system of integro-differential equations of nonstationary aeroelasticity
p 595 A91-35785
An approach to the numerical solution of two-dimensional Navier-Stokes equations by a finite difference method p 595 A91-35787
MHD drag and heat transfer of a sphere in supersonic flow of a partially ionized gas p 607 A91-35791
Calculation of a compressible laminar boundary layer on a tapered body of bielliptical cross section
p 553 A91-35796
Methods for the optimization of the testing and modeling of control systems for gas turbine engines
p 579 A91-35815
Control of the working cycle of gas turbine engines (2nd *revised and enlarged edition)* p 579 A91-35822

UNITED KINGDOM

START - A broad application spectrum gyro for the 1990's p 591 A91-33604
Terrain referenced navigation p 567 A91-33651
Terrain Aided Navigation - Current status, techniques for flat terrain and reference data requirements
p 567 A91-33663
Effects of heat transfer on aerodynamics and possible implications for wind tunnel tests p 545 A91-33802
Starship - Bright newcomer in a conservative firmament p 571 A91-34122
Cell-vertex, multigrid Euler scheme for use with multiblock grids p 547 A91-34128
Air safety regulation and its commercial impact
p 561 A91-34161
The final call: Why airline disasters continue to happen p 561 A91-34250
Mixing in axial flow compressors. I - Test facilities and measurements in a four-stage compressor. II - Measurements in a single-stage compressor and a duct
[ASME PAPER 90-GT-38] p 551 A91-34784
Tip leakage flow in axial compressors
[ASME PAPER 90-GT-127] p 552 A91-34792
High-speed compressor surge with application to active control
[ASME PAPER 90-GT-354] p 553 A91-34797
Vortex element methods for fluid dynamic analysis of engineering systems p 594 A91-35539
Computer program for the calculation of normal force and pitching moment of forebody-cylinder combinations at angles of attack up to 90 degrees and Mach numbers up to 5, including effects of conical boat-tailing
[ESDU-90034] p 555 N91-21102
Lift and rolling moment due to spoilers on wings at subsonic speeds
[ESDU-90030] p 572 N91-21129
Approximate methods for predicting the lifting characteristics of wing-body combinations
p 558 N91-22074
Effect of planform on induced drag
[BU-500] p 559 N91-22086
A leading-edge control surface
[BU-508] p 559 N91-22087
An investigation into the extent and effects of spanwise flow in the boundary layer of a helicopter rotor in hover
[BU-519] p 560 N91-22089
Oscillatory data for typical configurations
p 561 N91-22109
Variable camber wings for transport aircraft
p 574 N91-22112
The preliminary aerodynamic design of light aircraft
[BU-504] p 574 N91-22119
A quantitative investigation into the aerodynamic coupling effects in a coaxial contra-rotating rotor system
[BU-517] p 574 N91-22120
Experimental study of radiation from coated turbine blades p 580 N91-22122
Signal blending in control systems structural interactions
[BU-505] p 583 N91-22132
Flutter suppression of an aircraft wing using a control surface
[BU-506] p 583 N91-22133

Damage accumulation and degradation of composite laminates under aircraft service loading: Assessment and prediction, volumes 1 and 2 p 589 N91-22381
The flexural strength of unidirectional carbon fibre composites
[BU-509] p 589 N91-22399
Flow investigation of a ground effect vehicle
[BU-516] p 600 N91-22528
The use of axisymmetric flow for investigation of shock wave-boundary layer interactions
[BU-520] p 600 N91-22529

Y

YUGOSLAVIA
Solution method for viscous flows at all speeds in complex domains p 548 A91-34185

Typical Contract Number Index Listing

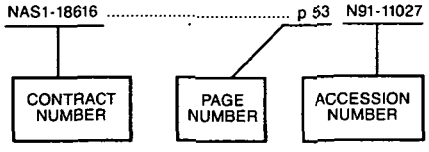

Listings in this index are arranged alphanumerically by contract number. Under each contract number, the accession numbers denoting documents that have been produced as a result of research done under the contract are shown. The accession number denotes the number by which the citation is identified in the abstract section. Preceding the accession number is the page number on which the citation may be found.

AF PROJ. 2307 ..... p 559 N91-22082
AF-AFOSR-0283-89 ..... p 559 N91-22082
AF-AFOSR-85-0126 ..... p 545 A91-33747
BMVG-T/R-760/K-0007/K-1707 ..... p 582 N91-21151
BMVG-T/RF41/E0010/E14 ..... p 574 N91-22118
DA PROJ. 1L1-62211-A-47-A ..... p 598 N91-21531
p 599 N91-21534
DAAG29-85-K-0255 ..... p 544 A91-33735
DAAL03-86-G-0044 ..... p 596 N91-21072
DAAL03-86-K-0056 ..... p 582 N91-21153
DAAL03-87-C-0008 ..... p 557 N91-21120
DAAL03-88-C-002 ..... p 570 A91-33531
DE-AC04-76DP-00789 ..... p 568 A91-33664
p 560 N91-22094
DFG-KO-956/1-1 ..... p 592 A91-34064
DFG-WA-424/4 ..... p 546 A91-34052
DRET-86-104 ..... p 550 A91-34216
DRET-88/214 ..... p 607 N91-21831
DTFA03-88-C-00024 ..... p 562 N91-21122
F19628-85-C-0002 ..... p 569 N91-22102
F33615-83-C-2331 ..... p 552 A91-34794
F33615-84-C-0519 ..... p 606 N91-22734
F33615-86-C-5139 ..... p 590 N91-22424
F33615-87-C-2755 ..... p 580 N91-22125
F33615-87-C-3607 ..... p 544 A91-33382
F33615-88-C-5504 ..... p 601 N91-22564
F33615-89-C-3610 ..... p 605 N91-21735
F49620-85-C-0027 ..... p 595 N91-21068
F49620-85-C-0049 ..... p 544 A91-32958
F49620-86-C-0113 ..... p 589 N91-22407
F49620-86-K-0020 ..... p 547 A91-34139
F49620-88-C-0022 ..... p 553 A91-34798
GRI-5084-271-0987 ..... p 601 N91-22550
MOESC-01550532 ..... p 593 A91-34439
NAGW-1809 ..... p 554 N91-21101
NAGW-674 ..... p 579 N91-21139
NAG1-1080 ..... p 559 N91-22080
NAG1-1119 ..... p 554 N91-21100
NAG1-1158 ..... p 560 N91-22095
NAG1-193 ..... p 583 N91-22127
NAG1-224 ..... p 602 N91-22578
NAG1-363 ..... p 557 N91-21117
NAG1-710 ..... p 558 N91-22078
NAG1-716 ..... p 547 A91-34130
NAG1-739 ..... p 570 A91-33529
p 570 A91-33531
NAG1-833 ..... p 570 A91-33527
NAG2-379 ..... p 607 N91-21829
NAG3-634 ..... p 598 N91-21485
NAG3-666 ..... p 562 A91-35107
NAG3-716 ..... p 595 N91-21068
NAG3-724 ..... p 547 A91-34135
NAG8-109 ..... p 593 A91-35117
NASA ORDER C-99066-G ..... p 596 N91-21071
NAS1-18444 ..... p 606 N91-22805
NAS1-18471 ..... p 571 A91-34144
NAS1-18585 ..... p 585 N91-21155
NAS1-18599 ..... p 596 N91-21089
NAS1-18605 ..... p 579 N91-21139
NAS1-18845 ..... p 586 N91-21198
NAS1-19000 ..... p 571 A91-33533
p 558 N91-22078
NAS1-19060 ..... p 608 N91-22830
NAS2-11934 ..... p 562 N91-21121
NAS2-12513 ..... p 547 A91-34179
NAS2-12640 ..... p 582 N91-21149
p 582 N91-21150
NAS2-12670 ..... p 574 N91-22117
NAS3-25266 ..... p 579 N91-21138
NAS8-36461 ..... p 590 N91-22416
NAS8-37821 ..... p 577 A91-32700
NAS8-40000 ..... p 595 N91-21070
NCA2-84 ..... p 571 A91-33534
NCC1-68 ..... p 557 N91-21117
NCC2-616 ..... p 558 N91-22071
NCC2-622 ..... p 600 N91-22475
NCC3-19 ..... p 589 A91-35949
NCC9-16 ..... p 605 N91-22728
NGL-22-009-640 ..... p 562 A91-35107
NSF DMR-90-13337 ..... p 589 A91-34841
NSF DMS-88-06099 ..... p 605 N91-22313
NSG-3208 ..... p 552 A91-34793
W-7405-ENG-48 ..... p 597 N91-21407
505-59-40-02 ..... p 559 N91-22080
505-59-85-01 ..... p 602 N91-22589
505-60-01-01 ..... p 558 N91-22070
505-61-01-05 ..... p 601 N91-22540
505-61-11 ..... p 607 N91-21828
505-61-51 ..... p 607 N91-21829
505-61-71 ..... p 558 N91-22077
505-62-0K ..... p 598 N91-21531
505-62-21 ..... p 554 N91-21062
505-62-50 ..... p 579 N91-21137
p 579 N91-21140
505-62-52 ..... p 554 N91-21060
p 598 N91-21458
505-62-71-01 ..... p 558 N91-22069
505-62-71 ..... p 556 N91-21116
505-63-1B ..... p 579 N91-21138
505-63-21 ..... p 572 N91-21127
505-63-31 ..... p 597 N91-21446
505-63-36-06 ..... p 558 N91-22078
505-63-41-02 ..... p 601 N91-22576
505-63-5B ..... p 601 N91-22567
505-63-50-06 ..... p 602 N91-22578
505-63-51 ..... p 599 N91-21534
505-64-00 ..... p 608 N91-22066
505-64-12 ..... p 573 N91-21132
505-64-20-01 ..... p 582 N91-21144
505-66-29 ..... p 572 N91-21131
505-66-71 ..... p 599 N91-21587
505-68-00 ..... p 583 N91-22131
505-68-11 ..... p 598 N91-21485
505-68-30-10 ..... p 563 N91-22096
505-68-84 ..... p 577 N91-21134
505-69-01-01 ..... p 573 N91-22103
505-90-52-01 ..... p 579 N91-21139
506-46-11-01 ..... p 587 N91-22331
506-62-21 ..... p 597 N91-21447
510-02-12-03 ..... p 606 N91-22805
533-02-01 ..... p 559 N91-22083
533-02-51 ..... p 577 N91-21135

Typical Report Number Index Listing

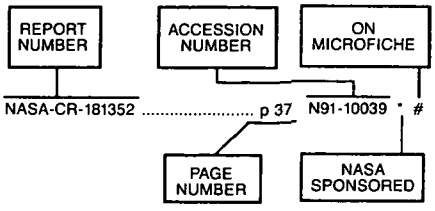

Listings in this index are arranged alphanumerically by report number. The page number indicates the page on which the citation is located. The accession number denotes the number by which the citation is identified. An asterisk (*) indicates that the item is a NASA report. A pound sign (#) indicates that the item is available on microfiche.

A-89038 p 607 N91-21828 * #
A-90137 p 560 N91-22091 * #
A-90142 p 558 N91-22077 * #
A-90178 p 572 N91-21131 * #
A-90269 p 607 N91-21829 * #
A-91058 p 577 N91-21134 * #
A-91088 p 608 N91-22066 * #

AAMRL-TR-90-015 p 606 N91-22734 #

ACD-20 p 563 N91-22096 * #

AD-A229932 p 605 N91-21735 #
AD-A230826 p 557 N91-21118 #
AD-A230868 p 577 N91-21136 #
AD-A230951 p 597 N91-21410 #
AD-A230995 p 573 N91-21133 #
AD-A231028 p 557 N91-21119 #
AD-A231077 p 585 N91-21158 #
AD-A231158 p 585 N91-22137 #
AD-A231191 p 562 N91-21124 #
AD-A231259 p 557 N91-21120 #
AD-A231353 p 580 N91-21143 #
AD-A231427 p 580 N91-22124 #
AD-A231433 p 606 N91-22734 #
AD-A231483 p 559 N91-22081 #
AD-A231490 p 586 N91-22138 #
AD-A231588 p 582 N91-21153 #
AD-A231666 p 601 N91-22564 #
AD-A231721 p 543 N91-22068 #
AD-A231750 p 589 N91-22407 #
AD-A231809 p 600 N91-22480 #
AD-A231899 p 580 N91-22125 #
AD-A231906 p 590 N91-22424 #
AD-A231946 p 559 N91-22082 #

AFIT/CI/CIA-90-126 p 585 N91-22137 #

AFIT/GAE/ENY/90D-07 p 557 N91-21118 #
AFIT/GAE/ENY/90D-14 p 557 N91-21119 #

AFIT/GE/ENG/90D-59 p 597 N91-21410 #

AFOSR-91-0012TR p 589 N91-22407 #
AFOSR-91-0026TR p 559 N91-22082 #

AGARD-AG-305(F) p 563 N91-22099 #

AGARD-AR-265 p 585 N91-21156 #
AGARD-AR-268 p 598 N91-21464 #

AGARD-R-776 p 573 N91-22104 #

AGARDOGRAPH-160 p 577 N91-21135 * #

AIAA PAPER 91-2987 p 577 A91-34111 #

AIAA-89-3519 p 579 N91-21137 * #
AIAA-90-2268 p 556 N91-21116 * #
AIAA-90-3121 p 582 N91-21144 * #
AIAA-91-0858 p 560 N91-22094 #

AR-005-607 p 600 N91-22511 #
AR-006-126 p 585 N91-22136 #

ARL-FLIGHT-MECH-R-179 p 600 N91-22511 #

ARL-PROP-R-177 p 585 N91-22136 #

ARO-23422.9-EL p 582 N91-21153 #
ARO-24788.7-EG p 557 N91-21120 #

ASME PAPER 90-GT-109 p 553 A91-34798 #
ASME PAPER 90-GT-113 p 578 A91-34815 #
ASME PAPER 90-GT-127 p 552 A91-34792 #
ASME PAPER 90-GT-133 p 551 A91-34788 #
ASME PAPER 90-GT-147 p 552 A91-34790 #
ASME PAPER 90-GT-151 p 552 A91-34794 #
ASME PAPER 90-GT-153 p 552 A91-34793 #
ASME PAPER 90-GT-155 p 551 A91-34787 #
ASME PAPER 90-GT-156 p 553 A91-34796 #
ASME PAPER 90-GT-157 p 552 A91-34795 #
ASME PAPER 90-GT-21 p 551 A91-34786 #
ASME PAPER 90-GT-23 p 578 A91-34811 #
ASME PAPER 90-GT-259 p 551 A91-34789 #
ASME PAPER 90-GT-266 p 593 A91-34810 #
ASME PAPER 90-GT-339 p 578 A91-34814 #
ASME PAPER 90-GT-341 p 578 A91-34813 #
ASME PAPER 90-GT-352 p 551 A91-34783 #
ASME PAPER 90-GT-354 p 553 A91-34797 #
ASME PAPER 90-GT-359 p 552 A91-34791 #
ASME PAPER 90-GT-38 p 551 A91-34784 #
ASME PAPER 90-JPGC/PTC-1 p 578 A91-34808 #
ASME PAPER 90-JPGC/PTC-2 p 578 A91-34809 #
ASME PAPER 90-WA/HT-4 p 544 A91-32958 #
ASME PAPER 90-WA/TS-1 p 591 A91-32961 #

AVSCOM-TR-90-A-005 p 577 N91-21134 * #
AVSCOM-TR-90-C-015 p 598 N91-21531 * #
AVSCOM-TR-90-C-022 p 599 N91-21534 * #

BU-500 p 559 N91-22086 #
BU-504 p 574 N91-22119 #
BU-505 p 583 N91-22132 #
BU-506 p 583 N91-22133 #
BU-508 p 559 N91-22087 #
BU-509 p 589 N91-22399 #
BU-516 p 600 N91-22528 #
BU-517 p 574 N91-22120 #
BU-519 p 560 N91-22089 #
BU-520 p 600 N91-22529 #

CONF-9104171-6 p 560 N91-22094 #
CONF-9105122-1 p 597 N91-21407 #

CRREL-90-3 p 586 N91-22138 #

DE91-007128 p 597 N91-21407 #
DE91-009166 p 560 N91-22094 #

DLR-FB-90-34 p 562 N91-21123 #
DLR-FB-90-37 p 598 N91-21466 #
DLR-FB-90-40 p 572 N91-21130 #
DLR-FB-90-41 p 555 N91-21108 #
DLR-FB-90-42 p 582 N91-21152 #

DOT/FAA/AS-90-3 p 585 N91-21158 #

DOT/FAA/CT-TN89/69 p 608 N91-21833 #
DOT/FAA/CT-TN90/25 p 563 N91-22096 * #
DOT/FAA/CT-TN90/28 p 587 N91-21238 #
DOT/FAA/CT-TN90/45 p 569 N91-22100 #
DOT/FAA/CT-TN90/60 p 569 N91-22101 #

DOT/FAA/CT-90/13 p 562 N91-21122 #

DOT/FAA/RD-91/8 p 569 N91-22102 * #

E-5296 p 554 N91-21062 * #
E-5689 p 597 N91-21447 * #
E-5690 p 556 N91-21116 * #
E-5722 p 598 N91-21531 * #
E-5895 p 579 N91-21137 * #
E-5916 p 599 N91-21534 * #
E-5942 p 601 N91-22567 * #
E-5984 p 554 N91-21060 * #
E-6053 p 598 N91-21458 * #
E-6081 p 579 N91-21138 * #
E-6113 p 579 N91-21140 * #

ESDU-90030 p 572 N91-21129
ESDU-90034 p 555 N91-21102

ETL-0567 p 600 N91-22480 #

ETN-91-98981 p 607 N91-21830 #
ETN-91-98983 p 582 N91-21151 #
ETN-91-98987 p 607 N91-21831 #
ETN-91-98988 p 608 N91-21832 #
ETN-91-98989 p 555 N91-21104 #
ETN-91-98990 p 555 N91-21105 #
ETN-91-98992 p 555 N91-21106 #
ETN-91-99031 p 562 N91-21123 #
ETN-91-99032 p 598 N91-21466 #
ETN-91-99034 p 582 N91-21152 #
ETN-91-99035 p 572 N91-21130 #
ETN-91-99036 p 555 N91-21108 #
ETN-91-99042 p 555 N91-21109 #
ETN-91-99043 p 599 N91-21568 #
ETN-91-99045 p 598 N91-21469 #
ETN-91-99047 p 556 N91-21110 #
ETN-91-99190 p 574 N91-22118 #
ETN-91-99193 p 559 N91-22086 #
ETN-91-99197 p 574 N91-22119 #
ETN-91-99198 p 583 N91-22132 #
ETN-91-99199 p 583 N91-22133 #
ETN-91-99201 p 559 N91-22087 #
ETN-91-99202 p 589 N91-22399 #
ETN-91-99209 p 600 N91-22528 #
ETN-91-99210 p 574 N91-22120 #
ETN-91-99212 p 560 N91-22089 #
ETN-91-99213 p 600 N91-22529 #

FAA-APO-91-1 p 543 N91-22068 #

FFA-TN-1990-24-PT-2 p 555 N91-21109 #
FFA-TN-1990-32 p 599 N91-21568 #
FFA-TN-1990-36 p 598 N91-21469 #
FFA-TN-1991-03 p 556 N91-21110 #

FTI-9042-001-PHASE-1 p 605 N91-21735 #

GAO/IMTEC-90-79 p 577 N91-21136 #

GRI-89/0201 p 601 N91-22550 #

H-1582-REV p 599 N91-21587 * #
H-1602 p 597 N91-21446 * #
H-1695 p 577 N91-21135 * #
H-1699 p 574 N91-22117 * #
H-1705 p 559 N91-22083 * #
H-1715 p 583 N91-22131 * #

IAR-89-15 p 609 N91-23020 #

ICASE-16 p 579 N91-21139 * #

INT-PATENT-CLASS-G01F-1/00 p 598 N91-21472 *

ISBN-0-85679-756-1 p 572 N91-21129
ISBN-0-85679-760-X p 555 N91-21102
ISBN-92-835-0597-2 p 585 N91-21156 #
ISBN-92-835-0607-3 p 573 N91-22104 #
ISBN-92-835-0608-1 p 598 N91-21464 #
ISBN-92-835-2116-1 p 563 N91-22099 #

ISL-CO-203/90 p 607 N91-21830 #
ISL-CO-209/90 p 582 N91-21151 #

ISL-R-119/89 p 607 N91-21831 #
ISL-R-120/89 p 608 N91-21832 #

ISL-R-122/89 ..... p 555 N91-21104 #
ISL-R-123/89 ..... p 555 N91-21105 #
ISL-R-125/89 ..... p 555 N91-21106 #

ISSN-0141-397X ..... p 555 N91-21102
ISSN-0141-397X ..... p 572 N91-21129
ISSN-0171-1342 ..... p 555 N91-21108 #
ISSN-0171-1342 ..... p 562 N91-21123 #
ISSN-0171-1342 ..... p 572 N91-21130 #
ISSN-0171-1342 ..... p 582 N91-21152 #
ISSN-0171-1342 ..... p 598 N91-21466 #
ISSN-0289-260X ..... p 596 N91-21379 #
ISSN-0389-4010 ..... p 556 N91-21111 #
ISSN-0389-4010 ..... p 556 N91-21112 #
ISSN-0389-4010 ..... p 556 N91-21113 #
ISSN-0389-4010 ..... p 556 N91-21114 #
ISSN-0389-4010 ..... p 600 N91-22520 #

L-16750 ..... p 601 N91-22576 * #
L-16765 ..... p 573 N91-22103 * #
L-16807 ..... p 572 N91-21127 * #
L-16823 ..... p 558 N91-22069 * #
L-16849 ..... p 558 N91-22070 * #
L-16877 ..... p 601 N91-22540 * #

MBB-FE122/S/PUB/375 ..... p 574 N91-22118 #

MCAT-91-003 ..... p 558 N91-22071 * #

MR-S-1800-PHASE-1 ..... p 580 N91-22125 #

NAL-SP-13 ..... p 596 N91-21379 #

NAL-TR-1059 ..... p 556 N91-21111 #
NAL-TR-1071 ..... p 556 N91-21112 #
NAL-TR-1072 ..... p 556 N91-21113 #
NAL-TR-1075-T ..... p 556 N91-21114 #
NAL-TR-1079 ..... p 600 N91-22520 #

NAS 1.15:101709-REV ..... p 599 N91-21587 * #
NAS 1.15:101739 ..... p 577 N91-21135 * #
NAS 1.15:101741 ..... p 559 N91-22083 * #
NAS 1.15:102672 ..... p 563 N91-22096 * #
NAS 1.15:102758 ..... p 582 N91-21144 * #
NAS 1.15:102813 ..... p 560 N91-22091 * #
NAS 1.15:102816 ..... p 558 N91-22077 * #
NAS 1.15:102830 ..... p 572 N91-21131 * #
NAS 1.15:103258 ..... p 556 N91-21116 * #
NAS 1.15:103276 ..... p 598 N91-21531 * #
NAS 1.15:103678 ..... p 579 N91-21137 * #
NAS 1.15:103695 ..... p 599 N91-21534 * #
NAS 1.15:103737 ..... p 601 N91-22567 * #
NAS 1.15:103742 ..... p 554 N91-21060 * #
NAS 1.15:103780 ..... p 598 N91-21458 * #
NAS 1.15:103791 ..... p 597 N91-21447 * #
NAS 1.15:103833 ..... p 577 N91-21134 * #
NAS 1.15:103844 ..... p 608 N91-22066 * #
NAS 1.15:104042 ..... p 602 N91-22578 * #
NAS 1.15:104053 ..... p 573 N91-21132 * #
NAS 1.15:104059 ..... p 602 N91-22589 * #
NAS 1.15:104232 ..... p 583 N91-22131 * #
NAS 1.15:104340 ..... p 579 N91-21140 * #
NAS 1.15:104956 ..... p 569 N91-22102 * #
NAS 1.15:4216 ..... p 597 N91-21446 * #
NAS 1.15:4254 ..... p 573 N91-22103 * #
NAS 1.15:4266 ..... p 601 N91-22540 * #
NAS 1.26:177372 ..... p 562 N91-21121 * #
NAS 1.26:177565 ..... p 607 N91-21829 * #
NAS 1.26:177571-VOL-1 ..... p 582 N91-21149 * #
NAS 1.26:177571-VOL-2 ..... p 582 N91-21150 * #
NAS 1.26:184114 ..... p 590 N91-22416 * #
NAS 1.26:185239 ..... p 598 N91-21485 * #
NAS 1.26:186011 ..... p 574 N91-22117 * #
NAS 1.26:187089 ..... p 579 N91-21138 * #
NAS 1.26:187503 ..... p 608 N91-22830 * #
NAS 1.26:187524 ..... p 558 N91-22078 * #
NAS 1.26:187539 ..... p 579 N91-21139 * #
NAS 1.26:187994 ..... p 605 N91-22728 * #
NAS 1.26:188011 ..... p 583 N91-22127 * #
NAS 1.26:188079 ..... p 554 N91-21101 * #
NAS 1.26:188083 ..... p 554 N91-21100 * #
NAS 1.26:188097 ..... p 558 N91-22071 * #
NAS 1.26:188116 ..... p 600 N91-22475 * #
NAS 1.26:188117 ..... p 560 N91-22093 * #
NAS 1.26:188153 ..... p 557 N91-21117 * #
NAS 1.26:188201 ..... p 560 N91-22095 * #
NAS 1.26:4352 ..... p 585 N91-21155 * #
NAS 1.26:4362 ..... p 606 N91-22805 * #
NAS 1.26:4369 ..... p 559 N91-22080 * #
NAS 1.55:10065-PT-2 ..... p 587 N91-22331 * #
NAS 1.55:3078 ..... p 554 N91-21062 * #
NAS 1.60:3040 ..... p 607 N91-21828 * #
NAS 1.60:3060 ..... p 558 N91-22069 * #
NAS 1.60:3073 ..... p 601 N91-22576 * #
NAS 1.60:3077 ..... p 572 N91-21127 * #
NAS 1.60:3086 ..... p 558 N91-22070 * #

NASA-CASE-LAR-13952-2-SB ..... p 598 N91-21472 *

NASA-CP-10045 ..... p 554 N91-21062 * #
NASA-CP-10065-PT-2 ..... p 587 N91-22331 * #
NASA-CP-3078 ..... p 554 N91-21062 * #

NASA-CR-177372 ..... p 562 N91-21121 * #
NASA-CR-177565 ..... p 607 N91-21829 * #
NASA-CR-177571-VOL-1 ..... p 582 N91-21149 * #
NASA-CR-177571-VOL-2 ..... p 582 N91-21150 * #
NASA-CR-184114 ..... p 590 N91-22416 * #
NASA-CR-185239 ..... p 598 N91-21485 * #
NASA-CR-186011 ..... p 574 N91-22117 * #
NASA-CR-187089 ..... p 579 N91-21138 * #
NASA-CR-187503 ..... p 608 N91-22830 * #
NASA-CR-187524 ..... p 558 N91-22078 * #
NASA-CR-187539 ..... p 579 N91-21139 * #
NASA-CR-187994 ..... p 605 N91-22728 * #
NASA-CR-188011 ..... p 583 N91-22127 * #
NASA-CR-188079 ..... p 554 N91-21101 * #
NASA-CR-188083 ..... p 554 N91-21100 * #
NASA-CR-188097 ..... p 558 N91-22071 * #
NASA-CR-188116 ..... p 600 N91-22475 * #
NASA-CR-188117 ..... p 560 N91-22093 * #
NASA-CR-188153 ..... p 557 N91-21117 * #
NASA-CR-188201 ..... p 560 N91-22095 * #
NASA-CR-4352 ..... p 585 N91-21155 * #
NASA-CR-4362 ..... p 606 N91-22805 * #
NASA-CR-4369 ..... p 559 N91-22080 * #

NASA-TM-101709-REV ..... p 599 N91-21587 * #
NASA-TM-101739 ..... p 577 N91-21135 * #
NASA-TM-101741 ..... p 559 N91-22083 * #
NASA-TM-102672 ..... p 563 N91-22096 * #
NASA-TM-102758 ..... p 582 N91-21144 * #
NASA-TM-102813 ..... p 560 N91-22091 * #
NASA-TM-102816 ..... p 558 N91-22077 * #
NASA-TM-102830 ..... p 572 N91-21131 * #
NASA-TM-103258 ..... p 556 N91-21116 * #
NASA-TM-103276 ..... p 598 N91-21531 * #
NASA-TM-103678 ..... p 579 N91-21137 * #
NASA-TM-103695 ..... p 599 N91-21534 * #
NASA-TM-103737 ..... p 601 N91-22567 * #
NASA-TM-103742 ..... p 554 N91-21060 * #
NASA-TM-103780 ..... p 598 N91-21458 * #
NASA-TM-103791 ..... p 597 N91-21447 * #
NASA-TM-103833 ..... p 577 N91-21134 * #
NASA-TM-103844 ..... p 608 N91-22066 * #
NASA-TM-104042 ..... p 602 N91-22578 * #
NASA-TM-104053 ..... p 573 N91-21132 * #
NASA-TM-104059 ..... p 602 N91-22589 * #
NASA-TM-104232 ..... p 583 N91-22131 * #
NASA-TM-104340 ..... p 579 N91-21140 * #
NASA-TM-104956 ..... p 569 N91-22102 * #
NASA-TM-4216 ..... p 597 N91-21446 * #
NASA-TM-4254 ..... p 573 N91-22103 * #
NASA-TM-4266 ..... p 601 N91-22540 * #

NASA-TP-3040 ..... p 607 N91-21828 * #
NASA-TP-3060 ..... p 558 N91-22069 * #
NASA-TP-3073 ..... p 601 N91-22576 * #
NASA-TP-3077 ..... p 572 N91-21127 * #
NASA-TP-3086 ..... p 558 N91-22070 * #

NATICK/TR-91/010 ..... p 573 N91-21133 #

NEAR-TR-418 ..... p 557 N91-21120 #

NIAR-91-11 ..... p 563 N91-22098 #

NOAA-TM-ERL-WPL-187 ..... p 604 N91-22670 #

PB91-128264 ..... p 543 N91-22067 #
PB91-131839 ..... p 604 N91-22670 #
PB91-136481 ..... p 601 N91-22550 #

RE-780 ..... p 606 N91-22805 * #

SAE PAPER 892608 ..... p 562 A91-34912

SAND-91-0531C ..... p 560 N91-22094 #

SDL-89-2532-13 ..... p 601 N91-22550 #

STI-TR-1254-1 ..... p 582 N91-21149 * #
STI-TR-1254-2 ..... p 582 N91-21150 * #

TUF-90-07 ..... p 608 N91-22830 * #

UCRL-JC-105984 ..... p 597 N91-21407 #

UDR-TR-90-15 ..... p 606 N91-22734 #
UDR-TR-90-23 ..... p 562 N91-21122 #

US-PATENT-APPL-SN-203178 ..... p 598 N91-21472 *
US-PATENT-APPL-SN-348223 ..... p 598 N91-21472 *
US-PATENT-CLASS-73-432.1 ..... p 598 N91-21472 *

US-PATENT-4,936,146 ..... p 598 N91-21472 *

WL-TR-91-4002 ..... p 590 N91-22424 #

WRDC-TR-90-2062-PHASE-1 ..... p 580 N91-22125 #
WRDC-TR-90-2083 ..... p 580 N91-21143 #
WRDC-TR-90-3067-PHASE-1 ..... p 605 N91-21735 #
WRDC-TR-90-4140 ..... p 601 N91-22564 #

Typical Accession Number Index Listing

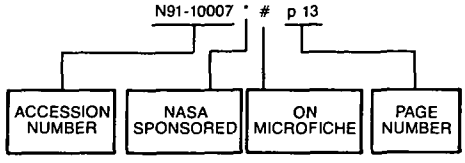

Listings in this index are arranged alphanumerically by accession number. The page number listed to the right indicates the page on which the citation is located. An asterisk (*) indicates that the item is a NASA report. A pound sign (#) indicates that the item is available on microfiche.

A91-32451 p 588
A91-32455 p 570
A91-32461 p 590
A91-32547 p 590
A91-32549 p 588
A91-32573 p 588
A91-32576 p 588
A91-32646 p 570
A91-32648 p 543
A91-32650 p 591
A91-32651 p 591
A91-32700 * # p 577
A91-32707 p 606
A91-32958 # p 544
A91-32961 # p 591
A91-33056 * p 604
A91-33227 # p 591
A91-33268 p 575
A91-33273 p 561
A91-33323 p 570
A91-33324 p 588
A91-33368 p 607
A91-33369 p 544
A91-33370 p 575
A91-33371 p 584
A91-33372 p 543
A91-33373 p 584
A91-33378 * # p 544
A91-33379 # p 544
A91-33380 * # p 544
A91-33382 # p 544
A91-33464 p 591
A91-33527 * # p 570
A91-33528 * # p 570
A91-33529 * # p 570
A91-33530 # p 570
A91-33531 * # p 570
A91-33532 * # p 571
A91-33533 * # p 571
A91-33534 * # p 571
A91-33535 * # p 580
A91-33536 * # p 580
A91-33601 p 586
A91-33604 p 591
A91-33607 # p 563
A91-33608 p 563
A91-33609 p 586
A91-33611 p 581
A91-33614 p 564
A91-33615 p 575
A91-33616 p 564
A91-33622 p 564
A91-33623 p 564
A91-33624 p 564
A91-33625 p 575
A91-33626 p 565
A91-33627 p 575
A91-33628 p 565
A91-33630 p 565
A91-33631 p 565
A91-33632 # p 565
A91-33633 # p 565
A91-33634 p 602
A91-33636 p 566
A91-33639 # p 581
A91-33640 p 581
A91-33644 p 566
A91-33645 p 566
A91-33646 p 566
A91-33647 p 566
A91-33648 p 602
A91-33649 p 566
A91-33650 p 576
A91-33651 p 567
A91-33652 p 567
A91-33653 p 567
A91-33655 p 576
A91-33656 p 576
A91-33657 p 576
A91-33660 p 567
A91-33661 p 567
A91-33663 p 567
A91-33664 p 568
A91-33665 p 568
A91-33666 p 568
A91-33667 p 568
A91-33668 p 561
A91-33674 p 591
A91-33675 p 544
A91-33725 p 588
A91-33735 p 544
A91-33747 p 545
A91-33775 p 568
A91-33802 p 545
A91-33803 p 545
A91-33868 p 568
A91-33919 p 584
A91-33920 p 545
A91-33932 p 604
A91-34011 p 568
A91-34014 p 592
A91-34015 p 592
A91-34033 p 545
A91-34034 p 545
A91-34052 p 546
A91-34055 p 546
A91-34057 p 546
A91-34063 p 546
A91-34064 p 592
A91-34070 p 546
A91-34073 p 546
A91-34074 p 546
A91-34111 # p 577
A91-34122 p 571
A91-34125 p 592
A91-34126 # p 547
A91-34127 # p 592
A91-34128 # p 547
A91-34130 * # p 547
A91-34135 * # p 547
A91-34136 * # p 547
A91-34139 # p 547
A91-34144 * # p 571
A91-34161 p 561
A91-34162 p 581
A91-34164 p 571
A91-34176 p 592
A91-34178 p 592
A91-34179 * p 547
A91-34180 p 547
A91-34181 p 593
A91-34185 p 548
A91-34187 p 548
A91-34191 p 548
A91-34192 * p 548
A91-34193 * p 548
A91-34194 p 548
A91-34195 * p 548
A91-34196 p 549
A91-34198 p 549
A91-34201 p 549
A91-34203 * p 549
A91-34206 p 549
A91-34210 p 549
A91-34213 p 549
A91-34215 p 550
A91-34216 p 550
A91-34218 p 550
A91-34220 p 550
A91-34229 p 550
A91-34230 p 605
A91-34250 p 561
A91-34260 p 571
A91-34287 p 588
A91-34341 p 561
A91-34375 p 571
A91-34398 p 550
A91-34439 # p 593
A91-34783 # p 551
A91-34784 # p 551
A91-34785 # p 551
A91-34786 # p 551
A91-34787 # p 551
A91-34788 # p 551
A91-34789 # p 551
A91-34790 # p 552
A91-34791 # p 552
A91-34792 # p 552
A91-34793 # p 552
A91-34794 # p 552
A91-34795 # p 552
A91-34796 # p 553
A91-34797 # p 553
A91-34798 # p 553
A91-34808 # p 578
A91-34809 # p 578
A91-34810 # p 593
A91-34811 # p 578
A91-34813 # p 578
A91-34814 # p 578
A91-34815 # p 578
A91-34816 # p 581
A91-34822 # p 593
A91-34841 p 589
A91-34912 p 562
A91-35100 p 605
A91-35107 # p 562
A91-35117 * # p 593
A91-35121 p 608
A91-35122 p 608
A91-35123 p 608
A91-35193 p 543
A91-35241 p 605
A91-35425 # p 571
A91-35427 * # p 572
A91-35498 p 593
A91-35516 p 594
A91-35529 p 594
A91-35536 * p 594
A91-35537 * p 594
A91-35539 p 594
A91-35576 p 581
A91-35660 p 553
A91-35738 p 576
A91-35742 p 594
A91-35743 p 594
A91-35784 p 553
A91-35785 p 595
A91-35787 p 595
A91-35791 p 607
A91-35796 p 553
A91-35815 p 579
A91-35822 p 579
A91-35902 p 569
A91-35949 * p 589
A91-35978 p 577
A91-35984 p 554
A91-35985 p 554
A91-35986 p 595
A91-36011 p 562
A91-36012 p 569
N91-21060 * # p 554
N91-21062 * # p 554
N91-21067 * # p 595
N91-21068 * # p 595
N91-21070 * # p 595
N91-21071 * # p 596
N91-21072 * # p 596
N91-21089 * # p 596
N91-21098 * # p 596
N91-21100 * # p 554
N91-21101 * # p 554
N91-21102 p 555
N91-21104 # p 555
N91-21105 # p 555
N91-21106 # p 555
N91-21108 # p 555
N91-21109 # p 555
N91-21110 # p 556
N91-21111 # p 556
N91-21112 # p 556
N91-21113 # p 556
N91-21114 # p 556
N91-21116 * # p 556
N91-21117 * # p 557
N91-21118 # p 557
N91-21119 # p 557
N91-21120 # p 557
N91-21121 * # p 562
N91-21122 # p 562
N91-21123 # p 562
N91-21124 # p 562
N91-21127 * # p 572
N91-21129 p 572
N91-21130 # p 572
N91-21131 * # p 572
N91-21132 * # p 573
N91-21133 # p 573
N91-21134 * # p 577
N91-21135 * # p 577
N91-21136 # p 577
N91-21137 * # p 579
N91-21138 * # p 579
N91-21139 * # p 579
N91-21140 * # p 579
N91-21143 # p 580
N91-21144 * # p 582
N91-21149 * # p 582
N91-21150 * # p 582
N91-21151 # p 582
N91-21152 # p 582
N91-21153 # p 582
N91-21155 * # p 585
N91-21156 # p 585
N91-21158 # p 585
N91-21197 * # p 586
N91-21198 * # p 586
N91-21199 * # p 585
N91-21208 * # p 587
N91-21209 * # p 587
N91-21210 * # p 587
N91-21238 # p 587
N91-21379 # p 596
N91-21381 # p 596
N91-21382 # p 596
N91-21383 # p 597
N91-21384 # p 597
N91-21407 # p 597
N91-21410 # p 597
N91-21446 * # p 597
N91-21447 * # p 597
N91-21458 * # p 598
N91-21464 # p 598
N91-21466 # p 598
N91-21469 # p 598
N91-21472 * p 598
N91-21485 * # p 598
N91-21531 * # p 598
N91-21534 * # p 599
N91-21568 # p 599
N91-21587 * # p 599
N91-21735 # p 605
N91-21828 * # p 607
N91-21829 * # p 607
N91-21830 # p 607
N91-21831 # p 607
N91-21832 # p 608
N91-21833 # p 608
N91-22047 # p 599
N91-22066 * # p 608
N91-22067 # p 543
N91-22068 # p 543
N91-22069 * # p 558
N91-22070 * # p 558
N91-22071 * # p 558
N91-22074 p 558
N91-22077 * # p 558
N91-22078 * # p 558
N91-22080 * # p 559
N91-22081 # p 559
N91-22082 # p 559
N91-22083 * # p 559
N91-22086 # p 559
N91-22087 # p 559
N91-22089 # p 560
N91-22091 * # p 560
N91-22093 * # p 560
N91-22094 # p 560
N91-22095 * # p 560
N91-22096 * # p 563
N91-22098 # p 563
N91-22099 # p 563
N91-22100 # p 569
N91-22101 # p 569
N91-22102 * # p 569
N91-22103 * # p 573
N91-22104 # p 573
N91-22105 # p 560
N91-22106 * # p 573
N91-22108 # p 561
N91-22109 # p 561
N91-22110 # p 573
N91-22112 p 574
N91-22117 * # p 574
N91-22118 # p 574
N91-22119 # p 574
N91-22120 # p 574
N91-22122 p 580
N91-22124 # p 580
N91-22125 # p 580
N91-22127 * # p 583
N91-22131 * # p 583
N91-22132 # p 583
N91-22133 # p 583
N91-22136 # p 585
N91-22137 # p 585
N91-22138 # p 586
N91-22313 * # p 605

N91-22318 * # p 574
N91-22331 * # p 587
N91-22332 * # p 583
N91-22333 * # p 575
N91-22334 * # p 583
N91-22335 * # p 584
N91-22337 * # p 584
N91-22380 # p 589
N91-22381 p 589
N91-22399 # p 589
N91-22407 # p 589
N91-22416 * # p 590
N91-22424 # p 590
N91-22475 * # p 600
N91-22480 # p 600
N91-22511 # p 600
N91-22520 # p 600
N91-22528 # p 600
N91-22529 # p 600
N91-22540 * # p 601
N91-22550 # p 601
N91-22564 # p 601
N91-22567 * # p 601
N91-22576 * # p 601
N91-22578 * # p 602
N91-22583 p 602
N91-22589 * # p 602
N91-22653 # p 603
N91-22654 # p 603
N91-22655 # p 603
N91-22656 # p 603
N91-22657 # p 603
N91-22658 # p 603
N91-22659 # p 603
N91-22661 # p 604
N91-22663 # p 604
N91-22670 # p 604
N91-22728 * # p 605
N91-22729 * # p 606
N91-22734 # p 606
N91-22792 * # p 606
N91-22794 * # p 606
N91-22805 * # p 606
N91-22830 * # p 608
N91-23020 # p 609
N91-23048 * # p 590
N91-23052 * # p 563
N91-23053 * # p 584

AVAILABILITY OF CITED PUBLICATIONS

IAA ENTRIES (A91-10000 Series)

Publications announced in *IAA* are available from the AIAA Technical Information Service as follows: Paper copies of accessions are available at $10.00 per document (up to 50 pages), additional pages $0.25 each. Standing order microfiche are available at the rate of $1.45 per microfiche for *IAA* source documents and $1.75 per microfiche for AIAA meeting papers.

Minimum air-mail postage to foreign countries is $2.50. All foreign orders are shipped on payment of pro-forma invoices.

All inquiries and requests should be addressed to: Technical Information Service, American Institute of Aeronautics and Astronautics, 555 West 57th Street, New York, NY 10019. Please refer to the accession number when requesting publications.

STAR ENTRIES (N91-10000 Series)

One or more sources from which a document announced in *STAR* is available to the public is ordinarily given on the last line of the citation. The most commonly indicated sources and their acronyms or abbreviations are listed below. If the publication is available from a source other than those listed, the publisher and his address will be displayed on the availability line or in combination with the corporate *source line.*

Avail: NTIS. Sold by the National Technical Information Service. Prices for hard copy (HC) and microfiche (MF) are indicated by a price code preceded by the letters HC or MF in the *STAR* citation. Current values for the price codes are given in the tables on NTIS PRICE SCHEDULES.

Documents on microfiche are designated by a pound sign (#) following the accession number. The pound sign is used without regard to the source or quality of the microfiche.

Initially distributed microfiche under the NTIS SRIM (Selected Research in Microfiche) is available at greatly reduced unit prices. For this service and for information concerning subscription to NASA printed reports, consult the NTIS Subscription Section, Springfield, VA 22161.

NOTE ON ORDERING DOCUMENTS: When ordering NASA publications (those followed by the * symbol), use the N accession number. NASA patent applications (only the specifications are offered) should be ordered by the US-Patent-Appl-SN number. Non-NASA publications (no asterisk) should be ordered by the AD, PB, or other *report number* shown on the last line of the citation, not by the N accession number. It is also advisable to cite the title and other bibliographic identification.

Avail: SOD (or GPO). Sold by the Superintendent of Documents, U.S. Government Printing Office, in hard copy. The current price and order number are given following the availability line. (NTIS will fill microfiche requests, as indicated above, for those documents identified by a # symbol.)

Avail: BLL (formerly NLL): British Library Lending Division, Boston Spa, Wetherby, Yorkshire, England. Photocopies available from this organization at the price shown. (If none is given, inquiry should be addressed to the BLL.)

Avail: DOE Depository Libraries. Organizations in U.S. cities and abroad that maintain collections of Department of Energy reports, usually in microfiche form, are listed in *Energy Research Abstracts*. Services available from the DOE and its depositories are described in a booklet, *DOE Technical Information Center - Its Functions and Services* (TID-4660), which may be obtained without charge from the DOE Technical Information Center.

Avail: ESDU. Pricing information on specific data, computer programs, and details on Engineering Sciences Data Unit (ESDU) topic categories can be obtained from ESDU International Ltd. Requesters in North America should use the Virginia address while all other requesters should use the London address, both of which are on the page titled ADDRESSES OF ORGANIZATIONS.

Avail: Fachinformationszentrum, Karlsruhe. Sold by the Fachinformationszentrum Energie, Physik, Mathematik GMBH, Eggenstein Leopoldshafen, Federal Republic of Germany, at the price shown in deutschmarks (DM).

Avail: HMSO. Publications of Her Majesty's Stationery Office are sold in the U.S. by Pendragon House, Inc. (PHI), Redwood City, CA. The U.S. price (including a service and mailing charge) is given, or a conversion table may be obtained from PHI.

Avail: NASA Public Document Rooms. Documents so indicated may be examined at or purchased from the National Aeronautics and Space Administration, Public Documents Room (Room 126), 600 Independence Ave., S.W., Washington, DC 20546, or public document rooms located at each of the NASA research centers, the NASA Space Technology Laboratories, and the NASA Pasadena Office at the Jet Propulsion Laboratory.

Avail: Univ. Microfilms. Documents so indicated are dissertations selected from *Dissertation Abstracts* and are sold by University Microfilms as xerographic copy (HC) and microfilm. All requests should cite the author and the Order Number as they appear in the citation.

Avail: US Patent and Trademark Office. Sold by Commissioner of Patents and Trademarks, U.S. Patent and Trademark Office, at the standard price of $1.50 each, postage free.

Avail: (US Sales Only). These foreign documents are available to users within the United States from the National Technical Information Service (NTIS). They are available to users outside the United States through the International Nuclear Information Service (INIS) representative in their country, or by applying directly to the issuing organization.

Avail: USGS. Originals of many reports from the U.S. Geological Survey, which may contain color illustrations, or otherwise may not have the quality of illustrations preserved in the microfiche or facsimile reproduction, may be examined by the public at the libraries of the USGS field offices whose addresses are listed in this Introduction. The libraries may be queried concerning the availability of specific documents and the possible utilization of local copying services, such as color reproduction.

Avail: Issuing Activity, or Corporate Author, or no indication of availability. Inquiries as to the availability of these documents should be addressed to the organization shown in the citation as the corporate author of the document.

FEDERAL DEPOSITORY LIBRARY PROGRAM

In order to provide the general public with greater access to U.S. Government publications, Congress established the Federal Depository Library Program under the Government Printing Office (GPO), with 52 regional depositories responsible for permanent retention of material, inter-library loan, and reference services. At least one copy of nearly every NASA and NASA-sponsored publication, either in printed or microfiche format, is received and retained by the 52 regional depositories. A list of the regional GPO libraries, arranged alphabetically by state, appears on the inside back cover. These libraries are *not* sales outlets. A local library can contact a Regional Depository to help locate specific reports, or direct contact may be made by an individual.

PUBLIC COLLECTION OF NASA DOCUMENTS

An extensive collection of NASA and NASA-sponsored publications is maintained by the British Library Lending Division, Boston Spa, Wetherby, Yorkshire, England for public access. The British Library Lending Division also has available many of the non-NASA publications cited in *STAR*. European requesters may purchase facsimile copy or microfiche of NASA and NASA-sponsored documents, those identified by both the symbols # and * from ESA – Information Retrieval Service European Space Agency, 8-10 rue Mario-Nikis, 75738 CEDEX 15, France.

STANDING ORDER SUBSCRIPTIONS

NASA SP-7037 supplements and annual index are available from the National Technical Information Service (NTIS) on standing order subscription as PB91-914100, at price code A04. Current values for the price codes are listed on page APP-5. Standing order subscriptions do not terminate at the end of a year, as do regular subscriptions, but continue indefinitely unless specifically terminated by the subscriber.

ADDRESSES OF ORGANIZATIONS

American Institute of Aeronautics and Astronautics
Technical Information Service
555 West 57th Street, 12th Floor
New York, New York 10019

British Library Lending Division,
Boston Spa, Wetherby, Yorkshire,
England

Commissioner of Patents and Trademarks
U.S. Patent and Trademark Office
Washington, DC 20231

Department of Energy
Technical Information Center
P.O. Box 62
Oak Ridge, Tennessee 37830

European Space Agency-Information Retrieval Service
ESRIN
Via Galileo Galilei
00044 Frascati (Rome) Italy

Engineering Sciences Data Unit International
P.O. Box 1633
Manassas, Virginia 22110

Engineering Sciences Data Unit International, Ltd.
251-259 Regent Street
London, W1R 7AD, England

Fachinformationszentrum Energie, Physik, Mathematik
GMBH
7514 Eggenstein Leopoldshafen
Federal Republic of Germany

Her Majesty's Stationery Office
P.O. Box 569, S.E. 1
London, England

NASA Center for AeroSpace Information
P.O. Box 8757
BWI Airport, Maryland 21240

National Aeronautics and Space Administration
Scientific and Technical Information Program (NTT)
Washington, DC 20546

National Technical Information Service
5285 Port Royal Road
Springfield, Virginia 22161

Pendragon House, Inc.
899 Broadway Avenue
Redwood City, California 94063

Superintendent of Documents
U.S. Government Printing Office
Washington, DC 20402

University Microfilms
A Xerox Company
300 North Zeeb Road
Ann Arbor, Michigan 48106

University Microfilms, Ltd.
Tylers Green
London, England

U.S. Geological Survey Library National Center
MS 950
12201 Sunrise Valley Drive
Reston, Virginia 22092

U.S. Geological Survey Library
2255 North Gemini Drive
Flagstaff, Arizona 86001

U.S. Geological Survey
345 Middlefield Road
Menlo Park, California 94025

U.S. Geological Survey Library
Box 25046
Denver Federal Center, MS914
Denver, Colorado 80225

NTIS PRICE SCHEDULES

(Effective January 1, 1991)

Schedule A
STANDARD PRICE DOCUMENTS AND MICROFICHE**

PRICE CODE	NORTH AMERICAN PRICE	FOREIGN PRICE
A01	$ 8.00	$ 16.00
A02	11.00	22.00
A03	15.00	30.00
A04-A05	17.00	34.00
A06-A09	23.00	46.00
A10-A13	31.00	62.00
A14-A17	39.00	78.00
A18-A21	45.00	90.00
A22-A25	53.00	106.00
A99	*	*
N01	60.00	120.00
N02	59.00	118.00
N03	20.00	40.00

Schedule E
EXCEPTION PRICE DOCUMENTS AND MICROFICHE**

PRICE CODE	NORTH AMERICAN PRICE	FOREIGN PRICE
E01	$10.00	$ 20.00
E02	12.00	24.00
E03	14.00	28.00
E04	16.50	33.00
E05	18.50	37.00
E06	21.50	43.00
E07	24.00	48.00
E08	27.00	54.00
E09	29.50	59.00
E10	32.50	65.00
E11	35.00	70.00
E12	38.50	77.00
E13	41.00	82.00
E14	45.00	90.00
E15	48.50	97.00
E16	53.00	106.00
E17	57.50	115.00
E18	62.00	124.00
E19	69.00	138.00
E20	80.00	160.00
E99	*	*

* Contact NTIS for price quote.

** Effective January 1, 1991, the microfiche copy of any new document entering the NTIS collection will be priced the same as the paper copy of the document.

IMPORTANT NOTICE

NTIS Shipping and Handling Charges

U.S., Canada, Mexico — ADD $3.00 per TOTAL ORDER

All Other Countries — ADD $4.00 per TOTAL ORDER

Exceptions — Does NOT apply to:

ORDERS REQUESTING NTIS RUSH HANDLING
ORDERS FOR SUBSCRIPTION OR STANDING ORDER PRODUCTS *ONLY*

NOTE: Each additional delivery address on an order requires a separate shipping and handling charge.

1. Report No.	2. Government Accession No.	3. Recipient's Catalog No.
NASA SP-7037(268)		

4. Title and Subtitle	5. Report Date
Aeronautical Engineering A Continuing Bibliography (Supplement 268)	August 1991
	6. Performing Organization Code NTT
7. Author(s)	8. Performing Organization Report No.
	10. Work Unit No.
9. Performing Organization Name and Address NASA Scientific and Technical Information Program	11. Contract or Grant No.
	13. Type of Report and Period Covered Special Publication
12. Sponsoring Agency Name and Address National Aeronautics and Space Administration Washington, DC 20546	14. Sponsoring Agency Code

15. Supplementary Notes

16. Abstract

This bibliography lists 406 reports, articles and other documents introduced into the NASA scientific and technical information system in July 1991.

17. Key Words (Suggested by Author(s))	18. Distribution Statement
Aeronautical Engineering Aeronautics Bibliographies	Unclassified - Unlimited Subject Category - 01

19. Security Classif. (of this report)	20. Security Classif. (of this page)	21. No. of Pages	22. Price *
Unclassified	Unclassified	134	A07/HC

*For sale by the National Technical Information Service, Springfield, Virginia 22161

NASA-Langley, 1991

FEDERAL REGIONAL DEPOSITORY LIBRARIES

ALABAMA

AUBURN UNIV. AT MONTGOMERY LIBRARY
Documents Dept.
7300 University Drive
Montgomery, AL 36117-3596
(205) 244-3650 FAX: (205) 244-0678

UNIV. OF ALABAMA
Amelia Gayle Gorgas Library
Govt. Documents
Box 870266
Tuscaloosa, AL 35487-0266
(205) 348-6046 FAX: (205) 348-8833

ARIZONA

DEPT. OF LIBRARY, ARCHIVES, AND PUBLIC RECORDS
Federal Documents
Third Floor State Capitol
1700 West Washington
Phoenix, AZ 85007
(602) 542-4121 FAX: (602) 542-4400; 542-4500

ARKANSAS

ARKANSAS STATE LIBRARY
State Library Services
One Capitol Mall
Little Rock, AR 72201
(501) 682-2869

CALIFORNIA

CALIFORNIA STATE LIBRARY
Govt. Publications Section
914 Capitol Mall - P.O. Box 942837
Sacramento, CA 94237-0001
(916) 322-4572 FAX: (916) 324-8120

COLORADO

UNIV. OF COLORADO - BOULDER
Norlin Library
Govt. Publications
Campus Box 184
Boulder, CO 80309-0184
(303) 492-8834 FAX: (303) 492-2185

DENVER PUBLIC LIBRARY
Govt. Publications Dept. BS/GPD
1357 Broadway
Denver, CO 80203
(303) 571-2135

CONNECTICUT

CONNECTICUT STATE LIBRARY
231 Capitol Avenue
Hartford, CT 06106
(203) 566-4971 FAX: (203) 566-3322

FLORIDA

UNIV. OF FLORIDA LIBRARIES
Documents Dept.
Library West
Gainesville, FL 32611-2048
(904) 392-0366 FAX: (904) 392-7251

GEORGIA

UNIV. OF GEORGIA LIBRARIES
Govt. Documents Dept.
Jackson Street
Athens, GA 30602
(404) 542-8949 FAX: (404) 542-6522

HAWAII

UNIV. OF HAWAII
Hamilton Library
Govt. Documents Collection
2550 The Mall
Honolulu, HI 96822
(808) 948-8230 FAX: (808) 956-5968

IDAHO

UNIV. OF IDAHO LIBRARY
Documents Section
Moscow, ID 83843
(208) 885-6344 FAX: (208) 885-6817

ILLINOIS

ILLINOIS STATE LIBRARY
Reference Dept.
300 South Second
Springfield, IL 62701-1796
(217) 782-7596 FAX: (217) 524-0041

INDIANA

INDIANA STATE LIBRARY
Serials/Documents Section
140 North Senate Avenue
Indianapolis, IN 46204
(317) 232-3678 FAX: (317) 232-3728

IOWA

UNIV. OF IOWA LIBRARIES
Govt. Publications Dept.
Washington & Madison Streets
Iowa City, IA 52242
(319) 335-5926 FAX: (319) 335-5830

KANSAS

UNIV. OF KANSAS
Govt. Documents & Map Library
6001 Malatt Hall
Lawrence, KS 66045-2800
(913) 864-4660 FAX: (913) 864-5380

KENTUCKY

UNIV. OF KENTUCKY LIBRARIES
Govt. Publications/Maps Dept.
Lexington, KY 40506-0039
(606) 257-3139 FAX: (606) 257-1563; 257-8379

LOUISIANA

LOUISIANA STATE UNIV.
Middleton Library
Govt. Documents Dept.
Baton Rouge, LA 70803
(504) 388-2570 FAX: (504) 388-6992

LOUISIANA TECHNICAL UNIV.
Prescott Memorial Library
Govt. Documents Dept.
305 Wisteria Street
Ruston, LA 71270-9985
(318) 257-4962 FAX: (318) 257-2447

MAINE

TRI-STATE DOCUMENTS DEPOSITORY
Raymond H. Fogler Library
Govt. Documents & Microforms Dept.
Univ. of Maine
Orono, ME 04469
(207) 581-1680

MARYLAND

UNIV. OF MARYLAND
Hornbake Library
Govt. Documents/Maps Unit
College Park, MD 20742
(301) 454-3034 FAX: (301) 454-4985

MASSACHUSETTS

BOSTON PUBLIC LIBRARY
Govt. Documents Dept.
666 Boylston Street
Boston, MA 02117
(617) 536-5400 ext. 226
FAX: (617) 267-8273; 267-8248

MICHIGAN

DETROIT PUBLIC LIBRARY
5201 Woodward Avenue
Detroit, MI 48202-4093
(313) 833-1440; 833-1409
FAX: (313) 833-5039

LIBRARY OF MICHIGAN
Govt. Documents Unit
P.O. Box 30007
Lansing, MI 48909
(517) 373-0640 FAX: (517) 373-3381

MINNESOTA

UNIV. OF MINNESOTA
Wilson Library
Govt. Publications Library
309 19th Avenue South
Minneapolis, MN 55455
(612) 624-5073 FAX: (612) 626-9353

MISSISSIPPI

UNIV. OF MISSISSIPPI
J.D. Williams Library
Federal Documents Dept.
106 Old Gym Bldg.
University, MS 38677
(601) 232-5857 FAX: (601) 232-5453

MISSOURI

UNIV. OF MISSOURI - COLUMBIA
Ellis Library
Govt. Documents
Columbia, MO 65201
(314) 882-6733 FAX: (314) 882-8044

MONTANA

UNIV. OF MONTANA
Maureen & Mike Mansfield Library
Documents Div.
Missoula, MT 59812-1195
(406) 243-6700 FAX: (406) 243-2060

NEBRASKA

UNIV. OF NEBRASKA - LINCOLN
D.L. Love Memorial Library
Documents Dept.
Lincoln, NE 68588
(402) 472-2562

NEVADA

UNIV. OF NEVADA
Reno Library
Govt. Publications Dept.
Reno, NV 89557
(702) 784-6579 FAX: (702) 784-1751

NEW JERSEY

NEWARK PUBLIC LIBRARY
U.S. Documents Div.
5 Washington Street - P.O. Box 630
Newark, NJ 07101-0630
(201) 733-7812 FAX: (201) 733-5648

NEW MEXICO

UNIV. OF NEW MEXICO
General Library
Govt. Publications Dept.
Albuquerque, NM 87131-1466
(505) 277-5441 FAX: (505) 277-6019

NEW MEXICO STATE LIBRARY
325 Don Gaspar Avenue
Santa Fe, NM 87503
(505) 827-3826 FAX: (505) 827-3820

NEW YORK

NEW YORK STATE LIBRARY
Documents/Gift & Exchange Section
Federal Depository Program
Cultural Education Center
Albany, NY 12230
(518) 474-5563 FAX: (518) 474-5786

NORTH CAROLINA

UNIV. OF NORTH CAROLINA - CHAPEL HILL
CB#3912, Davis Library
BA/SS Dept.—Documents
Chapel Hill, NC 27599
(919) 962-1151 FAX: (919) 962-0484

NORTH DAKOTA

NORTH DAKOTA STATE UNIV. LIBRARY
Documents Office
Fargo, ND 58105
(701) 237-8886 FAX: (701) 237-7138
In cooperation with Univ. of North Dakota, Chester Fritz Library
Grand Forks

OHIO

STATE LIBRARY OF OHIO
Documents Dept.
65 South Front Street
Columbus, OH 43266
(614) 644-7051 FAX: (614) 752-9178

OKLAHOMA

OKLAHOMA DEPT. OF LIBRARIES
U.S. Govt. Information Div.
200 NE 18th Street
Oklahoma City, OK 73105-3298
(405) 521-2502, ext. 252, 253
FAX: (405) 525-7804

OKLAHOMA STATE UNIV.
Edmon Low Library
Documents Dept.
Stillwater, OK 74078
(405) 744-6546 FAX: (405) 744-5183

OREGON

PORTLAND STATE UNIV.
Millar Library
934 SW Harrison - P.O. Box 1151
Portland, OR 97207
(503) 725-3673 FAX: (503) 725-4527

PENNSYLVANIA

STATE LIBRARY OF PENN.
Govt. Publications Section
Walnut St. & Commonwealth Ave. - P.O. Box 1601
Harrisburg, PA 17105
(717) 787-3752

SOUTH CAROLINA

CLEMSON UNIV.
Cooper Library
Public Documents Unit
Clemson, SC 29634-3001
(803) 656-5174 FAX: (803) 656-3025
In cooperation with Univ. of South Carolina, Thomas Cooper Library, Columbia

TENNESSEE

MEMPHIS STATE UNIV. LIBRARIES
Govt. Documents
Memphis, TN 38152
(901) 678-2586 FAX: (901) 678-2511

TEXAS

TEXAS STATE LIBRARY
United States Documents
P.O. Box 12927 - 1201 Brazos
Austin, TX 78711
(512) 463-5455 FAX: (512) 463-5436

TEXAS TECH. UNIV. LIBRARY
Documents Dept.
Lubbock, TX 79409
(806) 742-2268 FAX: (806) 742-1920

UTAH

UTAH STATE UNIV.
Merrill Library & Learning Resources Center, UMC-3000
Documents Dept.
Logan, UT 84322-3000
(801) 750-2684 FAX: (801) 750-2677

VIRGINIA

UNIV. OF VIRGINIA
Alderman Library
Govt. Documents
Charlottesville, VA 22903-2498
(804) 924-3133 FAX: (804) 924-4337

WASHINGTON

WASHINGTON STATE LIBRARY
Document Section
MS AJ-11
Olympia, WA 98504-0111
(206) 753-4027 FAX: (206) 753-3546

WEST VIRGINIA

WEST VIRGINIA UNIV. LIBRARY
Govt. Documents Section
P.O. Box 6069
Morgantown, WV 26506
(304) 293-3640

WISCONSIN

ST. HIST. SOC. OF WISCONSIN LIBRARY
Govt. Publications Section
816 State Street
Madison, WI 53706
(608) 262-2781 FAX: (608) 262-4711
In cooperation with Univ. of Wisconsin-Madison, Memorial Library

MILWAUKEE PUBLIC LIBRARY
Documents Div.
814 West Wisconsin Avenue
Milwaukee, WI 53233
(414) 278-2167 FAX: (414) 278-2137

WYOMING

WYOMING STATE LIBRARY
Supreme Court & Library Bldg.
Govt. Publications
Cheyenne, WY 82002
(307) 777-5920 FAX: (307) 777-6289

National Aeronautics and
Space Administration
Code NTT-4

Washington, D.C.
20546-0001

Official Business
Penalty for Private Use, $300

BULK RATE
POSTAGE & FEES PAID
NASA
Permit No. G-27

POSTMASTER: If Undeliverable (Section 158 Postal Manual) Do Not Return